

https://dspace.org/

An Investigation into the Effect of Advanced Gravity Separation on Platinum Group Metals (PGM) Flotation Concentrates

Nair, Taurean Jevaldo

2024
University of the Witwatersrand, Johannesburg
https://hdl.handle.net/10539/45398
Nair, Taurean Jevaldo . (2024). An Investigation into the Effect of Advanced Gravity Separation on Platinum Group Metals (PGM) Flotation Concentrates [Masters dissertation, University of the Witwatersrand, Johannesburg]. WIReDSpace. https://hdl.handle.net/10539/45398

Downloaded from a DSpace repository. https://dspace.org/

An Investigation into the Effect of Advanced Gravity Separation on Platinum Group Metals (PGM) Flotation Concentrates

MSc (50/50) RESEARCH REPORT

Prepared by

Taurean Nair

0603267E

Submitted to

School of Chemical and Metallurgical Engineering, Faculty of Engineering and the Built Environment, University of the Witwatersrand, Johannesburg, South Africa

Supervisor: Professor Vusumuzi Sibanda

JUNE 2024

Abstract

"It's the gravity that shapes the large-scale structure of the universe, even though it is the weakest of four categories of forces" - Stephen Hawking

Gravity concentration has been around since the dawn of mankind, and just as man has evolved so too has gravity concentration. The earliest records involved ancient cultures (Greeks, Romans, Mayans and Egyptians) using water to selectively separate precious metals from gangue. Gravity concentration has remained an integral part of many processes involving the recovery of native or alluvial precious metals and minerals which are amenable to this process. Developments in gravity concentration technology have led to the inception of advanced gravity separation devices. These advanced gravity separators can overcome the challenges associated with conventional gravity concentration as they are able to induce a high gravitational force that is capable of recovering fine and ultrafine heavy particles as well as particles with a complex mineralogy.

Decreasing feed grades and falling metal prices are placing an exorbitant amount of pressure on the PGM industry. As a price-taker, the industry is at the mercy of the prevailing market conditions. This means that the only levers the industry can use are cost cutting or optimization of the process to produce more PGMs at a better quality from the current feed source. The premise of this research project is to essentially find a way to optimize the PGM beneficiation process by the use of gravity concentration. This research specifically targeted the high-grade flotation concentrate stream of a UG2 tailings plant to understand how effective advanced gravity concentration would be in recovering PGMs, upgrading the resulting concentrate as well as rejecting chromite and gangue.

PGMs are associated with base-metal sulphides and are inherently complex. This complexity is further exacerbated by the fact that PGMs are in the fine to ultrafine particle size range which makes recovery of PGMs challenging. Gravity concentration is primarily a function of particle size, density and mineralogy. Separation of gangue and chromite from PGMs is another added complication as the gangue minerals are present in higher concentration than the PGMs, have a complex mineralogy and are also found in the fine and ultrafine particle sizes. Fire Assay/ICP-

MS, XRF, XRD and SEM all confirmed the complexity of the ore being treated. This ‘entanglement of complexity’ makes processing these ores very challenging.

A lab-scale Falcon gravity concentrator with an unfluidized (ultrafine) bowl was used in the main experimental work. The optimal parameters to run the gravity concentrator for PGMs was found to be a flow rate of 3 L/min, percent solids of 13.22% and a gravitational force of 300 G’s. These parameters were then applied to a multi-stage gravity concentration process. The feed to the gravity concentrator was found to have a grade of 131.02 g/t 4E PGM. The results indicated that a recovery of 48.90% and a final concentrate grade of 292.04 g/t 4E was achieved at a mass pull of 21.90%. The chromite in the final concentrate of the Falcon gravity concentrator was found to be 1.99% which did not exceed the maximum allowable chrome in concentrate of 3.00%. This proved that gravity concentration was indeed capable of recovering complex PGMs and rejecting chromite. The optimal parameters experiments indicated repeatability, and the assay results were validated by a statistical outlier test in the Minitab Software to ensure data integrity. The particle size analysis revealed that 97.07% of the feed to the Falcon was below 75µm and 66.29% below 25µm, thus confirming that the feed material was fine to ultrafine particles. The final gravity concentrate had a D_{90} of 42.24µm which was finer than the D_{90} for the feed, this demonstrates that fine and ultrafine heavy particles were more mineralized and recoverable by the Falcon. This analysis was further reinforced by the fractional analysis which confirmed that the majority of the PGMs were found in the fine to ultrafine fraction. The experiments were repeated using a fluidized bowl in the Falcon to see what the impact of fluidizing water would be. These experiments had lower overall recoveries and mass pulls than those done with an unfluidized bowl. The concentrate grade was, however, higher than the unfluidized bowl experiments possibly due to this bowl recovering PGMs in the coarser fraction.

This research provides a steppingstone to understanding the effect of advanced gravity concentration on PGM flotation concentrates and indeed on PGMs in general as well as providing an alternative unique processing option for PGMs. Ultimately advanced gravity concentration has been shown to be an uncomplicated process that can be viable in the recovery of fine and ultrafine complex PGMs. It is environmentally friendly, has low capital and operational costs and has a relatively high efficiency.

Declaration

I, Taurean Nair (Student number: 0603267E) am a student registered for MSc (50/50) in the year 2023/2024. I hereby declare the following:

- I am aware that plagiarism (the use of someone else's work without their permission and/or without acknowledging the original source) is wrong.
- I confirm that the work submitted for assessment for the above course is my own unaided work except where I have explicitly indicated otherwise.
- I have followed the required conventions in referencing the thoughts and ideas of others.
- I understand that the University of the Witwatersrand may take disciplinary action against me if there is a belief that this is not my own unaided work or that I have failed to acknowledge the source of the ideas or words in my writing.

Student Signature:  Date: 24-06-2024

Acknowledgements

I would like to thank almighty God for the strength and endurance to complete this research paper.

This endeavour would not have been possible without the financial support of Sibanye-Stillwater. I would like to express my deepest appreciation for the study grant that I was awarded.

I would like to thank my supervisor, Professor Vusumuzi Sibanda, for his guidance, encouragement, and patience throughout the course of this project. I would also like to thank him for the academic mentorship I received during the entire time I was doing my Masters.

I would like to thank the Lab manager, lab technicians and the administrative staff at the School of Chemical and Metallurgical Engineering for assisting me in ensuring that all the laboratory and academic resources were available when required at Wits University.

I would like to thank the laboratory staff at Marikana ETTP Operation as well as the shift personnel who assisted me with the ‘heavy lifting’ of preparing the bulk sample. I would also like to thank the ETTP plant management for allowing me to use their laboratory facilities to conduct the experimental work as well as the engineering team for ensuring that the Falcon was installed correctly and that all safety related protocols were followed.

I would like to thank Ashley Mmola for his metallurgical insight as well as his assistance with preparing the sample for the experimental work. I am grateful for his support throughout my Masters journey.

I would like to express my deepest gratitude to Wynand Erasmus of Sepro Mineral Systems South Africa, for allowing me to use the Falcon Gravity Concentrator for my experimental work. I would also like to thank him for sharing his expertise and knowledge with me.

I would like to thank my mother and father for their unwavering support during my Masters. I am deeply indebted to them for all the sacrifices they have made to give me a good education. I am also grateful for the passion for learning and drive to further my education that they have instilled in me. Words cannot express my gratitude to my brother and his fiancé as well as my fiancé who have all been pillars of strength throughout my Masters journey, thank you for motivating and encouraging me.

Table of Contents

Abstract i
Declaration iii
Acknowledgements iv
List of Figures ix
List of Tables xvi
Nomenclature xvii
1. Introduction 1
1.1. Background and Context 1
1.2. Problem Statement 3
1.3. Research Aim and Objective(s) 4
1.4. Hypothesis 4
1.5. Research Questions 5
1.6. Research Approach 5
1.7. Thesis Outline 5
2. Literature Review 7
2.1. Geological Context 7
2.1.1. Petrology and Mineralogy 7
2.1.2. Geometallurgical Characterization of Merensky Reef and UG2 Reef 13
2.2. Comminution of PGMs 21
2.2.1. Introduction to Comminution 21
2.2.2. Comminution Applied to PGM Containing Ore 22
2.2.3. Developments in PGM Comminution 24
2.3. Flotation of PGMs 25
2.3.1. Introduction to Flotation 25
2.3.2. Flotation Reagents 27
2.3.3. Developments in Flotation 29
2.3.4. Considerations for PGM Flotation 30
2.4. PGM Smelting 31
2.5. Gravity Concentration of Minerals 33
2.5.1. Principle of Gravity Concentration 34
2.5.2. Mechanisms of Gravity Concentration 36
2.6. Experimental Research and Application of Gravity Concentration 37

2.6.1. Conventional Gravity Separation 37
2.6.1.1. Jigging 37
2.6.1.2. Spirals 40
2.6.1.3. Shaking Tables 42
2.6.1.4. Reflux ® Classifier 44
2.6.2. Advanced/Enhanced Gravity Separation 47
2.7. The Falcon Gravity Concentrator 51
2.8. Gravity Concentration Applied to PGMs 54
2.9. A Theoretical Framework for Gravity Concentration of PGMs 56
3. Methodology 59
3.1. Sample Preparation 59
3.2. Experimental Setup 60
3.3. Feed Analysis 62
3.4. Experimental Work 62
3.4.1. Phase 1 – baseline tests 62
3.4.2. Phase 2 – variable % solids 63
3.4.3. Phase 3 – variable G-force 63
3.4.4. Phase 4 – variable flow rate 63
3.4.5. Phase 5 – multi-stage concentration 64
3.4.6. Phase 6 – PSA and Qualitative tests 65
3.4.7. Phase 7 – fluidized bowl tests 65
4. Results and Discussion 67
4.1. Introduction 67
4.2. Gravity Concentrator Feed Analysis 68
4.3. Falcon Parameter Determination Experiments 69
4.3.1. Phase 1: Recommended Parameters 69
4.3.2. Phase 2: Change in % Solids 70
4.3.3. Phase 3: Change in G-force 73
4.3.4. Phase 4: Change in Flow Rate 76
4.4. Falcon Experiments with Optimal Parameters 79
4.4.1. Phase 5: Optimized Parameters 79
4.4.2. Mass Pull/Recovery/Grade Relationship 85
4.4.3. PGM Recovery per Element 89

4.4.4. Chrome Rejection 90
4.4.5. Gangue Behavior 92
4.4.6. Particle Size Analysis 95
4.4.7. Fractional Analysis 98
4.4.8. Fluidized Bowl Experiments 109
4.5. Model for Additional Stages 115
4.6. SEM Results 118
4.7. XRF Results 129
4.8. XRD Results 133
5. Integrated Discussion 134
6. Conclusion and Recommendations 138
7. References 141
Appendices 158
Appendix A: Phase 1-4 Data 159
Appendix B: Phase 5 Data 162
Mass and Moisture Data 162
Outlier Control Charts 163
Phase 5: Assay and Mass yield/Recovery/Grade Data 208
Appendix C: PSD and Fractional Data 211
Malvern Data 211
Fractional Data 218
Appendix D: Phase 7 Data 219
Mass and Moisture Data 219
Phase 7: Assay and Mass yield/Recovery/Grade Data 220
Appendix E: XRF Raw Data 221
Appendix F: XRD Graphs 225
Appendix G: SEM Images and Graphs 228

List of Figures

Figure 1:Ternary Fo-Di-SiO_2 system showing parental magmas of the Stillwater Complex, Great Dyke, and Bushveld Complex plotted [Diagram from Chaumba (2022) with data from various authors compiled by McCallum (1996), Wilson (1996) and Cawthorn (2015). *8*

Figure 2: Sketches showing the formation of PGE-enriched reefs, PGE-enriched chromitite and magnetite reefs in layered intrusions (a) Crustal loading during magma emplacement causes central subsidence. Incompletely solidified cumulates slump towards the centre of intrusion, and disseminated sulphide, chromite and magnetite form massive layers. (b) Erosion exposes the variety of layered intrusions to various levels [Diagram from Chaumba (2022) simplified from Maier et al. (2013)]. *9*

Figure 3: Map of the Bushveld Igneous Complex (Watson et al., 2010) *11*

Figure 4: Stratigraphic Column Showing the Position of the UG-2 Reef Relative to the Merensky Reef (Schouwstra et al., 2000) *11*

Figure 5: Typical process flow Diagram for PGM Ore Processing (Jones, 1999; Cramer, 2008) *17*

Figure 6: Typical Grain Size of Merensky and UG2 Reefs (Hay & Roy, 2010) *18*

Figure 7: Photomicrographs sourced from an MLA investigation report on tailings from a Western Bushveld UG2 tailings sample showing the complexity of the liberation challenge; note that each particle shown has a PGM phase shown in red. These 'attached', 'middlings' and 'locked' composite particles are all sub 100 micron (Rule, 2008). *19*

Figure 8:Back scattered electron images showed the various types of PGM association in the Merensky (b–d) and UG2 platinum ores (a). (a) Liberated PGM; (b) PGM locked in liberated BMS; (c) PGM occluded in locked BMS; (d) PGM locked in silicate gangue. (Solomon et al., 2011). *19*

Figure 9: Different Breakage Mechanisms and the Resulting Product Size Distributions [In Lisso (2013) adapted from Varinot et al., (1997)] *22*

Figure 10: Typical MF2 Circuit (Cole & Ferron, 2002) *23*

Figure 11: Schematic of (a) Generic Mainstream Inert Grinding and (b) Generic Ultrafine Grinding (Rule, 2008) *23*

Figure 12: Flotation cell (Sefako, 2018) *26*

Figure 13: The froth flotation system illustrated as a three-cornered interactive system. (Klimpel, 2003) *26*

Figure 14: Typical industrial flotation collectors. R represents different hydrocarbon chains (and hydrogen atoms in cationic collectors). (Nguyen, 2012) *27*

Figure 15: Basic principles of a jig concentrator (Haldar, 2018) *38*

Figure 16: Basic principles of jigging (Yan & Gupta, 2006) *38*

Figure 17: Spiral Concentrator (FLSmidth, 2024) *40*

Figure 18: A standard spiral concentrator (Haldar, 2018) *41*

Figure 19: Typical Shaking Table Designs (Solo Resources, 2024) *43*

Figure 20: Gold Separation on a Shaking Table (source of photo: Taurean Nair, 2015) *43*

Figure 21: Reflux Classifier (FLSmidth, 2024) *46*
Figure 22: Standard Reflux Classifier Schematic (Galvin & Ivenson, 2014) *46*
Figure 23:Influence of rotation speed on the fluidized bowl and UF Falcon Bowl on various responses (a) yield, (b) WO_3 content and (c) recovery (Das et al., 2023) *49*
Figure 24: Influence of bowl speed on calcite rejection (Das et al., 2023) *49*
Figure 25: Falcon Ultrafine (UF) Concentrator (Sepro Mineral Systems, 2024) *52*
Figure 26: Falcon Fluidized Concentrator (Sepro Mineral Systems, 2024) *53*
Figure 27: Falcon Gravity Concentrator circuit with roughers and cleaners (Grewal & Neale, 2017) *53*
Figure 28: Bulk sample *59*
Figure 29: Homogenized sample *60*
Figure 30: Rotary splitter *60*
Figure 31: Experimental equipment showing (a) Falcon concentrator experimental equipment and feed pump, (b) Close up of Falcon Concentrator showing the controller for the g-force (frequency inverter) and (c) The Bowl fitted inside the Falcon *61*
Figure 32: Multistage Gravity Concentration *64*
Figure 33: Falcon gravity concentrator bowls showing the fluidized bowl (left) and unfluidized bowl (right) *66*
Figure 34: One stage gravity concentration *69*
*Figure 35: Phase 2 results indicating (a) mass pull, (b) recovery, (c) concentrate grade, (d) enrichment ratio, (e) chrome content and (f) gangue content (Please see **Appendix A** for raw data and calculation sheet)* *72*
*Figure 36: Phase 3 results indicating (a) mass pull, (b) recovery, (c) concentrate grade, (d) enrichment ratio, (e) chrome content and (f) gangue content as a function of G-force (Please see **Appendix A** for raw data and calculation sheet)* *75*
Figure 37: Phase 4 results indicating (a) mass pull, (b) recovery, (c) concentrate grade, (d) enrichment ratio, (e) chrome content and (f) gangue content *78*
Figure 38: Falcon gravity concentrator lab scale stages per run *80*
Figure 39: GC Concentrate images showing (a) GC concentrate 1. (b) GC concentrate 2. (c) GC concentrate 3. (d) GC concentrate 4. (e) GC concentrate 5 and (f) close-up image of GC concentrate 1 showing dark spiral lines. *81*
Figure 40: Phase 5 weighted PGM content in feed and concentrates *83*
Figure 41: Phase 5 weighted base metals and sulphur content in feed and concentrates *83*
Figure 42: Phase 5 weighted 4E and 6E recovery *84*
Figure 43: Phase 5 mass yield per stage *86*
Figure 44: Phase 5 cumulative mass yield *86*
Figure 45: Phase 5 4E recovery per stage *87*
Figure 46: Phase 5 cumulative 4E recovery *87*
Figure 47: Phase 5 4E grade per stage *88*

Figure 48: Phase 5 cumulative 4E grade *88*
Figure 49: Phase 5 PGM elemental recovery *90*
Figure 50: Phase 5 chrome content in GC feed, concentrates and tail *91*
Figure 51: Phase 5 chrome rejection per stage *91*
Figure 52: Phase 5 cumulative chrome rejection *92*
Figure 53: Phase 5 silicon dioxide content in GC feed, concentrates and tail *93*
Figure 54: Phase 5 magnesium oxide content in GC feed, concentrates and tail *93*
Figure 55: Phase 5 calcium oxide content in GC feed, concentrates and tail *94*
Figure 56: Phase 5 aluminium oxide content in GC feed, concentrates and tail *94*
Figure 57: Malvern Mastersizer 3000 ..... *95*
Figure 58: Cumulative percent passing *96*
Figure 59: GC feed 4E and 6E PGM content per size fraction *99*
Figure 60: GC feed Copper, Nickel and Sulphur per size fraction *99*
Figure 61: GC feed PGE content per size fraction *100*
Figure 62: GC feed Gangue content per size fraction *100*
Figure 63: GC feed Chromium per size fraction *101*
Figure 64: GC tail 4E and 6E PGM content per size fraction *101*
Figure 65: GC tail Copper, Nickel and Sulphur per size fraction *102*
Figure 66: GC tail PGE content per size fraction *102*
Figure 67: GC tail Gangue content per size fraction *103*
Figure 68: GC tail Chromium per size fraction *103*
Figure 69: GC concentrate 4E and 6E PGM content per size fraction *104*
Figure 70: GC concentrate Copper, Nickel and Sulphur per size fraction *104*
Figure 71: GC concentrate PGE content per size fraction *105*
Figure 72: GC concentrate Gangue content per size fraction *105*
Figure 73: GC concentrate Chromium per size fraction *106*
Figure 74: GC Concentrate fluidized bowl images showing (a) GC concentrate 1. (b) GC concentrate 2. (c) GC concentrate 3. (d) GC concentrate 4. (e) GC concentrate 5 and (f) close-up image of fluidizing water *111*
Figure 75: Phase 7 stage recovery at various fluidizing flow rates *112*
Figure 76: Phase 7 stage grade at various fluidizing flow rates *112*
Figure 77: Phase 7 base metals and sulphur content *113*
Figure 78: Phase 7 cumulative chrome rejection *113*
Figure 79: Phase 7 chrome content *114*
Figure 80: Relationship between feed grade and concentrate grade *115*
Figure 81: Modelled vs measured recovery per stage *117*

Figure 82: Zeiss SEM *118*
Figure 83: SEM image and composition of GC feed area *120*
Figure 84: SEM image and composition of GC feed gangue particle *120*
Figure 85: SEM image and composition of GC feed chrome particle *121*
Figure 86: SEM image and composition of GC feed PGM particle *121*
Figure 87: SEM image and composition of GC feed chrome particle *121*
Figure 88: SEM image and composition of GC tail sample area *122*
Figure 89: SEM image and composition of GC tail PGM particle *122*
Figure 90: SEM image and composition of GC tail gangue particle *122*
Figure 91: SEM image and composition of GC concentrate area (a) *124*
Figure 92: SEM image and composition of GC concentrate area (b) *124*
Figure 93: SEM image and composition of GC concentrate chrome particle (a) *124*
Figure 94: SEM image of GC concentrate magnified chrome particle *125*
Figure 95: SEM image and composition of GC concentrate chrome particle (b) *125*
Figure 96: SEM image and composition of GC concentrate gangue particle (a) *126*
Figure 97: SEM image and composition of GC concentrate gangue particle (b) *126*
Figure 98: SEM image and composition of GC concentrate PGM particle (a) *126*
Figure 99: SEM image and composition of GC concentrate PGM particle (b) *127*
Figure 100: SEM image and composition of GC concentrate PGM particle (c) *127*
Figure 101: SEM image and composition of GC concentrate particle (d) *127*
Figure 102: SEM image and composition of GC concentrate PGM particle (e) *128*
Figure 103: SEM image of GC concentrate magnified PGM particle *128*
Figure 104:pXRF device *129*
Figure 105: Phase 1 and 2 raw data *159*
Figure 106: Phase 3 raw data *160*
Figure 107: Phase 4 raw data *161*
Figure 108: GC concentrate 1 mass recovered outlier chart *163*
Figure 109: GC concentrate 1 platinum outlier chart *163*
Figure 110: GC concentrate 1 palladium outlier chart *164*
Figure 111: GC concentrate 1 gold outlier chart *164*
Figure 112: GC concentrate 1 rhodium outlier chart *165*
Figure 113: GC concentrate 1 ruthenium outlier chart *165*
Figure 114: GC concentrate 1 iridium outlier chart *166*
Figure 115: GC concentrate 1 copper outlier chart *166*
Figure 116: GC concentrate 1 nickel outlier chart *167*

Figure 117: GC concentrate 1 sulphur outlier chart *167*
Figure 118: GC concentrate 1 chrome outlier chart *168*
Figure 119: GC concentrate 1 silicon dioxide outlier chart *168*
Figure 120: GC concentrate 1 magnesium oxide outlier chart *169*
Figure 121: GC concentrate 1 calcium oxide outlier chart *169*
Figure 122: GC concentrate 1 aluminum oxide outlier chart *170*
Figure 123: GC concentrate 1 4E outlier chart *170*
Figure 124: GC concentrate 1 6E outlier chart *171*
Figure 125: GC concentrate 2 mass recovered outlier chart *172*
Figure 126: GC concentrate 2 platinum outlier chart *172*
Figure 127: GC concentrate 2 palladium outlier chart *173*
Figure 128: GC concentrate 2 gold outlier chart *173*
Figure 129: GC concentrate 2 rhodium outlier chart *174*
Figure 130: GC concentrate 2 ruthenium outlier chart *174*
Figure 131: GC concentrate 2 iridium outlier chart *175*
Figure 132: GC concentrate 2 copper outlier chart *175*
Figure 133: GC concentrate 2 nickel outlier chart *176*
Figure 134: GC concentrate 2 sulphur outlier chart *176*
Figure 135: GC concentrate 2 chrome outlier chart *177*
Figure 136: GC concentrate 2 silicon dioxide outlier chart *177*
Figure 137: GC concentrate 2 magnesium oxide outlier chart *178*
Figure 138: GC concentrate 2 calcium oxide outlier chart *178*
Figure 139: GC concentrate 2 aluminium oxide outlier chart *179*
Figure 140: GC concentrate 2 4E outlier chart *179*
Figure 141: GC concentrate 2 6E outlier chart *180*
Figure 142: GC concentrate 3 mass recovered outlier chart *181*
Figure 143: GC concentrate 3 platinum outlier chart *181*
Figure 144: GC concentrate 3 palladium outlier chart *182*
Figure 145: GC concentrate 3 gold outlier chart *182*
Figure 146: GC concentrate 3 rhodium outlier chart *183*
Figure 147: GC concentrate 3 ruthenium outlier chart *183*
Figure 148: GC concentrate 3 iridium outlier chart *184*
Figure 149: GC concentrate 3 copper outlier chart *184*
Figure 150: GC concentrate 3 nickel outlier chart *185*
Figure 151: GC concentrate 3 sulphur outlier chart *185*

Figure 152: GC concentrate 3 chrome outlier chart *186*
Figure 153: GC concentrate 3 silicon dioxide outlier chart *186*
Figure 154: GC concentrate 3 magnesium oxide outlier chart *187*
Figure 155: GC concentrate 3 calcium oxide outlier chart *187*
Figure 156: GC concentrate 3 aluminium oxide outlier chart *188*
Figure 157: GC concentrate 3 4E outlier chart *188*
Figure 158: GC concentrate 3 6E outlier chart *189*
Figure 159: GC concentrate 4 mass recovered outlier chart *190*
Figure 160: GC concentrate 4 platinum outlier chart *190*
Figure 161: GC concentrate 4 palladium outlier chart *191*
Figure 162: GC concentrate 4 gold outlier chart *191*
Figure 163: GC concentrate 4 rhodium outlier chart *192*
Figure 164: GC concentrate 4 ruthenium outlier chart *192*
Figure 165: GC concentrate 4 iridium outlier chart *193*
Figure 166: GC concentrate 4 copper outlier chart *193*
Figure 167: GC concentrate 4 nickel outlier chart *194*
Figure 168: GC concentrate 4 sulphur outlier chart *194*
Figure 169: GC concentrate 4 chrome outlier chart *195*
Figure 170: GC concentrate 4 silicon dioxide outlier chart *195*
Figure 171: GC concentrate 4 magnesium oxide outlier chart *196*
Figure 172: GC concentrate 4 calcium oxide outlier chart *196*
Figure 173: GC concentrate 4 aluminium oxide outlier chart *197*
Figure 174: GC concentrate 4 4E outlier chart *197*
Figure 175: GC concentrate 4 6E outlier chart *198*
Figure 176: GC concentrate 5 mass recovered outlier chart *199*
Figure 177: GC concentrate 5 platinum outlier chart *199*
Figure 178: GC concentrate 5 palladium outlier chart *200*
Figure 179: GC concentrate 5 gold outlier chart *200*
Figure 180: GC concentrate 5 rhodium outlier chart *201*
Figure 181: GC concentrate 5 ruthenium outlier chart *201*
Figure 182: GC concentrate 5 iridium outlier chart *202*
Figure 183: GC concentrate 5 chrome outlier chart *202*
Figure 184: GC concentrate 5 silicon dioxide outlier chart *203*
Figure 185: GC concentrate 5 magnesium oxide outlier chart *203*
Figure 186: GC concentrate 5 calcium oxide outlier chart *204*

Figure 187: GC concentrate 5 calcium oxide outlier chart *204*
Figure 188: GC concentrate 5 copper outlier chart *205*
Figure 189: GC concentrate 5 nickel outlier chart *205*
Figure 190: GC concentrate 5 sulphur outlier chart *206*
Figure 191: GC concentrate 5 4E outlier chart *206*
Figure 192: GC concentrate 5 6E outlier chart *207*
Figure 193: Phase 5 Run 1-5 Fire assay/ICP-MS results and analysis per run *208*
Figure 194: Phase 5 Run 6-10 Fire assay/ICP-MS results and analysis per run *209*
Figure 195: GC feed volume density vs size class *212*
Figure 196: GC feed cumulative volume density vs size class *212*
Figure 197: GC feed size class comparison with histogram *213*
Figure 198: GC tail volume density vs size class *214*
Figure 199: GC tail cumulative volume density vs size class *214*
Figure 200: GC tail size class comparison with histogram *215*
Figure 201: GC concentratel volume density vs size class *216*
Figure 202: GC concentrate cumulative volume density vs size class *216*
Figure 203: GC concentrate size class comparison with histogram *217*
Figure 204: Phase 7 mass yield/recovery/grade raw data *220*
Figure 205: XRF raw data *221*
Figure 206: GC feed XRD results *225*
Figure 207: GC concentrate XRD results *226*
Figure 208: GC tail XRD results *227*
Figure 209: SEM image and composition of GC feed gangue particle *228*
Figure 210: SEM image and composition of GC feed PGM particle *228*
Figure 211: SEM image and composition of GC tail PGM particle *229*
Figure 212: SEM image and composition of GC tail PGM particle *229*
Figure 213: SEM image and composition of GC concentrate PGM particle *230*
Figure 214: SEM image and composition of GC concentrate PGM particle *230*
Figure 215: SEM image and composition of GC concentrate chrome particle *230*
Figure 216: SEM image and composition of GC concentrate PGM particle *231*

List of Tables

Table 1: Composition of Some Common Minerals of the Bushveld Complex (Schouwstra et al., 2000) *10*

Table 2: Mineral PGM Speciation of the UG2 Chromitites (Penberthy et al., 2000) *13*

Table 3: List of Available Geometallurgical Tests [Lishchuka et al., (2020) modified after Lishchuka (2019)] *14*

Table 4: Some Mineralogical, Chemical and Other Characterization Techniques [Lishchuka et al., (2020) modified after Lishchuka (2019)] *14*

Table 5: Sulphide and Gangue Mineralogy of a Typical PGM Concentrate (Andrew et al., 2014) *16*

Table 6: Quantitative Mineralogy of the Merensky and UG2 Platinum Ore Samples. (Solomon et al., 2011) *18*

Table 7: Some PGMs Minerals Properties [In Xiao & Laplante (2004) from Cabri (2002)] *20*

Table 8: Gravity Concentrator Feed *56*

Table 9: Concentration criteria (CC) of PGMs *57*

Table 10: Phase 1 Parameters *62*

Table 11: Phase 2 Parameters *63*

Table 12: Gravity concentrator feed analysis *68*

Table 13: Weighted average assay results for optimized parameter runs *82*

Table 14: Weighted average mass yield, recovery and grade results for optimized parameter runs *82*

Table 15: Malvern Mastersizer average results *96*

Table 16: Gravity concentrate samples D_{10}, D_{50} and D_{90} *97*

Table 17: Summary of fluidized bowl experiments *109*

Table 18: Phase 7 gangue content *114*

Table 19: 10 stage gravity concentration modeled data *116*

Table 20: 10 stage gravity concentration measured data *116*

Table 21: XRF results *132*

Table 22: Phase 5 sample masses and moisture content *162*

Table 23: Elemental PGM and gangue recovery to GC concentrate *210*

Table 24: GC feed Malvern samples *211*

Table 25: GC tail Malvern samples *211*

Table 26: GC concentrate Malvern samples *211*

Table 27: GC feed fractional analysis *218*

Table 28: GC tail fractional analysis *218*

Table 29: GC concentration fractional analysis *218*

Table 30:Phase 7 mass and moisture raw data *219*

Nomenclature

µm	Micrometre
η	Viscosity of fluid
4E	The 4 main PGMs of economic value: platinum, palladium, rhodium and gold. Also called 3PGM+Au.
6E	The 6 main PGMs of economic value: platinum, palladium, rhodium, ruthenium, iridium and gold.
Al_2O_3	Aluminium Oxide
Au	Gold
BIC	Bushveld Igneous Complex
BMS	Base Metal Sulphides
CaO	Calcium oxide
Cr_2O_3	Chromium (III) oxide
Cu	Copper
d	Particle diameter
D_f	Density of the fluid
Ds	Density of the solid
GC Feed	Gravity Concentration Feed. This is the feed stream to the Falcon.
GC Tail	Gravity Concentration Tail. This is the tail stream of the Falcon.
GC Concentrate	Gravity Concentration Concentrate. This is the product stream of the Falcon.
G-force	Gravitational force
g	Gravitational acceleration
Hertz	Hz
ICP-MS	Inductively Coupled Plasma Mass Spectrometry
IPJ	Inline Pressure Jig
Ir	Iridium
IRUP	Iron Rich Ultramafic Pegmatite
kWh	kilowatt-hour
LGS	Lebowa Granite Suite
MML	Main Magnetite Layer

MR	Merensky Reef
MSZ	Main Sulphide Zone
MF1	Mill-Float
MF2	Mill-Float Mill-Float
MgO	Magnesium Oxide
Ni	Nickel
Oz	Ounce (Troy Ounce)
Pd	Palladium
PGE	Platinum Group Elements
PGM	Platinum Group Metals
pgm	Platinum Group Minerals (To avoid confusion with platinum group metals in this paper, *platinum group minerals* will not be abbreviated)
PSA	Particle size analysis
PSD	Particle size distribution
QEMSCAN	Quantitative Evaluation of Materials by Scanning Electron Microscopy
Rh	Rhodium
RLS	Rustenburg Layered Suite
Ru	Ruthenium
S	Sulphur
SEM	Scanning Electron Microscope.
SiO_2	Silicon dioxide
UG2	Upper Group 2 Chromitite layer
v	Terminal velocity
XCT	X-ray computed tomography
XRD	X-ray diffraction
XRF	X-ray fluorescence

1. Introduction

1.1. Background and Context

Platinum Group Metals (PGMs) are six noble precious metals which are clustered together in the periodic table and have similar properties (Renner et al., 2002). The six platinum- group metals are platinum, palladium, ruthenium, rhodium osmium and iridium (Harris & Cabri, 1991). In industry it is common practice to reference 4-Elements PGM which are platinum, palladium, gold and rhodium or also 6-Elements PGM which are platinum, palladium, gold, rhodium, iridium and ruthenium. The use of 4E or 6E is primarily for economic reasons as these occur in the highest and economically viable concentrations in platinum ores. It is also worth noting that gold is included in the 4E and 6E definitions as it occurs in significant concentrations and is of high economic value. There is some debate on the use of platinum group minerals, platinum group metals (PGM) and platinum group elements (PGE). Strictly speaking, PGEs refer to the transition precious metallic elements with similar physical and chemical properties grouped together in the D-block in Groups 8, 9, and 10; and Periods 5, 6, and 7 of the Periodic Table. Platinum group minerals refers to the complex minerals that are associated with PGEs and PGMs. Platinum group metals refers to the metals of significant quantity and which have economical benefits. This research paper is thus purposely titled ‘An investigation into the effect of advanced gravity separation on *Platinum Group Metals (PGM)* flotation concentrates’ as these metals are central to the outcomes of the research study.

The traditional method of PGM processing is comminution (milling), flotation, smelting and refining. This flowsheet is generally a cumbersome process with long lead times and potential for precious metal lock-up within processes. This flow sheet is also sensitive to small negative fluctuations in the PGM basket price which can negatively affect the economics of operations. Apart from this, the mining of UG2 ore with higher chromite content has become increasingly important as Merensky reef is fast depleting. The higher chrome content of the UG2 ore creates serious problems in smelters where the chrome spinel forms in the furnaces leading to higher temperatures required to ensure efficient separation of precious metals and slag (Jones, 2005).

The decreasing feed grades to PGM concentrators and the complexity of balancing mass pull, grade and recovery is becoming ever more challenging especially in circumstances where the PGM basket price is depressed. Flotation to recover and clean platinum concentrates also has limitations in terms of selectivity and entrainment of deleterious chrome especially in the case of UG2 ore processing. This leads to the postulation that an increase in the concentrate grade without negatively impacting on recovery and without entraining chrome can essentially improve the current process efficiency.

PGMs are complex minerals associated with base metal sulphides which makes these minerals particularly difficult to recover by any other methods apart from froth flotation. Apart from this complexity, PGMs are generally found in the fine to ultrafine fraction of the ore. For the purposes of this research paper, fine particles are those between 38 to 106µm and ultrafine particles are those below 38µm. The fine particles are a result of the milling process which is used in order to achieve effective liberation of minerals of interest. Most processing operations need fine to ultrafine grinding due to the complexity of the ore being treated as well as to ensure the process of recovering the said mineral(s) is efficient (Parry, 2006; Nayak et al., 2021). These complexities make finding appropriate economical processing routes and optimization just as complex.

One novel way of upgrading PGM concentrates can be the application of advanced (or enhanced) gravity separation. This technology utilizes a centrifugal force to separate particles potentially including ultra-fine particles, based on the particle densities (Sarkar et al., 2007). The primary gravity concentration of PGM ores was generally found to have been ineffective due to the large volume of ores that needs to be treated and that gravity concentrators are known to have throughput limitations in comparison to traditional milling and flotation. This research thus aims to apply advanced gravity concentration to further upgrade (enrich) the final flotation concentrate of a PGM plant post flotation. It is envisaged that the final plant concentrate from the flotation process will form a feed into a gravity separation unit which will increase the grade of the concentrate while rejecting gangue. The final concentrate streams from the flotation process have much smaller volumes compared to the fresh ore feed streams, this can be about 0.20-0.50% mass pull on tailings plants or 1-2% mass pull on reef plants. This indicates that the advanced

gravity concentration unit will be processing a much smaller throughput than the raw ore feed throughput. The typical concentrate grade on a tailing's flotation plant is 60-130 g/t 4E PGM, therefore an upgrade ratio of 1.5 or greater would be of economic value.

The question that may be asked is why further concentrate a flotation concentrate that is ready to be smelted and refined? The reasons are twofold: firstly, the concentrate can be upgraded without the need for additional flotation cells and without the need for reagents. Secondly, if a concentrator is able to economically upgrade its final concentrate with gravity separation, then it means that the overall plant mass pull can be increased and hence the plant can recover additional PGMs in the flotation section without the concern of a marked drop in concentrate grade and/or entrainment of chrome into the concentrate. The PGM industry is a price-taker and has no control on the PGM basket price hence when prices drop, they can only produce more PGM ounces or cut costs, this project ultimately looks to the former alternative. Producing more ounces from a plant ensures longer term sustainability for operations and using a relatively low-cost unit such as a gravity concentrator will ensure that no excessive capital or operational costs have to be incurred.

1.2. Problem Statement

PGM Concentrate grades cannot be economically and effectively improved through further cleaner flotation steps. The main problem that this research addresses is the limited upgradability of concentrates on traditional PGM flotation circuits. If concentrate needs to be upgraded further then large capital costs are required for infrastructure and equipment as well as increased operation costs for reagents, utilities, and labour. There is also an imminent loss in PGM recovery with additional upgrading of concentrates. Advanced gravity separation technology is thus seen as a potential novel method to improve the grade of PGM flotation concentrates without loss of recovery.

There is a clear gap in the research when it comes to the use of advanced gravity separation for upgrading PGM concentrates.

1.3. Research Aim and Objective(s)

The Aim of this research is to attempt further upgrading of a PGM flotation concentrate by use of an advanced gravity separation process. This entails the rejection of gangue components from the concentrate and further concentration of PGMs. Gravity separation is envisaged to be more economical for PGM concentration as no flotation cells or reagents are required.

The research objectives are:

- To determine the mineralogical composition of the flotation concentrate (that form the gravity concentrator feed). This will lead to an understanding of the mineral associations and mineral densities of the feed to the gravity concentrator.
- To determine the PGM recovery potential and the extent of Chrome rejection (as a deleterious constituent of the feed concentrate) of advanced gravity separation using a Falcon Gravity Concentrator.
- To determine the optimal parameters of advanced gravity separation for PGM recovery and grade improvement. The parameters tested include feed rate, feed density and G-force.
- To investigate the Particle Size Distribution and PGM content of the gravity separation product and tail (Fractional analysis).

1.4. Hypothesis

Research Hypothesis 1: Advanced Gravity Separation can further improve PGM concentrate grade.

Research Hypothesis 2: Chrome is not concentrated with the PGMs in the final concentrate though it is similarly contained in the fine and ultra-fine particles because it has a lower density than the platinum group minerals.

Research Hypothesis 3: Advanced Gravity Separation can recover dense fines and ultra-fines from a PGM flotation concentrate.

1.5. Research Questions

- Does advanced gravity concentration improve PGM concentrate grade?
- What is the extent of Chrome rejection using advanced gravity separation?
- What is the particle size distribution of the final concentrate and final tail from advanced gravity concentration?
- What is the mineralogy of the particle size distribution of the final concentrate and final tail from advanced gravity concentration?
- What are the mineralogical qualitative properties of the final concentrate and final tail from advanced gravity concentration?
- What are the optimal lab scale parameters to recover PGMs in a gravity concentrator?

1.6. Research Approach

This specific research will focus on a quantitative research strategy but will also be augmented with a qualitative view for greater clarity on the research topic and constructs, in essence a mixed approach will be used.

1.7. Thesis Outline

The thesis consists of six chapters. The summary and purpose of each chapter is given below:

Chapter 1: Introduction

This chapter introduces the PGM industry and gives an overview of the current metallurgical and economic challenges. This chapter also gives context for the research paper's aim, objectives, hypothesis and research questions. The tone, direction and framework for this research is contained in this chapter.

Chapter 2: Literature Review

This chapter provides a literature review covering the geological context, processing of PGM ores, gravity concentration applied to minerals, various types of gravity concentration and

advanced gravity concentration with particular focus on the Falcon gravity concentrator. The challenges associated with PGM ore in relation to gravity concentration are also discussed. Past studies are integrated with current technological advances in this chapter to give a conceptual framework for the study.

Chapter 3: Methodology

This chapter details the experimental set-up and procedures employed to achieve the aims and objectives of the research.

Chapter 4: Results and Discussion

This chapter meticulously presents the results from the experimental work as well as interpreting and analysing the results. The feed to the gravity concentrator is analysed and explained, the parameters for experimental results are detailed, the test work with optimised parameters are explained and verified, the particle size and fractional analysis are presented. This chapter also contains the fluidized bowl experiments as well as a simplified model to predict the results from additional gravity concentration stages. The SEM, XRD and XRF results are also presented in this chapter.

Chapter 5: Integrated Discussion

The purpose of this chapter is to bring all the preceding chapters together and have an overview of the significance and implication of this study based on what was found and achieved.

Chapter 6: Conclusion and Recommendations

This chapter includes the conclusions and recommendations that are underpinned by the results obtained as well as the inferences drawn from the study. This chapter also indicates the novelty of this study and gives direction for future research that is in the same vein as this research study.

2. Literature Review

2.1. Geological Context

2.1.1. Petrology and Mineralogy

The global supply of platinum and palladium as well as their associated elements is currently met from economically mining and processing four major layered igneous intrusions, namely, the Bushveld Igneous Complex (South Africa); the Stillwater Complex (U.S.A); the Great Dyke (Zimbabwe) and the Norilsk/Talnakh Complex (Russia) (Gruenewaldt, 1991; Peck & Huminicki, 2016). Approximately 94% of the world's economic platinum group elements (PGEs) reserves occur in the Bushveld Igneous Complex, the Stillwater Complex and the Great Dyke (U.S. Geological Survey, 2020). The formation of these deposits is believed to have happened in the Precambrian Era (Neoarchean to Paleoproterozoic) (Eckstrand & Hulbert, 2007). The formation of these intrusions is theorised to be a result of merging between an early ultramafic (U-type) parental magma and a subsequent tholeiitic (T-type) parental magma (Chaumba, 2022). The U-type magma contained high MgO, SiO_2 and Cr but low Al_2O_3 while the T-type magma contains plagioclase feldspar (labradorite), clinopyroxene (augite with pigeonite), and iron ore (magnetite and ilmenite) (Naldrett, 2010). The U-type magma is theorised to have interacted with the earth's crust leading to an enrichment of SiO_2 and this magma is also purported to be the PGE-rich component (Naldrett, 2010).

The compositions of parental magma's from the above mentioned intrusions are plotted on the Fo-Di-SiO_2 diagram depicted in Figure 1. Forsterite (Fo) is a magnesium-rich end-member of the olivine solid solution series, Diopside is a monoclinic pyroxene mineral with composition of $MgCaSi_2O_6$ and Silicon dioxide (SiO_2) which is commonly known as quartz and are all major components of the intrusions. The PGEs are concentrated in thin stratiform layers or reefs and are located in the stratums that occur close to the level at which the predominant crystallization is suggested to interchange between U-to T-type magma (Chaumba, 2022). The origin of the contained mineralisation of these reefs is still debated amongst experts and researchers with several models being put forward (Chaumba, 2022) but no single theory is able to fit the current state of the igneous intrusions. Due to the complexity of this ore body, it would seem more likely that a variety of factors influenced the current state of the layered igneous intrusions, including

but not limited to magma mixing, crustal contamination and high temperature magmatic fluids (Chaumba, 2022). The stratigraphic locations of PGE reefs are shown in Figure 2. The J-MR refers to the Stillwater Complex reef, the MSZ is the Main Sulphide Zone of the Great Dyke and the MR (Merensky Reef); UG-2 (Upper Group 2 Chromite Layer) and MML (Main Magnetite Layer) refers the BIC.

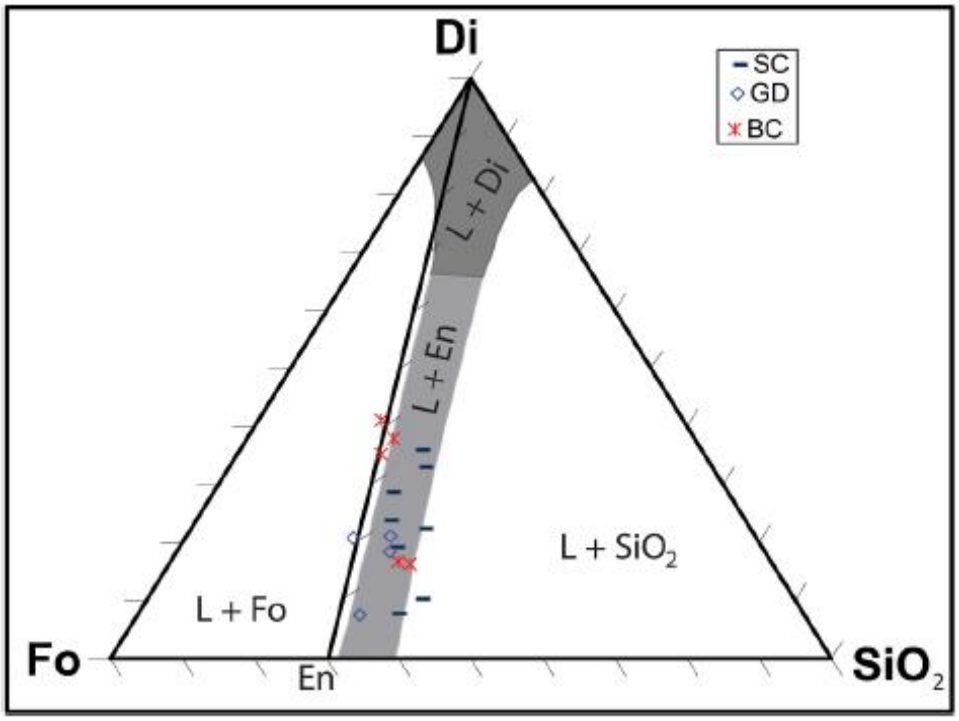

Figure 1:Ternary Fo-Di-SiO_2 system showing parental magmas of the Stillwater Complex, Great Dyke, and Bushveld Complex plotted [Diagram from Chaumba (2022) with data from various authors compiled by McCallum (1996), Wilson (1996) and Cawthorn (2015).

The genesis and mechanism of mineralisation of layered igneous intrusions can be grouped into either orthomagmatic and/or hydromagmatic in nature. "The orthomagmatic models consider the mineralization of the PGEs to be an integral part of magma chamber crystallization processes whereas hydromagmatic models attribute PGEs mineralization to volatile-rich fluids that are exsolved from cooling cumulates" (Chaumba, 2022, p.13). The amalgamating of a primitive magma and an evolved one is suggested to have been an initiating mechanism for the formation of PGE-enriched horizons in layered intrusions and ophiolite complexes (Naldrett & Gruenewaldt, 1989). The base-metal sulphides (BMS) such as pentlandite, pyrrhotite, and chalcopyrite, as well as pyrite are commonly found in the layered intrusions (Oberthür, 2011;

Osbahr et al., 2013). Table 1 indicates some common minerals found in the BIC. Godel et al. (2007) found that PGMs occur within or between base metal sulphides and silicates or oxides, with pentlandite being a major host to PGMs except for Platinum.

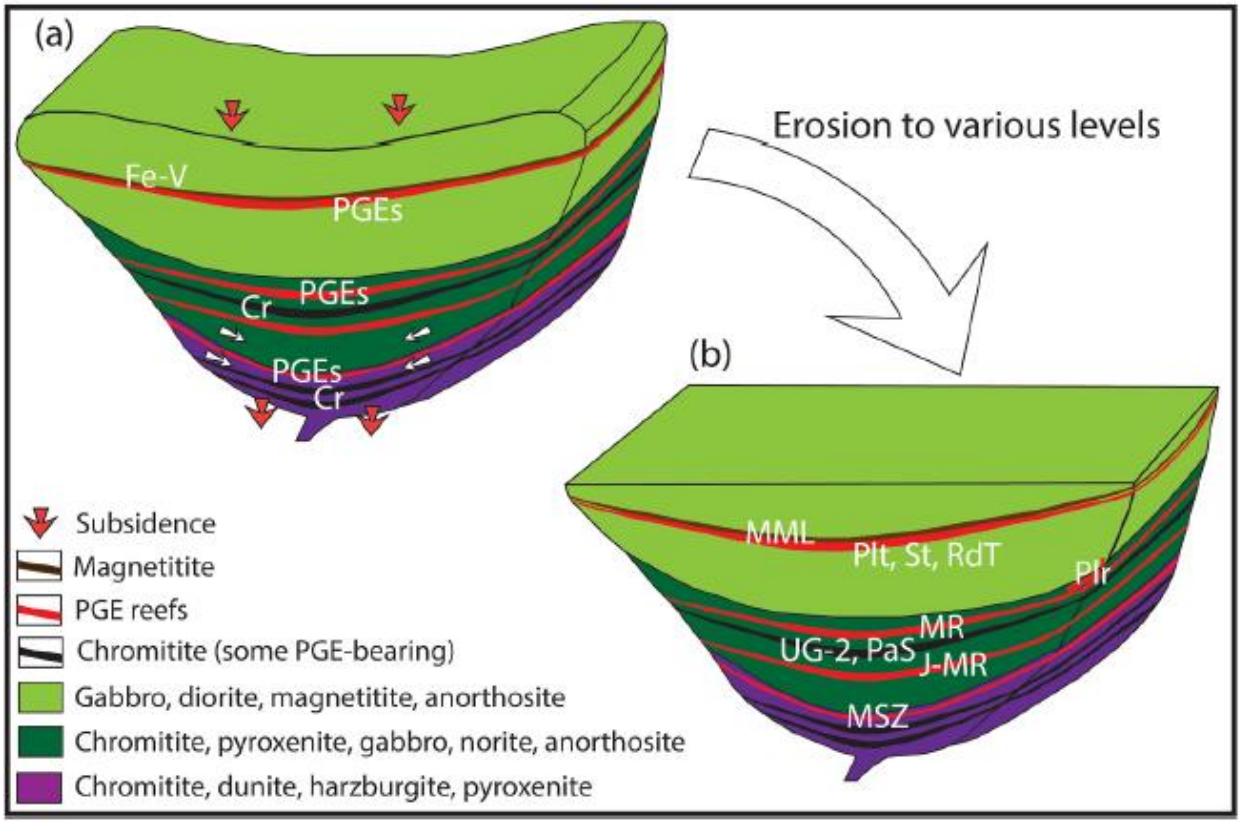

Figure 2: Sketches showing the formation of PGE-enriched reefs, PGE-enriched chromitite and magnetite reefs in layered intrusions (a) Crustal loading during magma emplacement causes central subsidence. Incompletely solidified cumulates slump towards the centre of intrusion, and disseminated sulphide, chromite and magnetite form massive layers. (b) Erosion exposes the variety of layered intrusions to various levels [Diagram from Chaumba (2022) simplified from Maier et al. (2013)].

The prior discussion focused on all the main deposits of PGMs and their genesis as well as overall mineralogy. This section will discuss the South African context of PGMs as this is fundamental to this current research. The Bushveld Igneous Complex (BIC) is the largest layered igneous intrusion (Oniyide, 2015) and is estimated at approximately 2 billion years old (Eriksson et al., 1995) within the Earth's crust. The mafic rocks of this intrusion were “emplaced into a stable cratonic shield well preserved from deformation, metamorphism and low temperature alteration, at least partly by its isostatic impact on the entire crustal thickness” (Cawthorn R. G., 2015, p. 1). The complex is divided into four different limbs: the northern, southern, eastern, and

western limbs (Oniyide, 2015), see Figure 3. The complex contains the world's largest reserves of platinum-group metals (PGMs) or platinum group elements (PGEs)—platinum, palladium, osmium, iridium, rhodium, and ruthenium (Mpinga et al., 2015). The BIC mainly consists of two main phases of igneous rocks, namely, a layered sequence of predominantly basic igneous rocks known as the Rustenburg Layered Suite (RLS) and a superimposing acidic phase of granite rocks known as the Lebowa Granite Suite (LGS) (Wansbury, 2016). The RLS has undergone little metamorphism or deformation after its solidification (Eales et al., 1993). Within the Bushveld Igneous Complex (BIC) there are mainly two different types of PGE dominant ores that are of economic interest, namely, Merensky type ore and UG2 Chromite type ore (Cole & Ferron, 2002). Figure 4 indicates the stratigraphic column of the layered intrusion part of the Bushveld igneous complex with all important reefs and the typical rock types for each zone. The location of the Merensky and UG-2 ores are in the critical zone.

Table 1: Composition of Some Common Minerals of the Bushveld Complex (Schouwstra et al., 2000)

Mineral group	Mineral	Composition
Pyroxene	Enstatite	Mg, Fe silicate
	Augite	Mg, Fe, Ca silicate
Feldspar	Plagioclase	Ca, Na, Al silicate
Mica	Phlogopite	K, Mg, Al silicate
	Biotite	K, Mg, Fe, Al silicate
Chlorite	Chlorite	Hydrated Mg, Fe, Al silicate
Clay	Talc	Hydrated Mg silicate
Serpentine	Serpentine	Hydrated Mg, Fe silicate
Spinel	Chromite	Cr, Fe, Mg oxide
	Pentlandite	Ni, Fe sulfide
Sulfide	Chalcopyrite	Cu, Fe sulfide
	Pyrrhotite	Fe mono-sulfide
	Pyrite	Fe di-sulfide

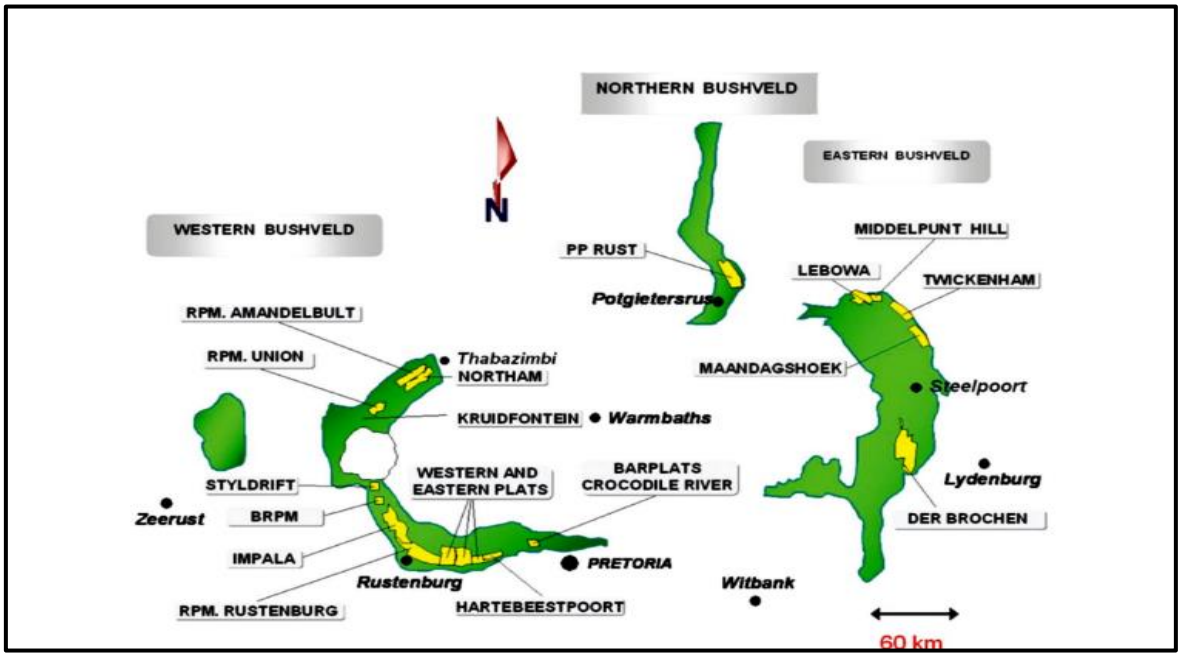

Figure 3: Map of the Bushveld Igneous Complex (Watson et al., 2010)

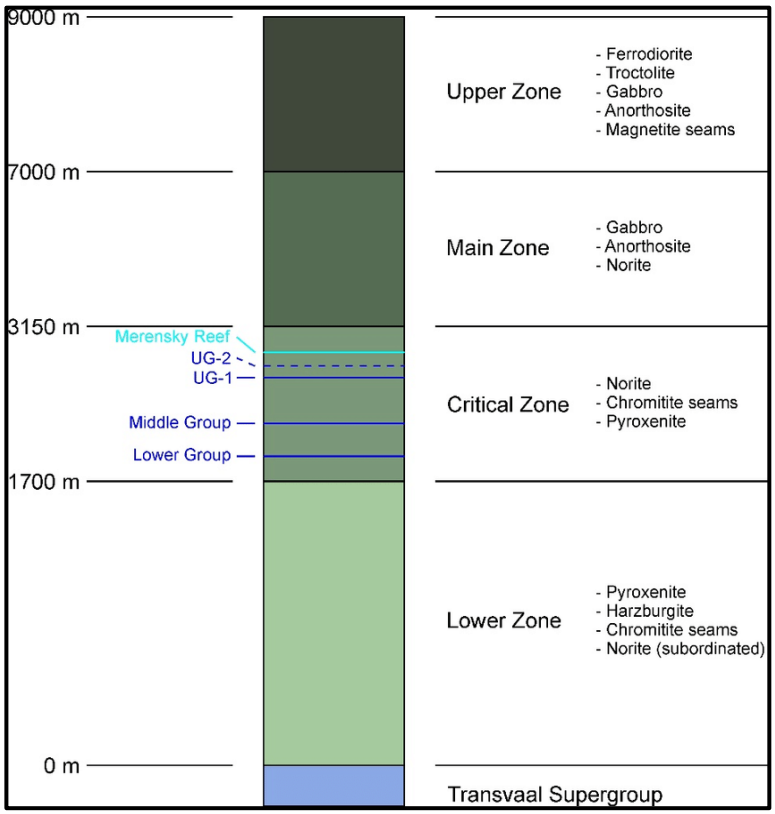

Figure 4: Stratigraphic Column Showing the Position of the UG-2 Reef Relative to the Merensky Reef (Schouwstra et al., 2000)

Merensky Reef is a predominantly sulphide-rich pyroxenite layer mostly found in the eastern and western parts of the BIC (Cawthorn, 2010). The Merensky Reef consists of equal parts of dark iron-magnesium silicate minerals and lighter calcium-aluminium-sodium silicate minerals (called a feldspathic pyroxenite) with interspersed chromite layers (Schouwstra et al., 2000). These can be further classified as predominantly of orthopyroxene (about 60%), plagioclase feldspar (about 20%), pyroxene (about 15%), phlogopite (about 5%), and occasional olivine (O'Connor & Aleksandrova, 2021). The base metal sulphide grains and associated PGMs are contained in the Merensky pegmatoid zone (Schouwstra et al., 2000). The base metal sulphides consist principally of pyrrhotite (approximately 40%), pentlandite (approximately 30%), and chalcopyrite (approximately 15%). The major PGMs are cooperite (PtS), braggite ((Pt,Pd)NiS), sperrylite ($PtAs_2$), PGE alloys and in some areas minerals such as laurite (RuS_2) (Schouwstra et al., 2000; Cole & Ferron, 2002).

The UG2 Ore is currently the most important source of PGE as the Merensky Reef deposits are becoming depleted and grades have become low. The UG2 ore also has Chromite which has become an important by-product of significant economic value. The UG2 Reef consists primarily of chromite (60 -90% by volume), orthopyroxene (5-25%) and plagioclase (5-15%) (McLaren & De Villiers, 1982). The accessory phases are mainly clinopyroxene, base metal sulphides (BMS), ilmenite, magnetite and rutile. PGEs are known to occur in association with chromite and BMS (Godel et al., 2007). Platinum group metals within UG2 chromite ores, typically occur in association with base metal sulphides (BMS) and will typically range in size between 1 and 2 µm (Cole & Ferron, 2002). Platinum group metals may also occur within chromite grain boundaries as grains and as inclusions in silicate gangue minerals (Cole & Ferron, 2002). The mineral PGM speciation of the UG2 Reef can be seen in Table 2.

“The vast majority of the platinum group minerals occur in association with BMS and silicates. The base metal sulphides occur almost entirely with interstitial silicate and are only rarely enclosed within the chromite particles” (Hay & Roy, 2010, p. 855). Less than 2% of the PGMs are associated with chromite but in altered ores this can increase to 10% (Hay & Roy, 2010). Laurite (RuS_2) does, however, seem to show an affinity for chromite grains (Schouwstra et al., 2000).

Table 2: Mineral PGM Speciation of the UG2 Chromitites (Penberthy et al., 2000)

PGM Mineral Species	Mineral	Composition	Common substitution
Antimonides	Geversite	$PtSb_2$	-
	Stibiopaladinite		-
Arsenides	Sperrylite	$PtAs_2$	Rh,Ir,Sb,S
Bismuthides	Insizwaite	$PtBi_2$	-
Sulphides	Cooperite	PtS	Pd,Ni
	Laurite	Ru,S_2	Ir,Os
	Braggite	(Pt,Pd)S	Ni
	Malanite	$(Pt,Rh,Ir)_2CuS_4$	-
	Rh sulphides		-
	Vysotskite	PdS	Pt,Ni
Tellurides	Merenskyite	$PdTe_2$	-
	Monocheite	$PtTe_2$	-
Alloy	Isoferroplatinum	Pt_3Fe	Ru,Rh,Ir,Pd,Os,Cu,Ni

2.1.2. Geometallurgical Characterization of Merensky Reef and UG2 Reef

Geometallurgy is at the cross-roads of geological, mining, metallurgical, environmental, and economic information to maximize the value of mined materials while minimizing the associated risks. Geometallurgy is intended to be a ‘golden thread’ to bring together the various complexities of a mining operation, thus leading to holistic solutions and greater economic benefits. The purpose of this section is to concisely bridge the gap between PGM geology & mineralogy with PGM Processing specifically. This will enable us to understand why certain processes have been successful in beneficiating PGMs and will also give guidance on what novel or innovative technologies can be used. This discussion will therefore focus on geometallurgical tests as well as mineralogical, chemical, and other characterization techniques as defined by (Lishchuka et al., 2020). Table 3 and Table 4 indicate the possible metallurgical tests and the characterization techniques respectively, that can be used on ores.

Table 3: List of Available Geometallurgical Tests [Lishchuka et al., (2020) modified after Lishchuka (2019)]

Process	Geometallurgical tests, i.e., can be used for variability study, require small amount of material and are cost efficient.	Metallurgical tests	Corresponding production scale equipment
Grinding	GCT (Mwanga et al., 2017, 2015, 2014), GeM Comminution index (GeMCi) (Kojovic et al., 2010), MinnovEX SAG Power Index Test (SPI) (Kosick et al., 2002), SMC Test® (Morrell, 2004), (Heiskari et al., 2019), SAG Variability Test (SVT) (Brissette et al., 2014)	Grindability test	Autogenous (AG) and Semiautogenous mills (SAG), ball mill, crushers, Isa mill, Vertimill etc.
Ore sorting	N/A	Sorting test	Ore sorter (XRT, hyperspectral, laser, etc.)
Flotation	Microflotation (Larsen et al., 2013), Julius Kruttschnitt Mineral Separability Indicator (JKMSI) (Hunt et al., 2011), "Shaker test" (Vos et al., 2014)	Conventional flotation test	Conventional self-aspirating and forced air flotation cells, pneumatic flotation cells etc.
Magnetic/electrical separation	Davis tube (DT) (Davis, 1918; Finch and Leroux, 1982; Murariu and Svoboda, 2003), Frantz separator (Oberteuffer, 1974)	Laboratory high-tension separator, dry and wet low intensity magnetic separator (LIMS), laboratory dry and wet high intensity magnetic separator (HIMS)	Dry and wet low and high intensity magnetic and electrical separators
Gravity separation	Mozley laboratory separator (Cordingley et al., 1994), Gravity Recoverable Gold (GRG) test (Dominy, 2013; Zhou and Cabri, 2004)	Shaking table, jig, spiral concentrators	Triple-deck table, Knelson separator, spiral concentrators, Reichert cone concentrator, jig, etc.
Leaching	Small-scale hydrometallurgical tests (Kuhar et al., 2011; Li et al., 2016; Turner et al., 2013)	Column leaching test, tank leach test, compacted granular leach test, pH- dependence leaching test	Heap leaching, bioleaching etc.

Table 4: Some Mineralogical, Chemical and Other Characterization Techniques [Lishchuka et al., (2020) modified after Lishchuka (2019)]

Information type	Characterization technique
Chemical information (chemical composition)	• X-ray fluorescence spectroscopy (XRF) (Dunne et al., 2019) • Dissolution + atomic absorption spectroscopy (AAS) (Dunne et al., 2019) • Inductively coupled plasma optical emission spectrometry (ICP-OES) (Dunne et al., 2019) • Inductively coupled plasma mass spectrometry (ICP-MS) (Dunne et al., 2019) • Electron probe micro-analysis (EPMA) with energy-dispersive spectrometer (EDS) (Williams et al., 1986) • EPMA with wavelength-dispersive spectrometer (WDS) (Reed, 1995)
Qualitative mineralogical (list of minerals) information	• Optical microscopy (Pirard, 2016) • X-ray diffraction (XRD) (Wicks et al., 1995)
Quantitative mineralogical (modal mineralogy) information	• Automated mineralogy, e.g., Mineral Liberation Analyser (MLA), Quantitative Evaluation of Minerals by SCANning electron microscopy (QEMSCAN) (Gottlieb et al., 2000), MinScan (ZEISS, 2018), INCAMineral (Oxford Instruments, 2018) • TESCAN (Tesla Scanning) Integrated Mineral Analyzer (Hrstka et al., 2018) • Quantitative X-ray diffraction (QXRD) with Rietveld refinement (Mandile and Johnson, 1998) • Element-to-mineral conversion (EMC) (Braun, 1986; Lamberg et al., 1997; Paktunc, 1998; Parian, 2015; Whiten, 2008) • Combined EMC and QXRD (Parian et al., 2015) • Hyperspectral imaging (e.g., Linton et al., 2013) • Semi- (Delbem et al., 2015) or automated optical microscopy (Donskoi et al., 2013) • Raman spectroscopy (Kauppinen, 2017; Wells and Ramanaidou, 2015)
Other methods	• X-ray computed tomography (XRT) e.g., (Dominy et al., 2011; Howard et al., 2011; Jardine et al., 2018; Reyes et al., 2017); hyperspectral core imaging (Linton et al., 2013); thermal infrared spectral analysis (Fox et al., 2017) • Visible light imaging (Koch et al., 2019; Tiu, 2017) • Density, P-wave velocity, electrical conductivity, magnetic susceptibility of (Vatandoost et al., 2008)

Crushing and Grinding is critical in any ore processing operation. Crushing is essentially the compression of ore against a rigid surface or by impact against a hard surface in a restricted motion path. Crushing is usually a dry process conducted on PGM ROM ore in sequence of two or three stages, namely, primary; secondary; and tertiary crushing (Haldar, 2018). Crushing is a size reduction process and alleviates the energy and equipment pressure on subsequent downstream processes. Most PGM reef plants have crushers due to the fine grinding that is required in the Milling stage and to reduce the size and number of Mills. The milling process liberates minerals of value for further concentration and extraction (Bahrami, et al., 2020). PGMs specifically require fine or even ultra-fine grinding as about 44% of the PGMs are locked in the sub 25µm fraction, 41% in the fine fraction (-106µm/+25µm) and the rest in the coarser fraction (Little, 2016). Milling is carried out using Primary and Secondary Ball or SAG Mills to ensure that sufficient liberation takes place. Tertiary milling is conducted using stirred mill detritor (SMD's), isaMills are also sometimes employed depending on the ore mineralogy, but these units are mostly used for regrinding the flotation tailings and thus liberating the particles for recirculation back into the process (Parry, 2004). The fine and ultra-fine particle size distributions of PGMs poses a challenge as the grinding intensity needed generates finer particles of chromite and gangue resulting in higher floatability and entrainment of these particles which are deleterious to the process (Hay & Roy, 2010). The MF2 circuit which entails primary and secondary milling and flotation is a perfect example of the application of geometallurgy to solve the comminution challenges of PGMs. The MF2 circuit is able to ensure fine grinding to liberate PGM particles for flotation but also coarse primary grind to liberate chromite crystals and minimize the impact of entrainment of chrome and gangue (Hay & Roy, 2010). It should also be noted that the primary and secondary mills are generally operated in open circuit to prevent overgrinding. Choosing the correct size reduction equipment is thus important to ensure effective extraction of valuable minerals in the PGM industry.

Flotation has been the most effective processing route to extract and concentrate PGMs (Rule & Anyimadu, 2007; Thethwayo, 2017). A sulphide-rich PGM concentrate is produced in the flotation cells due to the fact that the PGMs are actually associated within a matrix of the BMS (see Table 5). A typical Merensky concentrator can achieve recoveries of between 85-90% and a UG2 concentrator between 80-85% (Anglo American Platinum, 2001). Leaching is not

considered as an effective method of recovering PGMs due to low recoveries achieved, excessive costs and practical considerations due to the complexity of the ore (Mwase et al., 2012; Sefako et al., 2019). Gravity separation has been used sparingly on some Merensky plants such as the Anglo Platinum Retrofit Concentrator to upgrade concentrates but due to falling grades and volumes this process became uneconomical apart from being inefficient. Advanced Gravity concentration, however, may show promise for PGMs due to the density differences between the gangue and PGMs in a high gravitational force environment.

Table 5: Sulphide and Gangue Mineralogy of a Typical PGM Concentrate (Andrew et al., 2014)

Mineral		Formula
	Sulphide minerals	
Chalcopyrite		$CuFeS_2$
Pentlandite		$(Fe, Ni, Co)_9S_8$
Pyrite		FeS_2
Pyrrhotite		$Fe_{1-x}S_x$
	Gangue minerals	
Alteration silicates		Hydrated minerals
Chromite spinel		$FeCr_2O_4$
Pyroxenes		$(Mg, Fe)SiO_3 - Ca(Mg, Fe)Si_2O_6$
Olivine		$(Mg, Fe)_2SiO_4$
Plagioclase/feldspar		$NaAlSi_3O_8 - CaAl_2Si_2O_8$
Quartz		SiO_2
Haematite		Fe_2O_3

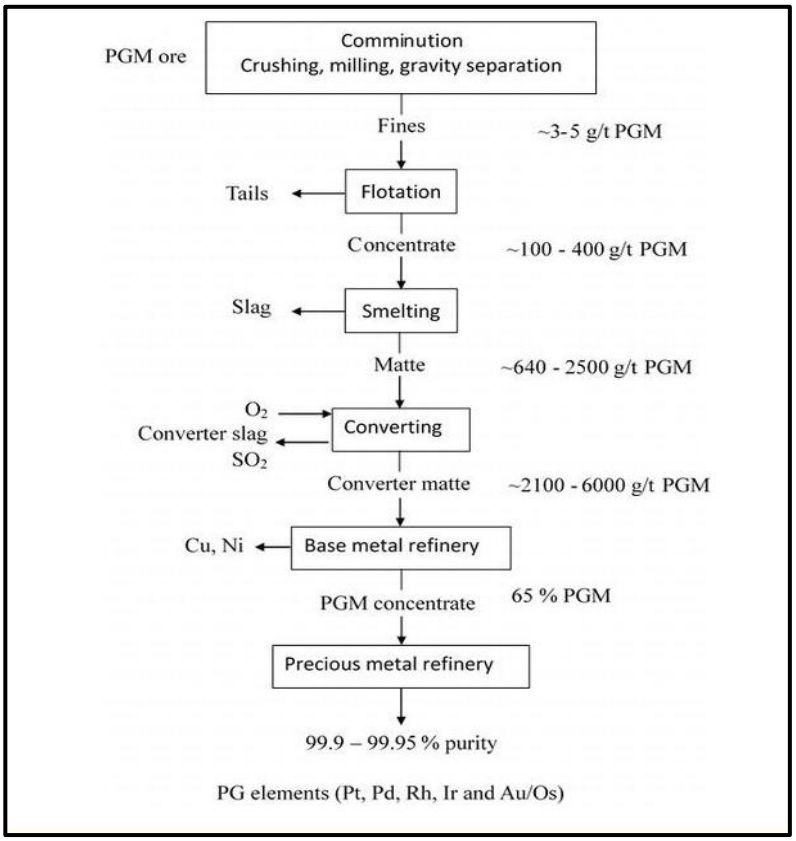

Figure 5: Typical process flow Diagram for PGM Ore Processing (Jones, 1999; Cramer, 2008)

A typical overall processing flowsheet for PGMs can be viewed in Figure 5. This shows the importance of the comminution and flotation processes to the downstream smelting and refining processes. Further discussion on these topics will be considered in subsequent sections of this report.

The characterization of PGM ore has been exhaustively studied due to the processing challenges of the ore, economic benefits of PGEs, applications of PGEs to daily life as well as the need from an academic perspective to understand PGM ore bodies as completely as possible. The grain size of PGMs are about 12µm but this can increase to 50µm and larger in the silicate pockets within the chromite region (Hay & Roy, 2010). The easily liberated PGMs associated with BMS are around 15-20µm in size and those associated with silicates are about 5µm in size (Hay & Roy, 2010). Figure 6 indicates the typical grain size of UG2 and Merensky reefs. The Photomicrographs in Figure 7 clearly show the complexity of PGM ore and how their associations with other minerals bring about challenges for processing. The mineralogical make-up of the Merensky and UG2 ores can be viewed in Table 6. The most abundant minerals present in the Merensky ore are orthopyroxene (46 wt.%), plagioclase (33 wt.%) and clinopyroxene (7.8 wt.%). These minerals are also present in the UG2 ore but constitute less than 30% in total. The

UG2 ore contains about 62% chromite and the Merensky about 5%. The BMS in the UG2 ore are also much less than that in the Merensky ore (Solomon et al., 2011). Figure 8 indicates the Back scattered electron (BSE) images for liberated PGM, PGM locked in floatable BMS, PGMs occluded in locked BMS and PGMs locked in gangue minerals.

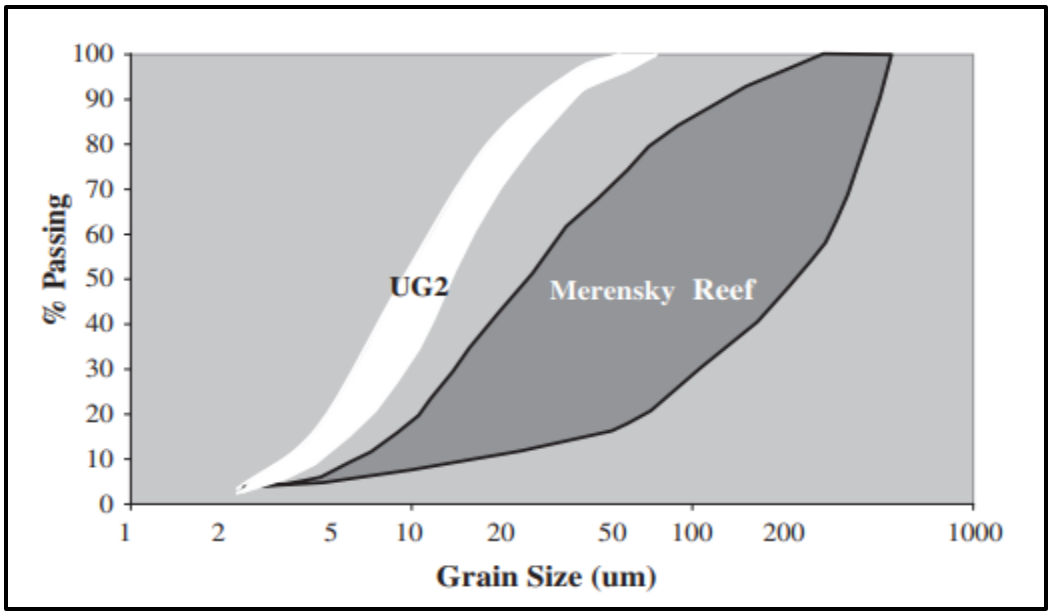

Figure 6: Typical Grain Size of Merensky and UG2 Reefs (Hay & Roy, 2010)

Table 6: Quantitative Mineralogy of the Merensky and UG2 Platinum Ore Samples. (Solomon et al., 2011)

Mineral (wt.%)	Merensky reef	UG2 reef
Pentlandite	0.6	<0.1
Pyrrhotite	0.4	<0.1
Pyrite	0.2	<0.1
Chalcopyrite	0.3	<0.1
Other sulfides	<0.01	<0.01
Orthopyroxene	45.9	12.8
Clinopyroxene	7.8	0.9
Olivine	0.6	0.2
Talc	0.1	0.3
Serpentine	1.2	1.6
Amphibole	0.7	0.2
Chlorite	1.5	2.8
Plagioclase	33.4	14.5
Mica	0.7	0.7
Chromite	5.0	62.1
Quartz	0.5	0.3
Oxides	0.6	1.1
Calcite	0.2	0.2
Other	0.6	2.3

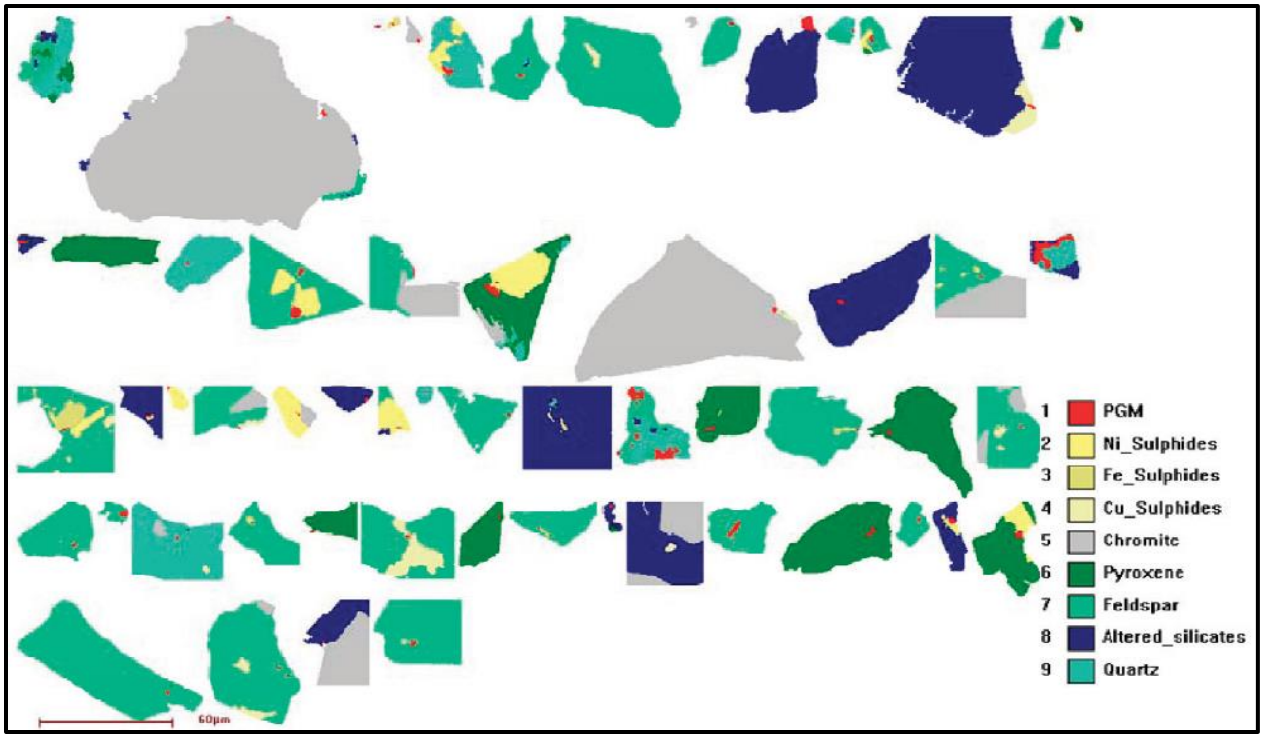

Figure 7: Photomicrographs sourced from an MLA investigation report on tailings from a Western Bushveld UG2 tailings sample showing the complexity of the liberation challenge; note that each particle shown has a PGM phase shown in red. These 'attached', 'middlings' and 'locked' composite particles are all sub 100 micron (Rule, 2008).

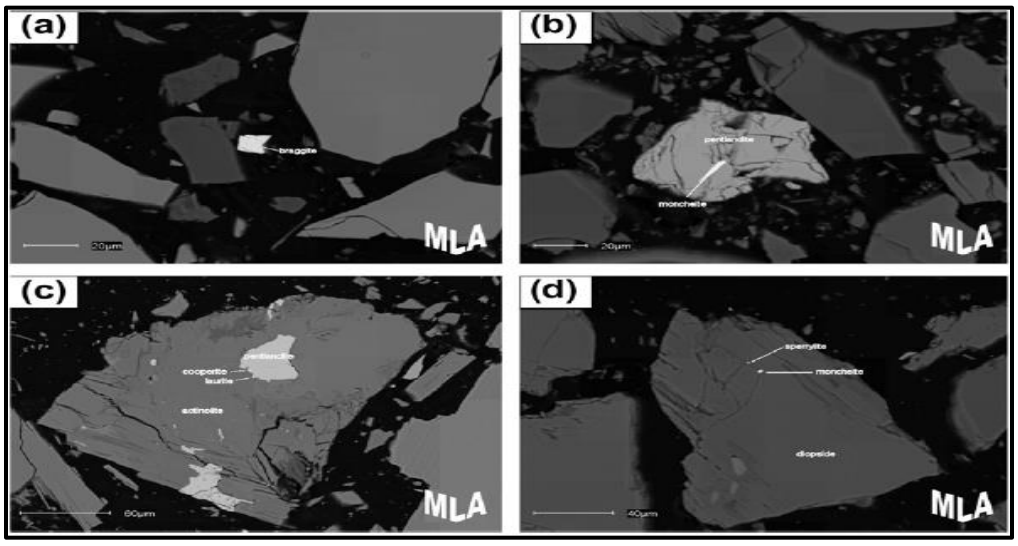

Figure 8:Back scattered electron images showed the various types of PGM association in the Merensky (b–d) and UG2 platinum ores (a). (a) Liberated PGM; (b) PGM locked in liberated BMS; (c) PGM occluded in locked BMS; (d) PGM locked in silicate gangue. (Solomon et al., 2011).

The densities of the various PGMs are detailed in Table 7. The high density of these minerals is quite apparent compared to the density of the gangue (mostly silicon dioxide) of 2.65 g/cm^3.

Table 7: Some PGMs Minerals Properties [In Xiao & Laplante (2004) from Cabri (2002)]

Name	Ideal formula	General appearance	Density (g/cm^3) (calculated)	Hardness (mohs)
Borovskite	Pd_3SbTe	Isolated grains up to 0.2 mm included in pyrrhotite and chalcopyrite	8.25	N/A
Braggite	(Pt,Pd)S	Fractured grains up to 8 mm long	9.36	5
Cherepanovite	RhAs	Grains and their aggregates up to 0.1 mm	9.72	Brittle
Cooperite	PtS	Euhedral to anhedral micrometer to 1.5 mm grains	10.10	4–4.5
Foodite	$PdBi_2$	Grains up to about 1 mm	11.62	Brittle
Genkinite	$(Pt,Pd)_4Sb_3$	Irregular grains from <0.005 up to about 0.165 mm × 0.165 mm in size	9.26	5.5
Geversite	$PtSb_2$	As small drop like inclusion	10.91	4.5–5
Insizwaite	$PtBi_2$	As small rounded grains up to 120 μm	12.86–13.59	5
Isoferroplatinum	Pt_3Fe	In placer deposits occurs as various size nuggets, usually containing chromite and many other mineral inclusion, varying from flakes to nugget size	18.23	N/A
Kotulskite	PdTe	Occurs as small rounded to anhedral inclusions in sulphides or intergrown with other PGM	9.18–10.54	N/A
Laurite	RuS_2	Grains and crystals from 0.0001 to few mm	6.39-6.43	7
Maslovite	PtBiTe	Grain up to 0.120 mm in size	11.23	4–5
Merenskyite	$PdTe_2$	As minute grains, intimately intergrown with other PGM, or as single-phase inclusions	8.30	3.5–4
Michenerite	PdBiTe	Grains from 0.0001 to 2 mm	9.81	4–4.5
Moncheite	$PtTe_2$	Crystals up to 1 mm and minute grains	10.24	3.5
Palladoarsenide	Pd_2As	Long and irregular grains	10.59	4.5
Sperrylite	$PtAs_2$	Micrometer to centimeter size crystals and rounded grains	10.8	6–7 Brittle
Stillwaterite	Pd_8As_3	Grains up to 0.12 mm × 0.265 mm	10.95	4.5–5
Sudburyite	PdSb	Elongated inclusions up to 55 μm × 120 μm	9.41	4–4.5
Tetraferroplatinum	PtFe	Irregular grains, rims on other Pt–Fe grains	15.81	N/A
Vysotskite	PdS	As intergrowths and lensoid inclusions in other sulphides	6.74	N/A
Ruthenium	Ru	The type material occurred as tabular grains (35 μm × 7 μm)	12.2	6.5
Rhodium	Rh	A grain from 0.175 to 0.195 mm in cross-section	16.5	3.5
Palladium	Pd	Commonly as loose grains, sometimes with a radial fibrous texture	12.0	4.5–5
Osmium	Os	Occurs as inclusions in Pt–Fe alloys	22.1	7
Iridium	Ir	Occurs as exsolutions in Pt–Fe alloys	22.2	6–6.5
Platinum	Pt	In placer deposits, it occurs as various size nuggets	19.1	4–4.5

This section has indicated in brief how geometallurgy is critical to interpret the characteristics of an ore in developing processing techniques and in generating business case for a processing route.

2.2. Comminution of PGMs

2.2.1. Introduction to Comminution

Comminution by grinding (or milling) is perhaps the most widely employed physical process to liberate minerals in the host matrix and hence increase the surface area of a given mass of solid (Rouquerol et al., 1999; Khan et al., 2022). During grinding of ore particles, the breakage required is achieved by the tumbling motion of the charge in the mill which is commonly mixed with grinding media that has a greater hardness than the ore. The mill load is carried upwards by the centrifugal forces and is brought down by gravitational effects. The point where the charge drops back down (leaves the mill lifters/liners) is called the shoulder and the point at which the charge lands is called the toe. This action imparts energy to the medium which then impacts the particles to cause grinding of the particles. Comminution occurs via three distinct mechanisms of breakage (Varinot et al., 1997; Hennart et al., 2009; Wills B. A., 2015):

- **Compression/Cleavage**: a particle is intensely compressed which results in fracture.
- **Abrasion/Attrition**: A particle experiences a shear stress by 'rubbing' against another particle or against a breakage surface.
- **Fracture by Impact**: The particle and a rigid surface or another particle undergo high energy impacts.

Figure 9 indicates different fragmentation mechanisms and the resulting product size distributions. When a mill is operating optimally the load will cataract and the dominant size reduction mechanism will be impact fracture with abrasion/attrition being the secondary reduction mechanisms.

Comminution is a vital processing step on PGM concentrators as PGMs are found in the sub 75µm fraction as mentioned previously. Primary milling of PGMs is able to achieve approximately 30-40% less than 75µm particles in the mill discharge and secondary milling can achieve more than 80% less than 75µm particles in the mill discharge (Hay & Schroeder, 2005; Liddell, 2009; Ilunga, 2014).

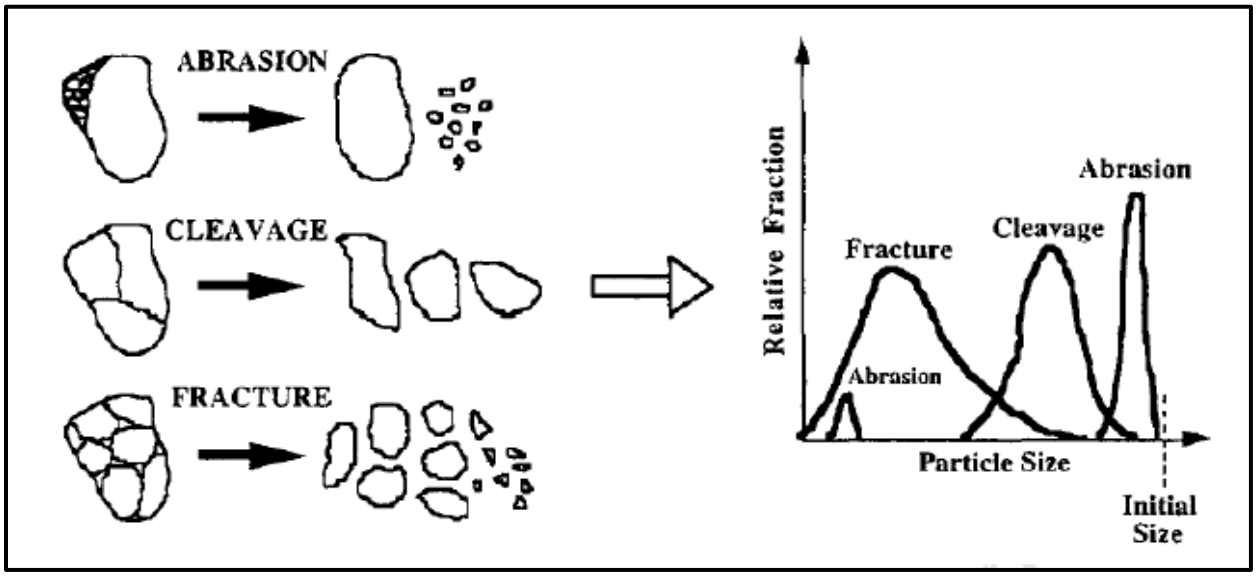

Figure 9: Different Breakage Mechanisms and the Resulting Product Size Distributions [In Lisso (2013) adapted from Varinot et al., (1997)]

2.2.2. Comminution Applied to PGM Containing Ore

The typical flow sheet of a PGM concentrator is referred to as an MF2, that is a primary mill and float followed by treatment of the primary rougher tails through a secondary mill and secondary float circuit (Cole & Ferron, 2002; Hay & Schroeder, 2005). The underlying principle behind a MF2 process flow sheet is to prevent overgrinding (Cole & Ferron, 2002). This is because the overgrinding of sulphides such as pentlandite can cause sliming in subsequent flotation stages (Cole & Ferron, 2002). This also prevents the overgrinding of gangue material such as talc, which can further hinder the efficiency of the subsequent process as well as chrome which may be entrained in the concentrate if it is ground too fine (Mpinga et al., 2015). The increased processing of UG2 ores with its complex PGM mineralogy and chromite spinel content has introduced a level of processing complexity to modern PGM processing compared to Merensky based processing techniques (Rule, 2008). This has led to the development of mainstream inert grind (MIG) and ultrafine grind (UFG) processes (Rule, 2008; Lisso, 2013). The main purpose of MIGs is to increase recovery in the mainstream flotation circuit. The main purpose of UFGs is to increase grade without losing recovery in the cleaner circuit (Rule et al., 2008). The generic flowsheets for this milling can be seen in Figure 10 and Figure 11.

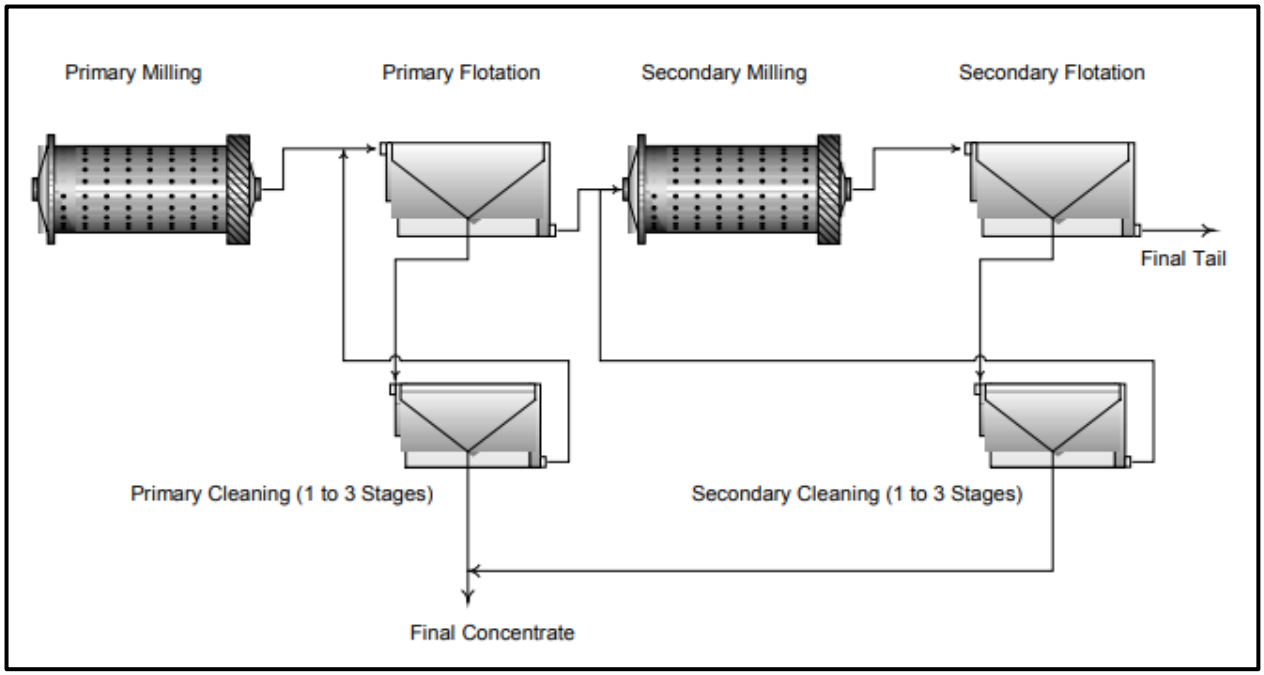

Figure 10: Typical MF2 Circuit (Cole & Ferron, 2002)

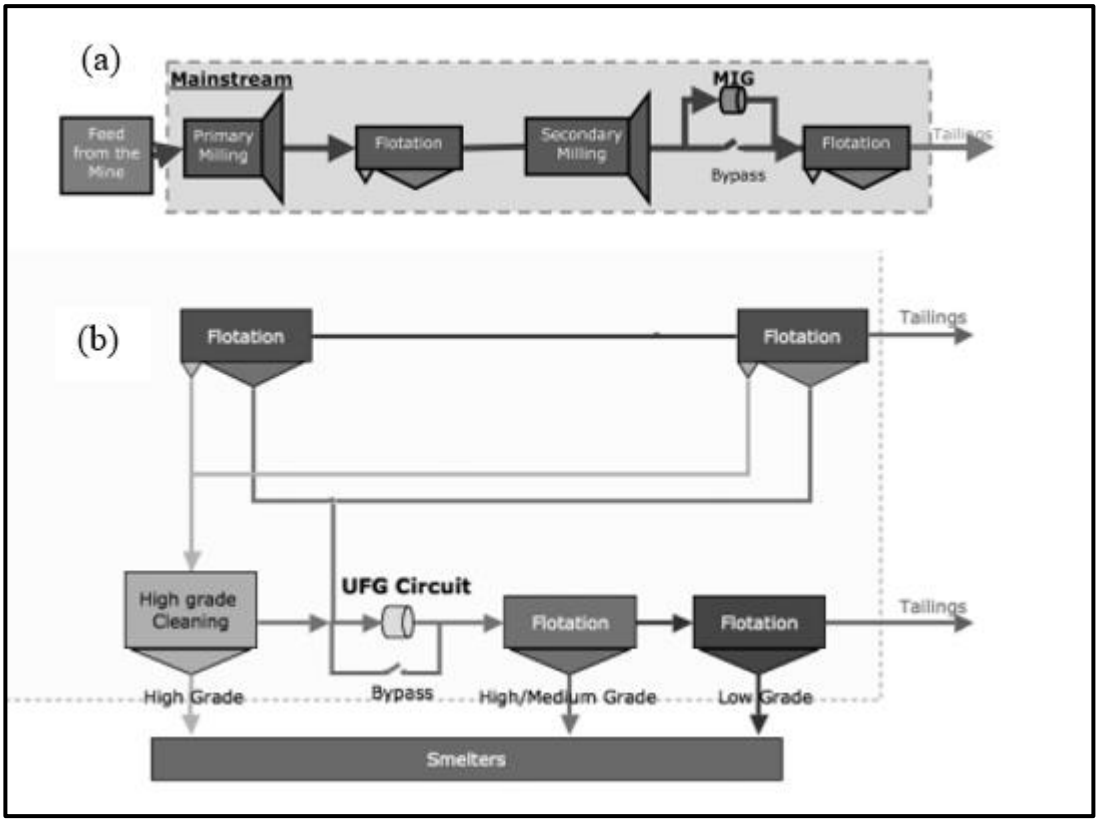

Figure 11: Schematic of (a) Generic Mainstream Inert Grinding and (b) Generic Ultrafine Grinding (Rule, 2008)

Fine grinding using MIG and UFG are energy intensive processes as smaller particles have a larger surface area and thus will require more unit energy to break further than larger ones for the same reduction ratio. As particles get smaller, their strength increases (Ehmer et al., 2006). Therefore, this leads to the postulation that it would take a larger amount of energy to produce fine and ultra-fine particles than coarser particles. Richardson et al. (2002) confirmed that since a much greater increase in surface results from crushing a given quantity of fines as opposed to coarse material, fine grinding requires much more power. The energy required to achieve a certain size reduction is a function of the internal structure of a given particle and is dependent on opening small pre-existing fissures in the particles as well as forming new surface area, therefore as particles become smaller these two criteria become harder to attain without additional energy.

2.2.3. Developments in PGM Comminution

A large body of research exists on optimizing PGM comminution by changing various parameters or process equipment. Solomon (2010) as well as Chapman et al. (2011) found that Ball Mill product had a better flotation response than high pressure grinding rolls (HPGR) product at various operating conditions, mainly due to the broader particle size distribution which results in a greater volume of fines (negatively impacting concentrate grade) and coarse particles (negatively affecting recovery). The type of grinding media also has a marked effect on downstream flotation kinetics as shown by Song et al. (2018) who tested five different grinding media namely, ceramic; forged steel; high chrome steel; stainless steel and a blend of stainless steel and high chrome steel to grind the same material. The research found that ceramic media resulted in the best flotation performance in terms of PGM recovery and low chrome recovery while high chrome grinding media performed second best. The other three types of media had poor results on flotation performance. These results are consistent with industry practice as high chrome steel balls are used in primary and secondary mills while ceramics are used in MIG/UFG grinding. Chimwani et al. (2013) investigated the most effective milling parameters for optimal mill product size distribution and found that understanding the selection and breakage functions were critical in ensuring optimal size distribution from a mill product, this research also created a simulation of the milling kinetics for various scenarios. Considerable research is still being

undertaken on comminution of PGM ores which demonstrates the importance of comminution in the PGM industry and that solutions are being pursued from multiple angles.

2.3. Flotation of PGMs

2.3.1. Introduction to Flotation

Flotation is a physicochemical process that allows for the separation of minerals of interest from gangue. The fundamental principle underpinning flotation is the differences in surface wettability of particles i.e. hydrophilicity or hydrophobicity of mineral particles. The process occurs in a wet chemical environment whereby the slurry flows through flotation cells. Various flotation reagents are added to the slurry to enhance and ensure flotation takes place and air is sparged through the cell to assist with bubble formation (Bethell, & Luttrell, 2004; Cisternas, et al., 2016; Carelse, et al., 2022). The main variables which influence the efficiency of the flotation process are reagent selection and quantity, fineness and composition of the slurry feed, pH of the solution, density of the slurry, air flow rate, intensity of agitation, froth depth and residence time (Wills & Napier-Munn, 2006; Santana, et al., 2008). A typical flotation circuit consists of Rougher, Cleaner, Recleaner and in some cases Scavenger cells. The rougher cells are typically employed to maximize recovery, while the cleaner cells are used to upgrade the final product (Metso, 2011). Scavenger cells are used to increase the retention time and extract any slow-floating PGMs before the slurry is sent to the Tailings Storage Facility (TSF). A typical flotation cell is depicted in Figure 12.

The three basic foundations of flotation are depicted in Figure 13. This indicates the dynamic relationship between various factors and how they work with each other but also how these factors can be self-compensating or capable of reinforcing desired or undesired system performance (Klimpel, 2003).

A critical point to be made about PGM flotation is that individual PGEs are not floated but rather the PGMs associated with BMS, which are either attached to the sulphides or in a solid solution with the sulphide matrix (Schouwstra et al., 2000; Ballhaus & Sylvester, 2000). The key to PGM flotation is thus intimately linked to base metal sulphides. Chalcopyrite has been shown to have a fast floating rate while pyrrhotite is considered slow-floating and the pentlandite flotation rate is

in between the other two sulphides, however it is important to note that varying plant and thermodynamic conditions can have a marked influence on flotation rates of various BMS species (Ekmekçi et al., 2005).

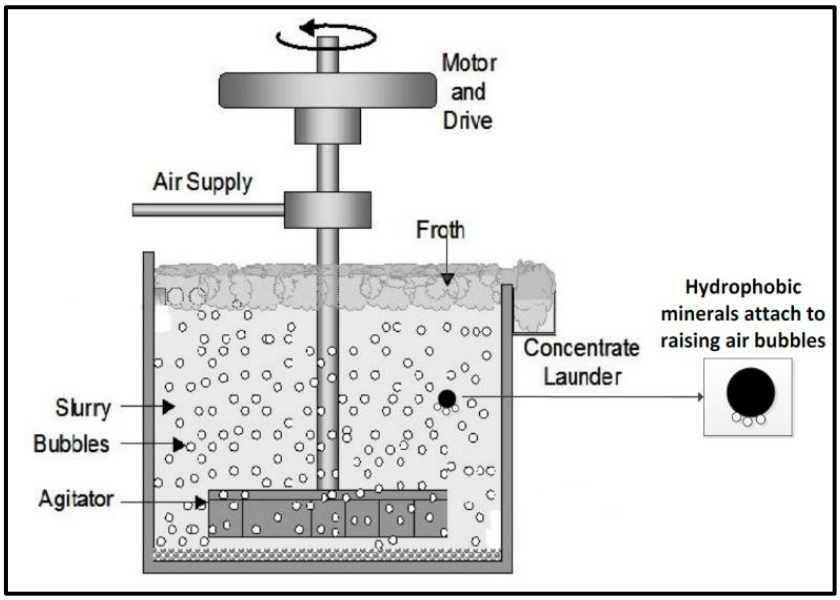

Figure 12: Flotation cell (Sefako, 2018)

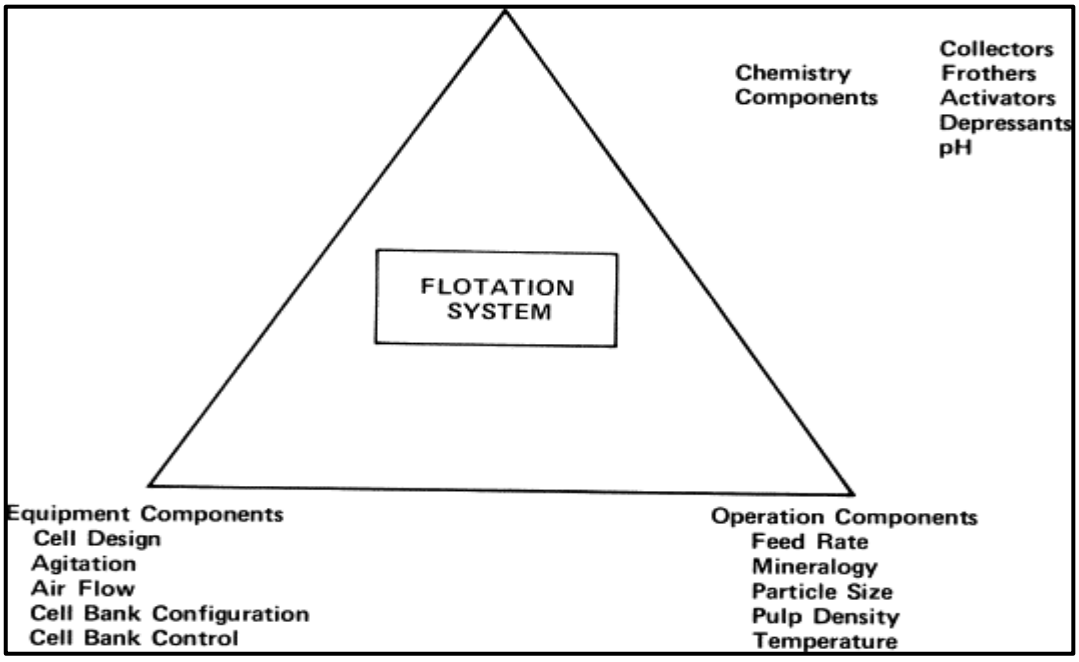

Figure 13: The froth flotation system illustrated as a three-cornered interactive system. (Klimpel, 2003)

2.3.2. Flotation Reagents

The purpose of flotation reagents is to ensure that a chemically and thermodynamically favourable condition exists for flotation kinetics. Each reagent performs a critical and specialized task in the froth flotation process.

Collectors are a group of organic chemical compounds whose purpose is to selectively form a hydrophobic surface film on the minerals of interest thus making the particles hydrophobic. These chemicals may be ionizing or non-ionizing (see Figure 14), the former have a complex asymmetric molecular structure which consists of a non-polar hydrocarbon chain and a functional polar head while the latter are largely insoluble in water and cover the particles surface making them hydrophobic (Nguyen, 2012). The collector also increases the contact angle between the particle and the air bubbles (Kawatra, 2011). Collectors can bond to particles by either chemisorption (chemically induced bonds) or physisorption (physical bonds) (Kawatra, 2011). Xanthates are the most used type of collector on PGM plants. Sodium isobutyl xanthate (SIBX) and sodium normal propyl xanthate (SNPX) are the specific xanthates used effectively on most PGM plants (Wiese et al., 2006).

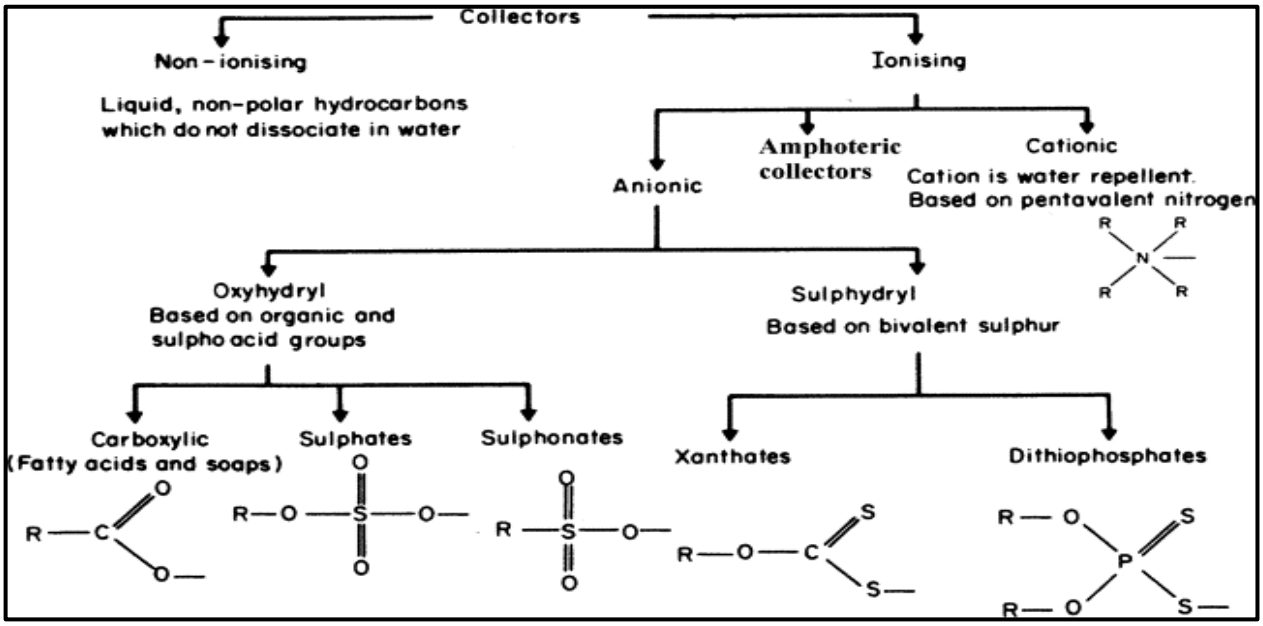

Figure 14: Typical industrial flotation collectors. R represents different hydrocarbon chains (and hydrogen atoms in cationic collectors). (Nguyen, 2012)

Frothers on the other hand are surfactants that produce small bubbles and stabilize the bubbles from the air introduced to the flotation cells. The smaller air bubbles have an increased surface area and thus improve the chances of hydrophobic particles being floated (Kumar & Kumar, 2018). The frother molecules have a heteropolar nature which lowers the water surface tension which results in stabilization of the froth zone (Gupta & Yan, 2006). In froth flotation it is critical that the bubbles do not break until the concentrate is removed from the flotation cell. Breakage of bubbles before that will result in the recovered minerals falling back into the pulp. The presence of a frothing agent in a slurry increases the air dispersion in the flotation cells (Nesset et al., 2006), reduces the coalescence of bubbles (Laskowski et al., 2003) and decreases the rate of rise of the bubbles (Rafiei et al., 2010) to ensure that the bubbles become sufficiently mineralized. The most common frothers are short chain aliphatic alcohols and polyglycols (Schlesinger et al., 2022).

Depressants are another family of flotation reagents that reduce the floatability of gangue minerals and thus increases the floating capacity difference between the gangue and minerals of value. Depressants are generally high-molecular-weight polymers that can render gangue particles hydrophilic, and this causes gangue minerals to have less of a chance of reporting to the froth. It has been shown that the creation of a strong electrostatic double-layer force is a major mechanism of the depressant action while suppression of the hydrophobic force is secondary (Xing et al., 2017). PGM ore from the BIC contains naturally floating gangue (NFG) which negatively impacts on PGM concentrate grade and recovery. Concentrators processing PGM ore make use of polysaccharide depressants to reduce the recovery of gangue minerals. Carboxymethyl cellulose (CMC) is a common depressant on PGM concentrators for carbonate gangue and pyroxene associated with talcaceous gangue (Leppinen, et al., 2004).

Activators promote the interaction of collectors with the surface of a valuable mineral which would otherwise not float. The activators essentially modify the target surface thus allowing the collector to attach to the particle. The complex interactions of activators for froth flotation are well known, for instance in the case of sulphide flotation where copper sulphate is used as an activator. The copper ions exchange with other surface ions and create the necessary conditions to float the target particles but under different thermodynamic conditions the copper sulphate

may complex as a hydroxyl species and depress particles of value (Bradshaw et al., 1998). The addition of copper sulphate in PGM flotation is an intensely debated topic although it has been shown that copper sulphate can activate sulphide minerals, more especially sphalerite. This happens under acidic conditions which is not the case with practical PGM flotation which occurs under neutral to basic conditions (Laskowski, 2004; Wiese et al., 2006). Another complication in the use of copper suphate is the inadvertent activation of gangue minerals (Martinovic et al., 2004). Merensky and UG-2 ores respond differently to the addition of copper sulphate as shown by Nyabeze & McFadzean (2016) who found that Merensky ore had better results than UG2 ore in terms of concentrate grade and recovery which may be attributed to the differences in BMS in the different ores. It was also found that the Merensky ore froth was stable during the tests while the collector interaction resulted in froth instability for the UG2 ore. The study also found, through zeta potential measurements that the copper species were associated with plagioclase, chromite, talc and pyrrhotite surfaces. This indicates that the activation capability of copper sulphate can also cause gangue flotation.

2.3.3. Developments in Flotation

Several developments have been made in PGM flotation over the years. Lotter & Bradshaw (2010) investigated the use of mixed collectors (xanthates, dithiophosphates (DTPs), and dithiocarbamates (DTCs)) in sulphide flotation. The researchers found that DTC had the greatest collector strength followed by xanthate and DTP while DTP had the best selectivity followed by xanthate and DTC (ceteris paribus). The unique properties of the collectors tested meant that a mixture of the collectors could possibly improve flotation performance. The synergy between different collectors showed an improvement in recovery of middling particles and could be configured for recovery or selectivity. The blending of frothers for PGM recovery was investigated by Ngoroma et al., (2013). The study found that a synergistic effect takes place when frothers are blended, more especially when a weaker and stronger frother are blended together. There was sufficient froth stability and bubble size control as well as higher mineral recoveries. This previous two studies on blending reagents point to the complex nature of PGMs and how using reagents with different characteristics can ensure optimal economical recovery and quality in PGM extraction. There have also been developments in flotation cells hardware such as the flotation column cell which has been shown to improve concentrate grade (Hurdeyal,

2012), high intensity flotation which improves both recovery and grade for ultra-fines (Eriez, 2024) and the direct flotation reactor which prevents the formation of a froth and slurry interface and rather allows individual loaded bubbles to be collected and making it more selective in mineral recovery (Woodgrove Technologies, 2024)

2.3.4. Considerations for PGM Flotation

Grade, Recovery and Mass Pull are the primary key performance indicators on a flotation plant. Mass pull refers to the total amount of final concentrate dry mass recovered compared to the feed to the circuit. Grade refers to the final concentrate grade. Recovery is the total PGM recovery from the circuit which is measured as 4E or 6E. Mass pull versus Recovery and Grade versus Recovery plots are critical in understanding the operation and limitations of a particular flotation plant. The general relationship between these variables is that as one increases mass pull, this will increase recovery as more PGMs report to the froth phase but concentrate grade decreases as this action also causes recovery of gauge. Increasing mass pull also increases entrained chrome which is deleterious to the smelting process. Each concentrator must therefore strike a balance between these variables based on what the downstream smelter will accept. It is therefore critical to mention that if a process was implemented to further upgrade the final concentrate selectively, then one would be able to shift the grade recovery curve to a more efficient position.

A discussion on PGM flotation would not be complete without discussing the ‘elephant in the room’…chrome. One of the main challenges for concentrators is the reduction of chrome in UG2 PGM concentrates due to its deleterious effects on the smelting process (Hay & Roy, 2010). Chromite is rather dense and naturally hydrophilic which leads to it being entrained in flotation concentrates rather than being recovered by true flotation, this is more especially true when the chromite is of a fine particle size i.e. less than 45µm (Song et al., 2018). Entrainment can be described as the phenomenon whereby hydrophilic particles are transported to the froth phase within the water that forms lamella between bubbles. It is therefore important to ensure operational parameters are set up to reduce entrainment as far as practically possible.

2.4. PGM Smelting

The conventional smelter-based process for PGMs is justifiable for high grade, low chromite, large resource and long life-of-mine operations. For lower grade ores (and even tailings materials) as well as ores with chrome levels more than 2.8%, pyro metallurgical process routes are not favourable. For the former the cost of smelting is restrictive and for the latter, the chrome forms a build-up of highly refractory chromite spinel layers in the furnace. Apart from this, the combination of high chrome, high talc and fineness of grind can lead to dangerously high matte temperatures (Mpinga et al., 2015).

Smelting of low Chrome PGM concentrates usually occur at temperatures between 1300-1400°C, while for UG2 concentrates which are high in Chrome the smelting temperature can be in excess of 1600°C (Jones, 2005). The electrical power consumption is approximately 600-1100KWH per ton of concentrate and accounts for 40-50% of the direct smelting costs (Newman, 1973) but of course this is highly dependent on the equipment as well concentrate grade and mineralogy.

Smelting essentially separates the charge into two distinct zones, slag and matte. The slag contains waste products such as oxides and silicates. Slag is either discarded as waste or milled and processed to recover any entrained residual precious metals. The matte phase on the other hand contains nickel, copper, cobalt, iron, sulphur, and the PGMs.

“During smelting, some magnetite and other spinels such as chromite, that are not reduced and fluxed, dissolve in the matte and slag. Magnetite sometimes forms an intermediate viscous zone between the matte and slag layers, causing an increase in entrainment. A build-up of magnetite or other spinels causes a reduction in operational furnace volume. Near the slag-matte interface, the concentration of matte particles in slag is at its highest, as is the concentration of chromium oxide in the slag” (Jones, 2005 , p. 10).

Subsequent to Smelting is a Converting process. This process removes Iron and Sulphur from the matte by oxidation. The converter matte contains base-metals as well as the PGMs in a much-

concentrated form. The converter matte is then sent to a base-metal refinery to remove base metals usually via leaching and the remaining leach residue is rich in PGMs and is sent for Refining. The complex and extensive processing routes and time-intensive nature of the process to get from concentrate to refined PGMs inevitably leads to greater lock-up of PGMs in the process units.

The chrome content of the concentrate has the most marked effect in the smelting stage of PGM processing. If there are recycle streams within the smelting and converting process the potential to build up chromite increases leading to premature equipment failure. “The UG2 concentrates contain significant quantities of chromite, which easily results in the build-up of highly refractory chromite spinel layers in the furnace. This affects furnace operation, and the accumulation reduces the working volume of the furnace over a period of time” (Jones, 2005, p. 12).

2.5. Gravity Concentration of Minerals

Gravity Concentration or Separation makes use of the inherent differences in the densities of minerals to bring about separation of the mineral of interest from other minerals and gangue (Singh et al., 1997).

The major limitation with gravity concentration is the treatment of fines and ultra-fines. In the fine size ranges, separation efficiency is negatively impacted by the fluid and viscous forces which become dominant relative to the gravitational force (Singh et al., 1997). For small particles the separation is dominated mainly by surface friction, and these respond poorly to conventional gravity separators. To reduce the size effect and for making the relative motion of the particle's specific gravity dependent, a closely sized feed is desirable (Sarkar et al., 2007). Research over the past few years suggests that advanced/enhanced gravity separation may be used to overcome challenges experienced with surface-based separation process, more especially if particles are fine and ultra-fine (Osborne, 1988). Advanced gravity separation technologies such as Knelson concentrators, Falcon Concentrators, Kelsey Jig, Multi-gravity Separators and Bartes Mozley Separator are able to process material in the finer size range. These units employ high gravitational forces at relatively high throughput volumes to recover fine and ultra-fine liberated particles in a slurry (Bunt, 1995; Peer et al., 2001). An operational site that utilizes gravity concentration for PGMs is the Norilsk nickel complex in Russia, in this plant a Knelson concentrator is utilized to recover PGMs as a by-product from the grinding circuit and final tails (Kozeyrev, et al., 2003). Jinchuan Company, the largest nickel–copper production company in China recovers PGMs by centrifugal gravity concentration as a by-product (Yao & Zhang, 2018). It is also pertinent to note that advanced gravity separators do not make use of any chemicals, use relatively little water and electricity and require minimal human supervision.

Mineral characterization for proposed applications of gravity concentration is critical to ensure that the correct process will be used to recover target minerals. The chemical and mineralogical compositions of the ore as well as the qualitative and quantitative aspects of the target minerals and associations, impurities, and by-products are very important at informing the potential success of advanced gravity separation (Perroton et al., 2020). This geo-metallurgical data can assist in determining the most optimal gravity concentration processing route.

2.5.1. Principle of Gravity Concentration

The gravity separation of two or more minerals with differing specific gravities in a fluid is influenced by their movement in response to gravity and the forces in the fluid (Singh et al., 1997). Inherent particle properties such as size, shape and relative weight also have an impact on separation efficiency. The Concentration Criterion describes the amenability of separation of two minerals and is given by

$$CC = \frac{(d_H - d_F)}{(d_L - d_F)}$$

Where:

d_H = Specific gravity of the heavy material

d_F = Specific gravity of the fluid

d_L = Specific gravity of the lighter material

A general rule is that when the quotient is greater than 2.5 then gravity separation is relatively easy but when the quotient goes below 1.25 then gravity separation is not feasible (Misra et al., 2004).

The efficiency of gravity concentration also increases with particle size as described by Newton's Law:

$$v = \left[3gd\frac{(D_s - D_f)}{D_f}\right]^{\frac{1}{2}}$$

Where:

v = terminal Velocity

D_s = density of the solid

D_f = density of the fluid

d = particle diameter

Newton's law holds for particles larger than 0.5 cm diameter and also assumes that particles are solid, smooth and spherical. Particles must also be of uniform density, should not interfere with each other during the fall and the fluid medium can have turbulent flow. Newton assumed that the drag the fluid imposes on particles is a result of turbulence.

The Stoke's law considers the forces acting on a particle as it sinks through a fluid under the influence of gravity. The force that hinders a particle from moving through a fluid is directly proportional to the velocity and radius of the sphere. Stokes law is considered valid for particles below 50 microns diameter, particles must be solid, smooth, and spherical, particles must be of uniform density, particles should not interfere with each other during the fall and the fluid medium must have laminar flow. Stoke's law is expressed mathematically as:

$$v = \frac{gd^2(D_s - D_f)}{18\eta}$$

Where:

g = gravitational acceleration

d = particle diameter

D_s = density of the solid

D_f = density of the fluid

η = viscosity of the fluid

Both laws mentioned above govern gravity concentration, at least in part.

Although density is a crucial factor in determining the possibility of separation of minerals one should also be aware that particle granularity and shape play a role in the effectiveness of gravity separation as well. The difficulty of gravity separation increases with a decrease in granularity of

the particles (Kroll-Rabotin et al., 2012; Maharaj et al., 2012). Particles with different shapes are subjected to different resistance forces and motion velocities which can complicate gravity separation (Aslan, 2008). It is therefore important to understand the nature of the mineral intended for gravity separation so that the most effective processing method can be used. If the main separation factor is density then a dense medium separation may be used to increase the density differences (Chu et al., 2009). If granularity of particles is the main separation factor then there may be a need for a classification process (Golyk et al., 2011). If shape is the main separation factor then the particles containing the minerals of interest should be protected from any deformation (Kademli & Gülsoy, 2012).

2.5.2. Mechanisms of Gravity Concentration

Fluid Density

This mechanism utilizes a fluid with apparent density between the particles to be separated. The difference in buoyancies causes some minerals to float and others to sink (Bulatovic, 2015). An example is heavy medium separation.

Stratification

The minerals are stratified by an intermittent fluidization caused by the pulsation of the fluid in a vertical plane (Ambrós et al., 2019). An example is a jig.

Flowing Film

The minerals are separated by their relative movement through a stream of slurry which is flowing down a plane by the action of gravity (Singh et al., 1997). An example is a sluice.

Shaking Surface

The various constituents are separated by superimposing a horizontal shear force on the flowing film (Gülsoy & Gülcan, 2019). An example is a shaking table.

Centrifugal Force: Advanced/Enhanced Gravity Separators

Advanced gravity separators are modern separators that have the ability to separate even fine particles. The general principle involves the application of a centrifugal field to the material (Sarkar et al., 2007). An example would be the Falcon concentrator.

2.6. Experimental Research and Application of Gravity Concentration

Although there is limited research on gravity concentrators applied to PGMs, there is a broad body of research on gravity concentration as applied to various other minerals. These investigations can shed light on why and how gravity concentration works on different minerals.

2.6.1. Conventional Gravity Separation

Various minerals processing industries have made use gravity concentrators that do not use a centrifugal force and are not defined as advanced/enhanced gravity concentrators but are 'traditional' due to their historic significance in processing particular ores. These include jigs, spirals and shaking tables. These types of gravity recovery process units become less effective with lower feed grades to the circuits, treatment of complex ore bodies and fine to ultrafine particles. Nonetheless these gravity separation techniques warrant discussion to add to the broader discourse around gravity concentration.

2.6.1.1. Jigging

Jigging is used to separate minerals with significant differences in specific gravity (Rao, 2006). The most basic form of a jig is depicted in Figure 15. The jig has a continuous pulsating action in the vertical plane while the feed material is fed to the unit from the top and fluidizing water is also added. A bed of heavy particles called ragging is placed on a perforated screen within the jig. The heavier particles or concentrate particles settle and move through the screen while the lighter or gangue particles cannot overcome the jigging action and are removed to the tailings (Haldar, 2018). The principle of jigging is essentially the process of particle stratification due to the continuous expansion or dilation and compaction of the particle bed by the vertical flow of the fluid (Bethell, & Luttrell, 2004). The bed of particles starts to dilate on the pulsation stroke, with separation of the particles which is induced by the difference in acceleration of the heavy

and light fractions followed by hindered settling. During the suction stroke, the bed is stratified based on density differences of the particles and consolidated trickling occurs as seen in Figure 16 (Kumar & Kumar, 2018). In a continuous jigging process performance is influenced by stratification dynamics as well as particle movement, horizontal fluid and particle mixing (King, 2001). The operational conditions within a jig can have a marked impact on the stratification kinetics and the stratification profile achieved at equilibrium (Woollacott et al., 2021). The four main variables that were found to have the largest impact on stratification are the pulsion time, pulsion hold-time, amplitude of the jig cycle and depth of the particle bed (Woollacott et al., 2021).

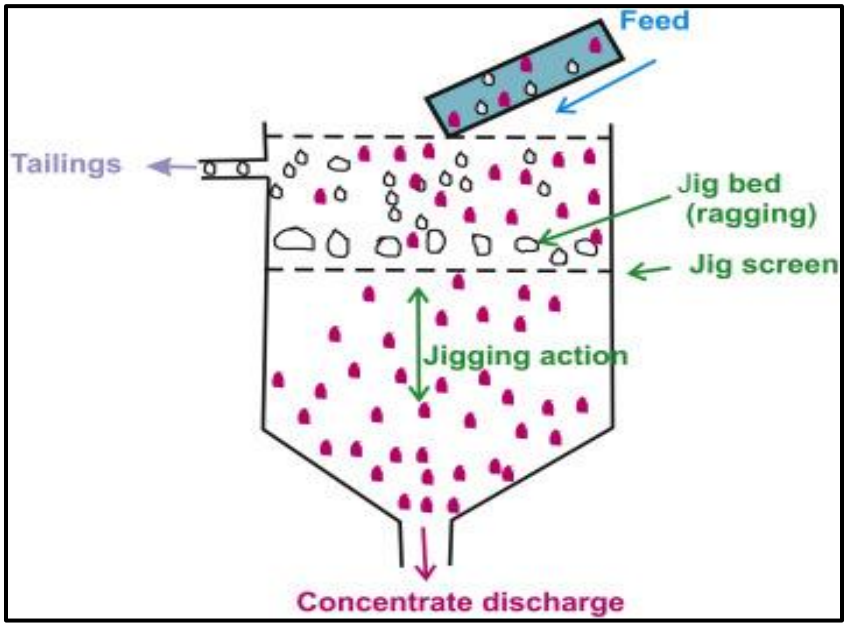

Figure 15: Basic principles of a jig concentrator (Haldar, 2018)

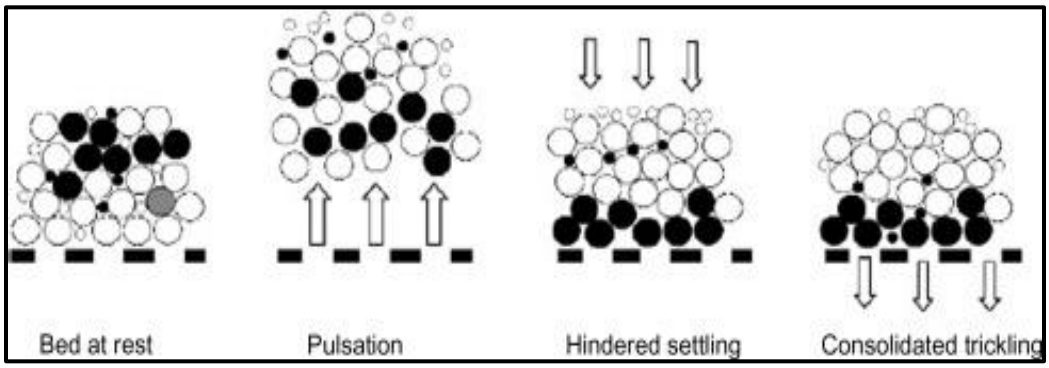

Figure 16: Basic principles of jigging (Yan & Gupta, 2006)

Several variations of the jig exist depending on the process requirements, two common units are the Inline Pressure Jig (IPJ) and the Kelsey Jig. The Inline Pressure Jig (IPJ) is said to be an improvement on the traditional jig by utilizing a pressurized unit that is completely filled with slurry and water, the air-water surface tension is removed and the slurry velocity is slowed for potentially improved recovery (Yan & Gupta, 2006). The Kelsey Jig incorporates a centrifugal force to jigging. The forces acting within the unit are capable of recovering fine particles with applications in coal, mineral sands, tin, base metals, iron and soil remediation (Richards & Jones, 2004). Complex ores with fine and ultrafine particles cannot be effectively recovered with jigging as the forces acting on the particles would lead to excessive valuable minerals reporting to the tailings. Jigs cannot be used in areas that are water scarce as large volumes of water are required to maintain operating conditions (Das et al., 2008).

The effectiveness of jigs in various industries has been studied and these studies have shown the type of feed material and parameters that are optimal and economical for this type of process unit. Das et al. (2008) studied the beneficiation of low-grade iron ore using jgging and found that 78.6% iron ore recovery was possible with production of a concentrate with a Fe grade of 63.7%. An investigation was also conducted by Olubambi & Potgieter (2005) on the effectiveness of jigging for Itakpe iron ore in Nigeria. The studied ore consisted mainly of hematite, magnetite and quartz and 71% of the iron was recoverable using a jig at an average particle size of 600µm in the concentrate. Heins et al. (2003) considered an inline pressure jig for recovery of diamonds and gold. The authors tested a number of ore deposits from the Witwatersrand and got recoveries of 70-85% at yields between 10-20%. The gold concentrate from a jig generally needs to be sent to a shaking table which has recoveries of less than 60%, this can make the process as a whole unfeasible. The use of intensive cyanidation in a leach reactor is an option to get above 95% recovery of jig gold concentrate. Diamonds have also been successfully recovered using jigging by application of synthetic ragging of uniform size and tightly controlled specific gravity (Heins et al., 2003). Boungou River Project in the Central African Republic and Williamson Diamond Mine in Tanzania are two known operations where diamonds have been successfully recovered using jigs.

2.6.1.2. Spirals

Spirals are high-capacity gravity concentration process units that separate mineral particles in a slurry based on their density and the hydrodynamic (quadratic) drag forces acting on the particles in the fluid medium. Spirals, as the name suggests, are vertical helical apparatus which may consist of a single or double conduit or sluice that allows a slurry to flow along its surface. Figure 17 indicates a typical spiral concentrator with multiple spirals. Slurry is pumped to the top of the spirals where a feed box or distributor is used to feed the spirals. The minerals in the slurry are separated through stratification by a combination of the centrifugal force (induced by gravity), differential settling and movement of denser particles to the inner section of the spiral conduit (Multotec, 2019). The spiral has a wash water channel and a number of concentrate off-take ports at specified intervals (Haldar, 2018). Figure 18 depicts a typical spiral, the larger and denser particles migrate to the bottom of the sluice as they experience more drag their velocity decreases and these particles move to the center edge of spiral (Moitra et al., 2021). The converse is true for light and relatively smaller particles, which stay on the outside edge of the spiral and are the rejects of the spiral. Spirals can be arranged in stacks of roughers, cleaners, and scavengers to ensure optimal recovery and grade of the final product (Gupta & Yan, 2006). Spiral concentrators are used for the beneficiation of rutile ore, monazite ore, zircon, iron ore, chromite and for the recovery of fine coal to name a few.



Figure 17: Spiral Concentrator (FLSmidth, 2024)

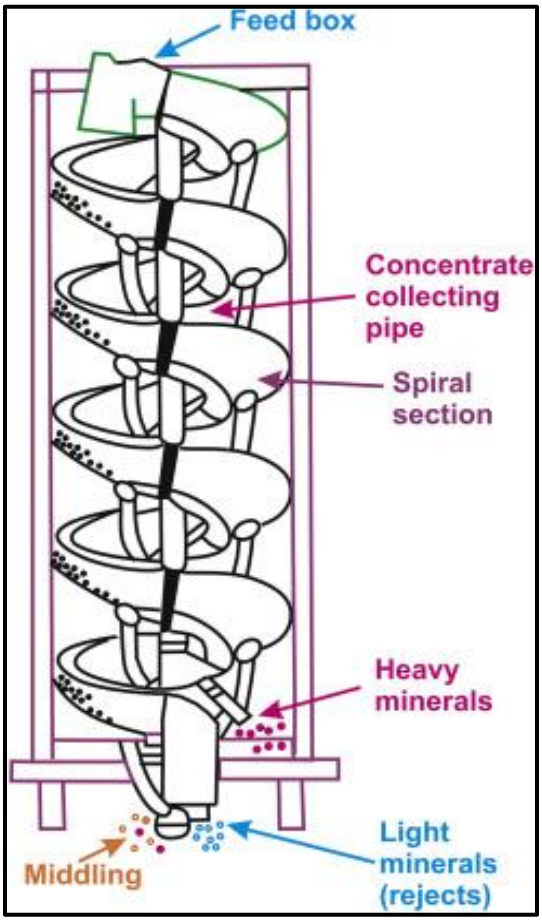

Figure 18: A standard spiral concentrator (Haldar, 2018)

Much research has been conducted on the effectiveness of spirals for various minerals. Richards Bay Minerals (RBM) processes heavy mineral sands to recover zircon, rutile, iron as well as producing titanium slag (Rio Tinto, 2024). Walklate & Fourie (2006) state that the non-magnetic fraction of the mineral sands (containing rutile, zircon, quartz and gangue) are fed to primary and scavenger wash-water spirals, the minerals of interest are successfully recovered and further processed via shaking tables. The site also makes use of Carpco wash-water spirals which introduce water on the inside of the spiral to improve separation efficiency. The successful use of spirals for mineral sands and specifically titanium have also been confirmed and discussed by Wright et al., (1986) and Holland-Batt (1995). Wang, et al. (2024) investigated the gravity separation of complex rutile ore using spirals. They found that spirals could achieve a zircon concentrate containing 33.18% ZrO_2 and a rutile concentrate containing 56.77% TiO_2, with further cleaning stages and the use of a shaking table these concentrations could be improved further. The fact that spirals could effectively recover a complex rutile placer deposit with the aid

of a shaking table downstream was a novel finding of the paper. A rather old paper by Guest & Dunne (1985) investigated the potential of spirals on a synthetic ore. The marker minerals were Casserite, Baddeleyite, Chromite, Magnesite and Apatite with Silica making up the gangue portion of the sample blend at 85% by weight. The various components of the synthetic ore were prepared in such a way as to ensure their particle size distribution was fairly similar though the deportation of each marker mineral in each particle size would differ due to the mineralogical differences between the markers. The results indicated that the multi-port spiral concentrator is more efficient than a pinched sluice at separating the gangue from the marker minerals. It was also noted that for finer particle sizes (less than 53μm), the efficiency of the spiral decreases.

2.6.1.3. Shaking Tables

Shaking tables are generally rectangular-shaped decks with water flowing over them, the decks are also ribbed allowing heavier particles to be directed to either a concentrate or middling's stream and lighter particles are directed to the tailings or rejects stream with the flowing water. The middling's stream can be recycled back to the table to ensure misallocated particles have an additional chance to flow to the concentrate stream. The table oscillates at regular intervals which assists with transferring momentum for particle movement along the bed. Wash water is added to the top or along the centre of the table. The main parameters that impact separation on a shaking table are particle size, particle density, shaking speed, and deck slope (Ferdana, et al., 2018). Shaking tables are used in myriad of industries due to their ability to produce high-quality concentrate products, workability, low maintenance and operating costs (Sierra et al., 2024). The separation performance of the shaking table increases as the grain size becomes narrower. Shaking tables are generally used for already concentrated material at low volumes that does not contain a complex mineralogy and serves to upgrade this material further (Houot et al., 1991; Fitzpatrick et al., 2016; Dehaine et al., 2017). Figure 19 indicates some typical shaking table designs, the one on the left being a Gemini table and the one on the right being a Desister multi-deck table. Figure 20 indicates gold separation from gangue material on a shaking table at a gold mining operation in the Witwatersrand, the gold ribbon/band is clearly visible from the gangue.

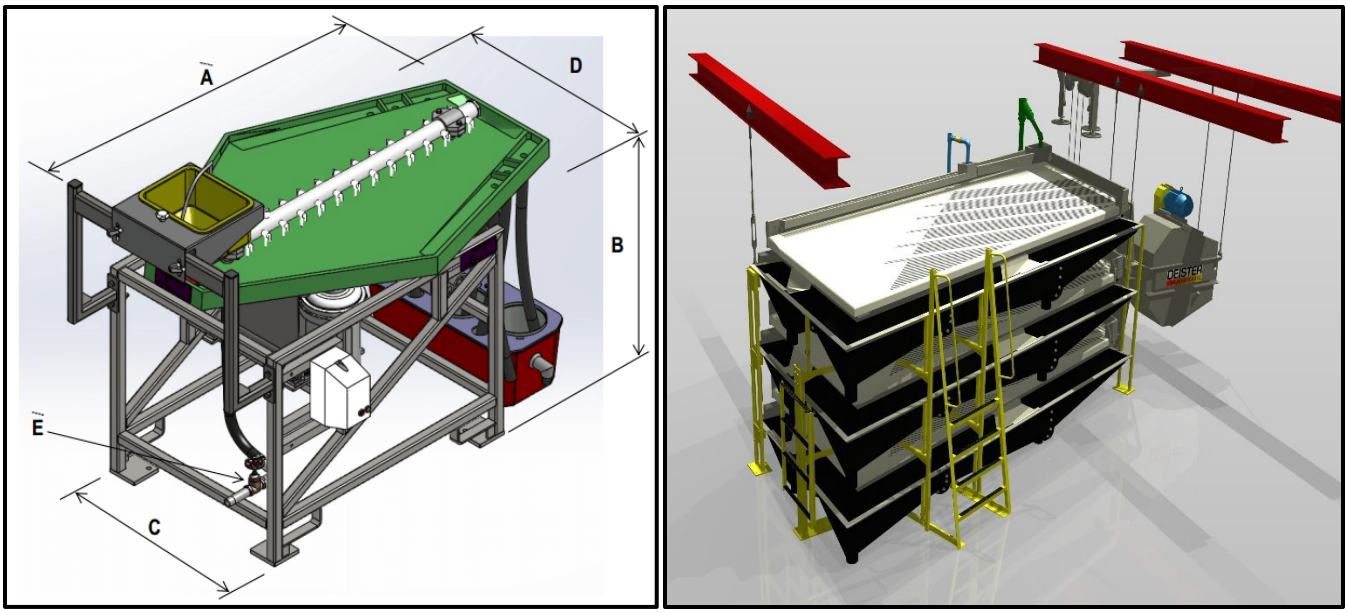

Figure 19: Typical Shaking Table Designs (Solo Resources, 2024)

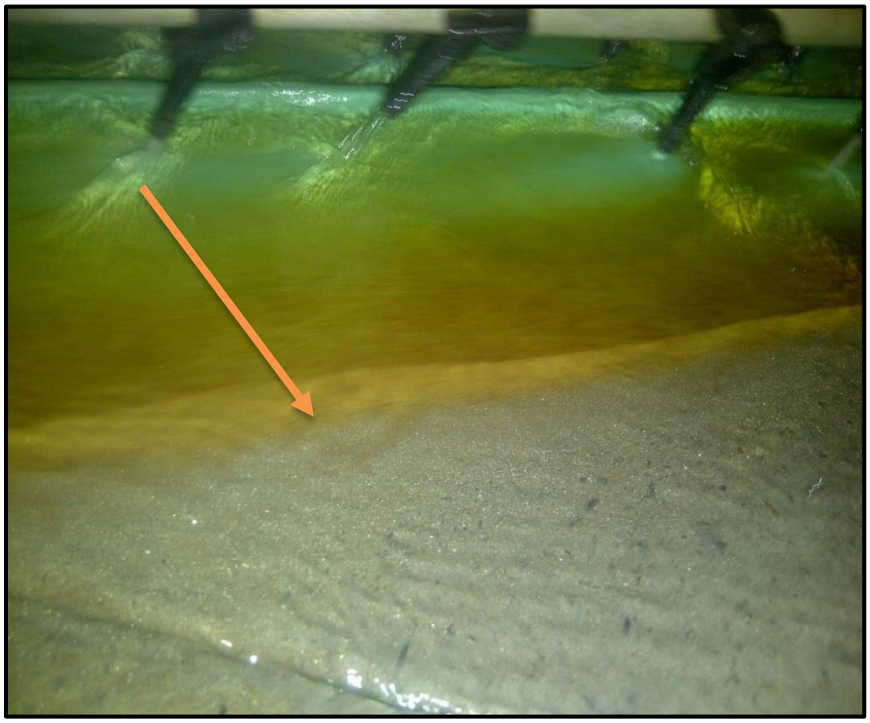

Figure 20: Gold Separation on a Shaking Table (source of photo: Taurean Nair, 2015)

Shaking tables have been extensively researched and applied to various minerals. Chromite ore has been successfully recovered and upgraded to a suitable grade using shaking tables as described by Seifelnasr et al. (2012) and Khakmardan et al. (2020). Seifelnasr et al. (2012) used

a Cr_2O_3 deposit from Sudan with a head grade of 30-35% chromite and achieved a 75% recovery at a chromium grade of 47.2% by using a shaking table. Khakmardan et al. (2020) utilised a combination of a shaking table and magnetic separation to recover Chromium from the shaking table tails and got mixed results as not all the chromite was magnetically separable, the mineralogy also had a negative impact on recovery and finally only alpine chromites were able to be recovered and not other forms of the mineral. An investigation by Fitzpatrick et al. (2016) utilised a synthetic ore consisting of wolframite, garnet, olivine and silica to try and model shaking table performance. QEMSCAN was used to develop a model for the synthetic ore. The research found that good prediction could be attained for wolframite and silica particles but less so for the olivine and garnet particles. Fitzpatrick et al. (2016) also found that smaller particles of value are difficult to recover using this method and modelling was idealized as naturally occurring ores would have particles which are a mix of various minerals and not fully liberated and separated as in the synthetic ore.

An investigation by Zhao, et al. (2013) revealed that the main separation factors for gravity concentration on a shaking table are density, shape and granularity of particles. For the specific case of vanadium pre-concentration from stone coal they found that density and granularity are not the main factors for particle concentration but rather the shape factor is the dominant separation factor. This suggests that the lamellar shape of the vanadium-bearing particles need to be protected from deformation during the grinding process of stone coal containing vanadium. Wet shaking tables have also been used to recover aluminium and copper from Incineration Bottom Ash (IBA) as described by Sierra et al. (2024). IBA from municipal solid waste was collected and subjected to a wet shaking table. The fine fraction (<2mm) which was the target size for this research accounted for 30-40% of the IBA and contained a significant amount of aluminium (20-40% by weight) and copper (45-80% by weight). Copper enrichment of up to 45 times was achieved in the finer than 500µm particles and up to 15 times in the 500-2000µm product with an overall recovery of 65% copper (Sierra et al., 2024).

2.6.1.4. Reflux ® Classifier

The reflux classifier (RC) is a patented technology invented by Professor Galvin of the University of Newcastle in Australia and subsequently commercialized by FLSmidth (Creamer

Media's Enginering News, 2017). The reflux classifier is a fairly new process unit that focuses on fine particle recovery. The RC comprises the lamella settler, the autogenous dense-medium separation, and the fluidized bed separator (Figure 21). Figure 22 is a schematic view of the RC showing the top section multiple parallel channels that create a laminar-shear separation zone, the flow in this section provides a conveying velocity that is proportional to the particle size thus decreasing the dependence of elutriation velocity on the size of the particle (Galvin & Ivenson, 2014). The channels also generate a hydrodynamic lifting force that lifts low density particles into the overflow (tailings). The particles that are not elutriated sink back into the channels and are given further opportunity to enter the next stage. A suspension of coarse and fine particles of value enter the fluidized bed zone, where large low-density particles are forced back to the overflow and fluidization water deslimes the concentrate (Galvin & Ivenson, 2014). In essence the operating principle consists of three mechanisms, namely, hindered settling, autogenous dense medium and lamella settling.

The RC has been tested on several minerals and coal. An agitated RC was used to determine the possibility of pre-concentrating antimony oxide tailings by Chu et al. (2020). The researchers found that by using an RC on oxidised antimony minerals particle properties (grade and particle size) could be significantly improved for subsequent recovery on a shaking table. The use of the RC on iron ores fines has been well documented as described by Amariei et al. (2014) as well as Rodrigues et al. (2023). Amariei et al. (2014) found that the RC could recover particles between 45 µm and 106 µm from spiral tailings which could otherwise be lost as final tails and in the process achieving a commercial grade iron oxide. Rodrigues et al. (2023) investigated a low-grade fine itabirite iron ore and the RC managed to achieve an iron recovery of 72.9-84.7% and an upgrade of approximately 66% from 37 - 41% in the feed. Campbell et al. (2015) described how coal could be effectively fractionated using a RC. The fractionation of coal becomes important in understanding the washability (or the density distribution) characteristics of the coal as well as to identify mineral content, maceral distribution and calorific value in narrow density ranges.



Figure 21: Reflux Classifier (FLSmidth, 2024)

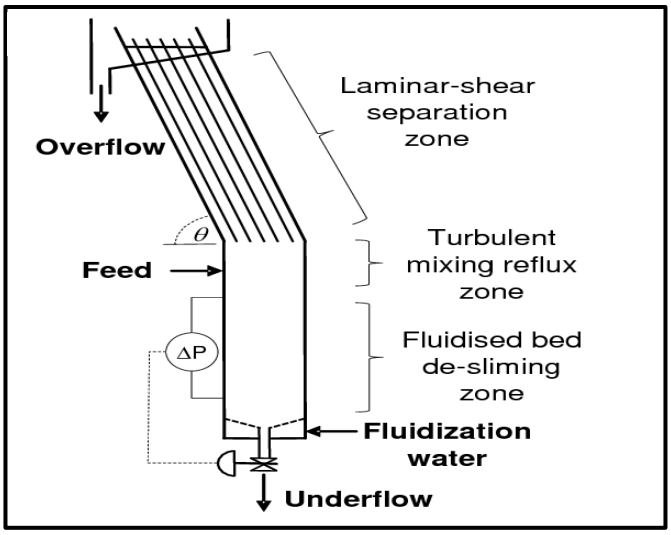

Figure 22: Standard Reflux Classifier Schematic (Galvin & Ivenson, 2014)

2.6.2. Advanced/Enhanced Gravity Separation

Centrifugal gravity concentrators are the most efficient type of advanced gravity separation technologies for processing mineral fines and ultrafines (Rath & Singh, 2007; Farajzadeh & Chelgan, 2022; Das et al., 2023) as well as overcoming challenges associated with surface-based separation processes (Osborne, 1988). Finer particles generally have a lower separation efficiency due to the negligible mass associated with this size fraction (Wills B. A., 1989). Fine particles are the most valuable in most mineral processing operations as they are the most liberated. The vast majority of minerals require grinding to micron size in order to be recovered in subsequent processes (Galvin & Ivenson, 2014). The fine and ultra-fine particles are, however, difficult and expensive to recover and concentrate. Processing ultrafine particles is a unique and complex challenge as the particles have a small mass, high specific surface area and high surface energy per surface area (Sivamohan, 1990). This entails that the natural gravitational force will not be adequate for particles classified as fine and ultrafine. To overcome this hurdle, the gravitational force must be enhanced by way of applying a centrifugal force. The high gravitational force results in differential settling and subsequent separation of particles (Fatahi & Farzanegan, 2017). When G-forces are applied to minerals, marked improvements in capacity and selectivity of fine minerals has been observed (Galvin & Ivenson, 2014). The application of this enhanced centrifugal field has been shown to recover coal particles finer than 44µm (Luttrell et al., 1995), scheelite particles finer than 10µm (Das et al., 2023), gold particles finer than 37µm (Laplante, 1993; Sepro Mineral Systems, 2024) as well as Magnetite and Hematite in the less than 75µm and less than 25µm ranges respectively (El-khalek et al., 2014). The use of gravity separation for ultra-fine liberated particles less than 20µm has also been document by Abela (1997) and Gee & Holtham (2005).

These separators can either be fluidized or unfluidized. A fluidised separator utilises water to fluidise the bed and an unfluidized separator does not use any additional water. The segregation and separation that occurs in a centrifugal gravity separator is primarily due to particle specific gravity (centrifugal force exerted on heavy and light particles) and size (Kroll-Rabotin & Sanders, 2014; Das et al., 2020) as well as separation bed fluidisation when fluidisation water is used (Koppalkar, 2009). The specific advanced gravity concentrator used in this research is the Falcon Gravity Concentrator.

Das et al. (2023) conducted research on the efficacy of a Falcon Concentrator (Lab Unit) for recovery of scheelite from a gold tailings storage facility. The feed material particle size consisted of a d_{50} of 37µm and a d_{80} of 76µm. X-ray Fluorescence (XRF) analysis indicated that most of the tungsten-bearing particles of the feed were finer than 33µm. The study first tested various rotational speeds (30, 50, 70 and 90 Hz) on both a fluidised and ultrafine Falcon bowl and found that the fluidised bowl was capable of producing a higher concentrate grade (higher content of WO_3) but lower mass yield and recovery whereas the ultrafine bowl was capable of achieving higher recoveries and mass yield but at a lower concentrate grade comparatively. These results are depicted in Figure 23. As the rotational speed was increased the ultrafine bowl showed a decrease in mass yield, increase in WO_3 content and an increase in recovery of WO_3 whereas the converse was true for the fluidised bowl. The ultrafine bowl was capable of capturing more of the finer denser particles (in the sub 10µm range) than the fluidised bowl. The reason for this is that the fluidising water washes away fine particles which cannot overcome the drag force and buoyancy force exerted by the fluid in the centrifugal environment, since most of the WO_3 is found in the fines fraction this means that the fluidised bowl is not as effective at recovering WO_3 compared to the ultrafine bowl. Another important parameter for this study was the rejection of calcite. The fluidised bowl performed better than the ultrafine bowl in this regard (see Figure 24).

The fluidized bowl performance is attributed to the effect of the drag force induced by the addition of fluidized water which ensures the concentrate bed is dilated and allows for reordering of the particles within the bed (Das et al., 2023) as well as the release of entrapped calcite which allows for further rejection of calcite (Yann et al., 2019). This phenomenon of rearrangement of particles in the concentrate bed is not possible in the ultrafine bowl hence the lower calcite rejection for those experiments. The authors of this paper conclude by stating that the fluidized bowl is more effective at recovering coarser particles and rejecting calcite whereas the ultrafine bowl is effective at recovering ultrafine particles. An integrated circuit is suggested that utilizes the properties of both bowls, this circuit could recover 85% of the scheelite with a WO_3 grade of 0.28% (Das et al., 2023).

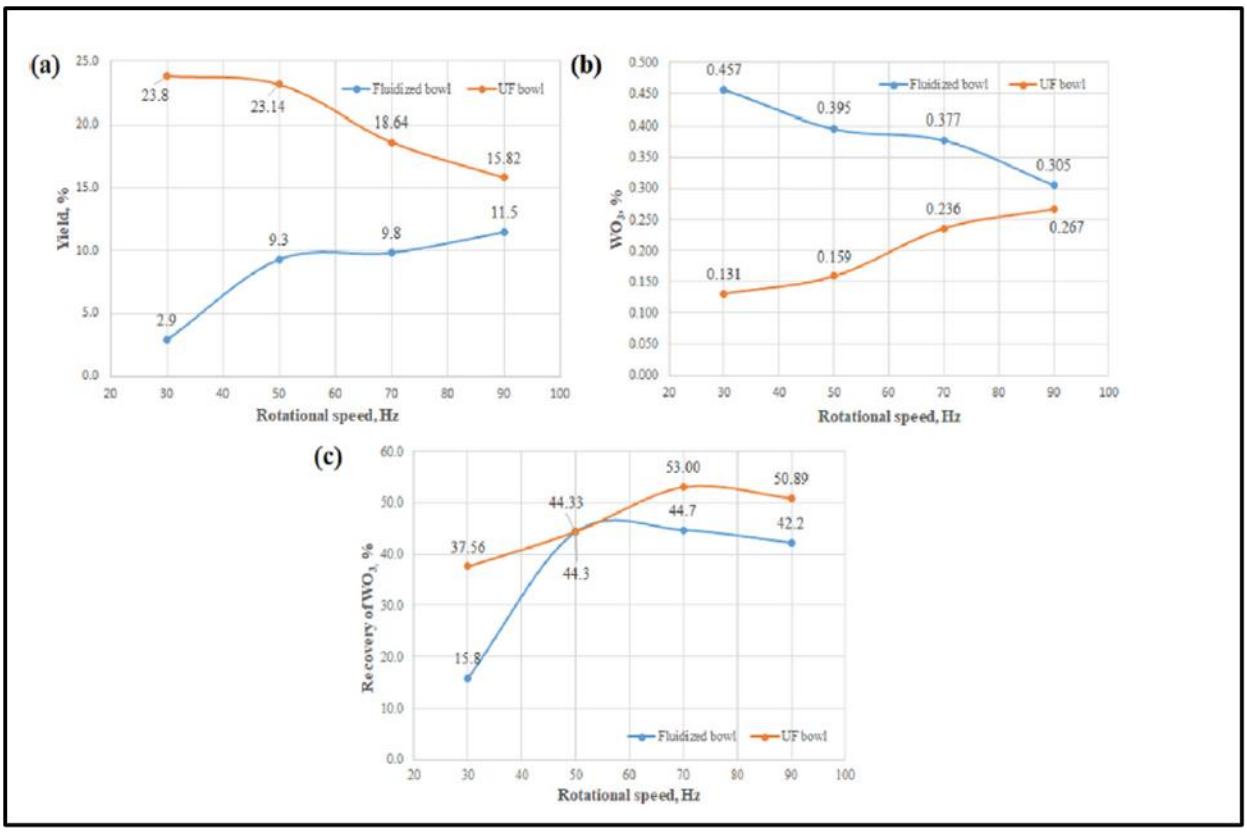

Figure 23:Influence of rotation speed on the fluidized bowl and UF Falcon Bowl on various responses (a) yield, (b) WO_3 content and (c) recovery (Das et al., 2023)

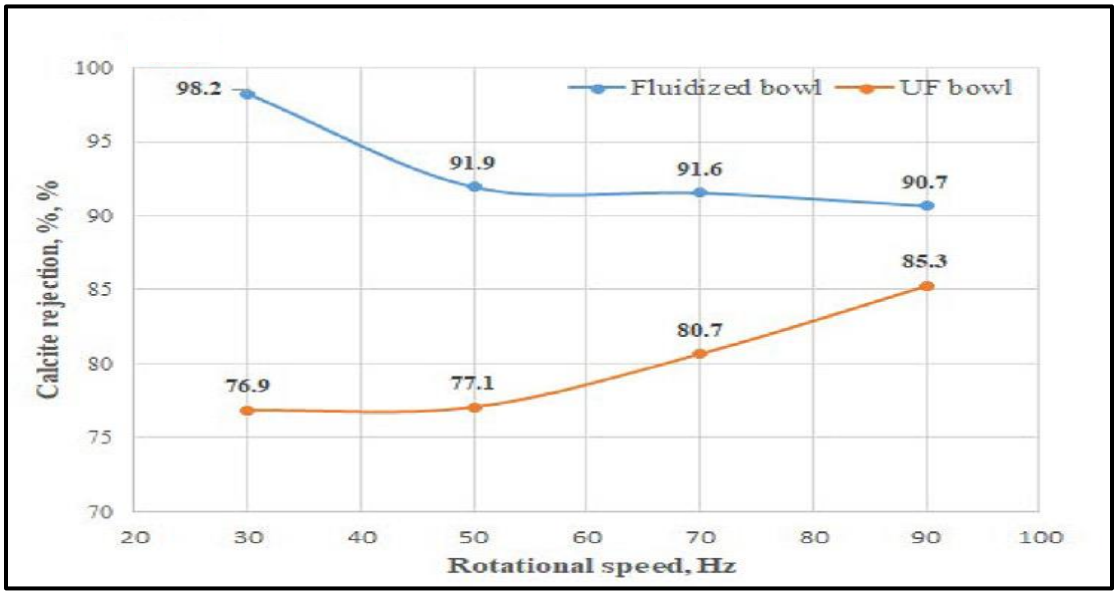

Figure 24: Influence of bowl speed on calcite rejection (Das et al., 2023)

The efficiency of centrifugal gravity separation has also been tested on coal with particle size less than 500µm, more specifically the ability to reduce the ash content and thus increase the quality of the saleable product as described by Peer et al. (2001). The researchers found that high mass recoveries could be obtained and that significant amounts of free mineral matter were rejected by the concentrator. The researchers did, however, also indicate that ash content was still relatively high in the final product and additional tests were recommended.

Grewal & Neale (2017) researched the application of non-fluidised bed gravity concentrators for various high density mineral recovery and their findings are listed below:

- Tantalum: A multi-stage gravity concentration was used for recovery and upgrade of fine tantalum (-100µm) at the TANCO Mine in Manitoba. The concentrators were able to achieve 70-80% recovery from the operations tailings. The gravity concentrator was also applied to the mines flotation concentrate (particle size of 80% less than 75µm) and achieved 80-90% recovery at a mass pull of 30% when the Falcon Gravity Concentrator was operated at 600 G's.
- Tin: The Renison Tin operation in Tasmania uses gravity concentration to recover tin. A multi-stage gravity concentration circuit consisting of gravity roughers and cleaners is used to upgrade tin concentrate from 14% to 28% with a corresponding recovery of 75%. The feed particle size to the Rougher concentrators is 98% passing 25µm.

Centrifugal concentration has also been applied to Rare Earth Minerals for the separation of the high density bastnaesite and monazite from calcite (gangue). This research found that from an initial feed of 6.7% barium, and 3.4% total rare earth elements, the final concentrate achieved after gravity concentration was 13.13% barium, and 7.8% rare earth elements (lanthanum, cerium, praseodymium, samarium, and neodymium) (Schriner & Anderson, 2015). This proved that gravity separation could be applied to rare earth minerals effectively to achieve better results than flotation of the minerals.

Gold concentration has been the 'flagship' for gravity concentration for many years. The ease of gravity concentration for most gold deposits comes down to the mineralogy of gold ore. Gold is much denser than its associated gangue in most ores and is also a 'free milling' ore. Free milling

gold ores can be defined as ores with a particle size distribution containing 80% less than 75µm particles from which direct cyanidation can extract at least 90% of the gold without excessive reagent consumption (Marsden, 2006; Zhou, 2004). Free milling gold ores are generally paleo-placers and quartz vein gold ores. This ore can be easily recovered via gravity concentration also termed GRG or Gravity Recoverable Gold. Both the Falcon and Knelson gravity concentrators have been successfully applied to gold recovery by using high G-force to recover coarse and fine gold attached to milling circuits. The performance of gravity concentrators as well as their low cost of installation and operation have made this equipment a viable option for the gold industry (Guerney et al., 2003; Grayson, 2007; Farajzadeh & Chelgan, 2022). The recoveries achieved by gravity concentration have been rather staggering: Alp et al. (2008) reported 81% recoverable gold at a grade of 262 g/t and a mass yield of 7.2% for a Iranian gold deposit; Sepro Mineral Systems (2024) reported a recovery of 77% on the gravity circuit installed and an overall plant recovery increase of 4% at Mazokwe mine in Zimbabwe; The GoldFields South Depp mine recovers approximately 15% of its total gold output from gravity concentration with recoveries exceeding 70% for the circuit (GoldFields, 2024).

2.7. The Falcon Gravity Concentrator

The Falcon gravity concentrator has a two types of bowls for recovering fine and ultrafine minerals, namely, the fluidized bowl (also called a continuous bowl) which is designed to allow fluidizing water to enter with the feed slurry and an unfluidized bowl also known as an ultrafine (UF) bowl (Sepro Systems, 2018). These bowls are designed to concentrate minerals of interest depending on whether water addition to fluidize the bed is required or not. The Falcon Semi-Batch (SB) concentrator is used for free-milling, usually non-complex ores (such as gold and silver). The SB type concentrators work by continuously accepting feed material while on the run cycle, but only produce concentrate during a pre-determined rinse cycle (Sepro Mineral Systems, 2024). The SB concentrator is not specified for processing fine and ultrafine minerals.

The Falcon UF bowl operates by receiving a feed stream into the central bowl where the feed slurry is distributed evenly. The feed slurry behaves like a flowing film allowing the segregation and separation of particles (Das et al., 2023). The heavier particles form a bed along the surface of the rotating bowl whereas the lighter particles remain at the periphery of the bowl wall and

flow out with the tailings (Singh et al., 2019; Foucaud et al., 2019). The fluidized bowl utilizes water to create a fluid drag force on the particles coupled with the buoyancy of the flowing film, this acts in opposition to the centrifugal force (Das et al., 2023). The interaction of these forces on the particles leads to heavier particles with higher centrifugal force being able to overcome the combined drag and buoyancy forces and gets collected as concentrate while the lighter particles succumb to the combined drag and buoyancy forces and report to the tailings of the bowl.

The main draw-back on the fluidized bowls is that when the feed material is classified as fine to ultra-fine particles, the force exerted by the flowing water also entrains and removes valuable particles and these end up in the tailings stream of the gravity concentrator. The un-fluidized bowl, however, can recover these particles more effectively and attain a high mass yield and concentrate grade (Grewal & Neale, 2017).

Figure 25 and Figure 26 depicts the plant scale schematic diagrams of the Falcon UF and Fluidized concentrators respectively. The main differences between the two units are the addition of fluidization water on the fluidized concentrator as well as the grooved design of the fluidized bowl which assists in retaining coarser particles.

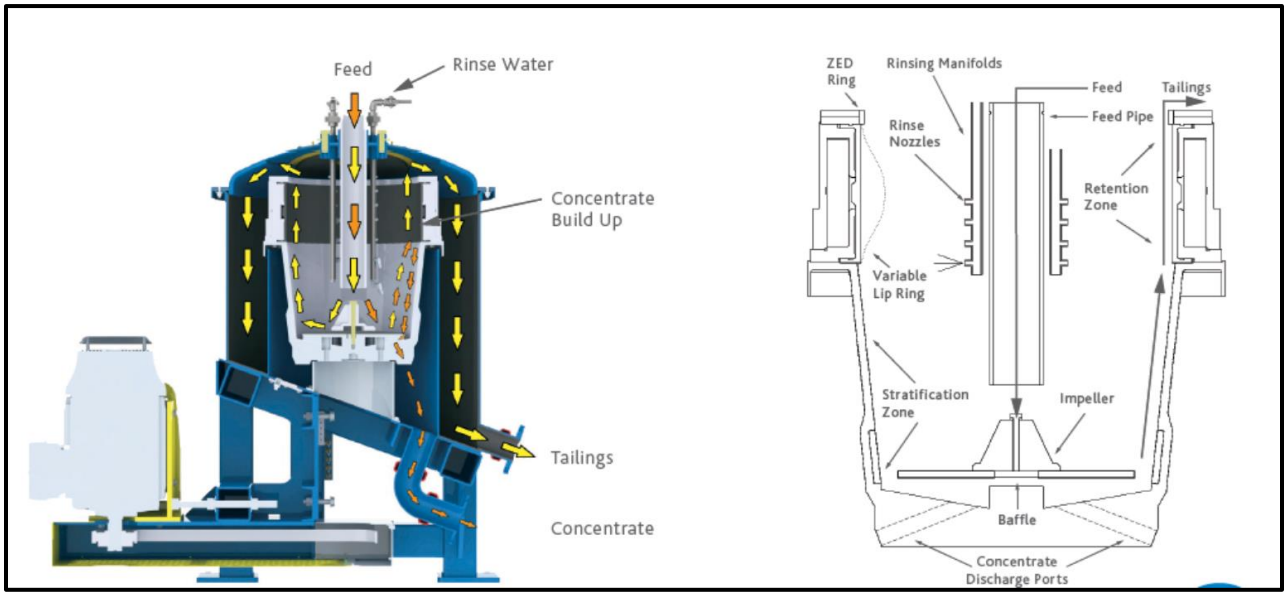

Figure 25: Falcon Ultrafine (UF) Concentrator (Sepro Mineral Systems, 2024)

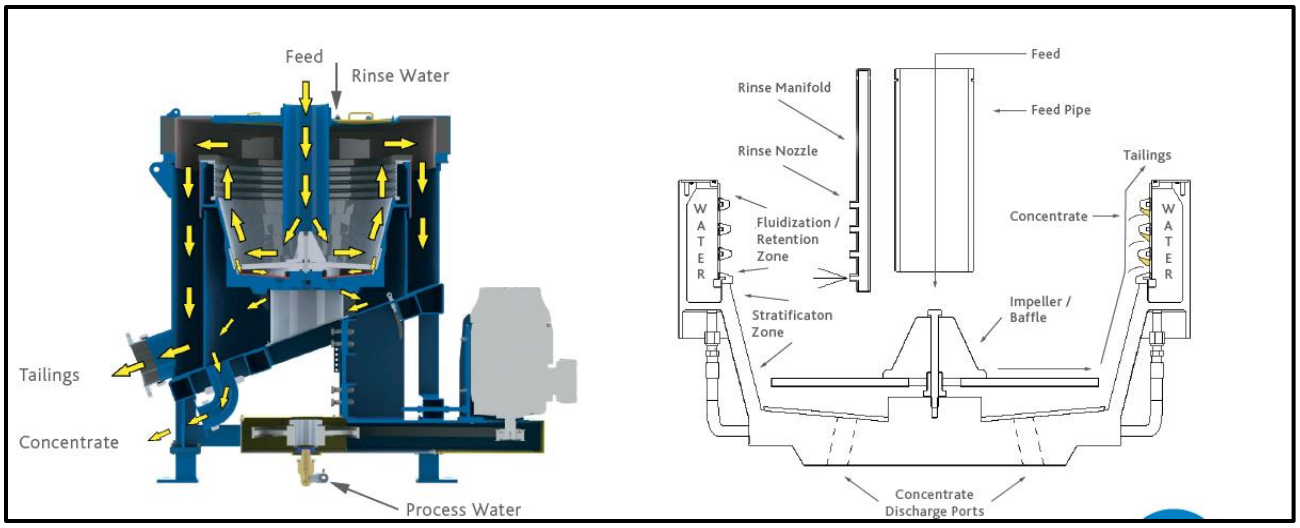

Figure 26: Falcon Fluidized Concentrator (Sepro Mineral Systems, 2024)

The Falcon concentrator can be set up in a circuit consisting of gravity concentrators that behave as roughers and those that behave as cleaners to maximize recovery and grade. Figure 27 indicates a typical circuit which includes roughers, cleaners and scavengers. The recycle stream increases the probability of additional valuable material reporting to the final product. This can move the overall grade-recovery curve of the circuit to a more optimal point (Grewal & Neale, 2017).

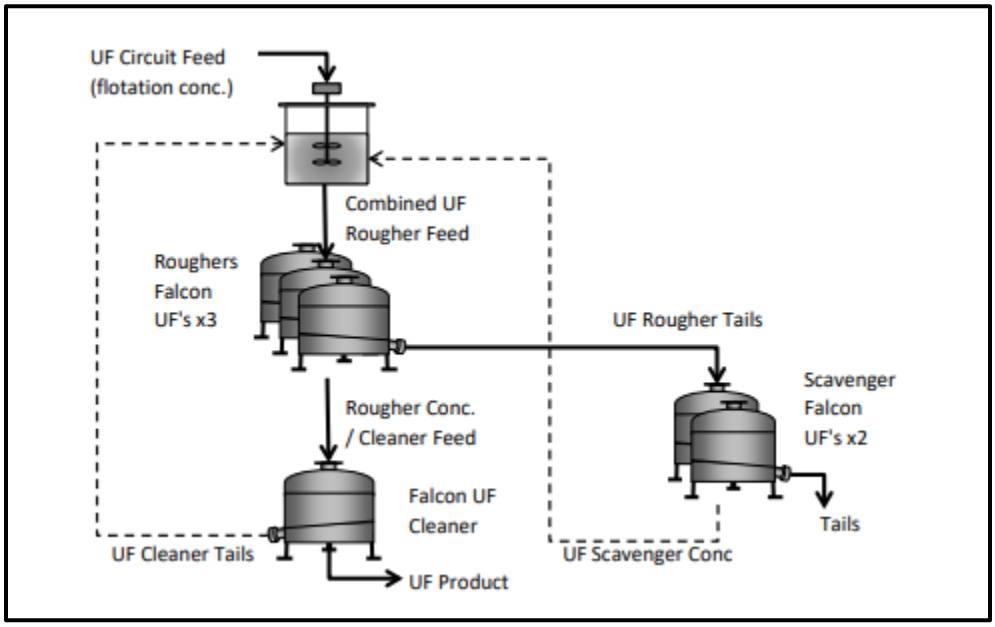

Figure 27: Falcon Gravity Concentrator circuit with roughers and cleaners (Grewal & Neale, 2017)

The Falcon UF overcomes the limitations posed by gravity concentration of fine and ultra-fine particles as well as limitations related to the other gravity concentration techniques mentioned previously. The Falcon is able to recover fine and ultra-fine complex minerals with high mass yield and high concentrate grades that are not possible with other technologies in the gravity concentration category.

2.8. Gravity Concentration Applied to PGMs

PGM associations with other minerals are diverse and include sulphides, oxides, silicates, sulpharsenides, arsenides and tellurides. The three main sulphide minerals associated with PGMs are pentlandite, chalcopyrite and pyrrhotite (Xiao et al., 2009). Pentlandite and chalcopyrite can be readily recovered, as they are associated (as blebs or in solid solution) with platinum group elements whereas PGEs present in pyrrhotite may be more difficult to recover by gravity concentration (Xiao et al., 2009).

Gravity concentration of PGMs faces a number of challenges, namely:

- The complex mineralogy of PGMs
- Low grade of feed material
- Fine and ultra-fine particle size distribution
- There is also no set method to determine whether a gravity concentrator is necessary or what the possible value-add of such a unit may be
- High mass pulls are required to achieve acceptable recoveries
- Granularity of feed
- Presence of Chromite
- From a business perspective, the capital and operational costs must not exceed the market price of PGMs recovered

Gravity Recoverable PGMs (GRPGM) is analogous to the term Gravity Recoverable Gold (GRG). Gravity recoverable PGM can include PGMs which are completely liberated and those locked in high density particles (Xiao et al., 2009). GRPGM prediction is based on 3 foundational components, namely, ore characteristics, behaviour in grinding and classification circuits and recovery unit performance (Xiao et al., 2009). Engelbrecht (2012) and Farajzadeh & Chelgan (2022) postulated the use of gravity concentration for PGMs based on the technology's

success with other minerals as long as the feed to the unit is dilute to ensure effective particle separation and only if coarse particles can be removed first to avoid affecting concentrate grade. A handful of authors have conducted extensive research on various aspects of GRPGM and found improved recoveries and grades, but these results were dependant on the complexity of the ore, feed density to the concentrator, particle size distribution and number of gravity stages to name a few (Huang & Mejiab, 2002; Jena et al., 2017; Chen, et al., 2020).

An interesting point to make is that UG-2 ore plants are commonly attached to chrome spiral plant for removal of chrome as a by-product, these spirals can be placed between primary and secondary milling or at the tail end of the plant. These spirals recover chrome with very minimal PGM recovery, the question would be why PGMs which are heavier do not report with the Chrome concentrate but rather report as a tail with the silica. An insight into this observation lies in the fact that the chrome is essentially free milling (high degree of liberation) and coarse while the PGMs are locked in a base metal sulphide matrix and are contained in much finer particle size and hosted in largely a lighter silica matrix (Holland-Batt et al., 1982; Osbahr et al., 2013; Sinisalo & Lundström, 2018).

Perroton et al. (2020) showed the importance of understanding particle density and particle size when making use of gravity concentration. Density separation can increase the concentrations of economic elements and hence the quality of the final concentrate. By understanding what size fractions various minerals are present in, one can make deductions on how effective gravity concentration will be for particular minerals.

The effectiveness of conventional gravity concentrators decreases as the particle size gets smaller this is due to the decreasing effect of gravity (Miettinen et al., 2010). It is for this reason that advanced gravity separation is postulated to have a better PGM recovery response as the high gravitational force will assist in retaining fine and ultrafine heavy particles.

Gravity concentration is one of the most economical and efficient methods to upgrade a mineral and improve recovery relative to other routes like hydrometallurgical routes (Loveday & Forbes, 1982). This technology, however, is not a ‘silver bullet’ and must be used in conjunction with

other processes. The gravity concentration adds to efficiency but will not be completely economical on its own for large volumes of feed.

2.9. A Theoretical Framework for Gravity Concentration of PGMs

The rationale for using advanced/enhanced gravity concentration to upgrade PGM concentrates stems from the hypothesis that gravity concentration with a Falcon concentrator is able to overcome the myriad challenges mentioned in the preceding sections.

The first crucial factor to consider is the composition of the feed to the gravity concentrator and secondly the density differences between PGMs and the associated gangue material.

Table 8 indicates the composition of the feed material which is a concentrate from a PGM tailings re-treatment operation in the Marikana area. The total 4E PGM is 131.02 g/t with 1.97% Chromium. The largest portion of the gangue in the sample is SiO_2 at 53.92% followed by MgO at 24.07%.

Table 8: Gravity Concentrator Feed

Element/Mineral	Unit	Concentration
Pt_Ave	g/T	80.35
Pd_Ave	g/T	34.99
Au_Ave	g/T	0.71
Rh_Ave	g/T	14.97
Ru_Ave	g/T	25.76
Ir_Ave	g/T	6.19
SUM 4E	g/T	131.02
SUM 6E	g/T	162.97
Cu_Ave	%	0.22
Ni_Ave	%	0.43
Fe_Ave	%	7.20
FeO_Ave	%	9.26
CO_Ave	%	0.02
Sulphur_Ave	%	0.78
Cr2O3_Ave	%	1.97
SiO_2_Ave	%	53.92
MgO_Ave	%	24.07
CaO_Ave	%	3.24
AlO_Ave	%	4.98

Based on the data in Table 8, it is evident that for concentration criteria calculations only the SiO_2 and MgO need to be considered as gangue due to their significant concentration in the sample. Chrome will also be considered as it is a deleterious material and has the highest density of all the gauge constituents. The individual PGE's will be considered for the calculation as well as the 3 platinum group minerals with the highest and lowest densities from Table 7. Although individual PGE's can give a good indication of possible separation with the gangue material, as previously mentioned, the complex mineralogy of PGMs means that most of the PGE's are locked in a BMS complex hence the need to consider the platinum group minerals. Only a few are chosen for comparison purposes in Table 9.

Table 9: Concentration criteria (CC) of PGMs

Description	Element/Mineral	Density (g/cm^3)	CC [PGM/SiO_2]	CC [PGM/MgO]	CC [PGM/Cr]
Platinum Group Metals	Pt	21.4	12.4	7.9	3.3
	Pd	11.99	6.7	4.3	1.8
	Rh	12.4	6.9	4.4	1.9
	Ru	12.41	6.9	4.4	1.9
	Ir	22.5	13.0	8.3	3.5
	Os	22.57	13.1	8.4	3.5
	Au	19.3	11.1	7.1	3.0
Platinum Group Minerals	Pt_3Fe	18.23	10.4	6.7	2.8
	PtFe	15.81	9.0	5.7	2.4
	$PtBi_2$	12.86	7.2	4.6	1.9
	Pd_3SbTe	8.25	4.4	2.8	1.2
	PdS	6.74	3.5	2.2	0.9
	RuS_2	6.39	3.3	2.1	0.9
Gangue	SiO_2	2.65	-	-	-
	Cr	7.15	-	-	-
	MgO	3.58	-	-	-
	CaO	3.34	-	-	-
	Al_2O_3	3.99	-	-	-
	$Mg_3Si_4O_{10}(OH)_2$	2.75	-	-	-

A general rule for effective separation below 75µm (fine and ultra-fine particles) is that the concentration criterion should be above 2.5. It is evident from Table 9 that the individual PGMs and the mineral complexes are able to be separated from the SiO_2 and MgO, although some less dense PGM minerals such as PdS and RuS_2 may have more difficulty in reporting to the concentrate. Chrome may report to both the concentrate and the tails of the Falcon concentrator as the concentration criterion is below 2.5 for certain minerals. This also means that chromite does not accumulate in the final concentrate of gravity separation.

At the back of previous studies, the concentration criterion analysis above as well as practical experience and ingenuity, the scope of this specific study will involve utilizing a lab scale falcon concentrator at high gravitational force to recover PGMs from a flotation concentrate. The first part of the study aims to determine the optimal parameters for the gravity concentrator (flowrate, G-force and density). The second part will focus on repeating the optimal parameters multiple times to obtain repeatability of results. Grade-Recovery and Mass Pull -Recovery relationships for the process will be established. The third part will aim to understand the fractional analysis and particle size distribution of the feed, concentrate and tails. This will give an understanding of the minerals and particle size recovered and rejected from the process. This study is unique in the sense that no reported studies have rigorously analysed the gravity concentration response of a South African PGM ore before. If it is proved that gravity concentration can effectively upgrade a PGM concentrate this study will greatly benefit PGM concentrators as more flexibility in the flotation circuit can be realized and this essentially increases recovery and grade of the precious metals.

3. Methodology

3.1. Sample Preparation

The sample for the test work was collected over 3-4 months and a composite was made. The sample was collected from the final concentrate stream of a PGM tailings processing plant that treats a UG2 tailings material. The concentrate stream is a continuous production stream from which representative samples were taken using a cross-cut sampler that is available on the stream. The slurry samples were collected in 20 L buckets daily and then filter pressed and dried. A total sample mass of 471.22kg was collected (Figure 28) and homogenized on a tarp (Figure 29). A rotary splitter was then used to obtain representative aliquot samples which were 5kg each for the test work (Figure 30) as per the operational procedure of the Falcon Concentrator.



Figure 28: Bulk sample



Figure 29: Homogenized sample



Figure 30: Rotary splitter

3.2. Experimental Setup

The experimental set-up consists of (i) the Falcon Gravity Concentrator provided by Sepro Systems. The Falcon Gravity Concentrator has a VFD Drive Inverter to adjust the G-force (centrifugal force) of the unit; (ii) A Watson-Marlow pump that is used to feed the Falcon to ensure continuous feed and at the correct density for each experimental run. The Watson-Marlow pump can pump a minimum of 3L/min and a maximum of 15L/min; (iii) The feed tank from

which the sample is pumped and is stirred continuously to prevent particles from settling and to ensure consistent density of the slurry. See Figure 31.

The experimental sample was prepared by first filling the feed tank with water to the required level and then adding the homogenized dry solids sample. The density was checked with a manual handheld density scale to ensure the density was correct for each test.

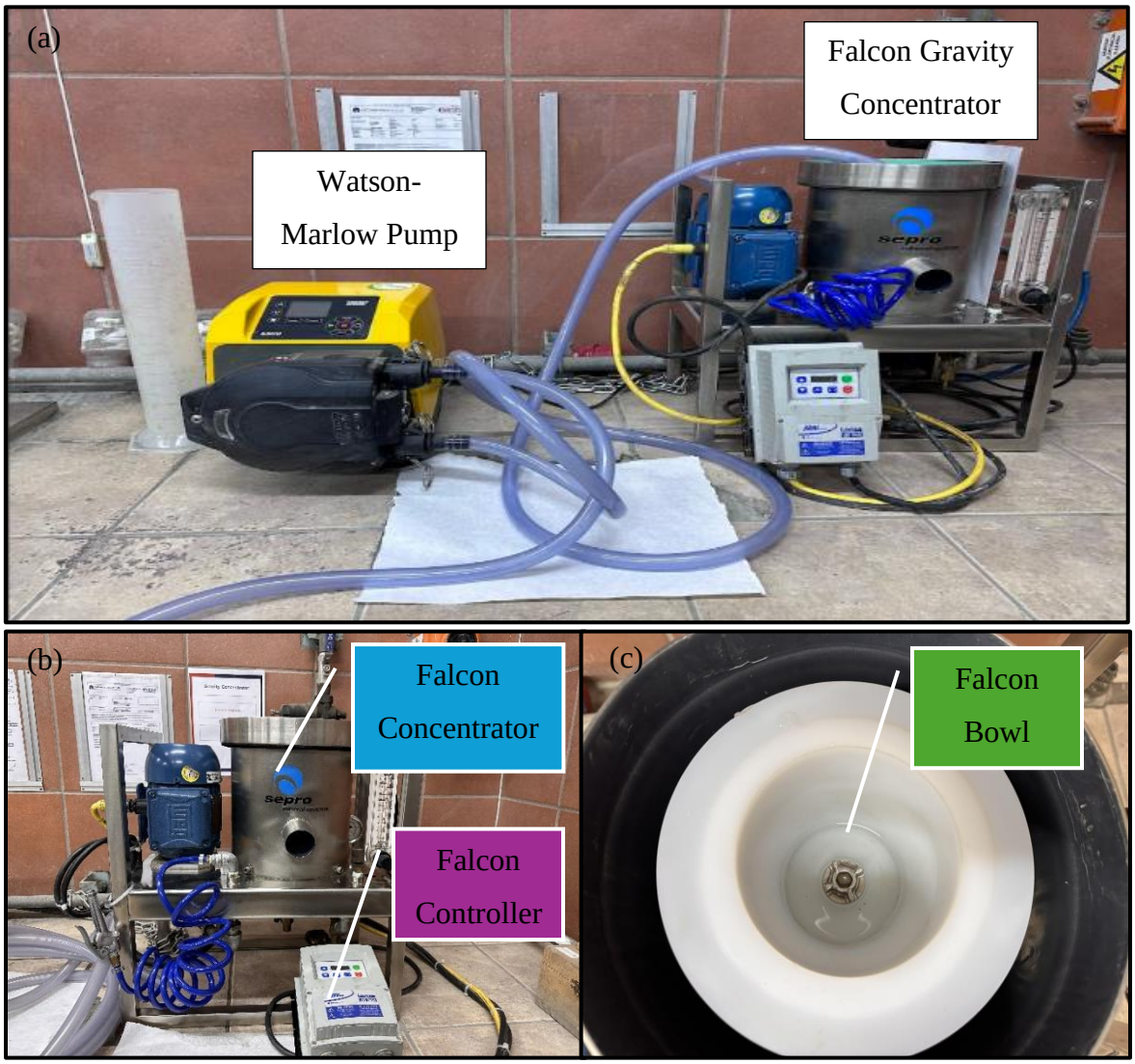

Figure 31: Experimental equipment showing (a) Falcon concentrator experimental equipment and feed pump, (b) Close up of Falcon Concentrator showing the controller for the g-force (frequency inverter) and (c) The Bowl fitted inside the Falcon

3.3. Feed Analysis

The feed sample was sent for 6E analysis as well as Chrome, Silica and Base Metals analysis. 6E refers to Platinum, Palladium, Gold, Rhodium, Ruthenium and Iridium which are the main precious metals of economic value. This analysis ensured that the individual mineral grades are accounted for in the feed sample and that the complete grade can be determined.

The feed sample was also subjected to Particle Size Distribution analysis so that particle size in the feed sample was understood from which different size classes/fractions were generated. Each size fraction was assayed for 6E, base metals, chrome and various gangue constituents. This analysis assisted in understanding which minerals and in what quantity are in different particle sizes. The PSD analysis was done at the mining operations laboratory.

Finally, XRF, XRD and SEM qualitative analysis were be carried out at Wits University.

3.4. Experimental Work

The experimental work was conducted in 7 phases. Each experimental subset was done in triplicates to ensure accuracy and consistency in results obtained. The feed SG was measured using a handheld density scale.

3.4.1. Phase 1 – baseline tests

Phase 1 was a baseline test and involved one stage gravity concentration. The concentrate and tails produced from the experiment were sent for 6E analysis as well as Chrome, Silica and Base Metals. Table 10 shows the experimental parameters used in Phase 1 of the test-work.

Table 10: Phase 1 Parameters

TEST NAME	SG	% Solids	Feed Solids Mass	RPM/G-force
Gravity Concentration - Run 1A_13.22%	1.10	13.22	5	78.3Hz/300G
Gravity Concentration - Run 1B_13.22%	1.10	13.22	5	78.3Hz/300G
Gravity Concentration - Run 1C_13.22%	1.10	13.22	5	78.3Hz/300G

3.4.2. Phase 2 – variable % solids

Phase 2 involved gravity concentration tests conducted at different % solids or density of the feed to determine the optimal density for gravity concentration. The water was added as per % solids calculation and a manual density scale used to verify that the desired density was attained. The minimum % solids of 13.22% was set as a baseline as this is the minimum practical concentrate density achieved on a typical PGM flotation concentrator. The concentrate and tails produced from the experiment were sent for 6E analysis as well as Chrome, Silica and Base Metals. Table 11 shows the experimental parameters used in Phase 2 of the test-work.

Table 11: Phase 2 Parameters

TEST NAME	SG	% Solids	Feed Solids Mass	RPM/G-force
Gravity Concentration - Run 1A_15%	1.10	13.22	5	78.3Hz/300G
Gravity Concentration - Run 1B_15%	1.10	13.22	5	78.3Hz/300G
Gravity Concentration - Run 1C_15%	1.10	13.22	5	78.3Hz/300G
Gravity Concentration - Run 2A_20%	1.17	21.12	5	78.3Hz/300G
Gravity Concentration - Run 2B_20%	1.17	21.12	5	78.3Hz/300G
Gravity Concentration - Run 2C_20%	1.17	21.12		78.3Hz/300G
Gravity Concentration - Run 3A_25%	1.22	26.40	5	78.3Hz/300G
Gravity Concentration - Run 3B_25%	1.22	26.40	5	78.3Hz/300G
Gravity Concentration - Run 3C_25%	1.22	26.40	5	78.3Hz/300G
Gravity Concentration - Run 4A_39,35%	1.40	41.56	5	78.3Hz/300G
Gravity Concentration - Run 4B_39,35%	1.40	41.56	5	78.3Hz/300G
Gravity Concentration - Run 4C_39,35%	1.40	41.56	5	78.3Hz/300G
Gravity Concentration - Run 5A_51,65%	1.60	54.55	5	78.3Hz/300G
Gravity Concentration - Run 5B_51,65%	1.60	54.55	5	78.3Hz/300G
Gravity Concentration - Run 5C_51,65%	1.60	54.55	5	78.3Hz/300G

3.4.3. Phase 3 – variable G-force

Phase 3 involved varying the G-force of the gravity concentrator. G-forces of 100, 200, 250 and 300 G were tested. The maximum G-force that this Falcon unit is capable of operating at is 300 G's. The concentrate and tails produced from the experiment under these conditions were sent for 6E analysis as well as Chrome, Silica and Base Metals.

3.4.4. Phase 4 – variable flow rate

Phase 4 involved varying the feed flow rate to the gravity concentrator to determine the optimal flow-rate. The feed rates used were 3L/min, 5l/min and 10 L/min. The maximum flow that the gravity concentrator can handle was 10L/min. At feed rates in excess of this design capacity, the

slurry overflows in the bowl. The concentrate and tails produced from the experiment under these conditions were sent for 6E analysis as well as Chrome, Silica and Base Metals.

3.4.5. Phase 5 – multi-stage concentration

Phase 1-4 were used to determine the optimal % solids, G-force and feed flow-rate parameters for the subsequent runs. Phase 5 involved multi-stage gravity concentration tests used to determine the total upgradeability of the concentrate and the total recovery as well as the mass pull. Multi-stage gravity concentration involved taking the same sample through a number of stages of gravity concentration to determine the experimental stages required for desired recovery and grade of the concentrate. A total of 5 concentrates were produced and weighed per run. A final tail was also produced and weighed. The concentrate and tails produced from this experiment were sent for 6E analysis as well as Chrome, Silica and Base Metals. The purpose of taking the feed through the concentrator 5 times was to get realistic data on the capability of the Falcon as the 5 stages are equivalent to a single plant scale unit which is a rule of thumb according to Sepro Minerals. The 5 stages lab scale tests also allow for sufficient data collection (and sample mass) per experimental run. The optimal parameters gravity concentration experiments are repeated ten times in order to ensure repeatability of results and ensure a robust data set. The assay results were subjected to a statistical outlier test in the Minitab Software to ensure data integrity. The repetition of experiments and statistical analysis performed are used to validate the results of these experiments.

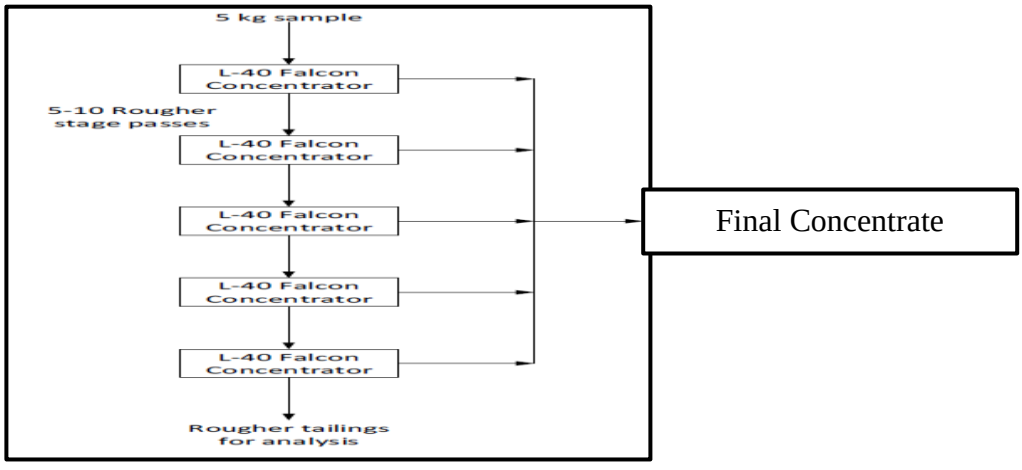

Figure 32: Multistage Gravity Concentration

3.4.6. Phase 6 – PSA and Qualitative tests

Phase 6 involved the same multi-stage gravity concentration test as those in Phase 5. The purpose of Phase 6 runs was to collect enough samples to do particle size analysis work as well as analytical tests performed at Wits University. The experimental gravity concentrator produces a small amount of concentrate at a time hence the need for this phase to ensure sufficient sample was generated for other critical analysis. Phase 5 only produced enough sample for overall 6E analysis whereas Phase 6 must produce enough sample for particle size analysis (approximately 500 grams per size fraction). Each size fraction was assayed for 6E, base metals, chrome and gangue constituents. This analysis assisted in understanding which minerals are found in different particle sizes. During the sieving process there is a possibility of mass loss, each sample was subjected to a stringent rule of not more than 1% mass loss in the wet and dry sieving process.

Finally, various confirmatory and exploratory tests were carried out at Wits University which included XRF, XRD and SEM to understand the mineralogy of the PGM concentrate.

3.4.7. Phase 7 – fluidized bowl tests

Phase 7 involved using a fluidized bowl to investigate the effects of a fluidized bed of water on the PGM concentrate. The fluidized bowl has riffles and ports along the circumference of the bowl to allow fluidizing water to enter the bowl whereas the ultra-fine (unfluidized bowl) does not. The fluidized bowl utilizes water to create a fluid drag force on the particles coupled with the buoyancy of the flowing film. This leads to heavier particles (in the gravity field) being able to overcome the combined drag and buoyancy forces and gets collected as concentrate while the lighter particles succumb to the combined drag and buoyancy forces and report to the tailings of the bowl. The optimised parameters from Phase 5 will be used.

Ultimately these tests were meant to prove or disprove that gravity separation can increase the grade of a PGM concentrate by rejecting gangue and increasing PGM content of the concentrate. The tests were meant to also prove or disprove whether rejection of chrome from the concentrate is possible and if economically viable recovery is possible and what particle sizes and associated minerals are recoverable.



Figure 33: Falcon gravity concentrator bowls showing the fluidized bowl (left) and unfluidized bowl (right)

4. Results and Discussion

4.1. Introduction

The Results and Discussion Section will expound on the experimental protocols that were followed in order to test the hypotheses that was put forward for advanced gravity concentration on PGM flotation concentrations. It is important to note that no previous studies exist in literature on advanced gravity concentration of PGM flotation concentrations and the literature explored in the studies was based on other minerals which were subjected to gravity concentration. The equipment supplier provided some advice which was useful in the development of an experimental framework to answer the critical research questions posed herein.

The samples were subjected to Fire Assay with Nickel-sulphide fusion/collection followed by ICP-MS. This method yields the most reliable results for PGE at low detection limits because these metals are quantitatively extracted into the nickel button. This method is also able to accurately quantify each PGE and associated metals and minerals without losses. Another method that is sometimes used is the lead collection method but this method, although faster than the Nickel-sulphide fusion, can only determine a total PGM content, which is taken as a summation of platinum, palladium rhodium and gold. The lead collection method suffers from losses in iridium, ruthenium and osmium during cupellation as well as losses in platinum, palladium, rhodium and gold as the metals are not collected quantitively (Matsau, 2003). The lead collection method is used if fast results are needed to make general inferences. The Nickel-sulphide fusion is used for a complete and accurate description of a PGM sample's contents hence this method was used for all samples requiring Fire Assay in this research.

This section will consist of the results of Phase 1-5 and Phase 7 as described in the methodology section. Phase 1-4 were tests conducted to determine the optimal parameters to run the Falcon gravity concentrator. Phase 5 tests applied the optimal parameters and repeated them to ensure repeatability of results. The Grade/Recovery curve will be described for the optimal parameters. The rejection of chrome and behaviour of the gangue will also be discussed in detail. The particle size analysis and fractional analysis will be discussed as per Phase 6. Phase 7 tests

applied the optimal parameters to the fluidized bowl. Finally, this section is concluded with findings from the XRF, XRD and SEM analysis.

4.2. Gravity Concentrator Feed Analysis

The chemical analysis results of the feed sample are shown in Table 12. The 6 PGE's are listed with their respective values in g/t. The 4E is the summation of the first 4 main PGE's (platinum, palladium, gold and rhodium). The 6E summation includes ruthenium and iridium. The various gangue materials, base metals, sulphur and chrome content are also listed. A total of 12 samples were sent from the homogenized and representative bulk sample which was split into smaller samples. The average results of the 12 samples were then used to obtain the feed content in Table 12.

Table 12: Gravity concentrator feed analysis

PGE/Mineral	Unit	Value
Pt_Ave	**g/T**	80.353
Pd_Ave	**g/T**	34.989
Au_Ave	**g/T**	0.708
Rh_Ave	**g/T**	14.971
Ru_Ave	**g/T**	25.757
Ir_Ave	**g/T**	6.192
SUM 4E	**g/T**	131.021
SUM 6E	**g/T**	162.971
Cu_Ave	**%**	0.222
Ni_Ave	**%**	0.432
Fe_Ave	**%**	7.200
FeO_Ave	**%**	9.262
Co_Ave	**%**	0.022
Sulphur_Ave	**%**	0.777
Cr_2O_3_Ave	**%**	1.966
SiO_2_Ave	**%**	53.923
MgO_Ave	**%**	24.066
CaO_Ave	**%**	3.235
Al_2O_3_Ave	**%**	4.977

The total 4E grade is 131.021 g/t. This is the value commonly used in industry to describe the PGM content for commercial purposes as it gives an indication of the content of PGMs for the top 4 constituents. The copper and nickel are 0.222% and 0.432% respectively. The sulphur content is 0.777%. Silicon dioxide is 53.923% and Magnesium oxide is 24.066% in the sample. The chrome content is 1.966%.

4.3. Falcon Parameter Determination Experiments

4.3.1. Phase 1: Recommended Parameters

Phase 1 was a baseline run using the Falcon suppliers' recommended settings. The parameters used were a flow rate of 3 L/min, gravitational force of 300 (78.3 Hz) and a density of 1.1 (13.22% solids). The tests were repeated 3 times to validate the data and weighted average values were used for calculations. In these experiments to investigate optimal parameters, only one stage gravity concentration was conducted (the same for Phase 3-4). Figure 34 shows the schematic diagram of the process. The feed material is fed to the Falcon unit using a pump as described in the methodology section, as the material enters the unit the dense particles settle in the concentrate bowl and the light fraction exits the unit as tailings.

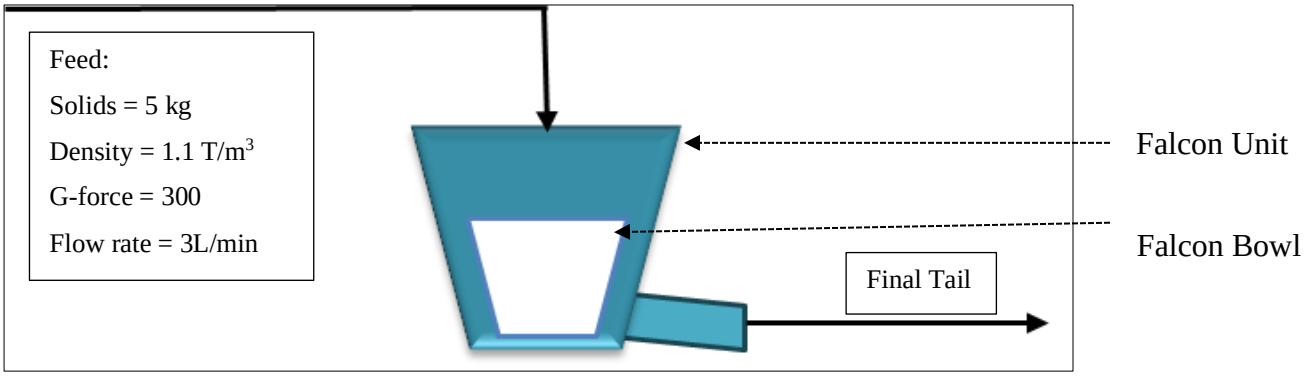

Figure 34: One stage gravity concentration

The baseline run results are incorporated into Phase 2-4 as data points for analysis.

4.3.2. Phase 2: Change in % Solids

The percentage solids or slurry density plays a role in how much solid particles enter the gravity concentrator at a point in time, the denser the slurry the greater the resultant solids into the gravity concentrator per unit time. The following % solids were used: 13.22%, 21.12%, 26.40%, 41.56% and 54.55% respectively. The minimum % solids of 13.22% was set as a baseline as this is the minimum practical concentrate density achieved on a typical PGM flotation concentrator.

Figure 35 (a) indicates the mass yield for each run. The data shows an increase in mass yield as the % solids increase. At 13.22% solids the mass yield is 4.8% whereas at 54.55% solids the mass yield is 8.3%. The increase in mass yield is due to the increased solids that is able to enter the Falcon gravity concentrator at a point in time. The higher density slurry allows more solids to form a bed as there is comparatively less water present to carry the solids away from the concentrate bowl.

Figure 35 (b) and (c) indicates that the recovery and grade decreases as the % solids increases. The base run of 13.22% solids indicated that the recovery is 17.7% and the concentrate grade is 488.07 g/t 4E. The highest % solids of 54.55% indicated that the recovery is 12.3% and the concentrate grade is 193.57 g/t 4E. This indicates that higher densities have a negative impact on recovery and concentrate grade as a result of the loss of selectivity in the concentrate bed. As the % solids increases, the gravity concentrator becomes unselective as lighter gangue particles (which would otherwise have reported to the tailings stream) become entrapped in the bed and possibly displace previously deposited PGM particles as well.

The enrichment ratio (Figure 35 (d)) is the ratio of the concentrate grade to the feed grade and is a parameter that determines efficiency of the gravity concentration for upgrading the feed material. The % solids of 13.22% has the highest enrichment ratio of 3.73 which means that this is the most effective % solids for upgrading the feed. There is a steep decline in the enrichment ratio as the % solids increases due to the loss in selectivity.

Figure 35 (e) indicates that the chrome content in the concentrate increases as the % solids increase. This is due to the entrapment of chrome particles in the concentrate bed as the amount

of solids entering the bowl increases and the volume of water in the slurry decreases, which would otherwise carry the chrome out of the concentrator to the tails.

The main gangue constituents which are silicon dioxide and magnesium oxide, had a similar concentration both in the feed and concentrates. Silicon dioxide was between 52.97% to 54.16% and magnesium oxide was between 23.78% to 25.67% in the Falcon concentrate. This indicates that due to the high mass concentrations of these gangue particles they also enter the concentrate bed at the same concentration as the feed.

The results for Phase 2 converge on a % solids of **13.22%** (SG of 1.10) as the most effective pulp density for gravity concentration of a PGM concentrate feed in the gravity concentrator. Though it has the lowest mass yield it achieved the best attainable recovery, concentrate grade, enrichment ratio and lowest chrome content in the concentrate product.

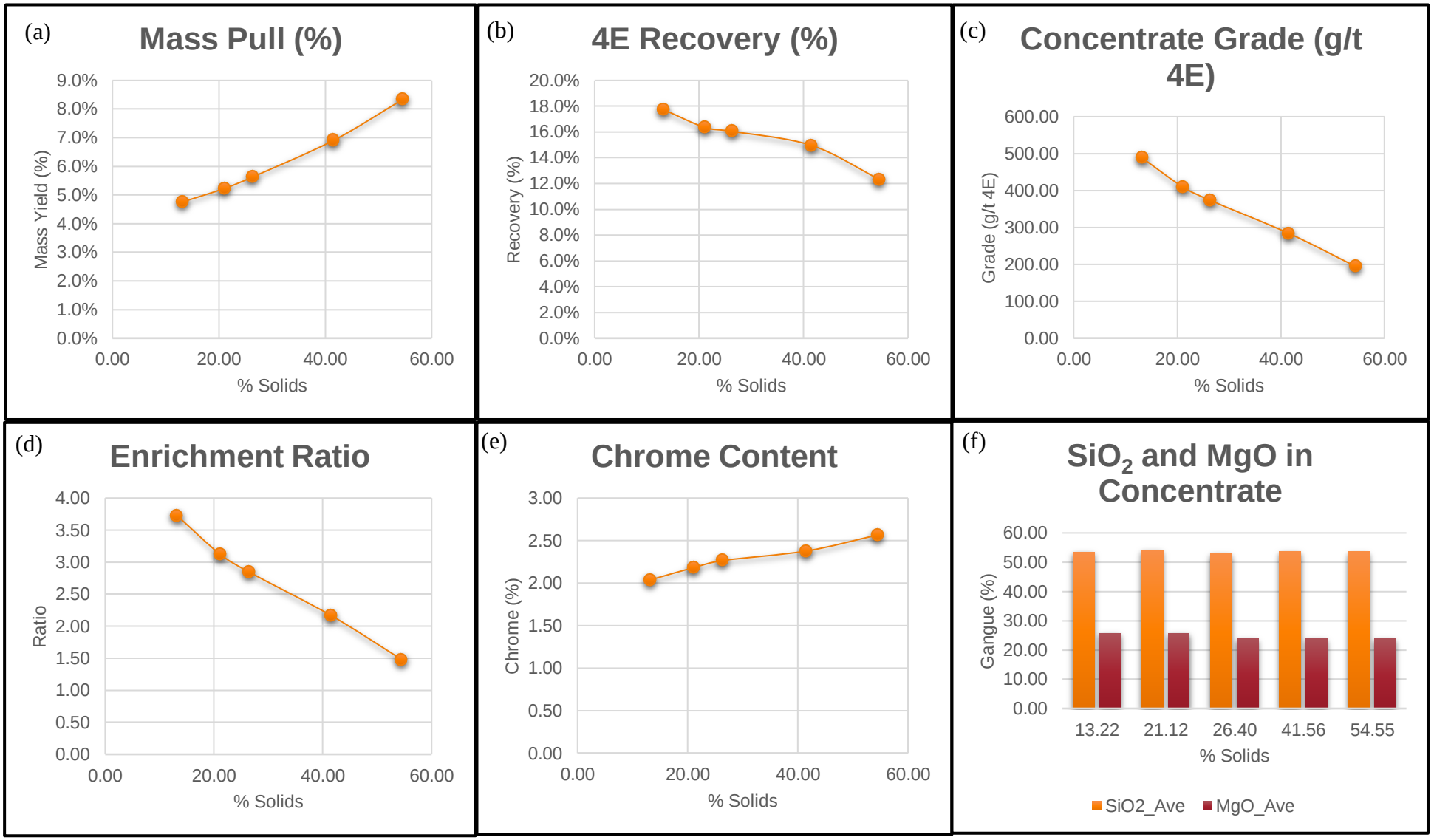

*Figure 35: Phase 2 results indicating (a) mass pull, (b) recovery, (c) concentrate grade, (d) enrichment ratio, (e) chrome content and (f) gangue content (Please see **Appendix A** for raw data and calculation sheet)*

4.3.3. Phase 3: Change in G-force

The gravitational force plays a role in how fast the Falcon concentrator spins as well as how much force is applied to the particles entering the concentrator. The energy imparted to denser particles is meant to keep those particles in the bowl while allowing lighter particles to leave in the tailings stream. The following gravitational forces were used; 100 G, 200 G, 250 G and 300 G. The maximum G-force that this Falcon unit is capable of operating at is 300 G's.

Figure 36 (a) indicates the mass pull to concentrate at each G force. The data shows a decrease in mass yield as the gravitational force increases. At 100 G the mass yield is 5.6% whereas at 300 G the mass yield is 4.8%. The decrease in mass yield as the gravitational field increases is due to the additional force acting on all the particles, the heavy particles remain in the bowl while more of the light fraction is removed by the centrifugal force. The lighter and finer particles cannot overcome the gravitational force and the velocity of the flowing slurry and are thus ejected from the gravity concentrator. At higher G-force the Falcon becomes more selective for denser particles and thus more gangue is removed.

Figure 36 (b) and (c) indicates that the recovery and grade increases as the gravitational force increases. The base run of 300 G's indicated that the recovery is 17.7% and the concentrate grade is 488.07 g/t 4E. The lowest G-force of 100 G's indicated that the recovery is 12.2% and the concentrate grade is 283.20 g/t 4E. This indicates that higher G-force has a positive impact on recovery and concentrate grade as a result of the improved selectivity in the concentrate bed at higher G-force. As the gravitational force increases the concentrator becomes more selective as lighter gangue particles are removed from the Falcon concentrator and heavier particles are favourably retained in the bowl.

The enrichment ratio (Figure 36 (d)) is the ratio of the concentrate grade to the feed grade and is a parameter that determines efficiency of the gravity concentration for upgrading the feed material. The G-force of 300 G's has the highest enrichment ratio of 3.73. There is a steep decline in the enrichment ratio as the G-force decreases due to the loss in selectivity.

Figure 36 (e) indicates that the chrome content in the concentrate increases as the G-force increase. This is due to the entrapment of chrome particles in the concentrate bed as the gravitational force increases there is some chrome that enters the concentrate bed due to the chrome being denser than the gangue constituents. This result is expected due to the density of chromite but it should be noted that on a mass basis, most of the chrome is rejected to the tailings.

The main gangue constituents, silicon dioxide and magnesium oxide, had a similar concentration in the feed and in the concentrates. Silicon dioxide was approximately between 52.04% to 53.46% and magnesium oxide was between 25.67% to 26.58% in the Falcon concentrate. This indicates that due to the high mass concentrations of these gangue particles they also enter the concentrate bed at the same concentration as the feed.

The results for Phase 3 show the gravitational force of **300 G's** as the most effective among the G forces tested for gravity concentration of a PGM concentrate feed to the gravity concentrator as this G-force has the lowest mass yield compared to the attainable recovery and concentrate grade as well as a highest enrichment ratio. It is also evident that there is an exponential increase in PGM recovery and grade at 300 G's, this shows that fine and ultra fine PGM particles require higher centrifugal force for more effective recovery and gangue rejection. Although the chrome content is higher at 300 G's, the concentration of 2.04% is still well below the maximum of 3% allowable in PGM concentrates for smelting purposes.

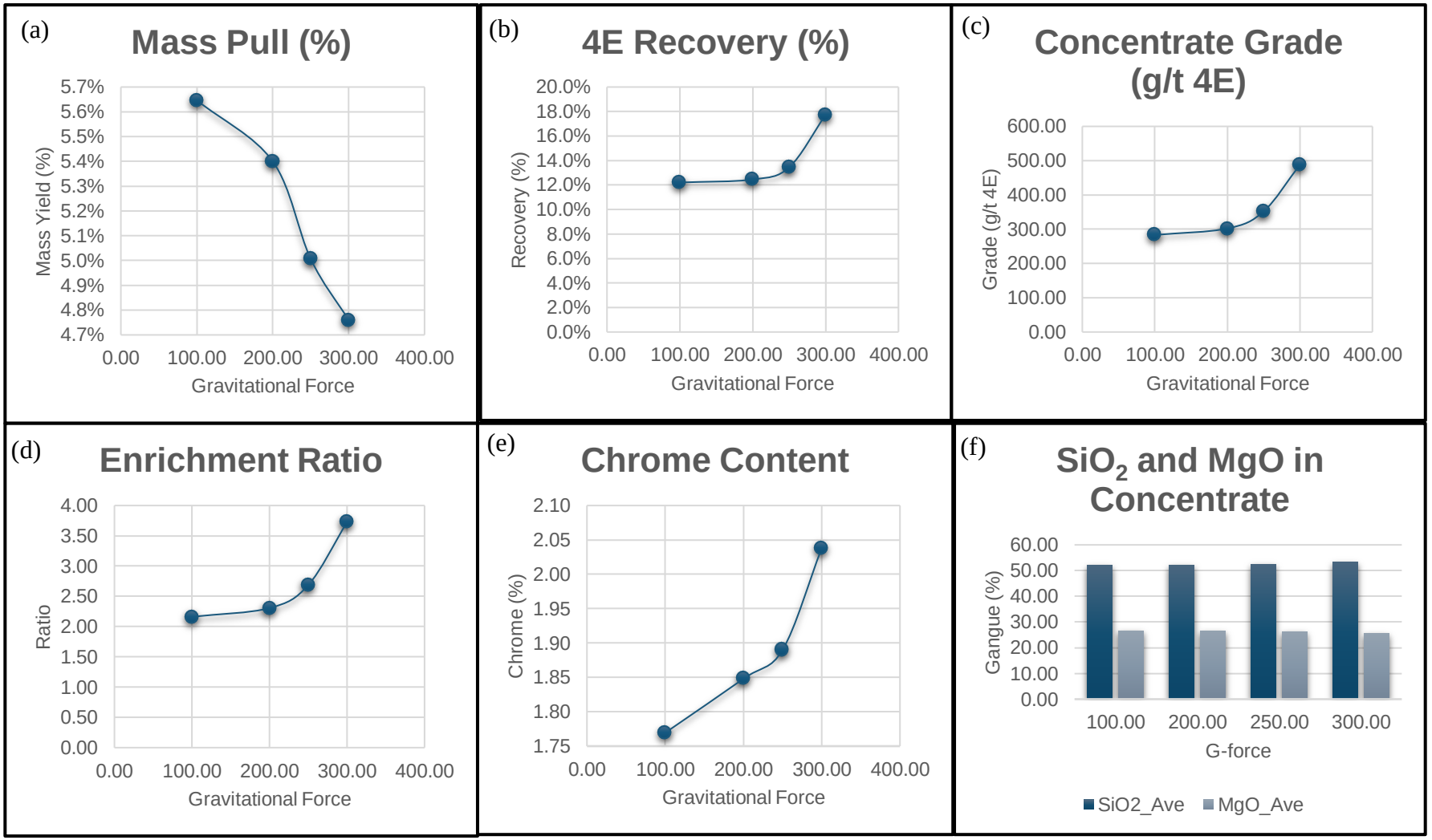

*Figure 36: Phase 3 results indicating (a) mass pull, (b) recovery, (c) concentrate grade, (d) enrichment ratio, (e) chrome content and (f) gangue content as a function of G-force (Please see **Appendix A** for raw data and calculation sheet)*

4.3.4. Phase 4: Change in Flow Rate

The feed flow rate determines the amount of slurry (water and solids) entering the concentrator per unit time. The higher the flow rate, the greater the amount of slurry passing through the Falcon bowl per unit time. An increased flow rate also increases the velocity of the slurry in the Falcon bowl. The following flow rates were used: 3 L/min, 5L/min and 10 L/min. It was found to be impractical to use flow rates less than 3L/min and flow rates above 10 L/min caused the Falcon bowl to overflow.

Figure 37 (a) indicates the mass yield vs flowrate and shows a decrease in mass yield as the flow rate increase. At 10 L/min the mass yield is 2.5% whereas at 3L/min the mass yield is 4.8%. The decrease in mass yield as the flow rate increases may be due to lower retention time experienced by the particles as well as the greater velocity of the slurry (fluid) which forces more particles out of the concentrate bowl. The greater velocity also erodes the concentrate bed thus leading to already settled particles being dislodged and reporting to the tailings stream.

Figure 37 (b) and (c) indicate that the recovery and grade decreases as the flow rate increases. The base run at 3 L/min resulted in a recovery of 17.7% and the concentrate grade is 488.07 g/t 4E. The highest flow rate of 10 L/min produced a recovery of 7.3% and the concentrate grade is 387.3 g/t 4E. This means that higher flow rates have a negative impact on both recovery and concentrate grade due to the decreased selectivity in the concentrate bed. As the flow rate increases the retention time a particle has in the Falcon decreases and the velocity of the fluid increases thus leading to lower recovery of heavy particles as they are ejected to the tailings stream.

The enrichment ratio (Figure 37 (d)) is the ratio of the concentrate grade to the feed grade and is a parameter that determines efficiency of the gravity concentration for upgrading the feed material. The flow rate of 3L/min has the highest enrichment ratio of 3.73 which means that this is the most effective flow rate for upgrading the feed. There is a steep decline in the enrichment ratio as the flow rate increases due to the loss in selectivity.

Figure 37 (e) indicates that the chrome content in the concentrate decreases as the flow rate increases. This is due to the lower retention time and higher fluid velocity which carries the chrome out of the Falcon bowl. The density of the chrome cannot overcome these forces and thus the chrome is rejected from the concentrate bed.

The main gangue constituents, silicon dioxide and magnesium oxide, had a similar concentration in the feed and in the concentrates. Silicon dioxide was approximately between 53.22% to 53.46% and magnesium oxide was between 25.07% to 25.67% in the Falcon concentrate. This indicates that due to the high mass concentrations of these gangue particles they also enter the concentrate bed at the same concentration as the feed.

The results for Phase 4 indicate that a flow rate of **3L/min** is the most effective flowrate for gravity concentration of a PGM concentrate feed using the Falcon concentrator. This suggests that fine and ultra fine PGM particles require a lower flow rate to be recovered and for gangue rejection. Although the chrome content is higher at 3L/min, the concentration of 2.04% is still well below the maximum of 3% allowable in PGM concentrates for smelting purposes.

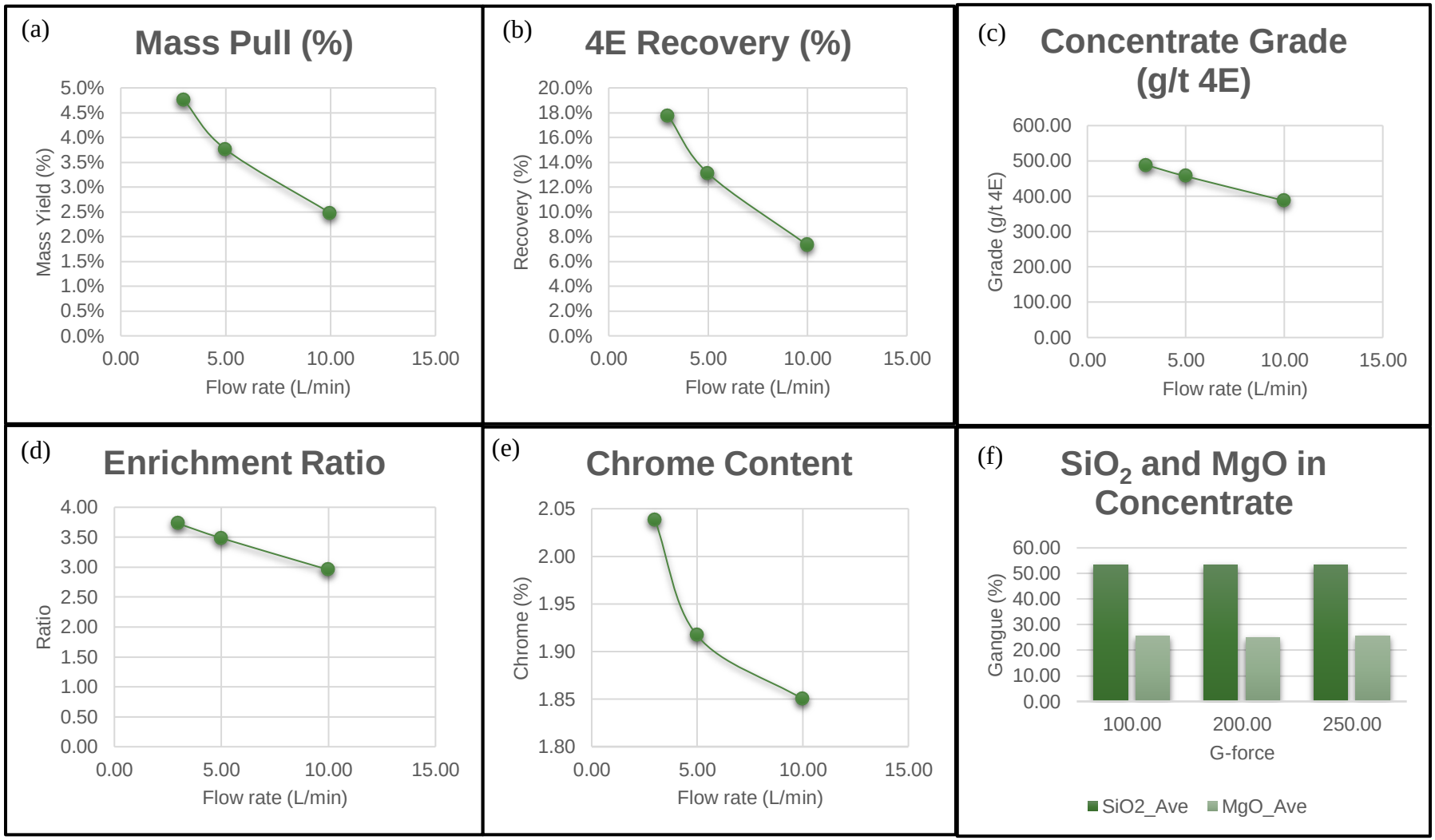

Figure 37: Phase 4 results indicating (a) mass pull, (b) recovery, (c) concentrate grade, (d) enrichment ratio, (e) chrome content and (f) gangue content

4.4. Falcon Experiments with Optimal Parameters

4.4.1. Phase 5: Optimized Parameters

The optimal parameters from Section 4.3 were used to determine the efficacy of gravity concentration for PGMs. The selected parameters were as follows; feed flow rate - 3L/min, the G-force - 300 (78.3 Hz) and density - 1.10 (13.22% solids). The feed samples were each fed through 5 stages of Falcon concentration as described in the methodology section. Figure 38 depicts this procedure, in which the original dry feed sample is initially mixed with water to create a slurry with the desired % solids and termed the Gravity concentration feed (GC feed). The tail of each stage is fed to the next stage until the fifth and final stage which produces a final tailings stream (essentially this process involved recycling the tail back to the Falcon 5 times). At each stage a concentrate is produced and collected. The purpose of the lab scale multi-stage gravity concentration was to simulate the expected results of a typical plant unit. The 5 concentrates were analysed individually for PGMs and then combined results yielded the mass pull (mass yield), recovery, grade and elemental composition of the final concentrate. The feed sample used was the same as described in Section 4.2 and the tail sample was also analysed. The process was repeated ten times in order to get repeatability of results and ensure a robust data set. The set of results from the assay were subjected to a statistical outlier test by comparing results from each run against one another in the Minitab Software to ensure data integrity, any individual result that is not within the tolerances (greater than 3 standard deviations from the mean, or less than 3 standard deviations) is termed an outlier. A total of 1000 individual analysis were performed all together from the 10 runs and of these only 4 individual results were outliers, hence 99.60% of the data was deemed as reliable to safely draw inferences and make decisions. The raw data for each run and outlier control charts can be found in **Appendix B**.

Figure 39 (a) - (e) show the 5 concentrates produced per experimental run. It is visually noticeable that concentrate 1 has a darker brown to grey/black colour and as the stages progress the colour becomes more light brown. The reason for this is that the first concentrate has the highest concentration of PGMs and as the stages progress the PGMs decrease accordingly. GC concentrate 5 is a light brown as it contains more gangue than the other concentrates. Figure 39 (f) is a close-up image of GC concentrate 1 showing the formation of dark spirals in the

concentrate bed. This is thought to be the heavy particles dragging along the concentrate bed due to the centrifugal motion of the Falcon bowl. The weighted average results for Phase 5 runs are shown in Table 13 and Table 14 . Table 13 shows the Fire Assay/ICP-MS results for PGMs, base metals, sulphur, chrome and gangue. Table 14 shows the weighted results and analysis of the 10 runs with mass pull (yield), recovery and concentrate grade.

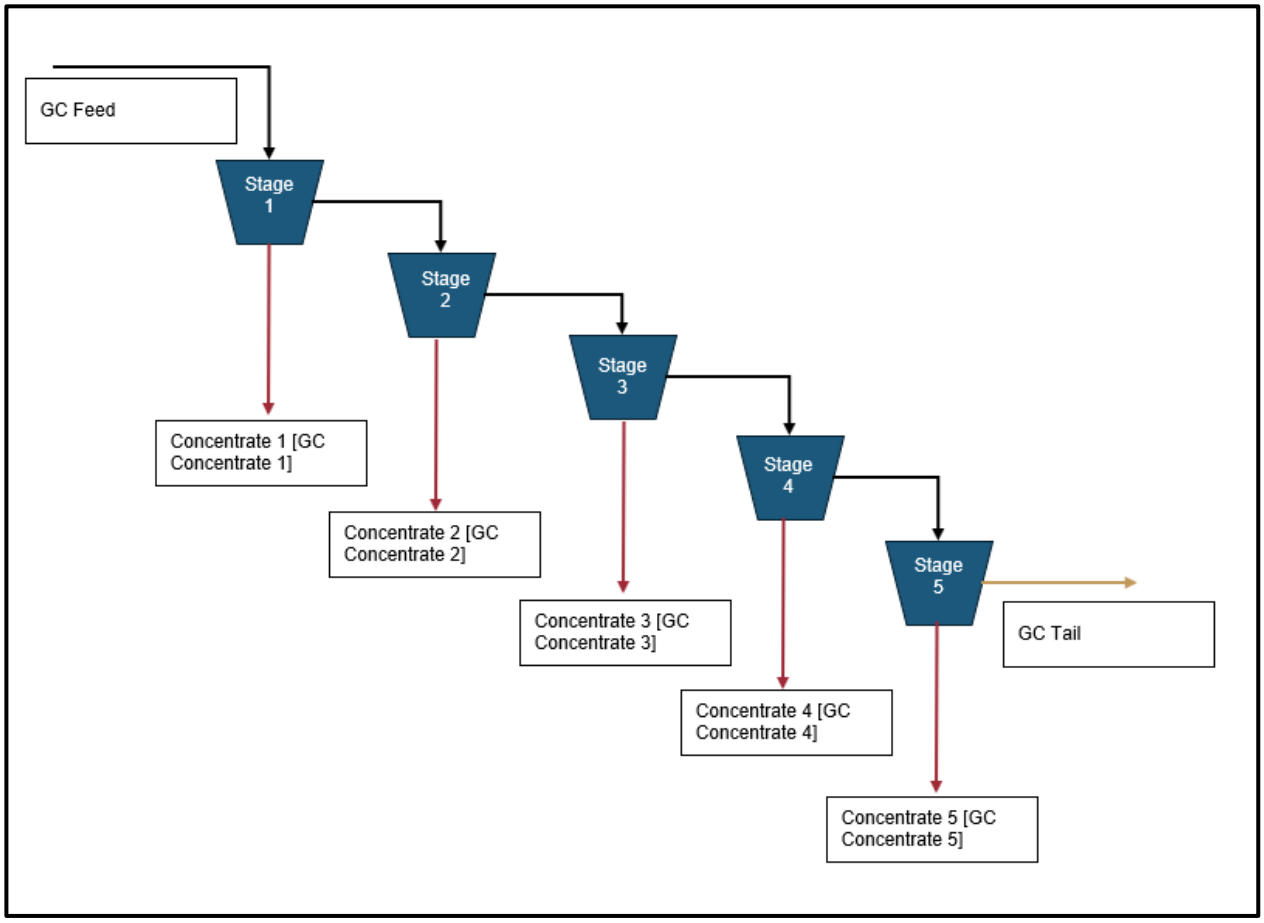

Figure 38: Falcon gravity concentrator lab scale stages per run

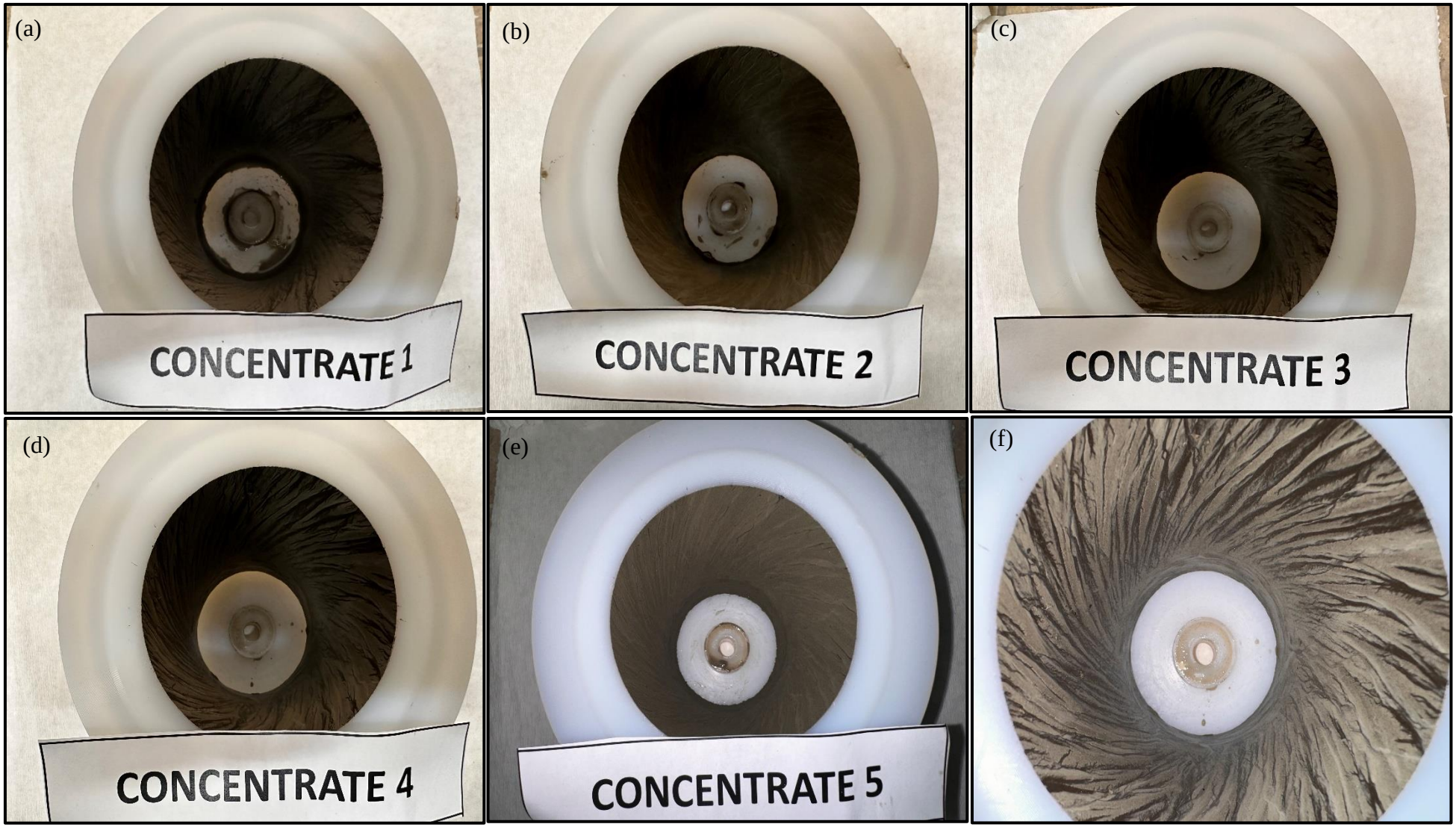

Figure 39: GC Concentrate images showing (a) GC concentrate 1. (b) GC concentrate 2. (c) GC concentrate 3. (d) GC concentrate 4. (e) GC concentrate 5 and (f) close-up image of GC concentrate 1 showing dark spiral lines.

Table 13: Weighted average assay results for optimized parameter runs

PGM	Pt_Ave	Pd_Ave	Au_Ave	Rh_Ave	Ru_Ave	Ir_Ave	SUM 4E	SUM 6E	Cu_Ave	Ni_Ave	Fe_Ave	FeO_Ave	Co_Ave	Sulphur_Ave	Cr_2O_3_Ave	SiO_2_Ave	MgO_Ave	CaO_Ave	Al_2O_3_Ave
	g/T	g/T	g/T	g/T	g/T	g/T	g/T	g/T	%	%	%	%	%	%	%	%	%	%	%
Gravity Concentrate Feed	80.35	34.99	0.71	14.97	25.76	6.19	131.02	162.97	0.22	0.43	7.20	9.26	0.02	0.78	1.97	53.92	24.07	3.24	4.98
Gravity Concentrate 1	356.31	132.35	3.95	34.61	131.20	21.78	527.22	680.20	0.31	0.80	8.25	10.62	0.04	1.24	2.18	53.52	24.49	2.65	4.33
Gravity Concentrate 2	232.81	93.63	2.04	31.76	92.88	17.81	360.25	470.94	0.32	0.82	8.26	10.63	0.04	1.28	2.16	53.37	24.42	2.72	4.42
Gravity Concentrate 3	145.48	63.87	1.24	25.11	57.22	13.42	235.70	306.34	0.30	0.72	8.06	10.37	0.03	1.13	1.93	53.66	24.49	2.77	4.37
Gravity Concentrate 4	119.34	54.56	1.17	23.06	42.24	10.91	198.13	251.28	0.30	0.72	7.98	10.26	0.03	1.13	1.87	52.85	24.56	2.78	4.33
Gravity Concentrate 5	87.74	41.67	0.89	18.12	30.10	9.31	148.42	187.83	0.29	0.67	7.98	10.27	0.03	1.08	1.80	53.90	24.55	2.79	4.38
Total Gravity Conc.	187.00	76.76	1.84	26.44	70.24	14.59	292.04	376.87	0.30	0.74	8.11	10.43	0.04	1.17	1.99	53.47	24.50	2.74	4.36

Table 14: Weighted average mass yield, recovery and grade results for optimized parameter runs

Phase 5: Multi-stage	Flow rate (L/min)	Mass (g)	Mass Recovery (%)	Cum Mass recovery (%)	Mass recovery (g)	4E PGM (g/t)	**4E PGM Recovery (%)**	4E PGM Cum Recovery (%)	4E PGM (g)	**4E PGM Upgrade**
Gravity Concentrate Feed	**3**	50000.00				131.02				
Gravity Concentrate 1		2149.13	4.3%	4.3%	2149.13	527.22	**17%**	17%	1.13	**4.02**
Gravity Concentrate 2		2154.88	4.3%	8.6%	2154.88	360.25	**12%**	29%	0.78	**2.75**
Gravity Concentrate 3		2295.50	4.6%	13.2%	2295.50	235.70	**8%**	37%	0.54	**1.80**
Gravity Concentrate 4		2103.75	4.2%	17.4%	2103.75	198.13	**6%**	44%	0.42	**1.51**
Gravity Concentrate 5		2266.38	4.5%	21.9%	2266.38	148.42	**5%**	49%	0.34	**1.13**
Total Gravity Conc.		*10969.63*	*21.9%*		*10969.63*	*292.04*	***49%***		*3.20*	**2.23**
Gravity Concentrate Tail		39030.38	78.1%		39030.38	85.77			3.35	
Totals		*50000.00*	*100%*		*50000.00*	***131.02***	***48.90%***		*6.55*	***2.23***

The above results are a combination of all 10 Falcon runs and are the weighted averages and totals from those runs. For instance, the gravity concentrate feed in Table 14 indicates 50 000 g which is derived from the 5 000g per run multiplied by the 10 runs. 4E recovery and grades are used as these specific PGMs are of highest economic value.

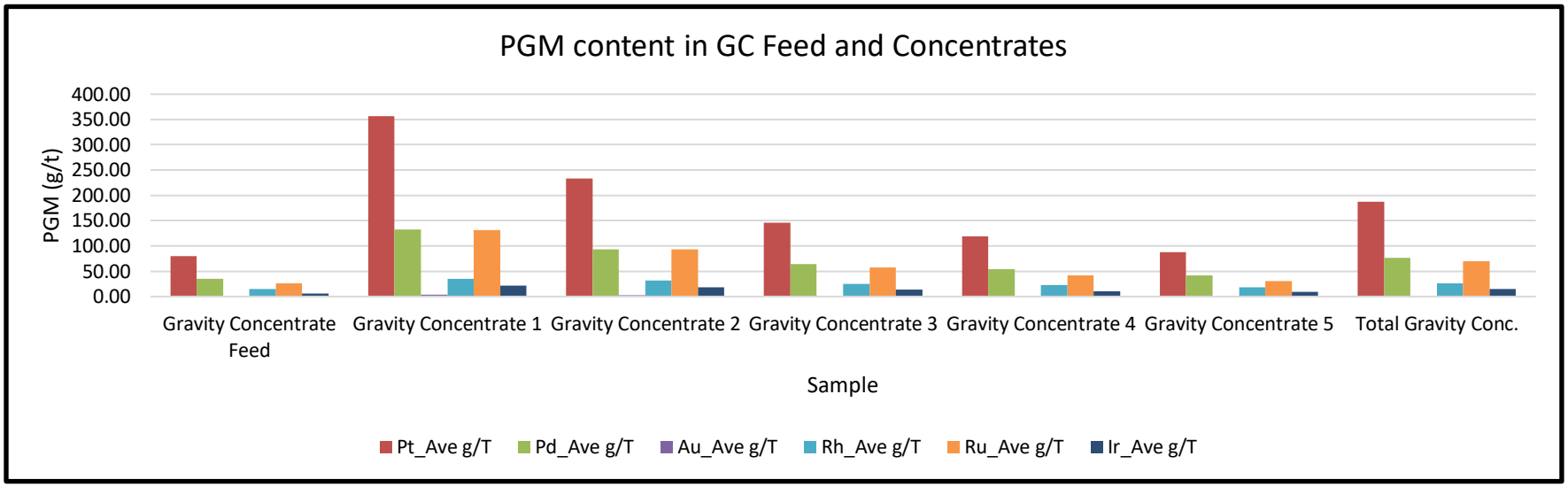

Figure 40: Phase 5 weighted PGM content in feed and concentrates

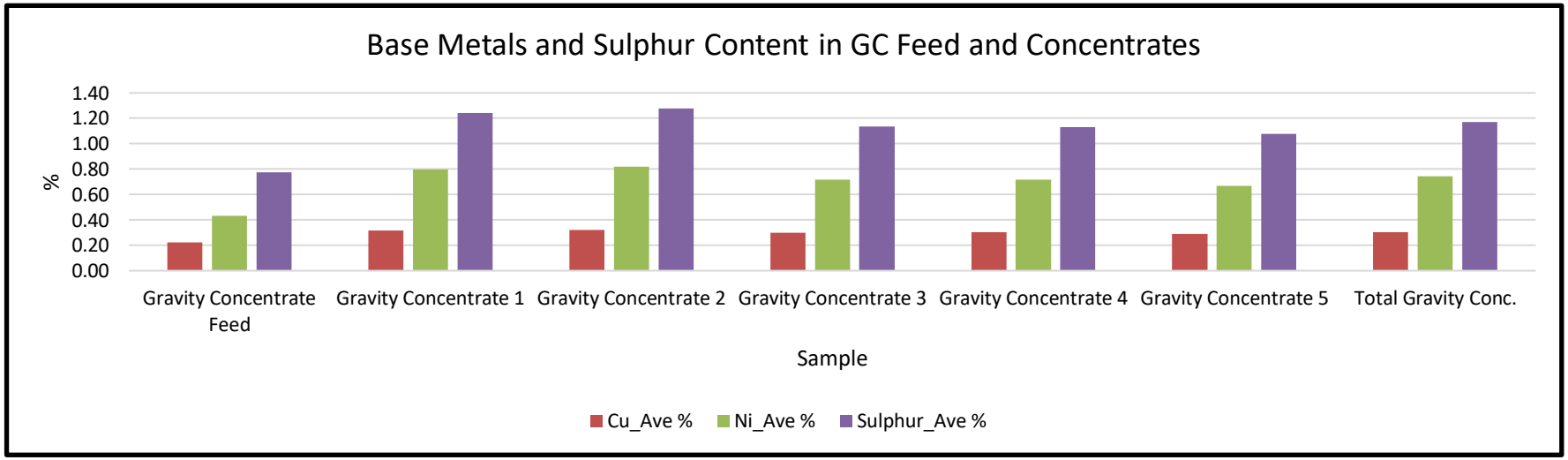

Figure 41: Phase 5 weighted base metals and sulphur content in feed and concentrates

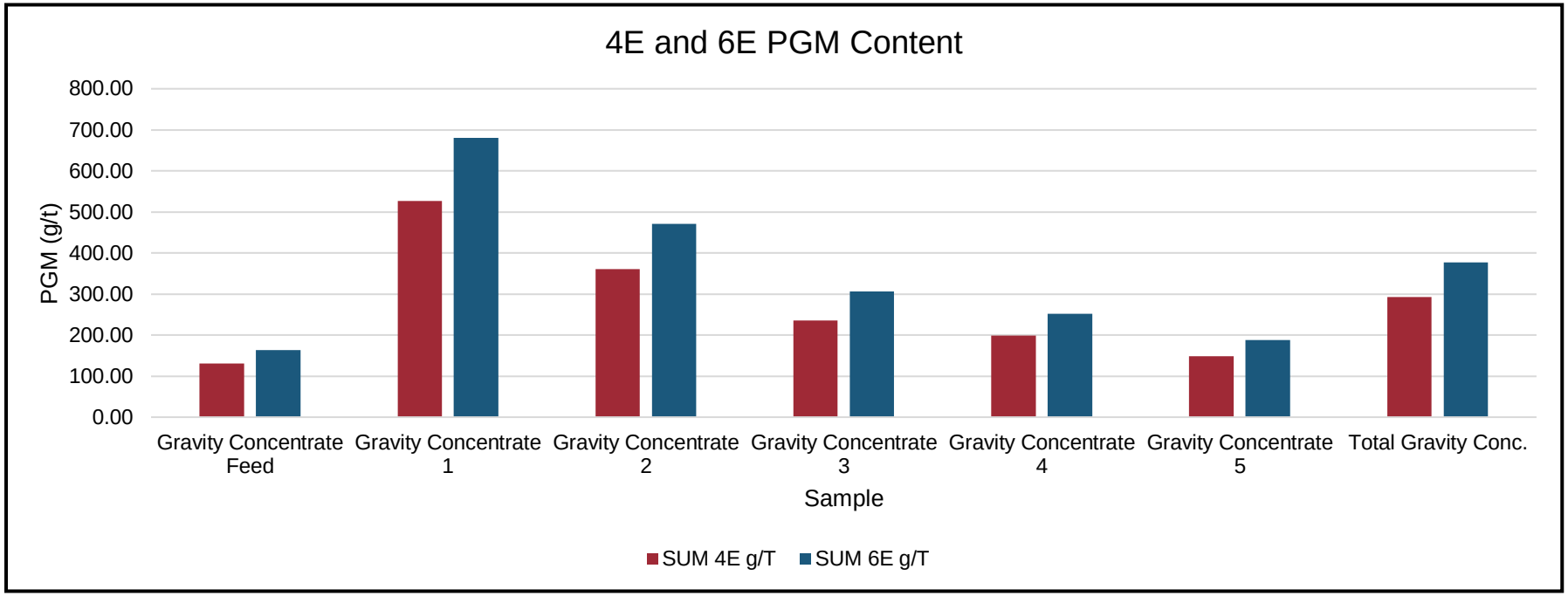

Figure 42: Phase 5 weighted 4E and 6E recovery

Figure 40 indicates the individual PGM content in the GC feed and each of the GC concentrates. The highest content is in the first two concentrates. Platinum, palladium and ruthenium have the highest concentrations in the 5 concentrates. Figure 42 indicates the 4E and 6E PGM recovery which gradually decreases over the 5 stages as the feed grade to the subsequent stages decreases, the weighted 4E grade is 292.04 g/t and 6E grade is 376.87 g/t. Figure 41 indicates the base metal and sulphur content per stage and in the feed. This clearly indicates that there is an increase in base metal and sulphur content from the feed to the concentrates and this is due to the association of PGMs with base-metal sulphides.

4.4.2. Mass Pull/Recovery/Grade Relationship

The mass pull (yield), recovery and grade relationship are critical metrics in determining the efficacy of gravity concentration for processing PGMs. Figure 43 indicates that each stage has a mass pull of approximately 4.4% and there is not much variance between the mass pull per stage. The likely reason why the mass pulls were similar could be the limited capacity of the bowl. Each concentration stage was run until the maximum capacity of the bowl was reached suggesting that the bowl could not retain any more solids beyond the 4.4% of the feed per stage at the optimal parameters. The cumulative mass yield was 21.9% (Figure 44). The average moisture content per stage in the concentrate bed was 25.74% indicating that not much moisture was retained in the concentrate bed. Excessive moisture retention could result in more fines and ultra-fine gangue remaining in the concentrate as moisture is not likely to be carried away to the tails by the centrifugal force.

Figure 45 indicates the recovery per stage which was 17%, 12%, 8%, 6% and 5% respectively. This indicates that as the stages progress the recovery decreased owing to the diminishing recoverable PGMs. The first and second stage of the gravity concentration showed highest grades and highest recoveries. The overall cumulative recovery is 48.9%, which indicates that about half the 4E PGMs present in the preconcentrated feed was able to be recovered using the gravity concentrator. Figure 46 also indicates that an increasing trend of recovery means that additional stages may be able to recover more PGMs, this aspect will be discussed further in **Section 4.5.**

The 4E concentrate grade for the runs are depicted in Figure 47 and Figure 48. These results indicate a gradual drop in concentrate grade after each subsequent stage. Stage 1 has the highest grade of 527.22 g/t 4E PGM and stage 5 has a grade of 148.42 g/t 4E PGM. The overall concentrate grade is 292.04 g/t 4E PGM which yields an upgrade ratio of 2.23 compared to the feed grade, essentially meaning that the feed grade was doubled.

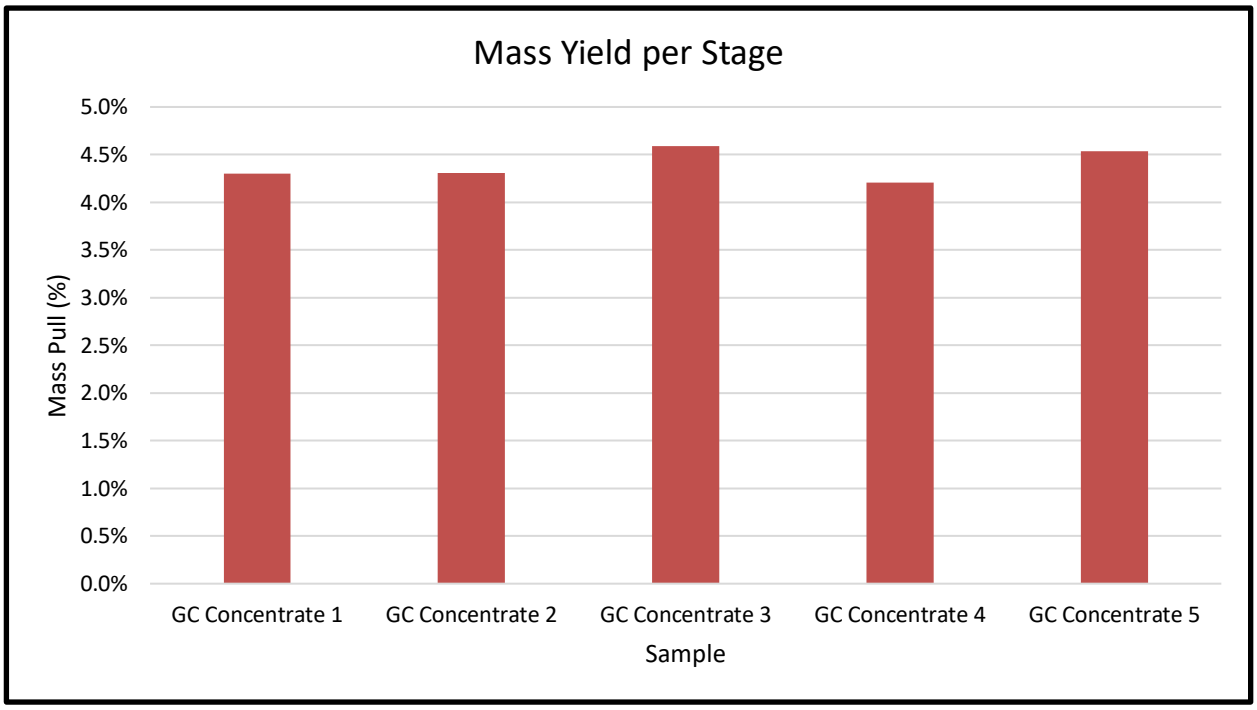

Figure 43: Phase 5 mass yield per stage

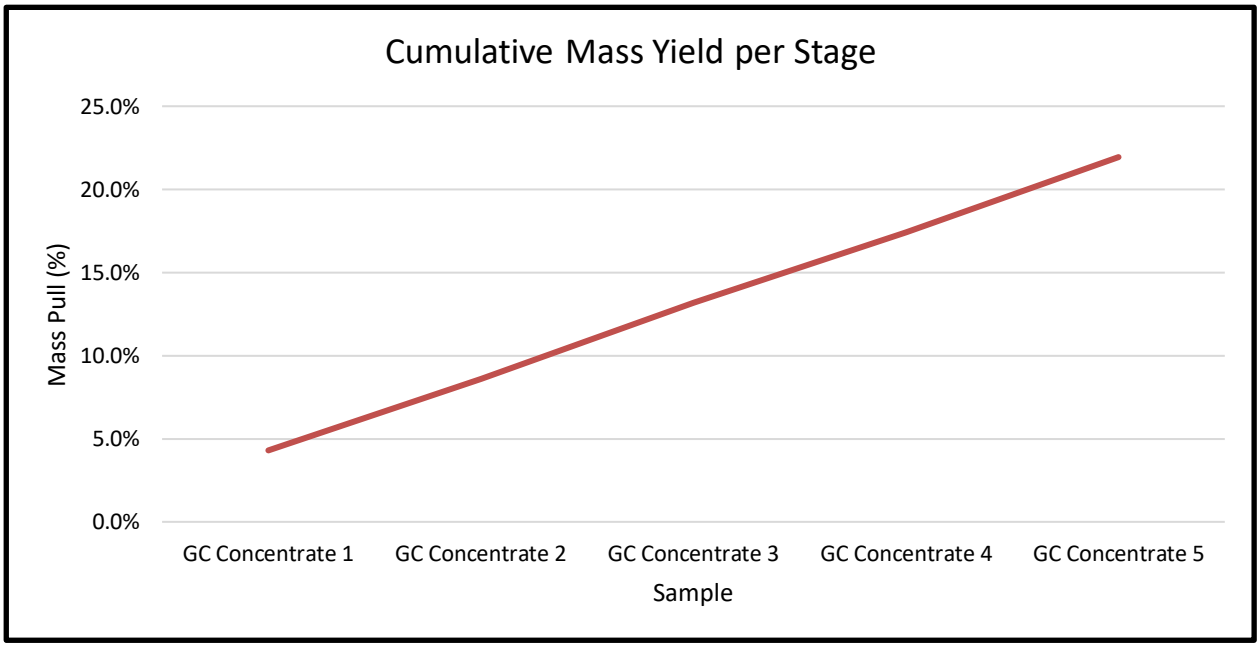

Figure 44: Phase 5 cumulative mass yield

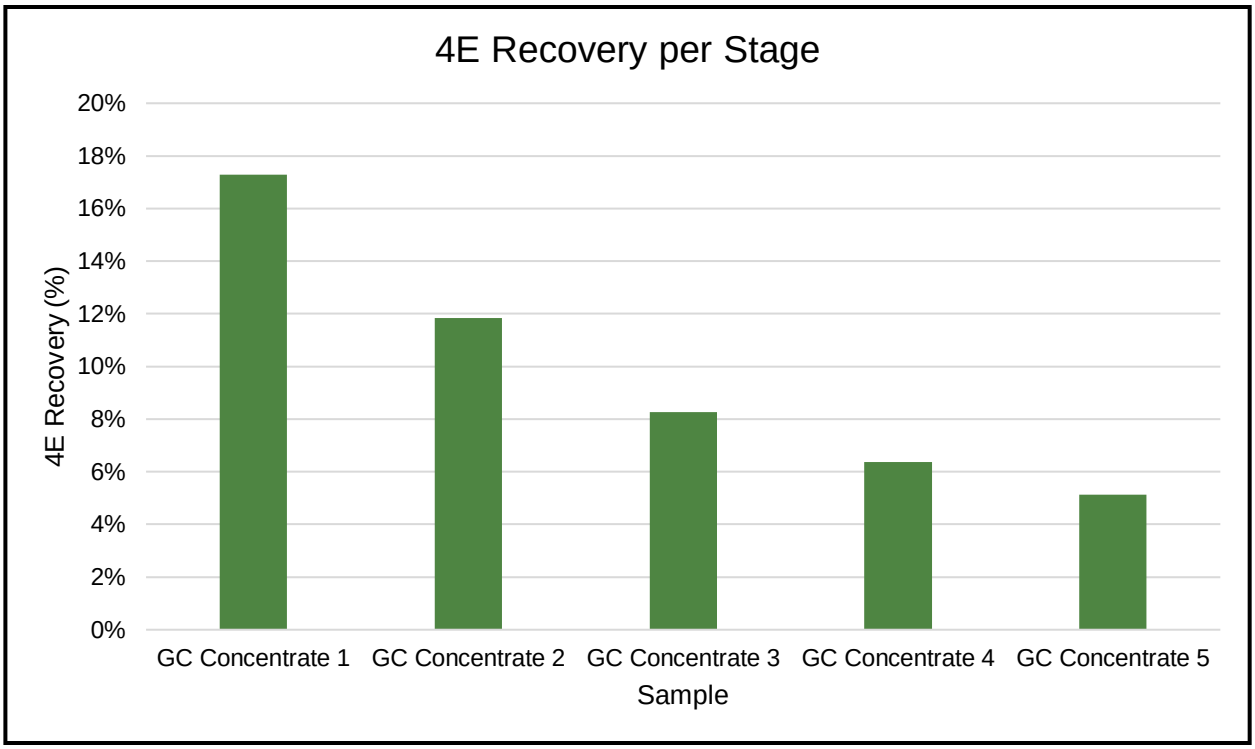

Figure 45: Phase 5 4E recovery per stage

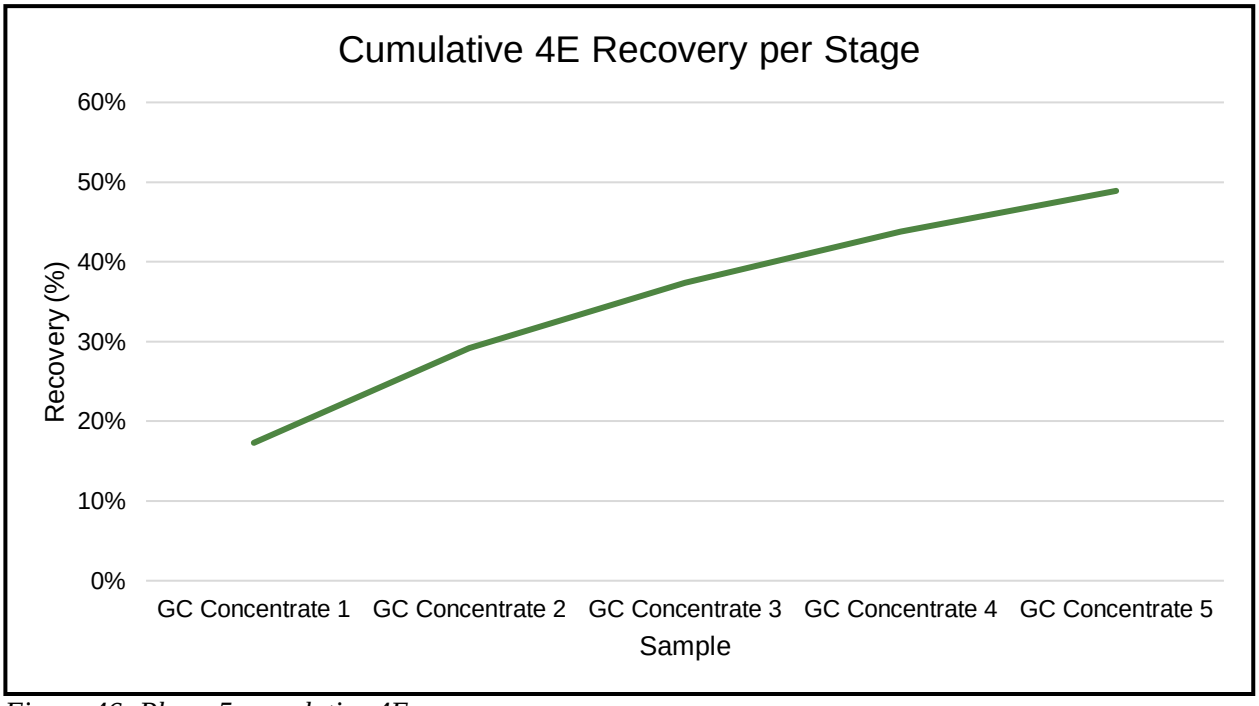

Figure 46: Phase 5 cumulative 4E recovery

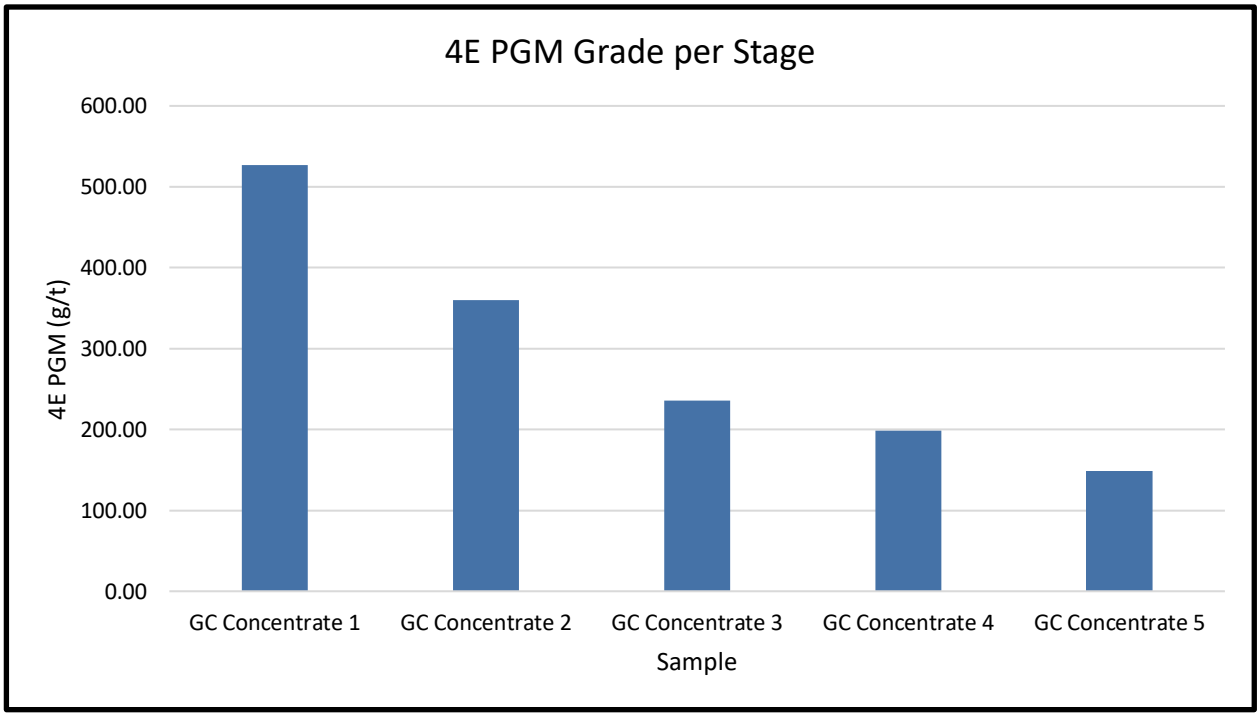

Figure 47: Phase 5 4E grade per stage

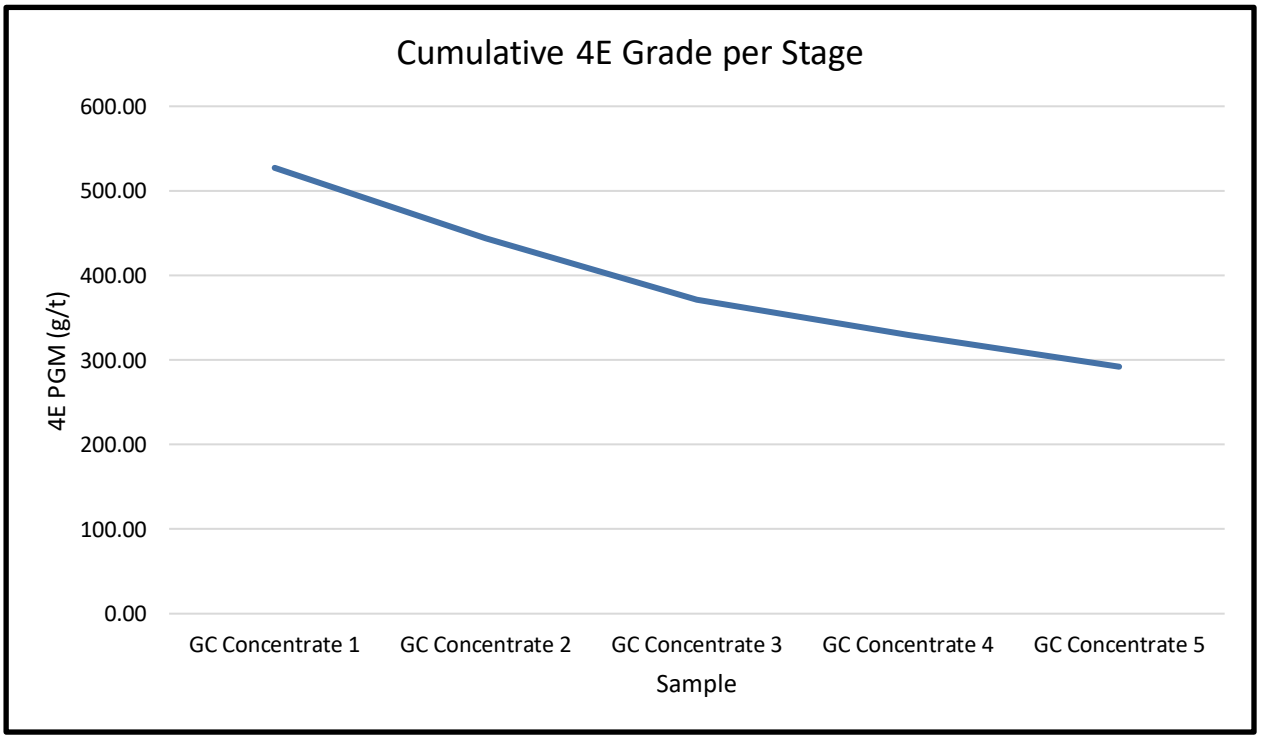

Figure 48: Phase 5 cumulative 4E grade

As the mass pull increases with the number of stages, the recovery increases and as the recovery increases the grade decreases. This relationship between mass pull, recovery and grade is well known and holds for gravity concentration as well. The experiments indicate that a total mass pull of 21.9% was able to recover 48.9% of the PGMs at a concentrate grade of 292.04 g/t 4E PGM. This proves the hypothesis that gravity concentration can indeed recover PGMs and upgrade PGM concentrates.

The fact that only 21.9% of the recovered mass contained approximately 50% of the PGMs also means that additional stages could possibly recover more PGMs. Another option would be to send the final gravity concentrate tail to an appropriate flotation section such as the cleaner or recleaner section thus creating a recycle stream and allowing the PGMs in the tail of the gravity concentrator to be recovered.

4.4.3. PGM Recovery per Element

The above section focused on the overall recovery of PGMs however, it is also important to consider the individual PGM recovery as depicted in Figure 49. Platinum and palladium have recoveries of 51.06% and 48.13% respectively. This is expected as these elements constitute the largest portion of the GC feed PGMs and have a high density, hence the greater recovery to the GC concentrate. Rhodium and iridium recoveries are 38.75% and 51.68% respectively. The iridium recovery is in line with the platinum and palladium recovery, but the rhodium recovery is rather low. This low rhodium recovery could be due to its lower density (12.4 g/cm^3) and mineral associations.

The most interesting results were those of gold and ruthenium which have the highest recoveries of 57.04% and 59.83% respectively. Gold has the lowest concentration of the GC feed (0.71 g/t) and ruthenium has the third highest concentration (25.76 g/t). Although the effect of concentration may play a role in ruthenium's ability to be recovered by gravity concentration it does not play a role in the high recovery of gold. Gold has a density of 19.3 g/cm^3 and ruthenium has a density of 12.41 g/cm^3, hence density differences may play a role in the recovery of gold but not necessarily ruthenium which has a lower density. This leads to the conjecture that most of the gold in the GC feed may be present in its native form rather than in the complex matrix

with the other PGMs and hence more amenable to gravity concentration. The same can be said for ruthenium, where the concentration may play a role, but it may also be postulated that most of the ruthenium may be in native form or may form more simple complexes than the other PGMs. Another possible reason that can be put forward is that the gold and ruthenium are in the coarser fraction and thus can be more easily recovered by gravity concentration, however this argument is disproved in **Section 4.4.7** where it is clear that these elements are present in the fine to ultra fine fraction.

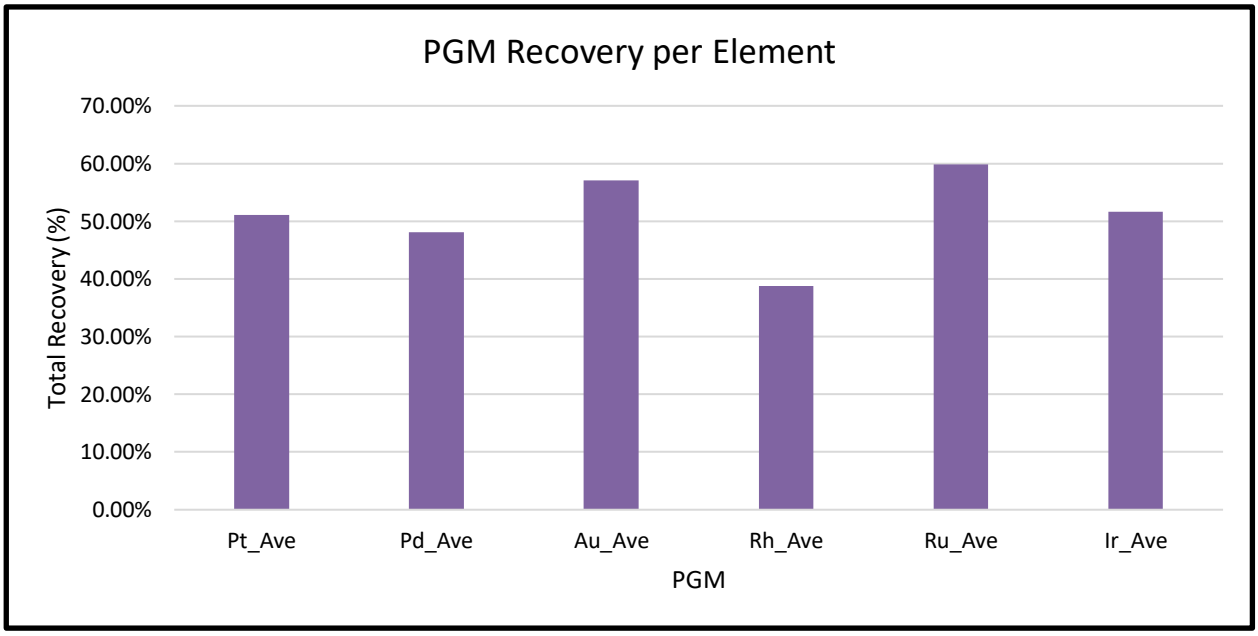

Figure 49: Phase 5 PGM elemental recovery

4.4.4. Chrome Rejection

Chrome rejection is a critical factor when considering gravity concentration for PGMs (specifically for UG-2 ore) as PGM smelters cannot take concentrates with a chrome content above 3% due to the formation of chrome spinel mentioned in the literature review section. It is therefore important to determine whether chrome is concentrated in the gravity concentrator with the PGMs.

Figure 50 indicates that the chrome in the feed was 1.97% and 1.99% in the overall concentrate. The chrome content gradually decreases from 2.18% in GC concentrate 1 to 1.80% in GC concentrate 5. The tail contains 1.4% chrome. Figure 51 indicates that about 95% of the chrome

is rejected at each stage and Figure 52 indicates that the total chrome rejection is 77.84%. This proves the hypothesis that chrome is not favourably concentrated in gravity concentration. This is due to its lower comparative density (7.15 g/cm^3) and that chrome is most likely in its native form or associated with silica.

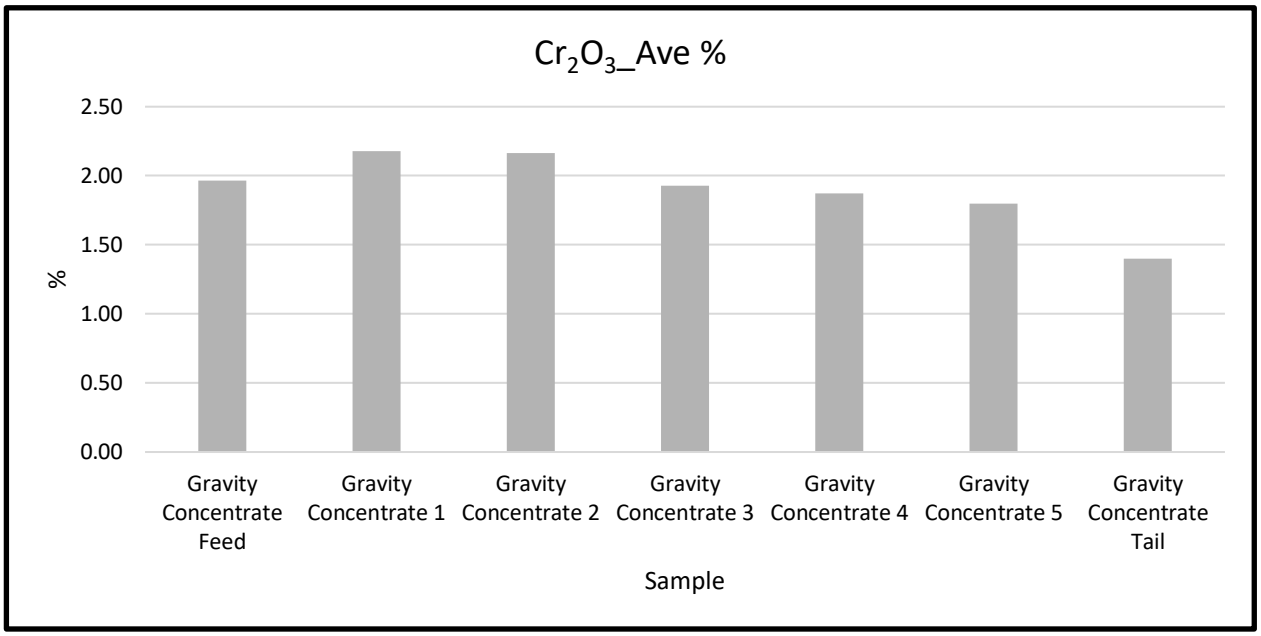

Figure 50: Phase 5 chrome content in GC feed, concentrates and tail

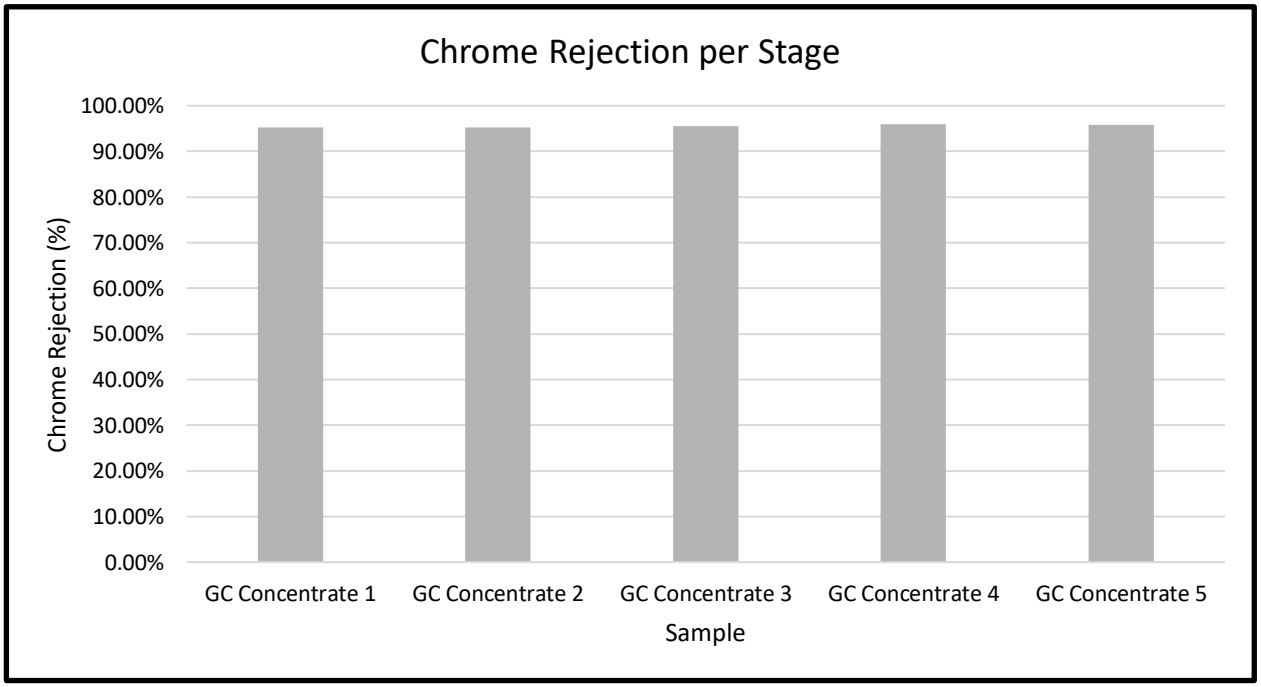

Figure 51: Phase 5 chrome rejection per stage

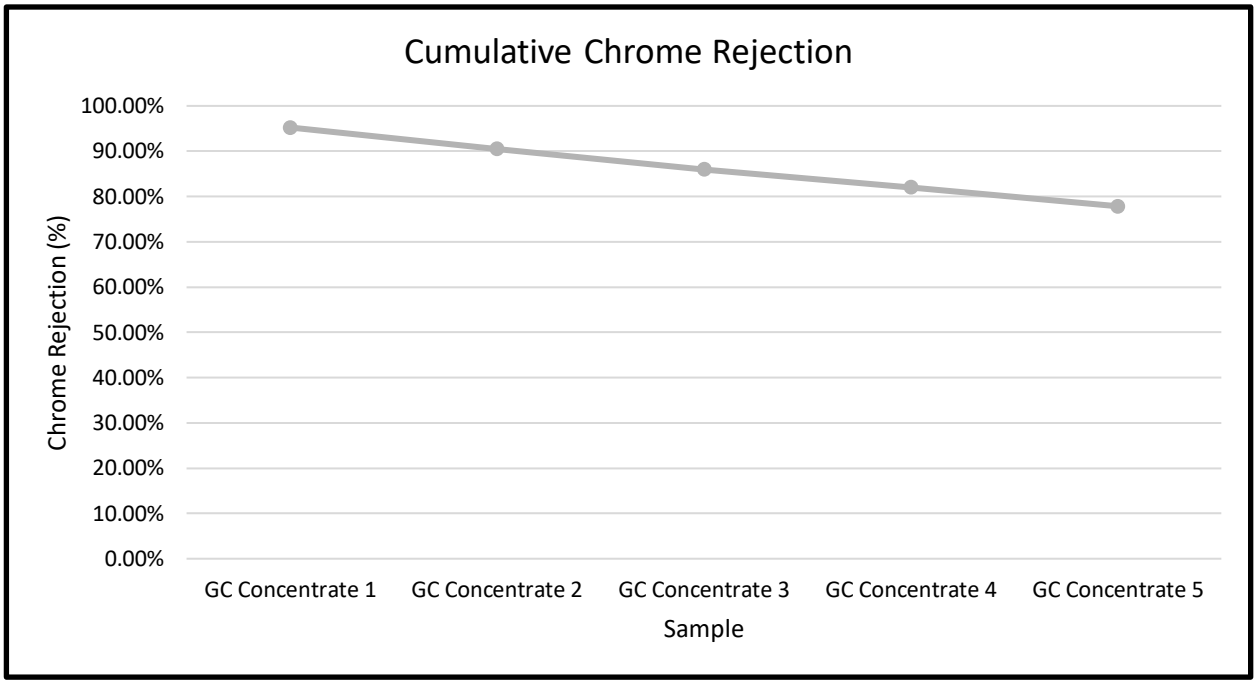

Figure 52: Phase 5 cumulative chrome rejection

4.4.5. Gangue Behavior

The concentration of the main gangue constituents in the GC feed, concentrates and tail seem to remain fairly constant. Silicon dioxide is the main gangue constituent making up 53.92% in the feed, 53.47% in the total concentrate and 54.83% in the final tail (Figure 53). The same trend was also observed for magnesium oxide (Figure 54) and calcium oxide (Figure 58), showing fairly the same concentrations in the feed; concentrate and tail. It should be mentioned, however, that on a mass basis 78.24% silicon dioxide, 77.66% magnesium oxide and 81.41% calcium oxide is rejected from the concentrate and reports to the tails. The behaviour of these three gangue constituents emanates from their large initial concentrations as well as their fine to ultra fine particle size which allows them to become trapped in the concentrate bed. The aluminium oxide concentration is 4.98 % and seems to follow a similar trend to the feed concentration but the content in the concentrate is 4.36%, which is a small decrease from feed to concentrator. The overall rejection for aluminium oxide is 80.76%.

The gangue does impact the final concentrate grade in terms of concentration of gangue but on a mass basis the majority of the gangue is rejected from the Falcon.

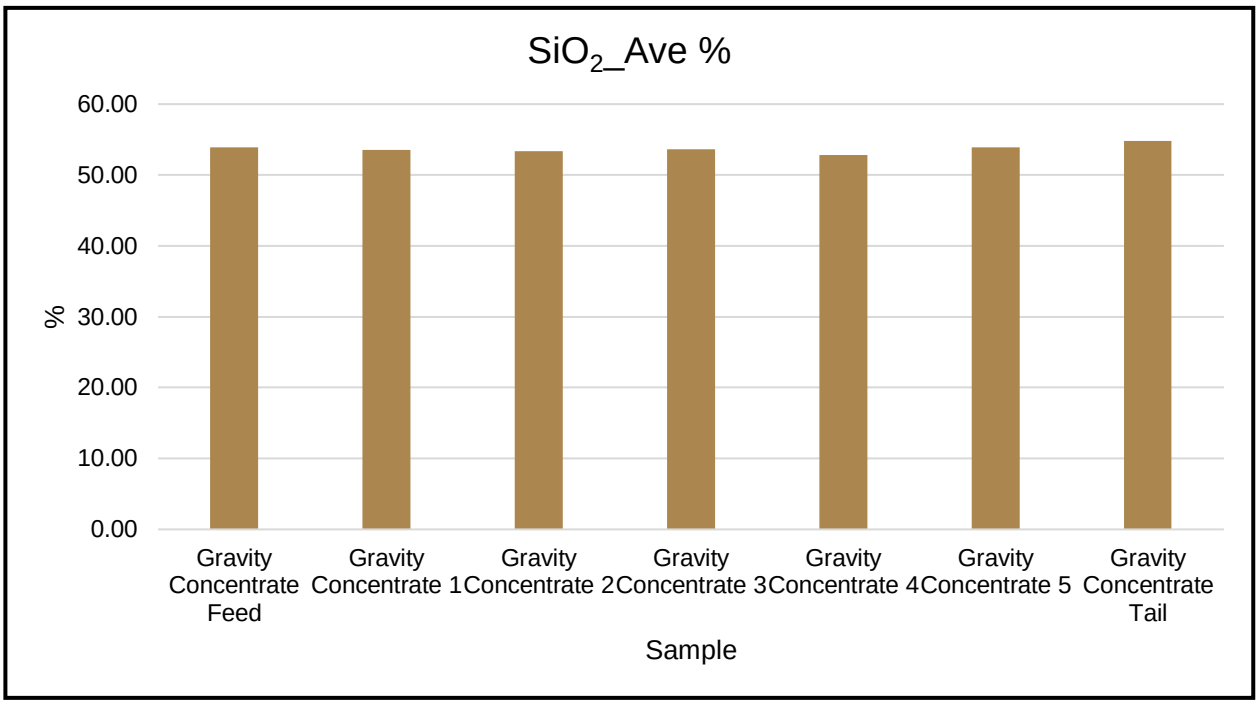

Figure 53: Phase 5 silicon dioxide content in GC feed, concentrates and tail

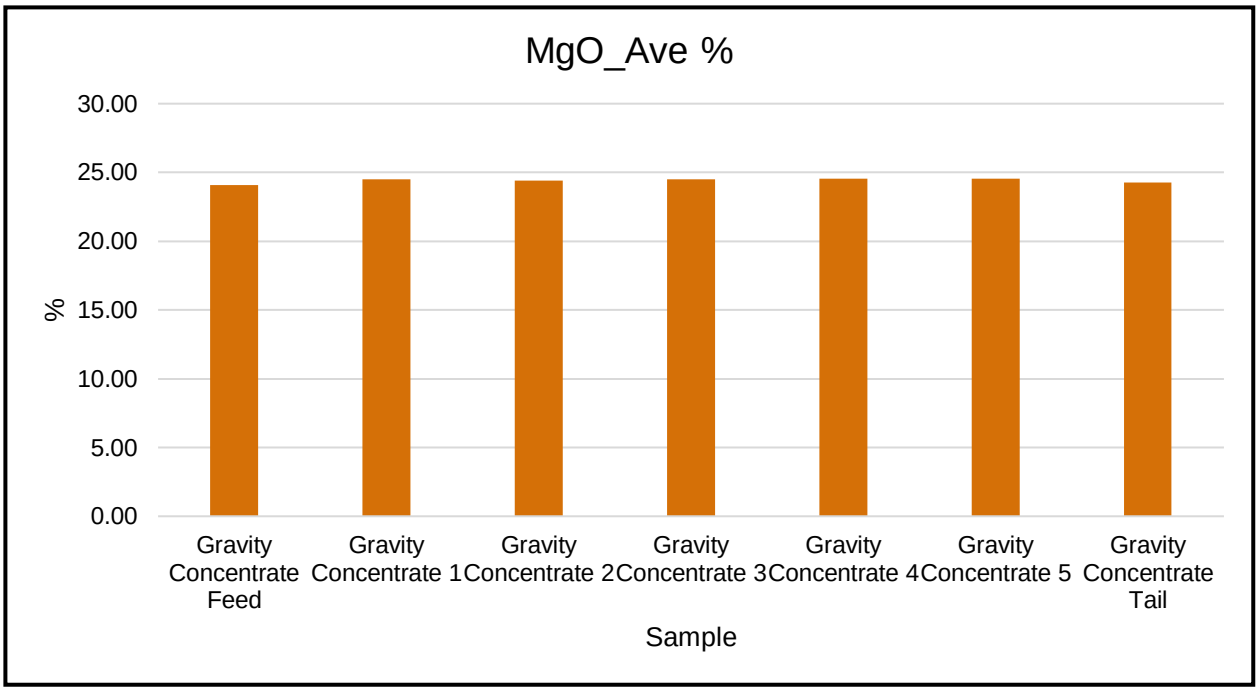

Figure 54: Phase 5 magnesium oxide content in GC feed, concentrates and tail

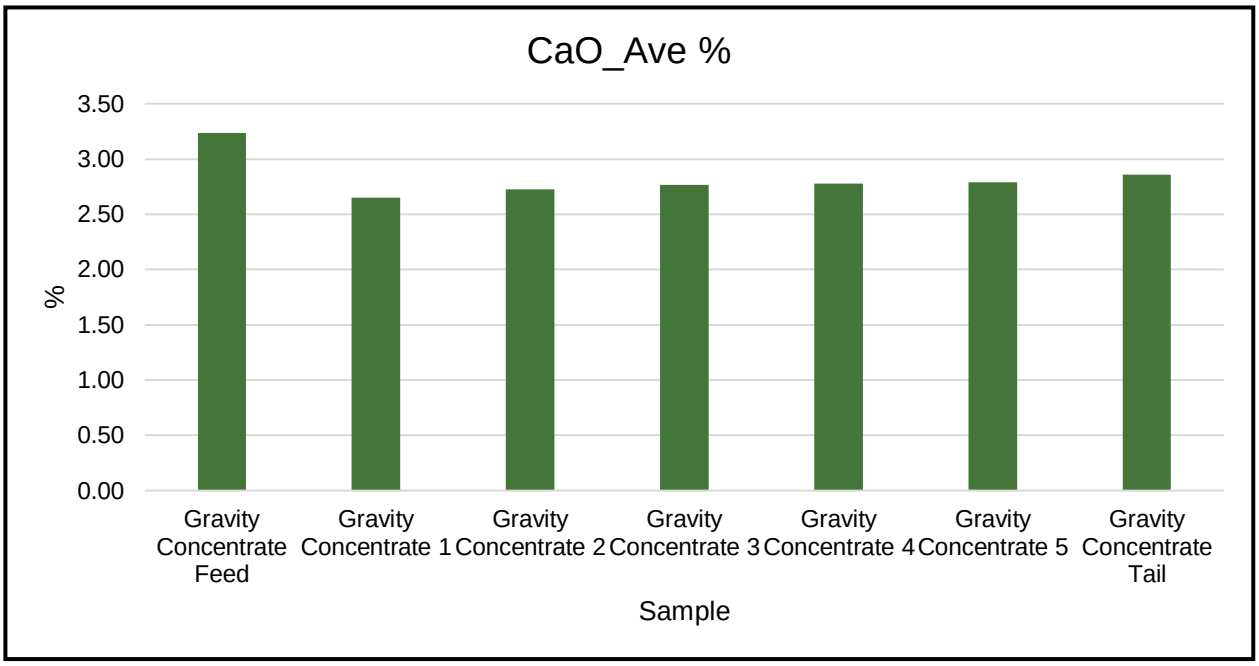

Figure 55: Phase 5 calcium oxide content in GC feed, concentrates and tail

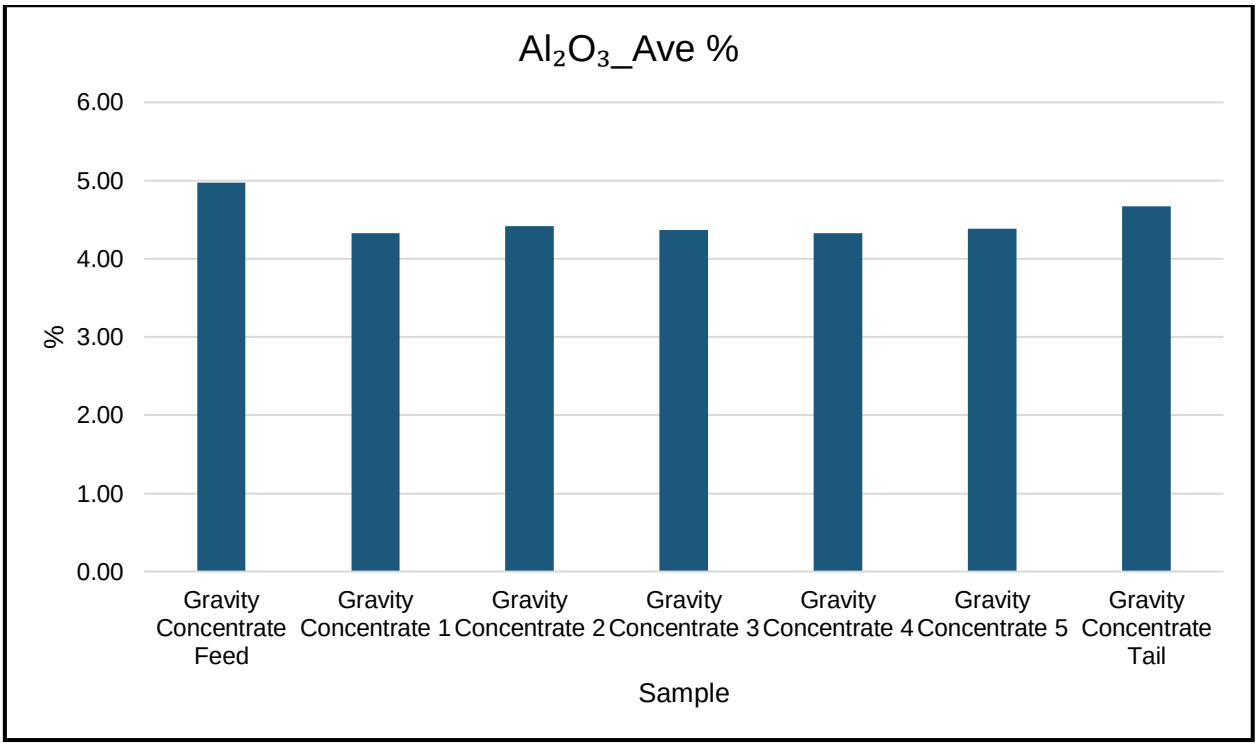

Figure 56: Phase 5 aluminium oxide content in GC feed, concentrates and tail

4.4.6. Particle Size Analysis

A Malvern Mastersizer 3000 (Figure 57) was used to obtain the particle size distribution of the gravity concentration feed (GC Feed), gravity concentration tail (GC Tail) and gravity concentration concentrate (GC concentrate). The GC feed is the initial feed sample as described in Section 3.1. The GC Tail and Concentrate were obtained after the Phase 5 tests as discussed in Section 4.4. The Malvern was used because it can accurately characterize particles of sizes below 25µm which is difficult with manual sieve screening. The samples were repeated three times to ensure repeatability of results obtained and an average was taken for final reporting. The particle size and deportment of PGMs in each particle size fraction and recovery thereof are critical aspects of this research.



Figure 57: Malvern Mastersizer 3000

Table 15: Malvern Mastersizer average results

Grain Size (µm)	1	2	5	8	12	15	20	25	30	38	45	53	62	75	88	106	150	212
GC Feed	0.00	0.88	13.13	24.95	37.49	45.56	57.03	66.29	73.64	82.21	87.41	91.45	94.44	97.07	98.49	99.46	100.00	100.00
GC Tail	0.00	1.39	16.28	28.64	40.65	48.18	58.95	67.75	74.83	83.19	88.28	92.24	95.12	97.60	98.86	99.65	100.00	100.00
GC Concentrate	0.00	0.37	9.55	21.73	36.85	46.84	60.61	71.04	78.76	87.02	91.56	94.76	96.88	98.54	99.32	99.77	100.00	100.00

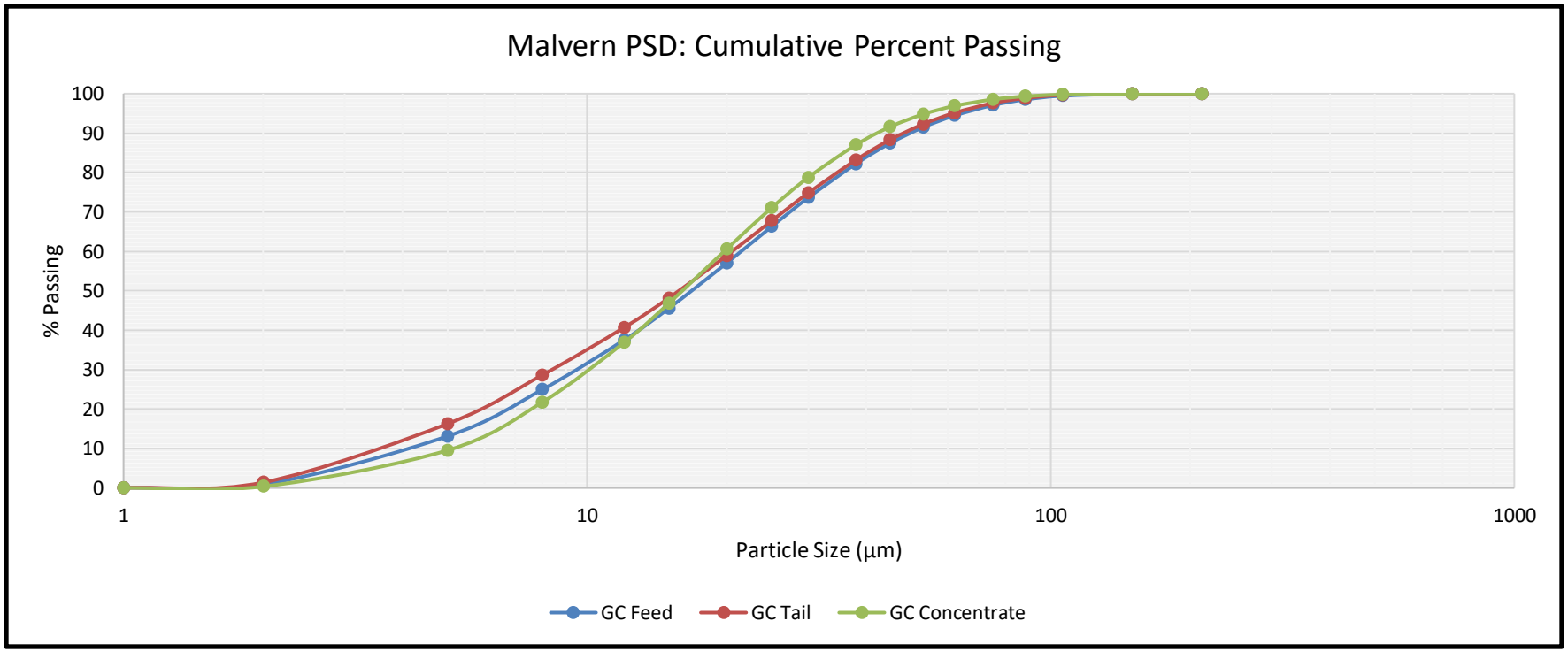

Figure 58: Cumulative percent passing

Table 16: Gravity concentrate samples D_{10}, D_{50} and D_{90}

Sample Category	Sample Name	Dx (10)	Dx (50)	Dx (90)
GC Feed	Average of 'GC Feed 1'	4.07	16.5	50
	Average of 'GC Feed 2'	4.54	17.3	50.2
	Average of 'GC Feed 3'	4.23	16.2	48.4
	Average of 'GC Feed 4'	4.47	17.3	50.5
	Average	**4.33**	**16.83**	**49.78**
GC Tail	Average of 'GC Tail 1'	3.86	16	48.1
	Average of 'GC Tail 2'	3.71	15.4	47.6
	Average of 'GC Tail 3'	3.86	15.9	48.7
	Average	**3.81**	**15.77**	**48.13**
GC Concentrate	Average of 'GC C1'	5.13	15.9	40.9
	Average of 'GC C2'	4.91	15.4	41
	Average of 'GC C3'	5.23	16.2	42.5
	Average of 'GC C4'	5.27	16.6	43.6
	Average of 'GC C5'	5.05	16.1	43.2
	Average	**5.12**	**16.04**	**42.24**

Table 15 and Figure 58 indicates the cumulative percent passing for each sample. It is visually evident from the graph that the GC Tail is finer than the GC Feed in the -53µm range but almost similar in the +62 -212µm range. The GC Concentrate is coarser that the GC feed in the -15µm range but finer in the +60 -212µm range. The GC concentrate particle size volume passing 75µm, 53µm and 25µm are all greater than the GC Feed and GC Tail which demonstrates that the GC is able to recover the fines and ultra-fines without the particles reporting completely to the tails.

The D_{10}, D_{50} and D_{90} of the samples were subjected to an ANOVA test in excel to determine whether statistical difference was present in the samples. The D_{10}, D_{50} and D_{90} all have a p-value < 0.05 which indicates a statistically significant differences between group means. This can be interpreted as an effective separation of particles as the expectation was for the process to recover fines and ultra-fines. Table 16 indicates that the D_{90} of the GC concentrate is 42.24µm compared to the GC feed which is 49.78µm and the GC tail which is 48.13µm, this shows that 90% of the GC concentrate is much finer overall. The D_{50} between samples are similar but

statistically different with the GC tail and GC concentrate being finer than the feed. The D_{10} indicates an interesting trend in that the GC concentrate is coarser (5.12µm) than the GC feed (4.33µm) and the GC tail (3.81 µm), this implies that the gravity concentration unit either rejects these particles due to lower density or cannot recover them due to the small size and hence this size fraction reports to the GC tail.

The particle size analysis proves the following:

- The feed to the gravity concentrator consists of fines and ultra-fines with 97.07% passing 75µm.
- The product of the gravity concentrator i.e. the GC concentrate recovers fines and ultra-fines.
- It becomes more difficult to recover particles less than 15µm, but the gravity concentrator is still able to recover some of these particles.

See **Appendix C** for all PSD data and statistical output.

4.4.7. Fractional Analysis

A fractional analysis was performed on the GC feed, GC tail and GC concentrate samples to determine the deportment of PGMs, gangue and chrome in the various particle sizes. Each sample was screened until a sufficient mass of sample was recovered for each particle size fraction to be assayed. A 6E analysis (Nickel-sulphide collection method), base metals, gangue and chrome was done at a South African National Accreditation System (SANAS) laboratory for PGMs. The analysis included fire assay and ICP-MS.

The results in this section are from Phase 6 of the experimental program in which the optimal parameters were utilized as in Phase 5 but the purpose of this phase was to collect enough sample for manual sieving (wet and dry) to obtain sufficient sample for analysis. The manual PSD analysis was comparable to the Malvern results with 97-98% passing 75µm and 66-70% passing 25µm for the GC feed, GC tail and GC concentrate. In general, Malvern results and manual sieving results do not agree to a high degree due to the fact that the Malvern measures the PSD based on volume whilst the manual sieving is based on diameter and particle shape. In this study the methods show similar results due to the narrow size range of the samples.

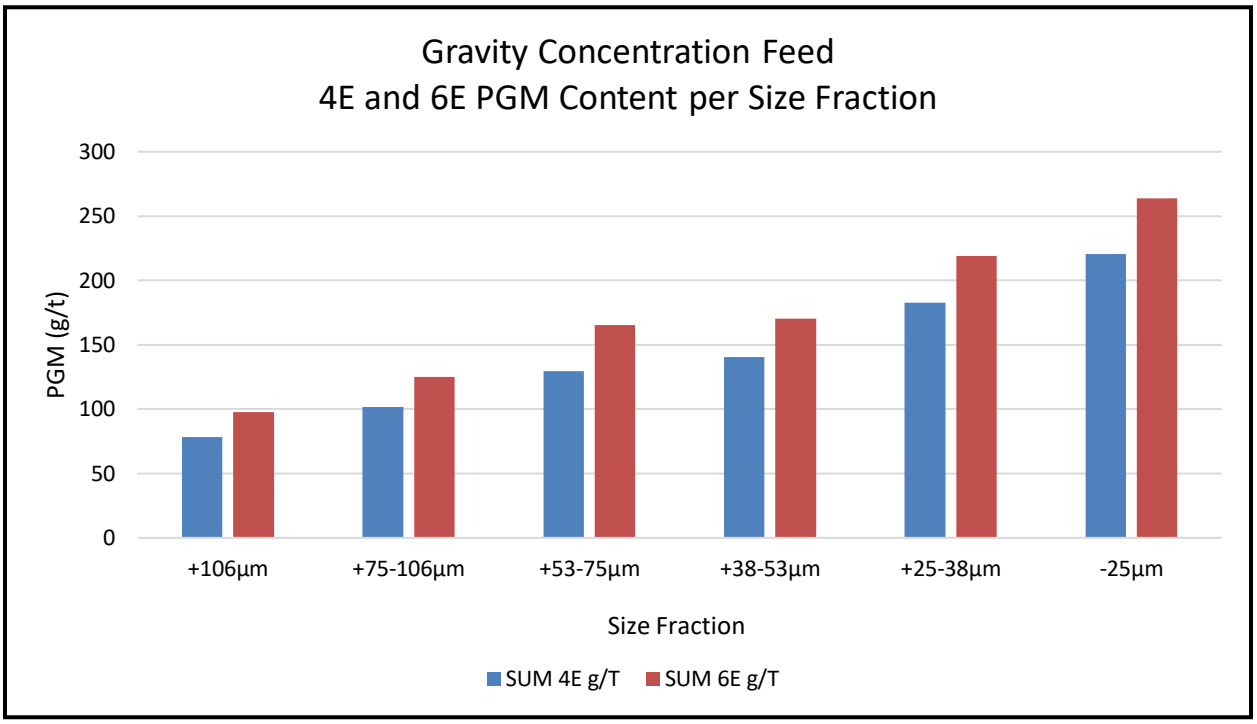

Figure 59: GC feed 4E and 6E PGM content per size fraction

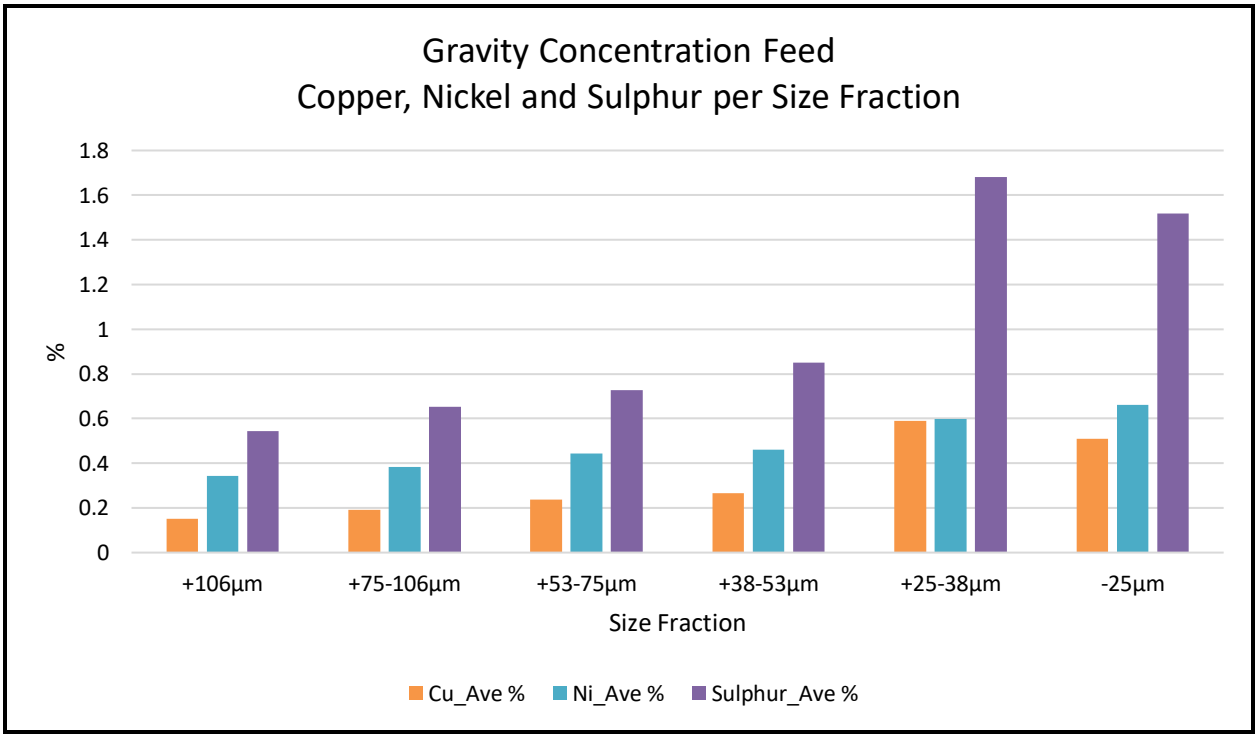

Figure 60: GC feed Copper, Nickel and Sulphur per size fraction

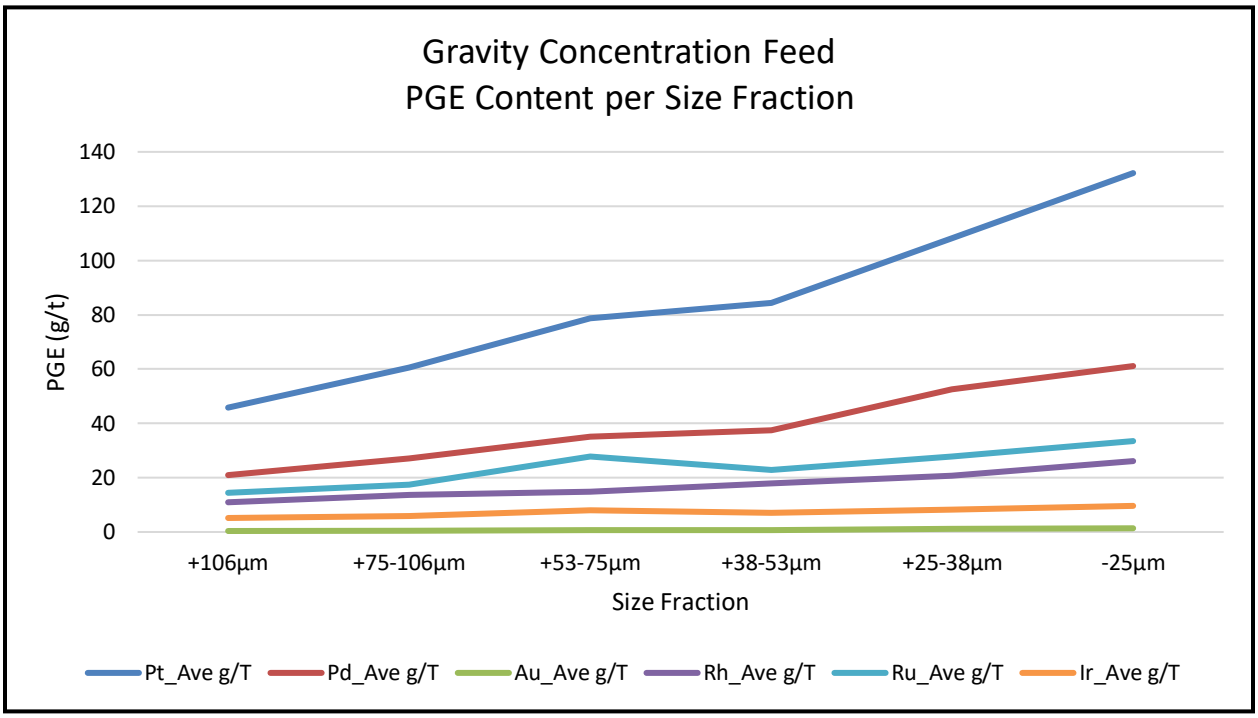

Figure 61: GC feed PGE content per size fraction

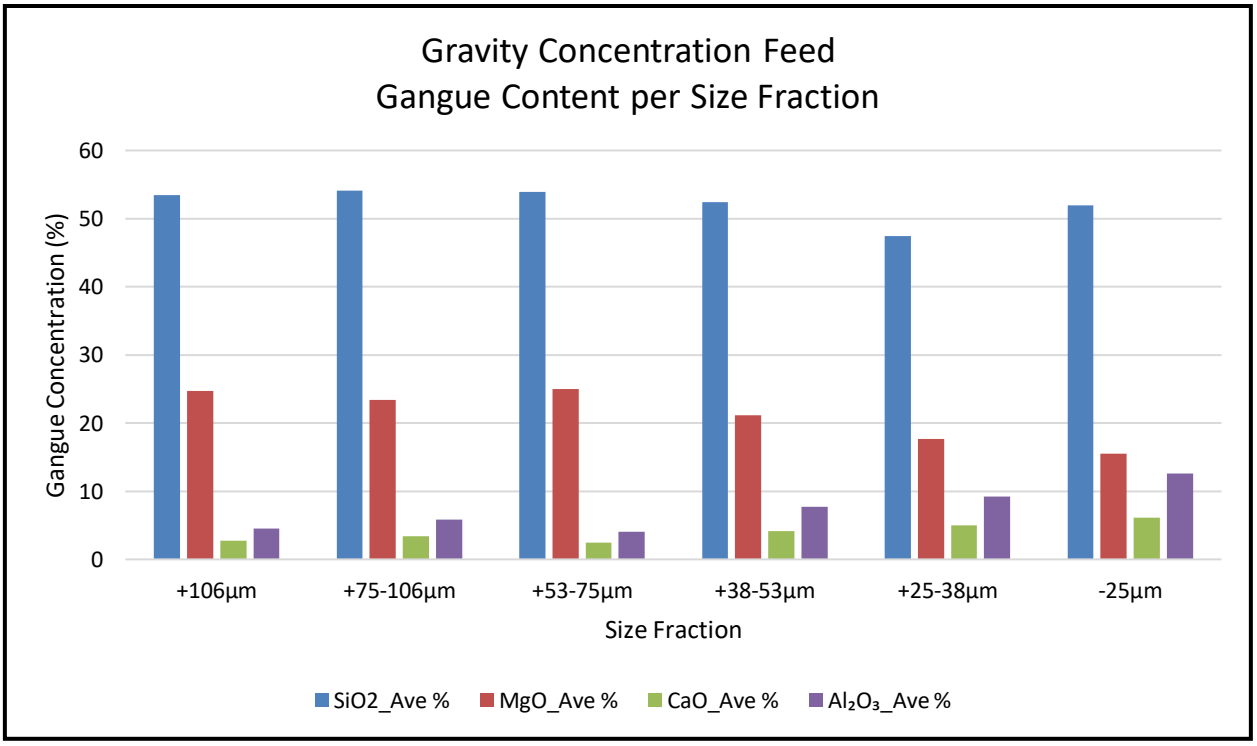

Figure 62: GC feed Gangue content per size fraction

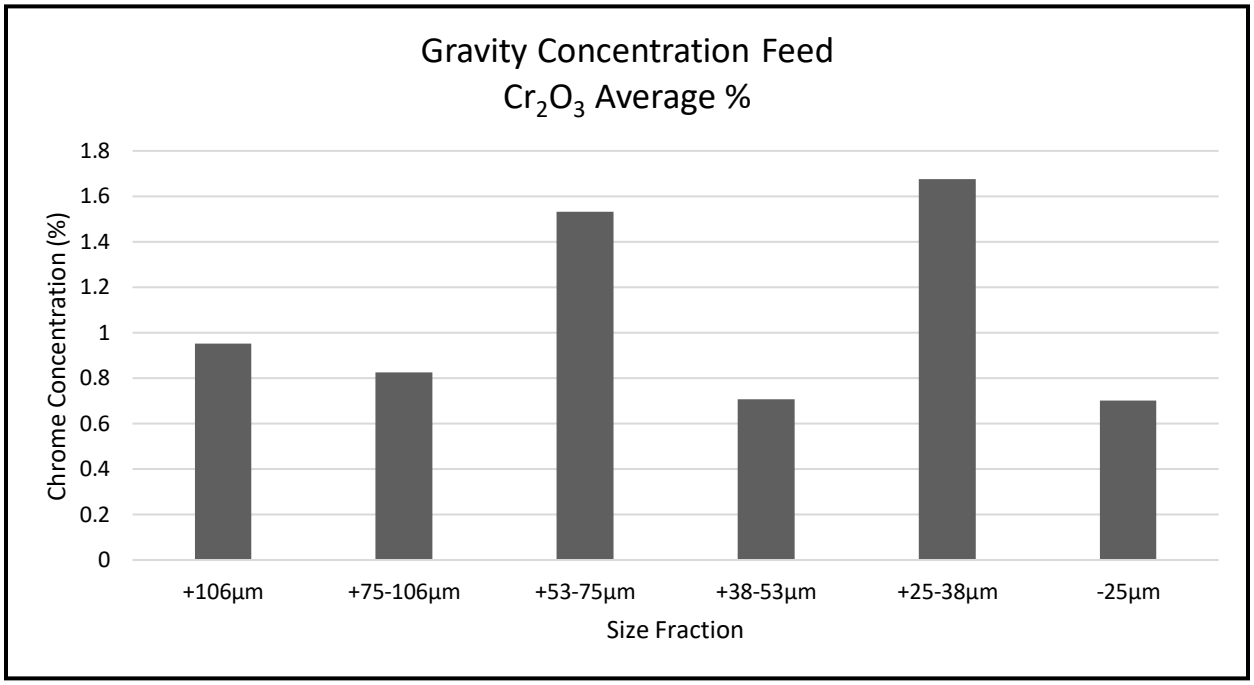

Figure 63: GC feed Chromium per size fraction

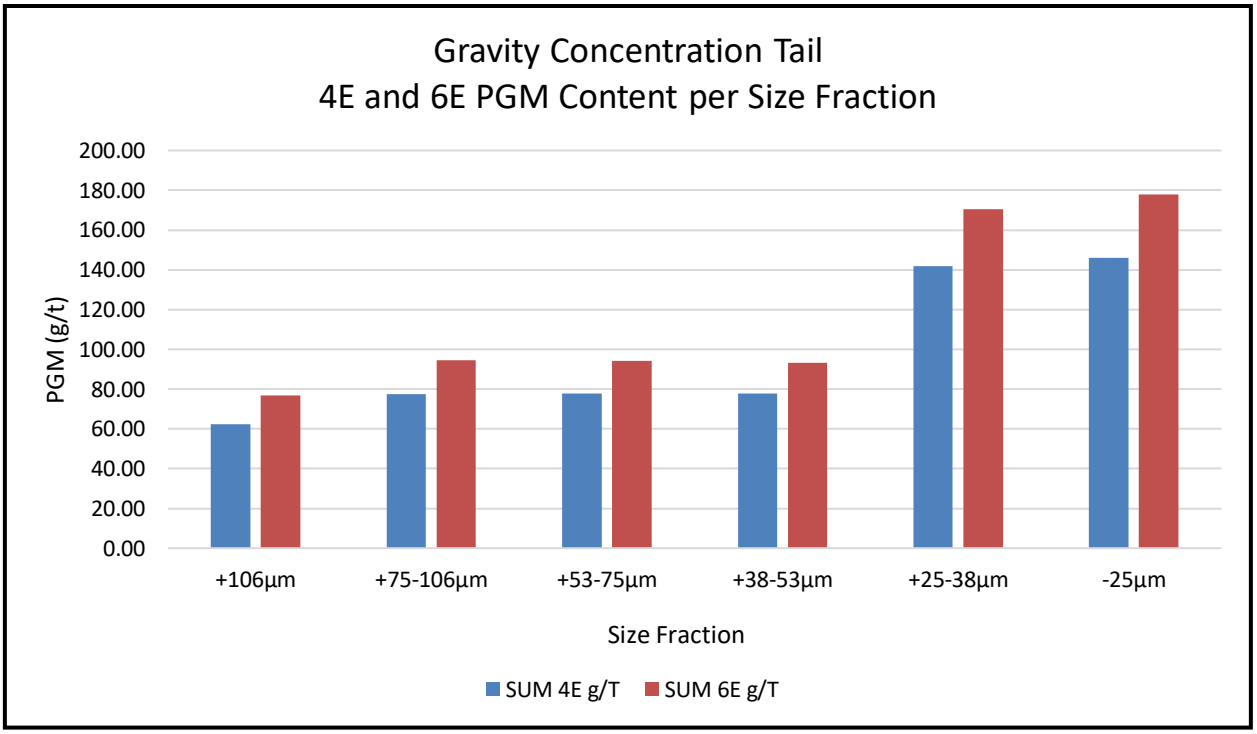

Figure 64: GC tail 4E and 6E PGM content per size fraction

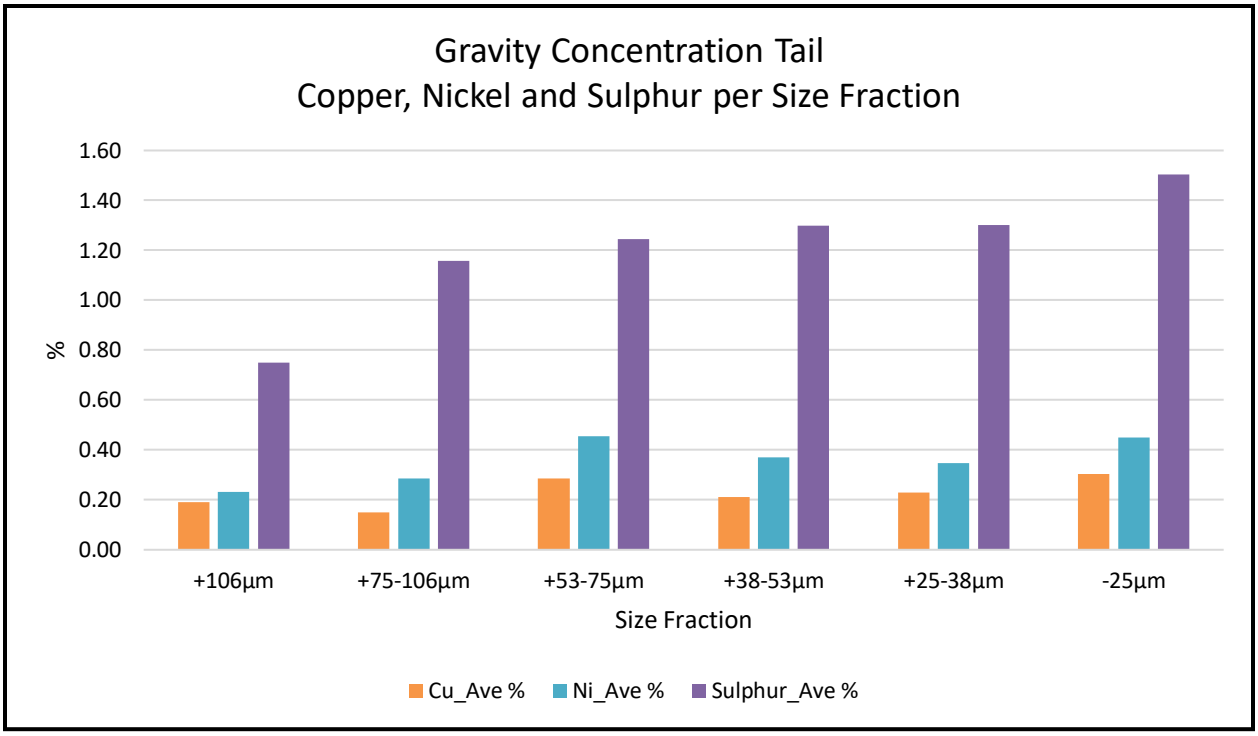

Figure 65: GC tail Copper, Nickel and Sulphur per size fraction

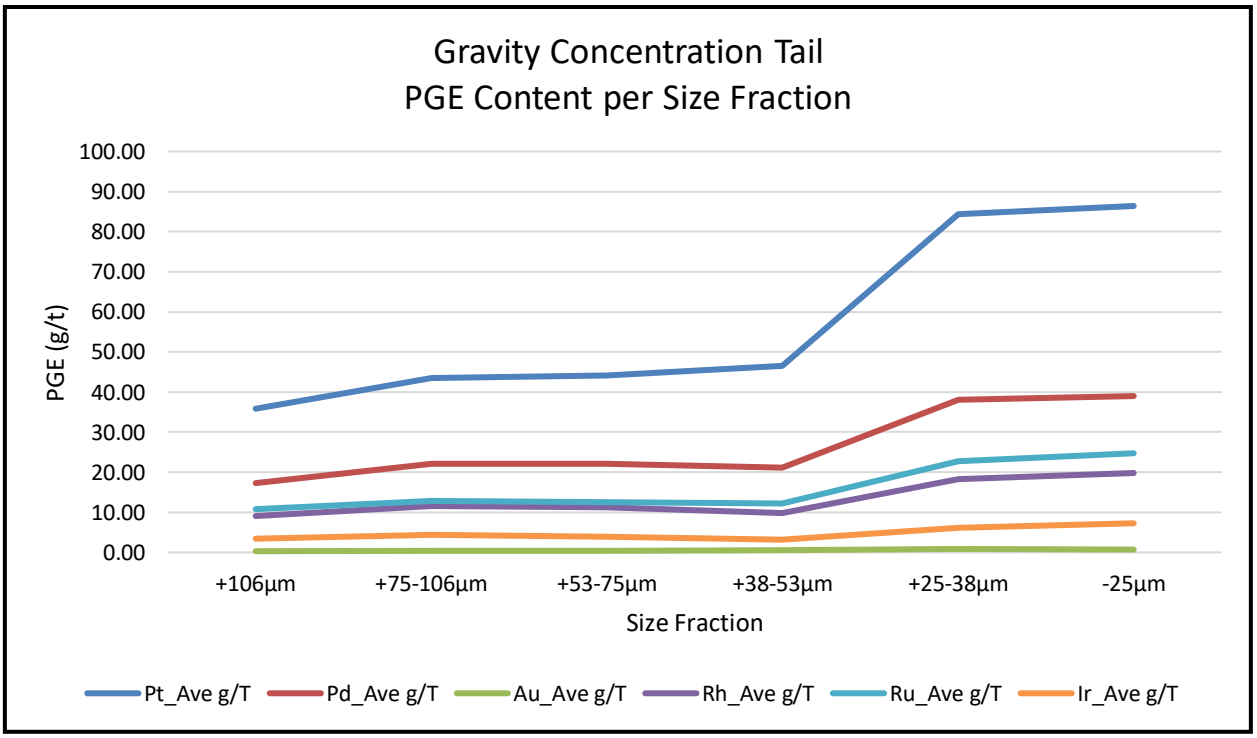

Figure 66: GC tail PGE content per size fraction

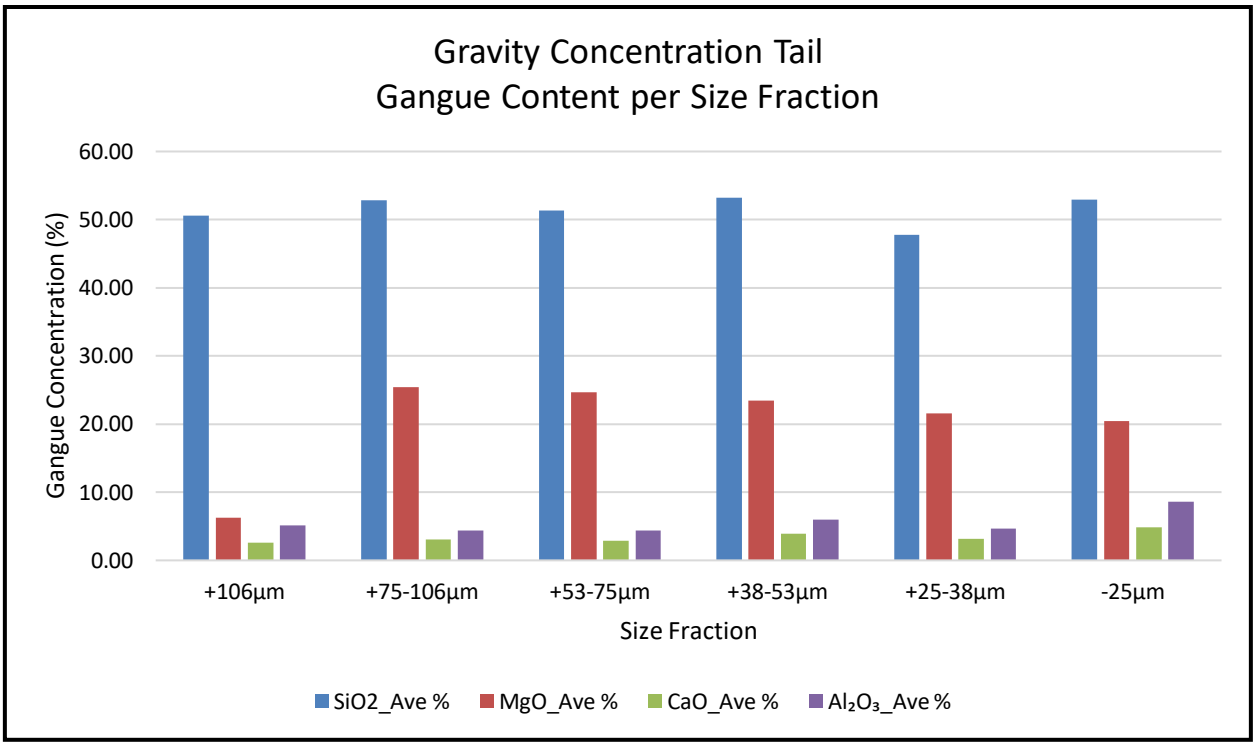

Figure 67: GC tail Gangue content per size fraction

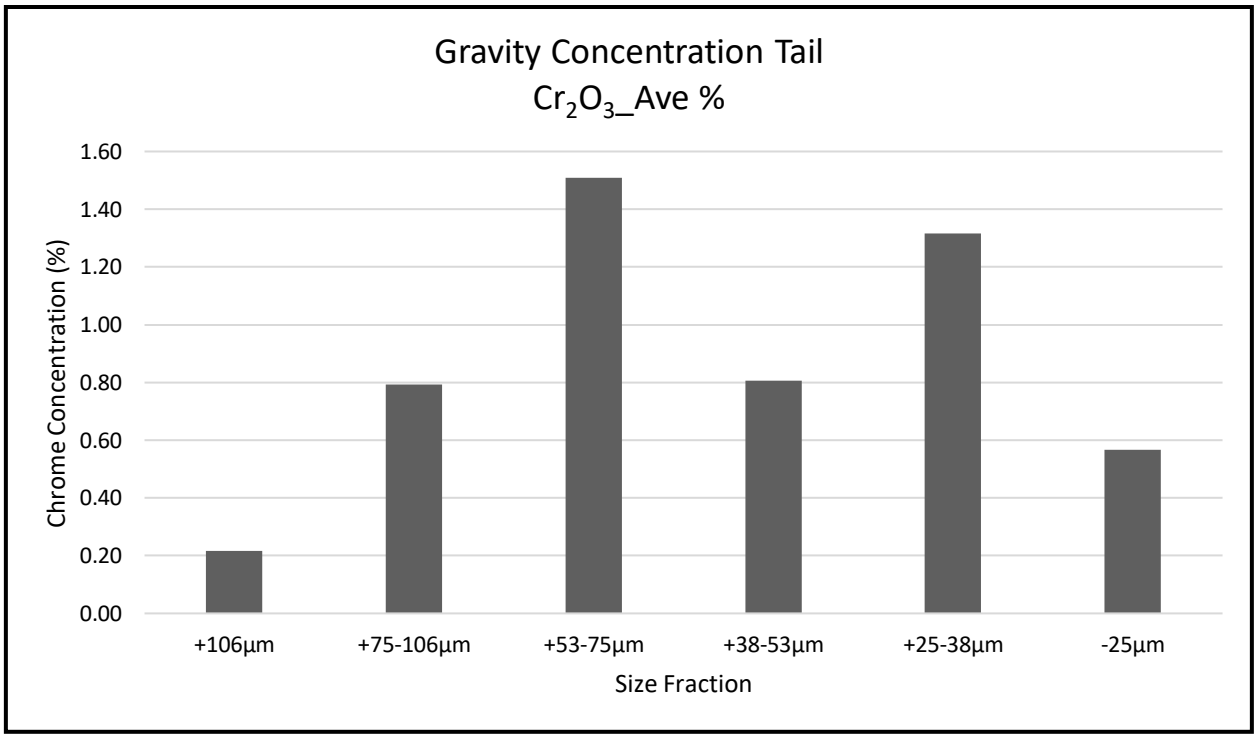

Figure 68: GC tail Chromium per size fraction

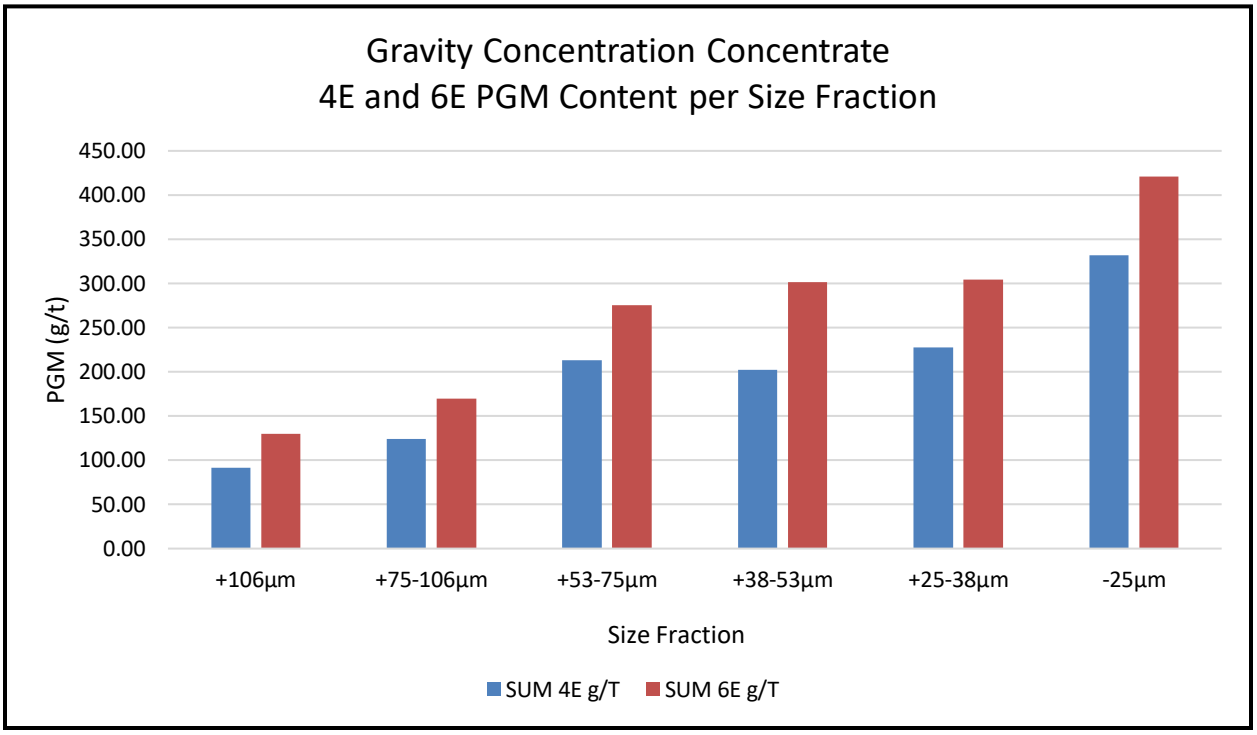

Figure 69: GC concentrate 4E and 6E PGM content per size fraction

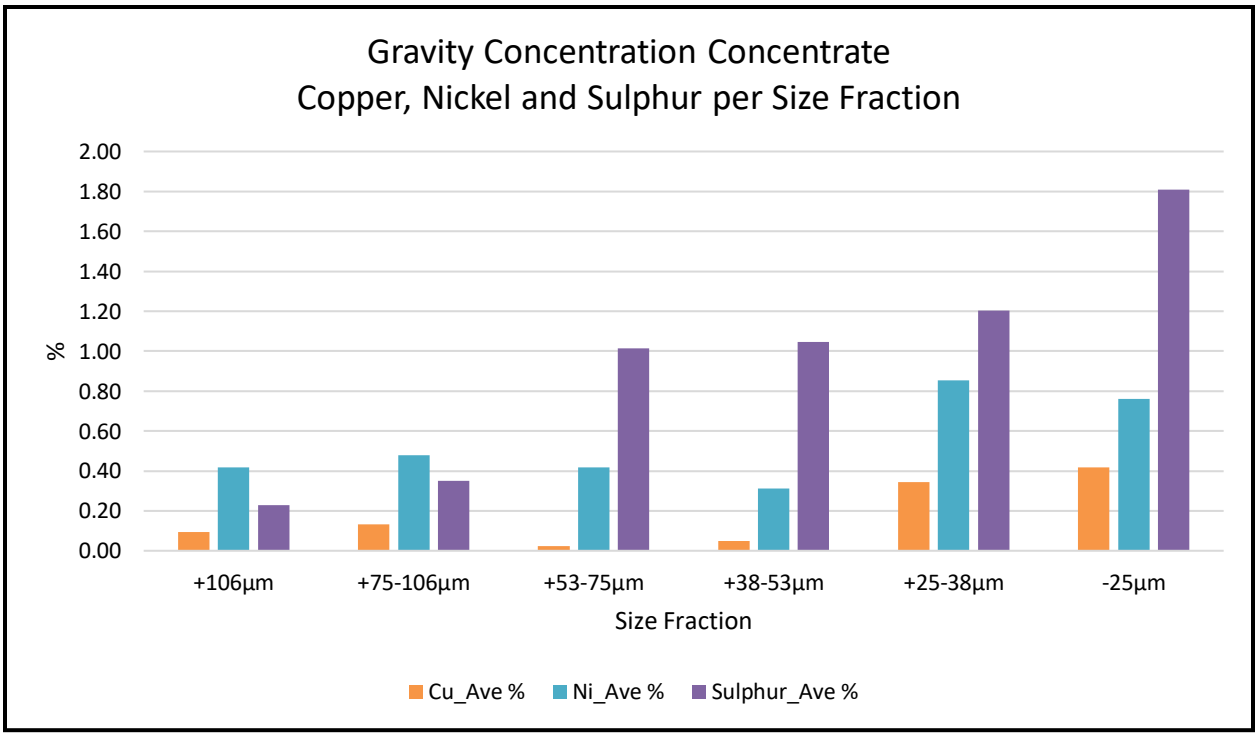

Figure 70: GC concentrate Copper, Nickel and Sulphur per size fraction

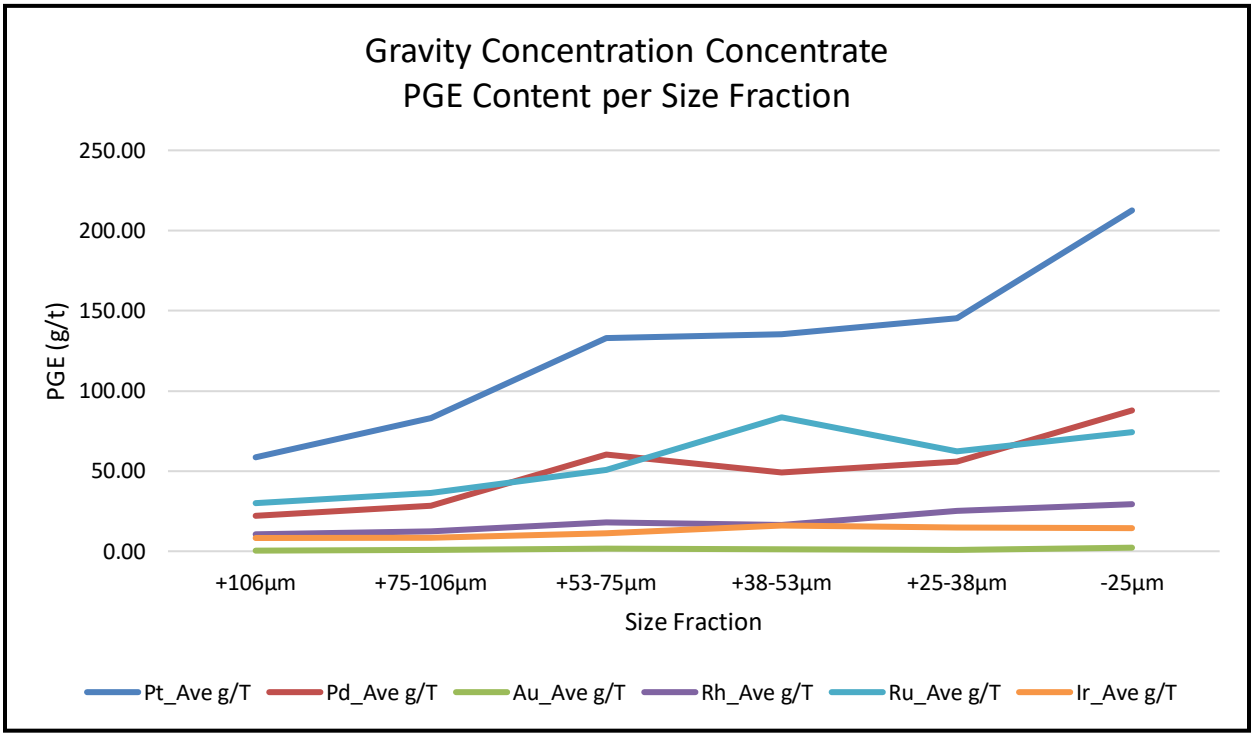

Figure 71: GC concentrate PGE content per size fraction

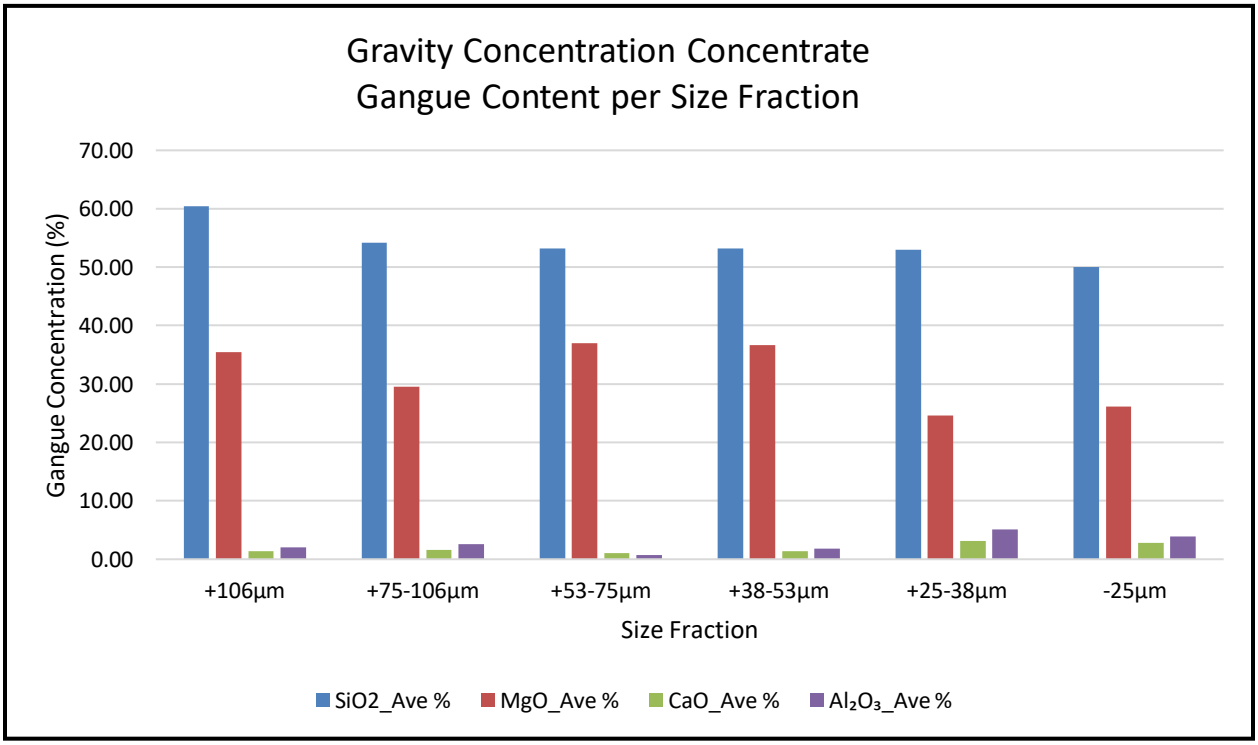

Figure 72: GC concentrate Gangue content per size fraction

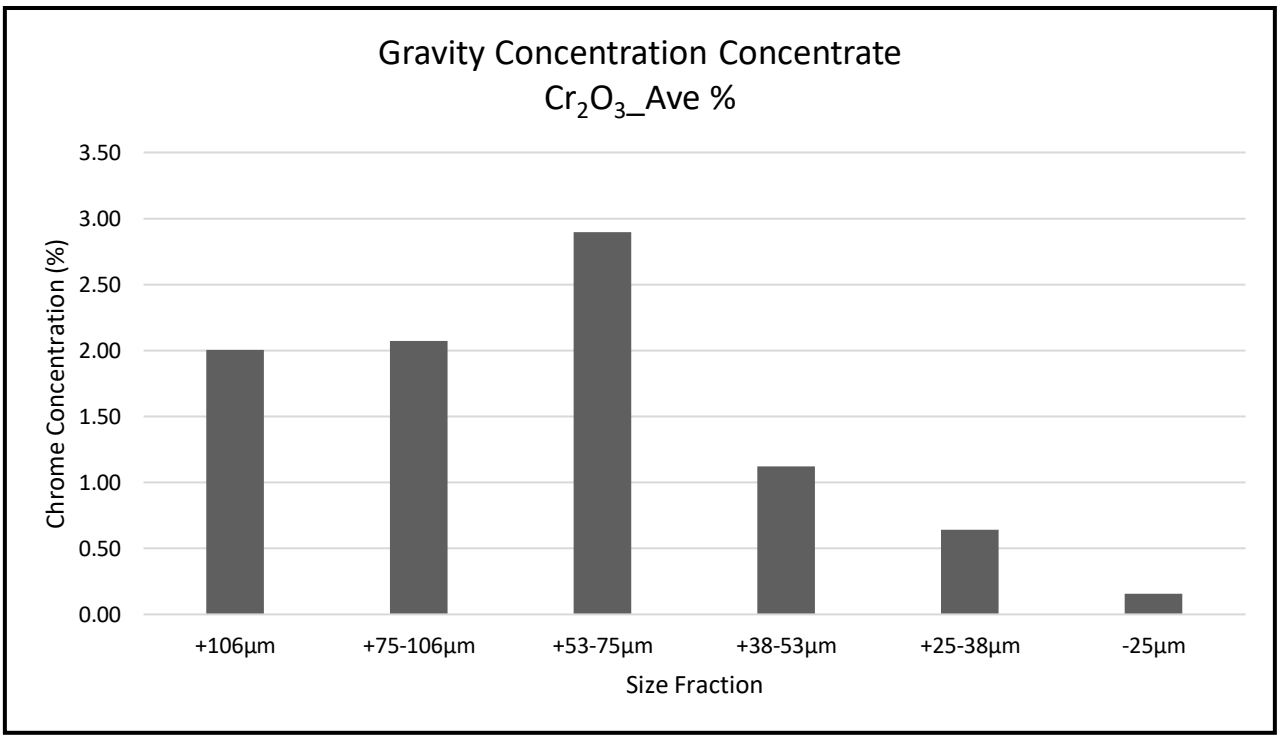

Figure 73: GC concentrate Chromium per size fraction

The results for 4E (platinum, palladium, gold and rhodium) and 6E (platinum, palladium, gold, rhodium, iridium and ruthenium) per size fraction are shown in Figure 59, Figure 64 and Figure 69. All samples indicate that the PGMs are concentrated in the fine and ultra-fine fractions and the lowest concentrations are found in the +106µm and -106+75µm fractions. The high PGM concentrations in the GC concentrate fines and ultra fines fraction indicates that the Falcon concentrator can recover PGMs in this fine size range (below 75µm and even below 25µm) successfully. The GC tail sample shows a similar trend; however the tail losses may possibly be due to retention time and number of runs that the lab unit can do, this will be discussed later in the report.

The results for copper, nickel and sulphur per size fraction are shown in Figure 60, Figure 65 and Figure 70. The data indicates that the highest concentrations of the base metal sulphides are in the fine and ultra-fine fraction. This correlation with 4E/6E graphs demonstrates that PGMs are strongly associated with base-metal sulphides in the fines and ultra-fines fractions. The individual PGE per size fraction are shown in Figure 61, Figure 66 and Figure 71. The GC feed,

GC tail and GC concentrate samples indicates that platinum is the most dominant PGE in all size fractions followed by palladium and ruthenium. Gold has the lowest concentration in all size fractions of the feed, tail and concentrate samples and Iridium has a fairly low concentration in all size classes. The GC tail indicates that most of the PGM tail losses are due to platinum and palladium in the fine to ultra-fine fraction. The GC concentrate indicates that more ruthenium than palladium is recovered from the -53+25µm fraction, this could be due to mineralogical associations of ruthenium with pentlandite and pyroxenite in that size fraction or free ruthenium in that size fraction that allows an ease in gravity concentration.

The gangue per size fraction data is shown in Figure 62, Figure 67 and Figure 72. The Silicon dioxide is approximately 50% in all size fractions except for the +106µm GC concentrate sample where it is higher at 60%. This is due to the gravity concentrator recovering the coarse silicon dioxide. The magnesium oxide is approximately 20-24% in the +106+38µm fraction of the GC feed. The -38µm fraction has the lowest concentration at approximately 15%. The GC tail has the lowest concentration of magnesium oxide in the +106µm fraction and 20-25% in the other size fractions. The GC concentrate has high magnesium oxide concentrations (over 30%) in the +106, +53-75 and +38-53µm particle sizes. The calcium oxide and aluminium oxide are fairly low in all size fractions and samples but show a minor increase in the -38µm fraction. These results indicate that gangue is not concentrated as such in the gravity concentrator but is split rather evenly between the feed, tail and concentrate. The fact that low density gangue reports to the concentrate of the gravity concentrator is based on statistical probability as 50% of the feed to the Falcon is Silicon dioxide and 24% is magnesium oxide hence it will be difficult to separate these gangue constituents completely. Higher concentrations of gangue in the coarser particle range of the concentrate are due to the larger particle size, shape and overall larger comparative mass.

The chrome content in the size fractions is shown in Figure 63, Figure 68 and Figure 73. The GC feed and GC tail seem to have a larger proportion of chrome in the +53-75µm and +25-38µm size ranges. The GC concentrate has a higher proportion of chrome in the +160, +75-106 and +53-75µm range, most probably due to the coarseness of the chrome in these ranges. The -53µm range has low chrome compared to the feed which means that the chrome in this fine fraction is

rejected from the concentrator. On a mass balance basis this means most of the chrome is rejected as the GC concentrate contains about 94.76% -53µm particles.

The fractional analysis therefore confirms that the majority of the PGMs are contained in the fine and ultra-fine fractions and that these fractions are recoverable by the gravity concentrator. The chrome from these fractions is also significantly rejected by the Falcon concentrator.

4.4.8. Fluidized Bowl Experiments

The optimal parameters were also applied to the fluidized bowl experiments. In these experiments the Falcon fluidized bowl was used to determine the effect of fluidizing water flow on the gravity concentration of the feed material. The fluidizing flowrate used was 1 L/min, 2 L/min and 4 L/min. The fluidizing bowl is generally not recommended for fine and ultra-fine material as the water velocity tends to carry high value particles in the fine size range to the tailings stream, nonetheless, these experiments were carried out to gain insight into the PGMs and gangue mineral recovery under fluidizing conditions.

The typical concentrates produced for each stage is shown in Figure 74 (a) – (e). Stage 1 has a darker grey/black to brown colour and this gradually gets lighter over the stages with stage 5 having a light grey/brown colour. The colour difference in these samples is due to the PGM concentration being higher in the first stage and gradually decreasing in subsequent stages. Figure 74 (f) indicates the action of the fluidizing water through the bowl water ports. This fluidizing water alters the concentrate bed and feed slurry by adding additional water velocity to the bowl and thus carries out lighter and smaller particles.

Table 17 indicates the summary of the results from Falcon fluidized bowl experiments. The mass pull remained constant at 8.7% for all runs, which indicates that this is the limiting volume available for solids. This mass pull is far less than the 21.9% achieved with the unfluidized bowl. The reason for the lower mass pull is the constant fluidizing water that essentially carries away fine and ultra fine particles of value and erodes the concentrate bed. The moisture content of the concentrates was approximately 30.24%, this is higher than in Phase 5 due to the addition of fluidizing water.

Table 17: Summary of fluidized bowl experiments

Experiment	Fluidising Water Flowrate (L/min)	Mass Pull (%)	Recovery (%)	Average Weighted Grade (g/t 4E)
Run 1	1	8.7%	36.3%	546.5
Run 2	2	8.7%	32.0%	481.8
Run 3	4	8.7%	20.2%	303.8

The overall recovery achieved for experiments conducted at fluidising water flowrate of 1, 2 and 4 L/min was 36.3%, 32.0% and 20.2% respectively. The results show that as the flow rate of fluidizing water increase the recovery decreases. The likely reason for this observation is that the increased velocity of the fluidizing water increases the drag forces on the fine and ultra fine heavier particles leading to much less PGMs reporting to the concentrate as the water flow rate increases. The overall weighted grade achieved with increasing fluidising water flowrate was 546.5, 481.8 and 303.8 g/t 4E respectively. These data indicate that higher grades are achievable with the Falcon fluidized bowl compared to the ultra-fine unfluidized bowl.

Figure 75 shows the cumulative stage 4E recovery for each run, it is evident that the lower fluidizing flow rate yields a higher recovery. Figure 76 shows the 4E grade per stage, it is evident that the lower fluidizing flow rate yields higher concentrate grade. The highest grades are achieved in the first stage (GC concentrate 1) and the grade gradually decreases with recovery stages.

The base metals and sulphur concentrations are considerably higher in the concentrates than in the feed which again proves the association of base metal sulphides with PGMs (Figure 77).

The cumulative chrome rejection for run 1, run 2 and run 3 are 90.85%, 91.16% and 92.18% respectively. This indicates that as the fluidizing flow increases there is a direct decrease in the chrome content in the concentrate. This is due to the action of the fluidizing water which acts on the chrome and chrome-silica complexes allowing the chrome to report to the tails stream. Figure 79 shows the chrome concentration in the feed and per stage, the results indicate that there is not a large variance in the chrome concentration from the feed to the concentrates except for run 3 which indicates lower chrome in concentrate due to the higher fluidizing water flow rate.

The largest gangue constituents (Table 18) have a very similar concentration in the feed and in the concentrates with silicon dioxide at 50% and magnesium oxide at 24%. The feed contains 3.24% and 4.98% calcium oxide and aluminium oxide respectively whereas the concentrates contain 2.4% and 4.1% calcium oxide and aluminium oxide respectively. This may be due to the presence of more calcium oxide and aluminium oxide in the fine fraction. On a mass basis the rejection of all gangue constituents was greater than 99%.

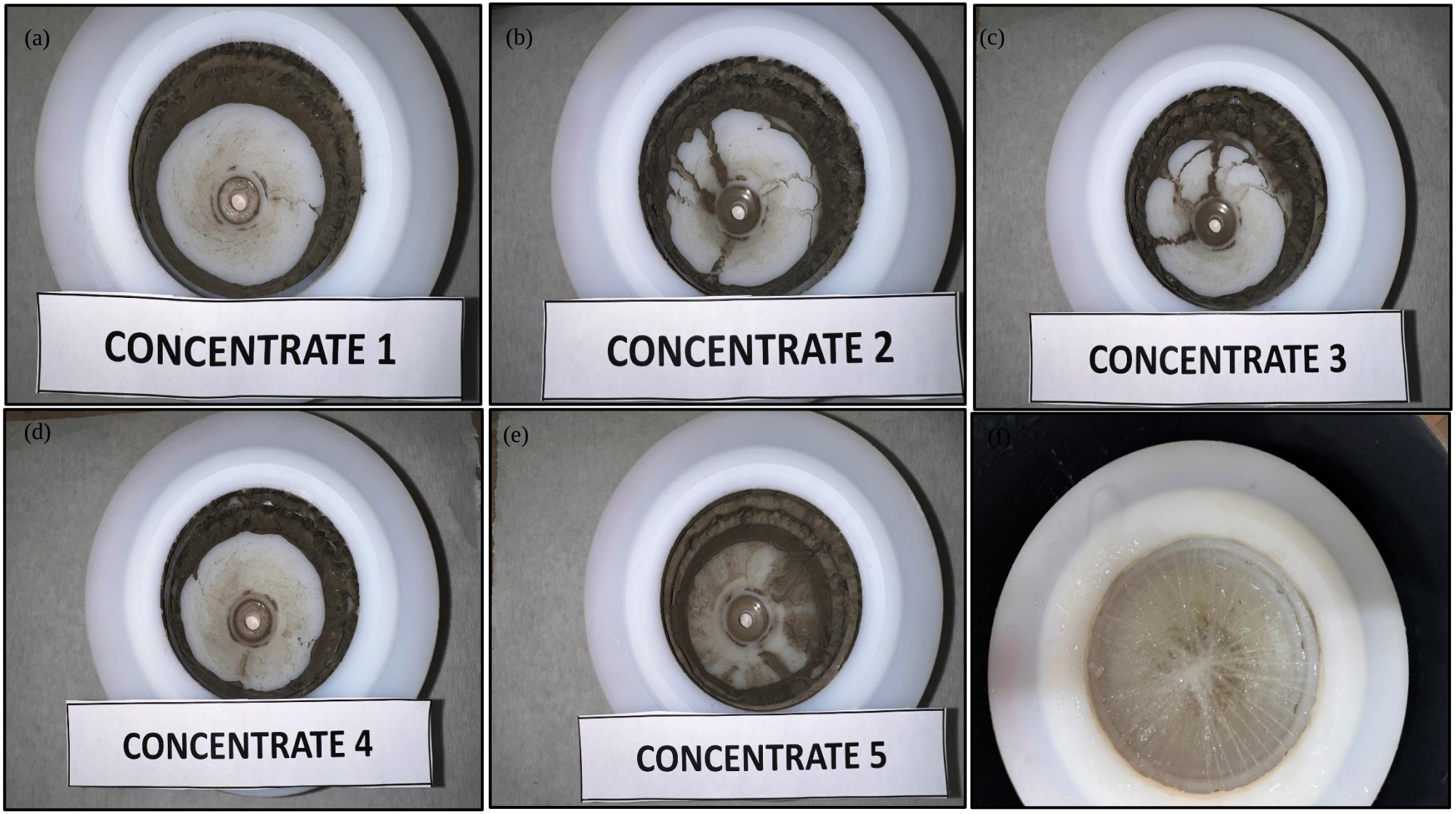

Figure 74: GC Concentrate fluidized bowl images showing (a) GC concentrate 1. (b) GC concentrate 2. (c) GC concentrate 3. (d) GC concentrate 4. (e) GC concentrate 5 and (f) close-up image of fluidizing water

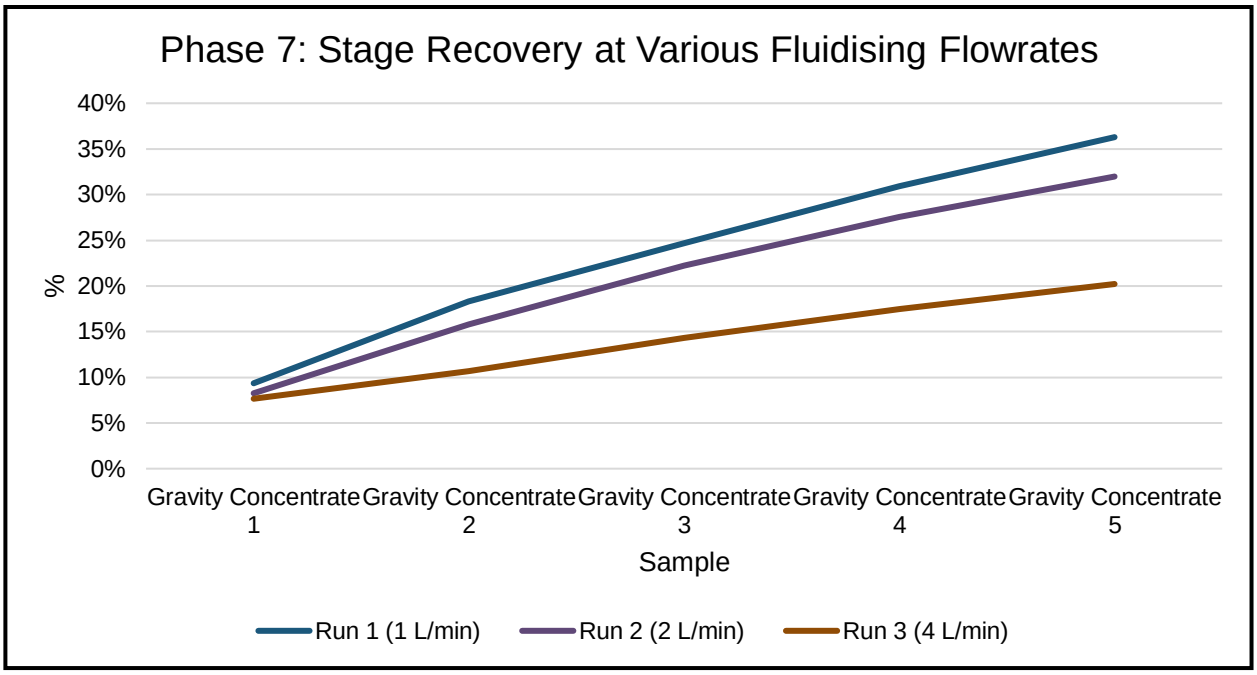

Figure 75: Phase 7 stage recovery at various fluidizing flow rates

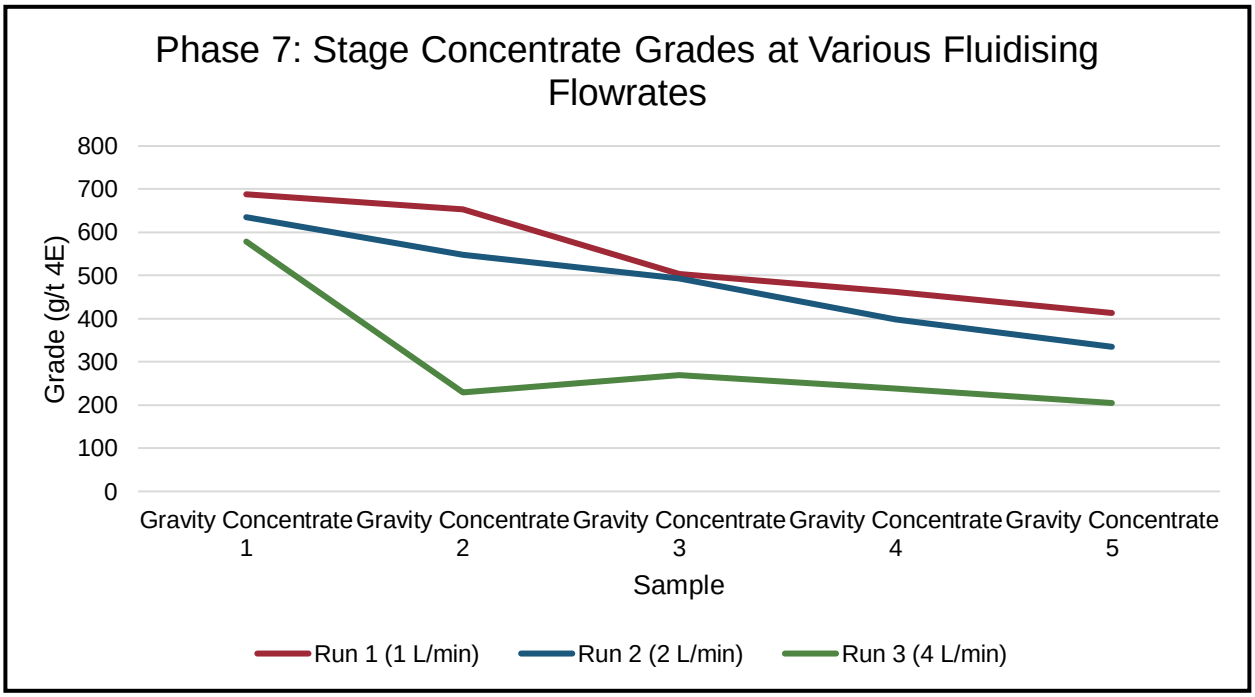

Figure 76: Phase 7 stage grade at various fluidizing flow rates

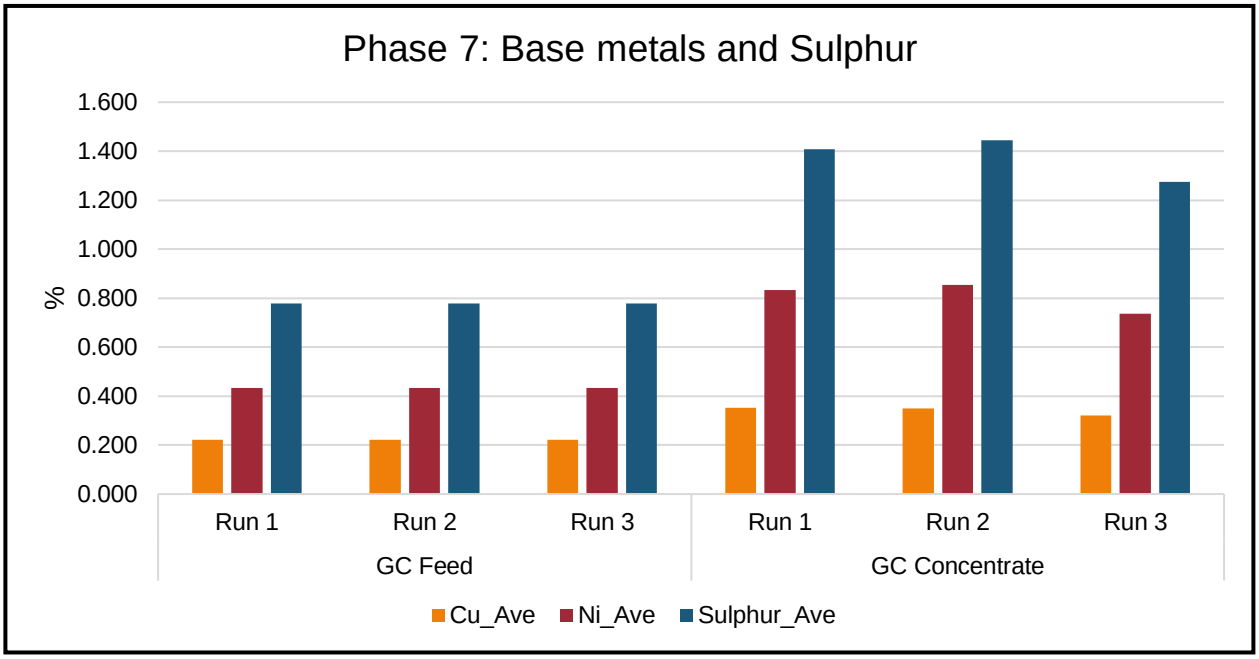

Figure 77: Phase 7 base metals and sulphur content

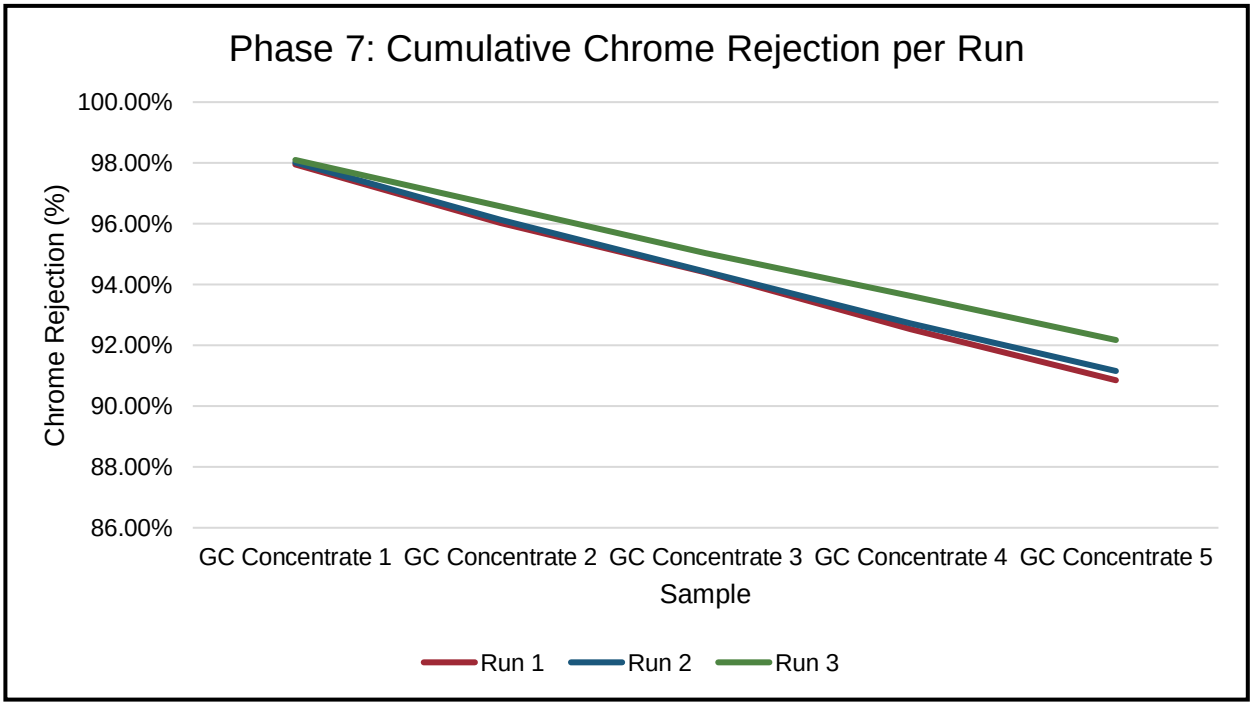

Figure 78: Phase 7 cumulative chrome rejection

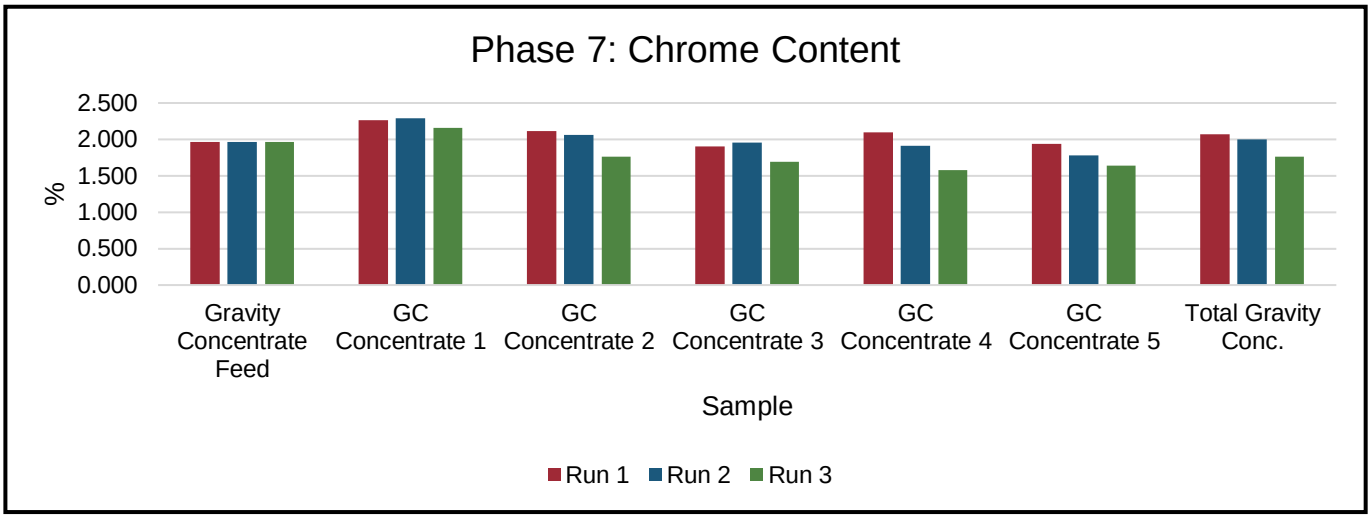

Figure 79: Phase 7 chrome content

Table 18: Phase 7 gangue content

Sample	SiO_2_Ave			MgO_Ave			CaO_Ave			Al_2O_3_Ave		
	Run 1	Run 2	Run 3	Run 1	Run 2	Run 3	Run 1	Run 2	Run 3	Run 1	Run 2	Run 3
Gravity Concentrate Feed	53.923	53.923	53.923	24.066	24.066	24.066	3.235	3.235	3.235	4.977	4.977	4.977
GC Concentrate 1	49.893	48.272	49.324	24.028	23.723	24.172	2.461	2.474	2.374	4.229	4.374	4.031
GC Concentrate 2	49.479	48.809	50.583	24.527	24.032	24.901	2.162	2.340	2.344	3.669	4.008	3.802
GC Concentrate 3	49.682	49.710	49.940	24.262	24.699	23.777	2.456	2.259	2.688	4.109	3.747	4.586
GC Concentrate 4	49.774	49.217	50.559	24.650	24.441	24.276	2.317	2.362	2.596	4.015	3.903	4.281
GC Concentrate 5	50.035	50.168	50.830	24.271	24.360	24.629	2.429	2.419	2.406	4.086	4.067	4.022
Total Gravity Conc.	49.771	49.233	50.245	24.349	24.251	24.346	2.363	2.370	2.483	4.019	4.018	4.148

The fluidized bowl experiments showed lower overall recoveries and lower mass yields than those obtained from the unfluidized (ultra fine) bowl but showed higher concentrate grades. The higher grades are possibly due to the bowl recovering heavy and coarse PGMs while allowing finer PGMs to report to the tail. The fluidizing water results in a fluid drag force which acts against the centrifugal force resultant from the rotation of the bowl leading to fewer and mostly heavier coarse particles reporting to the concentrate (Das et al., 2023). This analysis suggests that the fluidized bowl can be used as a ‘cleaner’ stage rather than a ‘rougher’ stage.

4.5. Model for Additional Stages

In Phase 5 of the experiments the results for a 5-stage gravity concentration run was discussed and this indicated that about 48.90% recovery could be achieved at a concentrate grade of 292.04 g/t 4E PGM. The pertinent question is how can additional stages of the Falcon lab unit be modelled to determine what recovery and grades can be achieved with further stages. In this section a model was developed using mass balance and the relationship between the feed and concentrate grade to predict what a 10-stage process could potentially achieve. This model was then validated with an actual 10 concentrator stage experimental run which was done by taking the feed material through the Falcon a total of 10 times.

Figure 80 indicates the linear relationship between the feed grade and the concentrate grade of the Falcon. This relationship had the best results compared to other relationships tested. The equation in Figure 80 has a R^2 value of 0.9948 which means that 99.48% of the variance of the dependent variable is explained by the variance of the independent variable. This equation was then used to complete the mass balance in Table 19.

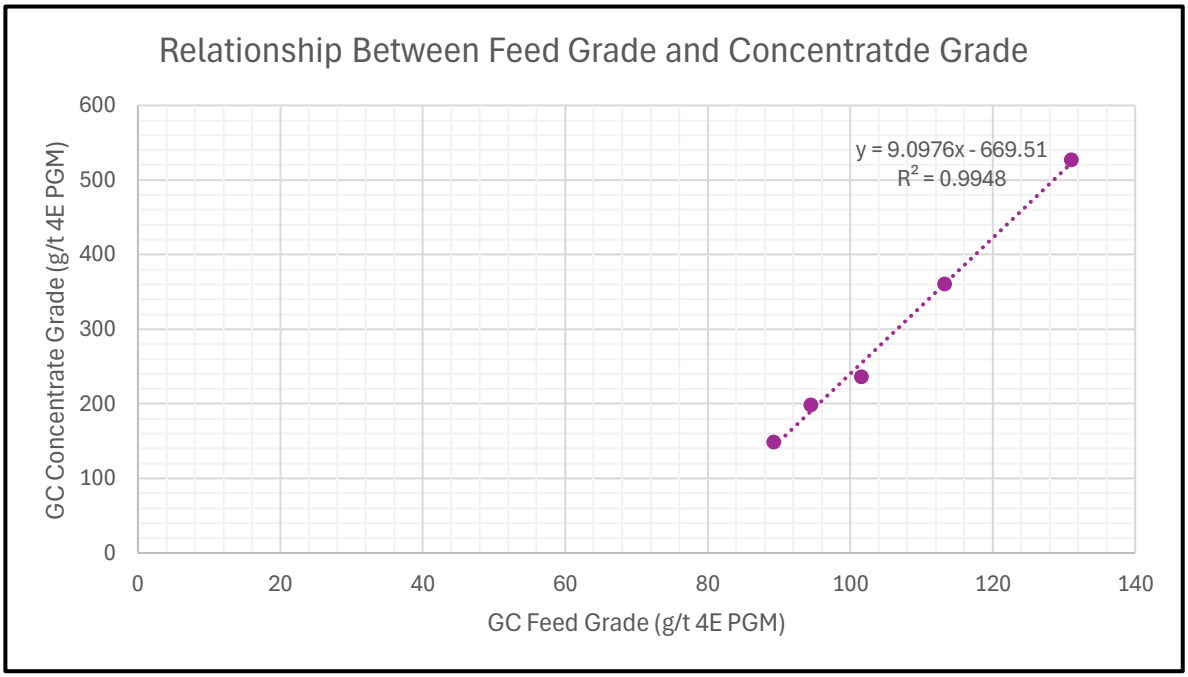

Figure 80: Relationship between feed grade and concentrate grade

Table 19: 10 stage gravity concentration modeled data

Parameter	Stage 1	Stage 2	Stage 3	Stage 4	Stage 5	Overall - 5 Stages	Stage 6	Stage 7	Stage 8	Stage 9	Stage 10	Overall - 10 Stages
Feed tons	0.005	0.005	0.005	0.004	0.004	0.005	0.004	0.004	0.003	0.003	0.003	0.005
Feed grade	131.021	113.226	101.577	94.484	89.204	131.021	85.765	84.237	83.435	83.020	82.819	131.021
Feed Content (g)	0.655	0.542	0.464	0.410	0.368	0.655	0.335	0.310	0.289	0.269	0.250	0.655
Concentrate tons	0.0002	0.0002	0.0002	0.0002	0.0002	0.001	0.0002	0.0002	0.0002	0.0002	0.0002	0.002
Concentrate grade	527.223	360.250	235.700	198.131	148.419	292.043	110.746	96.843	89.547	85.769	83.946	192.384
Concentrate Content (g)	0.113	0.078	0.054	0.042	0.034	0.320	0.025	0.021	0.020	0.019	0.018	0.424
Tail tons	0.005	0.005	0.004	0.004	0.004	0.004	0.004	0.003	0.003	0.003	0.003	0.003
Tail Grade	113.226	101.577	94.484	89.204	85.765	85.765	84.237	83.435	83.020	82.819	82.731	82.731
Tail Content (g)	0.542	0.464	0.410	0.368	0.335	0.335	0.310	0.289	0.269	0.250	0.231	0.231
4E Recovery	17.30%	14.33%	11.66%	10.16%	9.13%	48.90%	7.44%	6.88%	6.83%	7.02%	7.39%	64.66%
Mass Yield (%)	4.30%	4.50%	5.02%	4.85%	5.49%	21.94%	5.76%	5.98%	6.36%	6.79%	7.29%	44.04%

Table 20: 10 stage gravity concentration measured data

10 Stage										
Phase 5: Multi-stage	Flow rate (L/min)	Mass (g)	Mass Recovery (%)	Cum Mass recovery %	Mass recovery (g)	4E PGM (g/t)	**4E PGM Recovery (%)**	4E PGM Cum Recovery (%)	4E PGM (g)	**4E PGM Upgrade**
Gravity Concentrate Feed		5000.00				131.02				
Gravity Concentrate 1		216.00	4.3%	4.3%	216.00	505.92	**17%**	17%	0.11	**3.86**
Gravity Concentrate 2		212.00	4.2%	8.6%	212.00	409.29	**13%**	30%	0.09	**3.12**
Gravity Concentrate 3		230.00	4.6%	13.2%	230.00	226.74	**8%**	38%	0.05	**1.73**
Gravity Concentrate 4		229.00	4.6%	17.7%	229.00	198.03	**7%**	45%	0.05	**1.51**
Gravity Concentrate 5		265.00	5.3%	23.0%	265.00	139.32	**6%**	50%	0.04	**1.06**
Gravity Concentrate 6	**3**	250.00	5.0%	28.0%	250.00	103.34	**4%**	54%	0.03	**0.79**
Gravity Concentrate 7		225.00	4.5%	32.5%	225.00	107.23	**4%**	58%	0.02	**0.82**
Gravity Concentrate 8		225.00	4.5%	37.0%	225.00	106.56	**4%**	62%	0.02	**0.81**
Gravity Concentrate 9		209.00	4.2%	41.2%	209.00	109.23	**3%**	65%	0.02	**0.83**
Gravity Concentrate 10		206.00	4.1%	45.3%	206.00	101.47	**3%**	68%	0.02	**0.77**
Total Gravity Conc.		*2267.00*	*45.3%*		*2267.00*	*197.68*	***68.41%***		*0.45*	**1.51**
Gravity Concentrate Tail		2733.00	54.7%		2733.00	75.73			0.21	
Totals		*5000.00*	*100%*		*5000.00*	***131.02***	***68.41%***		*0.66*	***1.51***

Table 19 shows the first 5 stages as reported in Phase 5 results and the modelled subsequent 5 stages. The overall modelled 10 stages achieved a recovery of 64.66% and a concentrate grade of 192.384 g/t compared to 5 stages which achieved a recovery of 48.90% at a concentrate grade of 292.04 g/t. The 10 stage Falcon experiment was also conducted to determine the efficacy of the model. Table 20 shows the results from this experiment. Overall, the experiment achieved a recovery of 68.41% and concentrate grade of 197.68 g/t. The modelled versus the measured data is shown in Figure 81 and shows a good agreement between the model and measured data and thus it can be concluded that the modelled data can be used to predict the recovery of the Falcon at increased number of stages.

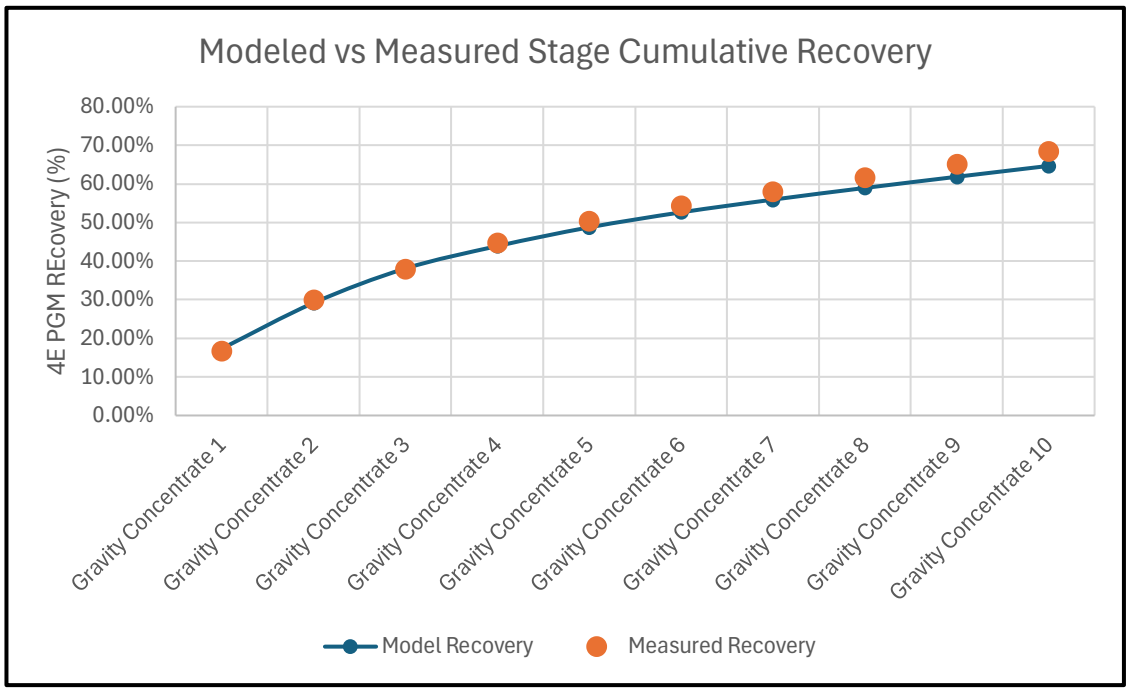

Figure 81: Modelled vs measured recovery per stage

The measured data and the modelled data indicate that with a mass pull of approximately 44-45%, it is possible to recover close to 70% of the PGMs that were in the fresh feed.

4.6. SEM Results

Scanning Electron Microscope (SEM) is able to scan a sample with a focused electron beam and obtain images with information about the samples' topography and composition (Zeiss, 2024). It is commonly necessary to coat the sample with a thin layer of gold-palladium alloy in order to prevent charging of the surface, promote the emission of secondary electrons, and provide a homogeneous surface for analysis and imaging (Heu et al., 2019). This coating is not always necessary and for this specific research no coating was added in order to avoid altering the sample which already contains gold and palladium. The magnification and composition results without a sample coating would be sufficient for the purposes of this research. Only Phase 5 composite samples were analysed with the SEM as this phase forms the basis for the postulations in this research report due to the positive outcomes achieved. The Zeiss SEM used can be seen in Figure 82.



Figure 82: Zeiss SEM

The GC feed sample (feed to the gravity concentrator) was subjected to SEM analysis, even though the PGM concentration was relatively low there were some interesting findings. Figure 83 indicates the area of a sample. The dark grey/black particles are gangue and the bright particles are high atomic mass particles. As expected, there is visually more gangue than PGM particles. The composition indicates PGE's, sulphur, base metals, silica, magnesium, aluminium, chrome, calcium and iron. All these elements are expected and were found in the Fire Assay/ICP-MS.

Figure 84 is a magnification of a gangue particle with a diameter of approximately 30µm. The particle composition indicates the presence of silica, magnesium, iron, chrome, calcium and aluminium. This is an interesting observation as it indicates that gangue particles themselves have a complex mineralogy and that chrome is associated with the silica particles. This is also confirmed by Figure 85 which shows a chrome particle and its association with silica, magnesium, aluminium, iron and in this case titanium as well.

Figure 86 and Figure 87 shows interesting results that have not been found in the previous literature on PGMs. These figures show a PGM particle and a chrome particle perfectly next to one another, this is a unique observation that has not been reported before. The chrome particle is irregular while the PGM particle is more rounded. The PGM particle indicates the presence of all PGMs as well as base metals, sulphur and iron which are all expected for the complex PGM matrix. Both particles are approximately 20µm in diameter. The PGM particle crystallography indicates oriented etch pits which have also been reported by Cabri et al. (2022).

The feed sample indicates presence of all the expected gangue minerals and PGMs as well as confirming the complexity of the PGM particles and the gangue particles. Most particles are in the fine and ultra fine size range as expected.

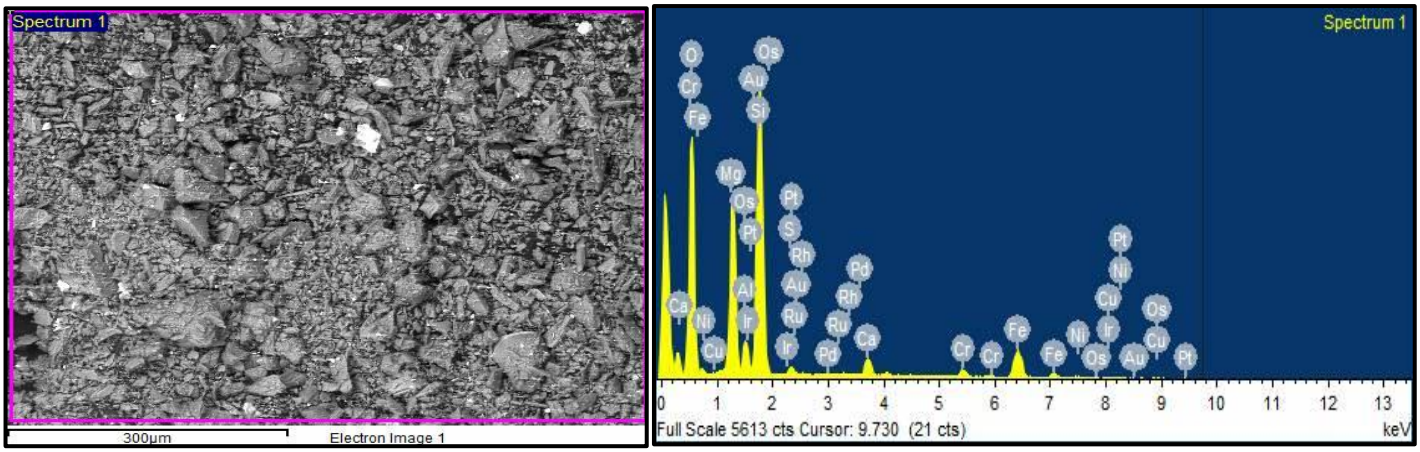

Figure 83: SEM image and composition of GC feed area

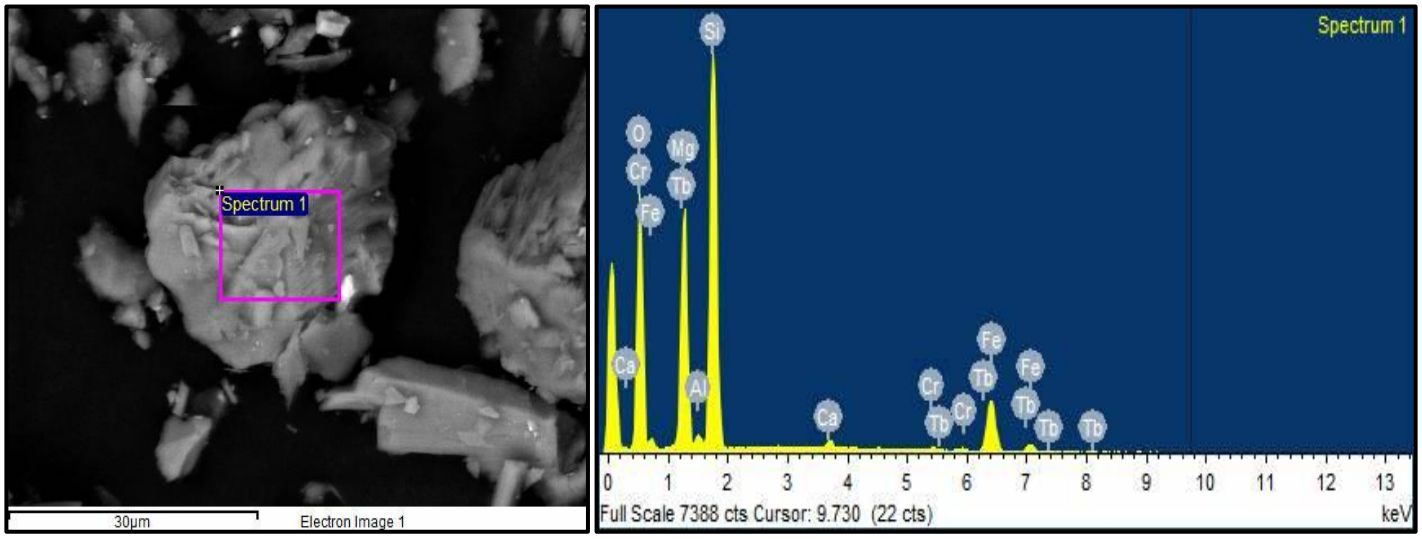

Figure 84: SEM image and composition of GC feed gangue particle

The GC tail sample contained a relatively low concentration of PGMs compared to the feed sample as a result it was difficult to find PGMs in this sample. Figure 88 indicates an area of the GC tail that is composed of silica, chrome, magnesium, aluminium and iron. The PGM concentration is too low for detection when analyzing an entire area. Figure 89 shows a PGM particle found in the GC tail, this indicates the PGMs present as well as sulphur and base metals. Figure 90 indicates a gangue particle containing silica, magnesium, aluminium, chrome and iron. Interestingly, this particle also contains some sulphur which could imply that this type of gangue particle is amenable to flotation as xanthate collectors act on sulphur.

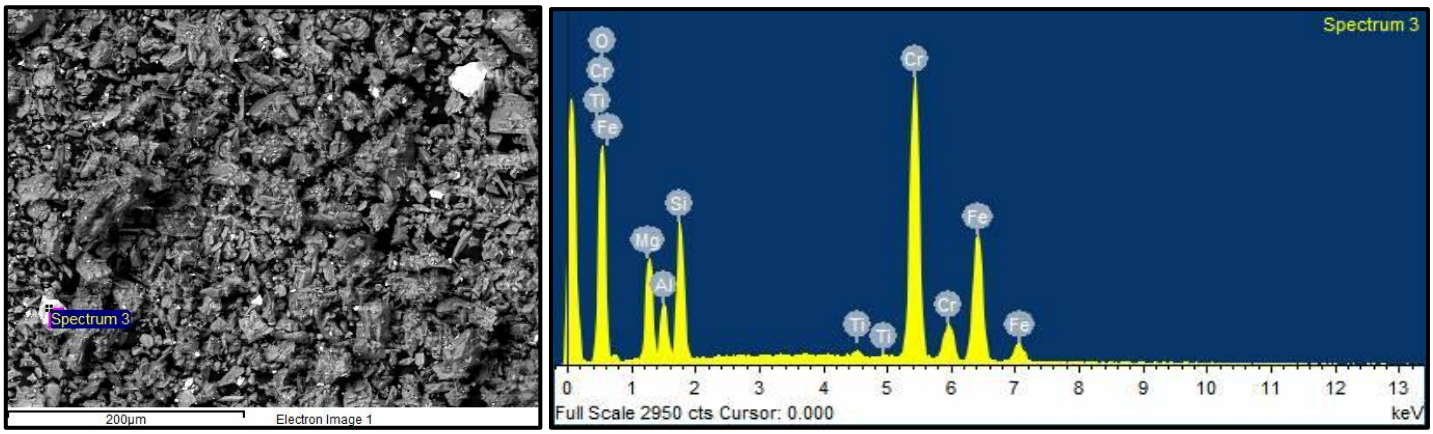

Figure 85: SEM image and composition of GC feed chrome particle

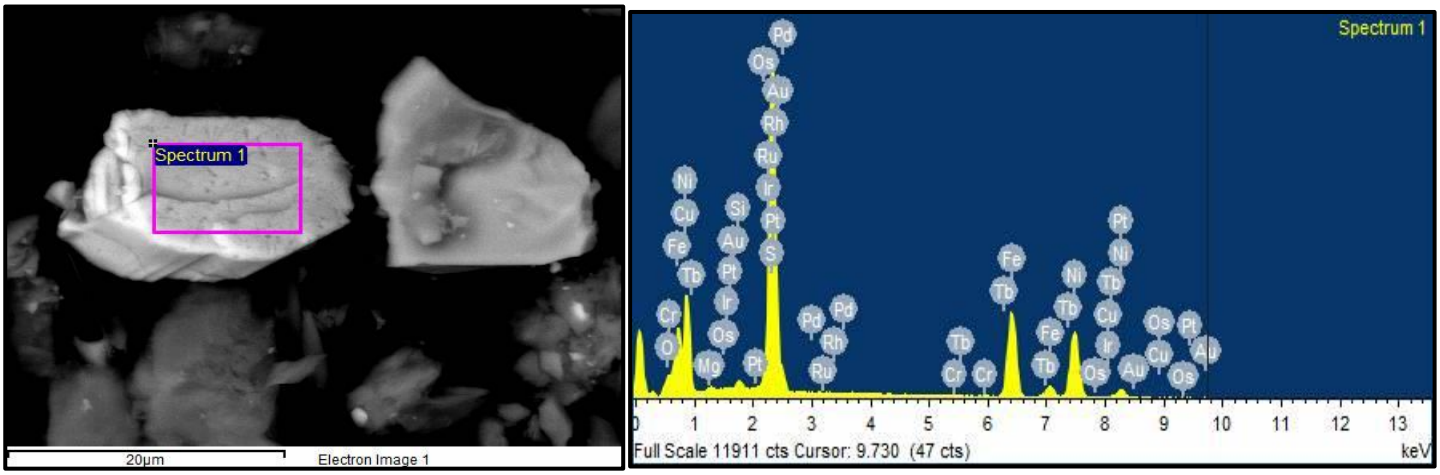

Figure 86: SEM image and composition of GC feed PGM particle

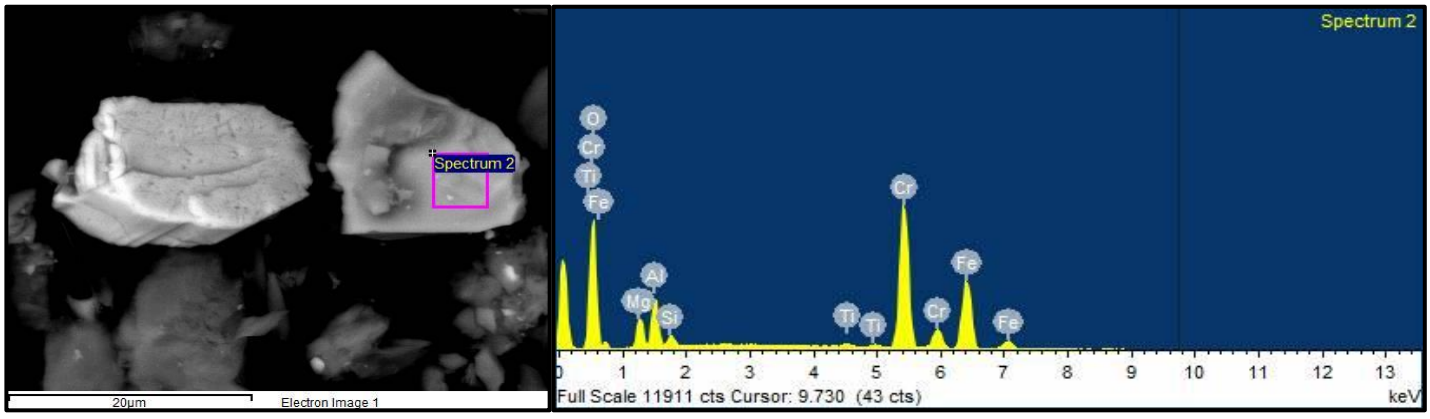

Figure 87: SEM image and composition of GC feed chrome particle

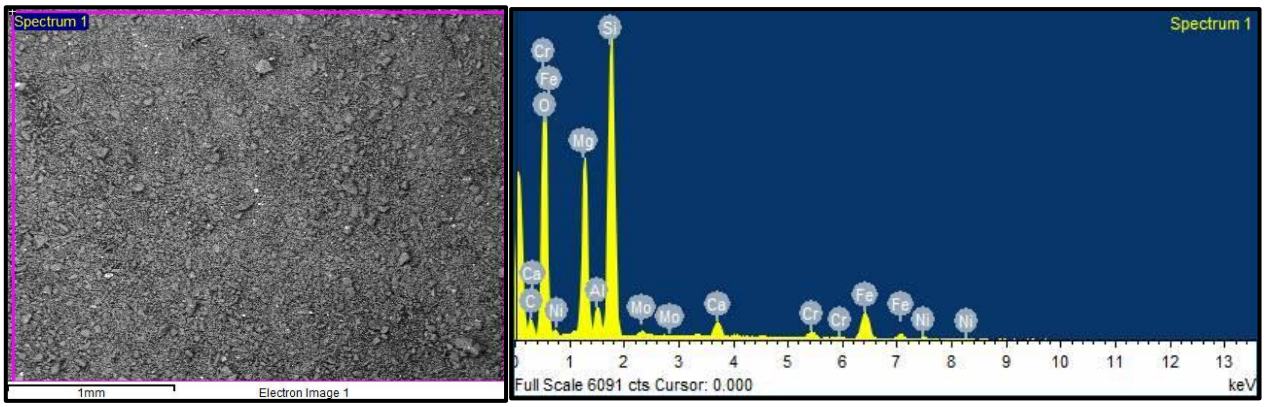

Figure 88: SEM image and composition of GC tail sample area

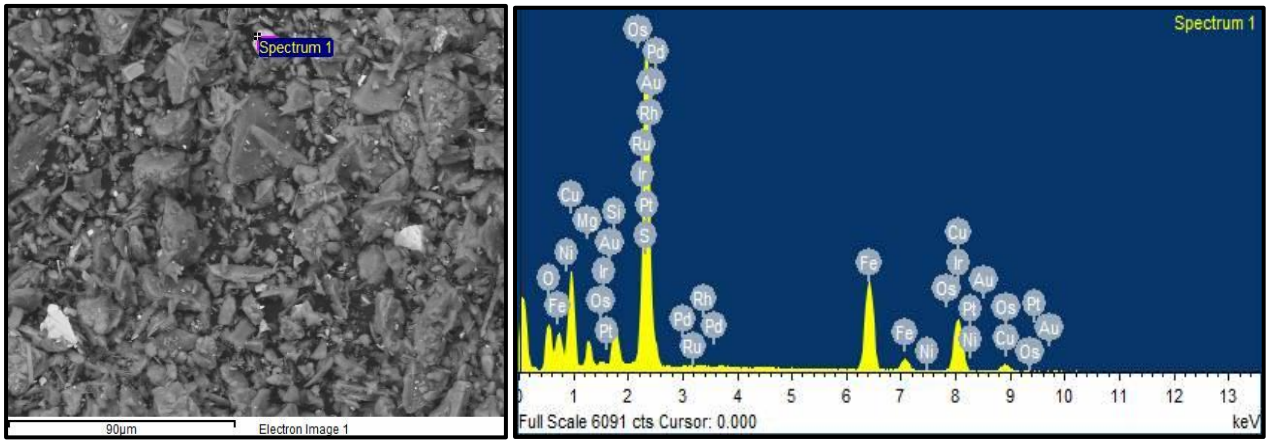

Figure 89: SEM image and composition of GC tail PGM particle

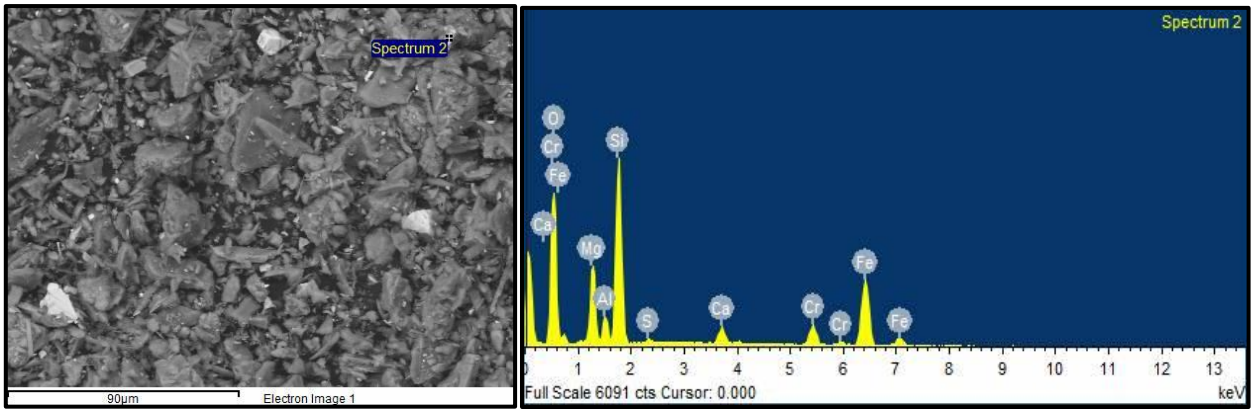

Figure 90: SEM image and composition of GC tail gangue particle

The 5 concentrates produced from the Falcon (GC concentrate samples) were also analyzed with the SEM, yielding some very interesting results. Due to the higher concentration of PGMs in these samples the PGMs could be identified by SEM images and compositions (Figure 91 and Figure 92). The compositions include all PGMs, sulphur, base metals, silica, magnesium, aluminium, calcium, chrome and iron. These results confirm the Fire Assay/ICP-MS results.

Chrome particles and compositions are shown in Figure 93 and Figure 95. The chrome particles appear to have association with silica, magnesium, iron, aluminium, and titanium. A magnified chrome particle is shown in Figure 94 and indicates an irregular and angular shape.

Figure 96 and Figure 97 indicates the gangue particles, which are approximately 50µm and 25µm in diameter. All expected gangue constituents are present and small amounts of chrome which indicates that chrome is also associated with the gangue minerals. The images also indicate that the gangue particles are a significant portion of the sample and are in the fine to ultra fine size fraction. The narrow particle size distribution of the gangue as well as the complexity of the gangue material is what makes it difficult to selectively upgrade PGM concentrates using gravity concentration.

Figure 98 to Figure 101 show the PGM particles in the samples. There is clear indication of all PGMs, sulphur and base metals present in each particle which suggests the complex nature of PGM particles. The presence of iron and arsenic in PGM particles is also expected and confirmed by this analysis. Figure 102 and Figure 103 depicts a PGM particle with all PGMs present, base metals and sulphur but what makes it unique is the shape. The particle has a spherical-hexagonal (hexagonal prism) type shape with smooth surfaces and could be a combination of a well-crystallized grain of Os-Ir-Ru alloy and isometric Pt-Fe alloy as reported by Cabri et al. (2022). The particle is approximately 12µm in diameter. These SEMs indicate the complexity of PGMs, proves the amorphous nature of the PGM particles as well as the fact that the majority of PGMs are in the fine to ultra-fine particle size range.

Appendix G contains additional SEM images and graphs.

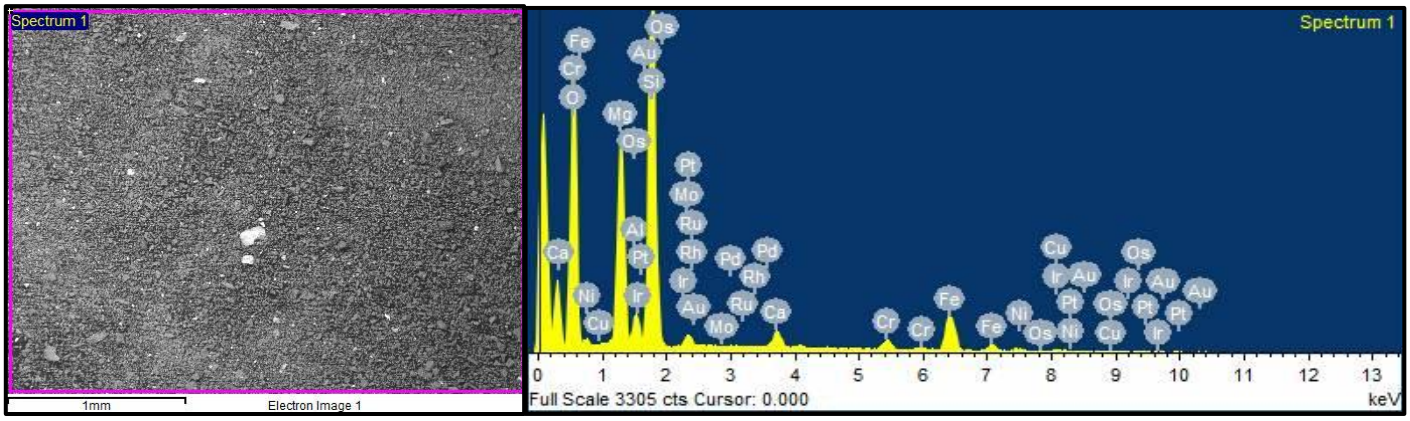

Figure 91: SEM image and composition of GC concentrate area (a)

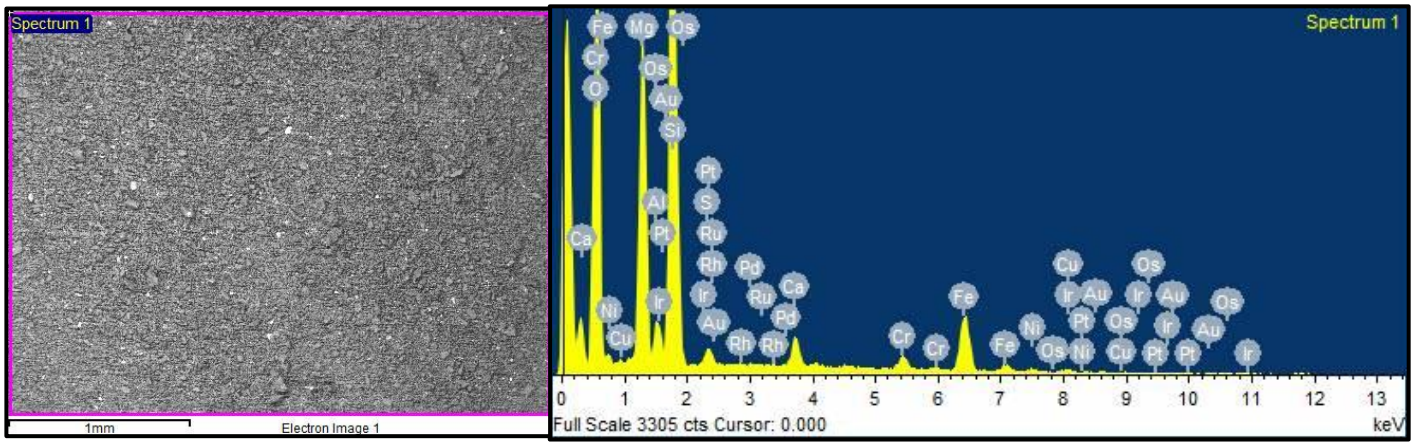

Figure 92: SEM image and composition of GC concentrate area (b)

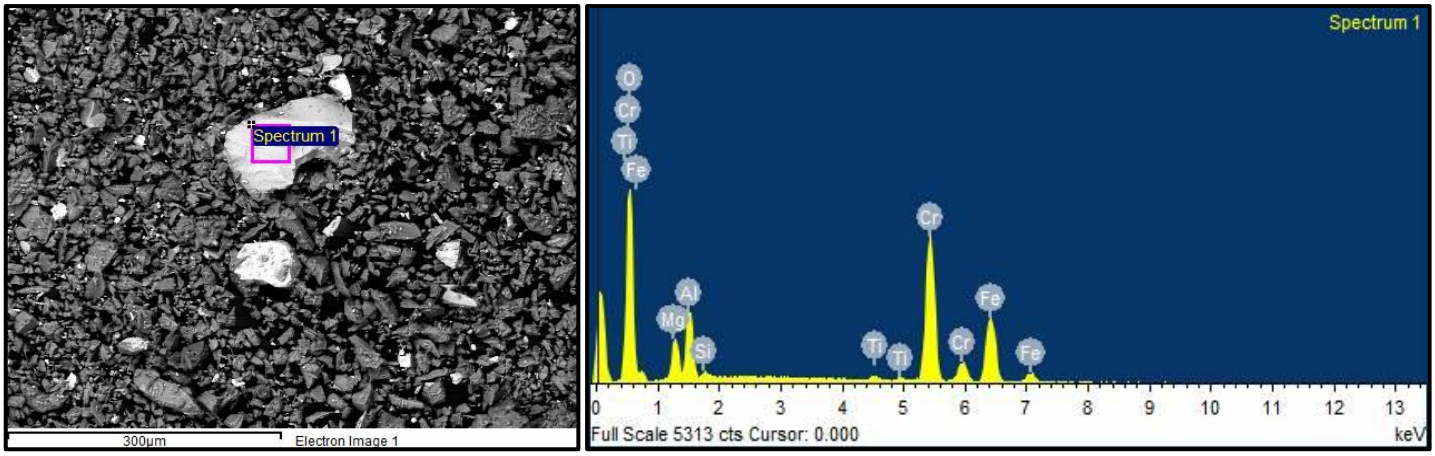

Figure 93: SEM image and composition of GC concentrate chrome particle (a)

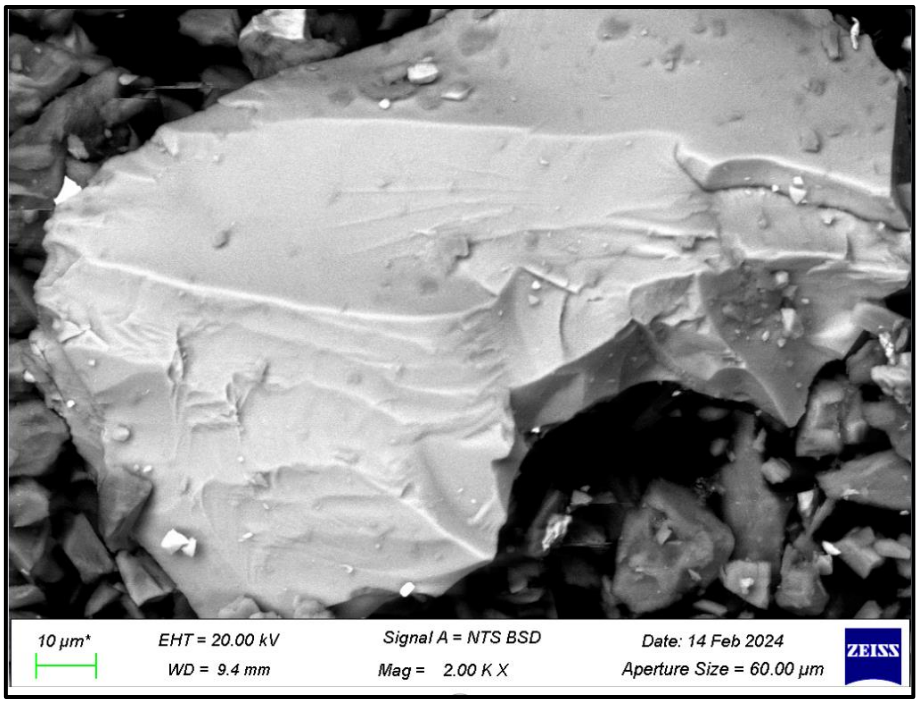

Figure 94: SEM image of GC concentrate magnified chrome particle

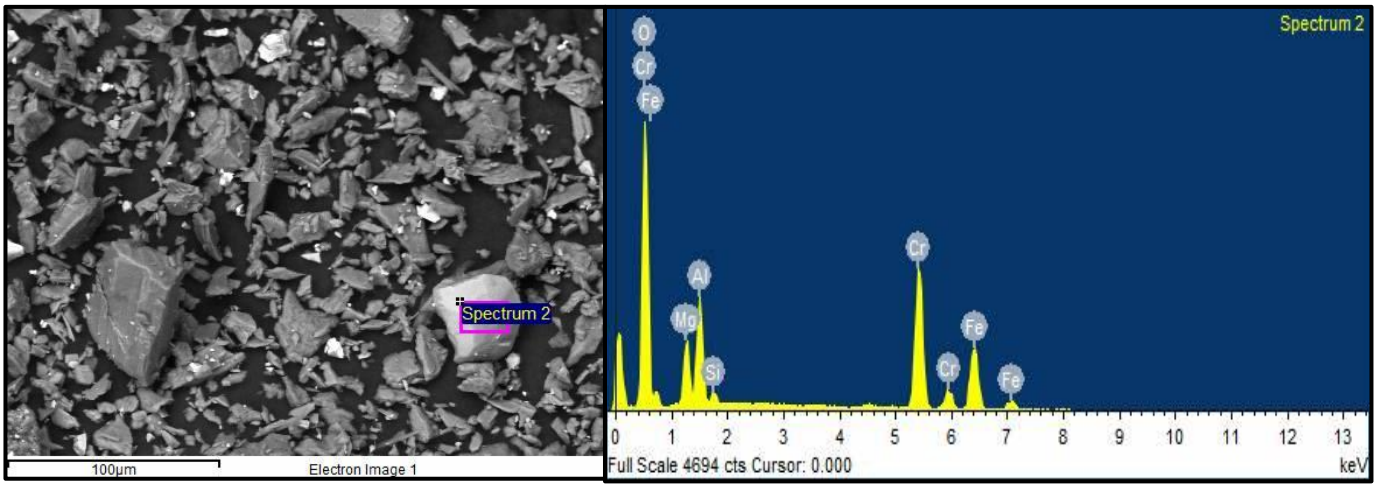

Figure 95: SEM image and composition of GC concentrate chrome particle (b)

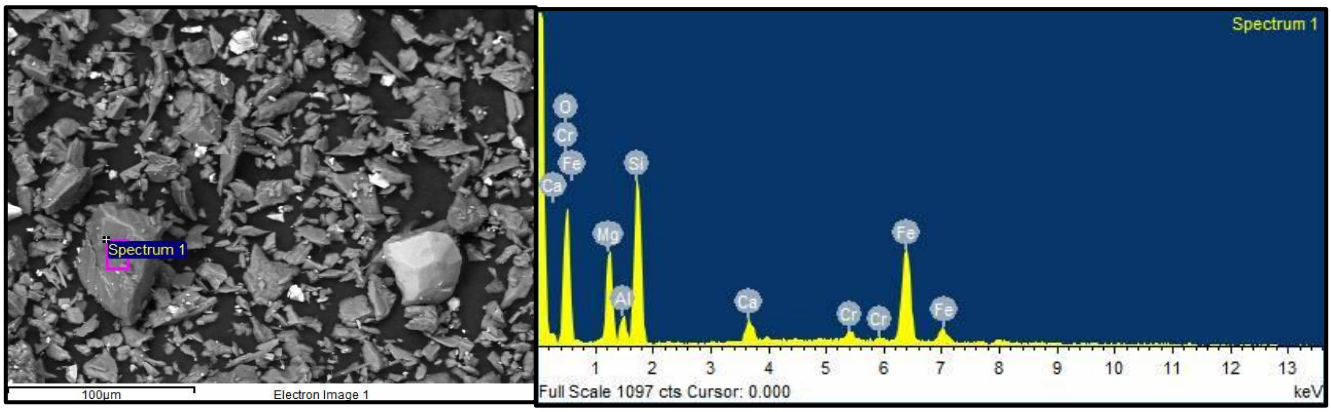

Figure 96: SEM image and composition of GC concentrate gangue particle (a)

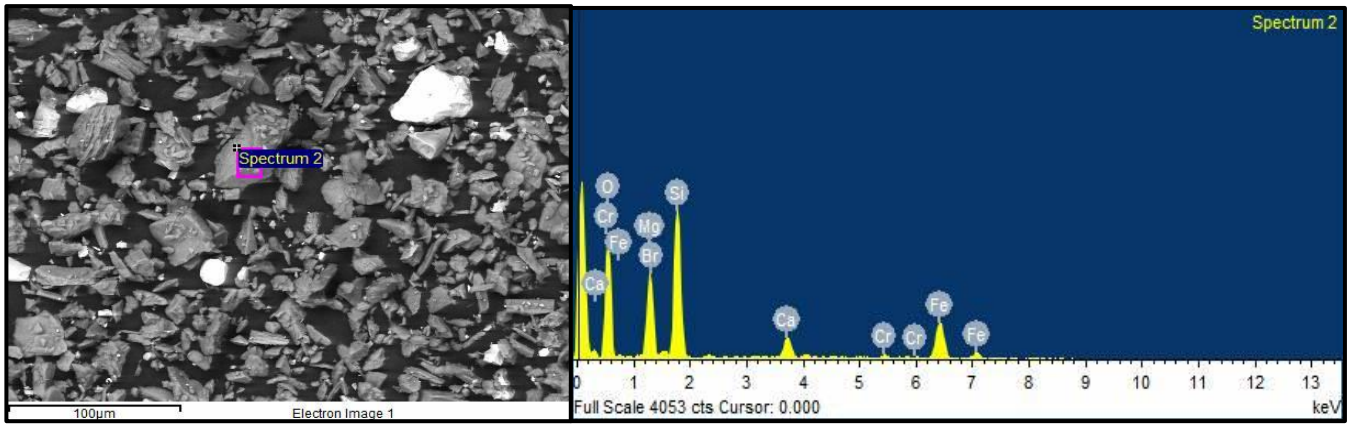

Figure 97: SEM image and composition of GC concentrate gangue particle (b)

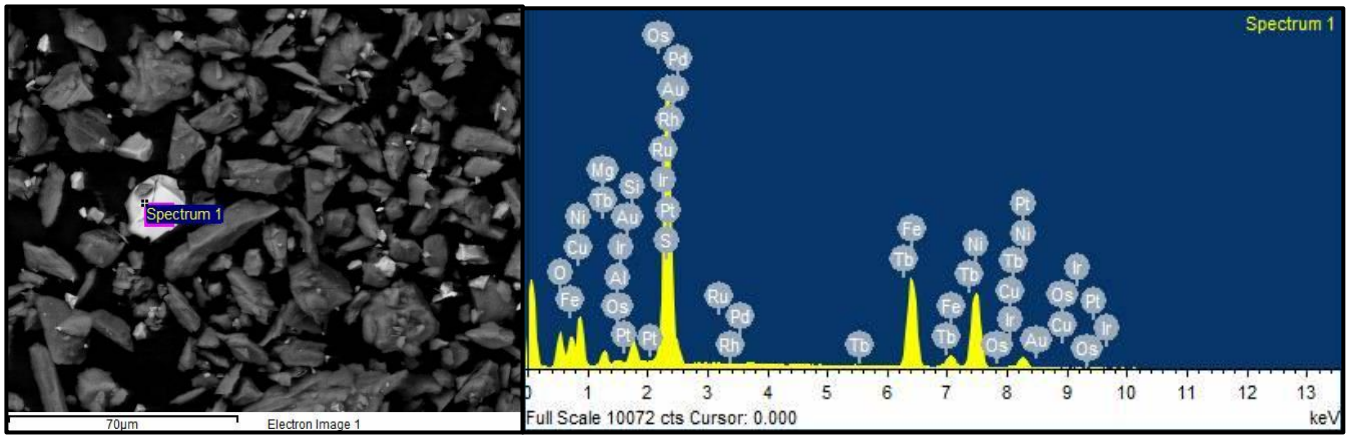

Figure 98: SEM image and composition of GC concentrate PGM particle (a)

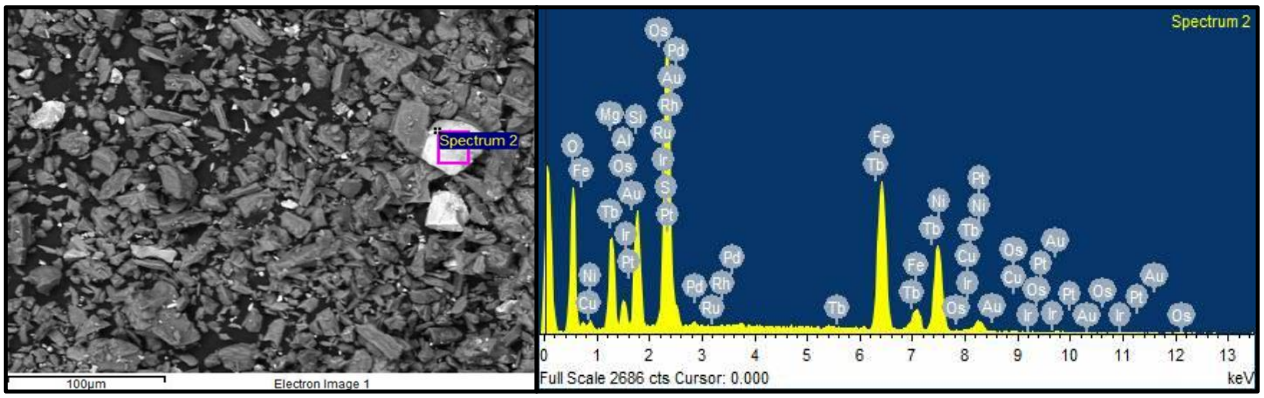

Figure 99: SEM image and composition of GC concentrate PGM particle (b)

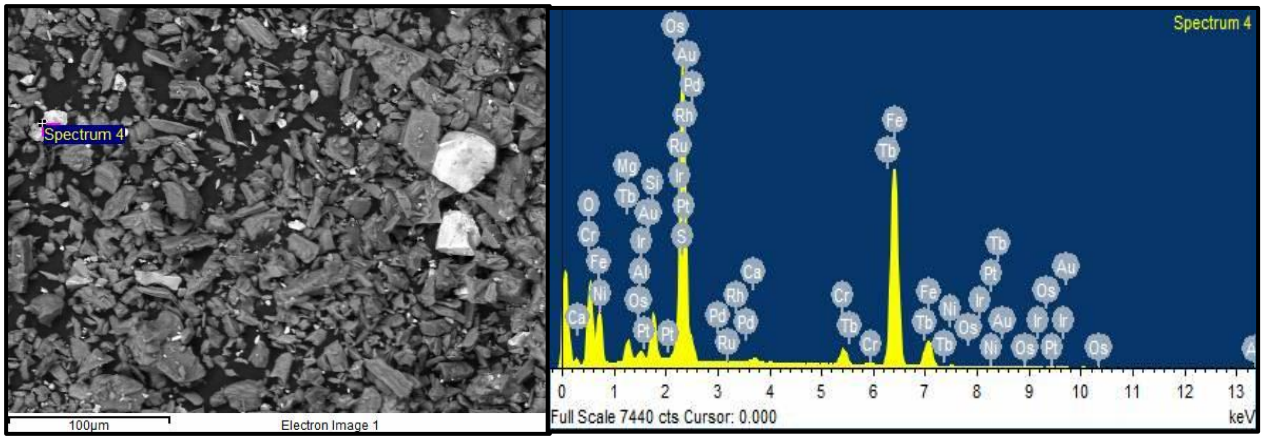

Figure 100: SEM image and composition of GC concentrate PGM particle (c)

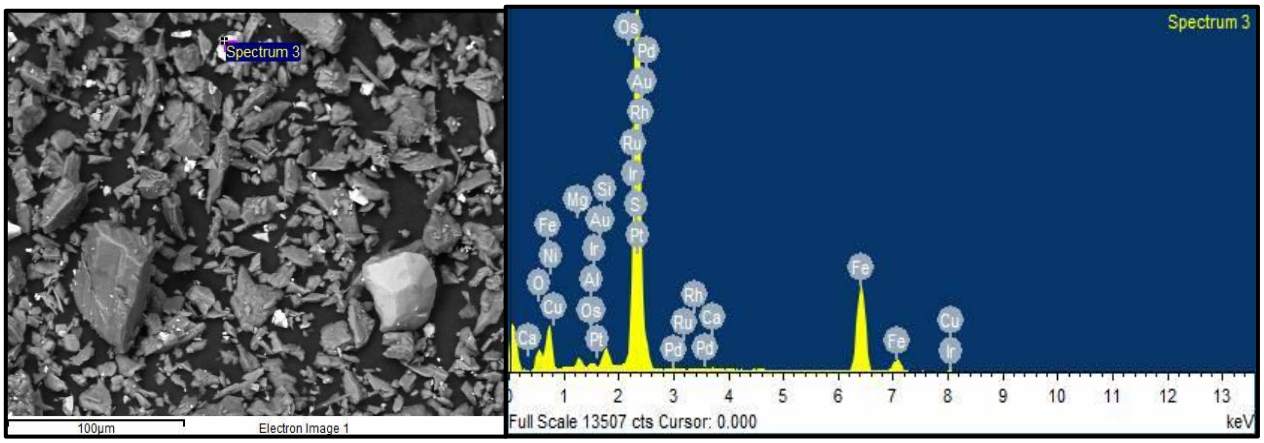

Figure 101: SEM image and composition of GC concentrate particle (d)

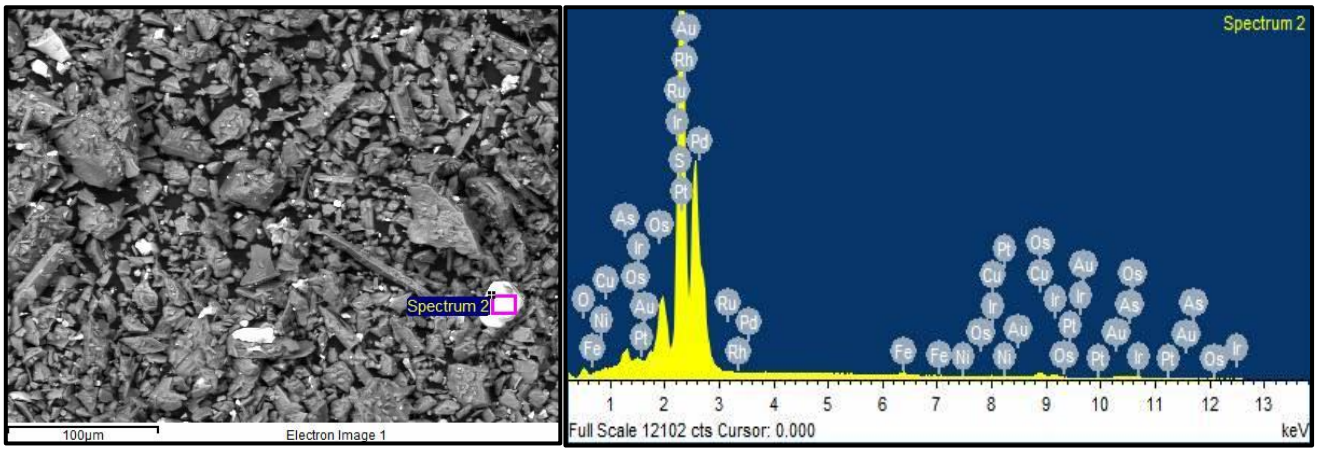

Figure 102: SEM image and composition of GC concentrate PGM particle (e)

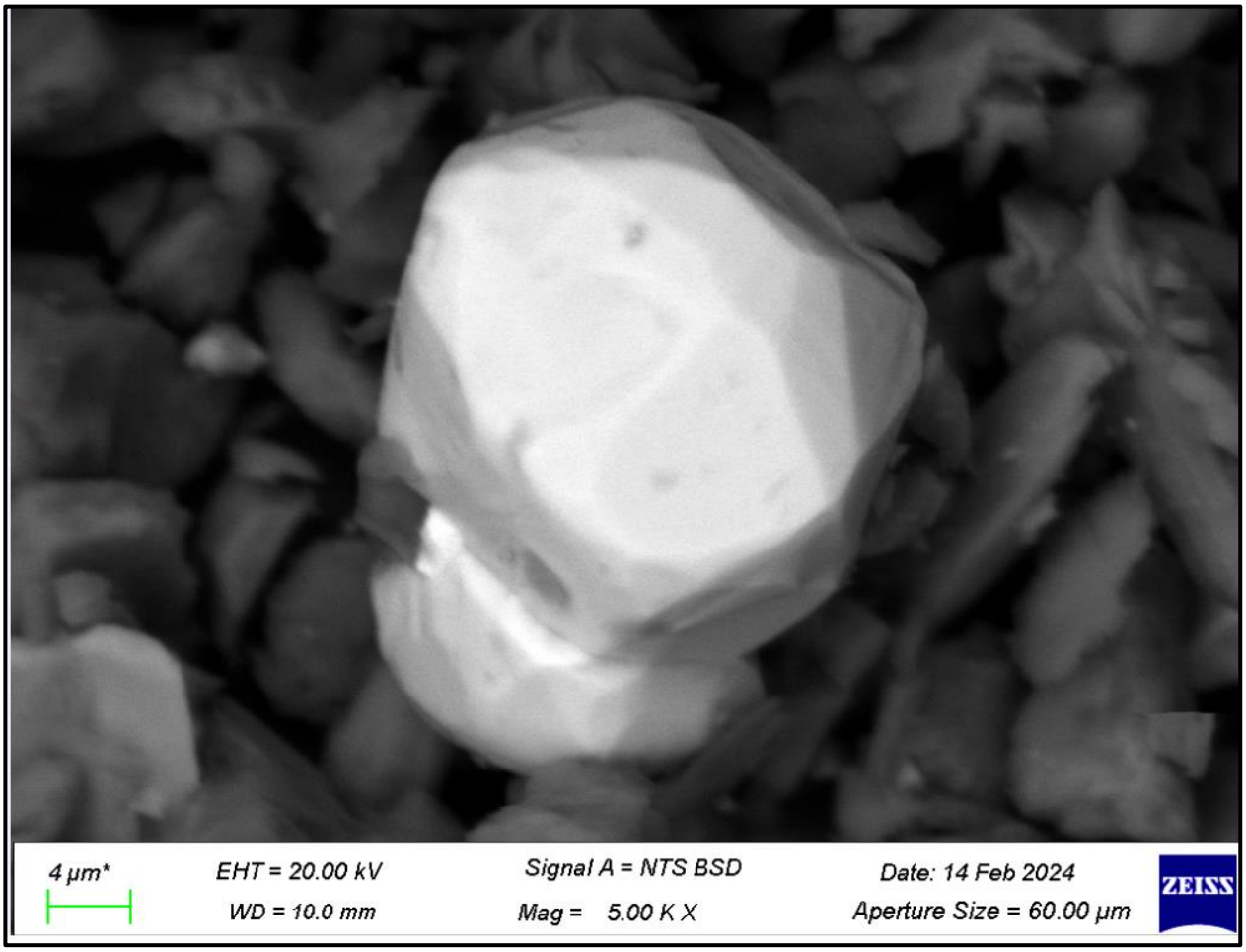

Figure 103: SEM image of GC concentrate magnified PGM particle

4.7. XRF Results

X-ray fluorescence (XRF) is a non-destructive analytical technique used to determine the elemental composition of materials. When a sample's atoms are excited by application of an X-ray source from the XRF analyser, the chemistry of the sample can be determined by measuring the fluorescent X-ray emitted from said sample. Each element produces a unique characteristic fluorescent X-ray and hence XRF can be used for qualitative and quantitative analysis. A portable XRF (pXRF) was utilized in this analysis (shown in Figure 104). The X-Ray Anode Tube was a rhodium anode which makes it particularly difficult to measure PGMs in small quantities, nonetheless, other compounds and elements can be detected which were not necessarily analysed in the Fire Assay/ICP-MS process.

The XRF analysis was used to verify findings and inferences from the Fire Assay/ICP-MS results as well as to explore additional facets of the samples that are not reported by the Fire Assay/ICP-MS. Only Phase 5 composite samples were analysed with the pXRF as this phase forms the basis for the postulations in this research report due to the positive outcomes achieved.



Figure 104:pXRF device

The XRF analysis was carried out on a composite from each of the 5 concentrates of the Falcon runs from Phase 5, 1 composite final tail and 3 feed samples. The results are shown in Table 21. The XRF results compare well with the Fire Assay/ICP results for SiO_2, MgO, Ni and Fe with a variance of 3%, 5%, 7% and 4% respectively. The other elements and compounds had higher variance. The chromite for instance was 0.99% on the XRF but 1.97% from Fire Assay/ICP, this indicates that the XRF does underestimate some elements, and this may be due to the content in the sample, crystal structure or interference from constituents which have a larger mass in the sample. Platinum and Palladium were also recognized by the pXRF but in very small amounts. The other PGMs were not recognized for reasons mentioned above.

Although the XRF data is not as accurate as the Fire Assay/ICP, inferences can be made from the data. The XRF data shows that the gangue compounds remain fairly constant in the feed, concentrate and tail. The concentrations of sulphur, nickel, copper, platinum and palladium all increase in the concentrates when compared to the feed concentrations and then decrease in the tail sample. This is evidence that the base metal sulphides and hence the PGMs are being recovered by the gravity concentrator. When comparing the 5 concentrates from each stage, there is a similar trend as reported by the Fire Assay/ICP where the first concentrate has the highest concentration of base metals, sulphur, platinum and palladium and this gradually decreases over the next 4 concentrates.

The XRF results also indicate the presence of the following elements and compounds in trace amounts that were not included in the Fire Assay/ICP method:

- Chlorite
- Potassium oxide
- Titanium
- Manganese
- Zinc
- Strontium
- Yttrium
- Zirconium
- Vanadium

The XRF confirms the presence of vanadium-iron-titanium-sulphide oxide formations which are associated with PGMs (O'Connor & Alexandrova, 2021). Although the above constituents are in small amounts, it does corroborate the discussion in the literature review section on the complexity of PGM ores.

Please see **Appendix E** for complete data.

Table 21: XRF results

Sample Name		GC Concentrate 1	GC Concentrate 2	GC Concentrate 3	GC Concentrate 4	GC Concentrate 5	GC Tail	GC Feed 1	GC Feed 2	GC Feed 3
Constituents (Wt %)	MgO	25.609	24.891	25.795	25.665	25.663	23.755	25.358	25.476	25.506
	Al_2O_3	3.410	3.376	3.529	3.601	3.516	3.576	3.712	3.668	3.830
	SiO_2	51.215	50.530	51.481	51.361	51.884	49.989	52.110	52.072	52.721
	S	1.078	1.254	0.905	0.963	0.932	0.490	0.631	0.619	0.630
	Cl	0.148	0.161	0.141	0.136	0.140	0.133	0.160	0.165	0.168
	K_2O	0.051	0.054	0.055	0.050	0.051	0.061	0.074	0.076	0.078
	Ca	1.653	1.612	1.665	1.683	1.703	1.602	1.726	1.692	1.735
	Ti	0.172	0.170	0.165	0.169	0.162	0.137	0.150	0.151	0.156
	Cr	1.481	1.454	1.224	1.238	1.182	0.819	0.992	0.981	1.012
	Mn	0.138	0.135	0.124	0.133	0.135	0.107	0.118	0.119	0.114
	Fe	8.809	8.604	8.374	8.435	8.295	6.626	7.521	7.517	7.535
	Co	0.035	0.036	0.026	0.028	0.028	0.016	0.019	0.017	0.018
	Ni	0.710	0.752	0.605	0.612	0.572	0.336	0.391	0.413	0.407
	Cu	0.283	0.305	0.268	0.264	0.256	0.180	0.191	0.202	0.200
	Zn	0.005	0.008	0.009	0.010	0.009	0.007	0.007	0.008	0.008
	Sr	0.003	0.003	0.003	0.003	0.003	0.003	0.003	0.003	0.003
	Y	0.001	0.001	0.001	0.001	0.001	0.001	0.000	0.001	0.001
	Zr	0.002	0.002	0.001	0.002	0.001	0.001	0.001	0.001	0.001
	Pd	0.011	0.007	0.006	0.005	0.005	0.003	0.005	0.004	0.002
	Pt	0.030	0.019	0.009	0.009	0.008	0.004	0.005	0.005	0.007

4.8. XRD Results

X-ray diffraction (XRD) is a non-destructive analytical method for phase identification of a crystalline material. Identification of phases is achieved by comparing the X-ray diffraction pattern obtained from an unknown sample with patterns of a reference database. The XRD cannot detect amorphous minerals and is primarily used to identify crystalline particles.

The XRD analysis was used to verify findings from the Fire Assay/ICP-MS results as well as to explore additional facets of the samples that are not reported by the Fire Assay/ICP-MS. Only Phase 5 composite samples were analysed with the XRD device as this phase forms the basis for the postulations in this research report due to the positive outcomes achieved. One feed, tail and composite concentrate were analysed. **Appendix F** contains the data for this section.

The mineral composition of the sample revealed significant concentrations of SiO_2 and MgO which confirms the XRF and Fire Assay/ICP-MS methods. Specifically, the crystalline gangue compounds found were Enstatite ($MgSiO_3$); Silicon dioxide (SiO_2) and Kyanite (Al_2SiO_5). The gangue is also associated with iron in some cases such as Rhomboclase ($H_5Fe^{3+}O_2(SO_4)_2 \cdot 2$) and Ferrosilite ($FeSiO_3$). The GC concentrate sample contained all PGMs except gold (possibly due to the much smaller concentration of gold in the concentrate). The PGMs were all in oxide form but this is not to say that all PGMs are in this crystalline form as the literature review suggest a number of PGM formations and even the possibility of small amounts of elemental (native) PGMs, nonetheless, Oberthür (2018) suggests that due to PGE-sulfide modification ill defined PGM-oxides may form. Apart from the gangue mentioned above, the concentrate sample also contained Fayalite (Fe_2SiO_4). Chromite was not detected by XRD possibly due to the low concentrations present in the sample

The XRD results confirm the presence of gangue and PGMs as shown by SEM, XRF and Fire Assay/ICP-MS with the addition of crystalline constituents which reveal the complexity of the gangue and PGM constituents of the PGM material.

5. Integrated Discussion

Platinum group metals in flotation concentrates are amenable to advanced gravity separation using a Falcon concentrator but due to the complexity of the PGM base metal sulphides matrix as well as the fine to ultra fine particle size of the flotation concentrate there are challenges with reducing the amount of gangue in the final concentrate product.

The complexity of the PGM flotation concentrate ore was shown by the Fire Assay/ICP-MS, XRF, XRD and SEM. The PGMs are proved to be associated with base metal sulphides as well as arsenic (for platinum) and possibly iron and titanium. It is very rare to find native PGMs as they preferentially form complexes but this research has shown the possibility of native or simple sulphides of gold and ruthenium as these have higher overall recoveries than all the other PGMs. Fire Assay/ICP-MS indicated that the feed to the Falcon consisted of all 6 PGMs, with platinum and palladium being the dominant PGMs. The overall 4E feed grade was 131.02 g/t. The XRF confirmed the presence platinum and palladium but not the other PGMs due to the lower concentrations and due to the XRF using a rhodium tube which makes it difficult to analyse for low quantities of PGMs. XRF did confirm the presence of vanadium-iron-titanium-sulphide oxide formations which are associated with PGMs. The XRD showed that some of the PGMs are in oxide form due to PGE-sulphide modification which induce the formation of ill-defined PGM-oxides. XRD could only detect crystalline particles but due to the complexity of PGM ore this report has also shown that most PGMs are in amorphous mineral complexes (as discussed in the literature review section). The SEM results reveal that all PGMs can be found in a matrix with base-metal sulphides. These results also indicate that a single PGM cannot be targeted for recovery but rather all six PGMs exhibit similar characteristics.

The density of the PGMs are much higher than the gangue constituents with only palladium, rhodium and ruthenium being lower than 19 g/cm^3 at 11.99, 12.4 and 12.41 g/cm^3 respectively. The concentration criteria for each PGM is greater than 2.5 which makes them amenable to gravity concentration on individual and overall basis.

The particle size distribution revealed that the feed to the gravity concentrator consists of fines and ultra-fines with 97.07% passing 75µm. The D90 of the GC concentrate is 42.24µm

compared to the GC feed which is 49.78µm, this showed that the Falcon gravity concentrator was able to recover the fine to ultra-fine particles as the concentrate is finer than the feed. The fractional analysis indicated that PGMs are concentrated in the fine and ultra-fine fractions and the lowest concentrations are found in the +106µm and -106+75µm fractions. The results also indicated that more ruthenium was recovered in the -53+25µm fraction which confirms the notion that ruthenium may be in native form or a simple sulphide that is more amenable to gravity concentration. The fractional analysis also revealed that PGMs in fine and ultra fine particle size ranges can be recovered by gravity concentration. The high gravitational force applied is able to preferentially recover the PGMs in this size range while rejecting lighter gangue particles.

The chrome content in the GC feed was 1.97%, this did not change appreciably in the GC concentrates which showed an average chrome content of 1.99% for the 5-stage optimized run. The GC feed seems to have a larger proportion of chrome in the +53-75µm and +25-38µm size ranges while the GC concentrate has a higher proportion of chrome in the +160, +75-106 and +53-75µm range, this indicates that the coarser chrome is being recovered by the falcon while the chrome associated with the finer particles is rejected. An interesting outcome is that 77.84% of the chrome is successfully rejected from the Falcon to the tailings stream on a mass basis. This proves that chrome is not concentrated in the Falcon. The SEM indicated that chrome was found in its native form but is also associated with silica, magnesium, aluminium and iron. The XRF also confirmed the presence of chrome in the GC feed, GC concentrate and GC tail.

The gangue constituents of the PGM flotation concentrate consisted primarily of silicon dioxide (53.92%), magnesium oxide (24.07%), calcium oxide (3.24%) and aluminium oxide (4.98%). This was corroborated with the XRF, XRD and SEM data. The SEM indicate that the gangue particles also form complexes with chrome and other gangue material. The XRD indicated that the crystalline gangue was Enstatite ($MgSiO_3$); Silicon dioxide (SiO_2), Kyanite (Al_2SiO_5). Rhomboclase ($H_5Fe^{3+}O_2(SO_4)_2 \cdot 2$) and Ferrosilite ($FeSiO_3$). The fractional analysis indicated that the GC concentrate recovered a greater portion of gangue in the +106µm range compared to the finer fractions which showed that particle size plays a role in gangue recovery in the Falcon. The gangue particles thus exhibit a complex mineralogy as well as complex behaviour when a gravity field is applied. Although the gangue particles are in the fine to ultra fine fraction on a mass basis

and are considerably less dense than the PGMs, the inherent complexity of the gangue as well as the relatively high concentrations of gangue compared to PGMs reduces the Falcon's effectiveness to completely reject the gangue particles. It is also postulated that the gangue becomes entrapped in the concentrate bed that is created in the bowl thus inhibiting its rejection.

The parameter optimization stage of the experiments converged at % solids, flowrate and gravitational force of 13.22%, 3 L/min and 300 G's respectively. These parameters were used in Phase 5 of the experimental protocol to determine the efficacy of gravity concentration for PGMs. The experimental results indicated that a 5-stage lab scale gravity concentration process achieves a mass pull of 21.9% with a 49.9% recovery and a concentrate grade of 292.04 g/t 4E PGM. This shows that close to 50% of the PGMs in the feed to the Falcon was recovered in 22% of the mass in the Falcon concentrate (GC concentrate). The Falcon is thus able to successfully recover PGMs by advanced gravity concentration at an improved concentrate grade. The mass yield per stage is approximately 4.4% which is the maximum capacity of the Falcon bowl, this means that additional stages or a larger unit could possibly recover additional PGMs.

The fluidized bowl was also tested with the same feed material. The results indicated that the fluidized bowl experiments had lower overall recoveries than those for the unfluidized (ultra fine) bowl and lower mass yields but higher grade concentrates were produced. The higher grades and lower recoveries are possibly due to the bowl recovering heavy and coarse PGMs while allowing finer PGMs to report to the tail. The fluidized bowl does seem to reject more gangue than the unfluidized bowl as greater than 99% on a mass basis of the gangue constituents were rejected. The fluidized bowl may therefore have utility as a cleaner stage when using gravity concentration for PGMs.

A simplified model was developed to understand what the effect of additional stages of the unfluidized bowl would be on the overall recovery of PGMs. The model was confirmed by measured data and indicated that by adding an additional 5 lab stages (total of 10 stages), the PGM recovery could get to approximately 68.41%.

The results prove that even though PGMs are complex and in the fine to ultra-fine size fraction, they can be recovered by advanced gravity concentration. The advanced gravity concentration is

also able to improve concentrate grade by rejecting gangue. Chrome is not concentrated with the PGMs in the Falcon which means that the chrome content remains below the acceptable level of 3% for smelting.

6. Conclusion and Recommendations

The overarching purpose of this study was to determine if advanced gravity concentration could successfully recover and upgrade the PGM flotation concentrates from a PGM tailings plant. In this respect, extensive experimental work and analysis was undertaken in order to prove this postulation and also to understand the behaviour and underlying principles governing gravity concentration of PGMs. This analysis was also extended to the gangue constituents and chromite in order to determine the behaviour of these minerals in the gravity concentrator. The novelty and significance of this study is underpinned by the fact that no research thus far has applied gravity concentration to PGM flotation concentrates; no study thus far has determined the interactions between PGMs, gangue and chromite in a gravity field; and finally, no previous study has had a multi-faceted approach to gravity concentration of PGMs by meticulously understanding the mineralogy of the ore, particle size distribution as well as gravity concentration of complex fine and ultra-fine PGMs. This study has investigated all of the above and added a unique perspective to current body of research of gravity separation processes.

Based on the findings in this thesis, the following conclusions can be drawn:

The complexity of PGM ore was proved as well as the association of PGMs with base metal sulphides. This complexity involved the PGMs being present together in a matrix in particles as well as being associated with other elements such as iron, titanium, arsenic and vanadium in some cases. Native PGMs are very rare but this research has shown that due to the higher recoveries of gold and ruthenium, that these particular elements may have higher concentrations as a result of being in their native form or may be associated with simple sulphides which makes these minerals easier to recover by gravity concentration.

The feed to the gravity concentrator was proved to be in the fine to ultra fine particle size range as 66.29% was below 25µm and 97.07% was below 75µm. The Falcon successfully recovered these fine and ultra fine particles as it was shown that 71.04% of the particles were below 25µm and 98.54% below 75µm in the gravity concentration concentrate. It was also proved that the vast majority of the PGMs lie in the fine to ultra fine size fraction and it was therefore critical to recover this fraction to the gravity concentrate stream. It was also shown that it becomes more

difficult to recover particles less than 15µm, though the gravity concentrator is still able to recover some of these particles. The reason for poor recoveries is due to the velocity of the fluid inducing a drag that is greater than the centrifugal force acting on fine particles causing the ultrafine PGM particles to be carried away with tailings.

The optimal parameters for lab scale gravity concentration with the Falcon were found to be a % solids of 13.22%, a flow rate of 3 L/min and a gravitational force of 300 G's. When these parameters were applied to a multi-stage gravity concentration process, the results achieved were: a mass pull of 21.9%, recovery of 48.9% and concentrate grade of 292.04 g/t 4E PGM. The enrichment ratio (upgrade ratio) was 2.23 which means that the original feed grade was doubled. This proved that advanced gravity concentration could be applied to PGM flotation concentrates successfully. The optimal parameters gravity concentration experiments were repeated ten times to ensure repeatability of results and to ensure a robust data set. The resulting assay results were subjected to a statistical outlier test by comparing results from each run against one another in the Minitab Software to ensure data integrity. The repetition of experiments and statistical analysis performed consequently validated the data used in this research.

A simplified model was created to determine the impact of additional gravity concentration stages and this model indicated a total recovery of 64.66% for a 10-stage process. These results were confirmed with measured data which indicated that a recovery of 68.41% was possible with a 10-stage process. This proves that additional stages can indeed recover a greater fraction of the PGMs. On a practical note, the tailings from the gravity concentrator can either be recycled back to the gravity circuit or the flotation cleaners to be re-cleaned and recovered.

The chrome content in the GC concentrate was well below the maximum 3% allowable by PGM smelters. The chrome content in the gravity concentrate was found to be 1.99% with an overall rejection of 77.84% of the chromite on a mass basis. This proves that chromite is not concentrated in the gravity concentration process and is rather rejected to the tailings stream.

The gangue constituents exhibit complexity in their mineralogy and behaviour in a gravity field. The silicon dioxide, magnesium oxide, calcium oxide and aluminium oxide had overall

concentrations of 53.47%, 24.50%, 2.74% and 4.63% respectively. These concentrations were similar to the gravity feed concentrations of gangue. The gangue rejection on a mass basis was 78.24%, 77.66%, 81.41% and 80.76% for silicon dioxide, magnesium oxide, calcium oxide and aluminium oxide respectively. This proves that gangue is rejected from the Falcon gravity concentrator but due to the high concentration of the gangue constituents in all size fractions and their complexity, it is challenging to appreciably reduce the concentration of these constituents in the concentrate.

Based on the findings and conclusions of this thesis, the following recommendations can be made

- Further research needs to be conducted on the effect of advanced gravity concentration on the PGM flotation concentrates of Merensky and UG-2 run-of-mine plants as this research only focussed on a UG-2 tailings plant concentrate.
- A combination of the Falcon unfluidized bowl as ‘roughers’ and the fluidised bowl as ‘cleaners’ needs to be tested. This would entail taking a feed through a multi-stage gravity concentration (as in Phase 5) and then cleaning this feed with a fluidised bowl to achieve higher grades. The unfluidized bowl will thus contribute to recovery while the fluidised bowl will contribute to concentrate grade.
- The application of gravity concentration can also be applied to the mainstream of flotation plant to treat either the feed or the tailings of the plant and essentially recover additional PGMs.
- A plant scale trial should be conducted which would lead to a business case on whether this technology is economically viable.

The implications of this research study for Academia and the PGM industry is that advanced gravity concentration should become an option in augmenting current and future process flow sheets to recover additional PGMs. The capital and operational costs of gravity concentrators are lower than the addition of flotation banks, but the economics of such decisions will have to be handled on a case-by-case basis.

7. References

Abela, R. L. (1997). Centrifugal Concentrators in Gold Recovery and Coal Processing. *Extraction Metallurgy Africa*.

Alp, I., Celep, O., & Deveci, H. (2008). Recovery of gold from a free-milling ore by centrifugal gravity separator. *Iranian Journal of Science and Technology*, 67-71.

Amariei, D., Michaud, D., Paquet, G., & Lindsay, M. (2014). The use of a Reflux Classifier for iron ores: Assessment of fine particles recovery at pilot scale. *Minerals Engineering*, 66-73.

Ambrós, W. M., Sampaio, C. H., Cazacliu, B. G., Conceição, P. N., & dos Reis, G. S. (2019). Some observations on the influence of particle size and size distribution on stratification in pneumatic jigs. *Powder Technology*, 594-606.

Andrew , N. J., van Beek , B., & Zietsman , L. A. (2014). Effect of Feed Composition Fluctuations on a Platinum Furnace Energy Balance and Slag Temperature. *The Southern African Institute of Minng and Metallurgy*, 4-5.

Anglo American Platinum. (2001). *investor-presentations.* Retrieved from www.angloamericanplatinum.com: https://www.angloamericanplatinum.com/~/media/Files/A/Anglo-American-Group-v5/Platinum/investor-presentations/2001/30-11-01.pdf

Aslan, N. (2008). Multi-objective optimization of some process parameters of a multi-gravity separator for chromite concentration. *Separation and Purification Technology*, 237-241.

Bahrami, A., Abdollahi, M., Mirmohammadi, M., Kazemi, F., Danesh, A., & Shokrzadeh, M. (2020). A process mineralogy approach to study the efficiency of milling of molybdenite circuit processing. *Scientific Reports*, Article number: 21211. Retrieved from https://www.nature.com/articles/s41598-020-78337-8#citeas

Ballhaus, C., & Sylvester, P. (2000). Noble metal enrichment processes in the Merensky Reef, Bushveld Complex. *Journal of Petrology, 41*, 545-561.

Bethell,, P. J., & Luttrell, G. H. (2004). Coal Preparation. In C. J. Cleveland (Ed.), *Encyclopedia of Energy.* Elsevier Inc.

Bradshaw, D. J., Harris, P. J., & O'Connor, C. T. (1998). Synergistic interactions betweenreagents in sulphide flotation reagents in sulphide flotation. *he Journal of The South African Institute of Mining and Metallurgy*, 189-194.

Brannen, J. (2016). *Mixing Methods: Qualitative and Quantitative Research.* New York: Routledge.

Bulatovic, S. M. (2015). *Handbook of Flotation Reagents: Chemistry, Theory and Practice.* Elsevier.

Bunt, J. R. (1995). *The Surface Characterisation of Twistdraai Ultrafine Coal.* Sastech R&D.

Cabri, L. J. (2002). *The Geology, Geochemistry, Mineralogy and Mineral Benefication of platinum-group elements* (Vol. 54). Canadian Institute of mining and metallurgy.

Cabri, L. J., Oberthür, T., & Keays, R. R. (2022). Origin and depositional history of platinum-group minerals in placers– A critical review of facts and fiction. *Ore Geology Reviews*.

Campbell, Q. P., le Roux, M., & Smith, I. G. (2015). Water-only laboratory coal fractionation using the reflux classifier. *Minerals Engineering*, 59-63.

Carelse, C., Manuel, M., Chetty, D., Taguta, J., Safari, M., & Youlton, K. (2022). The flotation behaviour of liberated Platinum Group minerals in Platreef ore under reduced reagent conditions. *Minerals Engineering*.

Cawthorn, G. R. (2010). The Platinum Group Element Deposits of the Bushveld Complex in South Africa. *Platinum Metals Review.*, 205-215.

Cawthorn, R. G. (2015). The Bushveld Complex, South Africa. In B. Charlier, O. Namur, R. Latypov, & C. Tegner, *Layered Intrusions* (pp. 1-12). Dordrecht: Springer Geology. Springer.

Chapman, N. A., Shackleton, N. J., Malysiak, V., & O'Connor, C. T. (2011). The effect of using different comminution procedures on the flotation of Platinum-Group Minerals. *Minerals Engineering*, 731-736.

Chaumba, J. B. (2022). A review of the emplacement and formation of magmatic platinum-group elements-enriched deposits in large layered mafic/ultramafic intrusions, with special reference to the "big three" (Stillwater Complex, Great Dyke, and Bushveld Complex). *Journal of African Earth Sciences*, 1-18.

Chen, Q., Yang, H.-y., Tong, L.-l., Niu, H.-q., Zhang, F.-s., & Chen, G.-m. (2020). Research and application of a Knelson concentrator: A review. *Minerals Engineering*, 1-15.

Chimwani, N., Glasser, D., Hildebrandt, D., Metzger, M. J., & Mulenga, F. K. (2013). Determination of the milling parameters of a platinum group minerals ore to optimize product size distribution for flotation purposes. *Minerals Engineering*, 67-78.

Chu, H., Wang, Y., Lu, D., Liu, Z., & Zheng, X. (2020). Pre-concentration of fine antimony oxide tailings using an agitated reflux classifier. *Powder Technology*, 565-572.

Chu, K. W., Wang, B., Yu, A. B., Vince, A., Barnett, G. D., & Barnett, P. J. (2009). CFD–DEM study of the effect of particle density distribution on the multiphase flow and performance of dense medium cyclone. *Minerals Engineering*, 893-909.

Cisternas, L. A., Acosta-Flores, R., Lucay, F., & Gálvez, E. D. (2016). Mineral Concentration Plants Design Using Rigorous Models. *Computer Aided Chemical Engineering*, 1461-1466.

Cole, S., & Ferron, C. J. (2002). A Review Of The Beneficiation And Extractive Metallurgy Of The Platinum Group Elements , Highlighting Recent Process Innovations. *SGS*.

Cramer , L. A. (2008). What is your PGM concentrate worth? In: Third International Platinum Conference, 'Platinum in Transformation. *South Africa: South African Institute of Mining and Metallurgy*, 5-9.

Creamer Media's Enginering News. (2017, November 29). *FLSmidth launches new, modular Reflux Classifier plant*. Retrieved 23 January, 2024, from www.engineeringnews.co.za: https://www.engineeringnews.co.za/print-version/flsmidth-launches-new-modular-reflux-classifier-plant-2017-11-29

Das, B., Prakash, S., Das, S. K., & Reddy, P. R. (2008). Effective Beneficiation of Low Grade Iron Ore Through Jigging Operation. *Journal of Minerals and Materials Characterization and Engineering*, 27-37.

Das, S. K., Angadi, S. I., Kundu, T., & Basu, S. (2020). Mineral Processing of Rare Earth Ores. In R. Jyothi, *Rare-Earth Metal Recovery for Green Technologies* (pp. 9-38). Springer.

Das, S. K., Tan, J., Kundu, T., Rath, S. S., & Angadi, S. I. (2023). Performance evaluation of Falcon fluidized bowl and ultrafine (UF) bowl concentrators for the recovery of ultrafine scheelite particles. *Advanced Powder Technology*, 1-12.

Davey , S. R. (1992). Lateral variations within the Upper Critical Zone of the Bushveld Complex on the farm Rooikoppies 297JQ Marikana, South Africa. *South African Journal of Geology*, 95(1), pp. 141–149.

Dehaine, Q., Filippov, L. O., & Joussemet, R. (2017). Rare earths (La, Ce, Nd) and rare metals (Sn, Nb, W) as by-products of kaolin production – Part 2: Gravity processing of micaceous residues. *Minerals Engineering*, 200-210.

Eales, H. V., Botha, W. J., de Klerk, W. J., Maier, W. D., & Odgers, A. T. (1993). The mafic rocks of the Bushveld complex: a review of emplacement and crystallization history, and mineralization, in the light of recent data. *Journal of African Earth Sciences (and the Middle East)*, 121-142.

Eckstrand, O. R., & Hulbert, L. J. (2007). Magmatic Nickel-Copper-Platinum Group Element Deposits. In W. D. Goodfellow, *Mineral Deposits of Canada: A Synthesis of Major Deposit Types, District Metallogeny, the Evolution of Geological Provinces, and Exploration Methods:* (pp. 205-222). Geological Association of Canada, Mineral Deposits Division.

Ehmer, A., Kolb, S., Teßmar, J., Blunk, T., & Göp, A. (2006). Micronization of Proteins by Jet Milling. *Material Science*.

Ekmekçi, Z., Bradshaw, D. J., & Harris, P. J. (2005). Interactive effects of the type of milling media and CuSO4 addition on the flotation Part II: Froth stability. *Mineral Processing*, 164-174.

El-khalek, N. A., Naser, M. I., Yassin, K. E., & Al Kelesh, H. (2014). Studying the Reduction Behavior of Eastern Desert Iron After Beneficiation using falcon concentrator. *Journal of ore dressing*, 11.

Engelbrecht, J. (2012). Potential changes in the physical beneficiation processes that can improve the recovery grade or costs for the platinum group metals. *The Southern African Institute of Mining and Metallurgy*, 343-360.

Eriez. (2024). *StackCell-Flotation*. Retrieved February 5, 2024, from Eriez: https://www.eriez.com/NA/EN/Flotation/StackCell-Flotation.htm

Eriksson, P. G., Hattingh, P. J., & Altermann, W. (1995). An overview of the geology of the Transvaal Sequence and Bushveld Complex, South Africa. *Mineralium Deposita*, 30 (2): 98–111.

Farajzadeh, S., & Chelgan, S. C. (2022). Gravity separation by falcon concentrator- an overview. *Separation Science and Technology*, 2145-2164.

Fatahi, M. R., & Farzanegan, A. (2017). DEM simulation of laboratory Knelson concentrator to study the effects of feed properties and operating parameters. *Advanced Powder Technology, 28*(6), 1443-1458.

Ferdana, A. D., Petrus, H. T., Bendiyasa, I. M., Prijambada, I. D., Hamada, F., & Sachiko, T. (2018). Optimization of gold ore Sumbawa separation using gravity method: Shaking table. *Proceedings of the 3rd International Conference on Materials and Metallurgical Engineering and Technology (ICOMMET 2017)*. Surabaya, Indonesia: AIP Publishing.

Fitzpatrick, R. S., Ghorbani, Y., Hegarty, P., & Rollinson, G. (2016). Quantitative Mineralogy for Improved Modelling of Shaking Tables. *International Mineral Processing Congress Proceedings* (pp. 1-19). Canadian Institute of Mining, Metallurgy and Petroleum.

FLSmidth. (2024). *centrifugation-and-classification*. Retrieved January 6, 2024, from FLSmidth: https://www.flsmidth.com/en-gb/products/centrifugation-and-classification/krebs-spirals

FLSmidth. (2024). *reflux-classifier*. Retrieved January 24, 2024, from www.flsmidth.com/: https://www.flsmidth.com/en-gb/products/centrifugation-and-classification/reflux-classifier

Foucaud, Y., Filippova, I., Dehaine, Q., Hubert, P., & Filippov, F. (2019). Integrated approach for the processing of a complex tungsten Skarn ore (Tabuaço, Portugal). *Minerals Engineering, 143*.

Galvin, K. P., & Ivenson, S. M. (2014). Gravity separation and flotation of fine particles using the Reflux Classifier platform. *Engineering Materials Science*.

Gee, B., & Holtham, P. (2005). Recovery of fine gold particles using a Falcon 'B' separator. Indooroopilly, Queensland, Australia: Julius Kruttschnitt Mineral Research Centre. Retrieved from file:///C:/MSc%202022/Course%20Work/CHMT7008A%20Research/Literature%20Review/Journals/Advanced%20Gravity%20Concentration/Holtham_Gee.pdf

Godel , B., Barnes, S.-J., & Maier, W. D. (2007). Platinum-Group Elements in Sulphide Minerals, Platinum-Group Minerals, and Whole-Rocks of the Merensky Reef (Bushveld Complex, South Africa): Implications for the Formation of the Reef. *Journal of Petrology, 48*(8), 1569-1604.

GoldFields. (2024). *goldfields-southdeep*. Retrieved November 9, 2023, from about-south-deep/how-we-process: https://www.goldfields-southdeep.co.za/about-us/about-south-deep/how-we-process

Golyk, V., Huber, S., Farghaly, M. G., Prölss, G., Endres, E., Neesse, T., & Hararah, M. A. (2011). Higher kaolin recovery with a water-injection cyclone. *Minerals Engineering*, 98-101.

Grayson, R. (2007). Fine Gold Recovery - Alternatives to Mercury and Cyanide. *World Placer Journal*, 66-161.

Grewal, I., & Neale, A. (2017). Enhanced gravity recovery of base metal and industrial minerals. *Annual Canadian Mineral Processors Operators Conference*, (pp. 362-373). Ottawa. Retrieved from file:///C:/MSc%202022/Course%20Work/CHMT7008A%20Research/Literature%20Review/Journals/Advanced%20Gravity%20Concentration/Enhanced-Gravity-Recovery-of-Base-Metal-and-Industrial-Minerals.pdf

Gruenewaldt, G. v. (1991). *Platinum Metals Review.* Retrieved November 8, 2023, from Johnson Matthey Technology Review: https://technology.matthey.com/content/journals/pmr/35/2

Guerney, P., Laplante, A., & O'Leary, S. (2003). . Gravity-recoverable gold and the Mineral Liberation Analyser. 401-416.

Guest, R. N., & Dunne, R. C. (1985). An evaluation of gravity separators by use of a synthetic ore. *Journal Of The South African Institute Of Mining And Metallurgy*, 187-195.

Gülsoy, Ö. Y., & Gülcan, E. (2019). A new method for gravity separation: Vibrating table gravity concentrator. *Separation and Purification Technology*, 124-134.

Gupta, A., & Yan, D. S. (2006). Chapter 16 - Flotation. In A. Gupta, & D. S. Yan, *Mineral Processing Design and Operation* (pp. 555-603). Elsevier.

Haldar, S. K. (2018). *Mineral Exploration: Principles and Applications* (2 ed.). Elsevier.

Harris, D. C., & Cabri, L. J. (1991). Nomenclature of platinum-group-element allopys; review and revision. *The Canadian Minerologist*, 231-237.

Hay , M. P., & Schroeder, G. (2005). Use of the SUPASIM flotation model in optimizing Impala's UG2 circuit. *Minerals Engineering*, 772-784.

Hay, M. P., & Roy, R. (2010). A case study of optimising UG2 flotation performance. Part 1: Bench, pilot and plant scale factors which influence Cr2O3 entrainment in UG2 flotation. *Minerals Engineering*, 855-867.

Heins, R., Spargo, R., & McCallum, A. (2003). Successful Applications Of The InLine Pressure Jig With Particular Reference To The Recovery Of Gold and Diamonds. *SAIMM Gravity Conference* (pp. 1-16). Hartebeespoort: Gekko Systems South Africa.

Hennart, S. L., Wildeboer, W., van Hee, P., & Meesters, G. (2009). Identification of thegrinding mechanisms and their origin in a stirred ball mill using population balances. *Chemical Engineering Science*, 4123-4130.

Heu, R., Shahbazmohamadi, S., Yorston, J., & Capeder, P. (2019). *Target Material Selection for Sputter Coating of SEM Samples* (Vol. 27). Cambridge University Press.

Holland-Batt, A. B. (1995). *Some Design Considerations for Spiral Separators.* Lake Tahoe: Minerals Engineering.

Holland-Batt, A. B., Balderson, G. F., & Cross, M. S. (1982). The application and design of wet-gravity circuits in the South African minerals industry. *Journal of the south african institute of mining and metallurgy*, 53-70.

Houot, R., Cuif, J. P., Mottot, Y., & Samama, J. C. (1991). Recovery of Rare Earth Minerals, with Emphasis on Flotation Process. *Materials Science Forum,*, 301-324.

Huang, L., & Mejiab, N. (2002). Characterising gravity recoverable PGMs and Gold in grinding circuit. *Iranian Journal of Science & Technology, Transaction*.

Hurdeyal, R. (2012). *A comparison between column and mechanical cell performance in platinum flotation.* Durban: University of Kwazulu-Natal.

Ilunga, M. K. (2014). *Binary Modelling the Milling of UG2 Ore.* Johannesburg : University of the Witwatersrand.

Jena, M. S., Mohanty, J. K., Sahu, P., Venugopal, R., & Mandre, N. R. (2017). Characterization and Pre-concentration of Low Grade PGE Ores of Boula Area, Odisha using Gravity Concentration Methods. *Trans Indian Inst Met*, 287-302.

Jones, R. T. (1999). Platinum smelting in South Africa. *South African Journal of Science*, 525-534.

Jones, R. T. (2005). An overview of Southern African PGM smelting. *44th Annual Conference of Metallurgists, Calgary, Alberta, Canada*, 147-178.

Kademli, M., & Gülsoy, Ö. (2012). The role of particle size and solid contents of feed on mica-feldspar separation in gravity concentration. *Physicochemical Problems of Mineral Processing*, 645-654.

Kawatra, S. (2011). Fundamental principles of froth flotation. Michigan , Michigan Technological University.

Khakmardan, S., Doodran, R., Shirazy, A., Shirazi, A., & Mozaffari, E. (2020). Evaluation of Chromite Recovery from Shaking Table Tailings by Magnetic Separation Method. *Open Journal of Geology*, 1153-1163.

Khan, W. S., Asmatulu, E., Uddin, N., & Asmatulu, R. (2022). *Recycling and Reusing of Engineering Materials.* Elsevier Inc. doi:https://doi.org/10.1016/C2019-0-04547-5

King, R. P. (2001). *Modeling and Simulation of Mineral Processing Systems.* Boston: Butterworth Heinmann.

Klimpel, R. R. (2003). Encyclopedia of Physical Science and Technology (Third Edition). In R. A. Meyers, *Froth Flotation* (pp. 219-234). Academic Press.

Koppalkar, S. (2009). *Effect of Operating Variables in Knelson Concentrators: A Pilot-Scale Study,*. McGill University.

Kozeyrev, S. M., Komarova, M. Z., Emelina,, L. N., Oleshkevich, O. I., Yakovleva, O. A., Lyalinov, D. V., & Maximov, V. I. (2003). The Mineralogy and Behavior of PGM during Processing of the Norilsk–Talnakh PGE–Cu–Ni Ore. *The Geology, Geochemistry, Mineralogy and Mineral Beneficiation of Platinum Group Elements.*, 675-679.

Kroll-Rabotin, J.-S., & Sanders, R. S. (2014). Implementation of a model for Falcon separation units using continuous size-density distributions. *Minerals Engineering*, 138-141.

Kroll-Rabotin, J.-S., Bourgeois, F., & Climent, É. (2012). Experimental validation of a fluid dynamics based model of the UF Falcon concentrator in the ultrafine range. *Separation and Purification Technology*, 129-135.

Kumar, D., & Kumar, D. (2018). Chapter 5 - Wet Cleaning Process by Major Unit Operations. In *Sustainable Management of Coal Preparation* (pp. 69-114). Woodhead Publishing.

Laplante, A. R. (1993). A comparative stuy of two centrifugal concentrators. *24th Annual Meeting of the Canadian Mineral Processors.* Ottawa: McGill University.

Laskowski, J. S. (2004). Activation in flotation circuits: Challenges and Opportunities. *International Mineral Processing Symposium*, (pp. 377-394).

Laskowski, J. S., Tlhone, T., Williams, P., & Ding, K. (2003). Fundamental properties of the polyoxypropylene alkyl ether flotation frothers. *International Journal of Mineral Processing*, 289-299.

Leppinen, J., Kreutzman, N., Moilanen, A., Kloow, G., Kalapudas, R., & Luukkanen, S. (2004). Depression of Gangue Minerals Using Tailor-Made CMCs in Sulfide Ore Flotation. *Centenary of Flotation Symposium.* AUSIMM. Retrieved from https://www.ausimm.com/publications/conference-proceedings/centenary-of-flotation-symposium/depression-of-gangue-minerals-using-tailor-made-cmcs-in-sulfide-ore-flotation/#:~:text=Carboxymethyl%20cellulose%2C%20CMC%2C%20is%20widely,Ni%20sulfide%20and%20PGM

Liddell, K. S. (2009). 25 Years of UG-2 concentrators. *Mintek 75' – A celebration of Technology Conference.* Mintek.

Lishchuk, V. (2019). *Bringing predictability into a geometallurgical program: An iron ore case study.* Luleå University of Technology.

Lishchuka, V., Kocha, P.-H., Ghorbania, Y., & Butcher, A. R. (2020). Towards integrated geometallurgical approach: Critical review of current practices and future trends. *Minerals Engineering*, 1-16.

Lisso, M. (2013). *Evaluating the Effect of Operating Variables on Energy Consumption in Stirred Mills.* Cape Town: University of Cape Town.

Little, L. (2016). *The Development and Demonstration of A Practical Methodology for Fine Particle Shape Characterisation in Minerals Processing.* Cape Town: University of Cape Town.

Lotter, N. O., & Bradshaw, D. J. (2010). The formulation and use of mixed collectors in sulphide flotation. *Minerals Engineering*, 945-951.

Loveday, B. K., & Forbes, J. E. (1982). Some considerations in the use of gravity concentration for the recovery of gold. *Journal of the south african institute of mining and metallurgy*, 121-124.

Luttrell, G. H., Phillips, D. I., & Honaker, R. Q. (1995). Enhanced gravity separators: New alternatives for fine coal cleaning. *International coal preparation exhibition and conference.* Lexington, KY: U.S. Department of Energy: Office of Scientific and Technical Information.

Maharaj, L., Loveday, B. K., & Pocock, J. (2012). Gravity separation of a UG-2 ore secondary sample for the reduction of chromite minerals. *Minerals Engineering*, 99-101.

Maier, W. D., Barnes, S. J., & Groves, D. I. (2013). The Bushveld Complex, South Africa: formation of platinum–palladium, chrome- and vanadium-rich layers via hydrodynamic sorting of a mobilized cumulate slurry in a large, relatively slowly cooling, subsiding magma chamber. *Miner Deposita, 48*, 1-56.

Marsden, J. O. (2006). *The Chemistry of Gold Extraction.* Littleton: Society for Mining, Metallurgy, and Exploration.

Martinovic, J., Bradshaw, D. J., & Harris, P. J. (2004). Investigation of surface properties of gangue minerals in platinum bearing ores. *Proceedings of Platinum adding Value.* Sun City.

Matsau, E. N. (2003). *Determination of platinum, palladimn, rhodium and gold in platiniferous ores using ICP-MS and microwave dissolution.* Stellenbosch: University of Stellenbosch.

McCallum, I. S. (1996). The Stillwater Complex. *Developments in Petrology*, 441-483.

McLaren, C. H., & De Villiers, J. P. (1982). The platinum-group chemistry and mineralogy of the UG-2 chromitite layer of the Bushveld Complex. *Economic Geology, 77*(6), 1348-1366.

Metso. (2011). *Basics in Minerals Processing. 8th edn.* Helsinki: Metso Corporation.

Miettinen, T., Ralston, J., & Fornasiero, D. (2010). The limits of fine particle flotation. *Minerals Engineering,, 23*(5), 420-437.

Misra, V. N., Reddy, P. S., & Mohapatra, B. K. (2004). *Mineral characterisation and processing.* Bhubaneswar, India, New Delhi: egional Research Laboratory, Council of Scientific and Industrial Research : Indian Institute of Mineral Engineers.

Moitra, A. K., Kayal, J. R., Mukerji, B., Bhattacharya, J., & Das, A. K. (2021). *Innovative Exploration Methods for Minerals, Oil, Gas, and Groundwater for Sustainable Development.* Elsevier Inc.

Mpinga, C. N., Eksteen, J. J., Aldrich, C., & Dyer, L. (2015). Direct leach approaches to Platinum Group Metal (PGM) ores and concentrates: A review. *Minerals Engineering*, 93-113.

Multotec. (2019). *how-do-spiral-concentrators-work.* Retrieved January 6, 2024, from Multotec Spirals: https://www.multotec.com/en/news-articles/how-do-spiral-concentrators-work

Mwase, J. M., Petersen, J., & Eksteen, J. J. (2012). A conceptual flowsheet for heap leaching of platinum group metals (PGMs) from a low-grade ore concentrate. *Hydrometallurgy*, 12-135.

Naldrett , A. J., & Gruenewaldt, G. v. (1989). Association of platinum-group elements with chromitite in layered intrusions and ophiolite complexes. *Economic Geology, 84*(1), 180-187.

Naldrett, A. J. (2010). Secular Variation of Magmatic Sulfide Deposits and Their Source Magmas. *Economic Geology, 105*(3), 669-688.

Nayak, A., Jena, M. S., & Mandre, N. R. (2021). Application of Enhanced Gravity Separators for Fine Particle Processing: An Overview. *Sustainable Metallurgy*, 315-339.

Nel, E., & et al. (2004). *PGM Ore Processing at Impala's UG-2 Concentrator in Rustenburg, South Africa.* SGS Minerals Services.

Nesset, J. E., Hernandez-Aguilar, J. R., Acuna, C., Gomez, C. O., & Finch, J. A. (2006). Some gas dispersion characteristics of mechanical flotation machines. *Minerals Engineering, 19*(6-8), 807-815.

Newman, S. C. (1973). *Transactions of the Institute of Mining and Metallurgy.* A52-A68.

Ngoroma, F., Wiese, J., & Franzidis, J.-P. (2013). The effect of frother blends on the flotation performance of selected PGM bearing ores. *Minerals Engineering*, 76-82.

Nguyen, A. V. (2012). Froth Flotation. In Elsevier, *Reference Module in Chemistry, Molecular Sciences and Chemical Engineering.* Elsevier.

Nyabeze, N., & McFadzean, B. (2016). Adsorption of copper sulphate on PGM-bearing ores and its influence on froth stability and flotation kinetics. *Minerals Engineering*, 28-36.

O'Connor, C., & Alexandrova, T. (2021). The Geological Occurrence, Mineralogy, and Processing by Flotation of Platinum Group Minerals (PGMs) in South Africa and Russia. *Minerals* .

Oberthür, T. (2011). Platinum-Group Element Mineralization of the Main Sulfide Zone, Great Dyke, Zimbabwe. In C. Li, & E. M. Ripley, *Magmatic Ni-Cu and PGE Deposits: Geology, Geochemistry, and Genesis* (Vol. 17). Society of Economic Geologists.

Oberthür, T. (2018). The Fate of Platinum-Group Minerals in the Exogenic Environment—From Sulfide Ores via Oxidized Ores into Placers: Case Studies Bushveld Complex, South

Africa, and Great Dyke, Zimbabwe. *Special Issue Platinum-Group Minerals: New Results and Advances in PGE Mineralogy in Various Ni-Cu-Cr-PGE Ore Systems*.

Olubambi, P. A., & Potgieter, J. H. (2005). Effectiveness Of Gravity Concentration For The Beneficiation Of Itakpe (Nigeria) Iron Ore Achieved Through Jigging Operation. *Journal of Minerals & Materials Characterization & Engineering*, 21-30.

Oniyide, G. (2015). *Thermo-mechanical behaviour of rocks from the bushveld igneous complex with relevance to deeper mining.* Johannesburg : Wits University.

Osbahr, I., Klemd, R., Oberthür, T., Brätz, H., & Schouwstra, R. P. (2013). Platinum-group element distribution in base-metal sulfides of the Merensky Reef from the eastern and western Bushveld Complex, South Africa. *Mineralium Deposita*, 211-232.

Osborne, D. G. (1988). *Coal Preparation Technology (Volume II).* . London: Graham & Trotman Ltd.

Östlund, U., Kidd, L., Wengström, Y., & Rowa-Dewar, N. (2011). Combining qualitative and quantitative research within mixed method research designs: A methodological review. *International Journal of Nursing Studies*, 369-383.

Parry, J. M. (2004). *Ultrafine Grinding or Improved Mineral Liberation in Flottaion Concentrates.* The University of British Columbia.

Parry, J. M. (2006). *Ultrafine grinding for improved mineral liberation in flotation concentrates.* British Columbia: The University of British Columbia.

Peck, D. C., & Huminicki, M. A. (2016). Value of mineral deposits associated with mafic and ultramafic magmatism: Implications for exploration strategies. *Ore Geology Reviews*, 269-298.

Peer, F., Mongwe, A., & van Heerden, J. H. (2001). A preliminary investigation into the metallurgical efficiency of an enhanced gravity separator. *The Journal of The South African Institute of Mining and Metallurgy*, 251-254.

Penberthy, C. J., Oosthuyzen, E. J., & Merkle, R. K. (2000). The recovery of platinum- group elements from the UG-2 chromitite, Bushveld Complex – a mineralogical perspective. *Mineralogy and Petrology, 68*(1-3), 213-222.

Perroton, A., Wallmach, T., Blancher, S. B., & Rameau, G. (2020). A geometallurgical approach to enhance the gravity beneficiation of a strontium deposit. *The Southern African Insitute of Mining and Metallurgy*, 131-138.

Rafiei, A. A., Robbertze, M., & Finch, J. A. (2010). Gas holdup and single bubble velocity profile. *International Journal of Mineral Processing*, *98*(1-2), 89-93.

Rao, S. R. (2006). *Resource Recovery and Recycling from Metallurgical Wastes.* Quebec, Canada: McGill University.

Rath, R. K., & Singh, R. (2007). Gravity Concentration of Iron Ore. *Processing of Iron Ore*.

Renner, H., Schlamp, G., Kleinwächte, I., Drost, E., Lüschow, H. M., & Tews, P. (2002). *"Platinum group metals and compounds". Ullmann's Encyclopedia of Industrial Chemistry.* Wiley.

Richards, R. G., & Jones, T. A. (2004). Kelsey Centrifugal Jig - An update on technology and application. *Minerals & Metallurgical Processing*, 179-182.

Richardson, J. F., Harker, J. H., & Backhurst, J. R. (2002). *Coulson and Richardson's CHEMICAL ENGINEERING.* Woburn: Butterworth-Heinemann.

Rio Tinto. (2024). *richards-bay-minerals*. Retrieved February 10, 2024, from Rio Tinto: https://www.riotinto.com/en/operations/south-africa/richards-bay-minerals

Rodrigues, A. F., Junior, O. M., Zhou, J., & Galvin, K. P. (2023). Gravity separation of fine itabirite iron ore using the Reflux Classifier – Part I – Investigation of continuous steady state separations across a wide range of parameters. *Minerals Engineering*, 1-12.

Rouquerol, F., Rouquerol, J., & Sing, K. (1999). CHAPTER 12 - Properties of Some Novel Adsorbents. In F. Rouquerol, J. Rouquerol, & K. Sing, *Adsorption by Powders and Porous Solids* (pp. 401-438). Academic Press.

Rule, C. M. (2008). Energy considerations in the current PGM processing flowsheet utilizing new technologies. *Third International Platinum Conference.* The Southern African Institute of Mining and Metallurgy.

Rule, C. M., & Anyimadu, A. K. (2007). Flotation cell technology and circuit design—an Anglo Platinum perspective. *The Journal of The Southern African Institute of Mining and Metallurgy*, 615-622.

Rule, C. M., Knopjes, L., Clermont, B., & Philippe, C. (2008). Fine grinding—developments in ceramic media technology and resulting improved plant performance at Anglo Platinum. *Third International Platinum Conference: Platinum in Transformation* (pp. 53-62). The Southern African Institute of Mining and Metallurgy.

Santana, R. C., Farnese, A. C., Fortes, M. C., & Ataíde, C. H. (2008). Influence of particle size and reagent dosage on the performance of apatite flotation. *Separation and Purification Technology*.

Sarkar, B., Sekhar , S. C., & Das, A. (2007). *Advanced gravity seperators - A review of state of the art technology.* Jamshedpur, India: NML.

Schlesinger, M. E., Sole, K. C., Davenport, W. G., Gerardo, R. F., & Flores, A. (2022). *Extractive Metallurgy of Copper.* Elsevier.

Schouwstra, R. P., Kinloch, E. D., & Lee, A. A. (2000). A Short Geological Review of the Bushveld Complex. *Platinum Metals Review*, 44(1), pp. 33–39.

Schriner, D., & Anderson, C. (2015). Centrifugal Concentration of Rare Earth Minerals from Calcitic Gangue. *Journal of Metallurgical Engineering*, 69-77. doi:10.14355/me.2015.04.009

Sefako, R. (2018). *Recovery of PGMs from an oxide ore by flotation and leaching.* Johannesburg: Wits University.

Sefako, R., Sibanda, V., & Sekgarametso, K. (2019). PGM extraction from oxidized ores using flotation and leaching. *Journal of the Southern African Institute of Mining and Metallurgy*.

Seifelnasr, A. A., Tammam, T., & Abouzeid, A. (2012). Gravity Concentration of Sudanese Chromite Ore Using Laboratory Shaking Table. *Physicochemical Problems of Mineral Processin*, 271-280.

Sepro Mineral Systems. (2024). *falcon-sb-gravity-concentrators*. Retrieved January 10, 2024, from minerals.seprosystems.com: https://minerals.seprosystems.com/

Sepro Mineral Systems. (2024, January 9). *hoose-a-falcon-gravity-concentrator-for-fine-gold-recovery*. Retrieved from minerals.seprosystems: https://minerals.seprosystems.com/choose-a-falcon-gravity-concentrator-for-fine-gold-recovery/

Sepro Mineral Systems. (2024). *minerals.seprosystems.com/knowledge/*. Retrieved January 21, 2024, from https://minerals.seprosystems.com/knowledge/: https://minerals.seprosystems.com/knowledge/

Sepro Systems. (2018, December). Falcon Laboratory Procedure: Falcon ‘C’ and ‘UF’ Test Procedure.

Sierra, H. M., Šyc, M., & Korotenko, E. (2024). Wet shaking table operating parameters optimization for maximizing metal recovery from incineration bottom ash fine fraction. *Waste Management*, 539-548.

Singh, R. K., Kishore, R., Sahu, K. K., Chalavadi , G., & Singh , R. (2019). Estimation of the Fluid Velocity Profile in the Stratification Zone of a Falcon Concentrator. *Mining, Metallurgy & Exploration*, 321-331.

Singh, R., Bhattacharyya, K., & Maulik, S. C. (1997). Gravity concentration of fines and ultrafines. (pp. 40-56). Jamshedpur: NML.

Sinisalo, P., & Lundström, M. (2018). Refining Approaches in the Platinum Group Metal Processing Value Chain—A Review. *Metals*, 8(4):203.

Sivamohan, R. (1990). The problem of recovering very fine particles in mineral processing — A review. *International Journal of Mineral Processing, 28*(3-4), 247-288.

Solo Resources. (2024). *deister-shaking-tables*. Retrieved December 11, 2023, from www.soloresources.co.za: https://www.soloresources.co.za/deister-shaking-tables/

Solomon, N. (2010). *Effect of HPGR on platinum bearing ores and the flotation response as compared to the conventional ball mill.* Cape Town: University of Cape Town.

Solomon, N., Becker, M., Mainza, A., Petersen, J., & Franzidis, J.-P. (2011). Understanding the influence of HPGR on PGM flotation behavior using mineralogy. *Minerals Engineering*, 1370-1377.

Song, Z. G., Corin, K. C., Wiese, J. G., & O'Connor, C. T. (2018). Effect of different grinding media composition on the flotation of a PGM ore. *Minerals Engineering*, 74-76.

Thethwayo, B. M. (2017). Extraction of Platinum Group Metals. *InTech*. doi:10.5772/intechopen.73214

U.S. Geological Survey. (2020). *Mineral Commodity Summaries 2020.* Reston, VA.

Varinot, C., Hiltgun, S., Pons, M. N., & Dodds, J. (1997). Identification of the fragmentation mechanisms in wet-phase fine grinding in a stirred bead mill. *Chemical Engineering Science*, 3605-3612.

Walklate, J. R., & Fourie, P. J. (2006). A history of gravity separation at Richards Bay Minerals. *The Journal of The Southern African Institute of Mining and Metallurgy*, 741-748.

Wang, Z., Zheng, Y., Huang, X., Wang, X., Peng, J., & Dai, Z. (2024). Gravity Separation Tests of a Complex Rutile Ore. *Minerals*. Retrieved from https://doi.org/10.3390/min14010068

Wansbury, N. T. (2016). *Mineral Chemistry of Merensky Reef Chromitite Layers in the Marikana District.* Johannesburg: University of the Witwatersrand.

Watson, B. P., Kuijpers, J. S., & Stacey, T. R. (2010). Design of Merensky Reef crush pillars. *The Journal of The Southern African Institute of Mining and Metallurgy*, 581-591.

Wiese, J. G., Becker, M., Bradshaw, D. J., & Harris, P. J. (2006). Interpreting the role of reagents in the flotation of platinum bearing Merensky ores. *The Southern African Institute of Mining and Metallurgy*, 175-180.

Wills, B. A. (1989). *Mineral Processing Technology, An introduction to the Practical aspect of ore treatment and mineral recovery* (3 ed.). New York: Pergamon.

Wills, B. A. (2015). *Wills' Mineral Processing Technology: An Introduction to the Practical Aspects of Ore Treatment and Mineral Recovery* (8 ed.). Butterworth-Heinemann.

Wills, B. A., & Napier-Munn, T. (2006). *Wills' Mineral Processing Technology* (7 ed.). Oxford, England: Butterworth-Heinemann.

Wilson, A. H. (1996). The Great Dyke of Zimbabwe. *Developments in Petrology*, 365-402.

Woodgrove Technologies. (2024). *Direct Flotation Reactor*. Retrieved February 15, 2024, from Woodgrove Tech: http://www.woodgrovetech.com/direct-flotation-reactor/

Woollacott, L. C., Tripathy, A., & Potgieter, H. (2021). The effect of operating conditions on density stratification in a batch jig I: The influence on the equilibrium stratification profile. *Minerals Engineering*, 1-11.

Wright, G., Richards, R. G., & Cross, M. S. (1986). The development of mineral sands separation technology—Solving today's problems, Anticipating Tomorrows's. *Proceedings: Australia: A Source of Ilmenite, Rutile, Monazite and Zircon Conference.* Perth. Western Autralia.

Xiao , Z., Laplante, A. R., & Finch, J. A. (2009). Quantifying the content of gravity recoverable platinum group minerals in ore samples. *Minerals Engineering*, 304-310.

Xiao, Z., & Laplante, A. R. (2004). Characterizing and recovering the platinum group minerals––a review. *Minerals Engineering*, 961-979.

Xing, Y., Gui, X., Karakas, F., & Cao, Y. (2017). Role of Collectors and Depressants in Mineral Flotation: A Theoretical Analysis Based on Extended DLVO Theory. *Minerals*.

Yan, D., & Gupta, A. (2006). *Mineral Processing Design & Operation: An Introduction.* Netherlands: Elsevier Publisher,.

Yann, F., Dehaine, Q., Filippov , L. O., & Filippova , I. V. (2019). Application of Falcon Centrifuge as a Cleaner Alternative for Complex Tungsten Ore Processing. *Minerals*, 1-20.

Yao, Z. Z., & Zhang, W. C. (2018). Application of Knelson concentrators in Jinchuan precious metals beneficiation. *World Nonferrous Metals*, 53-54.

Zeiss. (2024). *sem.* Retrieved March 5, 2024, from www.zeiss.com: https://www.zeiss.com/microscopy/en/products/sem-fib-sem/sem.html

Zhao, Y., Zhang, Y., Bao, S., Liu, T., Bian, Y., Liu, X., & Jiang, M. (2013). Separation factor of shaking table for vanadium pre-concentration from stone coal. *Separation and Purification Technology*, 92-99.

Zhou, J. B. (2004). Establishing the Process Mineralogy of Gold Ores. *SGS Minerals Technical Bulletin*.

Appendices

Appendix A: Phase 1-4 Data

Run 1

Phase 2	% Solids	Mass (g)	Mass Recovery (%)	Cum Mass recovery %	Mass recovery (g)	4E PGM (g/t)	4E PGM Recovery (%)	4E PGM Cum Recovery (%)	4E PGM (g)	4E PGM Upgrade
Gravity Concentrate Feed		15000.00				131.02				
Gravity Concentrate R1		241.00	1.6%	1.6%	241.00	514.53	6%	6.3%	0.12	3.93
Gravity Concentrate R2	13.22	221.00	1.5%	3.1%	221.00	458.56	5%	11.5%	0.10	3.50
Gravity Concentrate R3		252.00	1.7%	4.8%	252.00	488.64	6%	17.7%	0.12	3.73
Total Gravity Conc.		*714.00*	*4.8%*		*714.00*	*488.07*	***17.7%***		*0.35*	**3.73**
Gravity Concentrate Tail		14286.00	95.2%		14286.00	113.18			1.62	
Totals		*15000.00*	*100%*		*15000.00*	***131.02***	***17.73%***		*1.97*	***3.73***

PT_Ave	PD_Ave	AU_Ave	RH_Ave	SUM4E	Cr2O3_Av
g/T	g/T	g/T	g/T	g/T	%
80.353	34.989	0.708	14.971	131.021	1.966
347.93	129.85	3.58	33.17	514.534	2.161
313.06	110.88	3.36	31.25	458.558	1.978
333.50	118.99	3.35	32.80	488.635	1.973
332.04	120.14	3.43	32.45	488.07	2.04
				0	

131.0209167

Run 2

Phase 2	% Solids	Mass (g)	Mass Recovery (%)	Cum Mass recovery %	Mass recovery (g)	4E PGM (g/t)	4E PGM Recovery (%)	4E PGM Cum Recovery (%)	4E PGM (g)	4E PGM Upgrade
Gravity Concentrate Feed		5000.00				131.02				
Gravity Concentrate R1		257.00	1.7%	1.7%	257.00	408.43	5%	5%	0.10	3.12
Gravity Concentrate R2	21.12	265.00	1.8%	3.5%	265.00	368.30	5%	10%	0.10	2.81
Gravity Concentrate R3		263.00	1.8%	5.2%	263.00	451.06	6%	16%	0.12	3.44
Total Gravity Conc.		*785.00*	*5.2%*		*785.00*	*409.17*	***16.3%***		*0.32*	**3.12**
Gravity Concentrate Tail		14215.00	94.8%		14215.00	115.66			1.64	
Totals		*15000.00*	*100%*		*15000.00*	***131.02***	***16%***		*1.97*	***3.12***

PT_Ave	PD_Ave	AU_Ave	RH_Ave	SUM4E	Cr2O3_Av
g/T	g/T	g/T	g/T	g/T	%
80.353	34.989	0.708	14.971	131.021	1.966
295.963	79.384	2.684	30.399	408.430	2.239
243.919	92.976	2.421	28.987	368.303	2.12
303.71	112.231	3.073	32.044	451.058	2.192
280.99	94.98	2.73	30.47	409.17	2.18
				0	

Run 3

Phase 2	% Solids	Mass (g)	Mass Recovery (%)	Cum Mass recovery %	Mass recovery (g)	4E PGM (g/t)	4E PGM Recovery (%)	4E PGM Cum Recovery (%)	4E PGM (g)	4E PGM Upgrade
Gravity Concentrate Feed		5000.00				131.02				
Gravity Concentrate R1		267.00	1.8%	1.8%	267.00	360.47	5%	5%	0.10	2.75
Gravity Concentrate R2	26.40	293.00	2.0%	3.7%	293.00	375.27	6%	10%	0.11	2.86
Gravity Concentrate R3		285.00	1.9%	5.6%	285.00	382.83	6%	16%	0.11	2.92
Total Gravity Conc.		*845.00*	*5.6%*		*845.00*	*373.14*	***16.04%***		*0.32*	**2.85**
Gravity Concentrate Tail		14155.00	94.4%		14155.00	116.57			1.65	
Totals		*15000.00*	*100%*		*15000.00*	***131.02***	***16.04%***		*1.97*	***2.85***

PT_Ave	PD_Ave	AU_Ave	RH_Ave	SUM4E	Cr2O3_Av
g/T	g/T	g/T	g/T	g/T	%
80.353	34.989	0.708	14.971	131.021	1.966
243.6176	90.49095	2.6988	23.66409	360.471	2.281
253.6161	94.20485	2.809563	24.63531	375.266	2.254
258.7272	96.10334	2.866184	25.13178	382.828	2.266
252.18	93.67	2.79	24.50	373.14	2.27
				0	

Run 4

Phase 2	% Solids	Mass (g)	Mass Recovery (%)	Cum Mass recovery %	Mass recovery (g)	4E PGM (g/t)	4E PGM Recovery (%)	4E PGM Cum Recovery (%)	4E PGM (g)	4E PGM Upgrade
Gravity Concentrate Feed		5000.00				131.02				
Gravity Concentrate R1		346.00	2.3%	2.3%	346.00	284.54	5%	5%	0.10	2.17
Gravity Concentrate R2	41.56	348.00	2.3%	4.6%	348.00	290.71	5%	10%	0.10	2.22
Gravity Concentrate R3		342.00	2.3%	6.9%	342.00	275.69	5%	15%	0.09	2.10
Total Gravity Conc.		*1036.00*	*6.9%*		*1036.00*	*283.69*	***14.95%***		*0.29*	**2.17**
Gravity Concentrate Tail		13964.00	93.1%		13964.00	119.69			1.67	
Totals		*15000.00*	*100%*		*15000.00*	***131.02***	***15%***		*1.97*	***2.17***

PT_Ave	PD_Ave	AU_Ave	RH_Ave	SUM4E	Cr2O3_Av
g/T	g/T	g/T	g/T	g/T	%
80.353	34.989	0.708	14.971	131.021	1.966
192.3	71.4292	2.130303	18.6793	284.539	2.466
196.4674	72.97715	2.176469	19.0841	290.705	2.355
186.3193	69.20769	2.064048	18.09835	275.689	2.312
191.73	71.22	2.12	18.62	283.69	2.38
				0	

Run 5

Phase 2	% Solids	Mass (g)	Mass Recovery (%)	Cum Mass recovery %	Mass recovery (g)	4E PGM (g/t)	4E PGM Recovery (%)	4E PGM Cum Recovery (%)	4E PGM (g)	4E PGM Upgrade
Gravity Concentrate Feed		5000.00				131.02				
Gravity Concentrate R1		413.00	2.8%	2.8%	413.00	196.64	4%	4%	0.08	1.50
Gravity Concentrate R2	54.55	441.00	2.9%	5.7%	441.00	190.02	4%	8%	0.08	1.45
Gravity Concentrate R3		396.00	2.6%	8.3%	396.00	194.33	4%	12%	0.08	1.48
Total Gravity Conc.		*1250.00*	*8.3%*		*1250.00*	*193.57*	***12.31%***		*0.24*	**1.48**
Gravity Concentrate Tail		13750.00	91.7%		13750.00	125.33			1.72	
Totals		*15000.00*	*100%*		*15000.00*	***131.02***	***12%***		*1.97*	***1.48***

PT_Ave	PD_Ave	AU_Ave	RH_Ave	SUM4E	Cr2O3_Av
g/T	g/T	g/T	g/T	g/T	%
80.353	34.989	0.708	14.971	131.021	1.966
126.4263	51.08922	1.28466	17.84094	196.641	2.595
121.1036	49.8537	1.15284	17.90724	190.017	2.542
131.3347	48.78382	1.454927	12.75735	194.331	2.566
126.10	49.92	1.29	16.25	193.57	2.57
				0	

Figure 105: Phase 1 and 2 raw data

Run 1

Phase 3	G-force	Mass (g)	Mass Recovery (%)	Cum Mass recovery %	Mass recovery (g)	4E PGM (g/t)	4E PGM Recovery (%)	4E PGM Cum Recovery (%)	4E PGM (g)	4E PGM Upgrade		PT_Ave g/T	PD_Ave g/T	AU_Ave g/T	RH_Ave g/T	SUM4E g/T	Cr2O3_Av %
Gravity Concentrate Feed		15000.00				131.02						80.353	34.989	0.708	14.971	131.021	1.966
Gravity Concentrate R1		264.00	1.8%	1.8%	264.00	278.65	4%	3.7%	0.07	2.13	131.0209167	176.76	76.17	1.51	24.21	278.648	1.628
Gravity Concentrate R2	100.00	273.00	1.8%	3.6%	273.00	293.58	4%	7.8%	0.08	2.24		179.86	83.38	1.66	28.69	293.578	1.798
Gravity Concentrate R3		310.00	2.1%	5.6%	310.00	277.93	4%	12.2%	0.09	2.12		180.21	71.52	1.54	24.66	277.926	1.886
Total Gravity Conc.		*847.00*	*5.6%*		*847.00*	*283.20*	*12.2%*		*0.24*	2.16		179.02	76.79	1.57	25.82	283.20	1.77
Gravity Concentrate Tail		14153.00	94.4%		14153.00	121.91			1.73							0	
Totals		*15000.00*	*100%*		*15000.00*	***131.02***	*12.21%*		*1.97*	*2.16*							

Run 2

Phase 3	G-force	Mass (g)	Mass Recovery (%)	Cum Mass recovery %	Mass recovery (g)	4E PGM (g/t)	4E PGM Recovery (%)	4E PGM Cum Recovery (%)	4E PGM (g)	4E PGM Upgrade	PT_Ave g/T	PD_Ave g/T	AU_Ave g/T	RH_Ave g/T	SUM4E g/T	Cr2O3_Av %
Gravity Concentrate Feed		5000.00				131.02					80.353	34.989	0.708	14.971	131.021	1.966
Gravity Concentrate R1		278.00	1.9%	1.9%	278.00	285.10	4%	4%	0.08	2.18	193.096	68.049	1.956	21.997	285.098	1.971
Gravity Concentrate R2	200.00	258.00	1.7%	3.6%	258.00	323.86	4%	8%	0.08	2.47	213.52	81.462	2.127	26.75	323.859	1.904
Gravity Concentrate R3		274.00	1.8%	5.4%	274.00	298.86	4%	12%	0.08	2.28	192.055	82.799	2.209	21.794	298.857	1.694
Total Gravity Conc.		*810.00*	*5.4%*		*810.00*	*302.10*	*12.5%*		*0.24*	2.31	199.25	77.31	2.10	23.44	302.10	1.85
Gravity Concentrate Tail		14190.00	94.6%		14190.00	121.26			1.72						0	
Totals		*15000.00*	*100%*		*15000.00*	***131.02***	*12%*		*1.97*	*2.31*						

Run 3

Phase 3	G-force	Mass (g)	Mass Recovery (%)	Cum Mass recovery %	Mass recovery (g)	4E PGM (g/t)	4E PGM Recovery (%)	4E PGM Cum Recovery (%)	4E PGM (g)	4E PGM Upgrade	PT_Ave g/T	PD_Ave g/T	AU_Ave g/T	RH_Ave g/T	SUM4E g/T	Cr2O3_Av %
Gravity Concentrate Feed		5000.00				131.02					80.353	34.989	0.708	14.971	131.021	1.966
Gravity Concentrate R1		320.00	2.1%	2.1%	320.00	351.84	6%	6%	0.11	2.69	230.9685	88.2405	2.7975	29.836	351.843	1.890
Gravity Concentrate R2	250.00	201.00	1.3%	3.5%	201.00	347.52	4%	9%	0.07	2.65	235.142	83.686	2.473	26.217	347.518	1.920
Gravity Concentrate R3		230.00	1.5%	5.0%	230.00	356.17	4%	13%	0.08	2.72	226.795	92.795	3.122	33.455	356.167	1.890
Total Gravity Conc.		*751.00*	*5.0%*		*751.00*	*352.01*	*13.45%*		*0.26*	2.69	230.81	88.42	2.81	29.98	352.01	1.90
Gravity Concentrate Tail		14249.00	95.0%		14249.00	119.37			1.70						0	
Totals		*15000.00*	*100%*		*15000.00*	***131.02***	*13.45%*		*1.97*	*2.69*						

Run 4

Phase 3	G-force	Mass (g)	Mass Recovery (%)	Cum Mass recovery %	Mass recovery (g)	4E PGM (g/t)	4E PGM Recovery (%)	4E PGM Cum Recovery (%)	4E PGM (g)	4E PGM Upgrade	PT_Ave g/T	PD_Ave g/T	AU_Ave g/T	RH_Ave g/T	SUM4E g/T	Cr2O3_Av %
Gravity Concentrate Feed		15000.00				131.02					80.353	34.989	0.708	14.971	131.021	1.966
Gravity Concentrate R1		241.00	1.6%	1.6%	241.00	514.53	6%	6%	0.12	3.93	347.93	129.85	3.58	33.17	514.534	2.16
Gravity Concentrate R2	300.00	221.00	1.5%	3.1%	221.00	458.56	5%	11%	0.10	3.50	313.06	110.88	3.36	31.25	458.558	1.98
Gravity Concentrate R3		252.00	1.7%	4.8%	252.00	488.64	6%	18%	0.12	3.73	333.50	118.99	3.35	32.80	488.635	1.97
Total Gravity Conc.		*714.00*	*4.8%*		*714.00*	*488.07*	*17.73%*		*0.35*	3.73	332.04	120.14	3.43	32.45	488.07	2.04
Gravity Concentrate Tail		14286.00	95.2%		14286.00	113.18			1.62						0	
Totals		*15000.00*	*100%*		*15000.00*	***131.02***	*18%*		*1.97*	*3.73*						

Figure 106: Phase 3 raw data

Run 1

Phase 4	Flow rate (L/min)	Mass (g)	Mass Recovery (%)	Cum Mass recovery %	Mass recovery (g)	4E PGM (g/t)	**4E PGM Recovery (%)**	4E PGM Cum Recovery (%)	4E PGM (g)	**4E PGM Upgrade**
Gravity Concentrate Feed		15000.00				131.02				
Gravity Concentrate R1		241.00	1.6%	1.6%	241.00	514.53	**6%**	6.3%	0.12	**3.93**
Gravity Concentrate R2	**3.00**	221.00	1.5%	3.1%	221.00	458.56	**5%**	11.5%	0.10	**3.50**
Gravity Concentrate R3		252.00	1.7%	4.8%	252.00	488.64	**6%**	17.7%	0.12	**3.73**
Total Gravity Conc.		*714.00*	*4.8%*		*714.00*	*488.07*	*17.7%*		*0.35*	**3.73**
Gravity Concentrate Tail		14286.00	95.2%		14286.00	113.18			1.62	
Totals		*15000.00*	*100%*		*15000.00*	***131.02***	***17.73%***		*1.97*	***3.73***

PT_Ave	PD_Ave	AU_Ave	RH_Ave	Cr2O3_Av
g/T	g/T	g/T	g/T	%
80.353	34.989	0.708	14.971	1.966
347.93	129.85	3.58	33.17	2.16
313.06	110.88	3.36	31.25	1.98
333.50	118.99	3.35	32.80	1.97
332.04	120.14	3.43	32.45	2.04

131.0209167

Run 2

Phase 4	Flow rate (L/min)	Mass (g)	Mass Recovery (%)	Cum Mass recovery %	Mass recovery (g)	4E PGM (g/t)	**4E PGM Recovery (%)**	4E PGM Cum Recovery (%)	4E PGM (g)	**4E PGM Upgrade**
Gravity Concentrate Feed		5000.00				131.02				
Gravity Concentrate R1		188.00	1.3%	1.3%	188.00	459.53	**4%**	4%	0.09	**3.51**
Gravity Concentrate R2	**5.00**	193.00	1.3%	2.5%	193.00	454.72	**4%**	9%	0.09	**3.47**
Gravity Concentrate R3		183.00	1.2%	3.8%	183.00	455.32	**4%**	13%	0.08	**3.48**
Total Gravity Conc.		*564.00*	*3.8%*		*564.00*	*456.52*	*13.1%*		*0.26*	**3.48**
Gravity Concentrate Tail		14436.00	96.2%		14436.00	118.30			1.71	
Totals		*15000.00*	*100%*		*15000.00*	***131.02***	*13%*		*1.97*	***3.48***

PT_Ave	PD_Ave	AU_Ave	RH_Ave	Cr2O3_Av
g/T	g/T	g/T	g/T	%
80.353	34.989	0.708	14.971	1.966
324.79	97.971	3.774	32.991	1.92
324.065	93.881	3.867	32.903	1.93
325.767	91.722	4.031	33.801	1.9
324.86	94.54	3.89	33.22	1.92

Run 3

Phase 4	Flow rate (L/min)	Mass (g)	Mass Recovery (%)	Cum Mass recovery %	Mass recovery (g)	4E PGM (g/t)	**4E PGM Recovery (%)**	4E PGM Cum Recovery (%)	4E PGM (g)	**4E PGM Upgrade**
Gravity Concentrate Feed		5000.00				131.02				
Gravity Concentrate R1		122.00	0.8%	0.8%	122.00	368.42	**2%**	2%	0.04	**2.81**
Gravity Concentrate R2	**10.00**	128.00	0.9%	1.7%	128.00	428.24	**3%**	5%	0.05	**3.27**
Gravity Concentrate R3		121.00	0.8%	2.5%	121.00	363.03	**2%**	7%	0.04	**2.77**
Total Gravity Conc.		*371.00*	*2.5%*		*371.00*	*387.30*	*7.31%*		*0.14*	**2.96**
Gravity Concentrate Tail		14629.00	97.5%		14629.00	124.52			1.82	
Totals		*15000.00*	*100%*		*15000.00*	***131.02***	*7.31%*		*1.97*	***2.96***

PT_Ave	PD_Ave	AU_Ave	RH_Ave	Cr2O3_Av
g/T	g/T	g/T	g/T	%
80.353	34.989	0.708	14.971	1.966
256.35	74.462	3.587	34.024	1.850
292.912	94.102	3.935	37.289	1.850
258.583	68.792	3.761	31.895	1.850
269.69	79.39	3.76	34.46	1.85

Figure 107: Phase 4 raw data

Appendix B: Phase 5 Data

Mass and Moisture Data

Table 22: Phase 5 sample masses and moisture content

Sample ID	Gravity Concentrate			Gravity Tail	Moisture (g)	Moisture (%)
	Bowl	*Wet*	*Dry*	*Dry*		
Phase 5 run 1 Gc Conc 1	598	286	**210**		76.00	26.57%
Phase 5 run 1 Gc Conc 2	598	294	**218**		76.00	25.85%
Phase 5 run 1 Gc Conc 3	598	269	**197**		72.00	26.77%
Phase 5 run 1 Gc Conc 4	598	277	**206**		71.00	25.63%
Phase 5 run 1 Gc Conc 5	598	301	**223**		78.00	25.91%
Phase 5 run 1 Gc Tail				3946		
Phase 5 run 2 Gc Conc 1	598	316	**223**		93.00	29.43%
Phase 5 run 2 Gc Conc 2	598	277	**205**		72.00	25.99%
Phase 5 run 2 Gc Conc 3	598	318	**235**		83.00	26.10%
Phase 5 run 2 Gc Conc 4	598	292	**219**		73.00	25.00%
Phase 5 run 2 Gc Conc 5	598	284	**210**		74.00	26.06%
Phase 5 run 2 Gc Tail				3908		
Phase 5 run 3 Gc Conc 1	598	*302*	**227**		74.67	24.75%
Phase 5 run 3 Gc Conc 2	598	276	**206**		70.00	25.36%
Phase 5 run 3 Gc Conc 3	598	281	**211**		70.00	24.91%
Phase 5 run 3 Gc Conc 4	598	254	**191**		63.00	24.80%
Phase 5 run 3 Gc Conc 5	598	335	**252**		83.00	24.78%
Phase 5 run 3 Gc Tail				3913		
Phase 5 run 4 Gc Conc 1	598	303	**220**		83.00	27.39%
Phase 5 run 4 Gc Conc 2	598	294	**210**		84.33	28.68%
Phase 5 run 4 Gc Conc 3	598	281	**214**		66.67	23.72%
Phase 5 run 4 Gc Conc 4	598	294	**205**		88.67	30.16%
Phase 5 run 4 Gc Conc 5	598	298	**228**		69.67	23.38%
Phase 5 run 4 Gc Tail				3922		
Phase 5 run 5 Gc Conc 1	598	277	**215**		61.63	22.25%
Phase 5 run 5 Gc Conc 2	598	286	**215**		71.04	24.84%
Phase 5 run 5 Gc Conc 3	598	341	**228**		112.83	33.09%
Phase 5 run 5 Gc Conc 4	598	300	**210**		90.08	30.03%
Phase 5 run 5 Gc Conc 5	598	253	**227**		26.21	10.36%
Phase 5 run 5 Gc Tail				3905		
Phase 5 run 6 Gc Conc 1	598	254	**211**		43.25	17.03%
Phase 5 run 6 Gc Conc 2	598	269	**220**		48.75	18.12%
Phase 5 run 6 Gc Conc 3	598	265	**242**		23.00	8.68%
Phase 5 run 6 Gc Conc 4	598	290	**215**		75.50	26.03%
Phase 5 run 6 Gc Conc 5	598	281	**225**		55.75	19.84%
Phase 5 run 6 Gc Tail				3887		
Phase 5 run 7 Gc Conc 1	598	*290*	**212**		77.61	26.80%
Phase 5 run 7 Gc Conc 2	598	316	**230**		86.00	27.22%
Phase 5 run 7 Gc Conc 3	598	359	**280**		79.00	22.01%
Phase 5 run 7 Gc Conc 4	598	281	**210**		71.00	25.27%
Phase 5 run 7 Gc Conc 5	598	265	**197**		68.00	25.66%
Phase 5 run 7 Gc Tail				3871		
Phase 5 run 8 Gc Conc 1	598	271	**200**		71.00	26.20%
Phase 5 run 8 Gc Conc 2	598	281	**205**		76.00	27.05%
Phase 5 run 8 Gc Conc 3	598	268	**199**		69.00	25.75%
Phase 5 run 8 Gc Conc 4	598	282	**205**		77.00	27.30%
Phase 5 run 8 Gc Conc 5	598	335	**249**		86.00	25.67%
Phase 5 run 8 Gc Tail				3942		
Phase 5 run 9 Gc Conc 1	598	281	**199**		82.00	29.18%
Phase 5 run 9 Gc Conc 2	598	276	**205**		71.00	25.72%
Phase 5 run 9 Gc Conc 3	598	349	**258**		91.00	26.07%
Phase 5 run 9 Gc Conc 4	598	268	**201**		67.00	25.00%
Phase 5 run 9 Gc Conc 5	598	335	**251**		84.00	25.07%
Phase 5 run 9 Gc Tail				3886		
Phase 5 run 10 Gc Conc 1	598	316	**232**		84.00	26.58%
Phase 5 run 10 Gc Conc 2	598	326	**241**		85.00	26.07%
Phase 5 run 10 Gc Conc 3	598	308	**231**		77.00	25.00%
Phase 5 run 10 Gc Conc 4	598	324	**242**		82.00	25.31%
Phase 5 run 10 Gc Conc 5	598	273	**204**		69.00	25.27%
Phase 5 run 10 Gc Tail				3850		

Outlier Control Charts

GC Concentrate 1

Please note that the y-axes do not start at 0 in order to better depict the data.

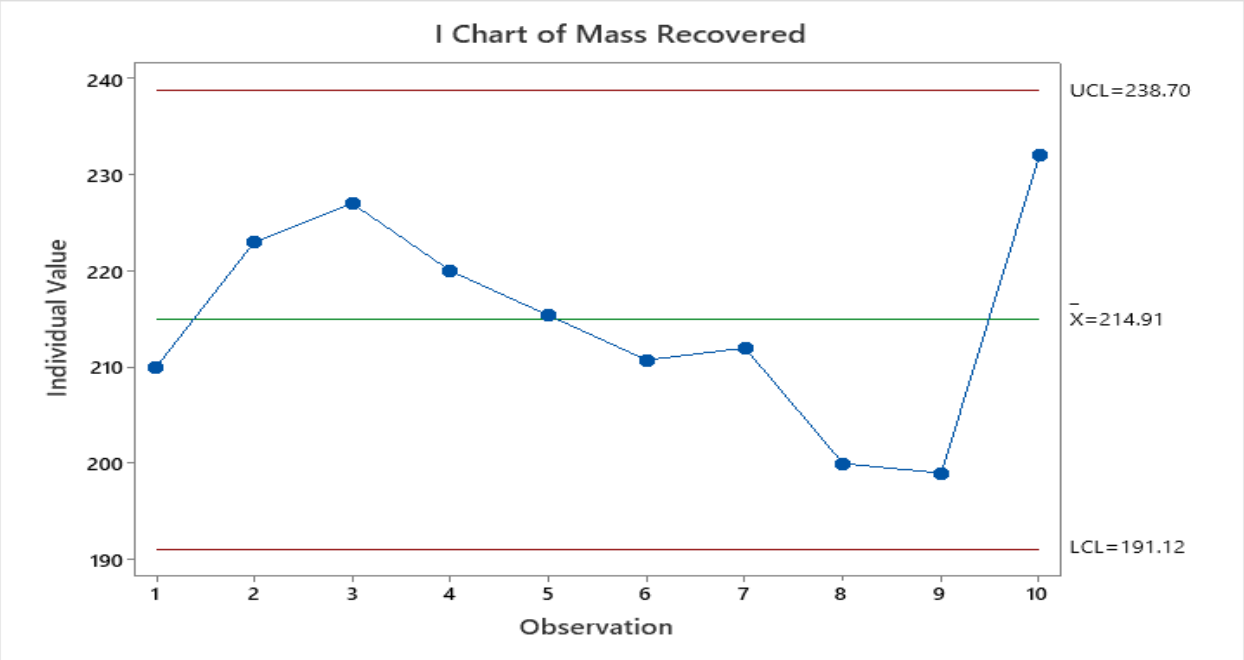

Figure 108: GC concentrate 1 mass recovered outlier chart

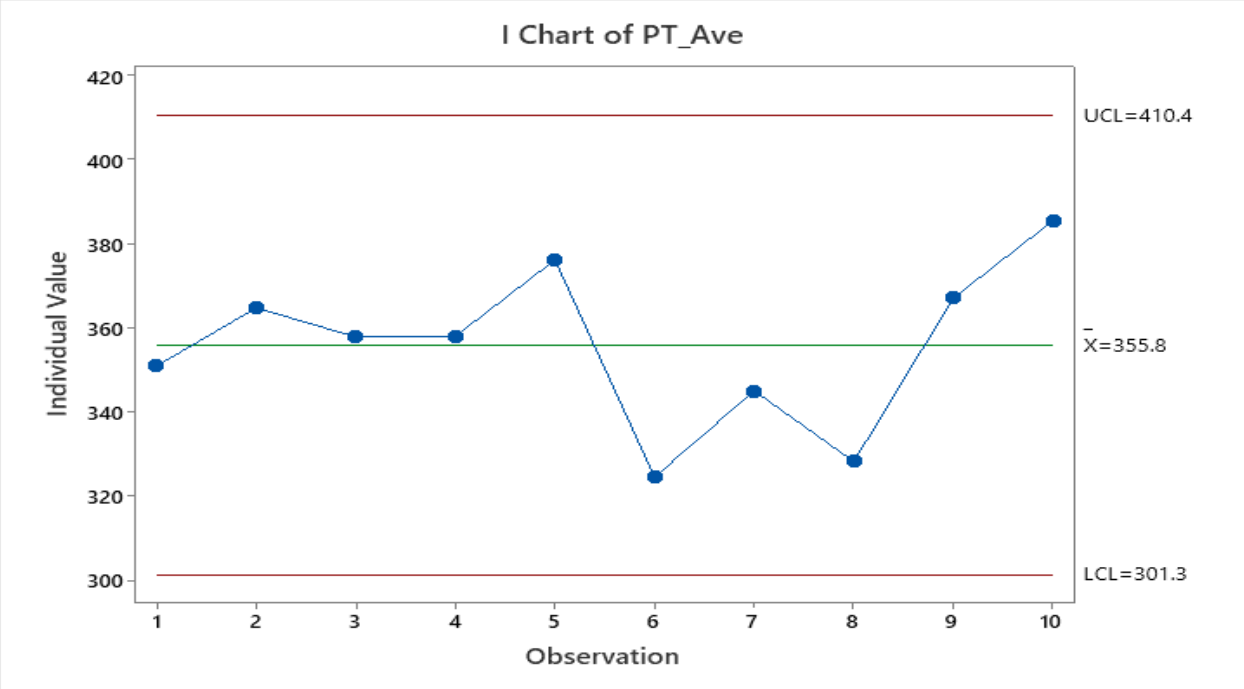

Figure 109: GC concentrate 1 platinum outlier chart

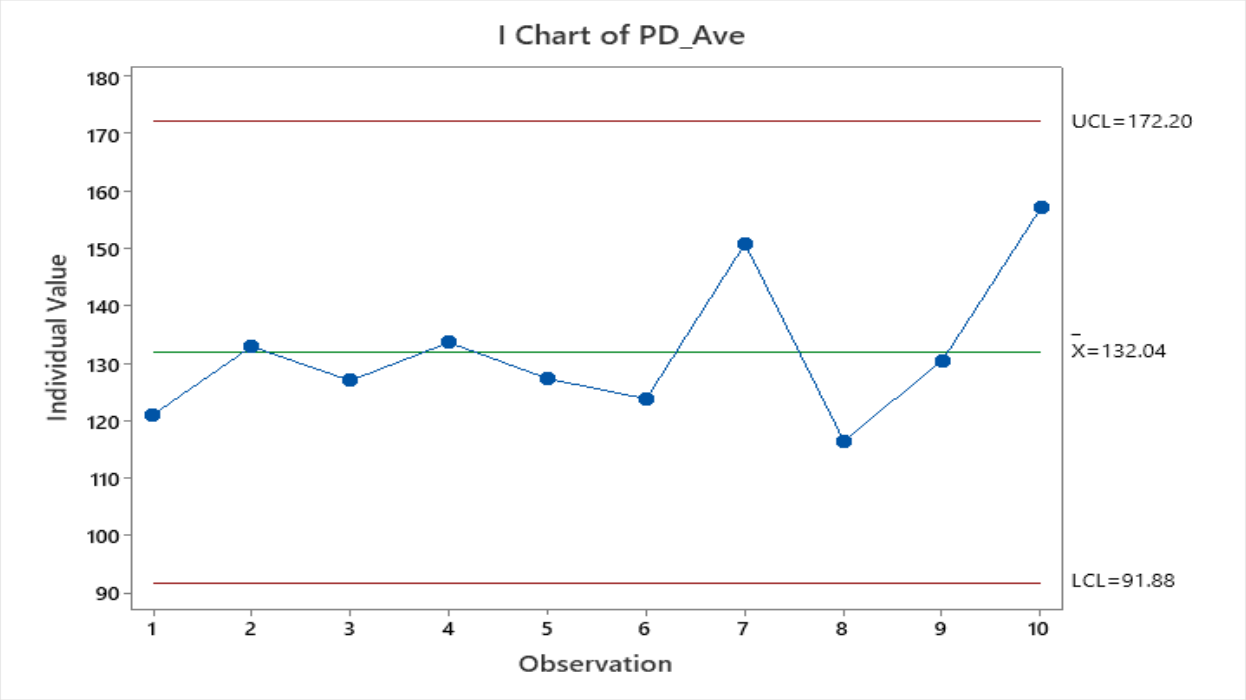

Figure 110: GC concentrate 1 palladium outlier chart

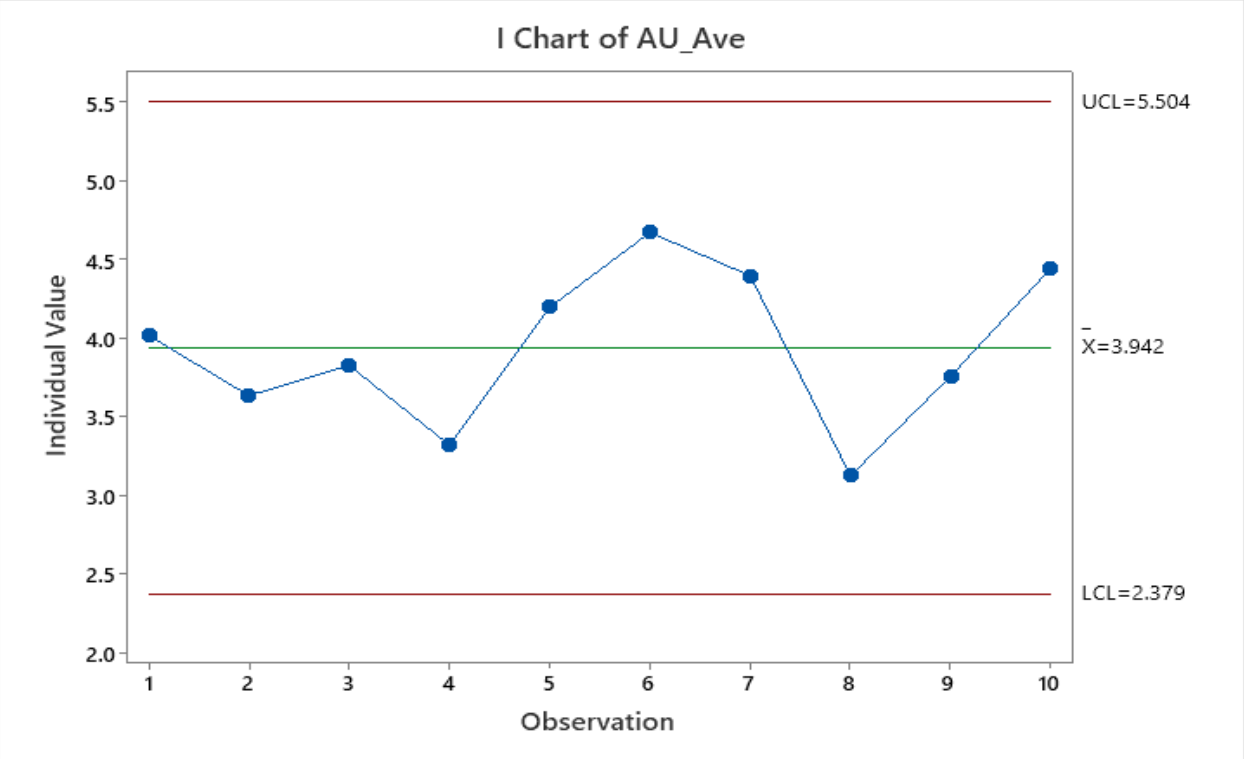

Figure 111: GC concentrate 1 gold outlier chart

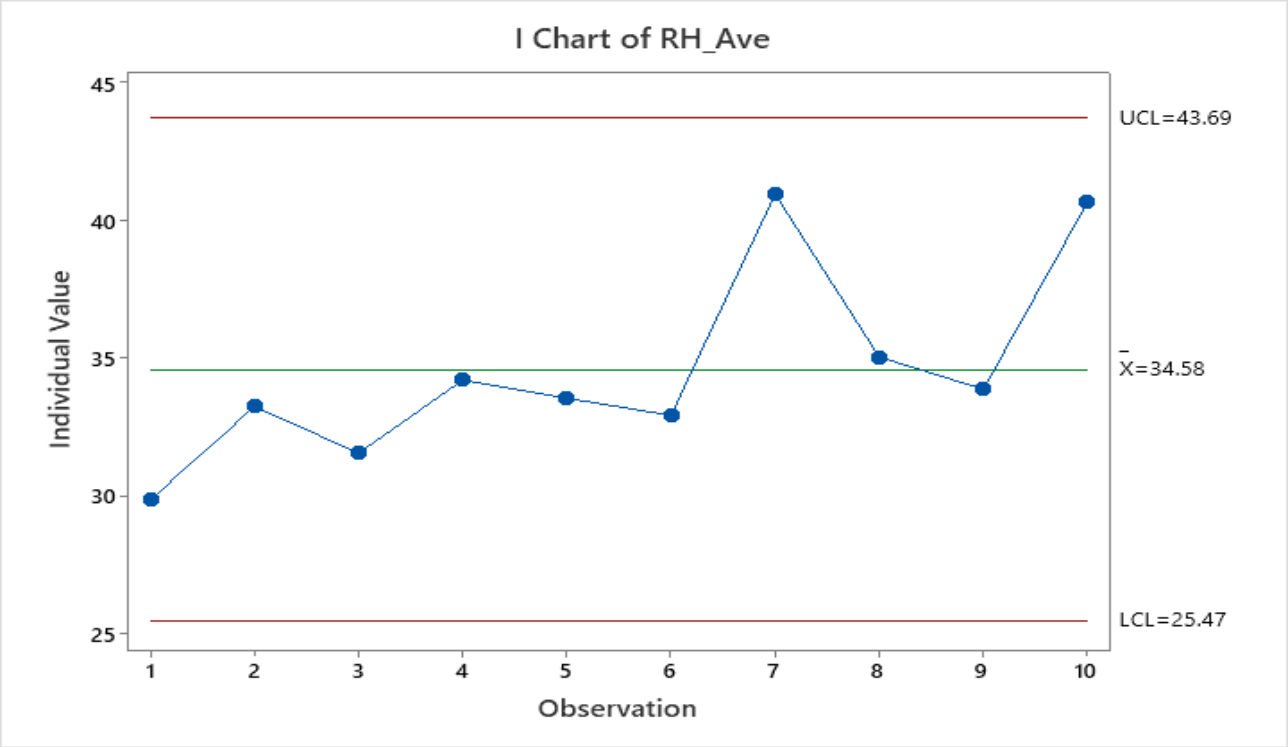

Figure 112: GC concentrate 1 rhodium outlier chart

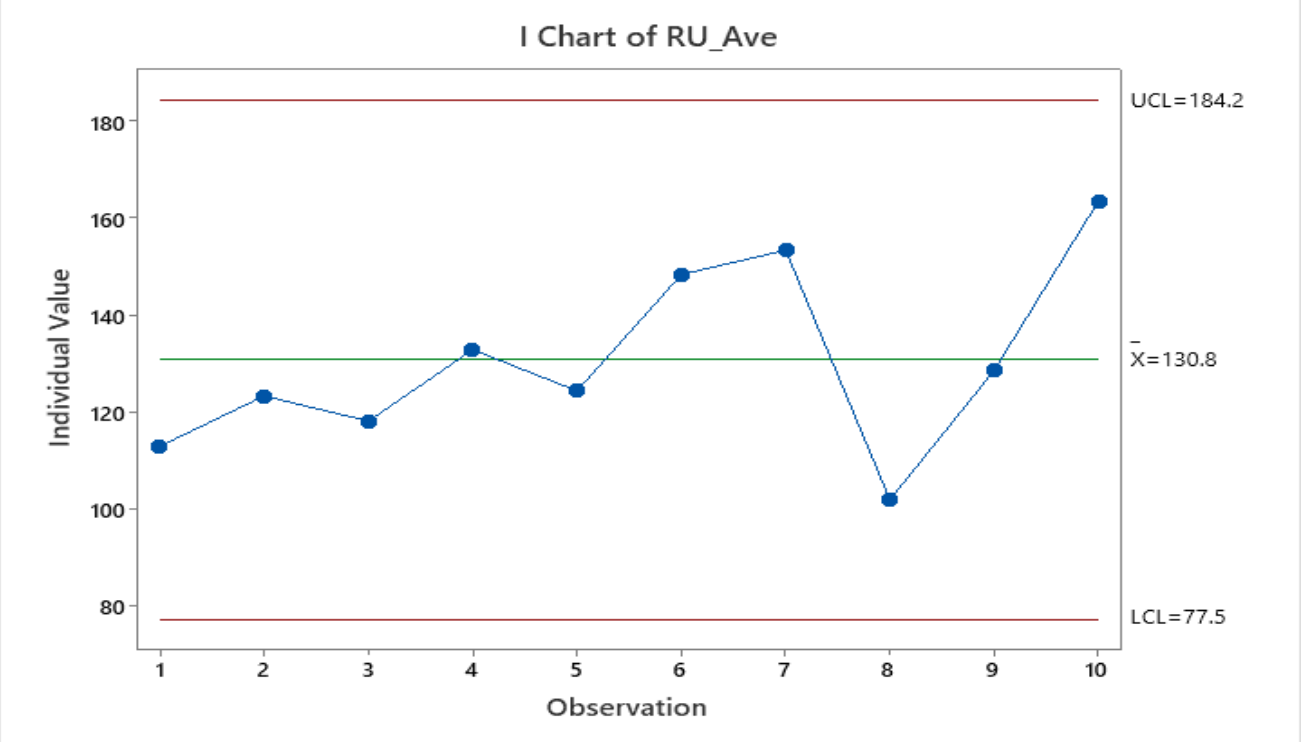

Figure 113: GC concentrate 1 ruthenium outlier chart

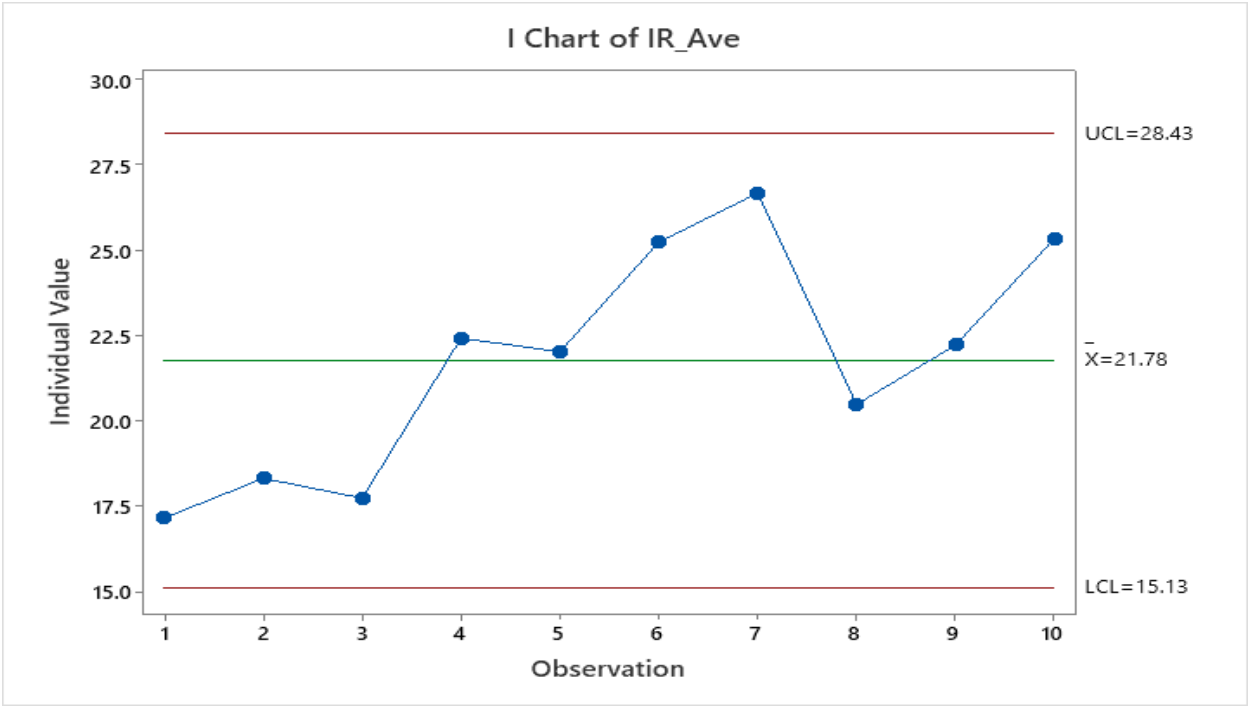

Figure 114: GC concentrate 1 iridium outlier chart

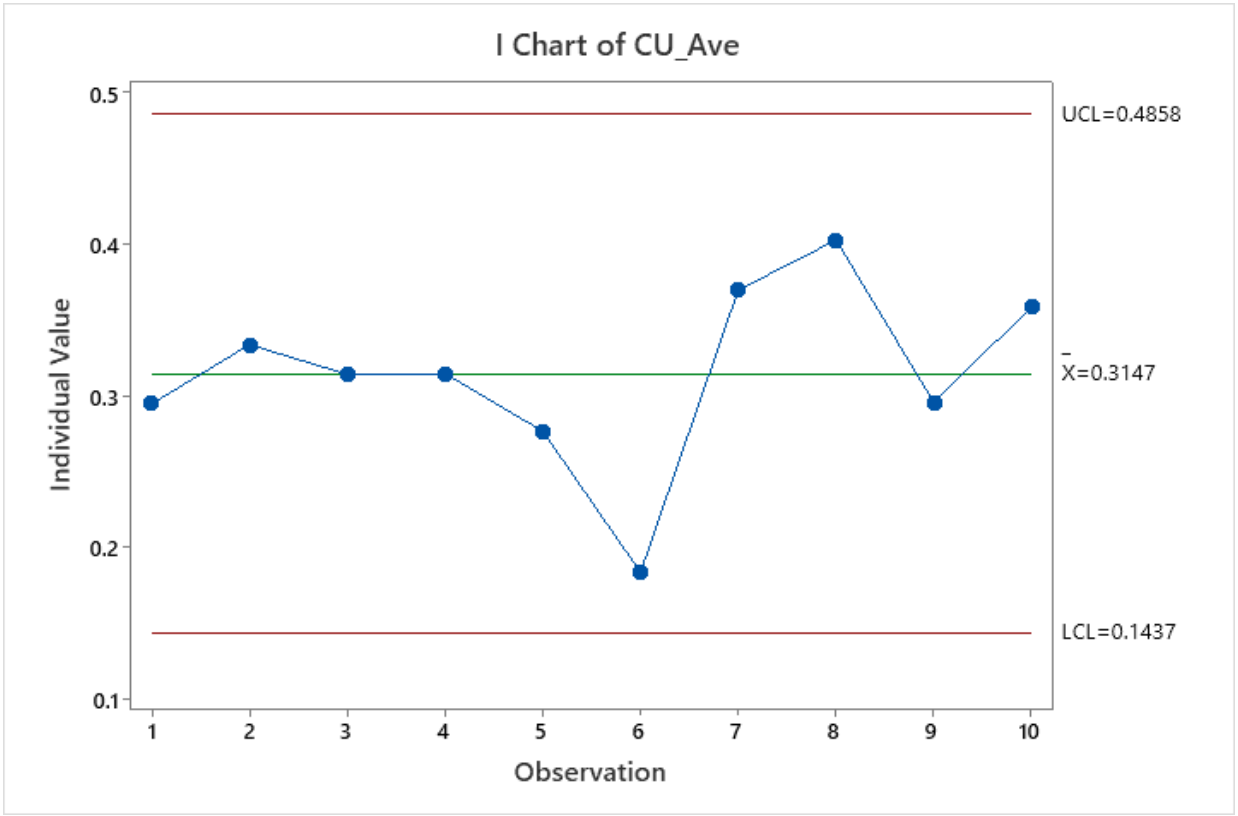

Figure 115: GC concentrate 1 copper outlier chart

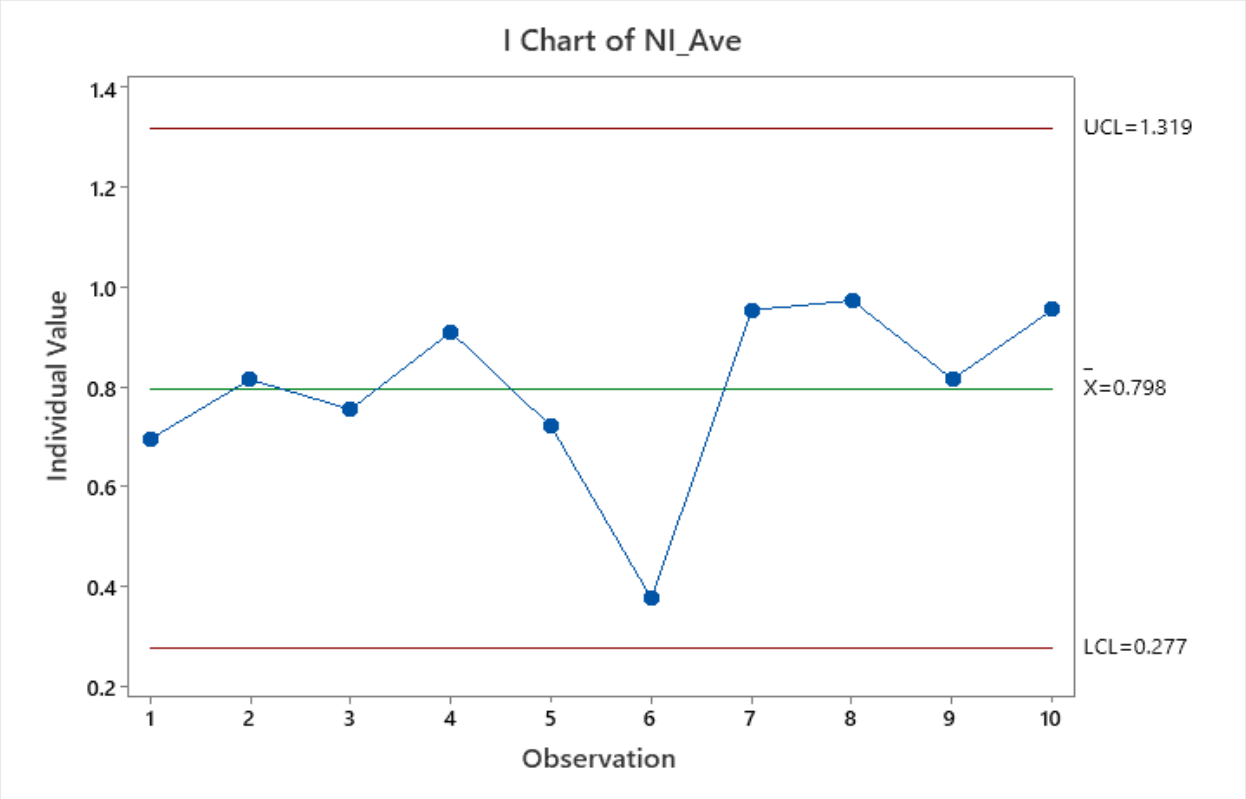

Figure 116: GC concentrate 1 nickel outlier chart

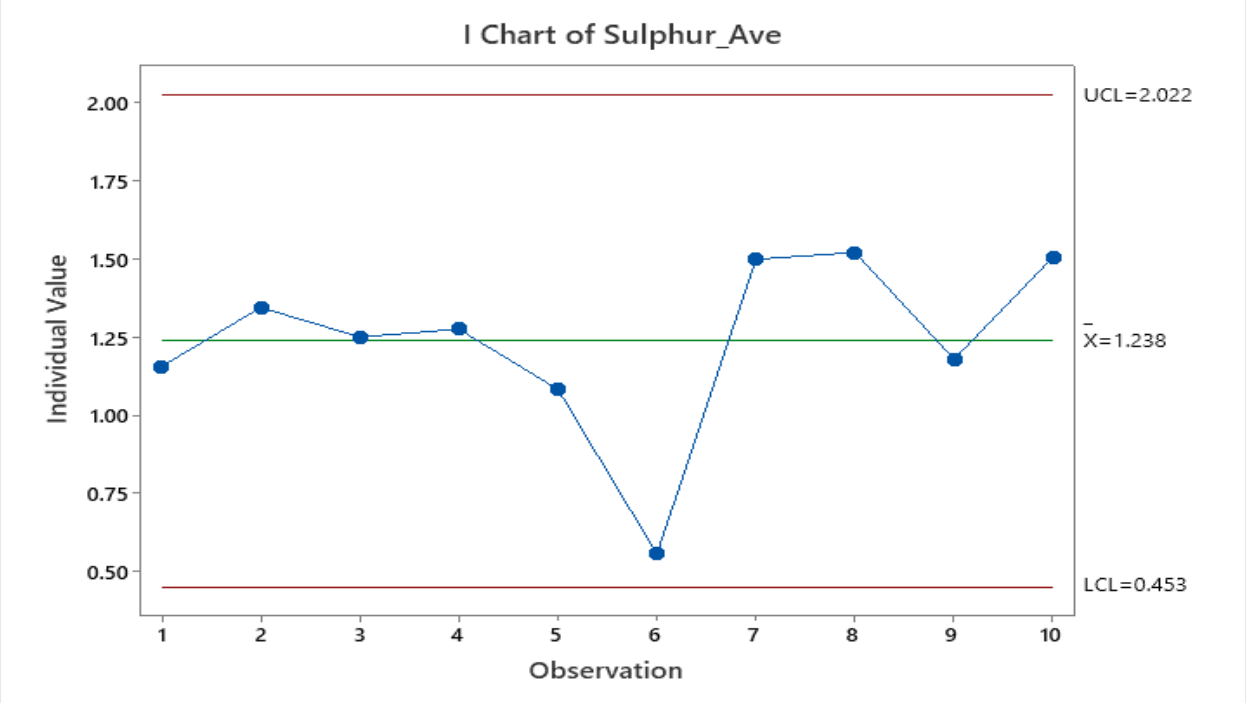

Figure 117: GC concentrate 1 sulphur outlier chart

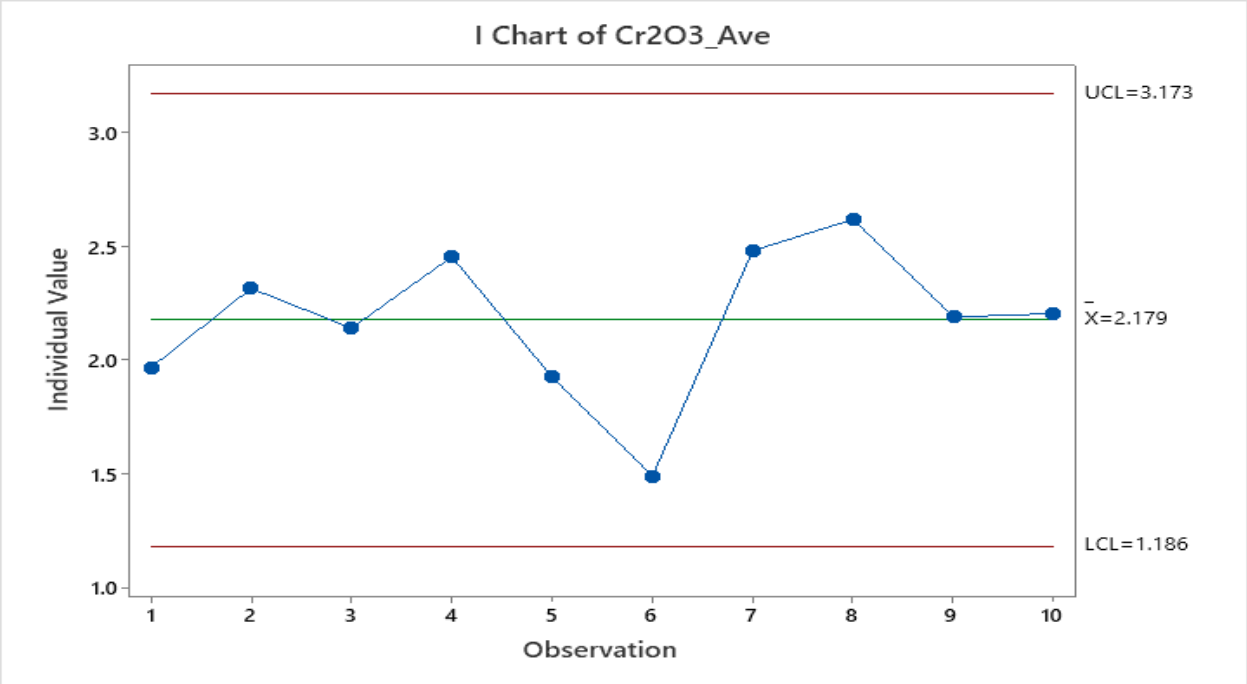

Figure 118: GC concentrate 1 chrome outlier chart

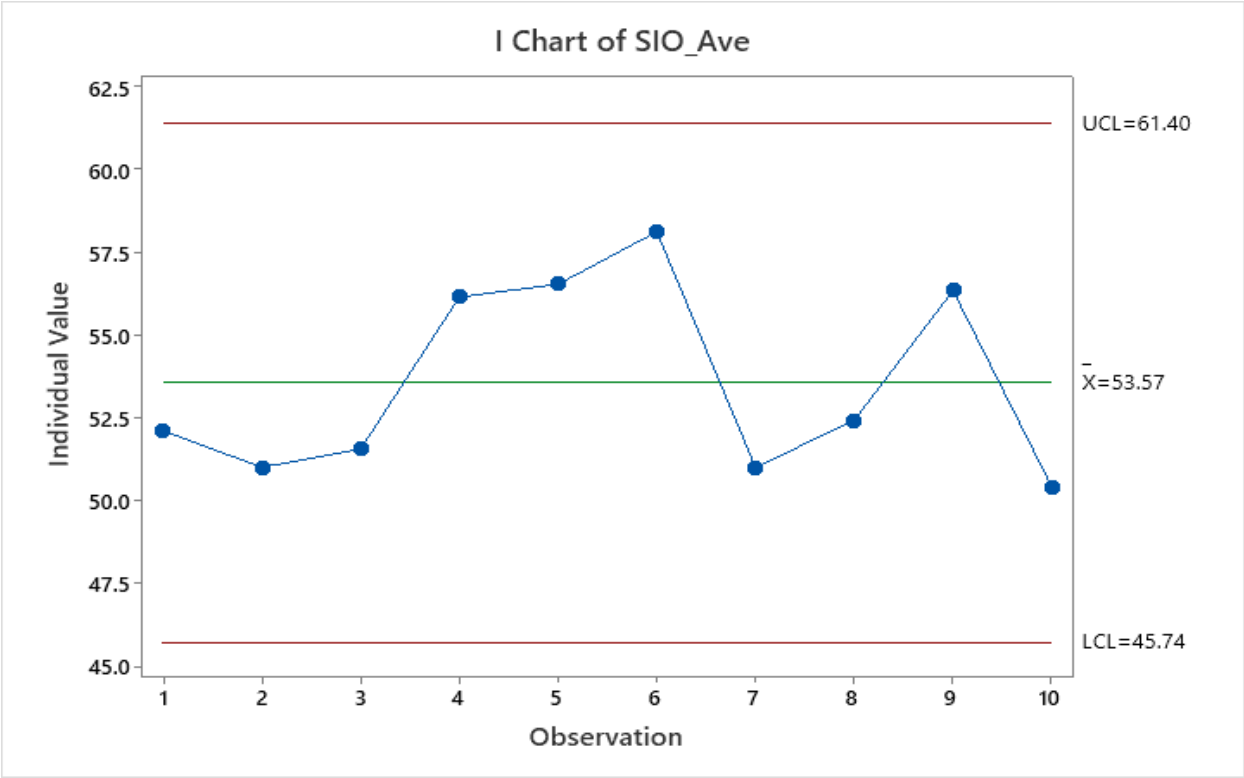

Figure 119: GC concentrate 1 silicon dioxide outlier chart

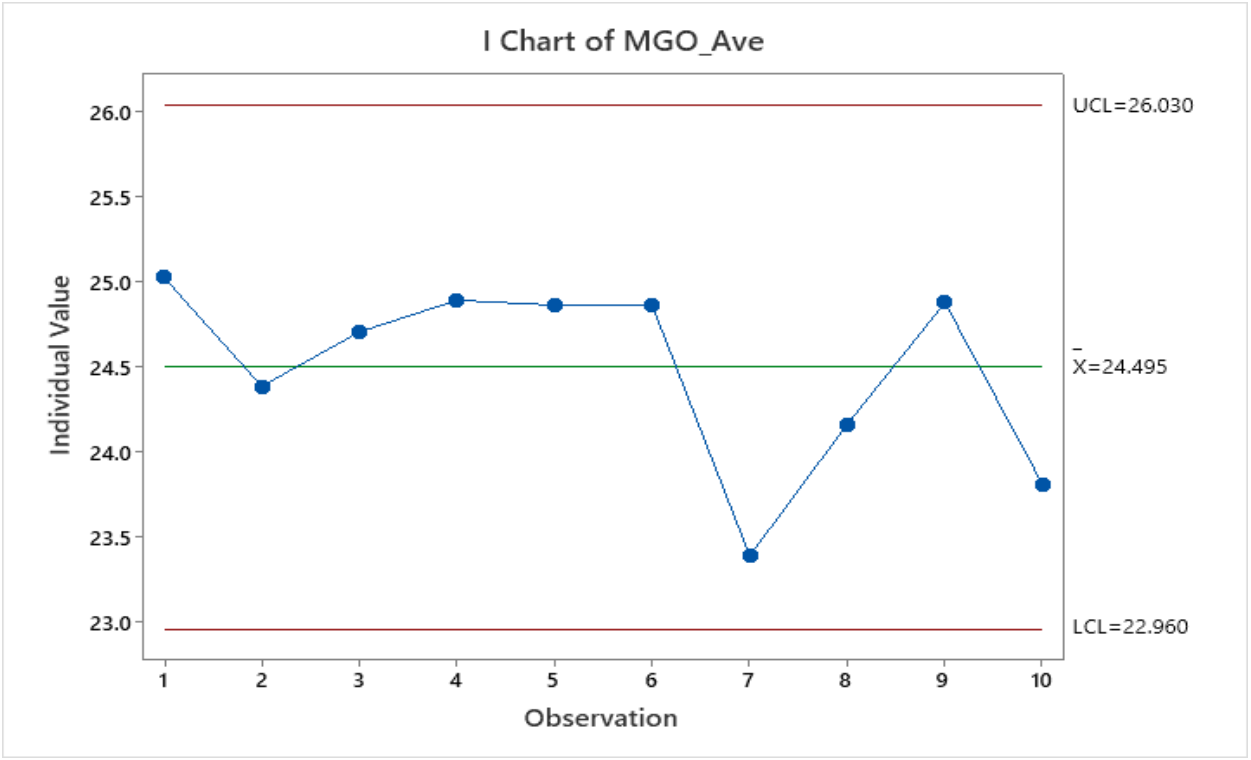

Figure 120: GC concentrate 1 magnesium oxide outlier chart

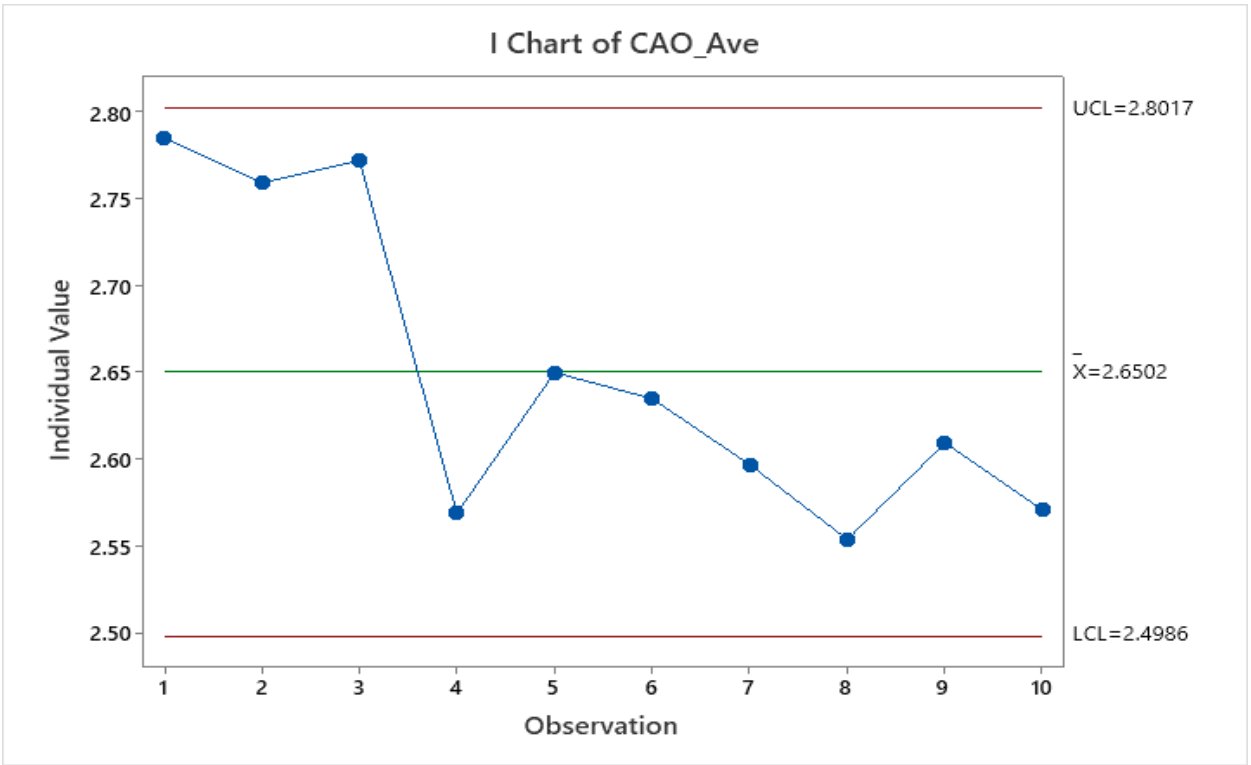

Figure 121: GC concentrate 1 calcium oxide outlier chart

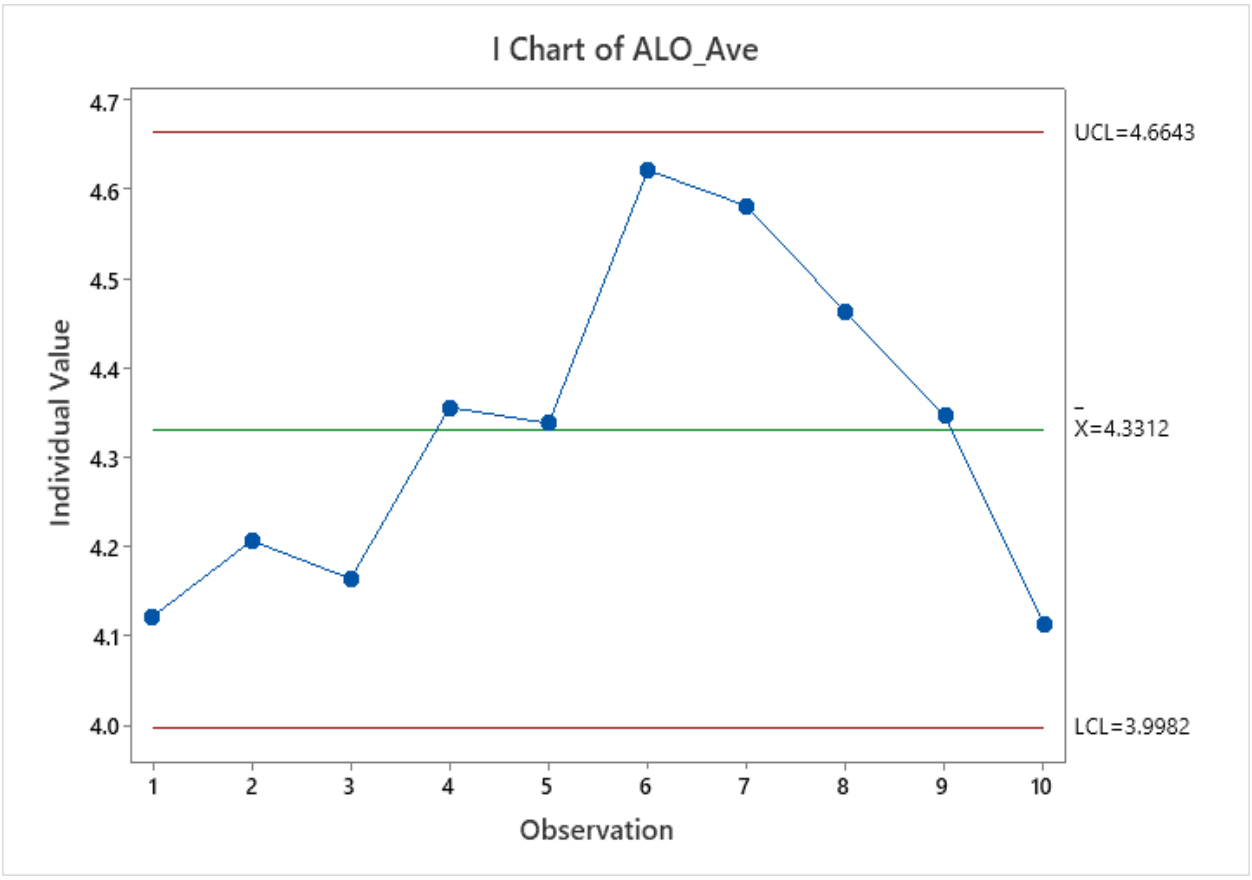

Figure 122: GC concentrate 1 aluminum oxide outlier chart

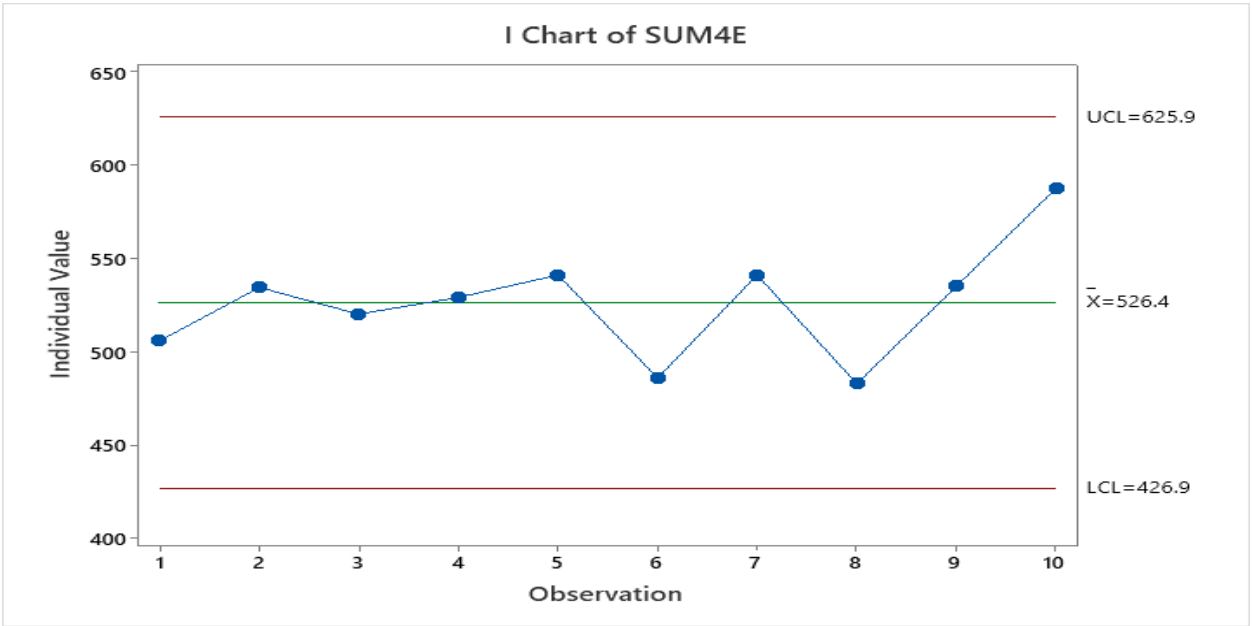

Figure 123: GC concentrate 1 4E outlier chart

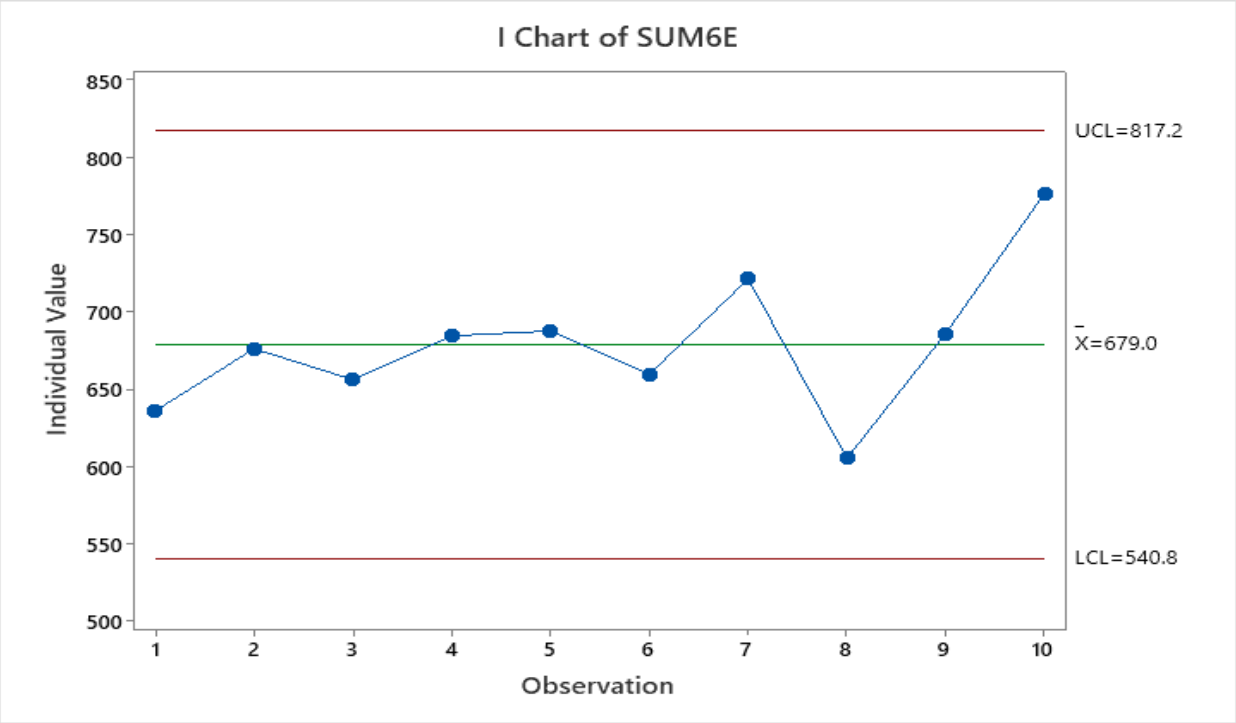

Figure 124: GC concentrate 1 6E outlier chart

GC Concentrate 2

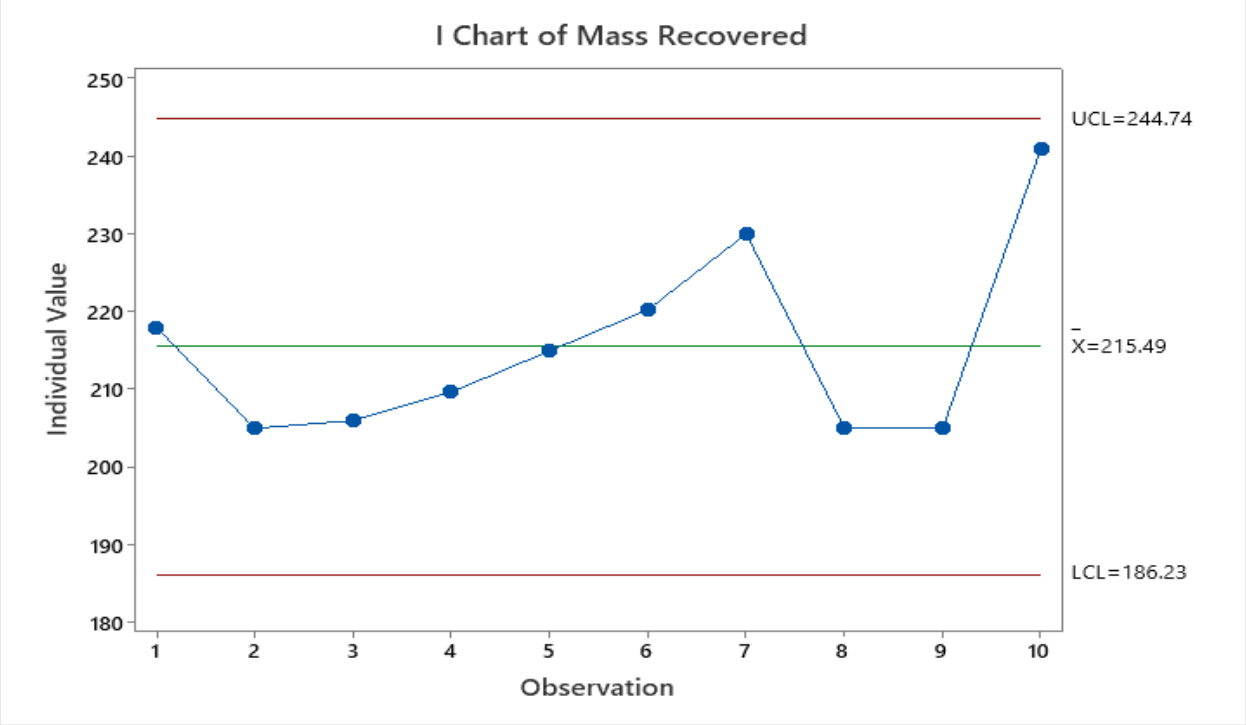

Figure 125: GC concentrate 2 mass recovered outlier chart

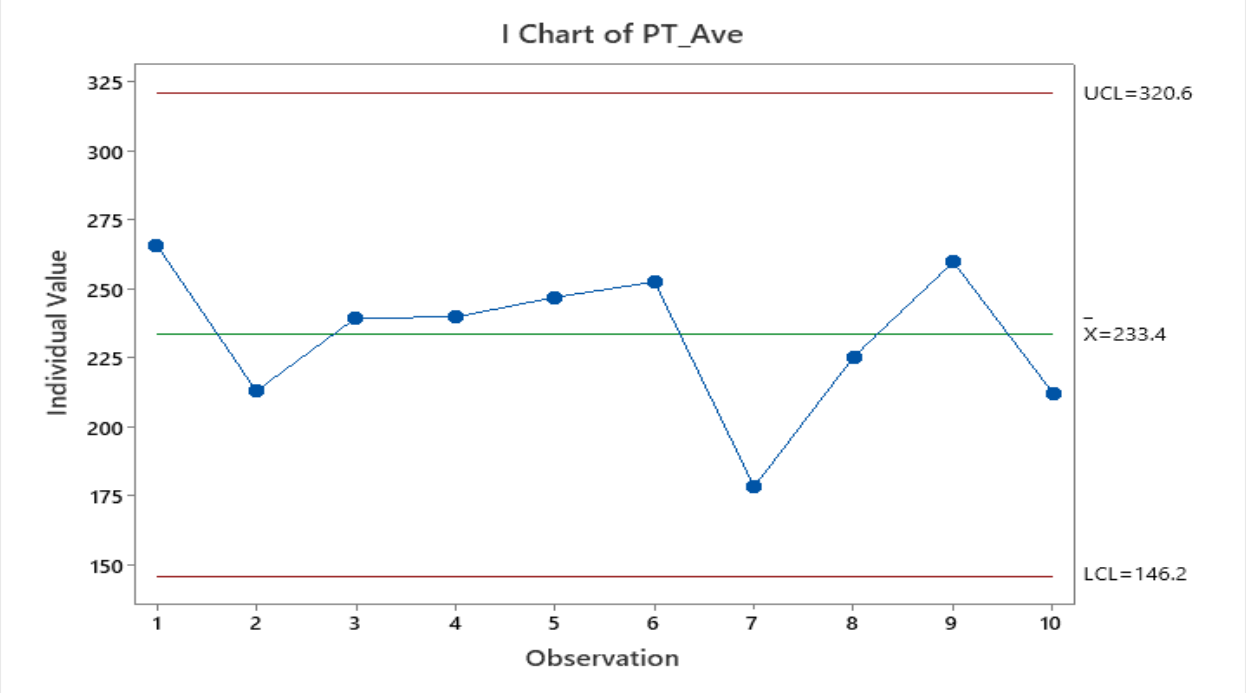

Figure 126: GC concentrate 2 platinum outlier chart

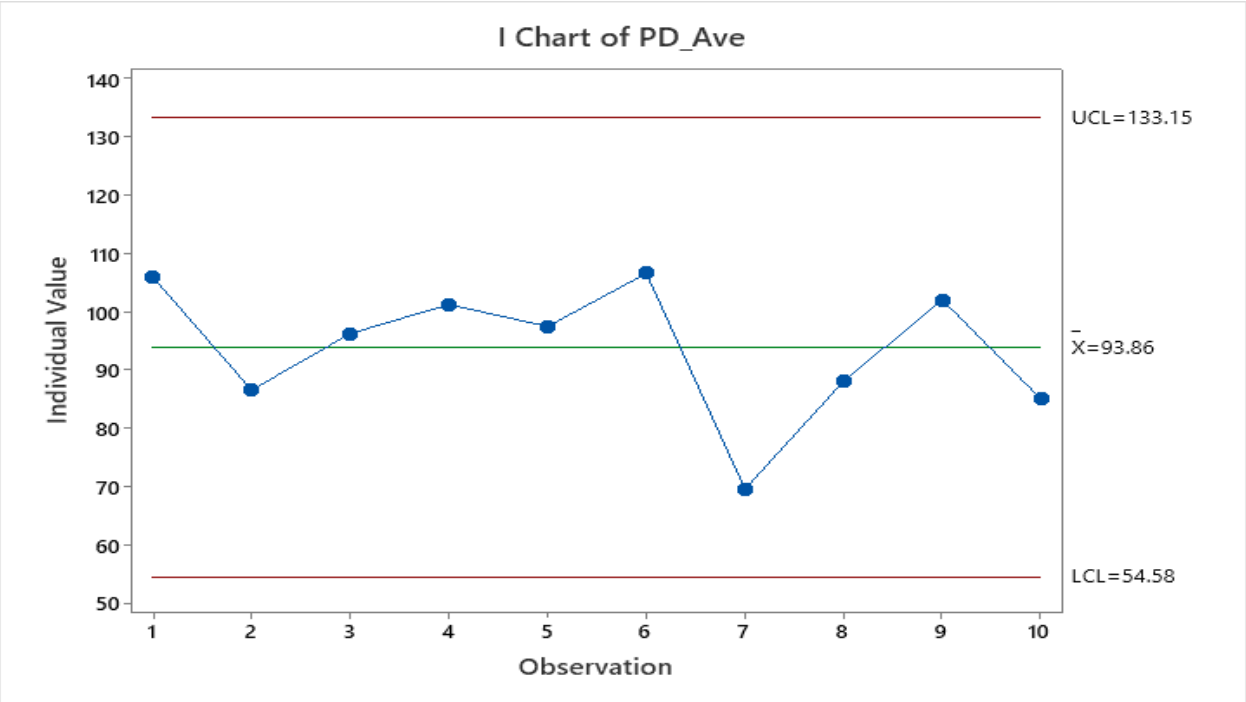

Figure 127: GC concentrate 2 palladium outlier chart

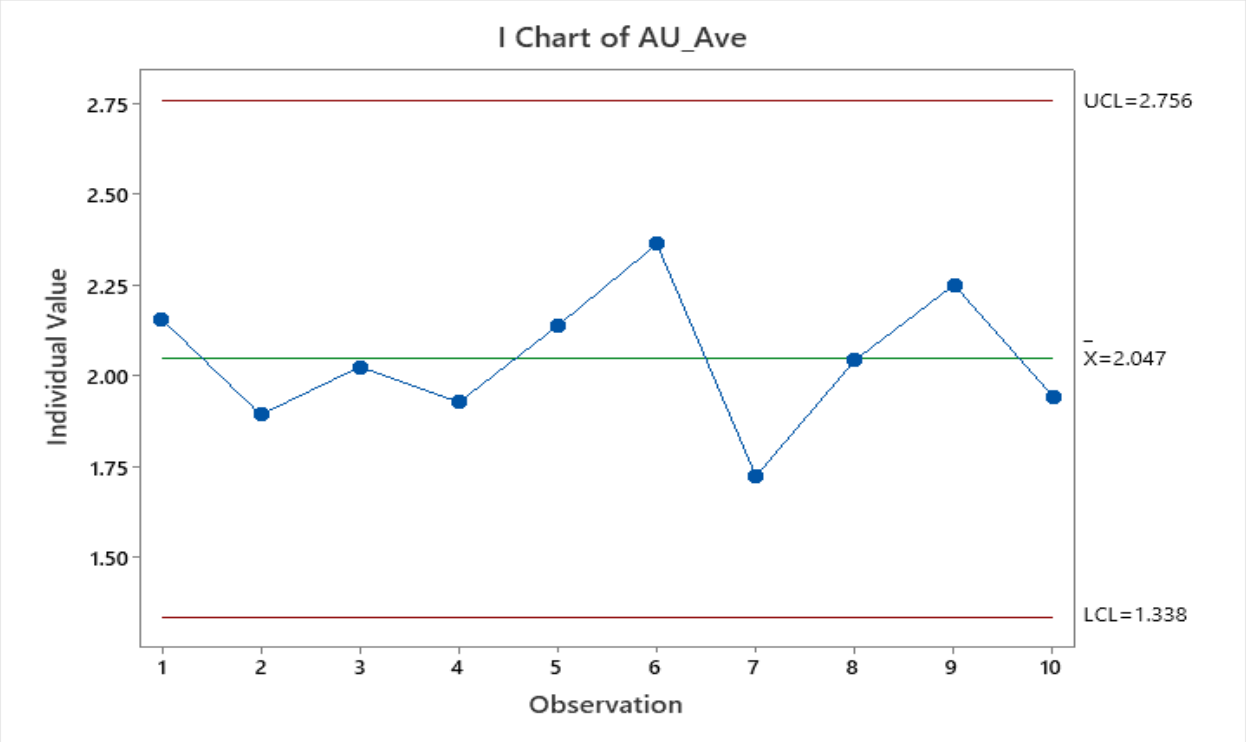

Figure 128: GC concentrate 2 gold outlier chart

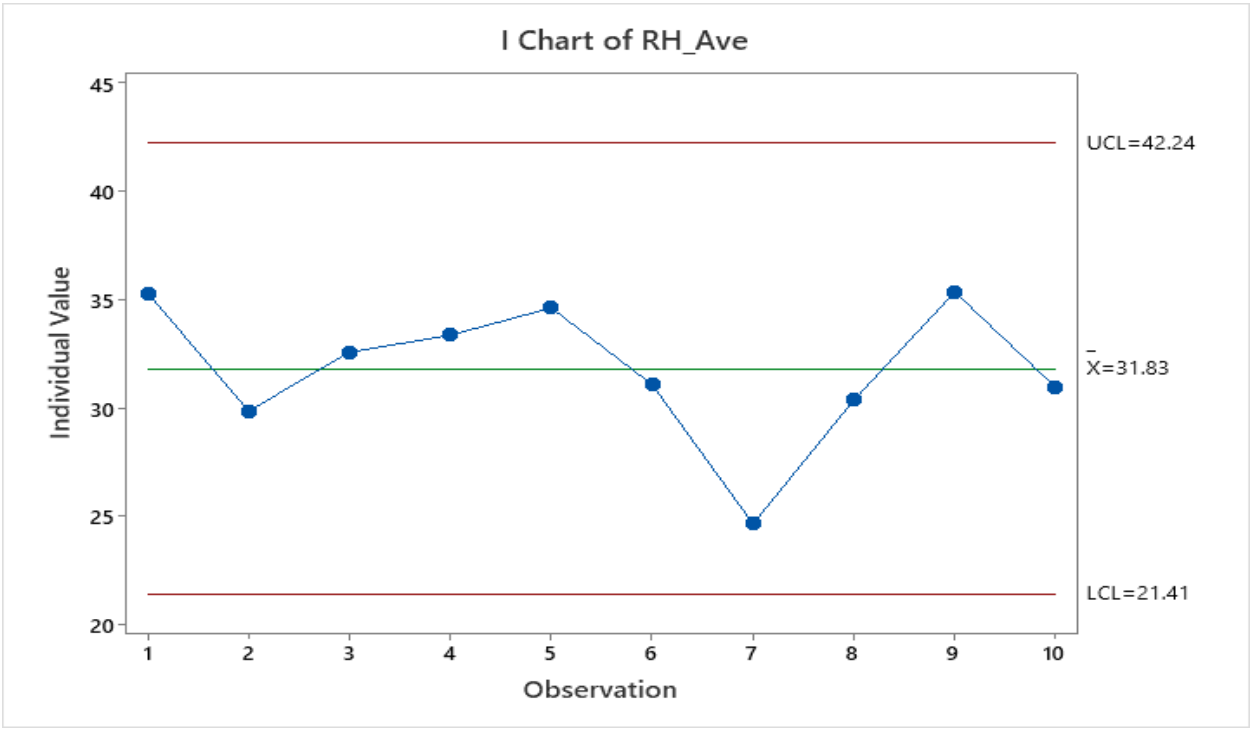

Figure 129: GC concentrate 2 rhodium outlier chart

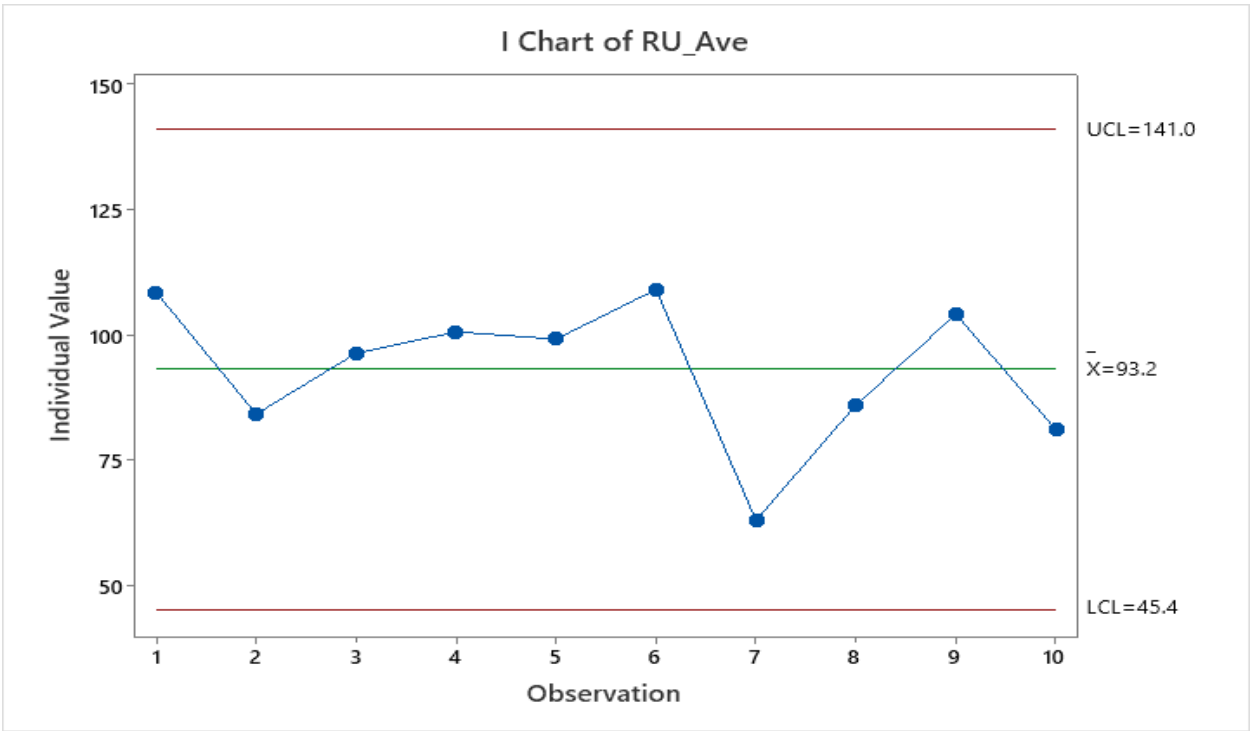

Figure 130: GC concentrate 2 ruthenium outlier chart

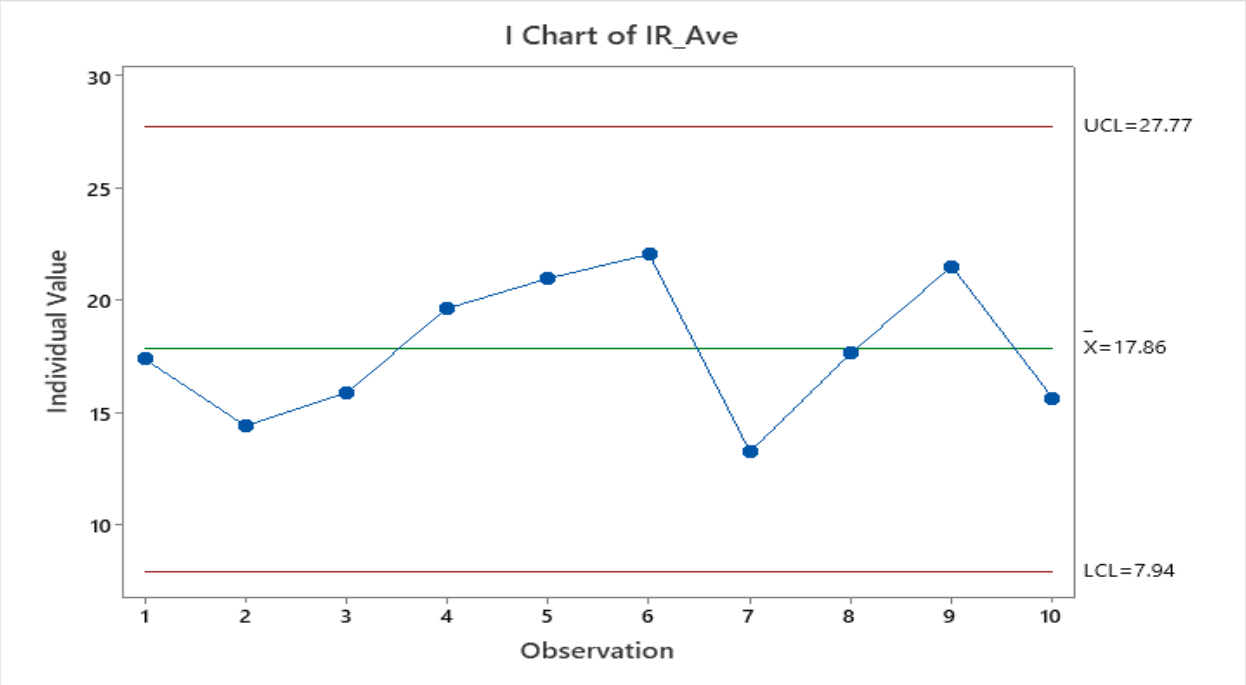

Figure 131: GC concentrate 2 iridium outlier chart

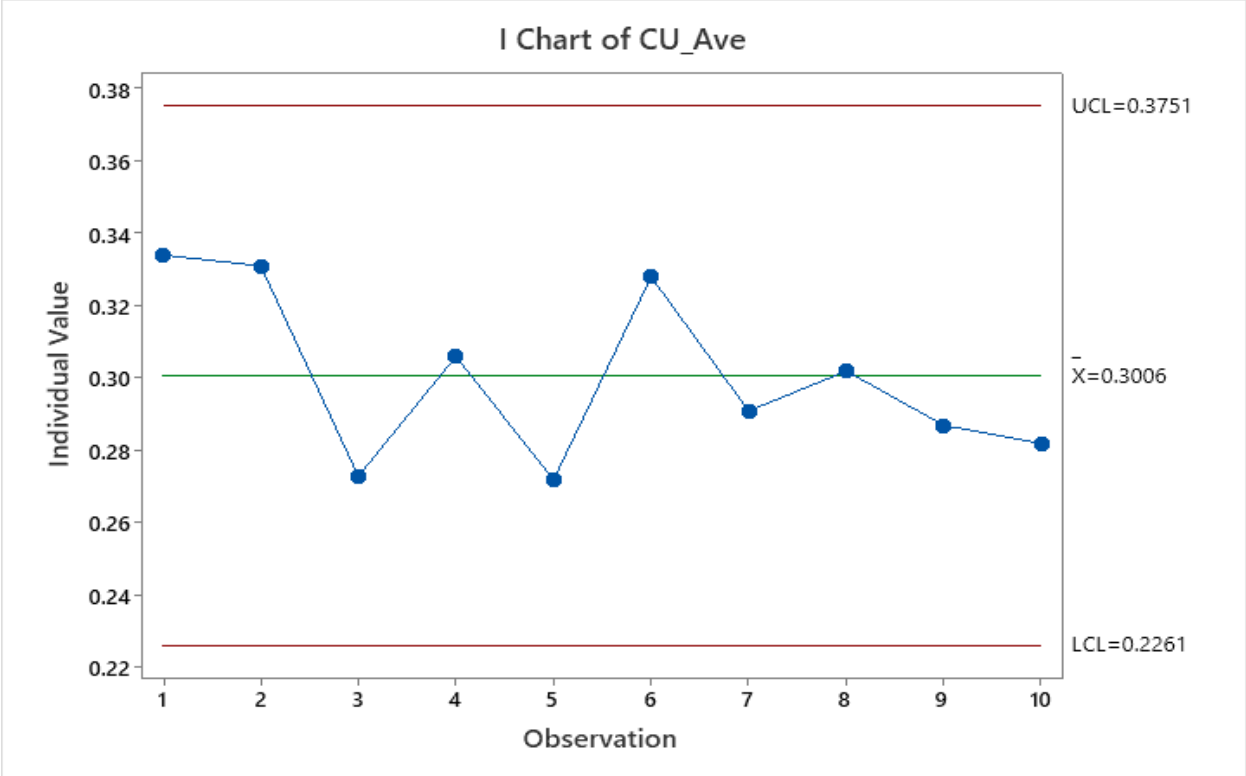

Figure 132: GC concentrate 2 copper outlier chart

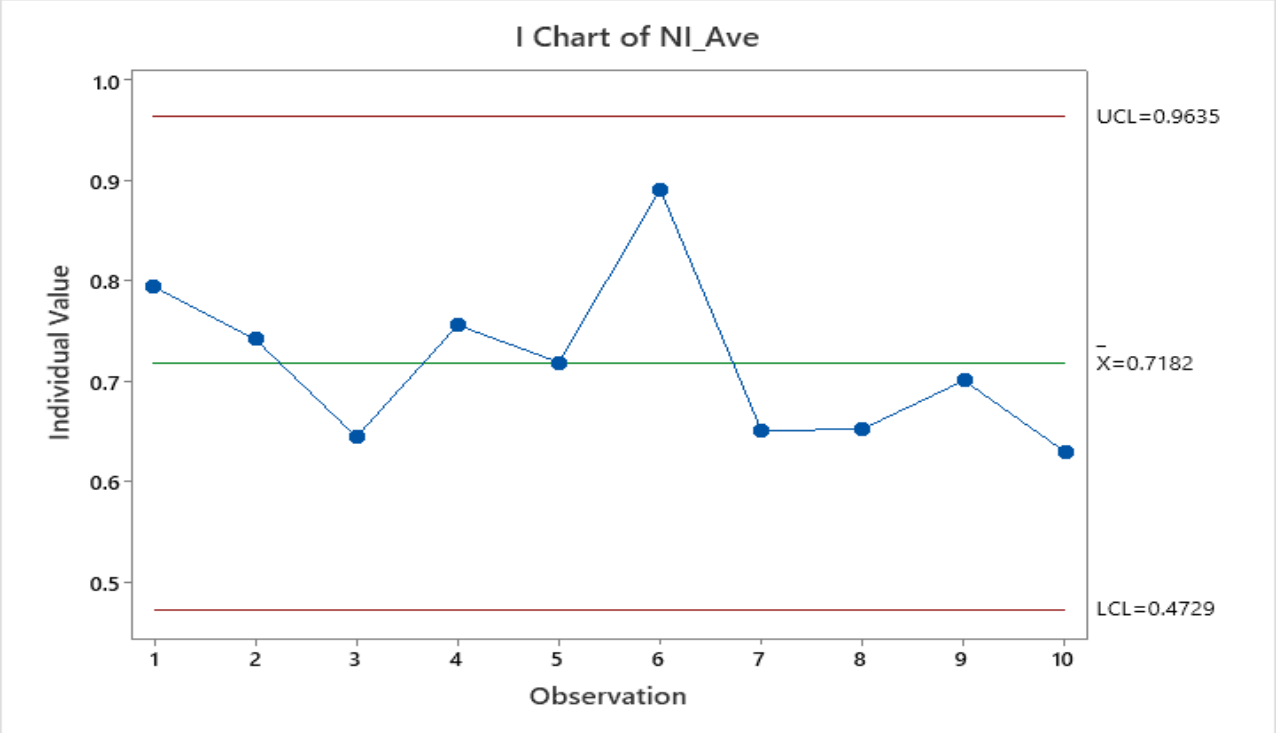

Figure 133: GC concentrate 2 nickel outlier chart

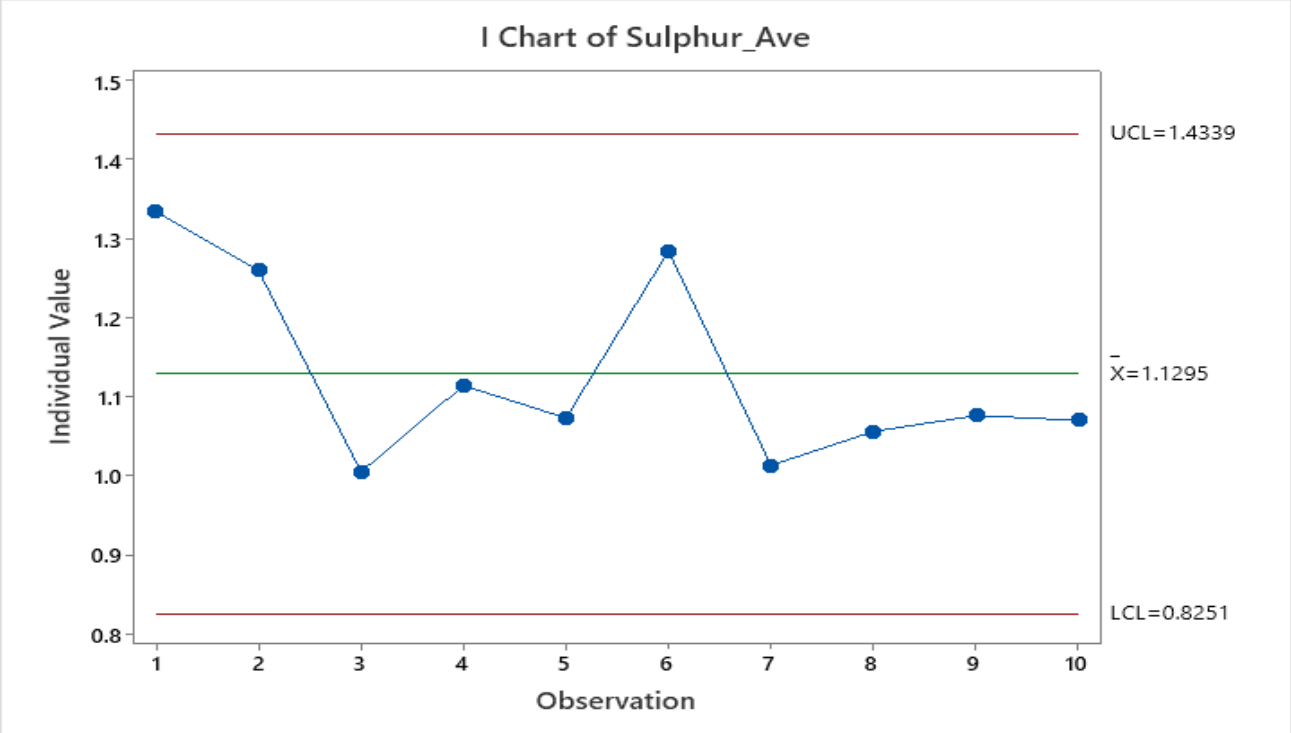

Figure 134: GC concentrate 2 sulphur outlier chart

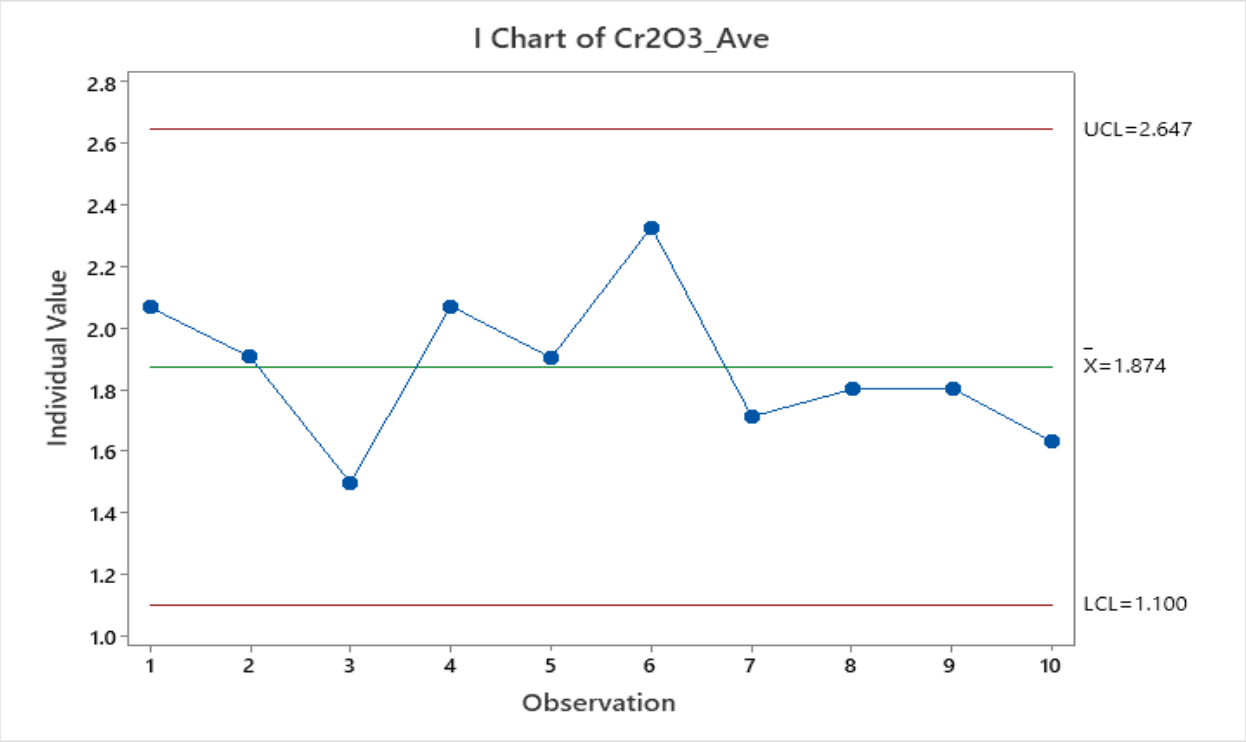

Figure 135: GC concentrate 2 chrome outlier chart



Figure 136: GC concentrate 2 silicon dioxide outlier chart

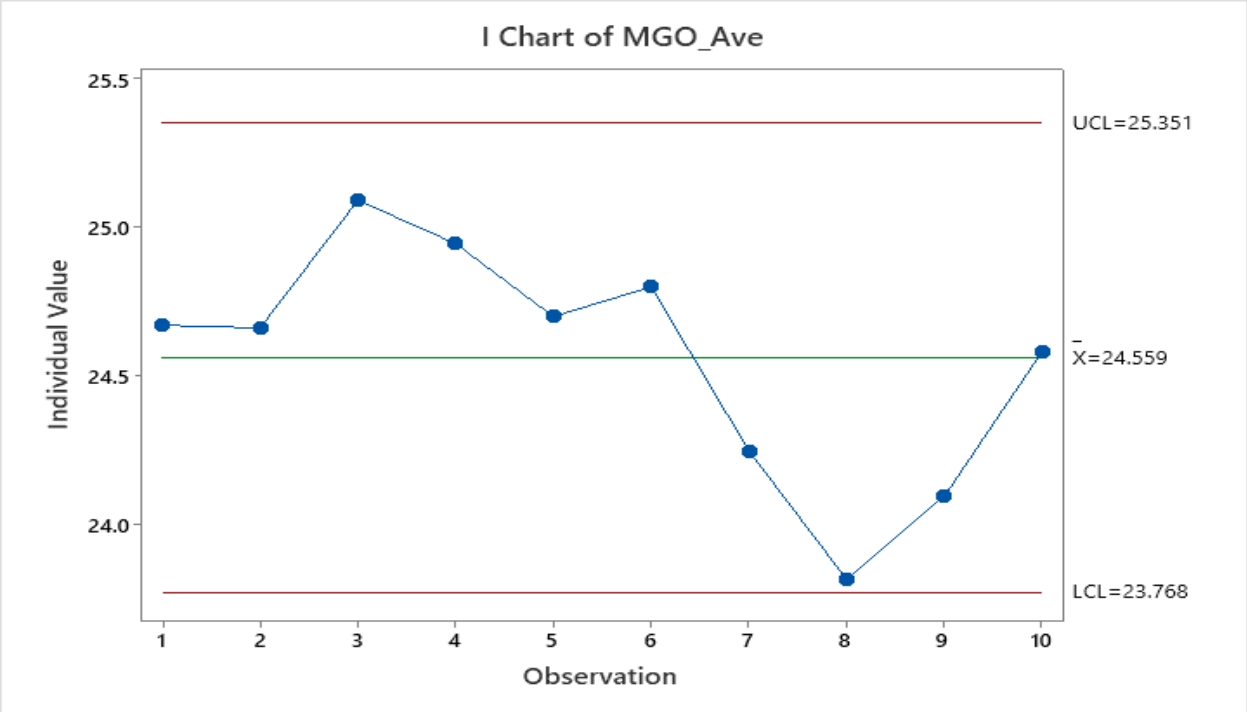

Figure 137: GC concentrate 2 magnesium oxide outlier chart

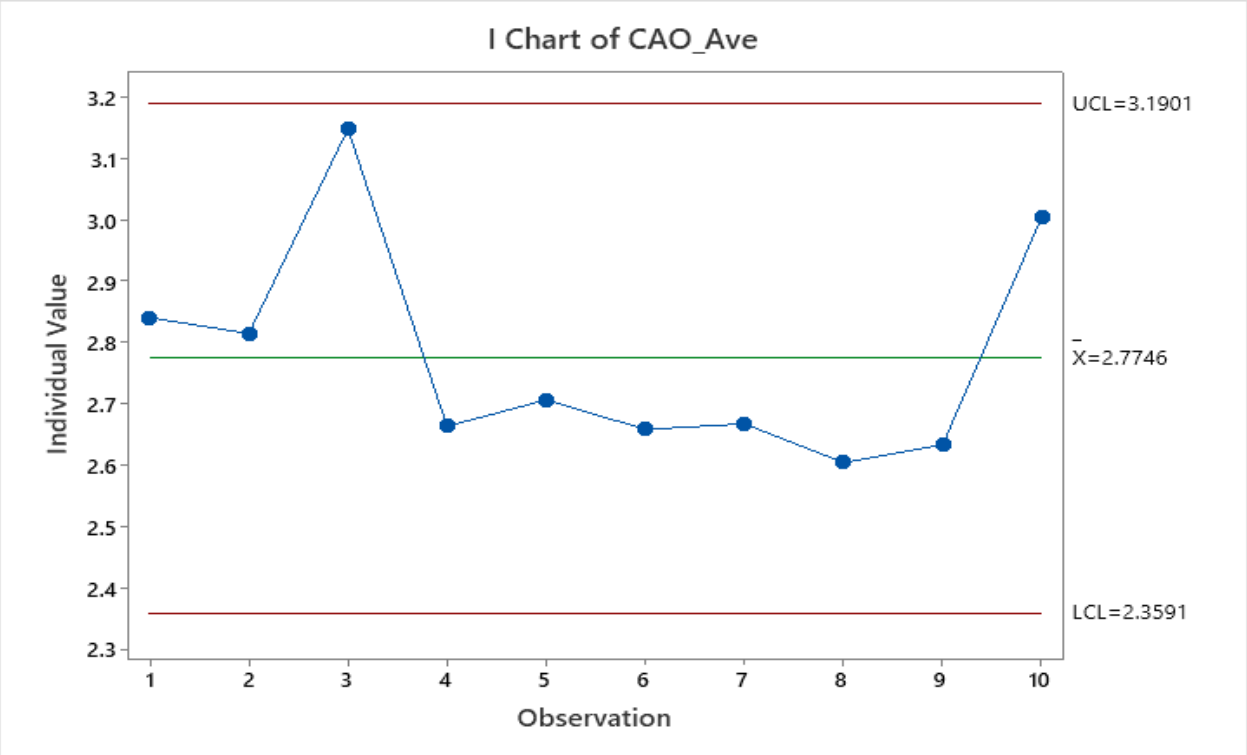

Figure 138: GC concentrate 2 calcium oxide outlier chart

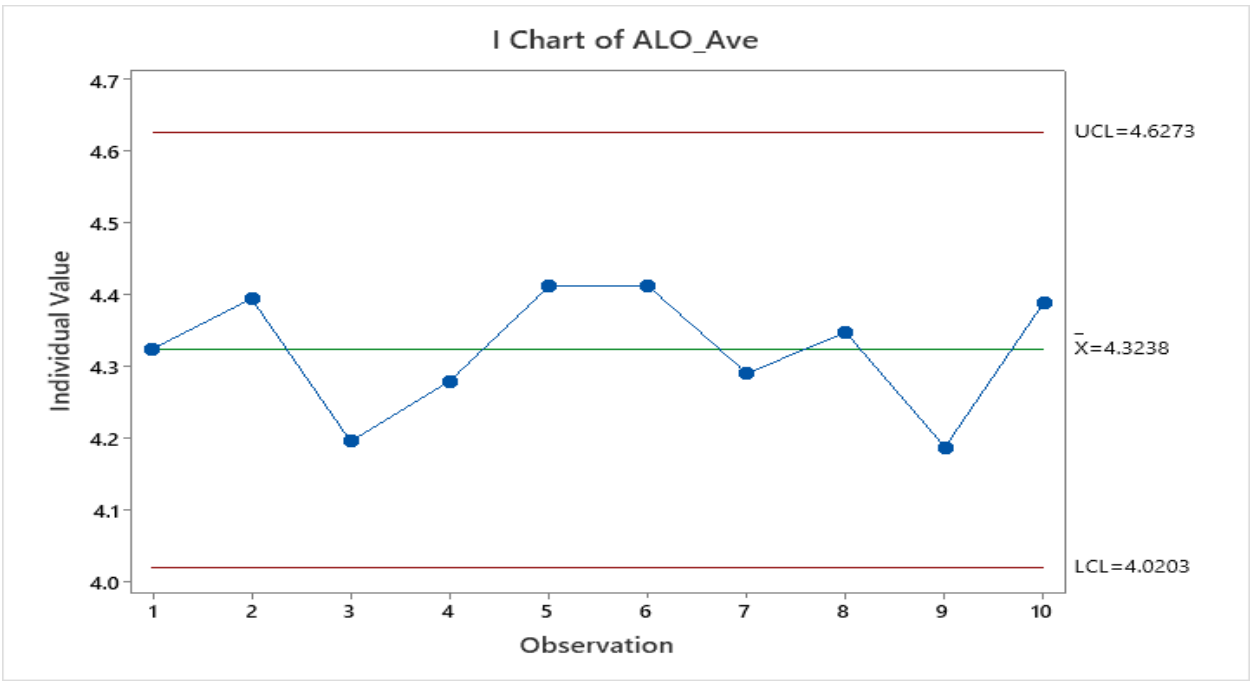

Figure 139: GC concentrate 2 aluminium oxide outlier chart

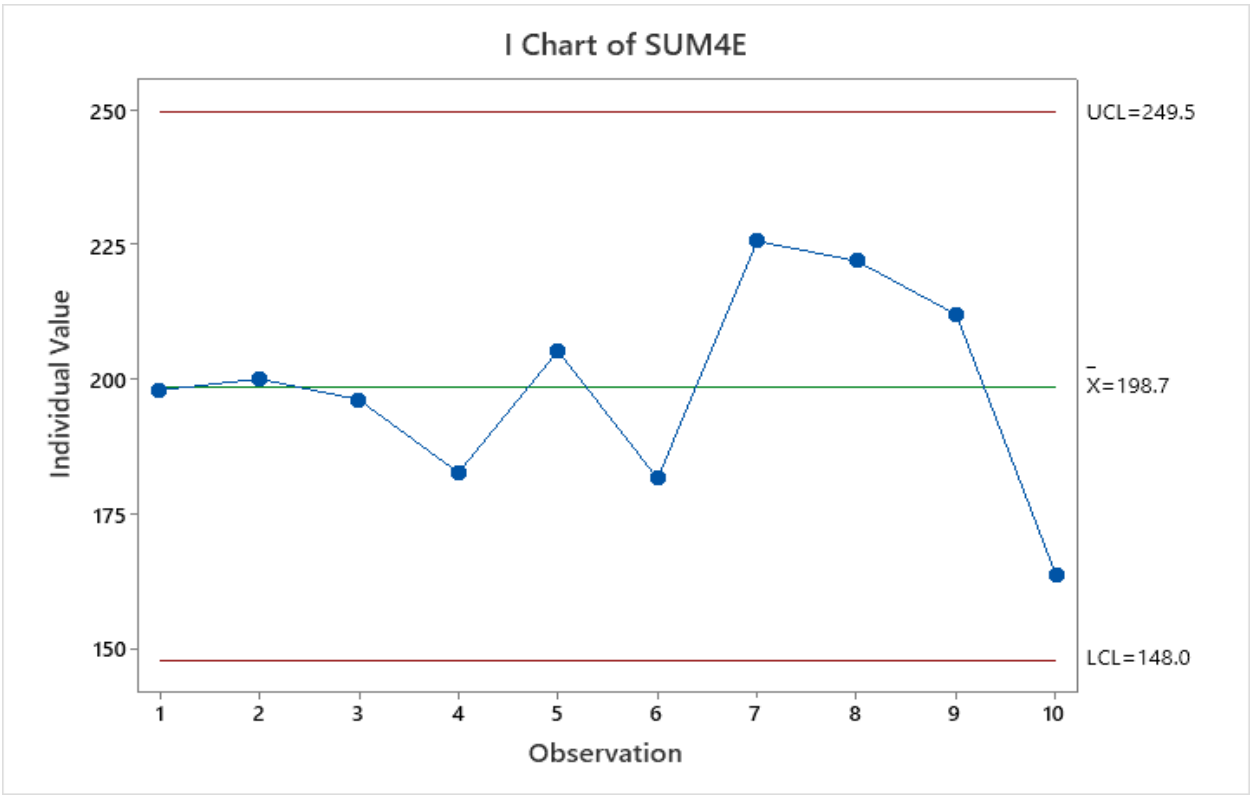

Figure 140: GC concentrate 2 4E outlier chart

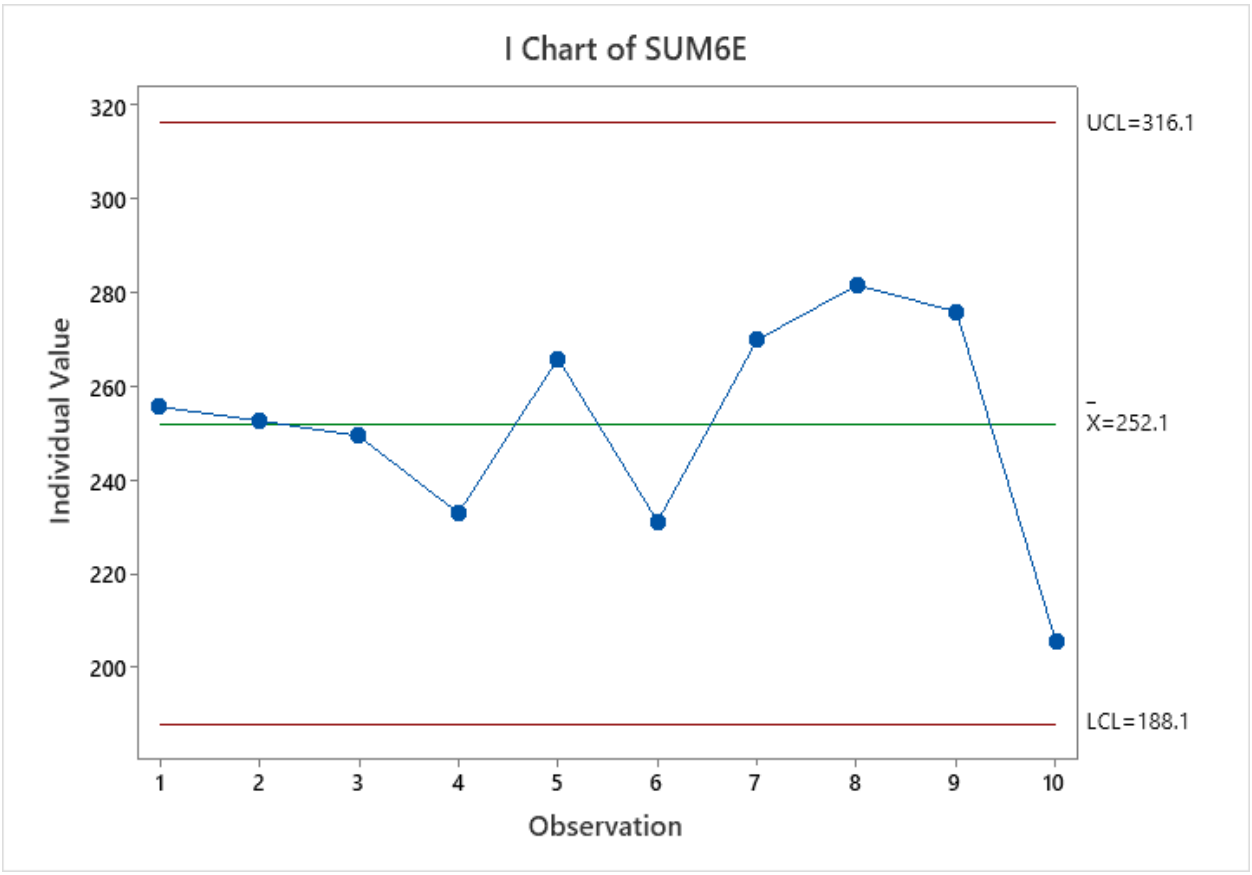

Figure 141: GC concentrate 2 6E outlier chart

GC Concentrate 3

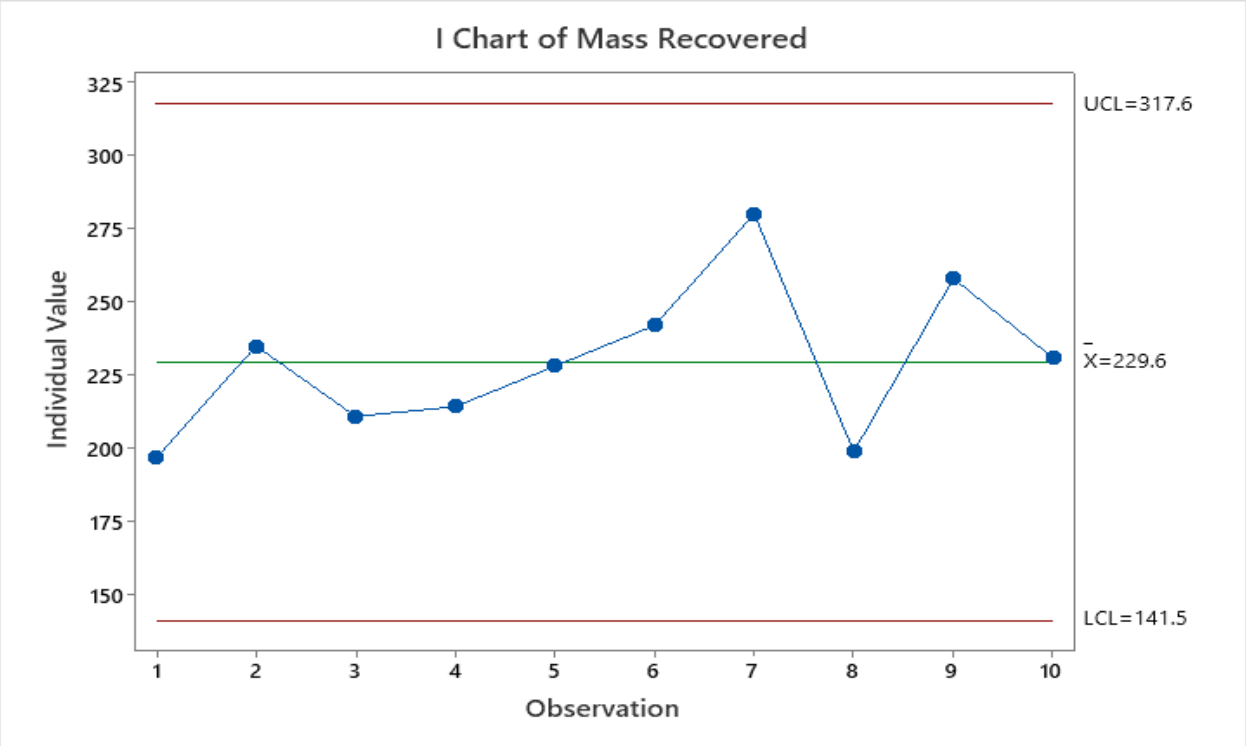

Figure 142: GC concentrate 3 mass recovered outlier chart

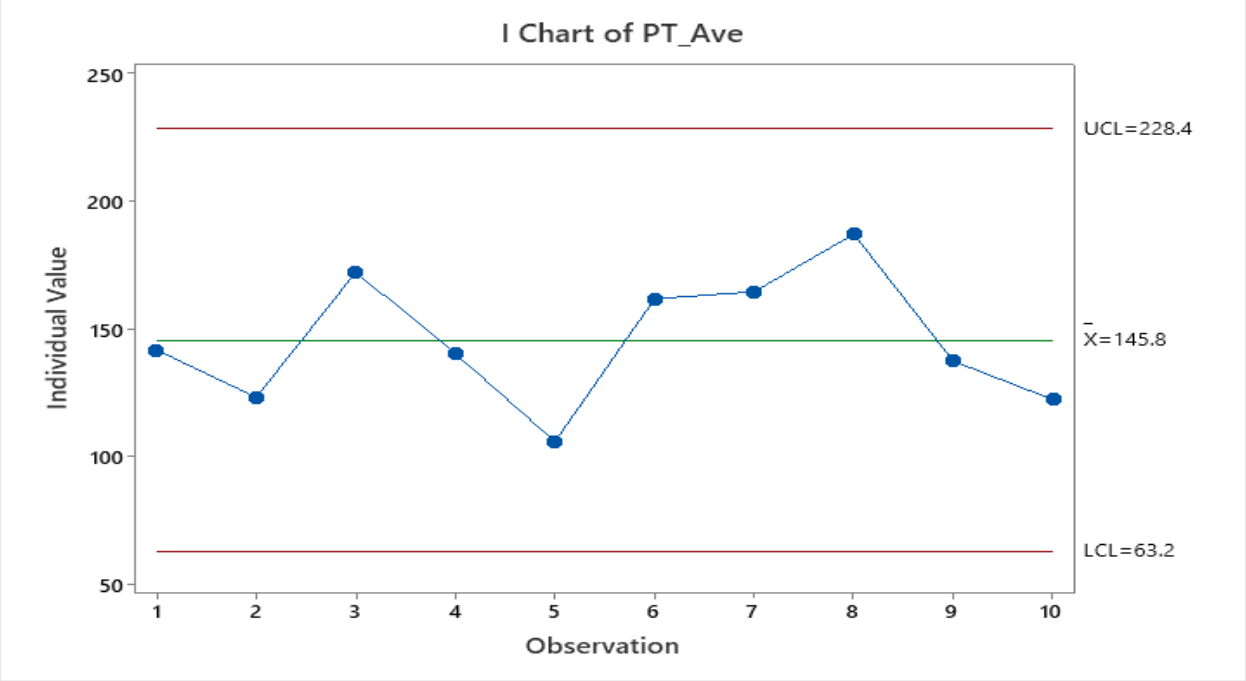

Figure 143: GC concentrate 3 platinum outlier chart

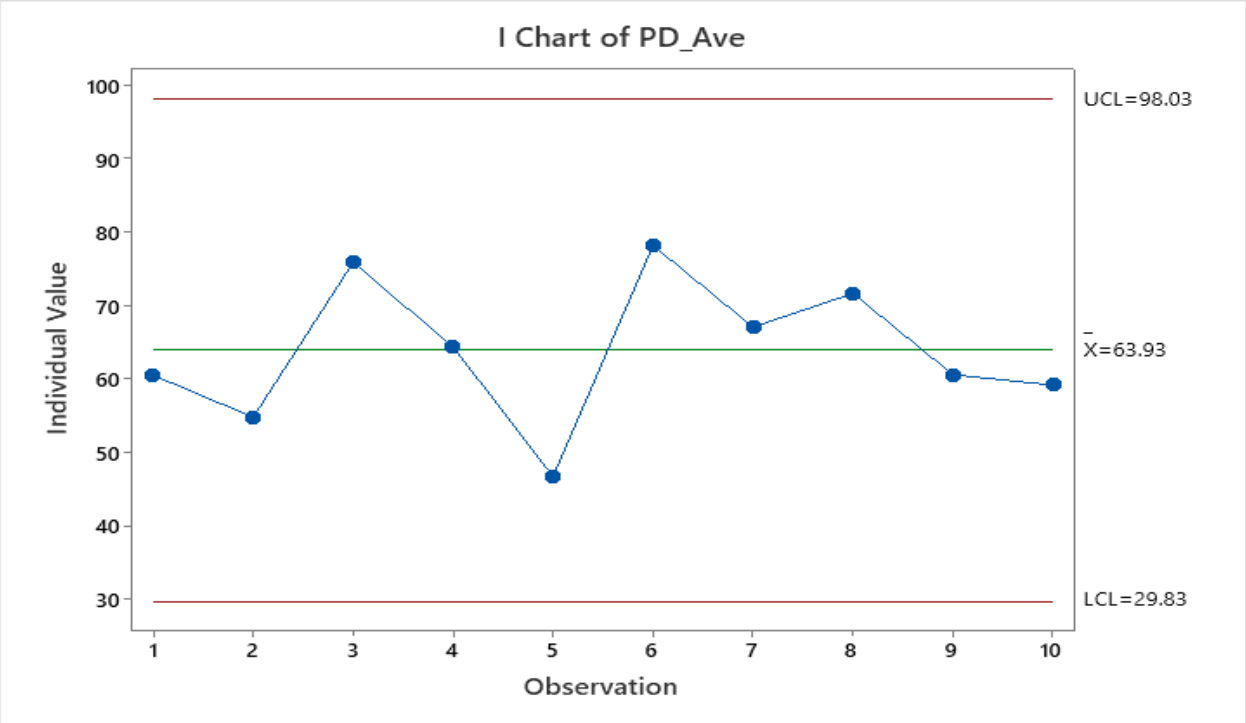

Figure 144: GC concentrate 3 palladium outlier chart

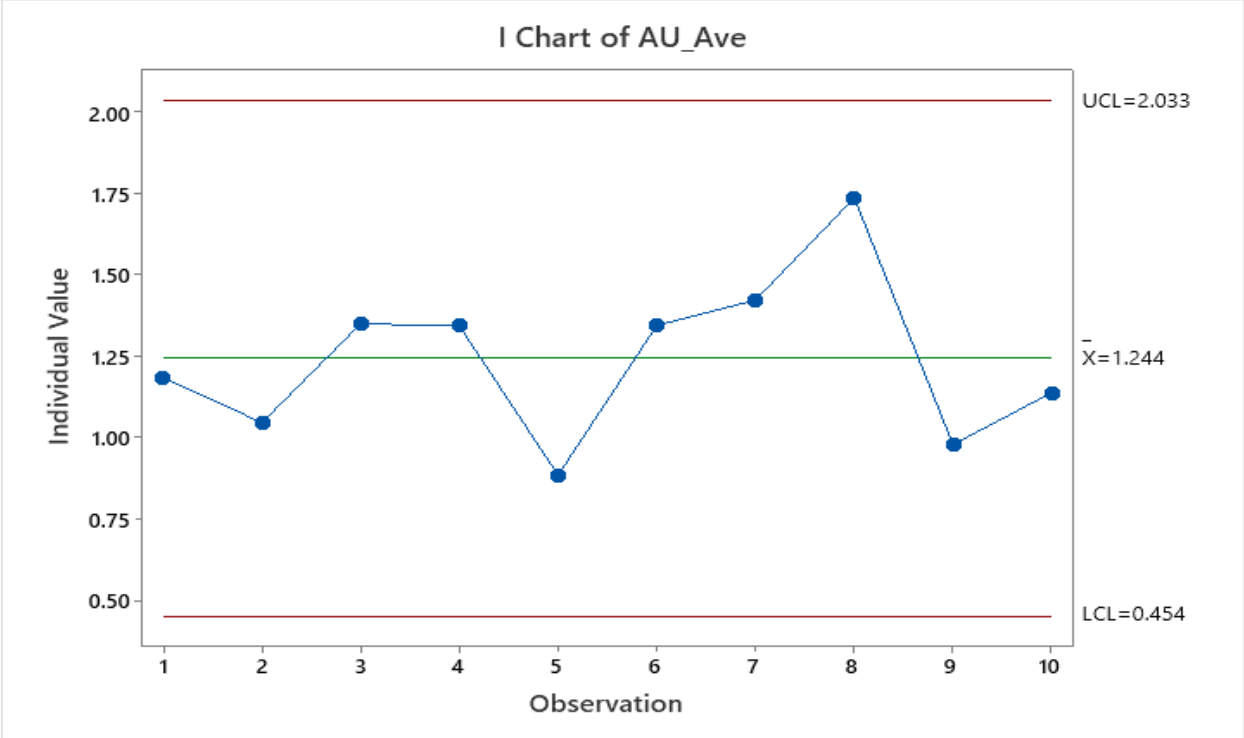

Figure 145: GC concentrate 3 gold outlier chart

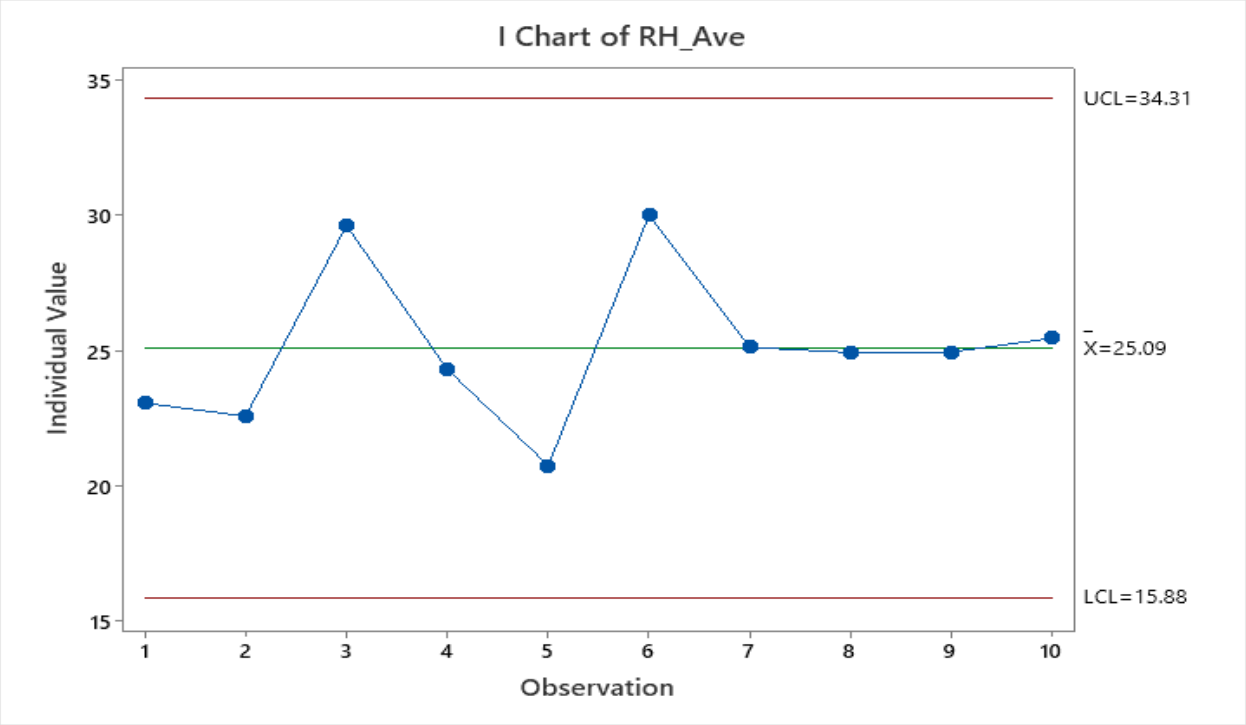

Figure 146: GC concentrate 3 rhodium outlier chart

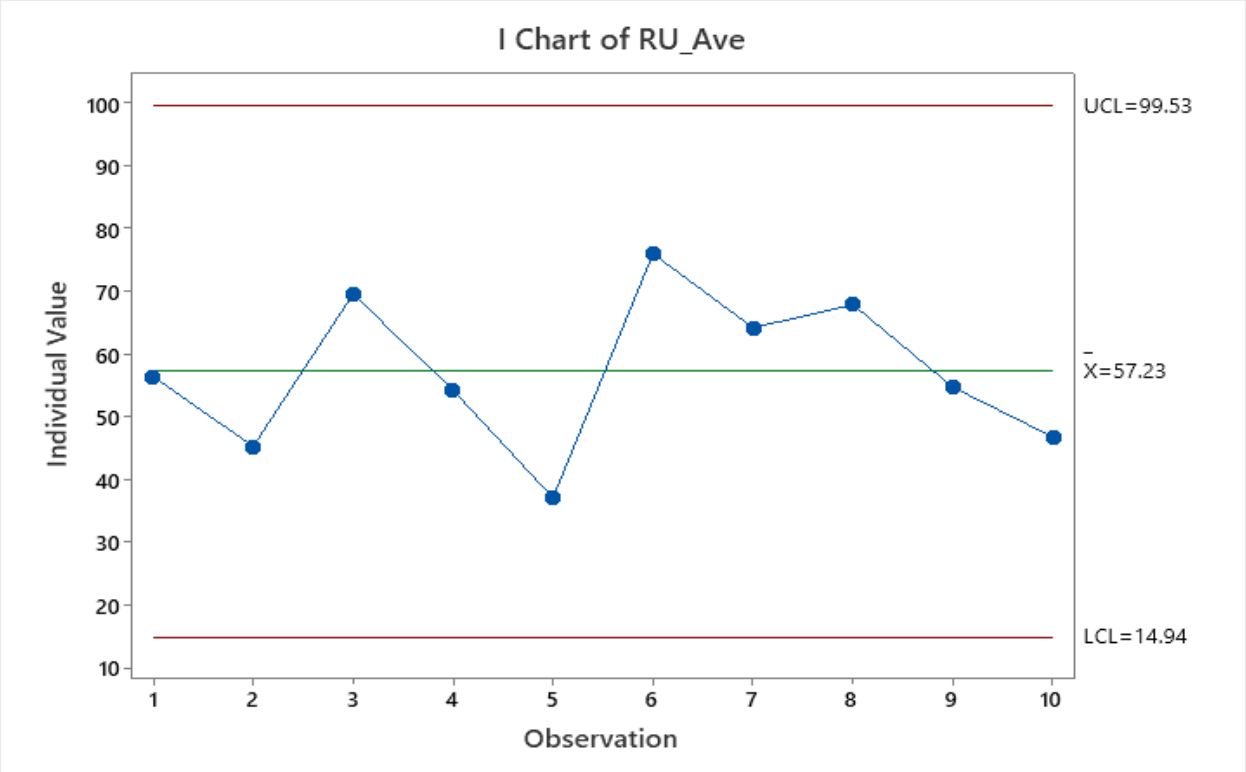

Figure 147: GC concentrate 3 ruthenium outlier chart

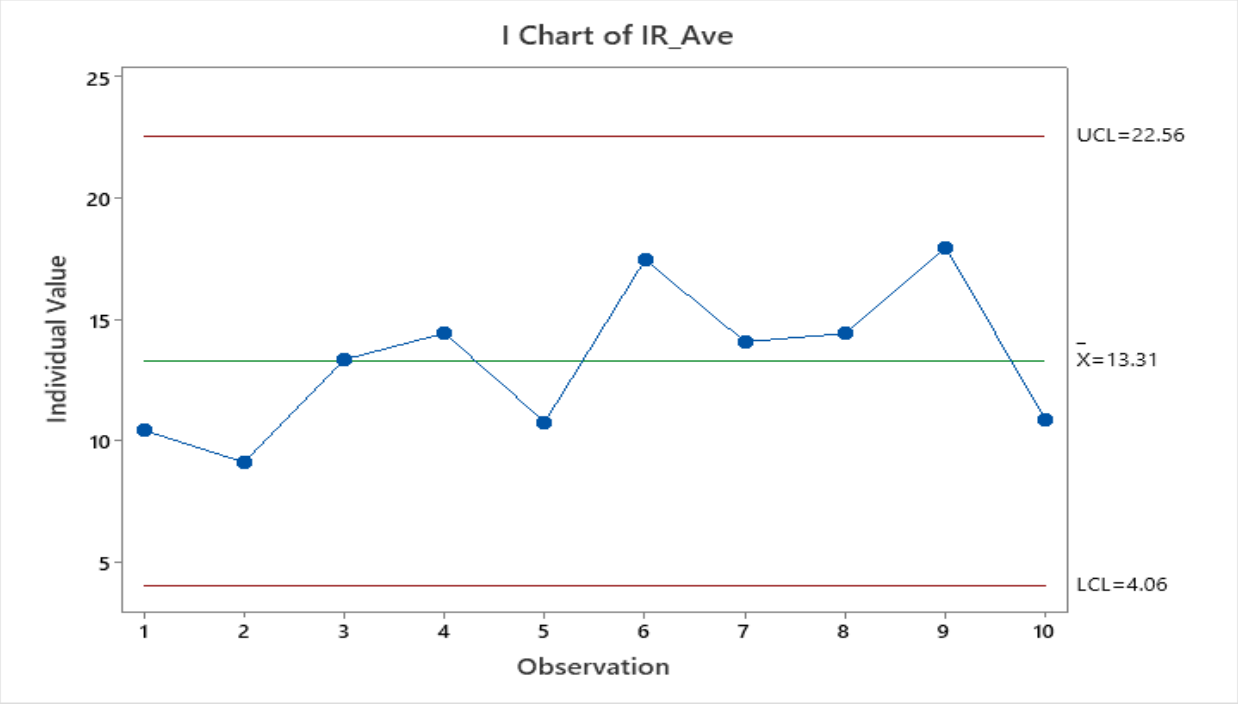

Figure 148: GC concentrate 3 iridium outlier chart

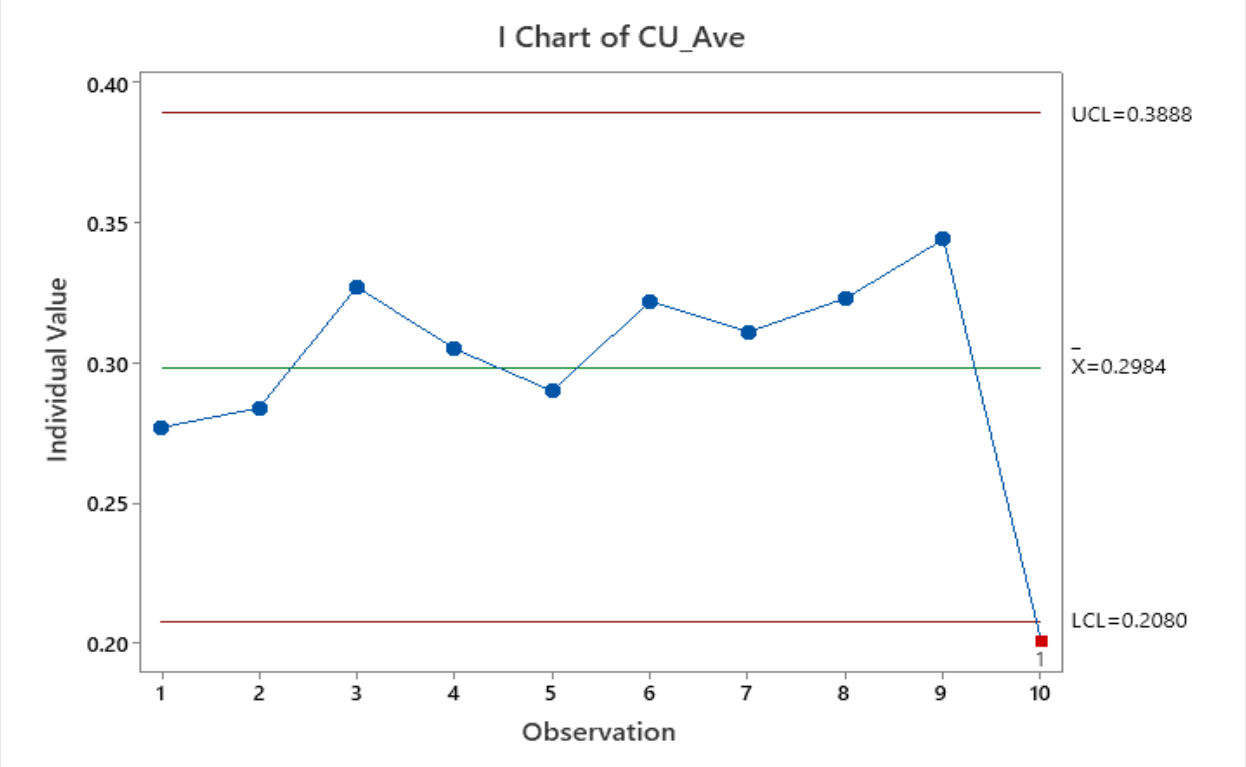

Figure 149: GC concentrate 3 copper outlier chart

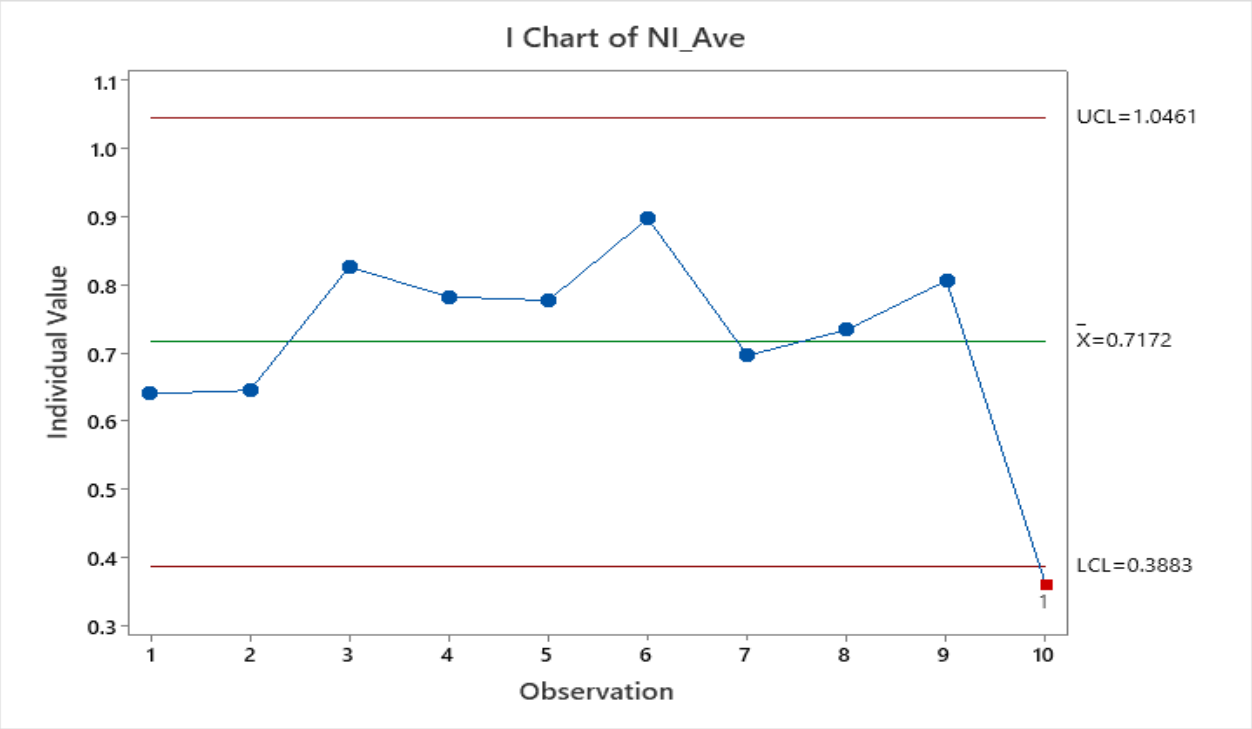

Figure 150: GC concentrate 3 nickel outlier chart

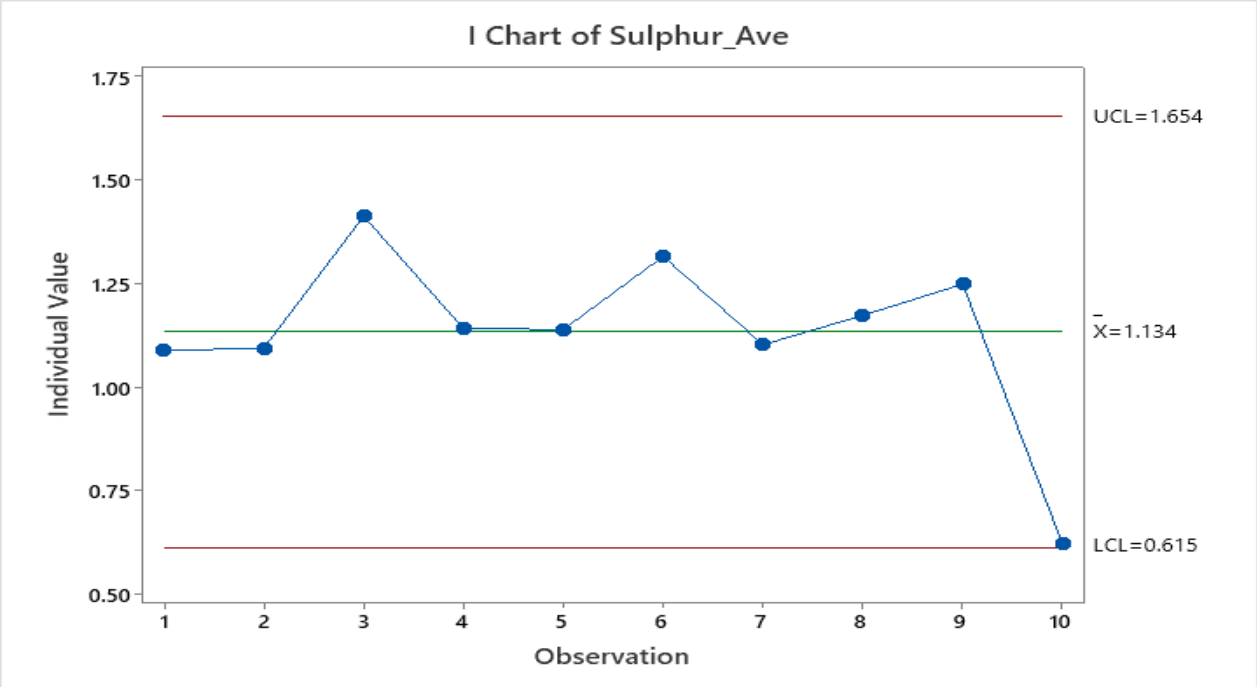

Figure 151: GC concentrate 3 sulphur outlier chart

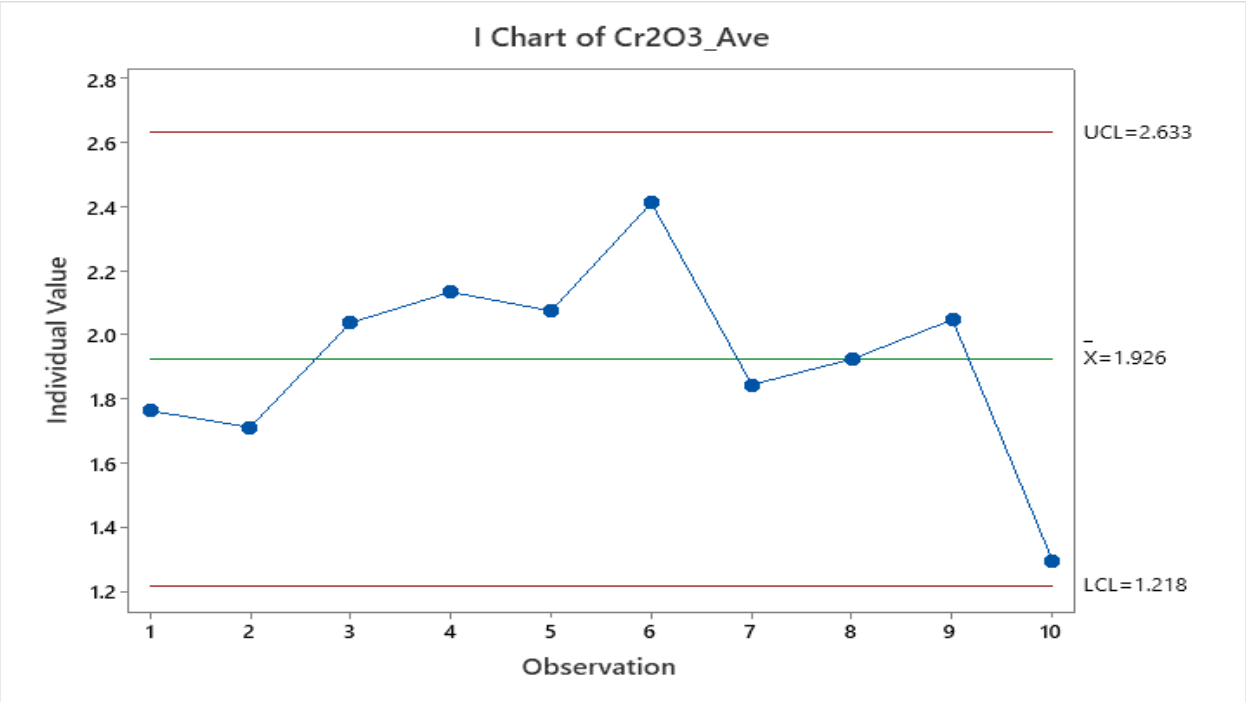

Figure 152: GC concentrate 3 chrome outlier chart

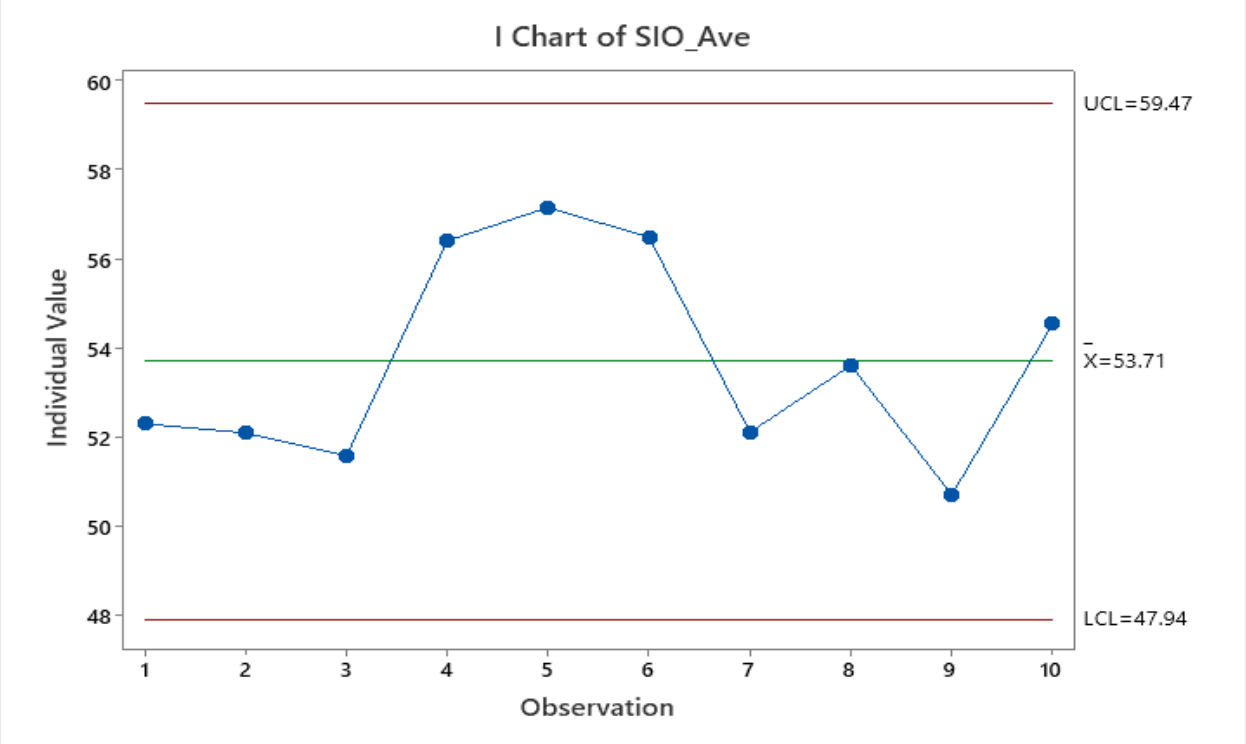

Figure 153: GC concentrate 3 silicon dioxide outlier chart

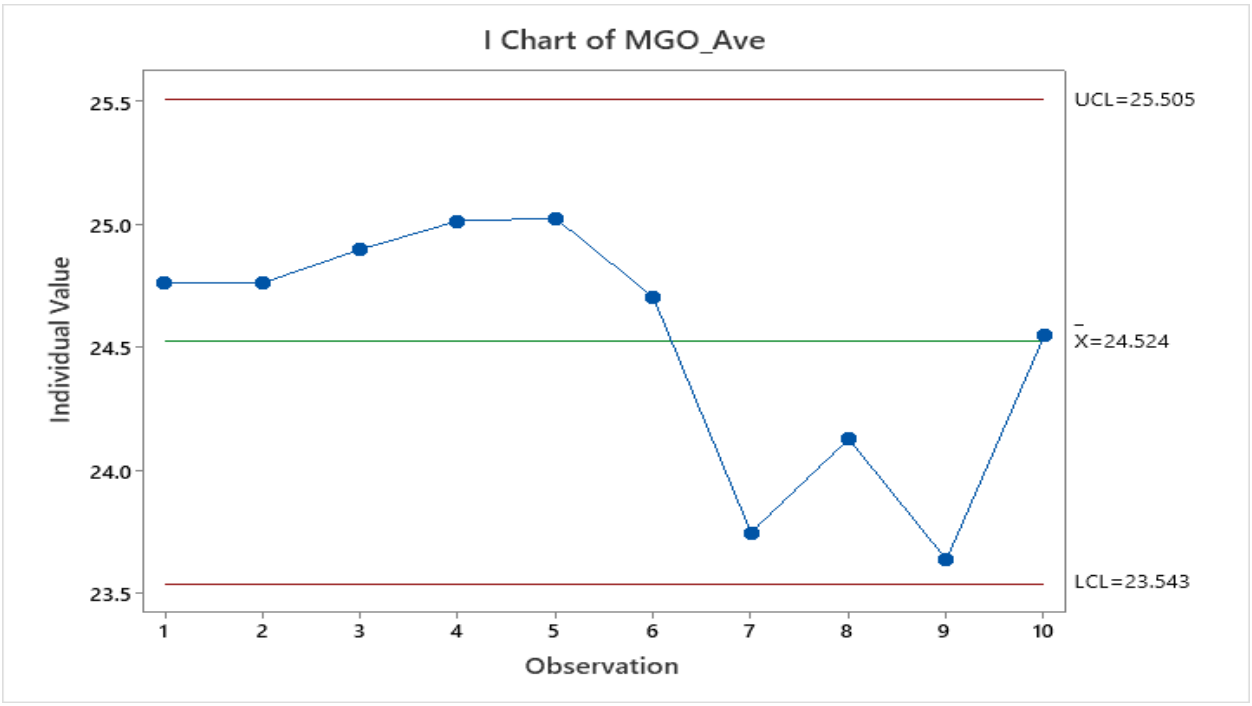

Figure 154: GC concentrate 3 magnesium oxide outlier chart

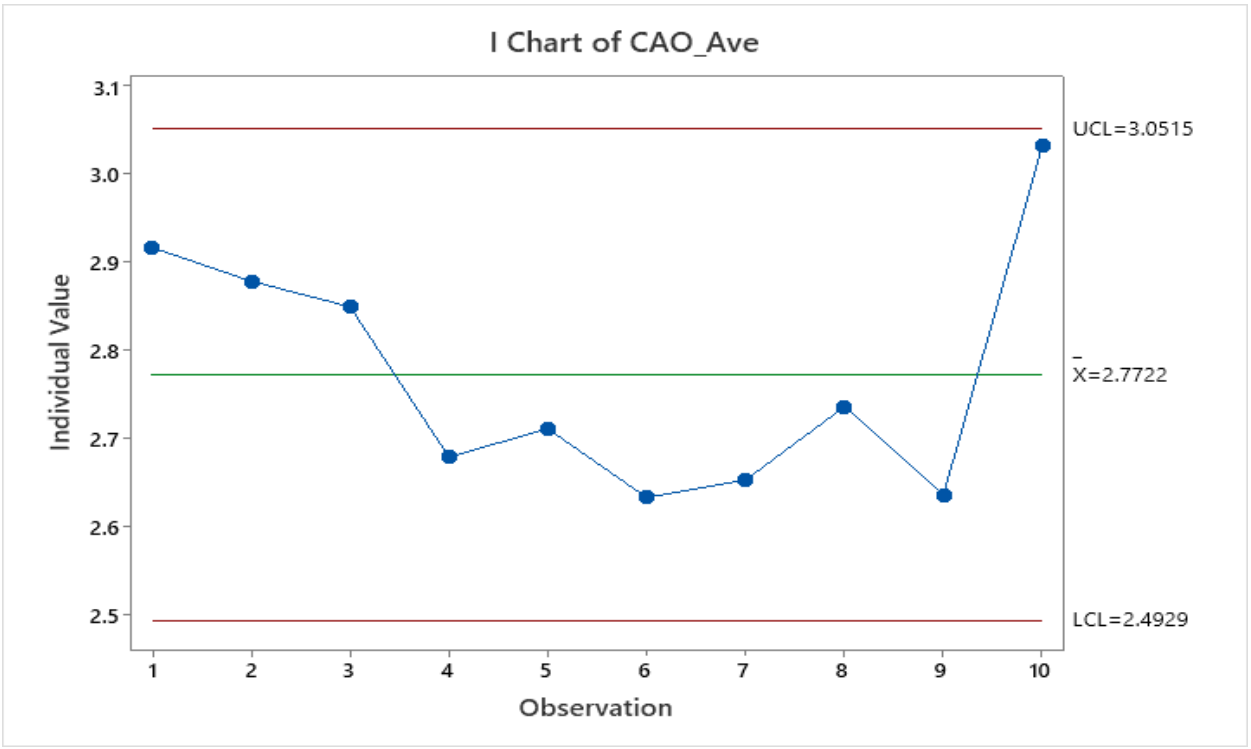

Figure 155: GC concentrate 3 calcium oxide outlier chart

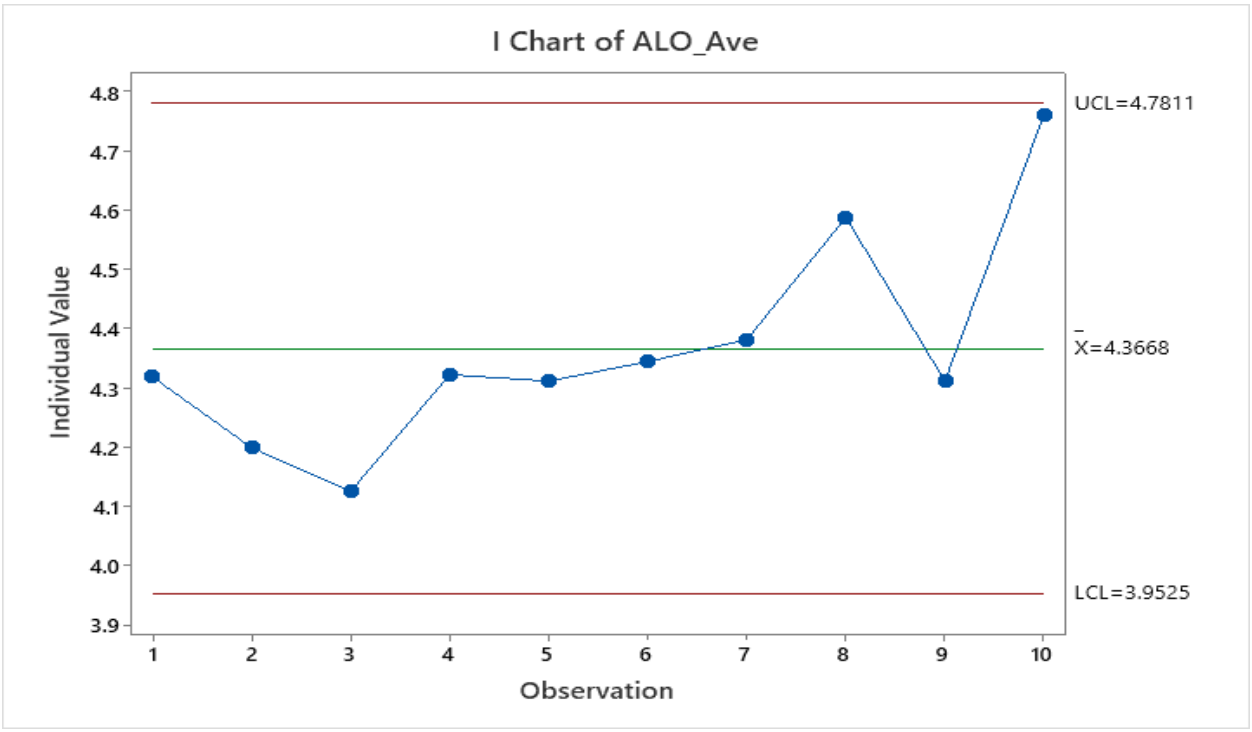

Figure 156: GC concentrate 3 aluminium oxide outlier chart

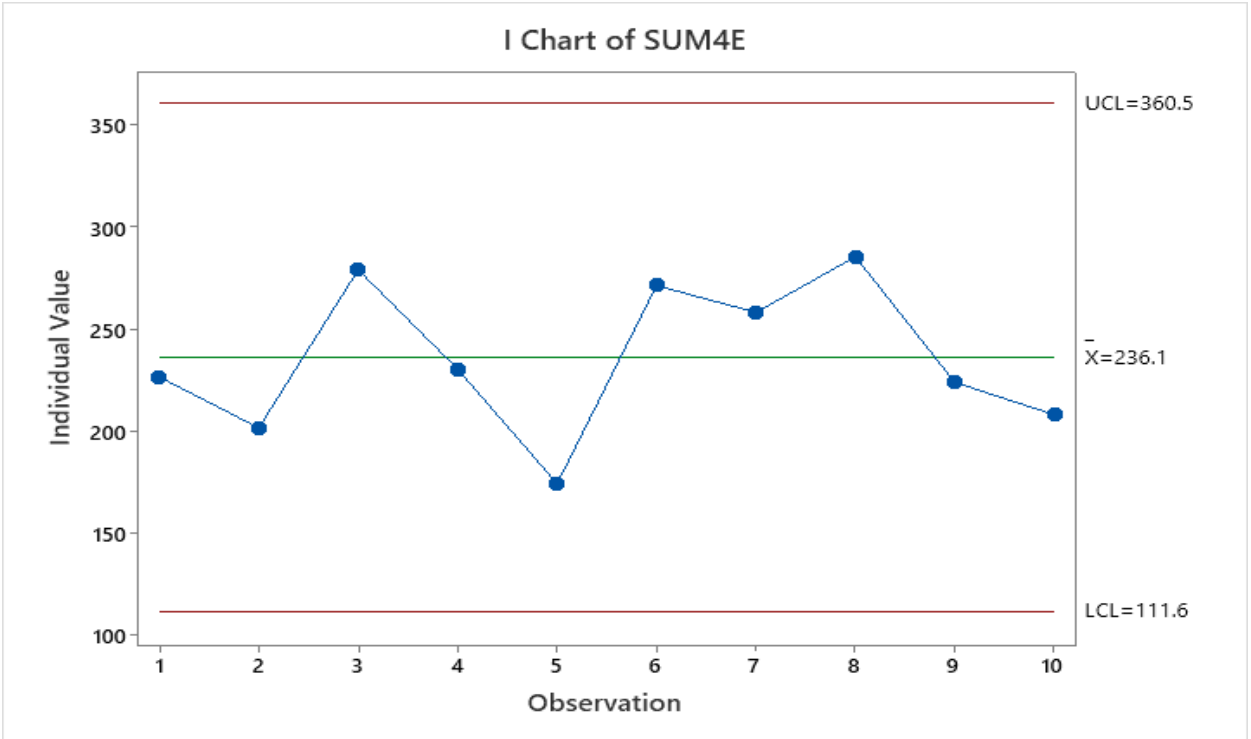

Figure 157: GC concentrate 3 4E outlier chart

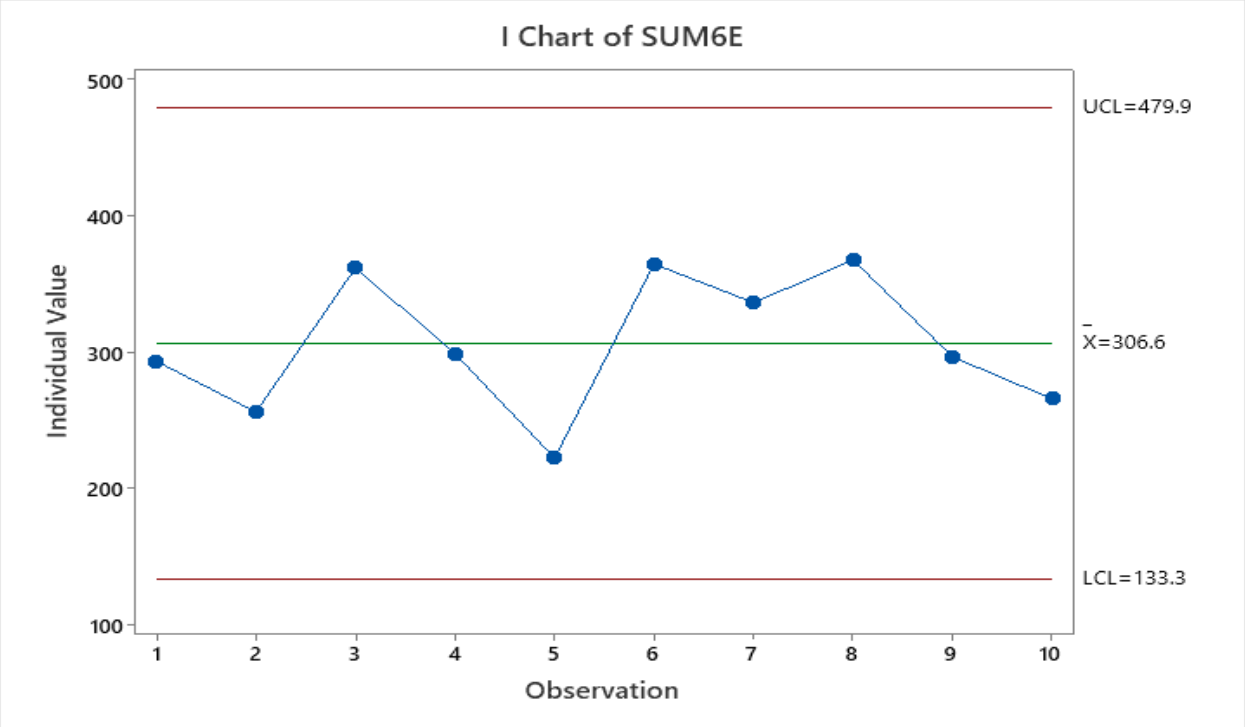

Figure 158: GC concentrate 3 6E outlier chart

GC Concentrate 4

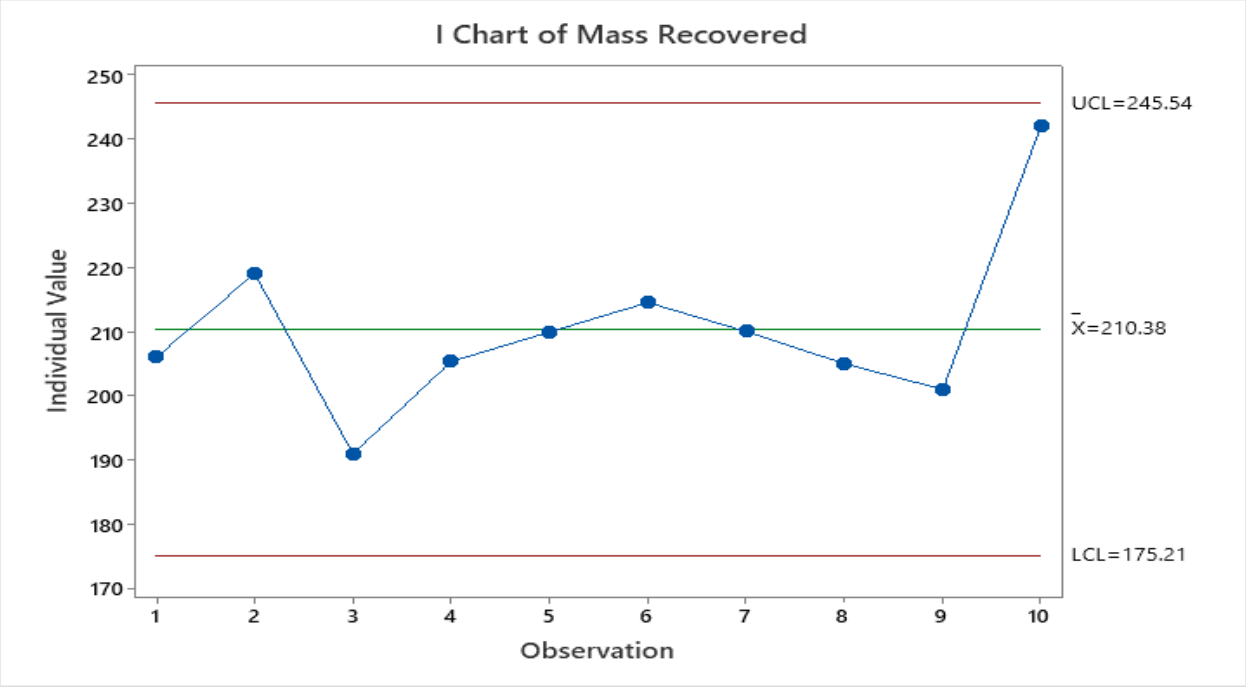

Figure 159: GC concentrate 4 mass recovered outlier chart

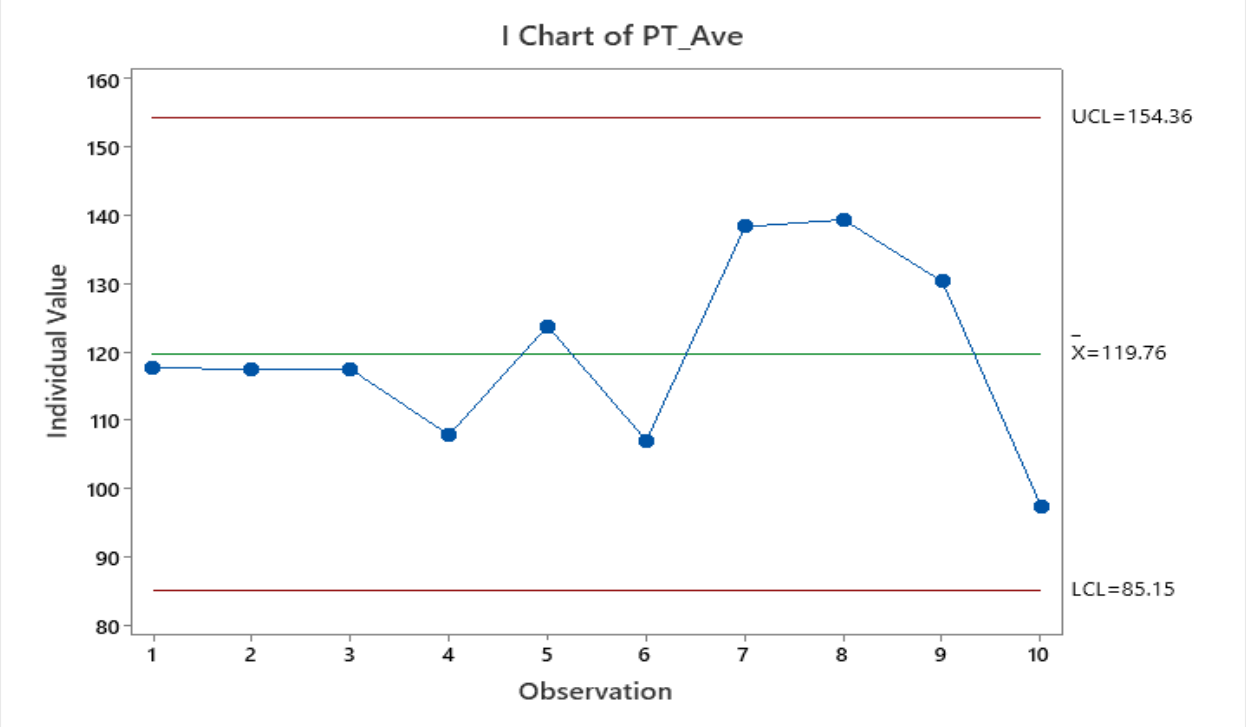

Figure 160: GC concentrate 4 platinum outlier chart

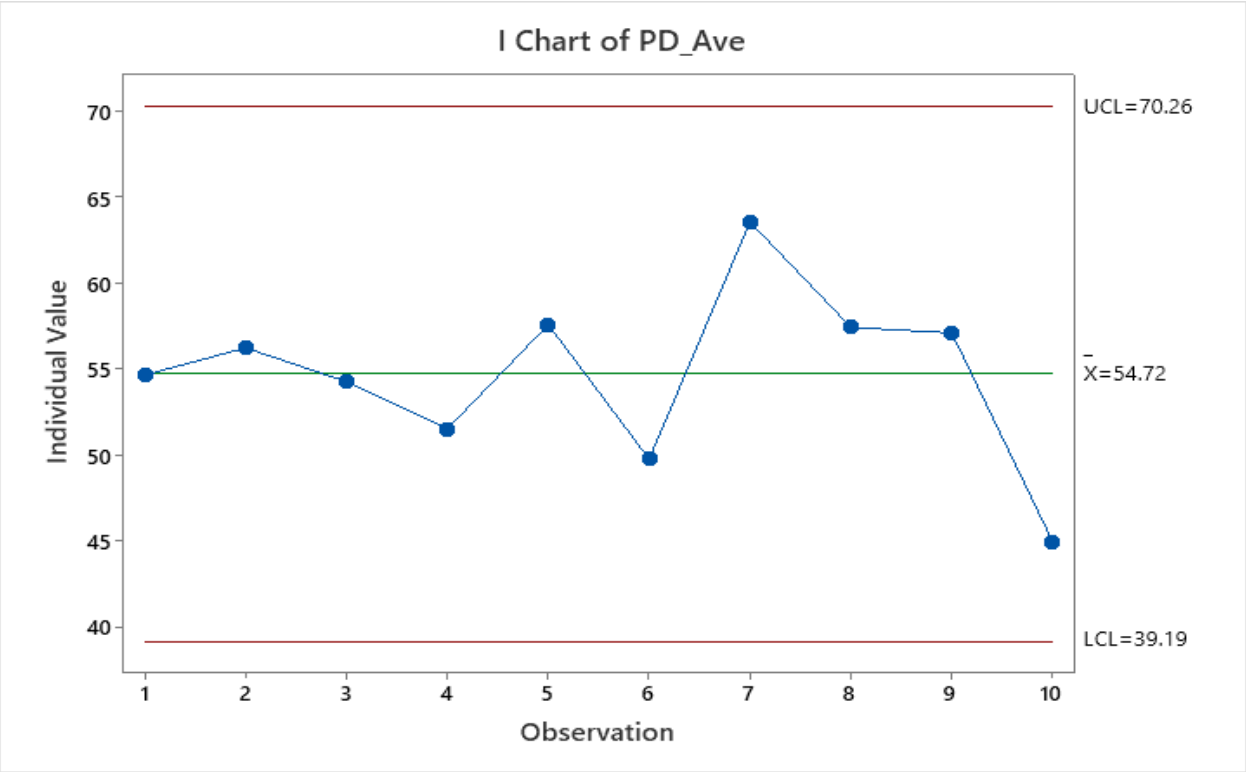

Figure 161: GC concentrate 4 palladium outlier chart

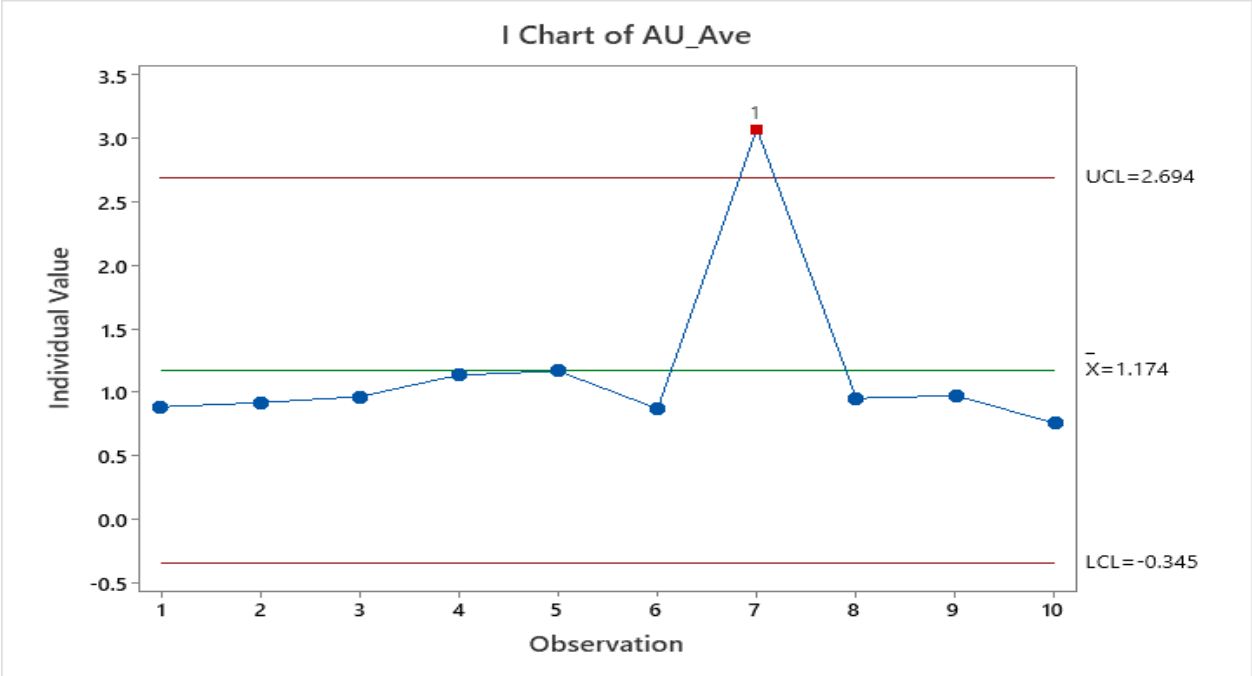

Figure 162: GC concentrate 4 gold outlier chart

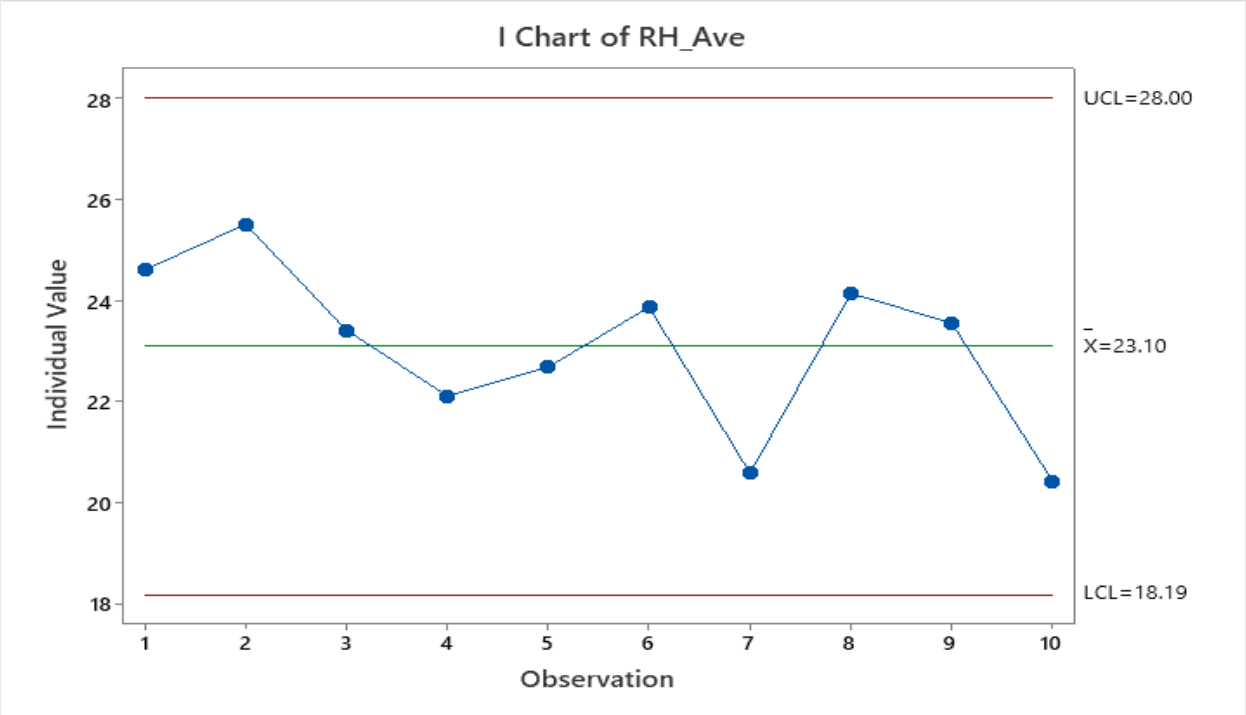

Figure 163: GC concentrate 4 rhodium outlier chart

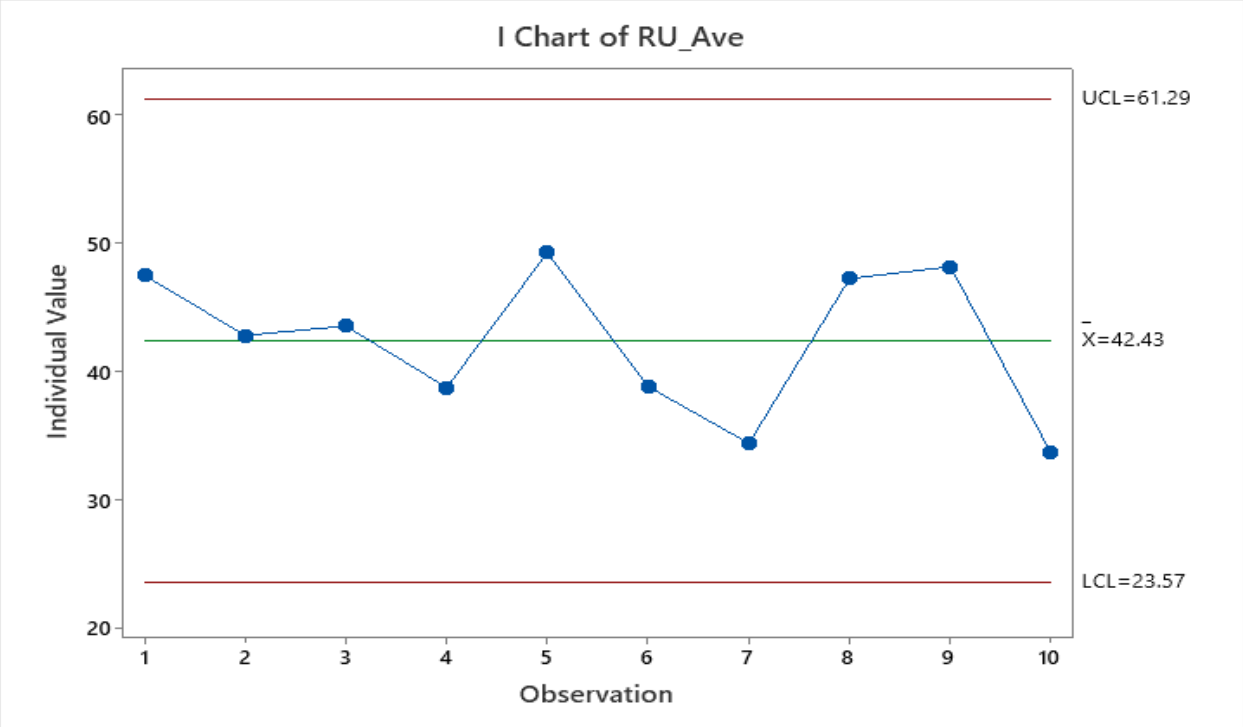

Figure 164: GC concentrate 4 ruthenium outlier chart

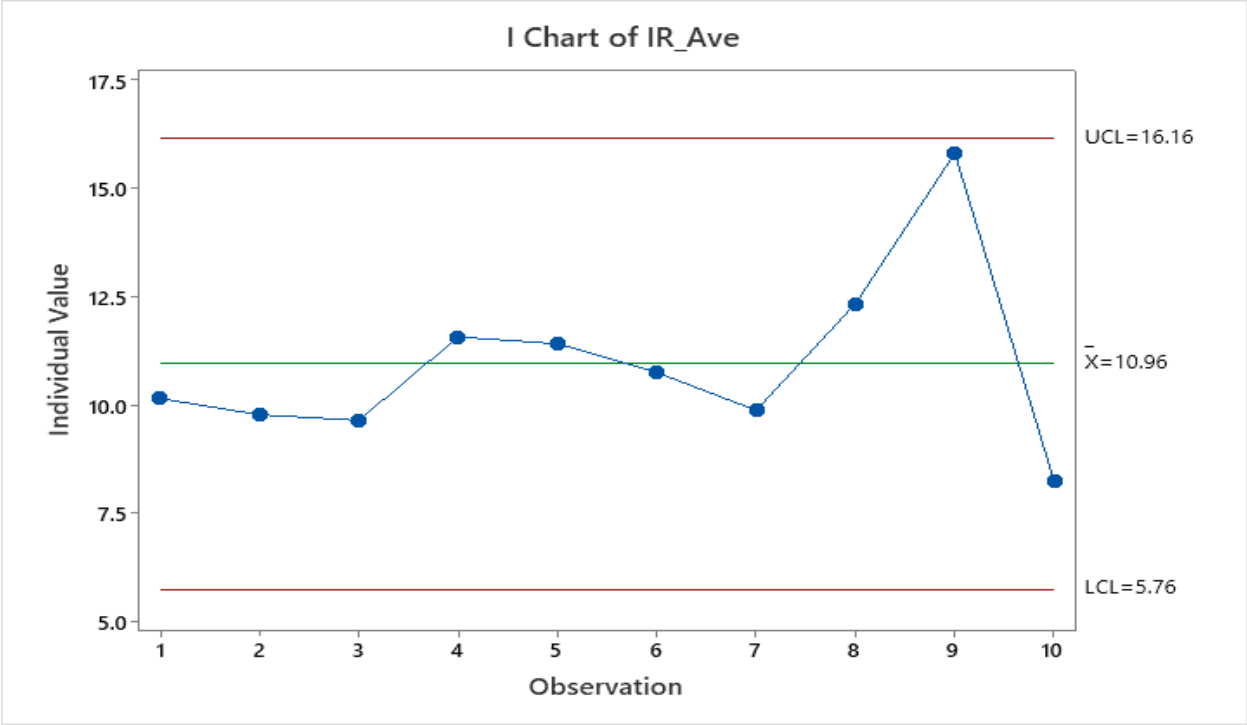

Figure 165: GC concentrate 4 iridium outlier chart

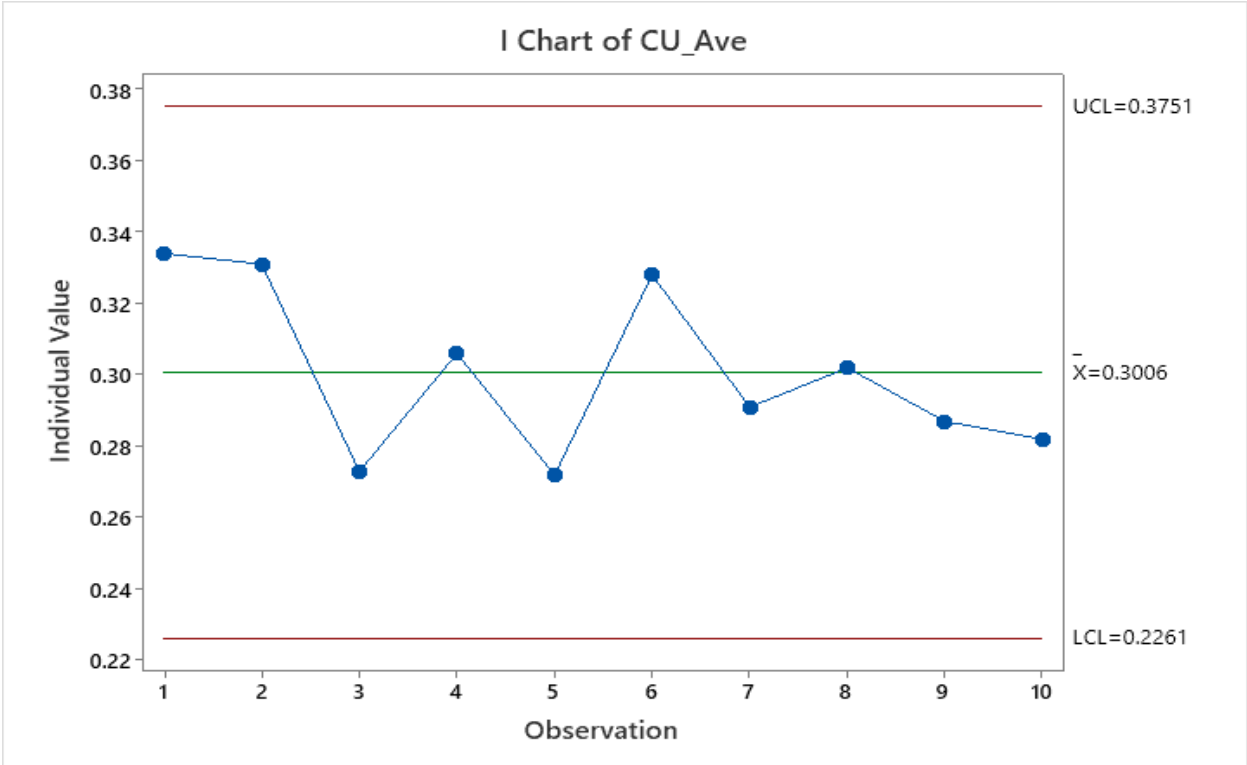

Figure 166: GC concentrate 4 copper outlier chart

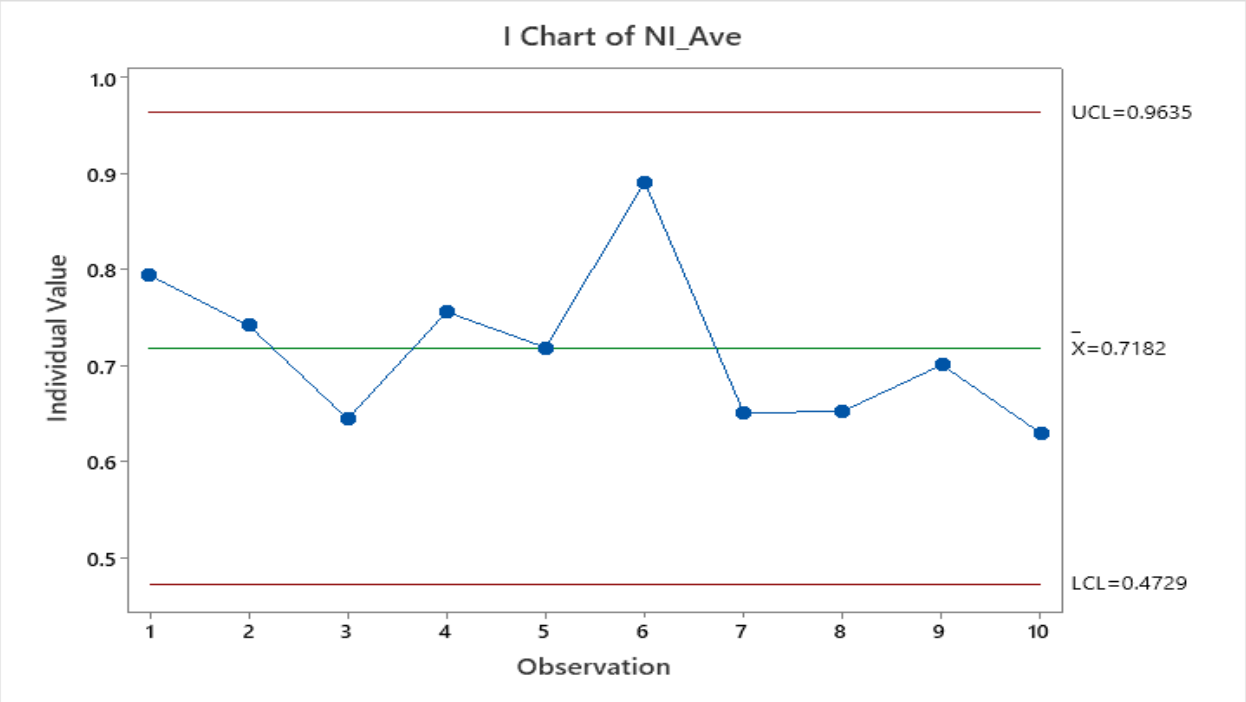

Figure 167: GC concentrate 4 nickel outlier chart

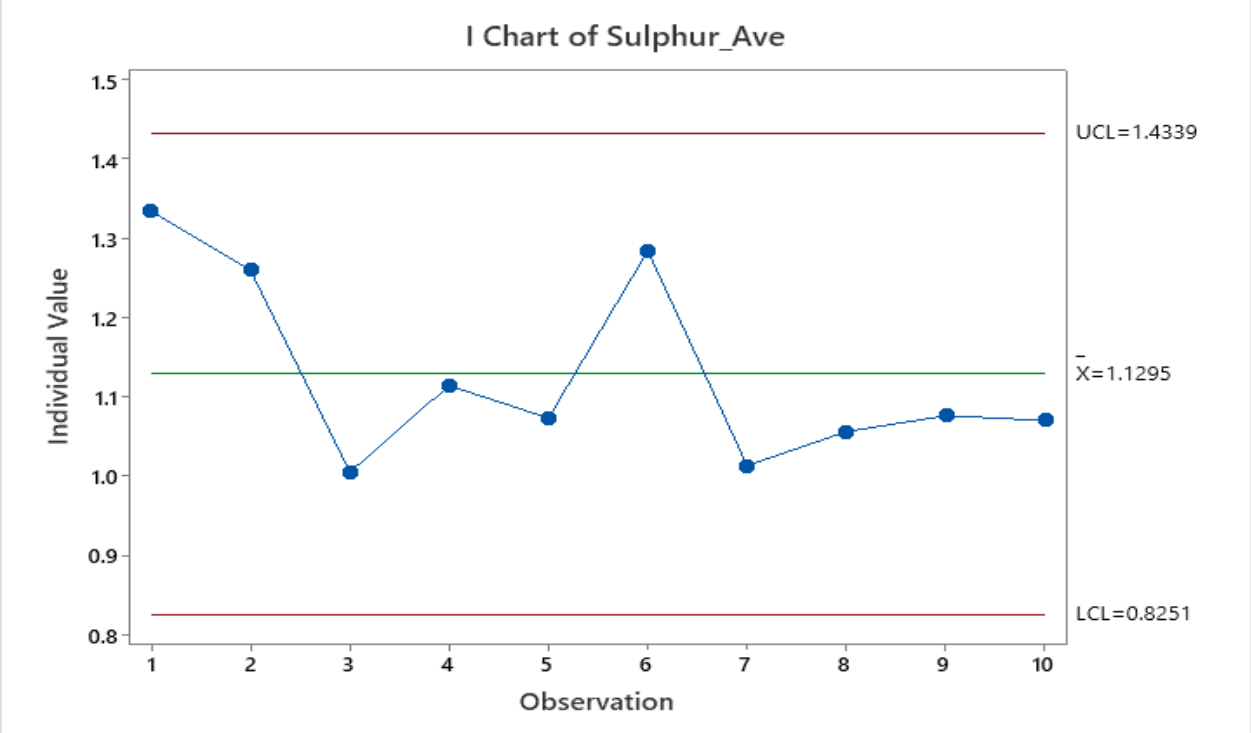

Figure 168: GC concentrate 4 sulphur outlier chart

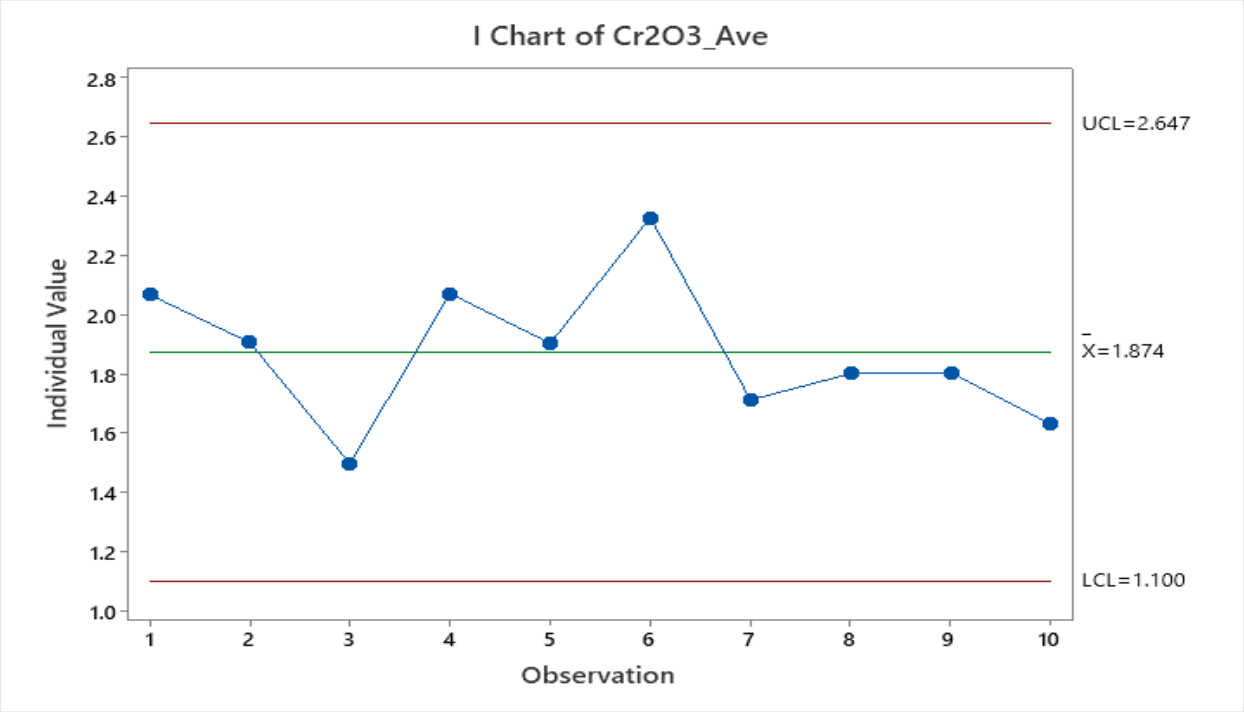

Figure 169: GC concentrate 4 chrome outlier chart



Figure 170: GC concentrate 4 silicon dioxide outlier chart

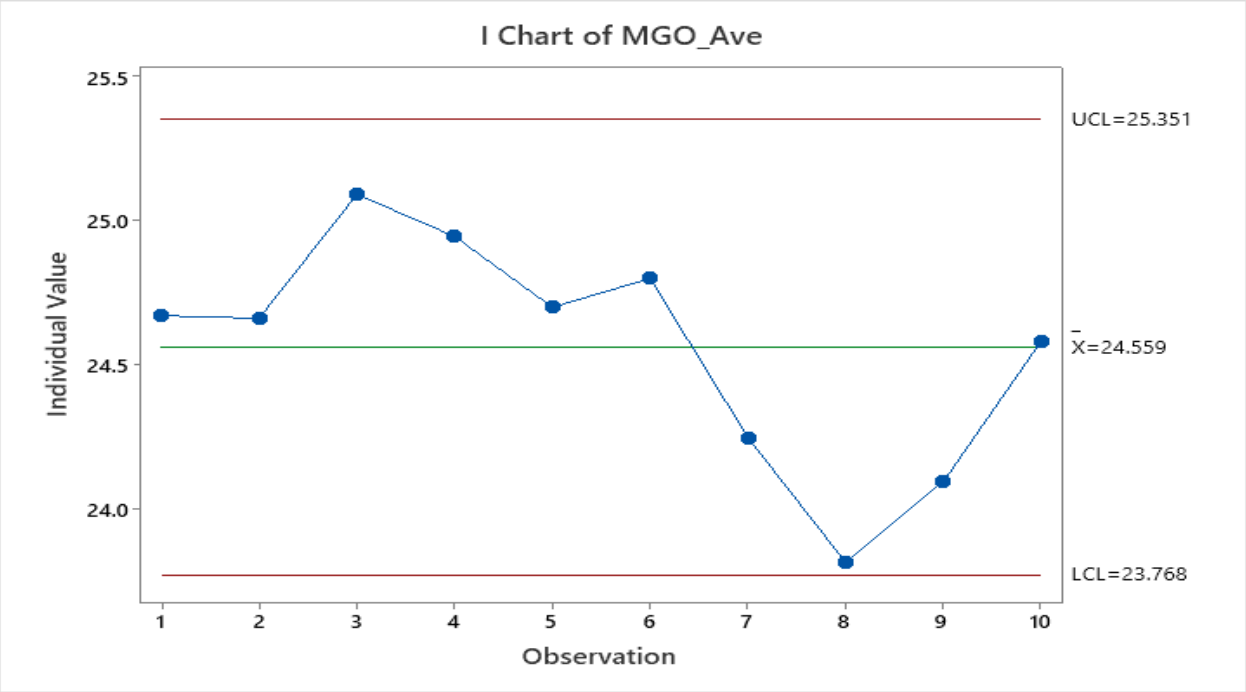

Figure 171: GC concentrate 4 magnesium oxide outlier chart

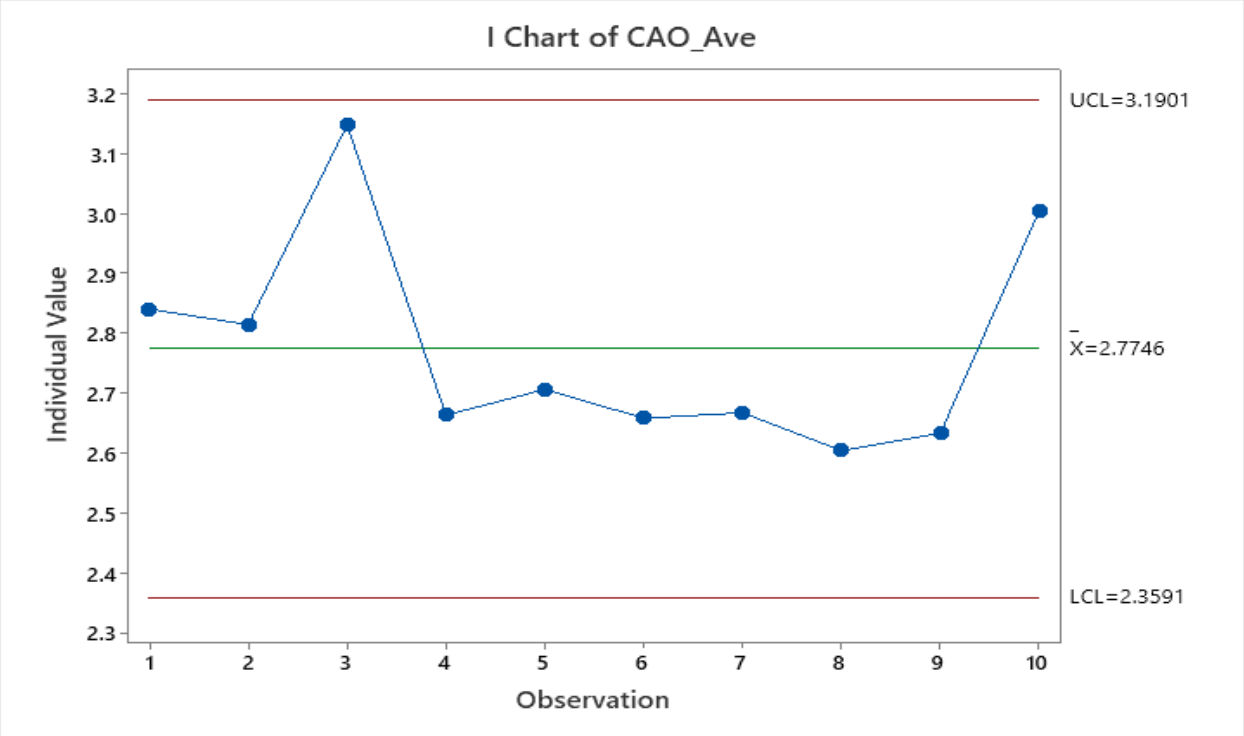

Figure 172: GC concentrate 4 calcium oxide outlier chart

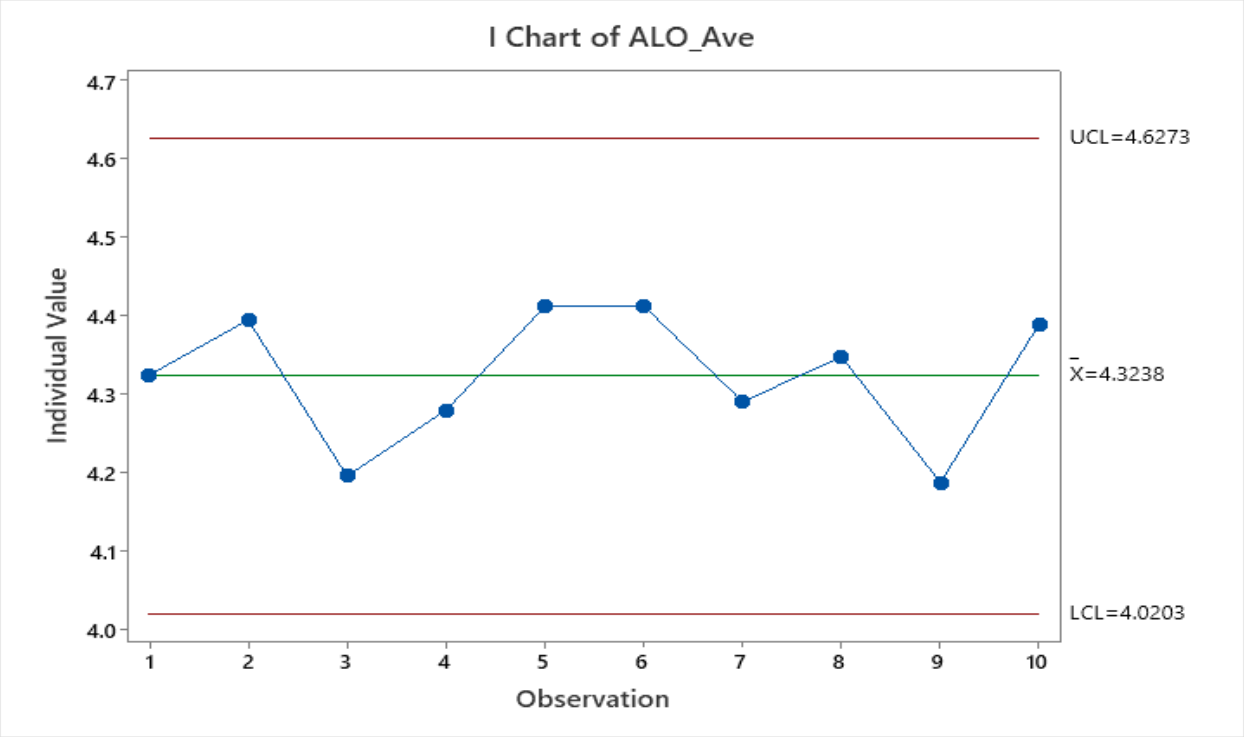

Figure 173: GC concentrate 4 aluminium oxide outlier chart

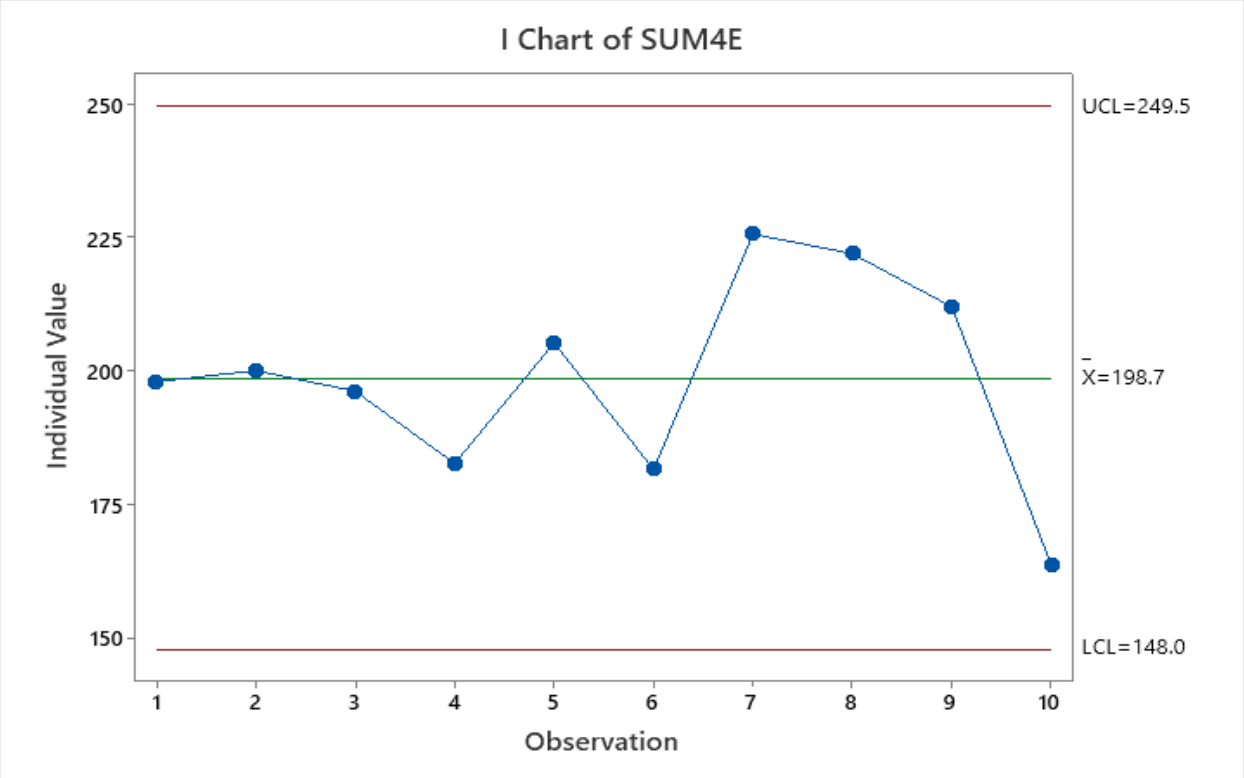

Figure 174: GC concentrate 4 4E outlier chart

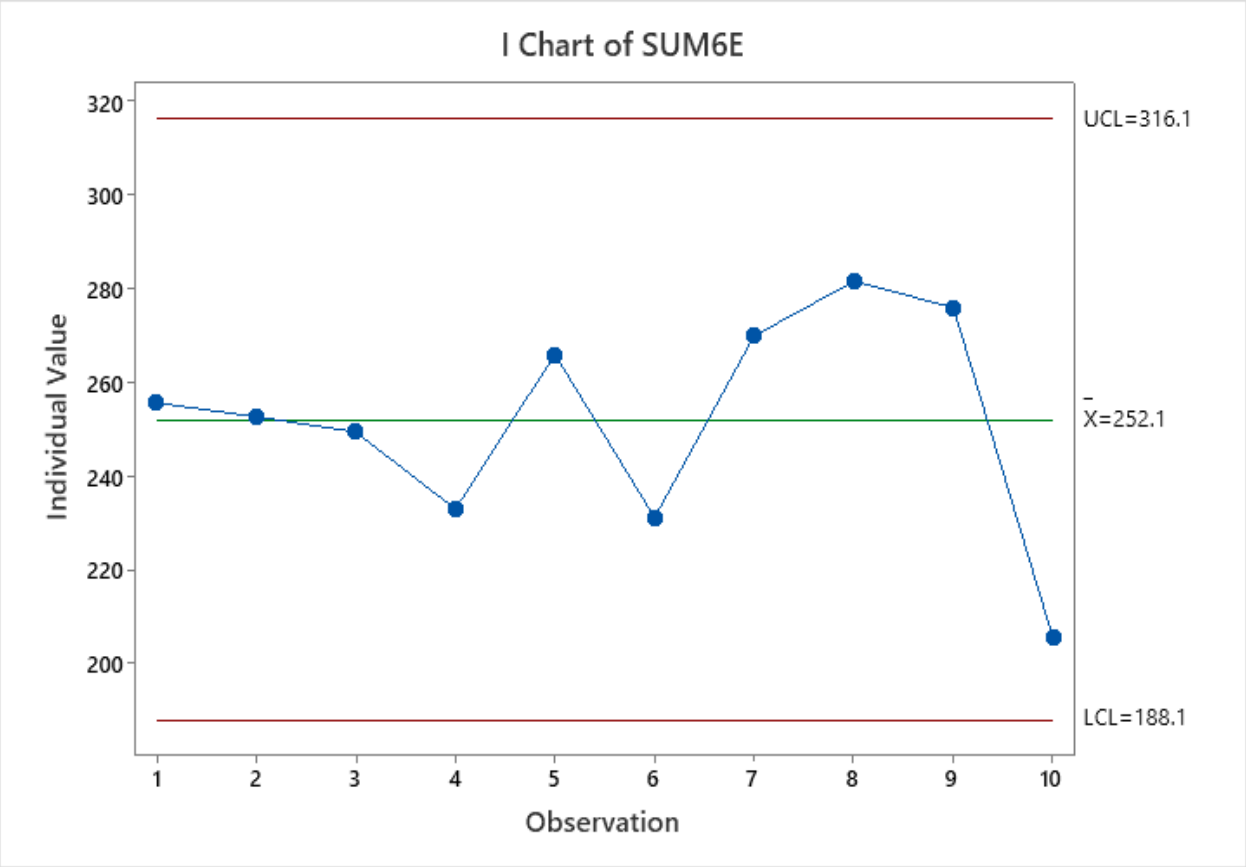

Figure 175: GC concentrate 4 6E outlier chart

GC Concentrate 5

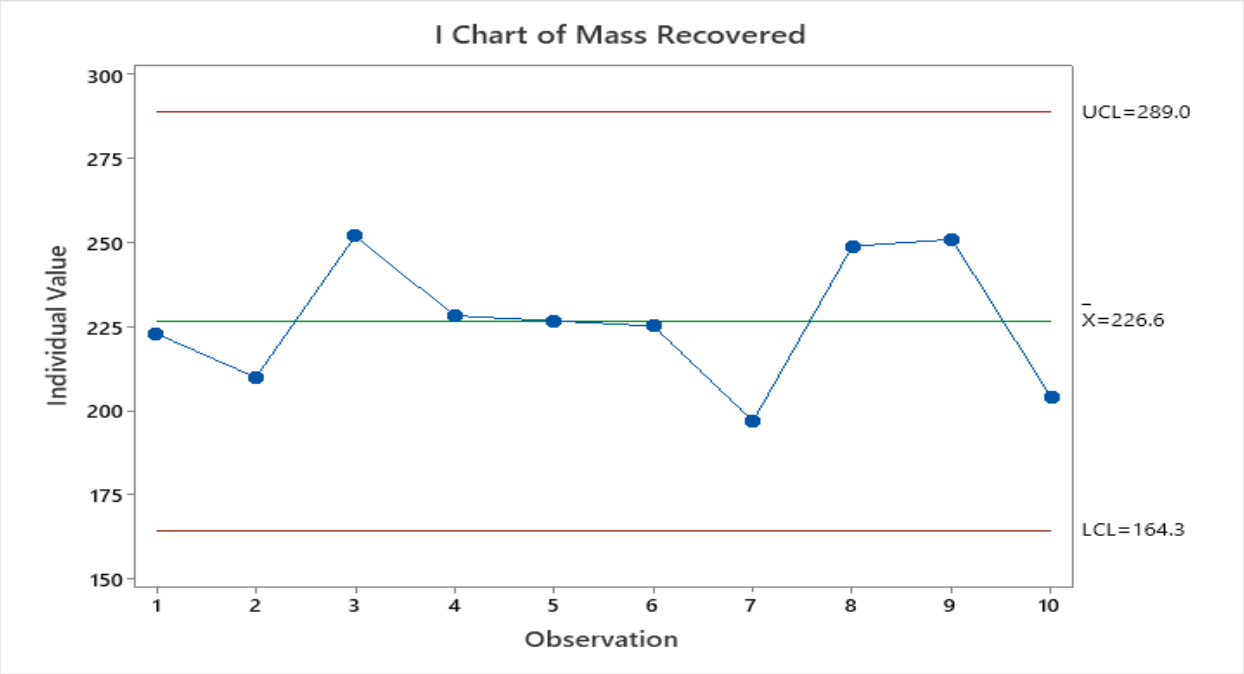

Figure 176: GC concentrate 5 mass recovered outlier chart

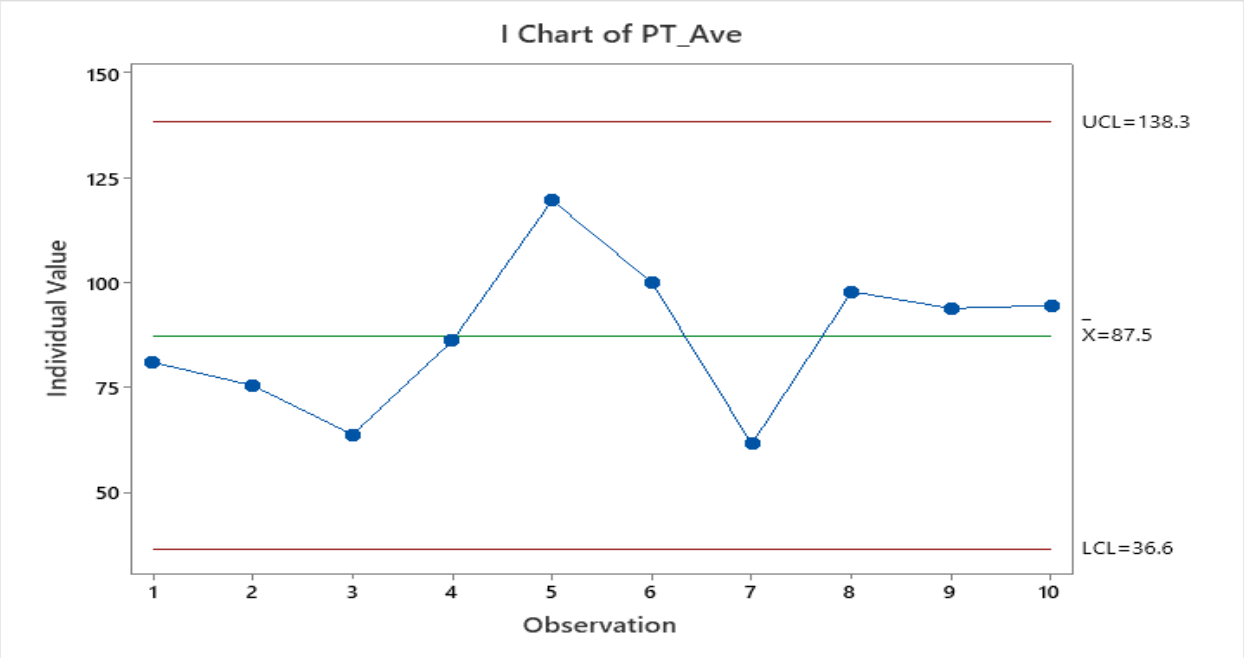

Figure 177: GC concentrate 5 platinum outlier chart

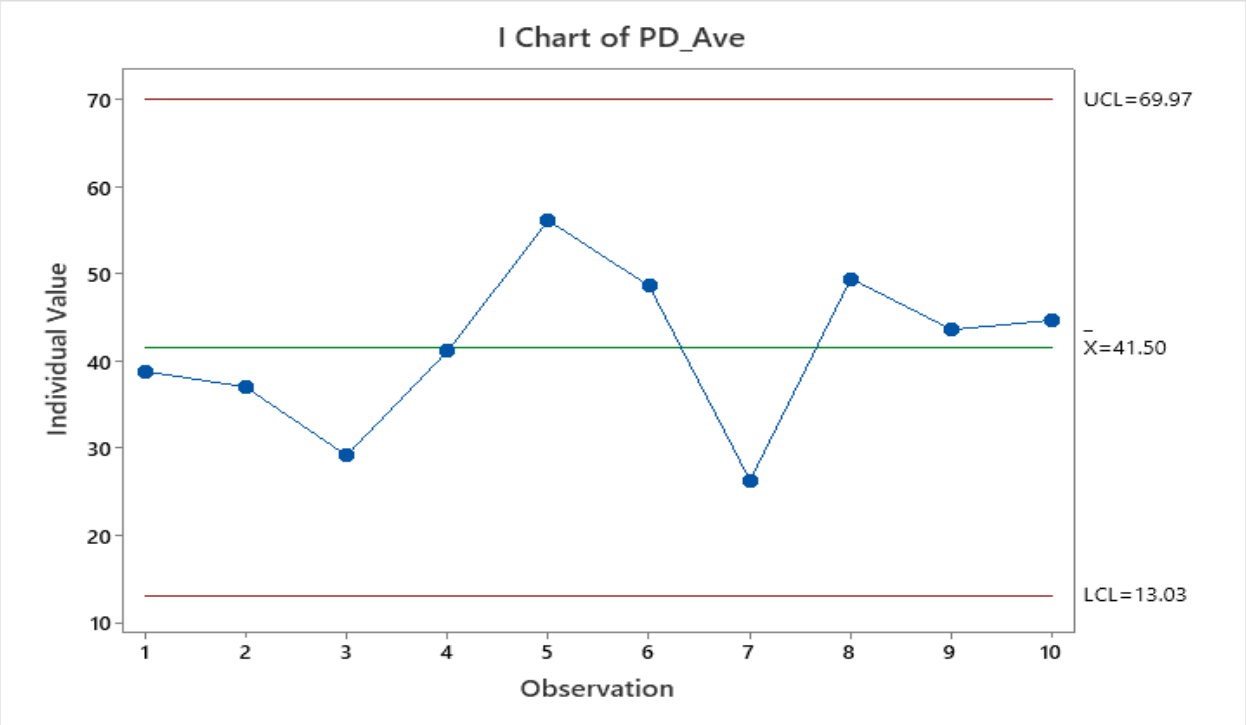

Figure 178: GC concentrate 5 palladium outlier chart

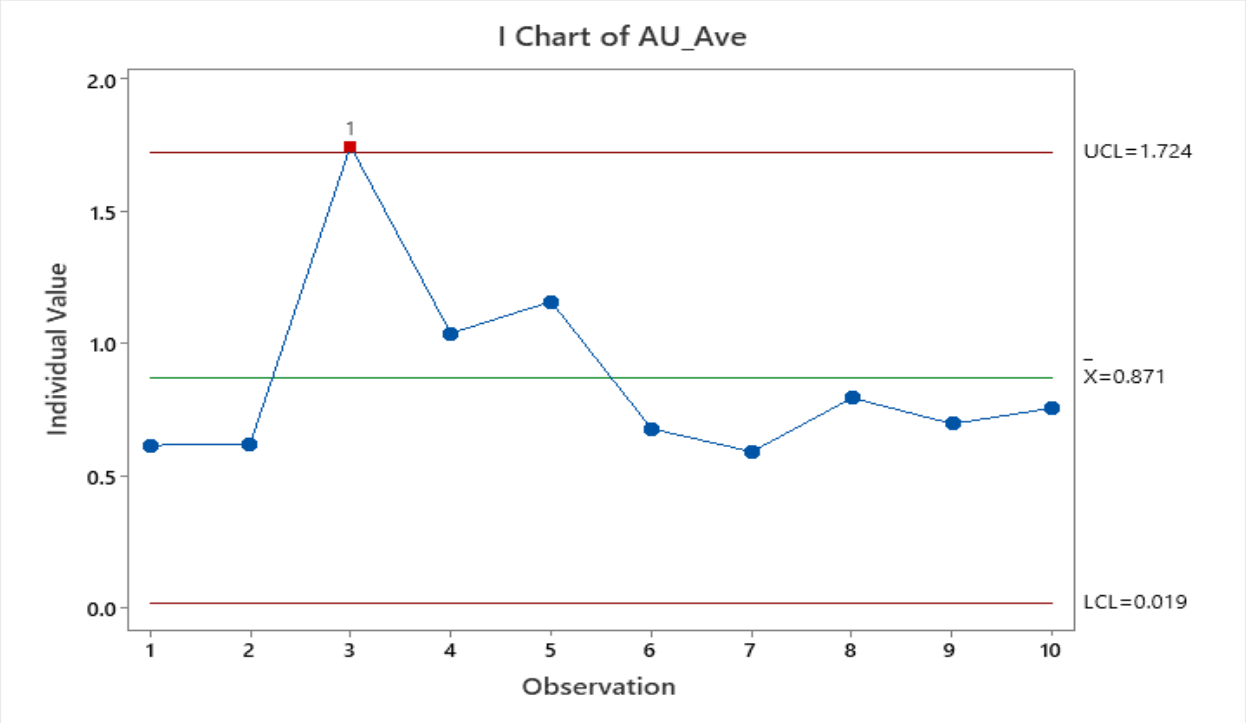

Figure 179: GC concentrate 5 gold outlier chart

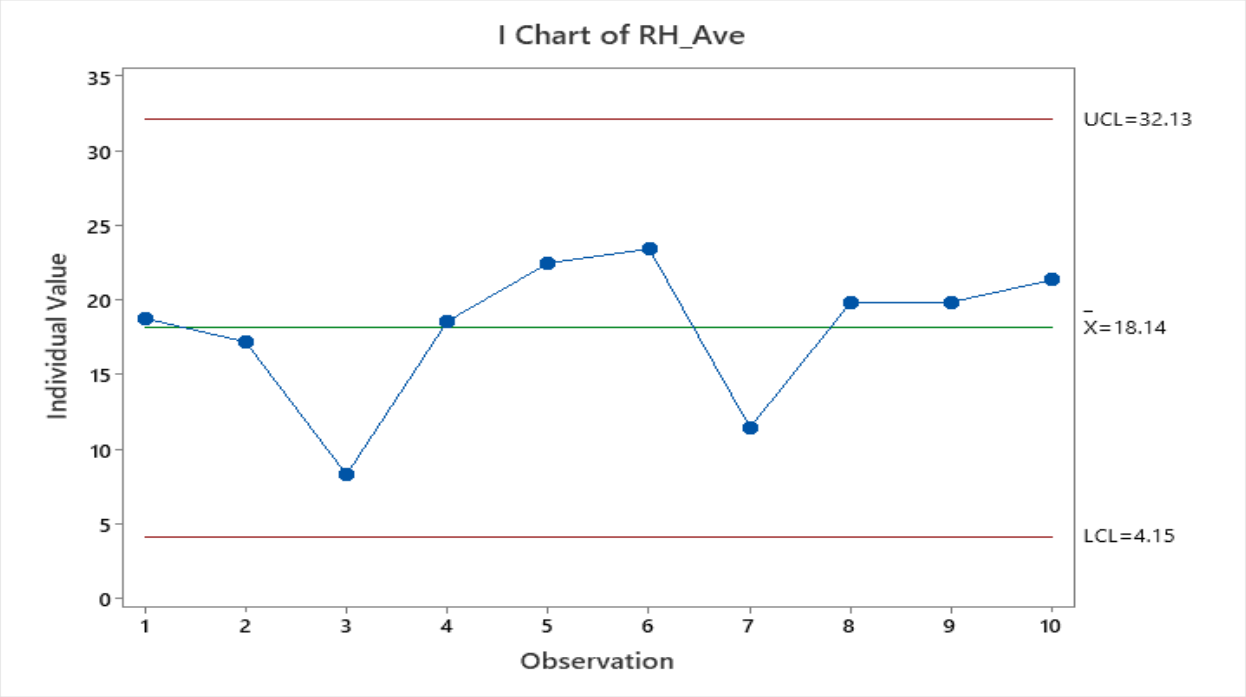

Figure 180: GC concentrate 5 rhodium outlier chart

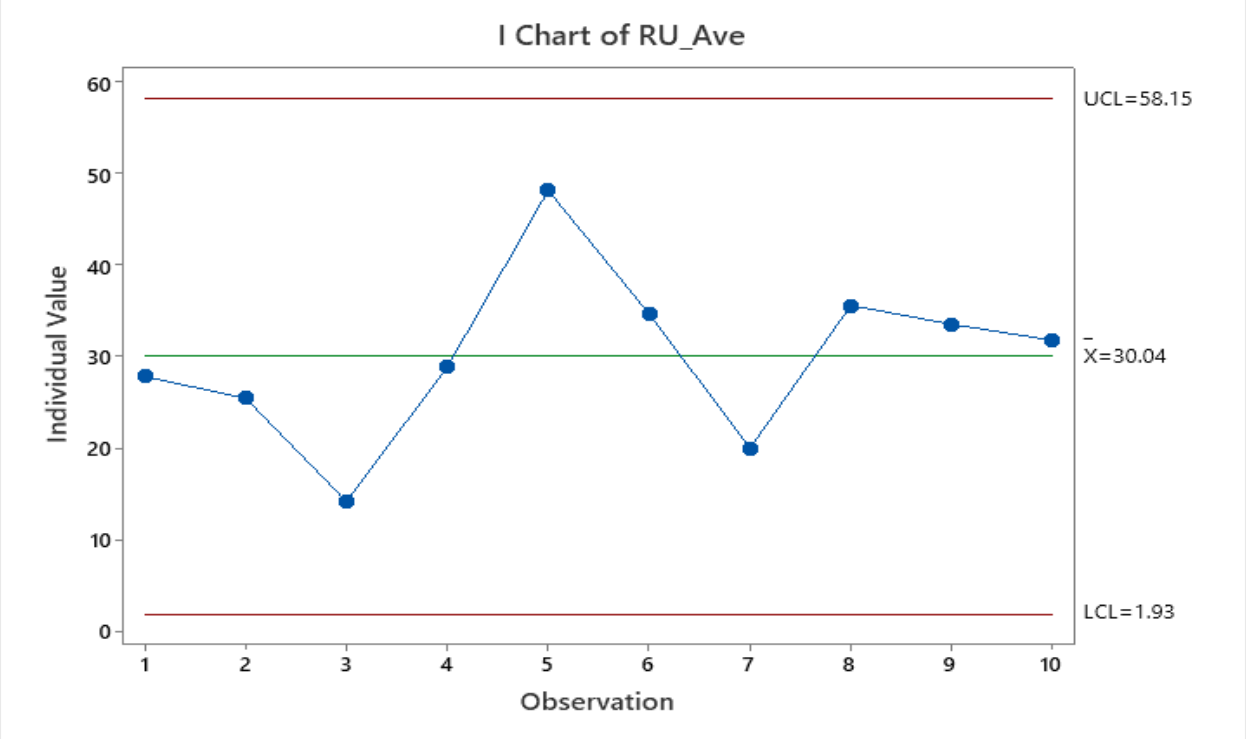

Figure 181: GC concentrate 5 ruthenium outlier chart

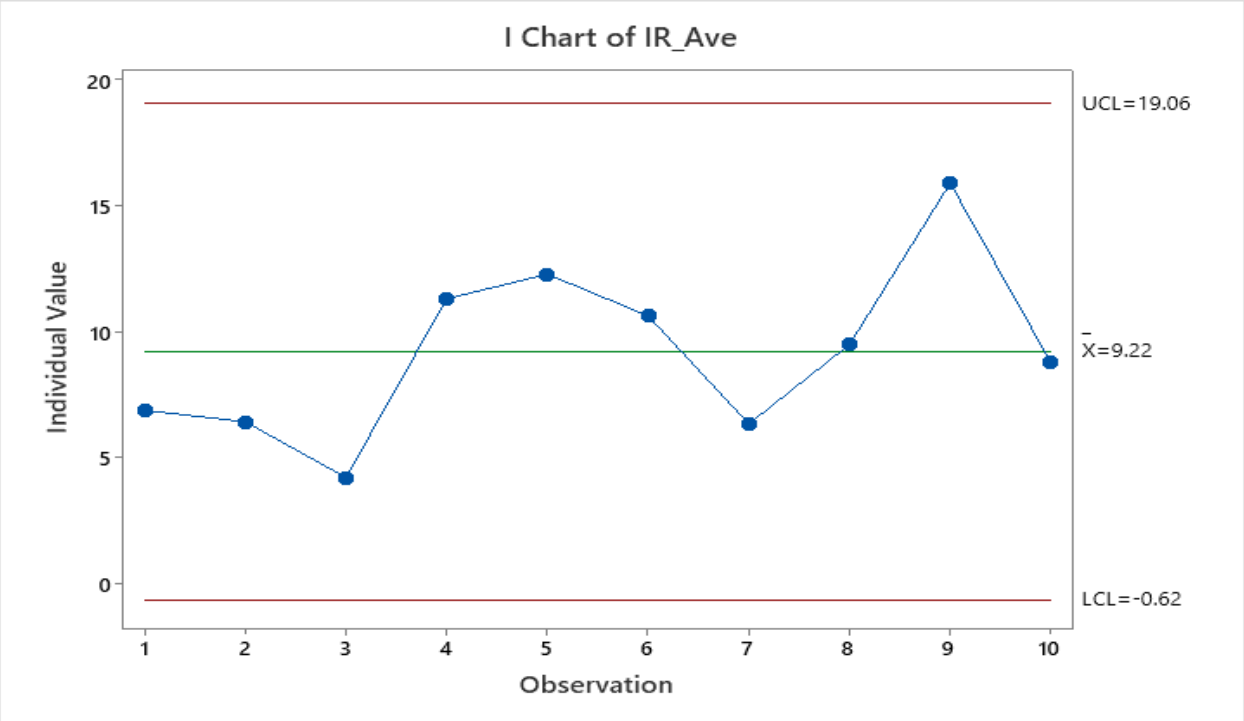

Figure 182: GC concentrate 5 iridium outlier chart

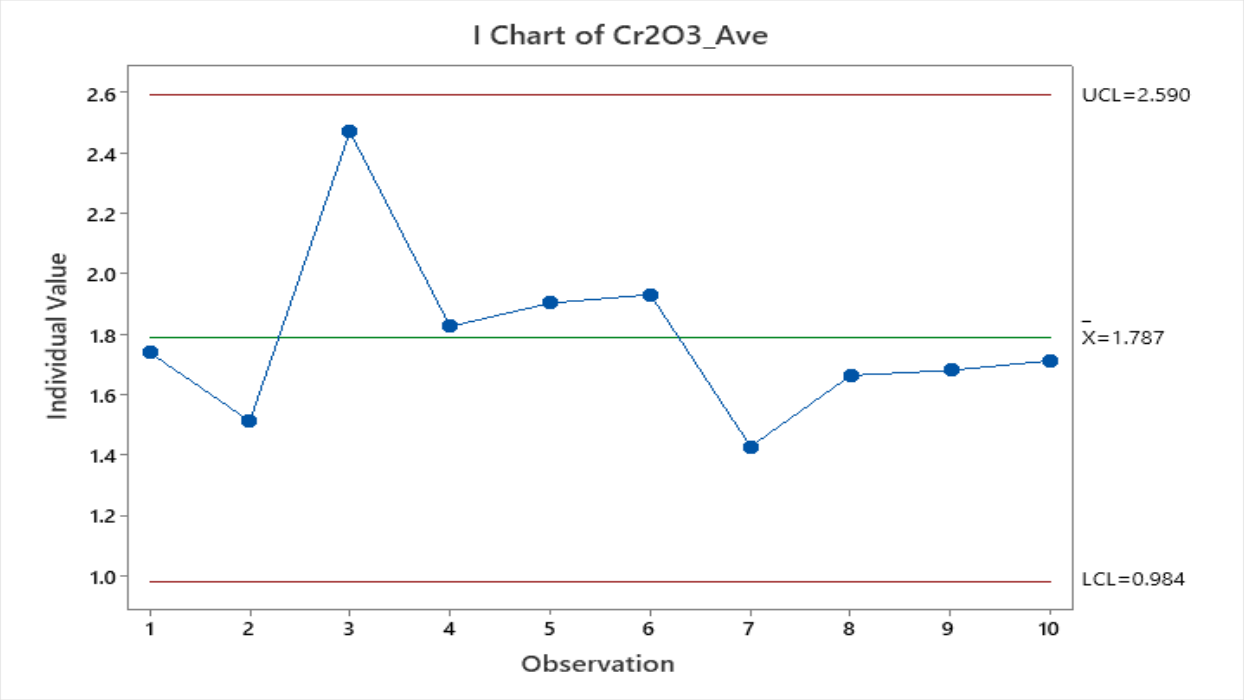

Figure 183: GC concentrate 5 chrome outlier chart

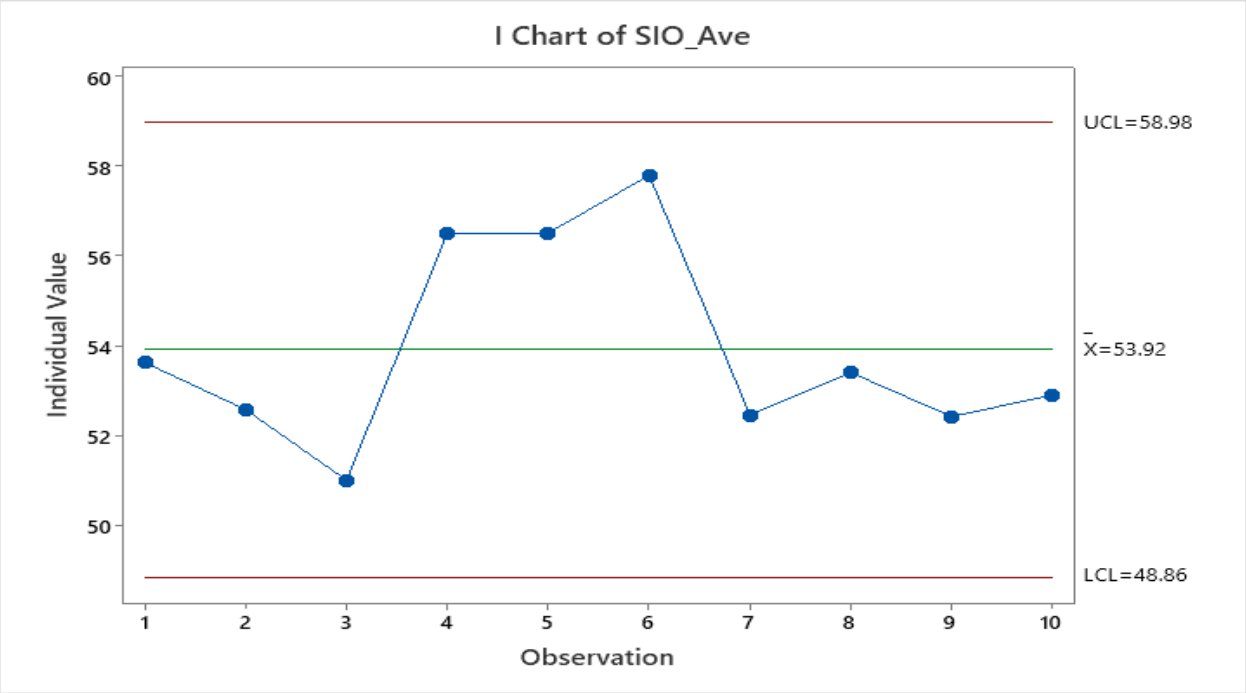

Figure 184: GC concentrate 5 silicon dioxide outlier chart

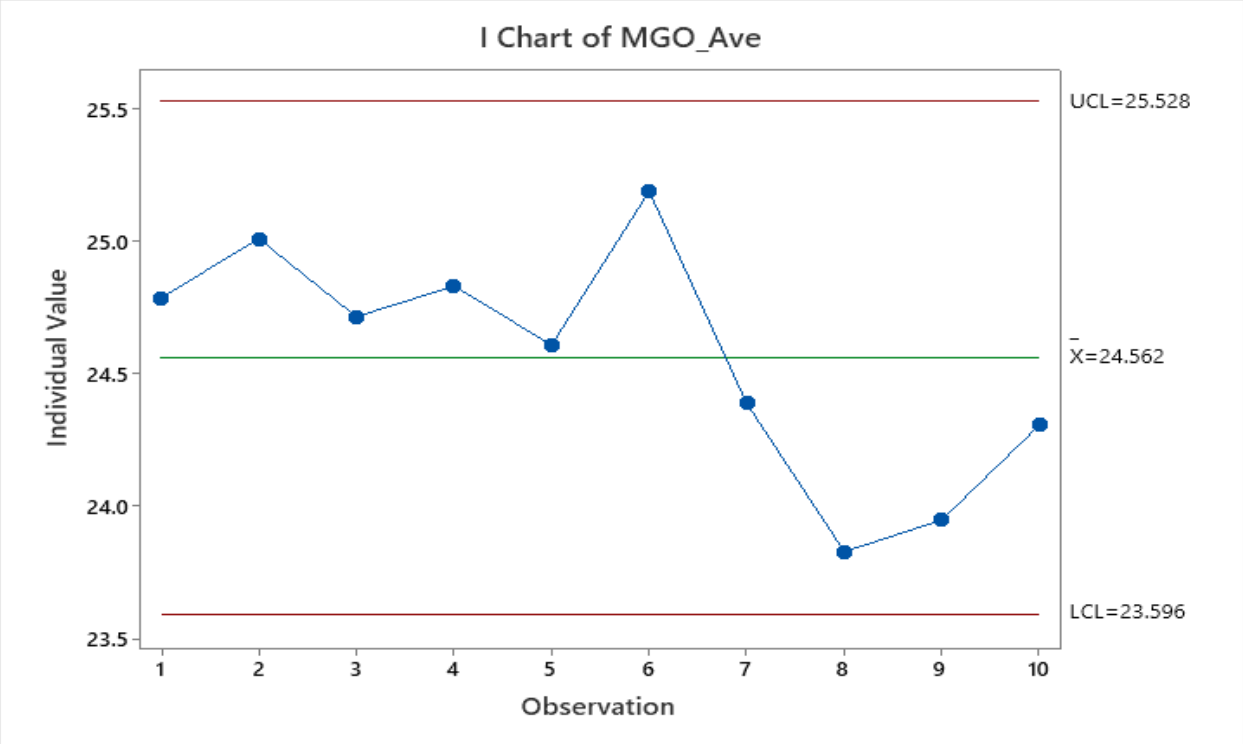

Figure 185: GC concentrate 5 magnesium oxide outlier chart

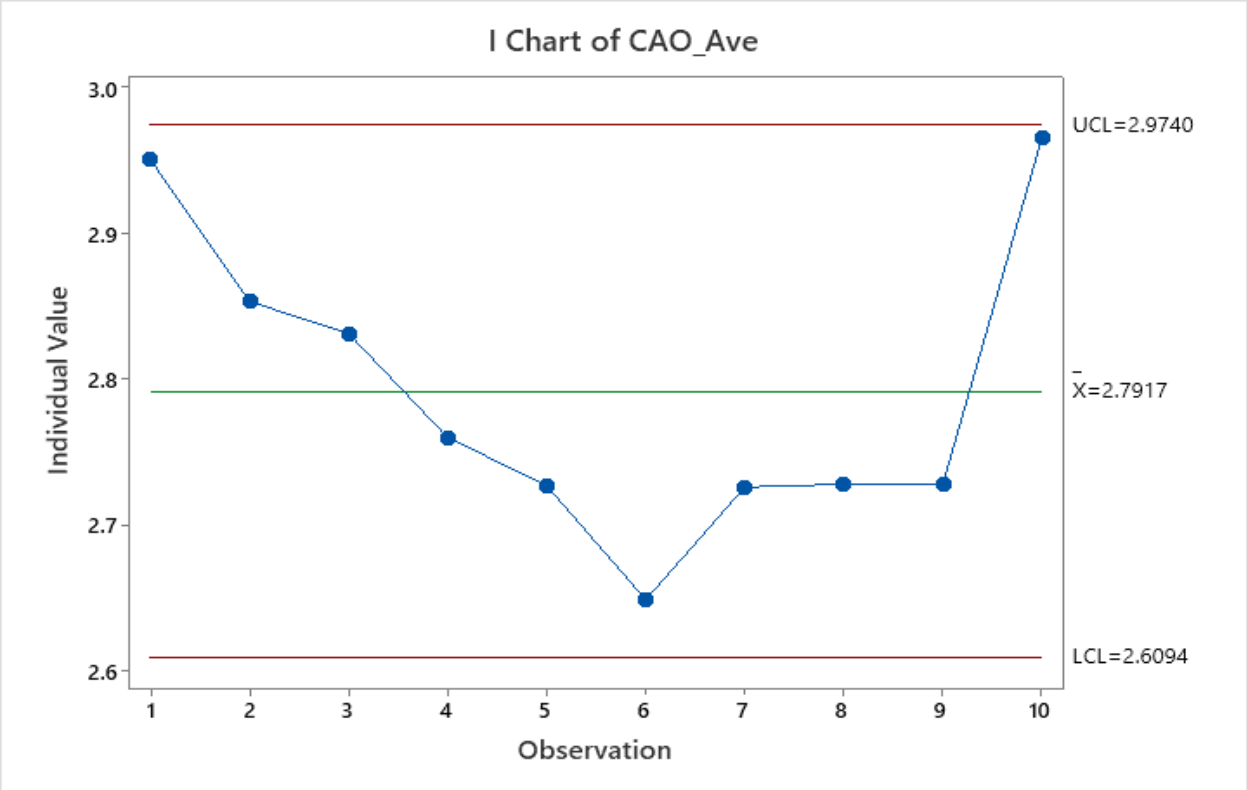

Figure 186: GC concentrate 5 calcium oxide outlier chart

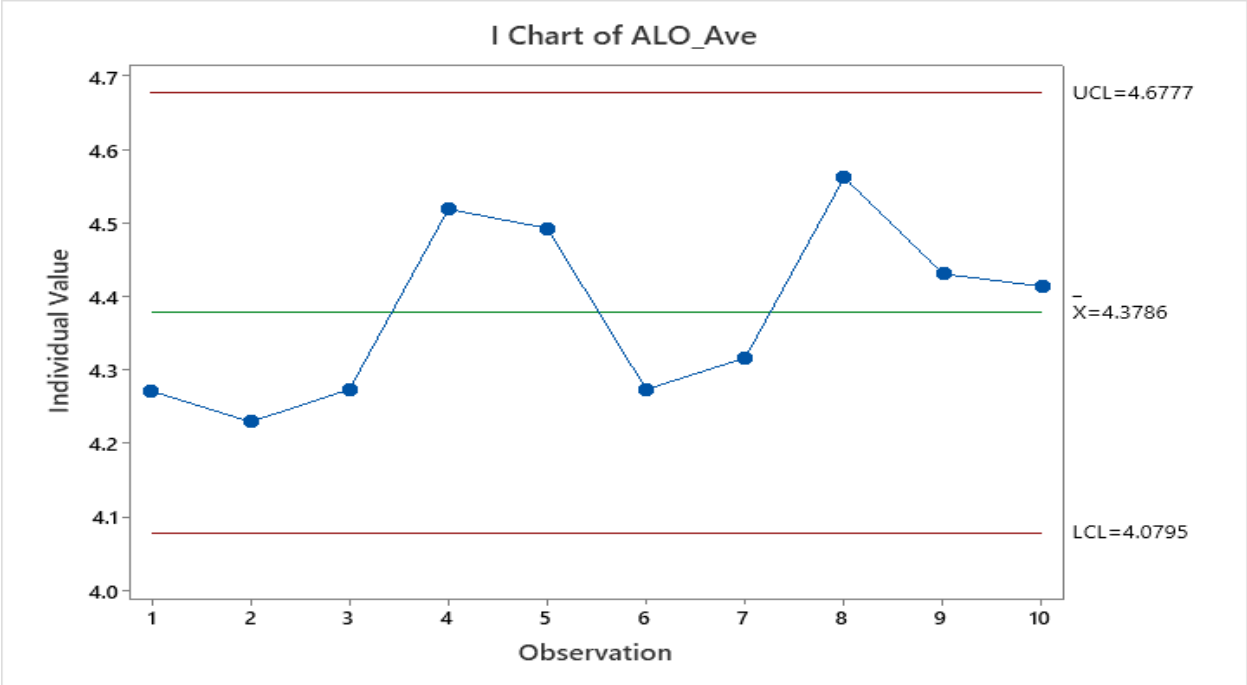

Figure 187: GC concentrate 5 calcium oxide outlier chart

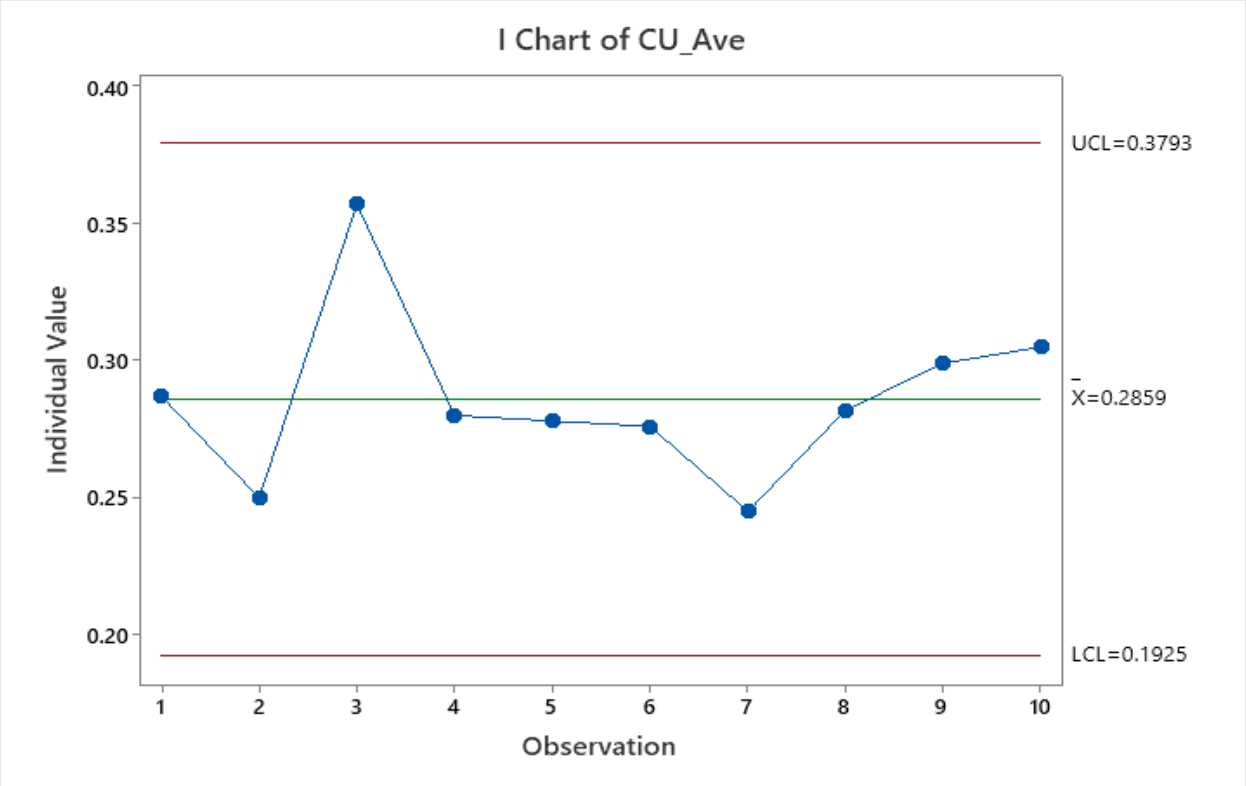

Figure 188: GC concentrate 5 copper outlier chart

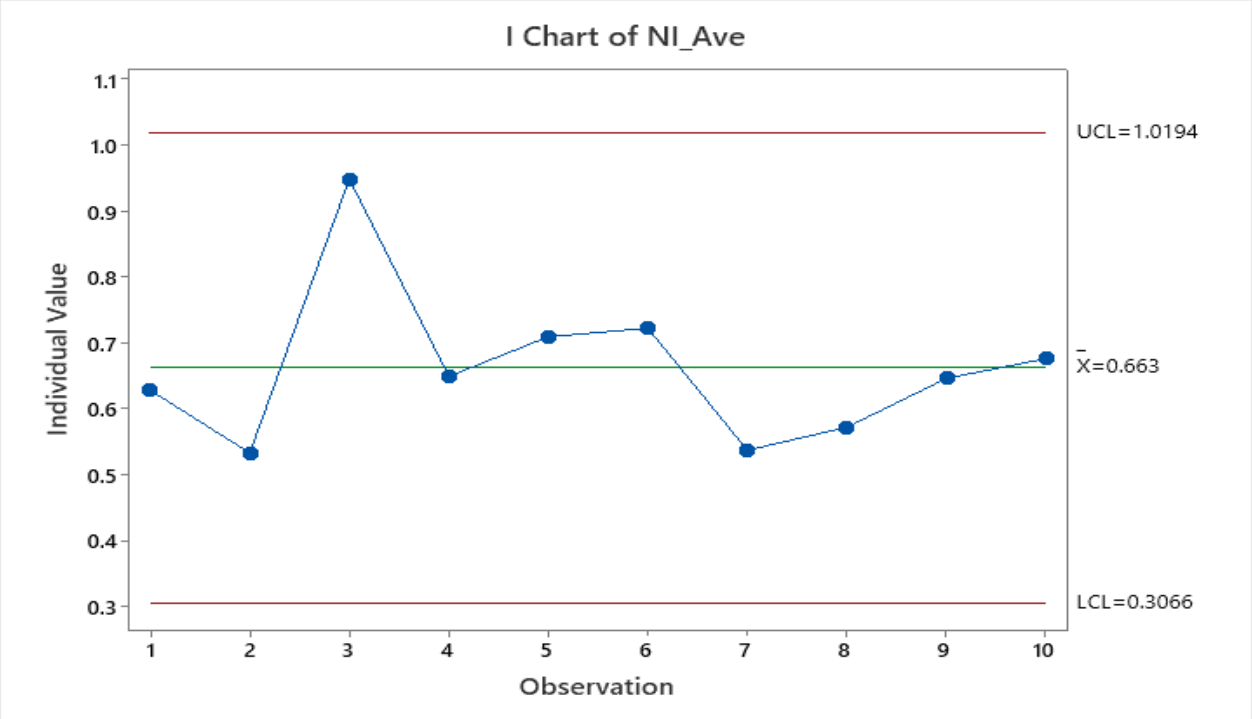

Figure 189: GC concentrate 5 nickel outlier chart

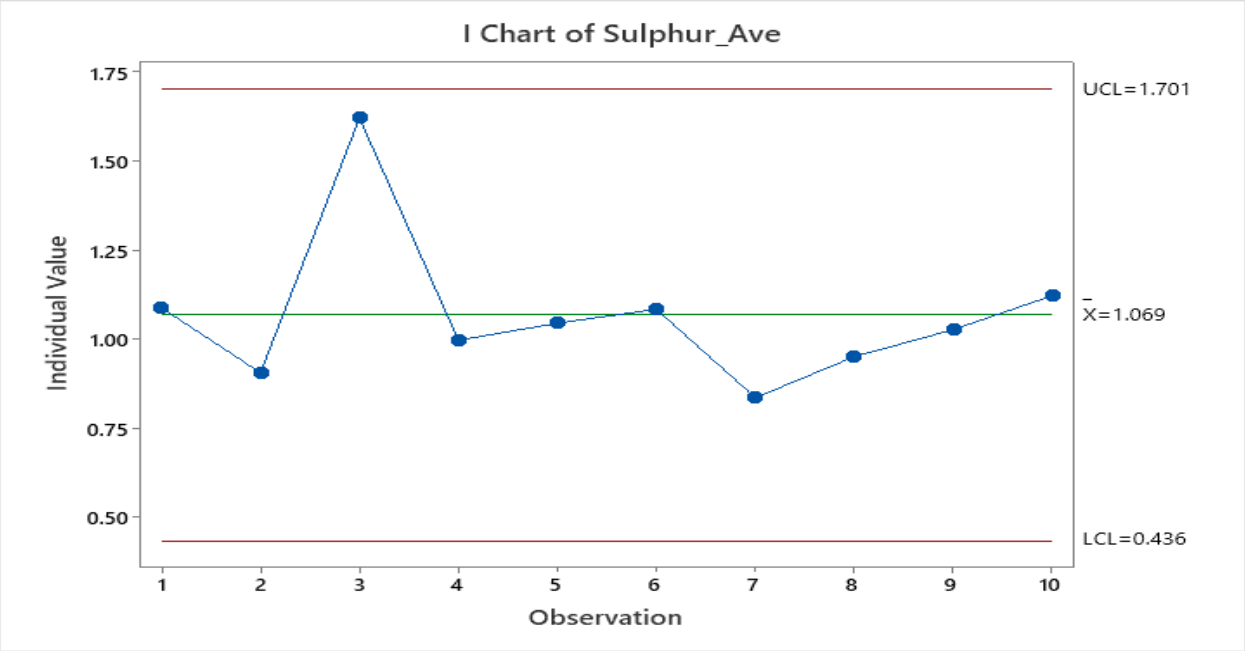

Figure 190: GC concentrate 5 sulphur outlier chart

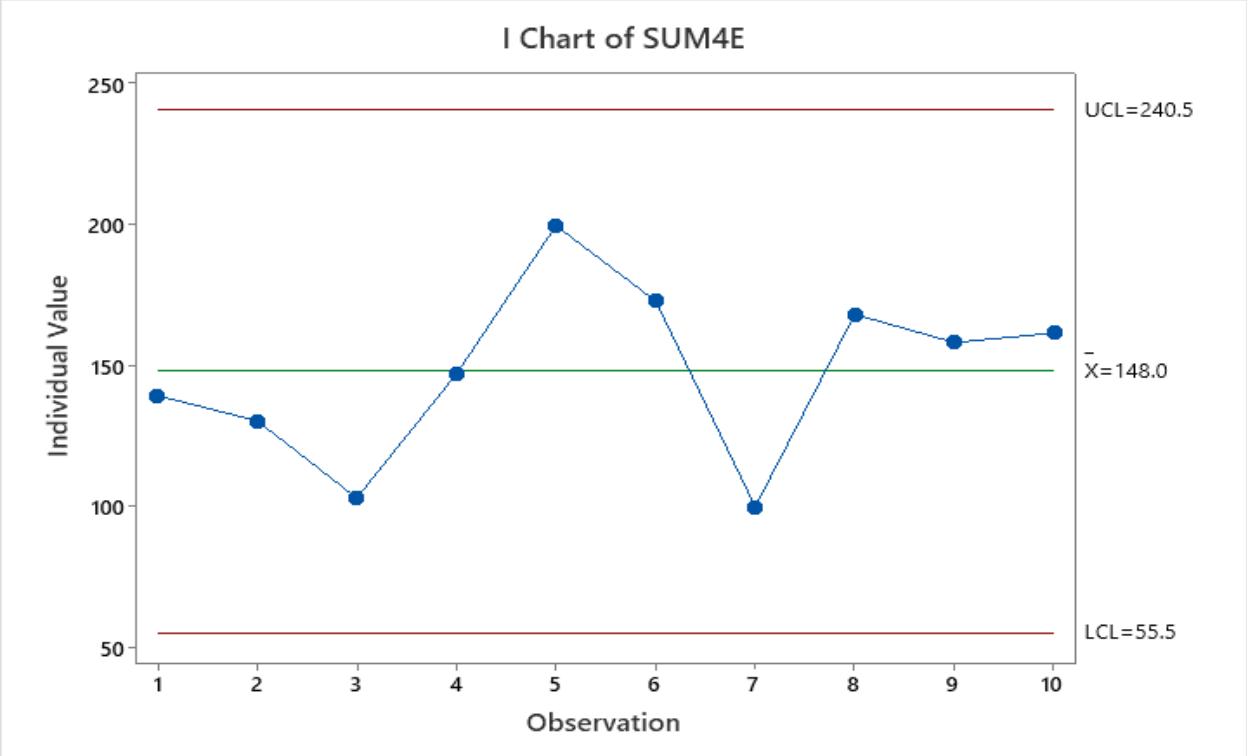

Figure 191: GC concentrate 5 4E outlier chart

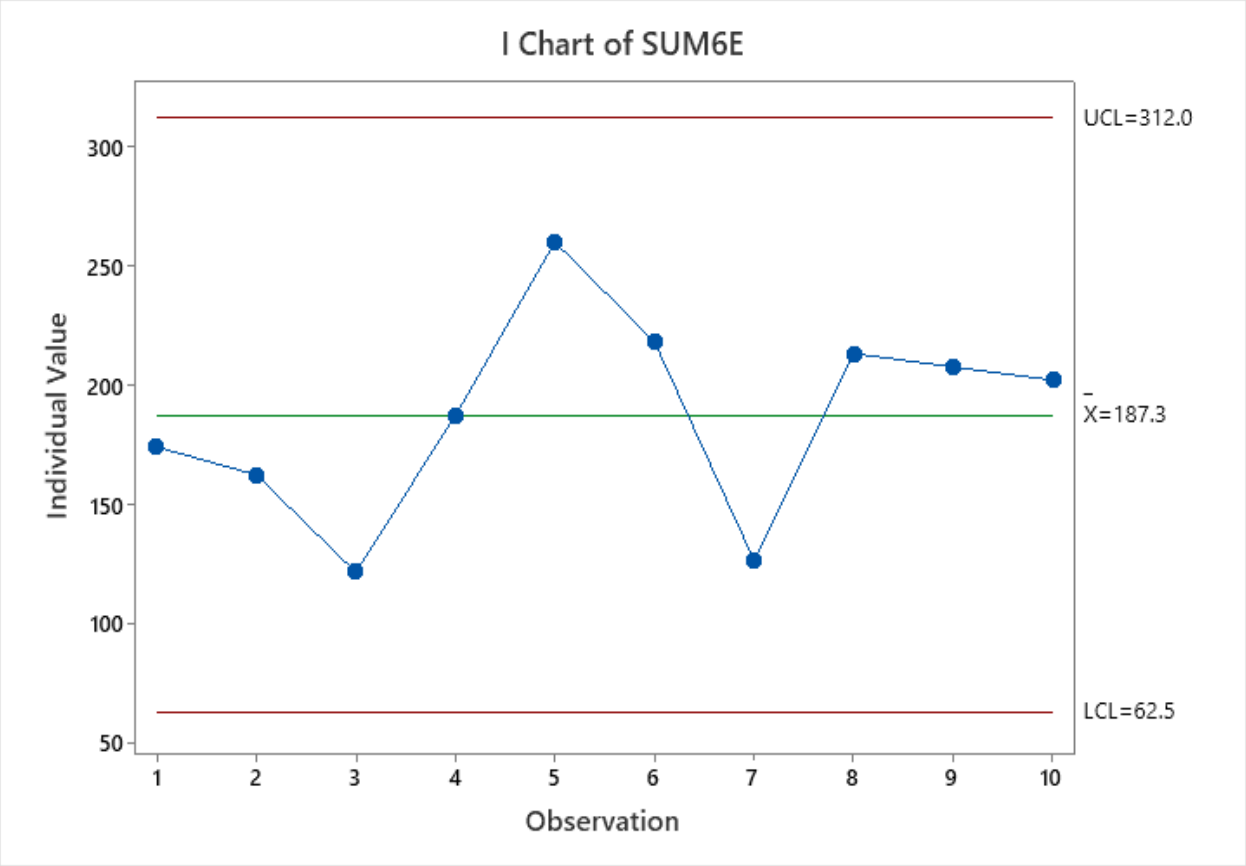

Figure 192: GC concentrate 5 6E outlier chart

Phase 5: Assay and Mass yield/Recovery/Grade Data

Run 1

Phase 5: Multi-stage	Flow rate (L/min)	Mass (g)	Mass Recovery (%)	Cum Mass recovery %	Mass recovery (g)	4E PGM (g/t)	4E PGM Recovery (%)	4E PGM Cum Recovery (%)	4E PGM (g)	4E PGM Upgrade
Gravity Concentrate Feed		5000.00				131.02				
Gravity Concentrate 1		210.00	4.2%	4.2%	210.00	505.92	**16%**	16%	0.11	**3.86**
Gravity Concentrate 2		218.00	4.4%	8.6%	218.00	409.29	**14%**	30%	0.09	**3.12**
Gravity Concentrate 3	**3**	197.00	3.9%	12.5%	197.00	226.74	**7%**	37%	0.04	**1.73**
Gravity Concentrate 4		206.00	4.1%	16.6%	206.00	198.03	**6%**	43%	0.04	**1.51**
Gravity Concentrate 5		223.00	4.5%	21.1%	223.00	139.32	**5%**	48%	0.03	**1.06**
Total Gravity Conc.		*1054.00*	*21.1%*		*1054.00*	*296.01*	*48%*		*0.31*	**2.26**
Gravity Concentrate Tail		3946.00	78.9%		3946.00	86.95			0.34	
Totals		*5000.00*	*100%*		*5000.00*	***131.02***	*47.63%*		*0.66*	*2.26*

PT_Ave	PD_Ave	AU_Ave	RH_Ave	RU_Ave	IR_Ave	SUM4E	SUM6E	CU_Ave	NI_Ave	FE_Ave	FEO_Ave	CO_Ave	Sulphur_A	Cr2O3_Av	SIO_Ave	MGO_Ave	CAO_Ave	ALO_Ave
g/T	g/T	g/T	g/T	g/T	g/T	g/T	g/T	%	%	%	%	%	%	%	%	%	%	%
80.353	34.989	0.708	14.971	25.757	6.192	131.021	162.971	0.222	0.432	7.200	9.262	0.008	0.777	1.966	53.923	24.066	3.235	4.977
350.992	121.04	4.019	29.866	113.084	17.179	505.917	636.180	0.295	0.696	7.877	10.133	0.036	1.157	1.968	52.113	25.022	2.785	4.122
265.944	105.873	2.157	35.312	108.411	17.4	409.286	535.097	0.366	0.929	8.196	10.544	0.048	1.531	2.336	50.748	24.342	2.839	4.46
141.919	60.562	1.186	23.077	56.434	10.461	226.744	293.639	0.277	0.641	7.633	9.82	0.033	1.089	1.765	52.31	24.766	2.916	4.319
117.861	54.667	0.889	24.611	47.5	10.157	198.028	255.685	0.334	0.794	7.996	10.287	0.04	1.335	2.069	51.969	24.669	2.841	4.325
81.082	38.843	0.617	18.78	27.852	6.882	139.322	174.056	0.287	0.629	7.822	10.064	0.032	1.089	1.74	53.624	24.787	2.95	4.272
191.65	76.24	1.77	26.35	70.68	12.42	296.01	379.11	0.31	0.74	7.91	10.18	0.04	1.24	1.98	52.16	24.71	2.87	4.30

Run 2

Phase 5: Multi-stage	Flow rate (L/min)	Mass (g)	Mass Recovery (%)	Cum Mass recovery %	Mass recovery (g)	4E PGM (g/t)	4E PGM Recovery (%)	4E PGM Cum Recovery (%)	4E PGM (g)	4E PGM Upgrade
Gravity Concentrate Feed		5000.00				131.02				
Gravity Concentrate 1		223.00	4.5%	4.5%	223.00	534.52	**18%**	18%	0.12	**4.08**
Gravity Concentrate 2		205.00	4.1%	8.6%	205.00	331.41	**10%**	29%	0.07	**2.53**
Gravity Concentrate 3	**3**	235.00	4.7%	13.3%	235.00	201.87	**7%**	36%	0.05	**1.54**
Gravity Concentrate 4		219.00	4.4%	17.6%	219.00	200.13	**7%**	42%	0.04	**1.53**
Gravity Concentrate 5		210.00	4.2%	21.8%	210.00	130.46	**4%**	47%	0.03	**1.00**
Total Gravity Conc.		*1092.00*	*21.8%*		*1092.00*	*280.04*	*47%*		*0.31*	**2.14**
Gravity Concentrate Tail		3908.00	78.2%		3908.00	89.38			0.35	
Totals		*5000.00*	*100%*		*5000.00*	***131.02***	*47%*		*0.66*	*2.14*

PT_Ave	PD_Ave	AU_Ave	RH_Ave	RU_Ave	IR_Ave	SUM4E	SUM6E	CU_Ave	NI_Ave	FE_Ave	FEO_Ave	CO_Ave	Sulphur_A	Cr2O3_Av	SIO_Ave	MGO_Ave	CAO_Ave	ALO_Ave
g/T	g/T	g/T	g/T	g/T	g/T	g/T	g/T	%	%	%	%	%	%	%	%	%	%	%
80.353	34.989	0.708	14.971	25.757	6.192	131.021	162.971	0.222	0.432	7.200	9.262	0.008	0.777	1.966	53.923	24.066	3.235	4.977
364.734	132.905	3.638	33.241	123.438	18.338	534.518	676.294	0.334	0.816	8.105	10.426	0.042	1.345	2.315	51.018	24.384	2.759	4.207
213.066	86.576	1.894	29.875	84.21	14.421	331.411	430.042	0.327	0.773	7.965	10.246	0.039	1.258	2.067	51.579	24.434	2.86	4.279
123.383	54.842	1.047	22.595	45.318	9.145	201.867	256.330	0.284	0.646	7.749	9.969	0.033	1.095	1.713	52.108	24.762	2.878	4.2
117.452	56.247	0.923	25.511	42.826	9.784	200.133	252.743	0.331	0.742	7.936	10.21	0.037	1.261	1.908	51.697	24.66	2.815	4.395
75.587	37.039	0.623	17.207	25.489	6.428	130.456	162.373	0.25	0.534	7.484	9.628	0.028	0.907	1.513	52.58	25.01	2.853	4.23
179.12	73.60	1.63	25.68	64.26	11.62	280.04	355.91	0.31	0.70	7.85	10.10	0.04	1.17	1.90	51.79	24.65	2.83	4.26

Run 3

Phase 5: Multi-stage	Flow rate (L/min)	Mass (g)	Mass Recovery (%)	Cum Mass recovery %	Mass recovery (g)	4E PGM (g/t)	4E PGM Recovery (%)	4E PGM Cum Recovery (%)	4E PGM (g)	4E PGM Upgrade
Gravity Concentrate Feed		5000.00				131.02				
Gravity Concentrate 1		227.00	4.5%	4.5%	227.00	520.22	**18%**	18%	0.12	**3.97**
Gravity Concentrate 2		206.00	4.1%	8.7%	206.00	370.35	**12%**	30%	0.08	**2.83**
Gravity Concentrate 3	**3**	211.00	4.2%	12.9%	211.00	279.15	**9%**	39%	0.06	**2.13**
Gravity Concentrate 4		191.00	3.8%	16.7%	191.00	196.26	**6%**	44%	0.04	**1.50**
Gravity Concentrate 5		252.00	5.0%	21.7%	252.00	103.16	**4%**	48%	0.03	**0.79**
Total Gravity Conc.		*1087.00*	*21.7%*		*1087.00*	*291.41*	*48%*		*0.32*	**2.22**
Gravity Concentrate Tail		3913.00	78.3%		3913.00	86.47			0.34	
Totals		*5000.00*	*100%*		*5000.00*	***131.02***	*48.35%*		*0.66*	*2.22*

PT_Ave	PD_Ave	AU_Ave	RH_Ave	RU_Ave	IR_Ave	SUM4E	SUM6E	CU_Ave	NI_Ave	FE_Ave	FEO_Ave	CO_Ave	Sulphur_A	Cr2O3_Av	SIO_Ave	MGO_Ave	CAO_Ave	ALO_Ave
g/T	g/T	g/T	g/T	g/T	g/T	g/T	g/T	%	%	%	%	%	%	%	%	%	%	%
80.353	34.989	0.708	14.971	25.757	6.192	131.021	162.971	0.222	0.432	7.200	9.262	0.009	0.777	1.966	53.923	24.066	3.235	4.977
357.863	126.9725	3.8285	31.5535	118.261	17.7585	520.218	656.237	0.3145	0.756	7.991	10.2795	0.039	1.251	2.1415	51.5655	24.703	2.772	4.1645
239.505	96.2245	2.0255	32.5935	96.3105	15.9105	370.349	482.570	0.3465	0.851	8.0805	10.395	0.0435	1.3945	2.2015	51.1635	24.388	2.8495	4.3695
172.298	75.879	1.35	29.622	69.563	13.375	279.149	362.087	0.327	0.827	8.033	10.335	0.041	1.413	2.039	51.593	24.898	2.849	4.126
117.587	54.284	0.97	23.417	43.562	9.654	196.258	249.474	0.273	0.645	6.731	8.659	0.028	1.006	1.499	48.536	25.089	3.148	4.196
63.872	29.205	1.747	8.333	14.211	4.219	103.157	121.587	0.357	0.949	8.408	10.817	0.047	1.621	2.469	51.01	24.716	2.831	4.274
189.04	75.79	2.02	24.56	67.40	11.99	291.41	370.80	0.33	0.81	7.89	10.15	0.04	1.35	2.10	50.83	24.75	2.88	4.23

Run 4

Phase 5: Multi-stage	Flow rate (L/min)	Mass (g)	Mass Recovery (%)	Cum Mass recovery %	Mass recovery (g)	4E PGM (g/t)	4E PGM Recovery (%)	4E PGM Cum Recovery (%)	4E PGM (g)	4E PGM Upgrade
Gravity Concentrate Feed		5000.00				131.02				
Gravity Concentrate 1		220.00	4.4%	4.4%	220.00	529.17	**18%**	18%	0.12	**4.04**
Gravity Concentrate 2		209.67	4.2%	8.6%	209.67	376.33	**12%**	30%	0.08	**2.87**
Gravity Concentrate 3	**3**	214.33	4.3%	12.9%	214.33	230.59	**8%**	37%	0.05	**1.76**
Gravity Concentrate 4		205.33	4.1%	17.0%	205.33	182.73	**6%**	43%	0.04	**1.39**
Gravity Concentrate 5		228.33	4.6%	21.6%	228.33	146.99	**5%**	48%	0.03	**1.12**
Total Gravity Conc.		*1077.67*	*21.6%*		*1077.67*	*293.07*	*48%*		*0.32*	**2.24**
Gravity Concentrate Tail		3922.33	78.4%		3922.33	86.50			0.34	
Totals		*5000.00*	*100%*		*5000.00*	***131.02***	*48%*		*0.66*	*2.24*

PT_Ave	PD_Ave	AU_Ave	RH_Ave	RU_Ave	IR_Ave	SUM4E	SUM6E	CU_Ave	NI_Ave	FE_Ave	FEO_Ave	CO_Ave	Sulphur_A	Cr2O3_Av	SIO_Ave	MGO_Ave	CAO_Ave	ALO_Ave
g/T	g/T	g/T	g/T	g/T	g/T	g/T	g/T	%	%	%	%	%	%	%	%	%	%	%
80.353	34.989	0.708	14.971	25.757	6.192	131.021	162.971	0.222	0.432	7.200	9.262	0.008	0.777	1.966	53.923	24.066	3.235	4.977
358.042	133.604	3.324	34.2	132.948	22.44	529.170	684.558	0.315	0.911	8.813	11.338	0.041	1.276	2.454	56.143	24.889	2.569	4.356
239.827	101.2	1.928	33.373	100.553	19.659	376.328	496.540	0.332	0.959	8.892	11.439	0.043	1.361	2.461	54.962	24.564	2.686	4.368
140.513	64.405	1.344	24.323	54.233	14.459	230.585	299.277	0.305	0.783	8.615	11.084	0.035	1.142	2.135	56.406	25.014	2.679	4.323
107.933	51.536	1.14	22.121	38.765	11.576	182.730	233.071	0.306	0.756	8.622	11.093	0.034	1.115	2.073	53.651	24.943	2.664	4.28
86.237	41.126	1.04	18.59	28.92	11.299	146.993	187.212	0.28	0.65	8.279	10.651	0.029	0.998	1.826	56.493	24.831	2.76	4.519
186.54	78.31	1.76	26.47	71.00	15.88	293.07	379.95	0.31	0.81	8.64	11.11	0.04	1.18	2.19	55.56	24.85	2.67	4.37

Run 5

Phase 5: Multi-stage	Flow rate (L/min)	Mass (g)	Mass	Cum	Mass	4E PGM (g/t)	4E PGM	4E PGM Cum	4E PGM	4E PGM
Gravity Concentrate Feed		5000.00				131.02				
Gravity Concentrate 1		215.38	4.3%	4.3%	215.38	541.17	**18%**	18%	0.12	**4.13**
Gravity Concentrate 2		214.96	4.3%	8.6%	214.96	381.19	**13%**	30%	0.08	**2.91**
Gravity Concentrate 3	**3**	228.17	4.6%	13.2%	228.17	174.56	**6%**	36%	0.04	**1.33**
Gravity Concentrate 4		209.92	4.2%	17.4%	209.92	205.32	**7%**	43%	0.04	**1.57**
Gravity Concentrate 5		226.79	4.5%	21.9%	226.79	199.44	**7%**	50%	0.05	**1.52**
Total Gravity Conc.		*1095.21*	*21.9%*		*1095.21*	*298.26*	*50%*		*0.33*	**2.28**
Gravity Concentrate Tail		3904.79	78.1%		3904.79	84.11			0.33	
Totals		*5000.00*	*100%*		*5000.00*	***131.02***	*50%*		*0.66*	*2.28*

PT_Ave	PD_Ave	AU_Ave	RH_Ave	RU_Ave	IR_Ave	SUM4E	SUM6E	CU_Ave	NI_Ave	FE_Ave	FEO_Ave	CO_Ave	Sulphur_A	Cr2O3_Av	SIO_Ave	MGO_Ave	CAO_Ave	ALO_Ave
g/T	g/T	g/T	g/T	g/T	g/T	g/T	g/T	%	%	%	%	%	%	%	%	%	%	%
80.353	34.989	0.708	14.971	25.757	6.192	131.021	162.971	0.222	0.432	7.200	9.262	0.007	0.777	1.966	53.923	24.066	3.235	4.977
376.112	127.319	4.198	33.54	124.481	22.046	541.169	687.696	0.277	0.722	8.41	10.819	0.033	1.084	1.926	56.528	24.86	2.65	4.338
246.976	97.445	2.139	34.633	99.128	20.991	381.193	501.312	0.26	0.735	8.362	10.758	0.034	1.064	2.033	56.413	24.87	2.567	4.379
106.104	46.798	0.886	20.776	37.152	10.804	174.564	222.520	0.29	0.778	8.77	11.283	0.035	1.14	2.076	57.15	25.025	2.711	4.312
123.857	57.599	1.172	22.69	49.268	11.42	205.318	266.006	0.272	0.719	8.324	10.709	0.032	1.074	1.905	56.61	24.698	2.707	4.412
119.689	56.111	1.16	22.476	48.18	12.278	199.436	259.894	0.278	0.71	8.278	10.649	0.033	1.046	1.903	56.505	24.61	2.727	4.493
193.07	76.57	1.89	26.72	71.10	15.44	298.26	384.79	0.28	0.73	8.43	10.85	0.03	1.08	1.97	56.65	24.81	2.67	4.39

Figure 193: Phase 5 Run 1-5 Fire assay/ICP-MS results and analysis per run

Run 6

Phase 5: Multi-stage	Flow rate (L/min)	Mass (g)	Mass	Cum	Mass	4E PGM (g/t)	4E PGM	4E PGM Cum	4E PGM	4E PGM
Gravity Concentrate Feed		5000.00				131.02				
Gravity Concentrate 1		210.75	4.2%	4.2%	210.75	486.06	16%	16%	0.10	3.71
Gravity Concentrate 2		220.25	4.4%	8.6%	220.25	392.53	13%	29%	0.09	3.00
Gravity Concentrate 3	3	242.00	4.8%	13.5%	242.00	271.45	10%	39%	0.07	2.07
Gravity Concentrate 4		214.50	4.3%	17.8%	214.50	181.64	6%	45%	0.04	1.39
Gravity Concentrate 5		225.25	4.5%	22.3%	225.25	172.80	6%	51%	0.04	1.32
Total Gravity Conc.		*1112.75*	*22.3%*		*1112.75*	*298.78*	*51%*		*0.33*	**2.28**
Gravity Concentrate Tail		3887.25	77.7%		3887.25	83.00			0.32	
Totals		*5000.00*	*100%*		*5000.00*	***131.02***	*51%*		*0.66*	***2.28***

PT_Ave	PD_Ave	AU_Ave	RH_Ave	RU_Ave	IR_Ave	SUM4E	SUM6E	CU_Ave	NI_Ave	FE_Ave	FEO_Ave	CO_Ave	Sulphur_A	Cr2O3_Av	SIO_Ave	MGO_Ave	CAO_Ave	ALO_Ave
g/T	g/T	g/T	g/T	g/T	g/T	g/T	g/T	%	%	%	%	%	%	%	%	%	%	%
80.353	34.989	0.708	14.971	25.757	6.192	131.021	162.971	0.222	0.432	7.200	9.262	0.021	0.777	1.966	53.923	24.066	3.235	4.977
324.658	123.805	4.673	32.921	148.408	25.253	486.057	659.718	0.184	0.377	7.349	9.454	0.017	0.558	1.493	58.107	24.859	2.635	4.621
252.537	106.532	2.363	31.093	108.977	22.068	392.525	523.570	0.289	0.834	8.42	10.832	0.039	1.178	2.258	55.359	24.69	2.563	4.342
161.888	78.202	1.345	30.014	75.98	17.477	271.449	364.906	0.322	0.898	8.823	11.35	0.041	1.316	2.413	56.481	24.706	2.633	4.345
107.113	49.781	0.875	23.874	38.841	10.758	181.643	231.242	0.328	0.891	8.704	11.198	0.041	1.285	2.329	56.15	24.798	2.659	4.413
100.081	48.614	0.68	23.428	34.697	10.623	172.803	218.123	0.276	0.723	8.584	11.043	0.033	1.085	1.931	57.784	25.189	2.649	4.274
187.59	80.98	1.95	28.26	80.71	17.18	298.78	396.67	0.28	0.75	8.39	10.80	0.03	1.09	2.09	56.77	24.85	2.63	4.40
42.886	22.126	0.368	10.912	11.966	3.994	76.292	92.252	0.183	0.379	7.291	9.380	0.017	0.541	1.466	58.001	24.687	2.655	4.696

Run 7

Phase 5: Multi-stage	Flow rate (L/min)	Mass (g)	Mass	Cum	Mass	4E PGM (g/t)	4E PGM	4E PGM Cum	4E PGM	4E PGM
Gravity Concentrate Feed		5000.00				131.02				
Gravity Concentrate 1		212.00	4.2%	4.2%	212.00	541.18	18%	18%	0.11	4.13
Gravity Concentrate 2		230.00	4.6%	8.8%	230.00	274.51	10%	27%	0.06	2.10
Gravity Concentrate 3	3	280.00	5.6%	14.4%	280.00	258.34	11%	38%	0.07	1.97
Gravity Concentrate 4		210.00	4.2%	18.6%	210.00	225.66	7%	45%	0.05	1.72
Gravity Concentrate 5		197.00	3.9%	22.6%	197.00	100.07	3%	48%	0.02	0.76
Total Gravity Conc.		*1129.00*	*22.6%*		*1129.00*	*281.05*	*48%*		*0.32*	**2.15**
Gravity Concentrate Tail		3871.00	77.4%		3871.00	87.26			0.34	
Totals		*5000.00*	*100%*		*5000.00*	***131.02***	*48%*		*0.66*	***2.15***

PT_Ave	PD_Ave	AU_Ave	RH_Ave	RU_Ave	IR_Ave	SUM4E	SUM6E	CU_Ave	NI_Ave	FE_Ave	FEO_Ave	CO_Ave	Sulphur_A	Cr2O3_Av	SIO_Ave	MGO_Ave	CAO_Ave	ALO_Ave
g/T	g/T	g/T	g/T	g/T	g/T	g/T	g/T	%	%	%	%	%	%	%	%	%	%	%
80.353	34.989	0.708	14.971	25.757	6.192	131.021	162.971	0.222	0.432	7.200	9.262	0.008	0.777	1.966	53.923	24.066	3.235	4.977
345.089	150.757	4.399	40.931	153.432	26.689	541.176	721.297	0.37	0.955	8.371	10.769	0.047	1.499	2.481	51.015	23.389	2.597	4.581
178.455	69.653	1.725	24.677	63.057	13.264	274.510	350.831	0.321	0.696	8.009	10.304	0.035	1.141	1.943	53.216	23.922	2.712	4.572
164.679	67.099	1.423	25.136	64.201	14.107	258.337	336.645	0.311	0.697	7.91	10.177	0.035	1.103	1.846	52.123	23.75	2.653	4.382
138.41	63.577	3.077	20.595	34.42	9.887	225.659	269.966	0.291	0.651	7.867	10.121	0.034	1.014	1.714	52.197	24.247	2.668	4.291
61.642	26.346	0.593	11.484	20.048	6.344	100.065	126.457	0.245	0.538	7.573	9.742	0.028	0.837	1.429	52.458	24.389	2.726	4.317
178.50	75.37	2.23	24.51	67.17	14.06	279.46	360.69	0.31	0.71	7.94	10.22	0.04	1.12	1.89	52.19	23.94	2.67	4.43

Run 8

Phase 5: Multi-stage	Flow rate (L/min)	Mass (g)	Mass	Cum	Mass	4E PGM (g/t)	4E PGM	4E PGM Cum	4E PGM	4E PGM
Gravity Concentrate Feed		5000.00				131.02				
Gravity Concentrate 1		200.00	4.0%	4.0%	200.00	483.01	15%	15%	0.10	3.69
Gravity Concentrate 2		205.00	4.1%	8.1%	205.00	346.02	11%	26%	0.07	2.64
Gravity Concentrate 3		199.00	4.0%	12.1%	199.00	285.53	9%	34%	0.06	2.18
Gravity Concentrate 4	3	205.00	4.1%	16.2%	205.00	221.98	7%	41%	0.05	1.69
Gravity Concentrate 5		249.00	5.0%	21.2%	249.00	168.07	6%	48%	0.04	1.28
Total Gravity Conc.		*1058.00*	*21.2%*		*1058.00*	*294.62*	*48%*		*0.31*	**2.25**
Gravity Concentrate Tail		3942.00	78.8%		3942.00	87.11			0.34	
Totals		*5000.00*	*100%*		*5000.00*	***131.02***	*47.58%*		*0.66*	***2.25***

PT_Ave	PD_Ave	AU_Ave	RH_Ave	RU_Ave	IR_Ave	SUM4E	SUM6E	CU_Ave	NI_Ave	FE_Ave	FEO_Ave	CO_Ave	Sulphur_A	Cr2O3_Av	SIO_Ave	MGO_Ave	CAO_Ave	ALO_Ave
g/T	g/T	g/T	g/T	g/T	g/T	g/T	g/T	%	%	%	%	%	%	%	%	%	%	%
80.353	34.989	0.708	14.971	25.757	6.192	131.021	162.971	0.222	0.432	7.200	9.262	0.008	0.777	1.966	53.923	24.066	3.235	4.977
328.319	116.53	3.129	35.035	102.094	20.503	483.013	605.610	0.403	0.974	8.789	11.307	0.047	1.521	2.618	52.434	24.162	2.554	4.462
225.496	88.0925	2.044	30.385	86.017	17.666	346.018	449.701	0.352	0.801	8.162	10.5	0.04	1.312	2.084	52.593	23.951	2.686	4.704
187.174	71.678	1.736	24.944	67.883	14.447	285.532	367.862	0.323	0.735	8.194	10.541	0.036	1.174	1.926	53.618	24.13	2.736	4.588
139.436	57.439	0.957	24.146	47.252	12.345	221.978	281.575	0.302	0.653	7.892	10.153	0.033	1.057	1.803	52.694	23.815	2.605	4.348
97.955	49.45	0.796	19.868	35.626	9.491	168.069	213.186	0.282	0.573	7.673	9.871	0.03	0.952	1.664	53.4	23.83	2.728	4.562
191.03	75.35	1.69	26.56	66.27	14.64	294.62	375.54	0.33	0.74	8.12	10.44	0.04	1.19	2.00	52.97	23.97	2.66	4.53

Run 9

Phase 5: Multi-stage	Flow rate (L/min)	Mass (g)	Mass	Cum	Mass	4E PGM (g/t)	4E PGM	4E PGM Cum	4E PGM	4E PGM
Gravity Concentrate Feed		5000.00				131.02				
Gravity Concentrate 1		199.00	4.0%	4.0%	199.00	535.17	16%	16%	0.11	4.08
Gravity Concentrate 2		205.00	4.1%	8.1%	205.00	399.36	12%	29%	0.08	3.05
Gravity Concentrate 3		258.00	5.2%	13.2%	258.00	224.11	9%	38%	0.06	1.71
Gravity Concentrate 4	3	201.00	4.0%	17.3%	201.00	212.03	7%	44%	0.04	1.62
Gravity Concentrate 5		251.00	5.0%	22.3%	251.00	158.13	6%	50%	0.04	1.21
Total Gravity Conc.		*1114.00*	*22.3%*		*1114.00*	*294.88*	*50%*		*0.33*	**2.25**
Gravity Concentrate Tail		3886.00	77.7%		3886.00	84.05			0.33	
Totals		*5000.00*	*100%*		*5000.00*	***131.02***	*50.14%*		*0.66*	***2.25***

PT_Ave	PD_Ave	AU_Ave	RH_Ave	RU_Ave	IR_Ave	SUM4E	SUM6E	CU_Ave	NI_Ave	FE_Ave	FEO_Ave	CO_Ave	Sulphur_A	Cr2O3_Av	SIO_Ave	MGO_Ave	CAO_Ave	ALO_Ave
g/T	g/T	g/T	g/T	g/T	g/T	g/T	g/T	%	%	%	%	%	%	%	%	%	%	%
80.353	34.989	0.708	14.971	25.757	6.192	131.021	162.971	0.222	0.432	7.200	9.262	0.008	0.777	1.966	53.923	24.066	3.235	4.977
367.077	130.4615	3.761	33.87	128.7145	22.243	535.170	686.127	0.296	0.8165	8.6115	11.0785	0.037	1.18	2.19	56.3355	24.8745	2.6095	4.347
259.757	101.9885	2.251	35.363	104.0525	21.5295	399.359	524.941	0.2745	0.7845	8.391	10.795	0.0365	1.121	2.1455	55.886	24.78	2.565	4.3605
137.54	60.622	0.98	24.967	54.735	17.978	224.109	296.822	0.344	0.807	8.144	10.477	0.041	1.249	2.049	50.72	23.64	2.636	4.312
130.375	57.115	0.979	23.558	48.185	15.811	212.027	276.023	0.287	0.701	7.979	10.266	0.036	1.077	1.806	51.33	24.095	2.634	4.188
93.942	43.609	0.698	19.881	33.562	15.882	158.130	207.574	0.299	0.647	7.864	10.117	0.033	1.028	1.681	52.423	23.95	2.728	4.431
189.92	76.24	1.65	27.07	71.07	18.53	294.88	384.48	0.30	0.75	8.18	10.52	0.04	1.13	1.97	53.17	24.22	2.64	4.33

Run 10

Phase 5: Multi-stage	Flow rate (L/min)	Mass (g)	Mass	Cum	Mass	4E PGM (g/t)	4E PGM	4E PGM Cum	4E PGM	4E PGM
Gravity Concentrate Feed		5000.00				131.02				
Gravity Concentrate 1		232.00	4.6%	4.6%	232.00	587.50	21%	21%	0.14	4.48
Gravity Concentrate 2		241.00	4.8%	9.5%	241.00	330.30	12%	33%	0.08	2.52
Gravity Concentrate 3		231.00	4.6%	14.1%	231.00	208.33	7%	40%	0.05	1.59
Gravity Concentrate 4	3	242.00	4.8%	18.9%	242.00	163.70	6%	46%	0.04	1.25
Gravity Concentrate 5		204.00	4.1%	23.0%	204.00	161.48	5%	51%	0.03	1.23
Total Gravity Conc.		*1150.00*	*23.0%*		*1150.00*	*292.68*	*51%*		*0.34*	**2.23**
Gravity Concentrate Tail		3850.00	77.0%		3850.00	82.73			0.32	
Totals		*5000.00*	*100%*		*5000.00*	***131.02***	*51.38%*		*0.66*	***2.23***

PT_Ave	PD_Ave	AU_Ave	RH_Ave	RU_Ave	IR_Ave	SUM4E	SUM6E	CU_Ave	NI_Ave	FE_Ave	FEO_Ave	CO_Ave	Sulphur_A	Cr2O3_Av	SIO_Ave	MGO_Ave	CAO_Ave	ALO_Ave
g/T	g/T	g/T	g/T	g/T	g/T	g/T	g/T	%	%	%	%	%	%	%	%	%	%	%
80.353	34.989	0.708	14.971	25.757	6.192	131.021	162.971	0.222	0.432	7.200	9.262	0.008	0.777	1.966	53.923	24.066	3.235	4.977
385.414	157.01	4.447	40.628	163.564	25.353	587.499	776.416	0.359	0.956	8.255	10.62	0.05	1.506	2.205	50.434	23.808	2.571	4.114
212.360	85.03	1.944	30.963	81.097	15.666	330.297	427.060	0.345	0.854	8.143	10.476	0.042	1.407	2.116	51.941	24.257	2.884	4.343
122.509	59.213	1.139	25.472	46.825	10.873	208.333	266.031	0.201	0.36	6.754	8.689	0.019	0.623	1.295	54.544	24.548	3.031	4.761
97.53	44.979	0.761	20.433	33.676	8.25	163.703	205.629	0.282	0.63	7.665	9.861	0.031	1.071	1.632	53.138	24.581	3.005	4.39
94.672	44.695	0.758	21.355	31.814	8.764	161.480	202.058	0.305	0.677	7.74	9.958	0.033	1.123	1.713	52.907	24.308	2.965	4.414
184.18	78.78	1.83	27.89	72.13	13.87	292.68	378.68	0.30	0.70	7.71	9.92	0.04	1.15	1.80	52.58	24.30	2.89	4.40

Figure 194: Phase 5 Run 6-10 Fire assay/ICP-MS results and analysis per run

Table 23: Elemental PGM and gangue recovery to GC concentrate

Description	Pt_Ave	Pd_Ave	Au_Ave	Rh_Ave	Ru_Ave	Ir_Ave	SUM 4E	SUM 6E	Cu_Ave	Ni_Ave	Fe_Ave	FeO_Ave	Co_Ave	Sulphur_	Cr_2O_3_Av	SiO_2_Ave	MgO_Ave	CaO_Ave	Al_2O_3_Av
Feed	4.018	1.749	0.035	0.749	1.288	0.310	6.551	8.149	0.011	0.022	0.360	0.463	0.001	0.039	0.098	2.696	1.203	0.162	0.249
Weighted Concentrate	2.051	0.842	0.020	0.290	0.771	0.160	3.204	4.134	0.003	0.008	0.089	0.114	0.000	0.013	0.022	0.587	0.269	0.030	0.048
Elemental Recovery	51.06%	48.13%	57.04%	38.75%	59.83%	51.68%	48.90%	50.74%	30.03%	37.73%	24.70%	24.70%	32.39%	33.05%	22.16%	21.76%	22.34%	18.59%	19.24%

Appendix C: PSD and Fractional Data

Malvern Data

Table 24: GC feed Malvern samples

Record Number	Sample Name	Dx (10)	Dx (50)	Dx (90)
4	Average of 'GC Feed 1'	4.07	16.5	50
8	Average of 'GC Feed 2'	4.54	17.3	50.2
12	Average of 'GC Feed 3'	4.23	16.2	48.4
16	Average of 'GC Feed 4'	4.47	17.3	50.5
	Average	**4.33**	**16.83**	**49.78**

Table 25: GC tail Malvern samples

Record Number	Sample Name	Dx (10)	Dx (50)	Dx (90)
20	Average of 'GC Tail 1'	3.86	16	48.1
24	Average of 'GC Tail 2'	3.71	15.4	47.6
28	Average of 'GC Tail 3'	3.86	15.9	48.7
	Average	**3.81**	**15.77**	**48.13**

Table 26: GC concentrate Malvern samples

Record Number	Sample Name	Dx (10)	Dx (50)	Dx (90)
32	Average of 'GC C1'	5.13	15.9	40.9
36	Average of 'GC C2'	4.91	15.4	41
44	Average of 'GC C3'	5.23	16.2	42.5
48	Average of 'GC C4'	5.27	16.6	43.6
52	Average of 'GC C5'	5.05	16.1	43.2
	Average	**5.12**	**16.04**	**42.24**

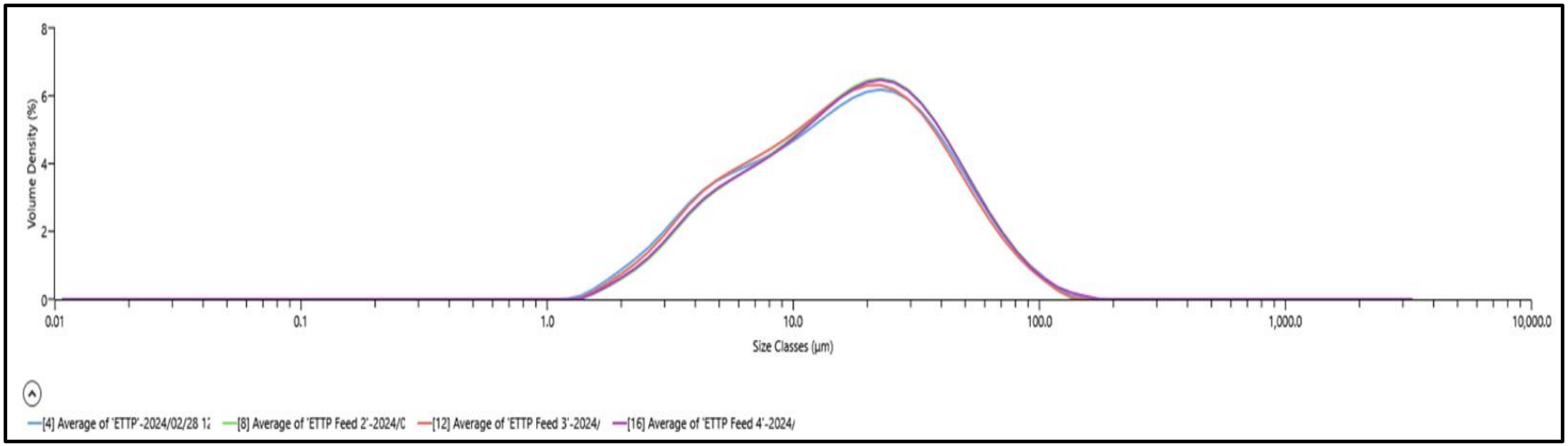

Figure 195: GC feed volume density vs size class

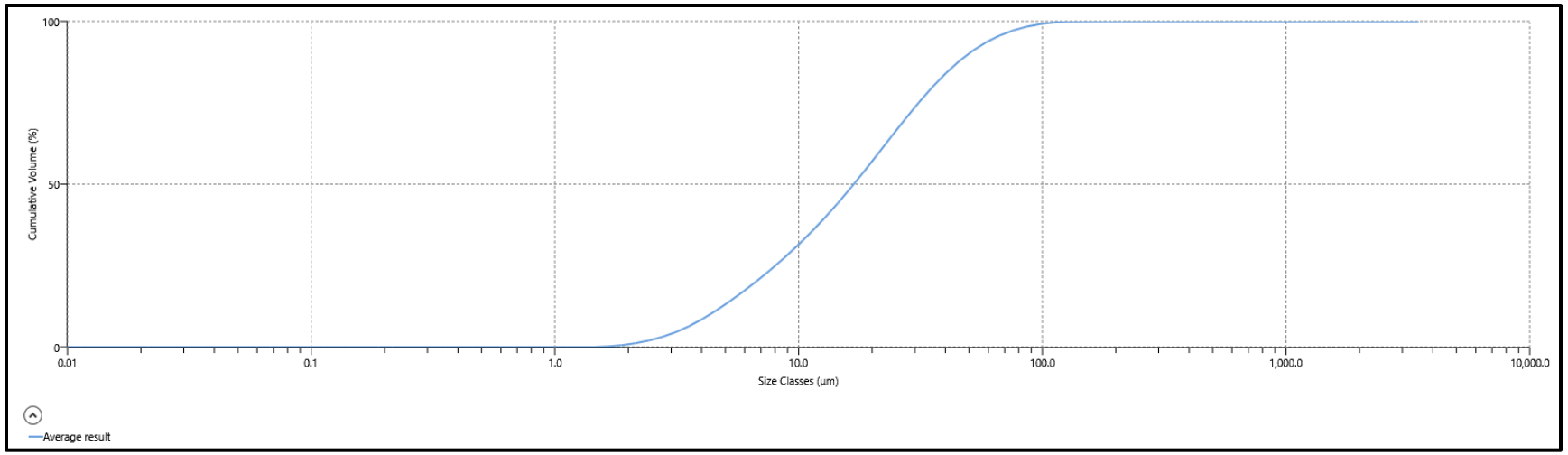

Figure 196: GC feed cumulative volume density vs size class

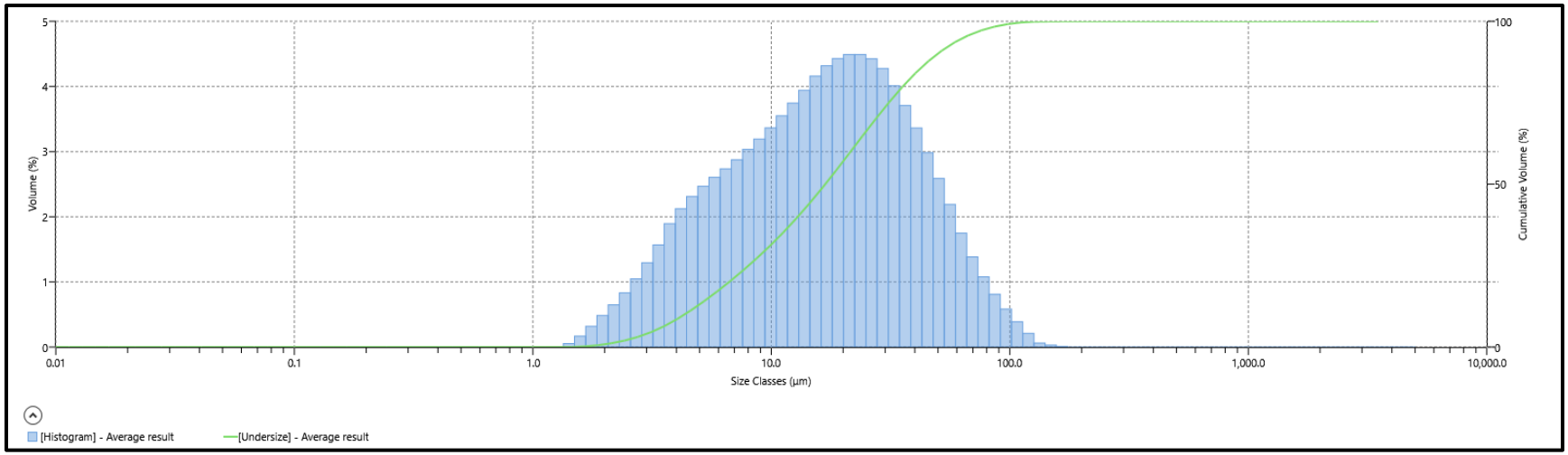

Figure 197: GC feed size class comparison with histogram

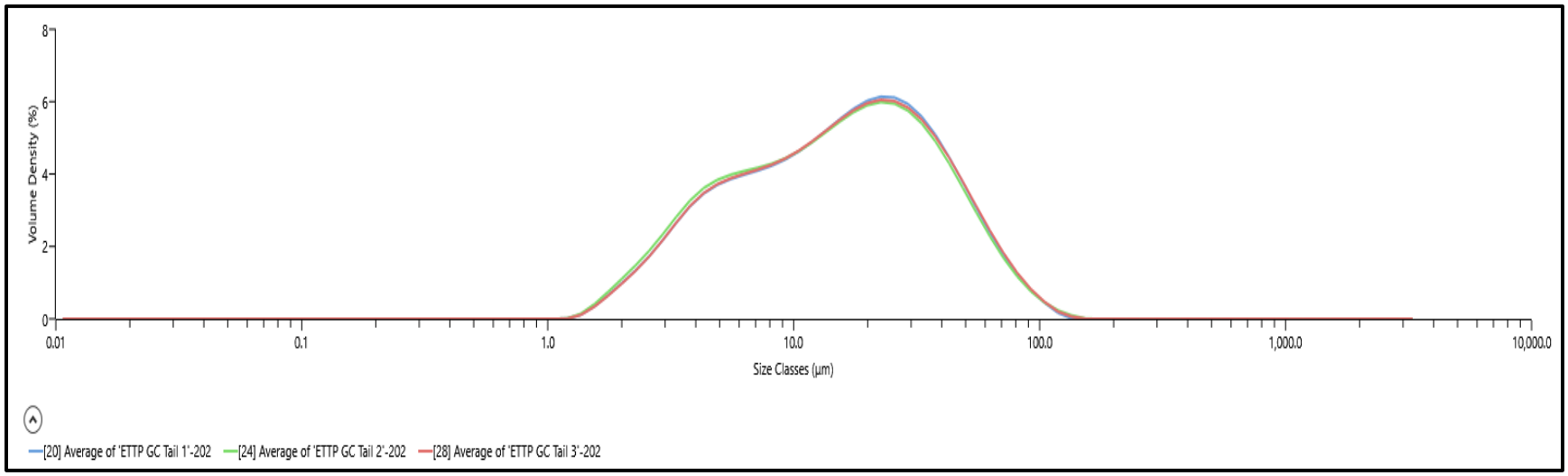

Figure 198: GC tail volume density vs size class

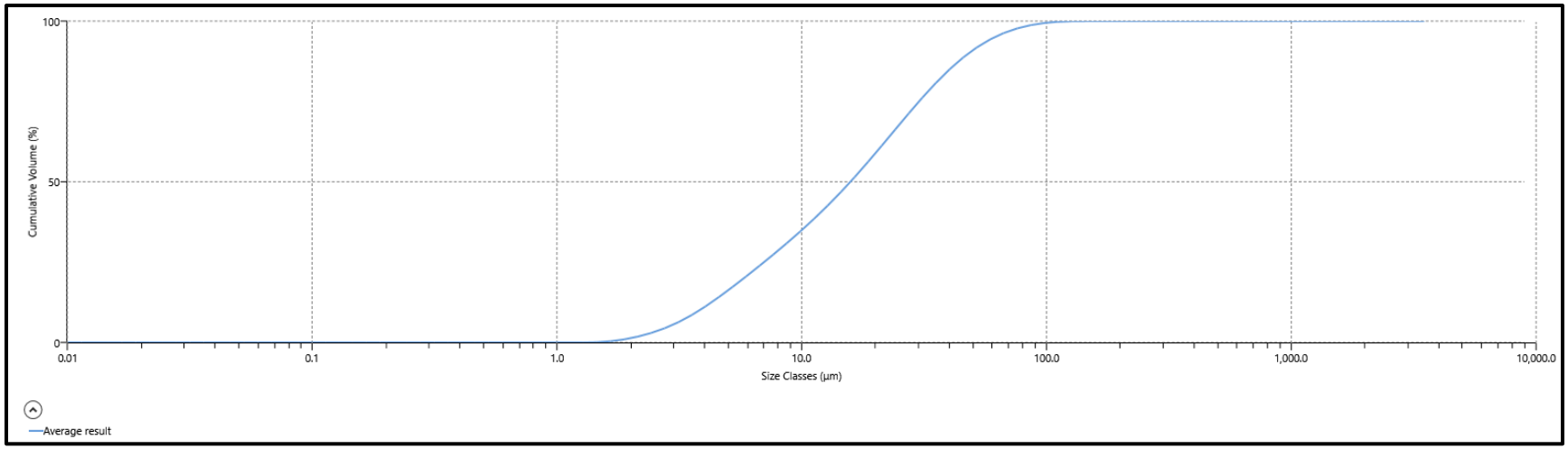

Figure 199: GC tail cumulative volume density vs size class

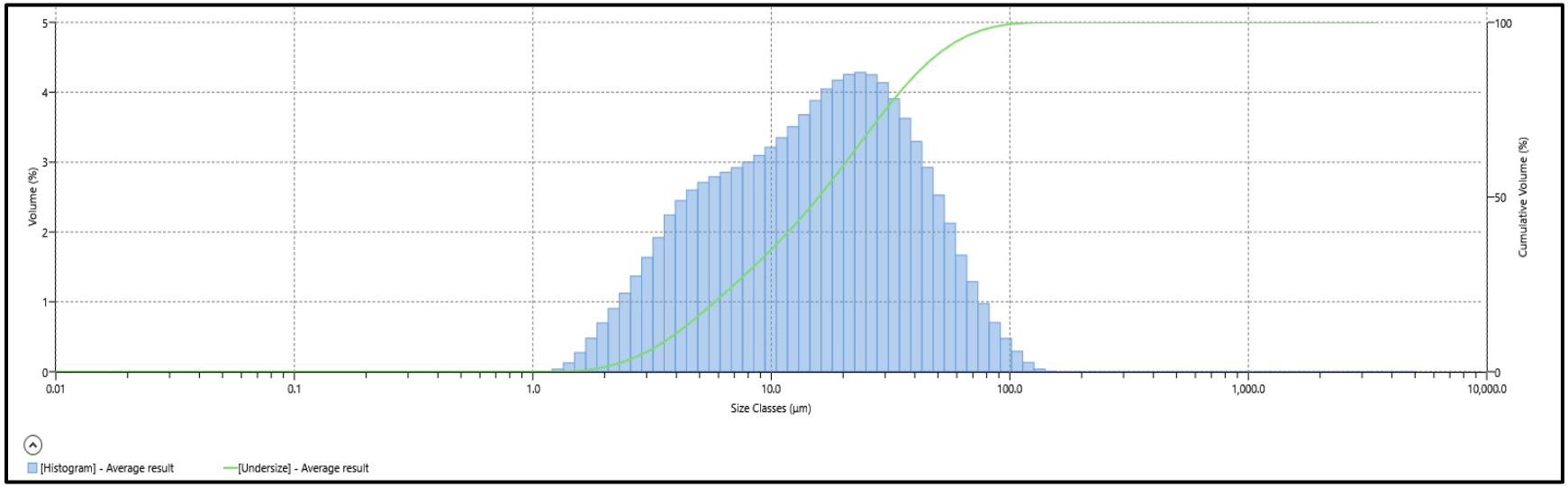

Figure 200: GC tail size class comparison with histogram

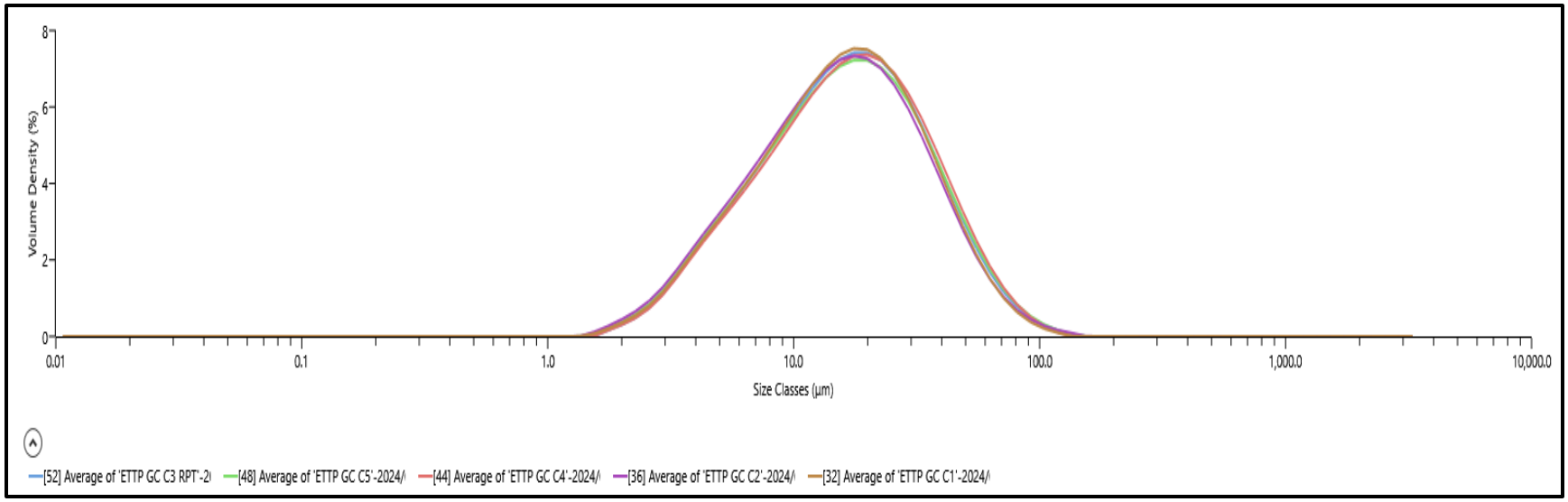

Figure 201: GC concentratel volume density vs size class

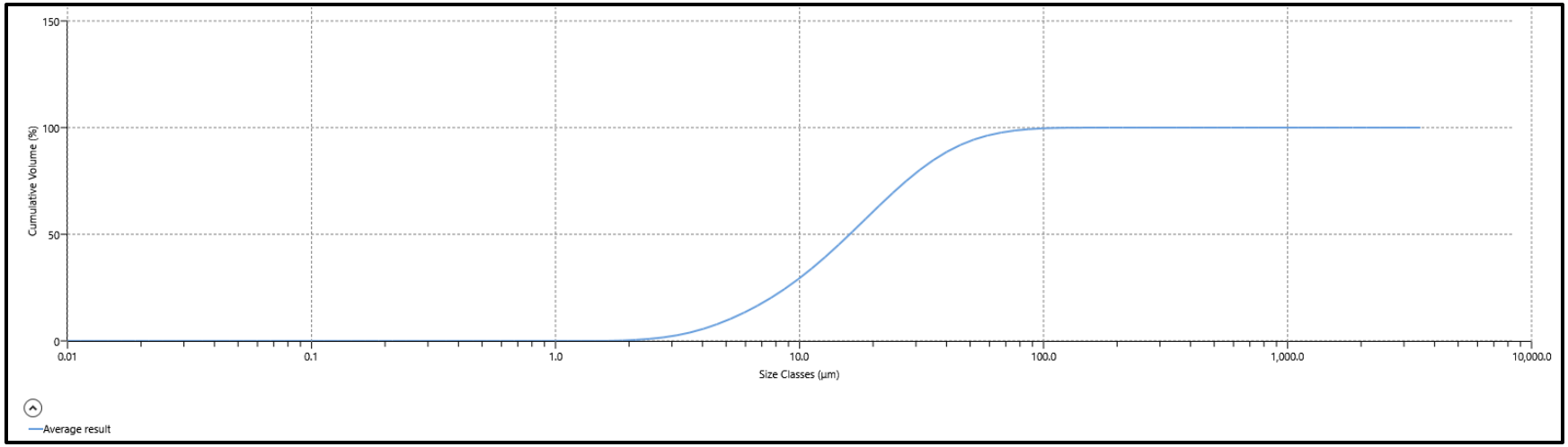

Figure 202: GC concentrate cumulative volume density vs size class

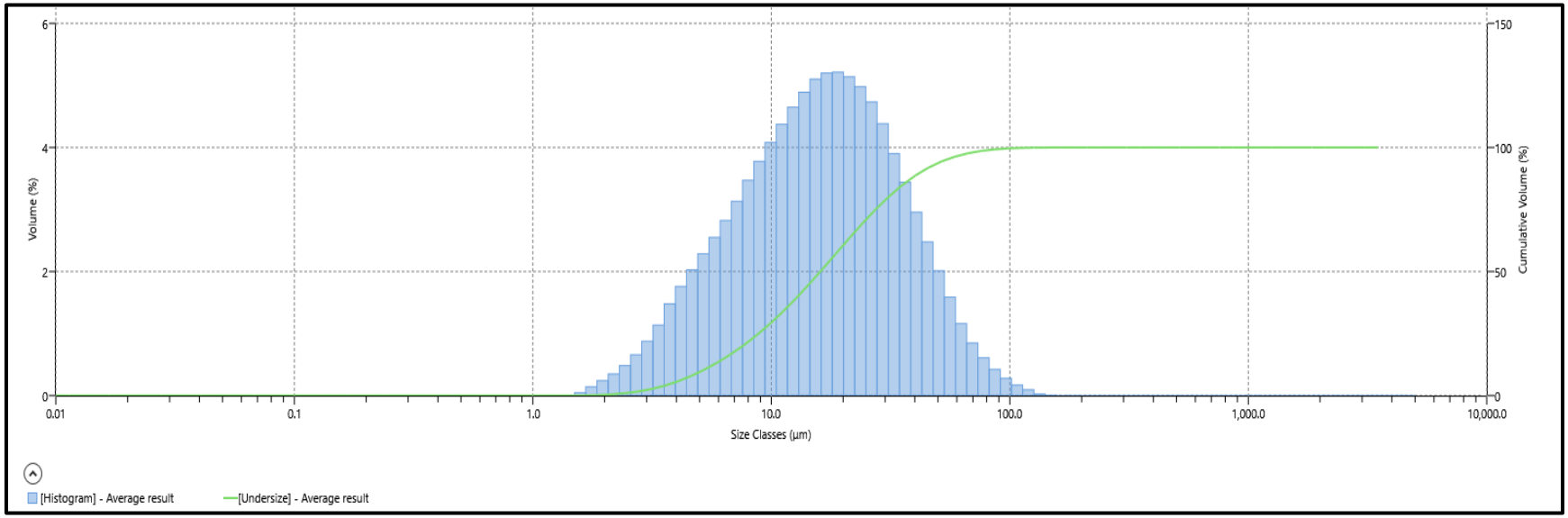

Figure 203: GC concentrate size class comparison with histogram

Fractional Data

Table 27: GC feed fractional analysis

Feed PSD																			
Size Fraction	Pt_Ave	Pd_Ave	Au_Ave	Rh_Ave	Ru_Ave	Ir_Ave	SUM 4E	SUM 6E	Cu_Ave	Ni_Ave	Fe_Ave	FeO_Ave	Co_Ave	Sulphur_Ave	Cr_2O_3_Ave	SiO_2_Ave	MgO_Ave	CaO_Ave	Al_2O_3_Ave
	g/T	g/T	g/T	g/T	g/T	g/T	g/T	g/T	%	%	%	%	%	%	%	%	%	%	%
+106µm	45.81	20.96	0.36	10.94	14.43	5.16	78.07	97.66	0.15	0.34	6.67	8.58	0.02	0.54	0.95	53.47	24.74	2.75	4.52
+75-106µm	60.50	26.97	0.53	13.56	17.50	5.94	101.56	125.00	0.19	0.38	6.39	8.23	0.02	0.65	0.82	54.14	23.40	3.36	5.84
+53-75µm	78.64	35.09	0.73	14.94	27.84	8.00	129.40	165.24	0.24	0.44	7.12	9.16	0.02	0.73	1.53	53.91	24.99	2.49	4.02
+38-53µm	84.26	37.50	0.74	18.00	22.84	7.16	140.50	170.50	0.27	0.46	5.86	7.54	0.02	0.85	0.71	52.44	21.13	4.16	7.72
+25-38µm	108.28	52.55	1.22	20.82	27.86	8.29	182.86	219.02	0.59	0.60	6.05	7.61	0.03	1.68	1.68	47.46	17.68	4.99	9.23
-25µm	132.18	61.11	1.37	26.11	33.49	9.61	220.76	263.86	0.51	0.66	5.19	6.67	0.03	1.52	0.70	51.91	15.49	6.17	12.62

Table 28: GC tail fractional analysis

Tail PSD																			
Size Fraction	Pt_Ave	Pd_Ave	Au_Ave	Rh_Ave	Ru_Ave	Ir_Ave	SUM 4E	SUM 6E	Cu_Ave	Ni_Ave	Fe_Ave	FeO_Ave	Co_Ave	Sulphur_Ave	Cr_2O_3_Ave	SiO_2_Ave	MgO_Ave	CaO_Ave	Al_2O_3_Ave
	g/T	g/T	g/T	g/T	g/T	g/T	g/T	g/T	%	%	%	%	%	%	%	%	%	%	%
+106µm	35.84	17.28	0.30	9.07	10.79	3.39	62.48	76.66	0.19	0.23	1.95	2.51	0.01	0.75	0.22	50.54	6.26	2.64	5.12
+75-106µm	43.46	22.17	0.38	11.51	12.82	4.32	77.52	94.65	0.15	0.29	6.55	8.43	0.01	1.16	0.79	52.82	25.44	3.05	4.35
+53-75µm	44.08	22.10	0.39	11.20	12.47	3.82	77.77	94.07	0.29	0.46	6.97	8.97	0.03	1.25	1.51	51.37	24.67	2.87	4.41
+38-53µm	46.45	21.12	0.49	9.76	12.14	3.18	77.81	93.13	0.21	0.37	6.35	8.17	0.02	1.30	0.81	53.25	23.49	3.87	6.00
+25-38µm	84.43	38.12	0.86	18.26	22.69	6.16	141.68	170.52	0.23	0.35	5.98	7.69	0.01	1.30	1.32	47.80	21.61	3.19	4.66
-25µm	86.41	38.99	0.75	19.80	24.73	7.26	145.95	177.94	0.30	0.45	5.58	7.18	0.02	1.50	0.57	52.89	20.49	4.89	8.56

Table 29: GC concentration fractional analysis

Concentrate PSD																			
Size Fraction	Pt_Ave	Pd_Ave	Au_Ave	Rh_Ave	Ru_Ave	Ir_Ave	SUM 4E	SUM 6E	Cu_Ave	Ni_Ave	Fe_Ave	FeO_Ave	Co_Ave	Sulphur_Ave	Cr_2O_3_Ave	SiO_2_Ave	MgO_Ave	CaO_Ave	Al_2O_3_Ave
	g/T	g/T	g/T	g/T	g/T	g/T	g/T	g/T	%	%	%	%	%	%	%	%	%	%	%
+106µm	58.58	22.11	0.38	10.57	30.00	8.27	91.64	129.91	0.09	0.42	17.31	22.65	0.02	0.23	2.00	60.41	35.48	1.35	2.00
+75-106µm	82.89	28.25	0.65	12.59	36.51	8.62	124.38	169.50	0.13	0.48	13.75	17.99	0.02	0.35	2.07	54.17	29.57	1.63	2.61
+53-75µm	132.99	60.33	1.47	18.17	50.80	11.39	212.96	275.15	0.02	0.42	45.33	59.30	0.02	1.01	2.89	53.20	37.00	1.02	0.77
+38-53µm	135.48	48.96	1.16	16.49	83.51	16.05	202.09	301.64	0.05	0.31	21.13	27.64	0.01	1.05	1.12	53.19	36.62	1.37	1.86
+25-38µm	145.19	55.88	1.01	25.30	62.31	14.70	227.37	304.38	0.34	0.85	3.27	4.27	0.04	1.20	0.64	52.97	24.59	3.13	5.07
-25µm	212.56	87.82	2.24	29.35	74.44	14.38	331.97	420.79	0.42	0.76	17.53	21.61	0.04	1.81	0.16	50.03	26.15	2.76	3.92

Appendix D: Phase 7 Data

Mass and Moisture Data

Table 30:Phase 7 mass and moisture raw data

Sample ID	Gravity Concentrate			Gravity Tail	Moisture (g)	Moisture (%)
	Bowl	*Wet*	*Dry*	*Dry*		
Phase 5 run 1 Gc Conc 1	787	126	**89**		37.00	29.37%
Phase 5 run 1 Gc Conc 2	787	130	**90**		40.00	30.77%
Phase 5 run 1 Gc Conc 3	787	117	**83**		34.00	29.06%
Phase 5 run 1 Gc Conc 4	787	126	**88**		38.00	30.16%
Phase 5 run 1 Gc Conc 5	787	125	**85**		40.00	32.00%
Phase 5 run 1 Gc Tail				4565		
Phase 5 run 2 Gc Conc 1	787	122	**85.156**		36.84	30.20%
Phase 5 run 2 Gc Conc 2	787	128	**89.728**		38.27	29.90%
Phase 5 run 2 Gc Conc 3	787	125	**86**		39.00	31.20%
Phase 5 run 2 Gc Conc 4	787	124	**88.164**		35.84	28.90%
Phase 5 run 2 Gc Conc 5	787	124	**85.808**		38.19	30.80%
Phase 5 run 2 Gc Tail				4565		
Phase 5 run 3 Gc Conc 1	787	*126*	**87**		39.31	31.20%
Phase 5 run 3 Gc Conc 2	787	123	**85**		37.64	30.60%
Phase 5 run 3 Gc Conc 3	787	127	**90**		37.47	29.50%
Phase 5 run 3 Gc Conc 4	787	124	**87**		36.95	29.80%
Phase 5 run 3 Gc Conc 5	787	125	**87**		37.75	30.20%
Phase 5 run 3 Gc Tail				4564		

Phase 7: Assay and Mass yield/Recovery/Grade Data

Run 1

Phase 7: Multi-stage	Flow rate (L/min)	Mass (g)	Mass Recovery (%)	Cum Mass recovery %	Mass recovery (g)	4E PGM (g/t)	4E PGM Recovery (%)	4E PGM Cum Recovery (%)	4E PGM (g)	4E PGM Upgrade
Gravity Concentrate Feed		5000				131.02				
Gravity Concentrate 1		89	1.8%	1.8%	89.00	688.16	9%	9%	0.06	**5.25**
Gravity Concentrate 2		90	1.8%	3.6%	90.00	653.80	9%	18%	0.06	**4.99**
Gravity Concentrate 3	1	83	1.7%	5.2%	83.00	503.97	6%	25%	0.04	**3.85**
Gravity Concentrate 4		88	1.8%	7.0%	88.00	462.49	6%	31%	0.04	**3.53**
Gravity Concentrate 5		85	1.7%	8.7%	85.00	413.25	5%	36%	0.04	**3.15**
Total Gravity Conc.		*435*	*8.7%*		*435.00*	*546.53*	*36%*		*0.24*	**4.17**
Gravity Concentrate Tail		4565	91.3%		4565.00	91.43			0.42	
Totals		*5000.00*	*100%*		*5000.00*	***131.02***	*36.29%*		*0.66*	*4.17*

PT_Ave	PD_Ave	AU_Ave	RH_Ave	RU_Ave	IR_Ave	SUM4E	SUM6E	CU_Ave	NI_Ave	FE_Ave	FEO_Ave	CO_Ave	Sulphur_A	Cr2O3_Av	SIO_Ave	MGO_Ave	CAO_Ave	ALO_Ave
g/T	g/T	g/T	g/T	g/T	g/T	g/T	g/T	%	%	%	%	%	%	%	%	%	%	%
80.353	34.989	0.708	14.971	25.757	6.192	131.021	162.971	0.222	0.432	7.200	9.262	0.022	0.777	1.966	53.923	24.066	3.235	4.977
448.061	185.615	6.267	48.213	195.23	30.333	688.156	913.719	0.351	0.978	8.41	10.819	0.047	1.622	2.264	49.893	24.028	2.461	4.229
436.259	167.851	5.098	44.589	176.616	28.037	653.797	858.450	0.361	0.772	7.903	10.167	0.04	1.288	2.114	49.479	24.527	2.162	3.669
316.793	142.479	4.497	40.202	152.126	25.561	503.971	681.658	0.336	0.835	7.901	10.165	0.042	1.397	1.907	49.682	24.262	2.456	4.109
316.856	109.393	3.397	32.846	111.904	19.291	462.492	593.687	0.356	0.757	7.912	10.178	0.04	1.284	2.1	49.774	24.65	2.317	4.015
247.875	124.173	3.686	37.515	123.925	21.958	413.249	559.132	0.36	0.828	8.026	10.325	0.044	1.446	1.936	50.035	24.271	2.429	4.086
354.91	146.28	4.60	40.74	152.36	25.08	546.53	723.98	0.35	0.83	8.03	10.33	0.04	1.41	2.07	49.77	24.35	2.36	4.02

Run 2

Phase 7: Multi-stage	Flow rate (L/min)	Mass (g)	Mass Recovery (%)	Cum Mass recovery %	Mass recovery (g)	4E PGM (g/t)	4E PGM Recovery (%)	4E PGM Cum Recovery (%)	4E PGM (g)	4E PGM Upgrade
Gravity Concentrate Feed		5000.00				131.02				
Gravity Concentrate 1		85	1.7%	1.7%	85.16	635.08	8%	8%	0.05	**4.85**
Gravity Concentrate 2		90	1.8%	3.5%	89.73	547.84	8%	16%	0.05	**4.18**
Gravity Concentrate 3	2	86	1.7%	5.2%	86.00	492.42	6%	22%	0.04	**3.76**
Gravity Concentrate 4		88	1.8%	7.0%	88.16	398.88	5%	28%	0.04	**3.04**
Gravity Concentrate 5		86	1.7%	8.7%	85.81	334.94	4%	32%	0.03	**2.56**
Total Gravity Conc.		*434.86*	*8.7%*		*434.86*	*481.75*	*32%*		*0.21*	**3.68**
Gravity Concentrate Tail		4565	91.3%		4565.14	97.61			0.45	
Totals		*5000.00*	*100%*		*5000.00*	***131.02***	*32%*		*0.66*	*3.68*

PT_Ave	PD_Ave	AU_Ave	RH_Ave	RU_Ave	IR_Ave	SUM4E	SUM6E	CU_Ave	NI_Ave	FE_Ave	FEO_Ave	CO_Ave	Sulphur_A	Cr2O3_Av	SIO_Ave	MGO_Ave	CAO_Ave	ALO_Ave
g/T	g/T	g/T	g/T	g/T	g/T	g/T	g/T	%	%	%	%	%	%	%	%	%	%	%
80.353	34.989	0.708	14.971	25.757	6.192	131.021	162.971	0.222	0.432	7.200	9.262	0.004	0.777	1.966	53.923	24.066	3.235	4.977
462.688	131.061	3.537	37.797	139.883	21.983	635.083	796.949	0.345	1.079	8.416	10.827	0.052	1.781	2.293	48.272	23.723	2.474	4.374
377.384	136.575	3.466	30.413	150.26	24.837	547.838	722.935	0.359	0.907	8.055	10.362	0.044	1.507	2.059	48.809	24.032	2.34	4.008
327.505	121.809	2.907	40.203	133.63	22.614	492.424	648.668	0.348	0.77	7.907	10.173	0.04	1.319	1.954	49.71	24.699	2.259	3.747
266.597	97.938	2.233	32.108	107.95	18.645	398.876	525.471	0.355	0.771	7.748	9.968	0.039	1.317	1.914	49.217	24.441	2.362	3.903
218.895	84.346	1.851	29.844	89.359	16.3	334.936	440.595	0.339	0.744	7.849	10.098	0.038	1.303	1.78	50.168	24.36	2.419	4.067
330.49	114.44	2.80	34.03	124.34	20.90	481.75	626.99	0.35	0.85	7.99	10.28	0.04	1.44	2.00	49.23	24.25	2.37	4.02

Run 3

Phase 7: Multi-stage	Flow rate (L/min)	Mass (g)	Mass Recovery (%)	Cum Mass recovery %	Mass recovery (g)	4E PGM (g/t)	4E PGM Recovery (%)	4E PGM Cum Recovery (%)	4E PGM (g)	4E PGM Upgrade
Gravity Concentrate Feed		5000.00				131.02				
Gravity Concentrate 1		87	1.7%	1.7%	86.69	578.63	8%	8%	0.05	**4.42**
Gravity Concentrate 2		85	1.7%	3.4%	85.36	229.18	3%	11%	0.02	**1.75**
Gravity Concentrate 3		90	1.8%	5.2%	89.54	269.76	4%	14%	0.02	**2.06**
Gravity Concentrate 4	4	87	1.7%	7.0%	87.05	237.61	3%	17%	0.02	**1.81**
Gravity Concentrate 5		87	1.7%	8.7%	87.25	204.73	3%	20%	0.02	**1.56**
Total Gravity Conc.		*435.88*	*8.7%*		*435.88*	*303.80*	*20%*		*0.13*	**2.32**
Gravity Concentrate Tail		4564	91.3%		4564.12	110.72			0.51	
Totals		*5000.00*	*100%*		*5000.00*	***127.55***	*20.21%*		*0.64*	*2.32*

PT_Ave	PD_Ave	AU_Ave	RH_Ave	RU_Ave	IR_Ave	SUM4E	SUM6E	CU_Ave	NI_Ave	FE_Ave	FEO_Ave	CO_Ave	Sulphur_A	Cr2O3_Av	SIO_Ave	MGO_Ave	CAO_Ave	ALO_Ave
g/T	g/T	g/T	g/T	g/T	g/T	g/T	g/T	%	%	%	%	%	%	%	%	%	%	%
80.353	34.989	0.708	14.971	25.757	6.192	131.021	162.971	0.222	0.432	7.200	9.262	0.003	0.777	1.966	53.923	24.066	3.235	4.977
429.93	89.792	4.718	54.189	213.037	31.663	578.629	823.329	0.337	0.921	8.127	10.455	0.046	1.545	2.158	49.324	24.172	2.374	4.031
151.217	60.384	1.233	16.345	60.252	12.725	229.179	302.156	0.325	0.632	7.697	9.902	0.034	1.111	1.762	50.583	24.901	2.344	3.802
172.307	69.279	1.294	26.876	73.051	14.195	269.756	357.002	0.328	0.785	7.738	9.955	0.039	1.363	1.691	49.94	23.777	2.688	4.586
149.884	61.217	1.046	25.459	61.538	12.556	237.606	311.700	0.304	0.689	7.677	9.877	0.036	1.206	1.575	50.559	24.276	2.596	4.281
126.258	53.607	1.114	23.751	49.526	12.258	204.730	266.514	0.312	0.652	7.628	9.813	0.034	1.146	1.643	50.83	24.629	2.406	4.022
205.72	66.87	1.88	29.34	91.38	16.67	303.80	411.84	0.32	0.74	7.77	10.00	0.04	1.28	1.77	50.25	24.35	2.48	4.15

Figure 204: Phase 7 mass yield/recovery/grade raw data

Figure 204: Phase 7 mass yield/recovery/grade raw data

Appendix E: XRF Raw Data

Figure 205: XRF raw data

File #	DateTime	Operator	Name	ID	Application	Method	Elapsed Time	Alloy 1	Match Qual 1	Alloy 2	Match Qual 2	Alloy 3	Match Qual 3	MgO	MgO Err	Al2O3	Al2O3 Err	SiO2	SiO2 Err	P	P Err	S	S Err	Cl	Cl Err	K2O	K2O Err	Ca	Ca Err	Ti	Ti Err	V	V Err	Cr	Cr Err
379	02-15-2024 11:31	Supervisor	c1	unk	GeoExploration	Oxide3phase	90.0		0.0		0.0		0.0	25.6094	0.8851	3.4096	0.1862	51.2149	0.3848	< LOD	0.0114	1.0783	0.0216	0.1476	0.0155	0.0510	0.0071	1.6527	0.0143	0.1724	0.0044	0.0095	0.0059	1.4814	0.0258
File #	DateTime	Operator	Name	ID	Application	Method	Elapsed Time	Alloy 1	Match Qual 1	Alloy 2	Match Qual 2	Alloy 3	Match Qual 3	MgO	MgO Err	Al2O3	Al2O3 Err	SiO2	SiO2 Err	P	P Err	S	S Err	Cl	Cl Err	K2O	K2O Err	Ca	Ca Err	Ti	Ti Err	V	V Err	Cr	Cr Err
380	02-15-2024 11:40	Supervisor	c2	unk	GeoExploration	Oxide3phase	90.0		0.0		0.0		0.0	24.8913	0.8754	3.3758	0.1845	50.5297	0.3816	< LOD	0.0114	1.2536	0.0229	0.1612	0.0155	0.0543	0.0069	1.6124	0.0141	0.1703	0.0043	< LOD	0.0059	1.4537	0.0255
File #	DateTime	Operator	Name	ID	Application	Method	Elapsed Time	Alloy 1	Match Qual 1	Alloy 2	Match Qual 2	Alloy 3	Match Qual 3	MgO	MgO Err	Al2O3	Al2O3 Err	SiO2	SiO2 Err	P	P Err	S	S Err	Cl	Cl Err	K2O	K2O Err	Ca	Ca Err	Ti	Ti Err	V	V Err	Cr	Cr Err
381	02-15-2024 12:05	Supervisor	c3	unk	GeoExploration	Oxide3phase	90.0		0.0		0.0		0.0	25.7952	0.8748	3.5293	0.1844	51.4811	0.3855	< LOD	0.0110	0.9047	0.0200	0.1408	0.0153	0.0554	0.0070	1.6648	0.0143	0.1650	0.0043	0.0079	0.0059	1.2243	0.0236
File #	DateTime	Operator	Name	ID	Application	Method	Elapsed Time	Alloy 1	Match Qual 1	Alloy 2	Match Qual 2	Alloy 3	Match Qual 3	MgO	MgO Err	Al2O3	Al2O3 Err	SiO2	SiO2 Err	P	P Err	S	S Err	Cl	Cl Err	K2O	K2O Err	Ca	Ca Err	Ti	Ti Err	V	V Err	Cr	Cr Err
382	02-15-2024 12:10	Supervisor	c4	unk	GeoExploration	Oxide3phase	90.0		0.0		0.0		0.0	25.6649	0.8764	3.6007	0.1865	51.3605	0.3851	< LOD	0.0112	0.9631	0.0205	0.1362	0.0153	0.0498	0.0069	1.6830	0.0144	0.1690	0.0043	0.0081	0.0058	1.2382	0.0237
383	02-15-2024 12:14	Supervisor	c5	unk	GeoExploration	Oxide3phase	90.0		0.0		0.0		0.0	25.6631	0.8794	3.5162	0.1864	51.8839	0.3873	< LOD	0.0113	0.9322	0.0203	0.1396	0.0153	0.0509	0.0071	1.7027	0.0145	0.1616	0.0043	0.0060	0.0058	1.1817	0.0230
File #	DateTime	Operator	Name	ID	Application	Method	Elapsed Time	Alloy 1	Match Qual 1	Alloy 2	Match Qual 2	Alloy 3	Match Qual 3	MgO	MgO Err	Al2O3	Al2O3 Err	SiO2	SiO2 Err	P	P Err	S	S Err	Cl	Cl Err	K2O	K2O Err	Ca	Ca Err	Ti	Ti Err	V	V Err	Cr	Cr Err
384	02-15-2024 12:18	Supervisor	gct	unk	GeoExploration	Oxide3phase	89.0		0.0		0.0		0.0	23.7550	0.8512	3.5761	0.1809	49.9890	0.3829	< LOD	0.0106	0.4895	0.0161	0.1332	0.0153	0.0614	0.0069	1.6018	0.0141	0.1366	0.0041	< LOD	0.0052	0.8185	0.0192
File #	DateTime	Operator	Name	ID	Application	Method	Elapsed Time	Alloy 1	Match Qual 1	Alloy 2	Match Qual 2	Alloy 3	Match Qual 3	MgO	MgO Err	Al2O3	Al2O3 Err	SiO2	SiO2 Err	P	P Err	S	S Err	Cl	Cl Err	K2O	K2O Err	Ca	Ca Err	Ti	Ti Err	V	V Err	Cr	Cr Err
387	02-15-2024 12:25	Supervisor	r1	unk	GeoExploration	Oxide3phase	90.0		0.0		0.0		0.0	26.3173	0.8703	3.8426	0.1866	53.1386	0.3919	< LOD	0.0106	0.5187	0.0162	0.1189	0.0150	0.0728	0.0071	1.6860	0.0143	0.1496	0.0042	0.0071	0.0055	0.9424	0.0207
File #	DateTime	Operator	Name	ID	Application	Method	Elapsed Time	Alloy 1	Match Qual 1	Alloy 2	Match Qual 2	Alloy 3	Match Qual 3	MgO	MgO Err	Al2O3	Al2O3 Err	SiO2	SiO2 Err	P	P Err	S	S Err	Cl	Cl Err	K2O	K2O Err	Ca	Ca Err	Ti	Ti Err	V	V Err	Cr	Cr Err
412	03-04-2024 11:40	Supervisor	r2	unk	GeoExploration	Oxide3phase	90.0		0.0		0.0		0.0	24.6417	0.8450	3.6630	0.1794	50.6633	0.3806	< LOD	0.0102	0.5306	0.0162	0.1540	0.0152	0.0765	0.0070	1.6572	0.0142	0.1494	0.0042	< LOD	0.0054	0.8925	0.0201
413	03-04-2024 11:44	Supervisor	r3	unk	GeoExploration	Oxide3phase	90.0		0.0		0.0		0.0	24.4502	0.8489	3.5754	0.1811	51.4473	0.3842	< LOD	0.0107	0.5020	0.0161	0.1476	0.0152	0.0757	0.0071	1.6839	0.0143	0.1542	0.0042	0.0080	0.0055	0.8981	0.0202
File #	DateTime	Operator	Name	ID	Application	Method	Elapsed Time	Alloy 1	Match Qual 1	Alloy 2	Match Qual 2	Alloy 3	Match Qual 3	MgO	MgO Err	Al2O3	Al2O3 Err	SiO2	SiO2 Err	P	P Err	S	S Err	Cl	Cl Err	K2O	K2O Err	Ca	Ca Err	Ti	Ti Err	V	V Err	Cr	Cr Err
415	03-04-2024 11:48	Supervisor	f1	unk	GeoExploration	Oxide3phase	90.0		0.0		0.0		0.0	25.3578	0.8649	3.7124	0.1851	52.1095	0.3875	< LOD	0.0110	0.6306	0.0174	0.1602	0.0154	0.0735	0.0071	1.7256	0.0145	0.1497	0.0042	< LOD	0.0056	0.9918	0.0212
File #	DateTime	Operator	Name	ID	Application	Method	Elapsed Time	Alloy 1	Match Qual 1	Alloy 2	Match Qual 2	Alloy 3	Match Qual 3	MgO	MgO Err	Al2O3	Al2O3 Err	SiO2	SiO2 Err	P	P Err	S	S Err	Cl	Cl Err	K2O	K2O Err	Ca	Ca Err	Ti	Ti Err	V	V Err	Cr	Cr Err
416	03-04-2024 11:52	Supervisor	f2	unk	GeoExploration	Oxide3phase	90.0		0.0		0.0		0.0	25.4759	0.8653	3.6681	0.1842	52.0720	0.3872	< LOD	0.0109	0.6190	0.0173	0.1645	0.0154	0.0764	0.0071	1.6918	0.0143	0.1506	0.0042	< LOD	0.0054	0.9812	0.0211
File #	DateTime	Operator	Name	ID	Application	Method	Elapsed Time	Alloy 1	Match Qual 1	Alloy 2	Match Qual 2	Alloy 3	Match Qual 3	MgO	MgO Err	Al2O3	Al2O3 Err	SiO2	SiO2 Err	P	P Err	S	S Err	Cl	Cl Err	K2O	K2O Err	Ca	Ca Err	Ti	Ti Err	V	V Err	Cr	Cr Err
419	03-04-2024 11:56	Supervisor	f3	unk	GeoExploration	Oxide3phase	90.0		0.0		0.0		0.0	25.5063	0.8681	3.8298	0.1883	52.7207	0.3905	< LOD	0.0110	0.6296	0.0175	0.1675	0.0155	0.0783	0.0073	1.7348	0.0145	0.1564	0.0043	< LOD	0.0056	1.0117	0.0214

Mn	Mn Err	Fe	Fe Err	Co	Co Err	Ni	Ni Err	Cu	Cu Err	Zn	Zn Err	Ga	Ga Err	As	As Err	Se	Se Err	Rb	Rb Err	Sr	Sr Err
0.1379	0.0078	8.8094	0.0323	0.0348	0.0040	0.7099	0.0075	0.2830	0.0039	0.0054	0.0009	< LOD	0.0005	0.0009	0.0004	0.0009	0.0004	< LOD	0.0002	0.0025	0.0003
Mn	Mn Err	Fe	Fe Err	Co	Co Err	Ni	Ni Err	Cu	Cu Err	Zn	Zn Err	Ga	Ga Err	As	As Err	Se	Se Err	Rb	Rb Err	Sr	Sr Err
0.1349	0.0078	8.6036	0.0319	0.0360	0.0040	0.7522	0.0080	0.3052	0.0042	0.0079	0.0009	< LOD	0.0005	0.0010	0.0005	0.0007	0.0003	< LOD	0.0002	0.0026	0.0003
Mn	Mn Err	Fe	Fe Err	Co	Co Err	Ni	Ni Err	Cu	Cu Err	Zn	Zn Err	Ga	Ga Err	As	As Err	Se	Se Err	Rb	Rb Err	Sr	Sr Err
0.1239	0.0073	8.3744	0.0313	0.0259	0.0039	0.6051	0.0071	0.2676	0.0039	0.0092	0.0009	< LOD	0.0005	0.0006	0.0005	0.0005	0.0003	< LOD	0.0002	0.0026	0.0003
Mn	Mn Err	Fe	Fe Err	Co	Co Err	Ni	Ni Err	Cu	Cu Err	Zn	Zn Err	Ga	Ga Err	As	As Err	Se	Se Err	Rb	Rb Err	Sr	Sr Err
0.1327	0.0074	8.4347	0.0314	0.0276	0.0039	0.6118	0.0071	0.2637	0.0038	0.0095	0.0009	< LOD	0.0005	0.0008	0.0005	0.0009	0.0003	< LOD	0.0002	0.0028	0.0003
0.1351	0.0073	8.2951	0.0311	0.0281	0.0039	0.5715	0.0068	0.2555	0.0038	0.0090	0.0008	< LOD	0.0005	< LOD	0.0005	< LOD	0.0003	< LOD	0.0002	0.0030	0.0003
Mn	Mn Err	Fe	Fe Err	Co	Co Err	Ni	Ni Err	Cu	Cu Err	Zn	Zn Err	Ga	Ga Err	As	As Err	Se	Se Err	Rb	Rb Err	Sr	Sr Err
0.1070	0.0064	6.6261	0.0275	0.0157	0.0035	0.3361	0.0054	0.1804	0.0032	0.0070	0.0008	< LOD	0.0005	0.0007	0.0005	0.0003	0.0002	0.0004	0.0002	0.0031	0.0003
Mn	Mn Err	Fe	Fe Err	Co	Co Err	Ni	Ni Err	Cu	Cu Err	Zn	Zn Err	Ga	Ga Err	As	As Err	Se	Se Err	Rb	Rb Err	Sr	Sr Err
0.1213	0.0067	7.6007	0.0296	0.0135	0.0036	0.3583	0.0053	0.1945	0.0032	0.0109	0.0008	< LOD	0.0004	0.0008	0.0005	< LOD	0.0002	< LOD	0.0002	0.0034	0.0003
Mn	Mn Err	Fe	Fe Err	Co	Co Err	Ni	Ni Err	Cu	Cu Err	Zn	Zn Err	Ga	Ga Err	As	As Err	Se	Se Err	Rb	Rb Err	Sr	Sr Err
0.1147	0.0067	7.3793	0.0292	0.0183	0.0037	0.3688	0.0055	0.1946	0.0033	0.0104	0.0008	< LOD	0.0004	0.0005	0.0005	< LOD	0.0003	< LOD	0.0002	0.0034	0.0004
0.1193	0.0067	7.4033	0.0292	0.0175	0.0036	0.3591	0.0054	0.1909	0.0032	0.0089	0.0008	< LOD	0.0004	0.0009	0.0005	< LOD	0.0002	0.0005	0.0002	0.0036	0.0004
Mn	Mn Err	Fe	Fe Err	Co	Co Err	Ni	Ni Err	Cu	Cu Err	Zn	Zn Err	Ga	Ga Err	As	As Err	Se	Se Err	Rb	Rb Err	Sr	Sr Err
0.1182	0.0069	7.5213	0.0295	0.0185	0.0037	0.3913	0.0056	0.1914	0.0032	0.0072	0.0008	< LOD	0.0004	0.0007	0.0005	< LOD	0.0003	0.0004	0.0002	0.0033	0.0003
Mn	Mn Err	Fe	Fe Err	Co	Co Err	Ni	Ni Err	Cu	Cu Err	Zn	Zn Err	Ga	Ga Err	As	As Err	Se	Se Err	Rb	Rb Err	Sr	Sr Err
0.1191	0.0068	7.5174	0.0295	0.0172	0.0036	0.4127	0.0058	0.2023	0.0033	0.0076	0.0008	< LOD	0.0005	< LOD	0.0005	0.0003	0.0003	0.0002	0.0002	0.0032	0.0003
Mn	Mn Err	Fe	Fe Err	Co	Co Err	Ni	Ni Err	Cu	Cu Err	Zn	Zn Err	Ga	Ga Err	As	As Err	Se	Se Err	Rb	Rb Err	Sr	Sr Err
0.1141	0.0068	7.5345	0.0296	0.0177	0.0036	0.4072	0.0058	0.2004	0.0034	0.0078	0.0008	< LOD	0.0004	0.0008	0.0005	< LOD	0.0003	< LOD	0.0002	0.0034	0.0004

Y	Y Err	Zr	Zr Err	Nb	Nb Err	Mo	Mo Err	Pd	Pd Err	Ag	Ag Err	Cd	Cd Err	Sn	Sn Err	Sb	Sb Err	Ba	Ba Err	La	La Err
0.0008	0.0003	0.0015	0.0002	< LOD	0.0003	< LOD	0.0010	0.0109	0.0009	< LOD	0.0006	< LOD	0.0004	< LOD	0.0014	< LOD	0.0021	< LOD	0.0036	< LOD	0.0043
Y	Y Err	Zr	Zr Err	Nb	Nb Err	Mo	Mo Err	Pd	Pd Err	Ag	Ag Err	Cd	Cd Err	Sn	Sn Err	Sb	Sb Err	Ba	Ba Err	La	La Err
0.0007	0.0003	0.0015	0.0002	< LOD	0.0003	< LOD	0.0010	0.0069	0.0009	< LOD	0.0007	< LOD	0.0005	< LOD	0.0015	< LOD	0.0019	0.0049	0.0037	< LOD	0.0044
Y	Y Err	Zr	Zr Err	Nb	Nb Err	Mo	Mo Err	Pd	Pd Err	Ag	Ag Err	Cd	Cd Err	Sn	Sn Err	Sb	Sb Err	Ba	Ba Err	La	La Err
0.0006	0.0003	0.0013	0.0002	< LOD	0.0003	< LOD	0.0010	0.0057	0.0008	< LOD	0.0007	0.0005	0.0005	< LOD	0.0017	< LOD	0.0020	0.0046	0.0043	< LOD	0.0050
Y	Y Err	Zr	Zr Err	Nb	Nb Err	Mo	Mo Err	Pd	Pd Err	Ag	Ag Err	Cd	Cd Err	Sn	Sn Err	Sb	Sb Err	Ba	Ba Err	La	La Err
0.0007	0.0003	0.0018	0.0003	< LOD	0.0003	< LOD	0.0010	0.0047	0.0008	< LOD	0.0007	< LOD	0.0005	< LOD	0.0017	< LOD	0.0020	< LOD	0.0042	< LOD	0.0049
0.0006	0.0003	0.0013	0.0002	< LOD	0.0003	< LOD	0.0010	0.0047	0.0008	< LOD	0.0007	0.0008	0.0005	< LOD	0.0017	< LOD	0.0020	0.0046	0.0043	< LOD	0.0050
Y	Y Err	Zr	Zr Err	Nb	Nb Err	Mo	Mo Err	Pd	Pd Err	Ag	Ag Err	Cd	Cd Err	Sn	Sn Err	Sb	Sb Err	Ba	Ba Err	La	La Err
0.0009	0.0003	0.0012	0.0003	< LOD	0.0003	< LOD	0.0009	0.0030	0.0008	< LOD	0.0008	< LOD	0.0006	< LOD	0.0018	< LOD	0.0018	< LOD	0.0045	< LOD	0.0050
Y	Y Err	Zr	Zr Err	Nb	Nb Err	Mo	Mo Err	Pd	Pd Err	Ag	Ag Err	Cd	Cd Err	Sn	Sn Err	Sb	Sb Err	Ba	Ba Err	La	La Err
0.0006	0.0003	0.0011	0.0002	< LOD	0.0003	< LOD	0.0009	0.0029	0.0008	< LOD	0.0007	0.0006	0.0005	< LOD	0.0017	< LOD	0.0019	0.0050	0.0040	< LOD	0.0045
Y	Y Err	Zr	Zr Err	Nb	Nb Err	Mo	Mo Err	Pd	Pd Err	Ag	Ag Err	Cd	Cd Err	Sn	Sn Err	Sb	Sb Err	Ba	Ba Err	La	La Err
0.0006	0.0003	0.0010	0.0003	< LOD	0.0003	< LOD	0.0010	0.0022	0.0008	< LOD	0.0008	< LOD	0.0005	< LOD	0.0017	< LOD	0.0019	0.0057	0.0044	< LOD	0.0050
0.0004	0.0003	0.0011	0.0003	< LOD	0.0003	< LOD	0.0010	0.0027	0.0008	< LOD	0.0008	< LOD	0.0005	< LOD	0.0018	< LOD	0.0020	0.0052	0.0045	< LOD	0.0051
Y	Y Err	Zr	Zr Err	Nb	Nb Err	Mo	Mo Err	Pd	Pd Err	Ag	Ag Err	Cd	Cd Err	Sn	Sn Err	Sb	Sb Err	Ba	Ba Err	La	La Err
0.0003	0.0003	0.0010	0.0002	< LOD	0.0003	< LOD	0.0010	0.0045	0.0008	< LOD	0.0007	< LOD	0.0005	< LOD	0.0017	< LOD	0.0020	< LOD	0.0042	< LOD	0.0049
Y	Y Err	Zr	Zr Err	Nb	Nb Err	Mo	Mo Err	Pd	Pd Err	Ag	Ag Err	Cd	Cd Err	Sn	Sn Err	Sb	Sb Err	Ba	Ba Err	La	La Err
0.0006	0.0003	0.0011	0.0002	< LOD	0.0003	< LOD	0.0010	0.0035	0.0008	< LOD	0.0008	< LOD	0.0005	< LOD	0.0018	< LOD	0.0020	0.0075	0.0044	< LOD	0.0050
Y	Y Err	Zr	Zr Err	Nb	Nb Err	Mo	Mo Err	Pd	Pd Err	Ag	Ag Err	Cd	Cd Err	Sn	Sn Err	Sb	Sb Err	Ba	Ba Err	La	La Err
0.0005	0.0003	0.0012	0.0002	< LOD	0.0003	< LOD	0.0009	0.0023	0.0008	< LOD	0.0008	< LOD	0.0005	< LOD	0.0017	< LOD	0.0019	0.0069	0.0042	< LOD	0.0048

Ce	Ce Err	Hf	Hf Err	Ta	Ta Err	W	W Err	Pt	Pt Err	Hg	Hg Err	Tl	Tl Err	Pb	Pb Err	Bi	Bi Err	Th	Th Err	U	U Err
< LOD	0.0052	< LOD	0.0004	< LOD	0.0078	0.0020	0.0019	0.0301	0.0029	< LOD	0.0011	< LOD	0.0007	0.0062	0.0009	0.0008	0.0007	< LOD	0.0009	< LOD	0.0004
Ce	Ce Err	Hf	Hf Err	Ta	Ta Err	W	W Err	Pt	Pt Err	Au	Au Err	Hg	Hg Err	Tl	Tl Err	Pb	Pb Err	Bi	Bi Err	Th	Th Err
< LOD	0.0052	< LOD	0.0005	< LOD	0.0069	< LOD	0.0020	0.0192	0.0024	< LOD	0.0006	< LOD	0.0011	< LOD	0.0007	0.0065	0.0010	< LOD	0.0007	< LOD	0.0008
Ce	Ce Err	Hf	Hf Err	Ta	Ta Err	W	W Err	Pt	Pt Err	Hg	Hg Err	Tl	Tl Err	Pb	Pb Err	Bi	Bi Err	Th	Th Err	U	U Err
< LOD	0.0061	< LOD	0.0004	< LOD	0.0063	< LOD	0.0020	0.0090	0.0021	< LOD	0.0012	< LOD	0.0008	0.0059	0.0010	< LOD	0.0008	< LOD	0.0007	< LOD	0.0004
Ce	Ce Err	Hf	Hf Err	Ta	Ta Err	W	W Err	Pt	Pt Err	Au	Au Err	Hg	Hg Err	Tl	Tl Err	Pb	Pb Err	Bi	Bi Err	Th	Th Err
< LOD	0.0059	< LOD	0.0004	< LOD	0.0060	0.0023	0.0019	0.0089	0.0020	< LOD	0.0006	< LOD	0.0011	< LOD	0.0007	0.0039	0.0009	< LOD	0.0008	< LOD	0.0008
< LOD	0.0061	< LOD	0.0004	< LOD	0.0058	0.0030	0.0019	0.0076	0.0020	< LOD	0.0006	< LOD	0.0011	< LOD	0.0008	0.0039	0.0009	< LOD	0.0008	< LOD	0.0008
Ce	Ce Err	Hf	Hf Err	Ta	Ta Err	W	W Err	Pt	Pt Err	Hg	Hg Err	Tl	Tl Err	Pb	Pb Err	Bi	Bi Err	Th	Th Err	U	U Err
< LOD	0.0060	< LOD	0.0004	< LOD	0.0049	< LOD	0.0019	0.0035	0.0017	< LOD	0.0010	< LOD	0.0008	0.0035	0.0010	< LOD	0.0008	< LOD	0.0007	< LOD	0.0004
Ce	Ce Err	Hf	Hf Err	Ta	Ta Err	W	W Err	Pt	Pt Err	Hg	Hg Err	Tl	Tl Err	Pb	Pb Err	Bi	Bi Err	Th	Th Err	U	U Err
< LOD	0.0055	< LOD	0.0004	< LOD	0.0053	< LOD	0.0019	0.0038	0.0017	< LOD	0.0010	< LOD	0.0008	0.0028	0.0009	< LOD	0.0008	< LOD	0.0007	< LOD	0.0004
Ce	Ce Err	Hf	Hf Err	Ta	Ta Err	W	W Err	Pt	Pt Err	Au	Au Err	Hg	Hg Err	Tl	Tl Err	Pb	Pb Err	Bi	Bi Err	Th	Th Err
< LOD	0.0060	< LOD	0.0004	< LOD	0.0054	< LOD	0.0019	0.0060	0.0018	< LOD	0.0006	< LOD	0.0010	< LOD	0.0008	0.0036	0.0009	< LOD	0.0008	< LOD	0.0007
< LOD	0.0062	< LOD	0.0004	< LOD	0.0054	< LOD	0.0019	0.0030	0.0017	< LOD	0.0006	< LOD	0.0010	< LOD	0.0008	0.0031	0.0009	< LOD	0.0008	< LOD	0.0007
Ce	Ce Err	Hf	Hf Err	Ta	Ta Err	W	W Err	Pt	Pt Err	Au	Au Err	Hg	Hg Err	Tl	Tl Err	Pb	Pb Err	Bi	Bi Err	Th	Th Err
< LOD	0.0059	< LOD	0.0004	< LOD	0.0056	< LOD	0.0018	0.0051	0.0018	< LOD	0.0006	< LOD	0.0011	< LOD	0.0008	0.0047	0.0010	< LOD	0.0007	< LOD	0.0007
Ce	Ce Err	Hf	Hf Err	Ta	Ta Err	W	W Err	Pt	Pt Err	Hg	Hg Err	Tl	Tl Err	Pb	Pb Err	Bi	Bi Err	Th	Th Err	U	U Err
< LOD	0.0061	< LOD	0.0004	< LOD	0.0056	< LOD	0.0019	0.0045	0.0018	< LOD	0.0011	< LOD	0.0008	0.0033	0.0009	< LOD	0.0008	< LOD	0.0007	< LOD	0.0004
Ce	Ce Err	Hf	Hf Err	Ta	Ta Err	W	W Err	Pt	Pt Err	Hg	Hg Err	Tl	Tl Err	Pb	Pb Err	Bi	Bi Err	Th	Th Err	U	U Err
< LOD	0.0058	< LOD	0.0004	< LOD	0.0057	< LOD	0.0019	0.0066	0.0019	< LOD	0.0010	< LOD	0.0008	0.0040	0.0010	< LOD	0.0008	< LOD	0.0007	< LOD	0.0004

Appendix F: XRD Graphs

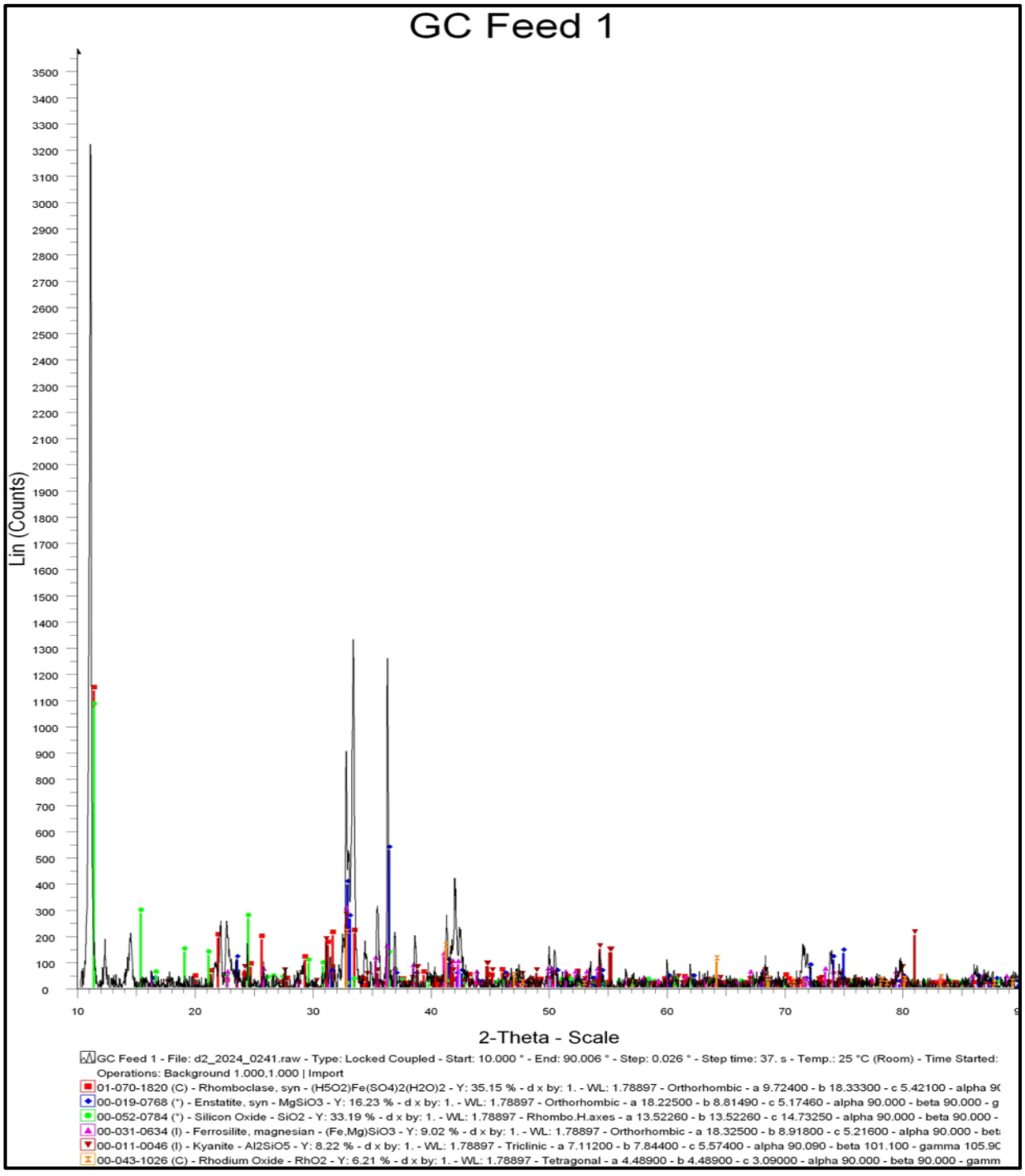

Figure 206: GC feed XRD results

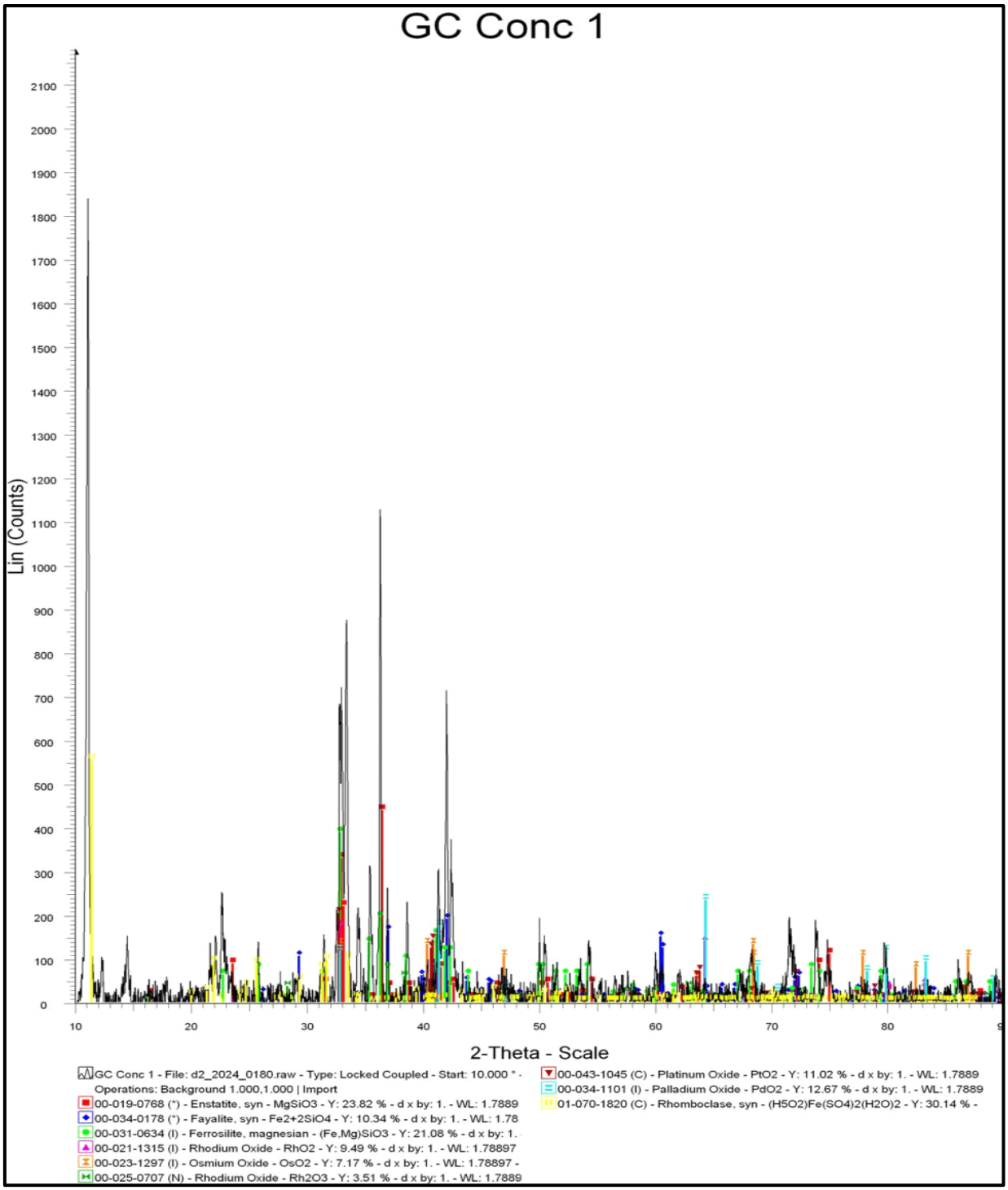

Figure 207: GC concentrate XRD results

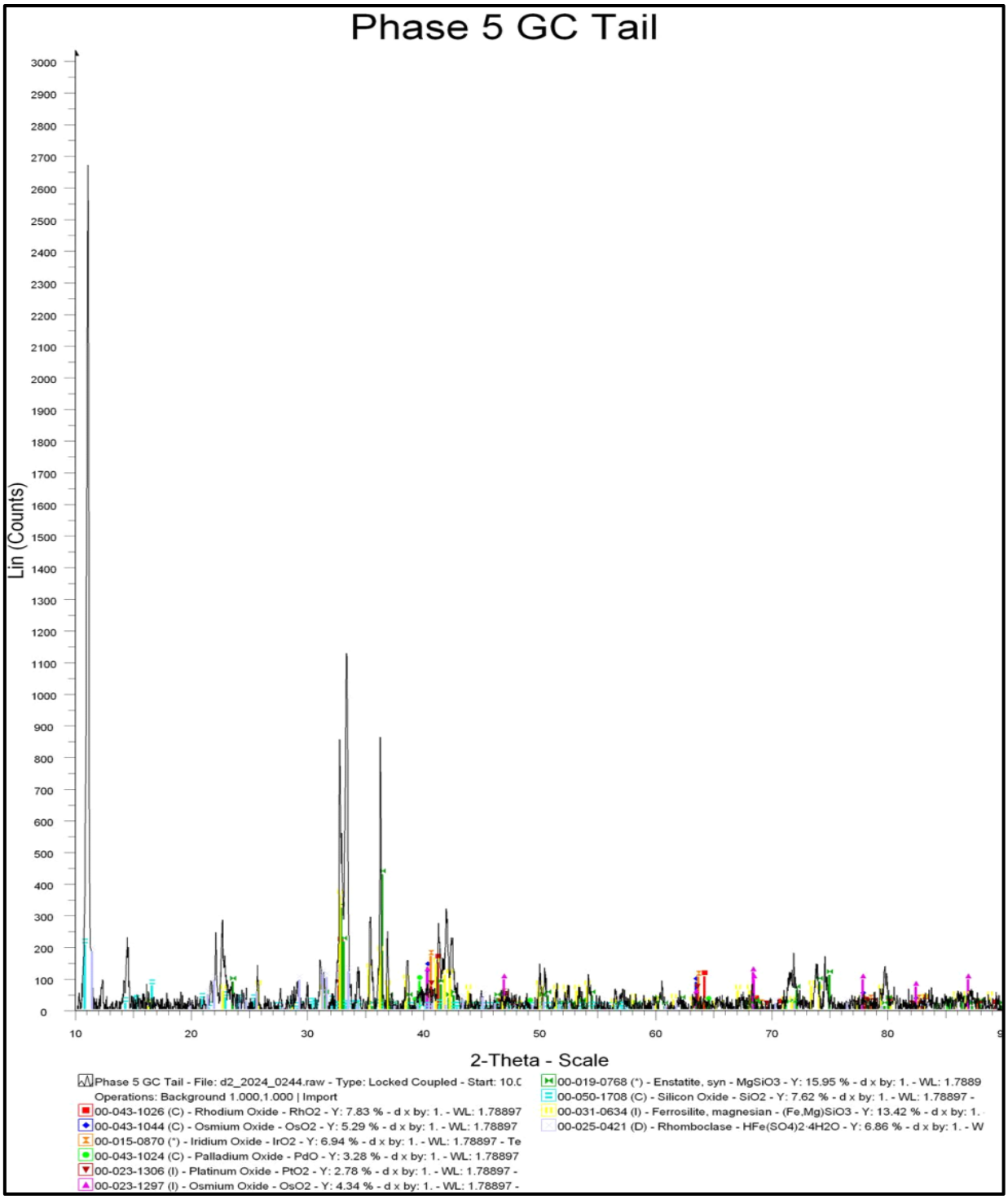

Figure 208: GC tail XRD results

Appendix G: SEM Images and Graphs

GC Feed

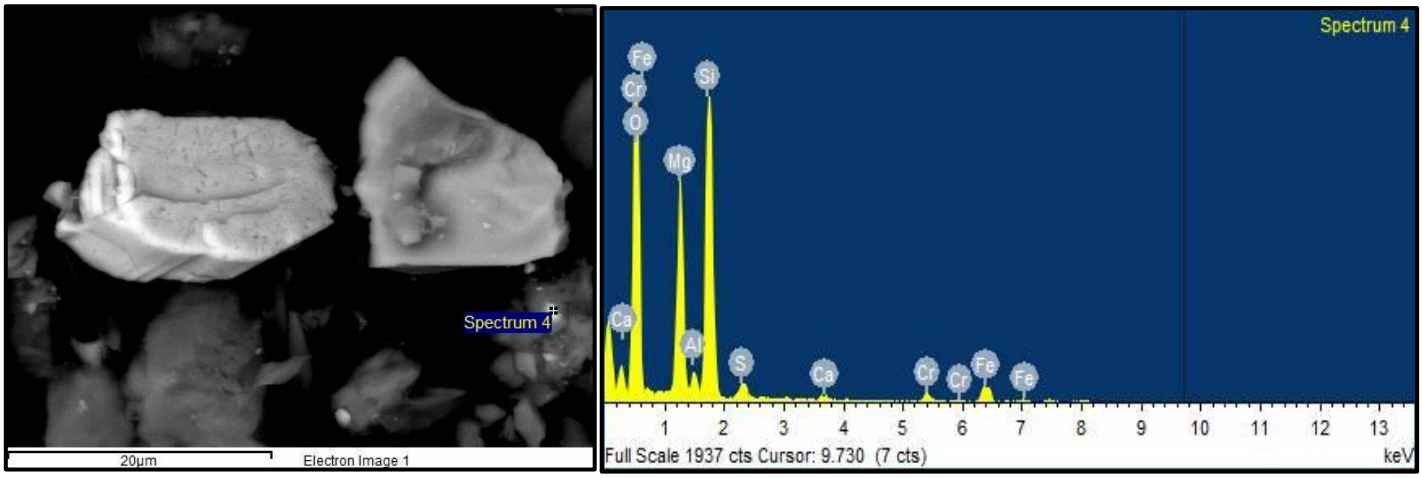

Figure 209: SEM image and composition of GC feed gangue particle

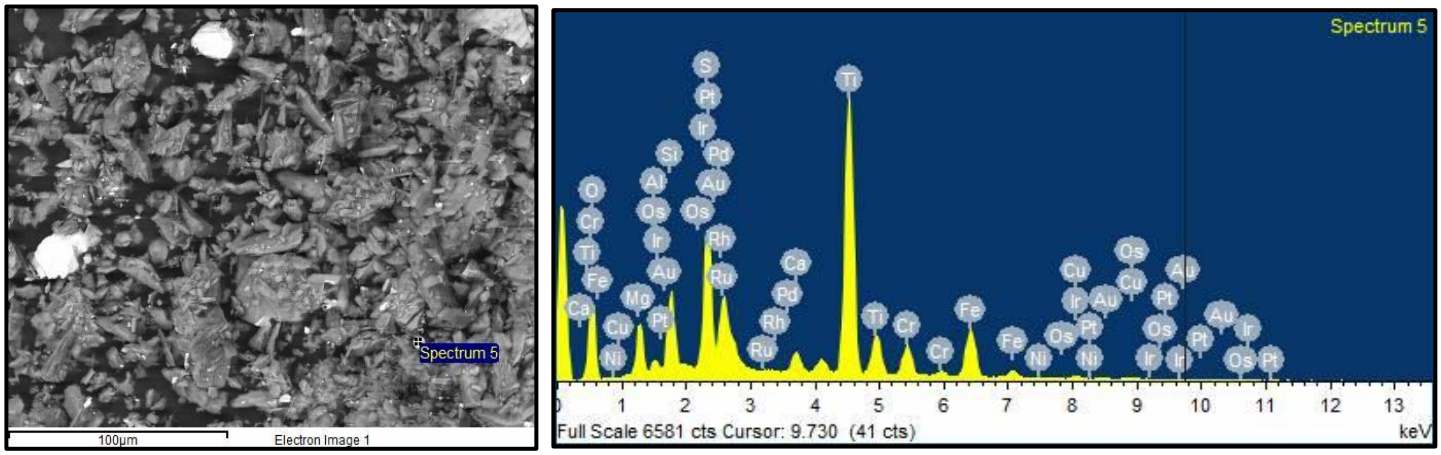

Figure 210: SEM image and composition of GC feed PGM particle

GC Tail

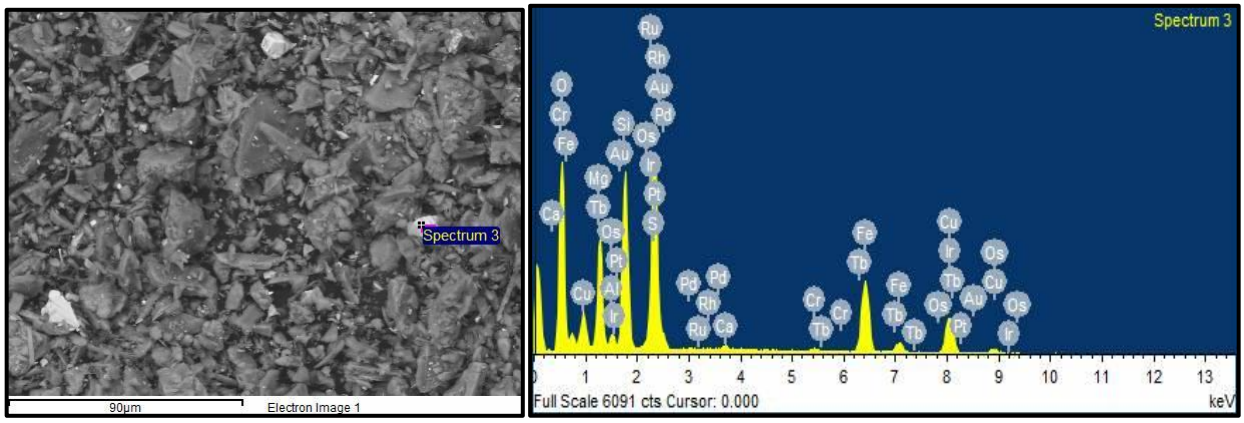

Figure 211: SEM image and composition of GC tail PGM particle

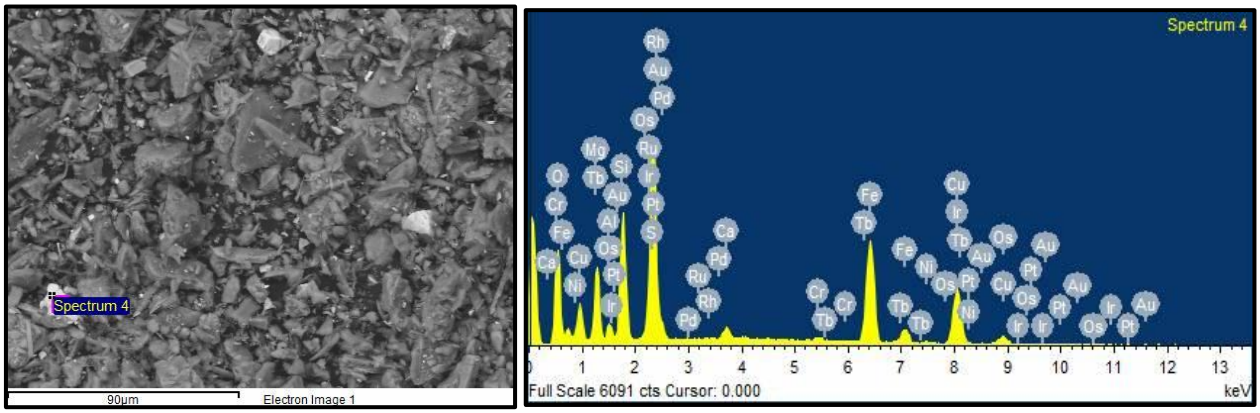

Figure 212: SEM image and composition of GC tail PGM particle

GC Concentrate

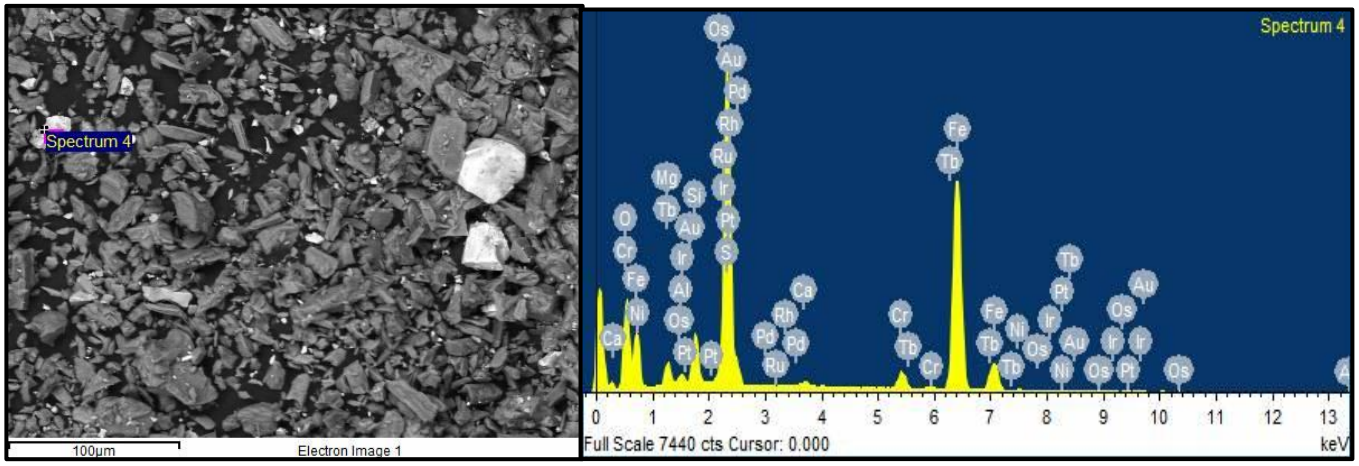

Figure 213: SEM image and composition of GC concentrate PGM particle

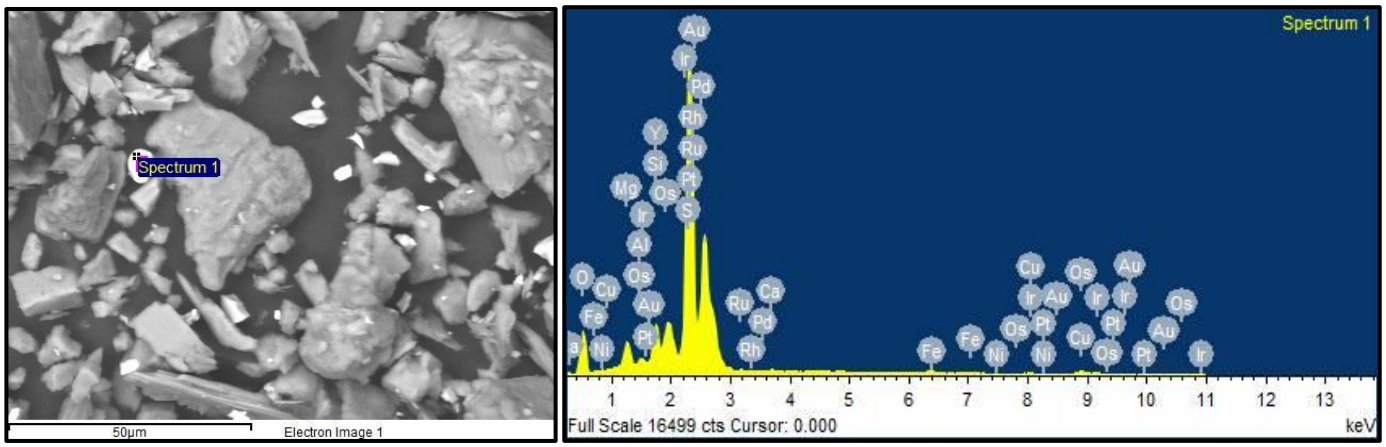

Figure 214: SEM image and composition of GC concentrate PGM particle

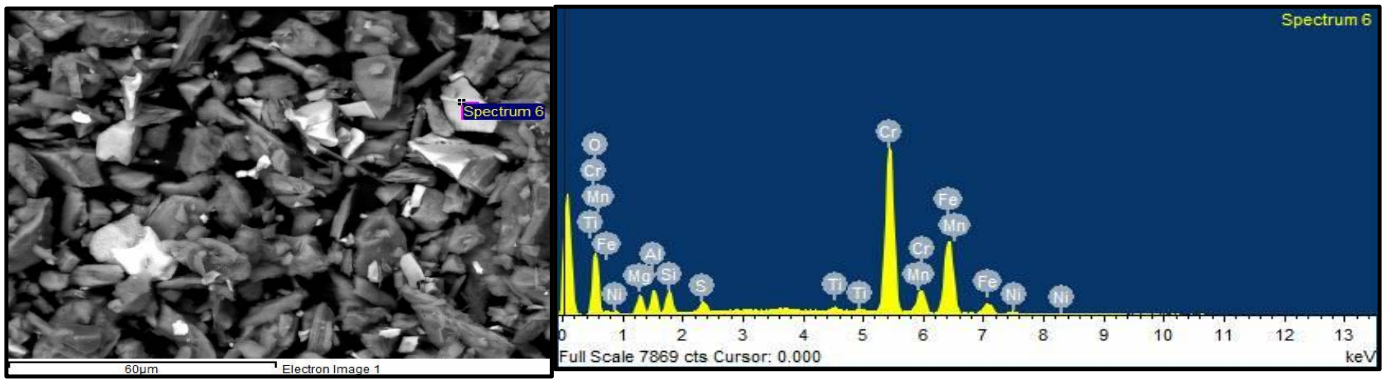

Figure 215: SEM image and composition of GC concentrate chrome particle

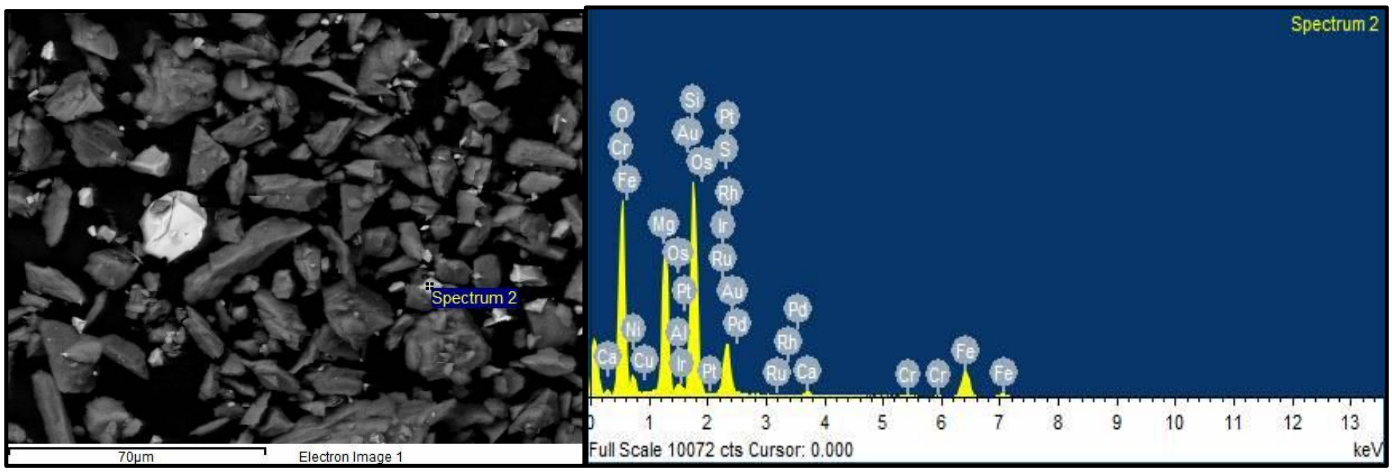

Figure 216: SEM image and composition of GC concentrate PGM particle